THE UNIVERSITY *of* EDINBURGH

The effect of rare and common single amino acid substitutions on DISC1 subcellular targeting and functional interaction with ATF4

Elise Linda Victoria Malavasi

PhD

The University of Edinburgh

2012

Declaration

I declare that, except for where noted, all work contained in this thesis was performed and composed by myself. Where others have contributed to elements of the work, this is clearly stated in the text. No element of this work has been submitted for any other degree or professional qualification.

Elise L.V. Malavasi

Acknowledgements

It has been a very long journey from the day I was recruited as a PhD student to the day I write these words, and the people who have contributed to making this a very pleasant one are far too many to aknowledge here!

Going back to the very beginning, I wish to thank Karen Chapman for encouraging me to start this journey, as well as Margarete Heck and all the organisers of the Wellcome Trust 4-year PhD programme in Edinburgh for taking me on board, and for putting a great deal of pressure on us students, particularly during the first year of this course! I must admit that, while experiencing over-the-roof cortisol levels was not particularly fun back then, I now realise how much this has helped my personal and professional development.

Next, I would like to thank my supervisors Kirsty Millar and David Porteous for the guidance and inspiration they have provided me during my PhD adventure. You have always supported my initiatives, and you have always encouraged me to develop and test my own ideas, for which I am extremely grateful. Thank you also for patiently and closely assisting me during the production of this thesis, and for doing so with a smile.

My thanks also go to all my fellow students and co-workers in the lab, for creating a very positive, supportive and inspirational environment to be in. Among them, Shaun Mackie and Fumiaki Ogawa deserve an extra special thank you for having been infinitely patient and kind teachers, and also for all the drinks they have bought me at the pub!

A big thank you to my beloved "Wellcome family": Robert Ekiert, Lynne Harris, Hayden Selvadurai and Tom Nowakowski for the unforgettable times we shared. I very much hope that there are many more awaiting us in the future.

Thanks to my dear "benchmate" and fellow student Gareth Briggs for his friendship, understanding, encyclopaedic culture and good sense of humour, which made for very interesting conversations and lightened my spirit in many occasions.

Needless to say, I thank my family with all my heart for constantly believing in me and supporting my education and personal growth, you are the driving force behind all my achievements.

Finally, thanks to the one who has always been at my side, through the good times and the bad times. Thank you for making me tea and putting things into perspective whenever I felt disheartened. You have all my love and gratitude, and even though I am the one who carried it in her laptop for 6 months, this thesis is your baby too!

Abstract

DISC1, a strong genetic candidate for psychiatric illness, is a molecular scaffold residing in multiple subcellular compartments, where it regulates the function of interacting proteins with key roles in neurodevelopment and plasticity. Both common and rare DISC1 missense variants are associated with risk of mental illness and/or brain abnormalities in healthy carriers, but the underlying mechanisms are unclear. In this thesis, I initially examine the effect of a panel of common and rare single amino acid substitutions on DISC1 subcellular targeting, establishing that the rare mutation R37W and the common variant L607F disrupt DISC1 nuclear targeting in a dominant-negative fashion. This finding predicts that DISC1 nuclear expression is severely impaired in 37W and 607F carriers. In addition, I show that the L607F substitution results in aberrant cytoplasmic and cytoskeletal distribution of DISC1. In the nucleus, DISC1 interacts with the transcription factor ATF4, which is involved in the regulation of cellular stress responses and memory consolidation. Here I show that at basal cAMP levels, wild-type DISC1 strongly inhibits the transcriptional activity of ATF4, and this effect is ablated by 37W and 607F, most likely as a consequence of their defective nuclear targeting. 607F additionally reduces DISC1/ATF4 interaction, which likely contributes to its weakened inhibitory effect. I also demonstrate that DISC1 modulates transcriptional responses to endoplasmic reticulum stress, and that this modulatory effect is also ablated by 37W and 607F. By providing evidence that single amino acid substitutions of DISC1 associated with psychiatric illness impair its regulatory function on ATF4-dependent transcription, I highlight a potential mechanism by which these protein variants may impact on molecular pathways underlying cognition and stress responses, two processes of direct relevance to psychiatric disease.

Table of contents

List of figures

List of tables

List of abbreviations used in this thesis

Genes and proteins

αCaMKII	Calcium/calmodulin-dependent protein kinase II alpha
βTrCP	Beta-transducin repeat containing E3 ubiquitin protein ligase
Akt1	V-akt murine thymoma viral oncogene homolog 1
AP-1	Activator protein 1
ApCREB2	Aplysia cAMP-responsive element-binding protein 2
APP	Amyloid beta (A4) precursor protein
ASNS	Asparagine synthetase
ATF4	Activating transcription factor 4, aka CREB2
ATF4ΔRK	ATF4 mutant lacking the DNA binding region
ATF5	Activating transcription factor 5
BBS4	Bardet-Biedl syndrome 4
BGH	Bovine growth hormone
BSA	Bovine serum albumin
C/EBP	CCAAT/enhancer binding protein
CAMD1	Coiled-coil protein associated with myosin II and DISC1
CBP	CREB-binding protein
CENPF	Centromere protein F, 350/400kDa (mitosin)
CEP290	Centrosomal protein, 290kDa
CHOP	CCAAT/enhancer-binding protein homologous protein
CIT	Citron (rho-interacting, serine/threonine kinase 21)
CK1	Casein kinase 1
CREB1	cAMP responsive element binding protein 1, aka CREB
CREB2	cAMP-responsive element-binding protein 2, aka ATF4
CREM	cAMP responsive element modulator
DISC1	Disrupted-In-Schizophrenia 1

DISC1ΔLZ9	DISC1 mutant lacking the leucine zipper in exon 9
DISC1FP1	DISC1 Fusion Partner 1
DISC2	Disrupted-In-Schizophrenia 2
Dixdc1	DIX domain containing 1
EIF2B	Eukaryotic translation initiation factor 2B
eIF2α	Eukaryotic translation initiation factor 2 alpha
ERK1	Extracellular signal-regulated kinase 1
FOS	FBJ murine osteosarcoma viral oncogene homolog
Gal4	Lectin, galactoside-binding, soluble, 4
GAPDH	Glyceraldehyde-3-phosphate dehydrogenase
GCN2	General control nonrepressed 2
GFAP	Glial fibrillary acidic protein
GFP	Green fluorescent protein
GluR1	Glutamate receptor, ionotropic, AMPA 1
Grb2	Growth factor receptor-bound protein 2
Grp78	Glucose-regulated protein, 78kDa
GSK3β	Glycogen synthase kinase 3 beta
H3	Histone 3
HRI	Heme regulated initiation factor 2 alpha kinase
HRP	Horseradish peroxidase
HSP90	Heat-shock protein, 90 kDa
JUN	*Jun* proto-oncogene
Kal7	Kalirin-7
Ki67	Antigen identified by monoclonal antibody Ki-67
LIS1	Lissencephaly 1
MAG	Myelin-associated glycoprotein
MAPK	Mitogen-activated protein kinase
MBP	Myelin basic protein
mTOR	Mammalian target of rapamycin

mTORC1	Mammalian target of rapamycin complex 1
N-CoR	Nuclear receptor corepressor
NDE1	Nuclear Distribution factor E homologue 1
NDEL1	Nuclear Distribution factor E homologue-Like 1
NEK6	NIMA (never in mitosis gene a)-related kinase 6
NIPK	Neuronal cell death inducible putative kinase, aka TRIB3
NMDAR	N-Methyl-D-aspartic acid receptor
Nrf2	Nuclear factor (erythroid-derived 2)-like 2
NRG1	Neuregulin 1
p84	Nuclear matrix protein, 84 kDa
PCM1	Pericentriolar Material 1
PDE4	Phosphodiesterase 4
PERK	RNA-dependent protein kinase-like endoplasmic reticulum kinase
PHD3	Prolyl-4-hydroxylase 3, aka EGLN3 (egl nine homolog 3)
PKA	Protein kinase A, aka cAMP-dependent protein kinase
PKG	cGMP-dependent protein kinase
PKIα	Protein kinase inhibitor alpha
PKR	Protein kinase RNA-activated
PLP	Proteolipid protein
PML	Promyelocytic leukemia
PP2A	Protein phosphatase 2, regulatory subunit A
PS1	Presenilin 1
PSD-95	Postsynaptic density protein 95
Puma	p53-upregulated modulator of apoptosis
PV	Parvalbumin
Rac1	Ras-related C3 botulinum toxin substrate 1
RankL	Receptor activator of nuclear factor kappa B ligand
RPL41	Ribosomal protein L41
RSK2	Ribosomal protein S6 kinase 2, 90kDa, polypeptide 3

SAP	Shrimp alkaline phosphatase
Satb2	Special AT-rich sequence-binding homeobox 2
SCF	Skp1/cullin/F-box protein
SLC7A11	Sodium-independent aspartate/glutamate/cystine transporter, aka xCT
SMARCE1	SWI/SNF related, matrix associated, actin dependent regulator of chromatin, subfamily e, member 1
SNAT2	System A neutral amino acid transporter 2
Sox2	SRY (sex determining region Y)-box 2
SP6	Sp6 transcription factor
TBB	TATA-binding protein
TFIIB	General transcription factor IIB
TFIIF	General transcription factor IIF
TK	Thymidine kinase
TNIK	TRAF2 and NCK interacting kinase
TRAX	Translin-associated factor X, aka TSNAX

Units

°C	Degree centigrade
b	Base (nucleic acid)
Da	Dalton
g	Gram
l	Litre
m	Metre
M	Molar (mols per liter)
mol	Mols
RPM	Revolutions per minute
V	Volt
n	Nano ($x10^{-9}$)
µ	Micro ($x10^{-6}$)

m	Milli ($x10^{-3}$)
k	Kilo ($x10^{3}$)
M	Mega ($x10^{6}$)

Amino acids

A/ala	Alanine
C/cys	Cysteine
F/phe	Phenylalanine
G/gly	Glicine
H/his	Histidine
I/ile	Isoleucine
L/leu	Leucine
M/met	Methionine
P/pro	Proline
Q/gln	Glutamine
R/arg	Arginine
S/ser	Serine
T/thr	Threonine
V/val	Valine
W/trp	Tryptofan

Nucleotides

A	Adenine
C	Cytosine
G	Guanine
T	Thymidine

Chemical compounds and biomolecules

Aβ	Amyloid beta
AMPA	α-amino-3-hydroxy-5-methyl-4-isoxazolepropionic acid
APS	Ammonium persulphate
ATP	Adenosine Triphosphate
BAC	Bacterial artificial chromosome
cAMP	Cyclic Adenosine Monophosphate
cDNA	Complementary DNA
CTP	Cytidine Triphosphate
DABCO	1,4-diazabicyclo[2.2.2]octane
DAPI	4',6-diamidino-2-phenylindole
DMSO	Dimethyl sulfoxide
DNA	Deoxyribonucleic Acid
dNTP	Deoxyribonucleotide triphosphate
DTT	Dithiothreitol
EDTA	Ethylenediaminetetraacetic Acid
ENU	N-nitroso-ethylurea
FSK	Forskolin
GABA	Gamma-Aminobutyric acid
GDP	Guanosine diphosphate
GST	Glutatione S-transferase (tag)
GTP	Guanosine triphosphate
HCY	Homocysteine
HEPES	4-(2-Hydroxyethyl)piperazine-1-ethanesulfonic acid
HisOH	Histidinol
IBMX	3-isobutyl-1-methylxanthine
mPKI	Myristoylated protein kinase inhibitor peptide (14-22)
mRNA	Messenger RNA
MTT	3-(4,5-Dimethylthiazol-2-yl)-2,5-diphenyltetrazolium
NAD(P)H	Nicotinamide adenine dinucleotide phosphate

NMDA	N-Methyl-D-aspartic acid
OA	Okadaic acid
PDVF	Polyvinylidene difluoride
PFA	Paraformaldehyde
PolyI:C	Polyinosinic:polycytidylic acid
RNA	Ribonucleic acid
SDS	Sodium Dodecyl Sulphate
shRNA	Short hairpin RNA
siRNA	Small interfering RNA
TEMED	Tetramethylethylenediamine
TG	Thapsigargin
tRNA	Transfer RNA
TTP	Thymidine triphosphate

Other abbreviations

(f)MRI	(Functional) magnetic resonance imaging
3D	Three-dimensional
AARE	Amino acid response element
ANOVA	Analysis of variance
Bt	*Bos taurus*
BTF	Basic transcription factors
bZIP	Basic region-leucine zipper
CARE	C/EBP-ATF4 response element
CBNE	Chromatin-bound nuclear extract
CCD	Charge coupled device
CD-CV	Common disease-common variant
CE	Cytoplasmic extract
Cf	*Canis familiaris*

ChIP-seq	Chromatin immunoprecipitation and sequencing
CMV	Cytomegalovirus
CNV	Copy number variant
Co-IP	Co-immunoprecipitation
CRE	cAMP response element
CSKE	Cytoskeletal extract
DALY	Disability Adjusted Life Year
DISC1LZ9	Leucine zipper in DISC1 exon 9
DMEM	Dulbecco Modified Eagle's minimum essential Medium
DN	Dominant-negative
DPF	Days post fertilisation
Dr	*Danio rerio*
DSM	Diagnostic and Statistical Manual of Mental Illness
DZ	Dizygotic
E	Embryonic day
EC_{50}	Half maximal effective concentration
ECACC	European Collection of Cell Cultures
EMSA	Electrophoretic mobility shift assay
ER	Endoplasmic reticulum
ERP	Event-related potential
FA	Fractional anisotropy
FBS	Foetal bovine serum
GWAS	Genome-wide association study
HBSS	Hank's balanced salt solution
HGU	Human Genetics Unit
HPA	Hypothalamus-pituitary-adrenal
HPLC	High-performance liquid chromatography
Hs	Homo sapiens
IC_{50}	Half maximal inhibitory concentration

ICC	Immunocytochemistry
ICD	International Classification of Disease
IP	Immunoprecipitation
iPS	Induced pluripotent stem (cells)
ISR	Integrated stress response
KD	Knock-down
KO	Knock-out
LB	Luria-Bertani
LI	Latent inhibition
LOD	Logarithm of odds
LTD	Long-term depression
LTF	Long-term facilitation
LTP	Long term potentiation
M2H	Mammalian-two-hybrid
Ma	*Macaca mulatta*
ME	Membrane extract
Mm	*Mus musculus*
MRC	Medical Research Council
MTOC	Microtubule-organising centre
MZ	Monozygotic
NA	Nucleus accumbens
NC	Negative control
NES	Nuclear export signal
NLS	Nuclear localisation signal
O/N	Overnight
ODDD	Oxygen-dependent degradation domain
ORF	Open reading frame
PBS	Phosphate buffered saline
PCR	Polymerase chain reaction

PFC	Prefrontal cortex
PLA	Proximity ligation assay
PPI	Prepulse inhibition
PSD	Post-synaptic density
Pt	*Pan troglodytes*
Q-PCR	Quantitative PCR
RACE	Rapid amplification of cDNA ends
RIPA	Radio immuno precipitation assay
Rn	*Rattus norvegicus*
RNS	Reactive nitrogen species
ROI	Region of interest
ROS	Reactive oxygen species
RT	Room temperature
SCN	Suprachiasmatic nucleus
SF	Serine/phenylalanine-rich motif of DISC1
SNE	Soluble nuclear extract
SNP	Single nucleotide polymorphism
SPR	Surface plasmon resonance
SV40	Simian virus 40
TAE	Tris-Acetate-EDTA
TE	Tris-EDTA
TGS	Tris-Glysine-SDS
Tr	*Takifugu rubripes*
UCR	Upstream conserved region
uORF	Upstream ORF
UTR	Untranslated region
UV	Ultra violet
VWM	Vanishing white matter
WB	Western blotting

WHO	World Health Organisation
WM	White matter
WT	Wild-type
Y2H	Yeast-two-hybrid
YLD	Years lived with Disability
YLL	Years Lost to Premature Mortality

1 Introduction

1.1 Introduction to psychiatric illness

1.1.1 *The global burden of psychiatric illness*

Psychiatric disorders are defined by the World Health Organisation (WHO) as "clinically significant conditions characterised by alterations in thinking, mood (emotions) or behaviour associated with personal distress and/or impaired functioning" (WHO World Health Report 2001). Psychiatric diseases are heterogeneous in the nature, severity, persistence and age of onset of the symptoms, which are often disabling and can severely impair the quality of life of the affected individuals and their close relatives. It is estimated that more than 25% of people worldwide are affected by psychiatric illness at some point during their life (WHO, 2001). Due to their relatively high prevalence and disabling symptoms, psychiatric disorders are a major economic burden for society (Gustavsson *et al*, 2011; Ormel *et al*, 2008). A new parameter has been introduced by the WHO to quantify the global burden of disease: the Disability Adjusted Life Year (DALY). DALY is the sum of the Years of Life Lost to Premature Mortality (YLL) and the Years Lived with Disability (YLD). Thus, one DALY corresponds to one lost year of healthy life. In the year 2000, psychiatric disorders accounted for 12% of DALYs and 31% of YLDs worldwide, and it is estimated that by the year 2015 they will be responsible for 15% of DALYs globally (Murray & Lopez, 1996). Depression, schizophrenia and bipolar disorder rank among the top ten causes of disability worldwide at all ages, and among the top five in individuals aged 15 to 44 (WHO, 2001).

With an estimated global lifetime prevalence of 16%, anxiety disorders are the most common mental illnesses (Kessler *et al*, 2009). Mood disorders follow, with an overall lifetime prevalence of about 12% (Kessler *et al*, 2009). Depression is the most prevalent mood disorder (estimated lifetime prevalence between 8.3% and 16.2%), and represents the leading cause of YLDs and the fourth leading cause of DALYs worldwide (Richards, 2011) and (WHO, 2001). Bipolar disorder, another relatively common mood disorder with a lifetime prevalence of 4-6% (Kessler *et al*,

2009), ranks fifth and ninth among the causes of YLDs and DALY, respectively, in the younger population (15 to 44 years of age) (WHO, 2001). Finally, with a lifetime prevalence of 0.4-0.8% (Perala *et al*, 2007; Saha *et al*, 2005), Schizophrenia also features among the top causes of disability worldwide, ranking third and eighth leading cause of YLDs and DALYs, respectively, among individuals aged 15 to 44 (WHO, 2001).

Despite the significant burden it represents for the affected individuals and society, psychiatric illness is still poorly understood. As a result, no radically new drugs or alternative therapeutic strategies have been identified since the introduction of antidepressants and antipsychotics in the 50s (Hyman, 2008). It is hoped that a better understanding of the molecular pathogenesis of psychiatric disorders will pave the way for the development of improved preventative and therapeutic approaches.

1.1.2 *Major depression, bipolar disorder and schizophrenia*

Due to our still limited understanding of the neurobiology of mental illness and the lack of specific biomarkers, diagnosis of psychiatric conditions is currently solely based on clinical observations such as symptoms, signs and course of illness (Hyman, 2007; Hyman, 2008). Based on expert consensus, two manuals have been compiled that list the currently recognised psychiatric conditions and define the criteria to diagnose them: the Diagnostic and Statistical Manual of Mental Disorders, (DSM), and the International Classification of Disease (ICD). The DSM, currently at its fourth edition, focuses on mental illness and is produced by The American Psychiatric Association. The ICD, now at its tenth edition, is produced by the WHO and covers all human diseases, with chapter V being dedicated to psychiatric diagnoses. Both manuals are in current use, but the DSM-IV is used much more frequently in research settings. The DSM-IV diagnostic criteria for major depression, bipolar disorder and schizophrenia are briefly summarised below. The clinical features of schizophrenia will be described in more detail in the next section.

Major depression, also referred to as unipolar depression, is characterised by prolonged depressive episodes during which the sufferer experiences feelings of sadness, worthlessness and emptiness and loses interest or pleasure in everything. A

major depressive episode can also include sleep disturbances, altered appetite, loss of energy and reduced ability to concentrate, and can lead to recurrent suicidal thoughts.

Bipolar disorder, also known as manic-depressive disorder, is characterised by major depressive episodes alternating with manic or mixed episodes. A manic episode is defined as a period of abnormally and persistently elevated mood, during which the sufferer experiences inflated self-esteem, decreased need for sleep, increased distractibility, increased talkativeness and flights of ideas. Bipolar patients experiencing a manic episode are more likely to engage in pleasurable activities and risky behaviours. A mixed episode is defined as meeting both the criteria for a major depressive episode and a manic episode nearly every day for at least one week.

Schizophrenia is characterised by the concomitant occurrence of "positive" and "negative" symptoms. Positive symptoms include delusions, hallucinations and/or disorganised thoughts, whereas negative symptoms are manifested as blunted emotional responses, loss of motivation and speech decline. For the diagnostic criteria for schizophrenia to be met, the above symptoms must be accompanied by a social or occupational dysfunction that compromises the sufferer's ability to work, live independently and/or maintain interpersonal relations.

1.1.2.1 *Clinical features of schizophrenia*

Schizophrenia is a highly heterogeneous syndrome in terms of clinical presentation, severity of the symptoms, course of illness, response to treatment and long-term outcome (Peralta & Cuesta, 2001). Due to the high variability of its clinical profile, the nosological boundaries between schizophrenia and other psychiatric disorders, especially mood disorders, are not clearly demarked, which led to the proposition that schizophrenia and bipolar disorder may be better conceptualised as a spectrum of clinical manifestations rather than distinct diseases (Kendell & Brockington, 1980; Owen *et al*, 2007). In general, the schizophrenia syndrome includes several distinct clusters or dimensions of signs and symptoms, which can be classified as positive symptoms, negative symptoms, disorganised thought and behaviour, mood symptoms and cognitive impairment (Tandon *et al*, 2009). Positive symptoms involve a distorted perception of reality, and they are typically manifested as

hallucinations (false perceptions) and delusions (false beliefs) (Tandon *et al*, 2009). Hallucinations can affect all senses, although auditory hallucinations (hearing voices) are the most common in schizophrenia patients (Waters *et al*, 2012). The nature of delusions can vary broadly between patients, and it is influenced by the social and cultural setting of the affected individual, but persecutory delusions and delusions of reference (i.e. the belief that irrelevant and innocuous events or phenomena have a specific significance for oneself) are particularly common in schizophrenia (Tandon *et al*, 2009). Negative symptoms are described as a severe impairment or complete loss of affective and conative functions (e.g. volition, drive, desire), and can be manifested as emotional bluntness, anhedonia, lack of motivation, initiative and interest, speech impairment and social withdrawal (Tandon *et al*, 2009). Disorganised thought constitutes a further clinical dimension of schizophrenia, and consists in the inability to formulate logical and sequential thoughts, often resulting in inconsistent, incongruous and disorganised behaviour (Tandon *et al*, 2009). Mood alterations, and in particular depression, are an integral part of the disease for many schizophrenia patients, and they can occur at any stage of the illness, although they tend to become more pronounced during psychotic exacerbations (Tandon *et al*, 2009). Schizophrenia is also characterised by a generalised cognitive impairment, which is a highly prevalent feature of the disease, although its extent varies significantly between patients (Tandon *et al*, 2009). This cognitive impairment is commonly present before the onset of positive symptoms, and it precedes the beginning of antipsychotic treatment, indicating that it is a core feature of the disease, which persists throughout the course of illness (Tandon *et al*, 2009). However, the question of whether cognitive abilities remain stable in schizophrenia patients or instead decline gradually as the disease progresses is still under debate (Napal *et al*, 2012). Importantly, similar cognitive defects, albeit of attenuated severity, are present in a subgroup of unaffected first-degree relatives of schizophrenia patients, indicating that these deficits are a hallmark of disease susceptibility (Tandon *et al*, 2009). Although the intellectual impairment in schizophrenia is of a generalised nature (i.e. schizophrenia patients have, on average, a lower IQ compared to healthy controls), some spheres of cognition, such as episodic memory, processing speed, verbal fluency, attention, executive functions

and working memory, are more affected than others (Tandon *et al*, 2009). Unlike positive symptoms, the impairment of cognitive function in schizophrenia is not significantly improved by antipsychotic treatment, and together with negative symptoms, which also respond poorly to medication, it underlies the poor social integration and long-term disability of the patients (Tandon *et al*, 2009).

The evolution of schizophrenia typically follows a sequential trajectory in which a premorbid phase and a prodromal phase precede the onset of illness (Tandon *et al*, 2009) (Figure 1.1, taken from Tandon *et al*, 2009). In the premorbid phase, individuals who will later develop schizophrenia often present a range of behavioural, cognitive and emotional abnormalities, including impaired attention, language deficits, poor academic performance, social withdrawal and emotional detachment (Schenkel & Silverstein, 2004). However, it is important to emphasize that not all schizophrenia patients experience a premorbid phase, and not all individuals that show the typical signs and symptoms of premorbid schizophrenia will later develop the disease (Tandon *et al*, 2009). In the prodromal phase, mood alterations, cognitive impairment and negative symptoms are accompanied by mild psychotic symptoms (Cornblatt *et al*, 1999). Between one sixth and one half (depending on the population studied and the inclusion criteria) of the individuals presenting the signs and symptoms of prodromal schizophrenia will later develop the disease (Tandon *et al*, 2009). The onset of schizophrenia is marked by the first full-blown psychotic episode, which may include hallucinations, delusions and disorganised speech and behaviour, and often results in hospitalisation (Tandon *et al*, 2009). The onset of schizophrenia typically occurs during adolescence or early adulthood, with earlier age of onset, which is more common in males than females, being associated with more severe symptoms and poorer outcome (Tandon *et al*, 2009). After the first psychotic episode, positive symptoms typically go through intermittent phases of exacerbation and remission, with highly variable patterns between patients (Haro *et al*, 2008). Symptom exacerbation can be triggered by stress, substance abuse or non-compliance to treatment (Tandon *et al*, 2009). In the years following the disease onset, positive symptoms tend to become milder, while negative symptoms become more prominent and mood remains very variable, leading to a progressive decline of social function, after which a plateau is frequently

reached (Tandon *et al*, 2009) (Figure 1.1). The long-term disease outcome varies substantially, with some patients showing partial or complete remission, and others deteriorating to a state of severe social and functional deficit (Tandon *et al*, 2009). In general, schizophrenia patients have higher mortality rates, a significant proportion of which is due to high rates of suicide, but that can also be reconducted to a high prevalence of substance abuse, including nicotine and alcohol, and severe comorbidities like cardiovascular disease (Tandon *et al*, 2009). All together, these factors account for the elevated individual and societal burden of schizophrenia.

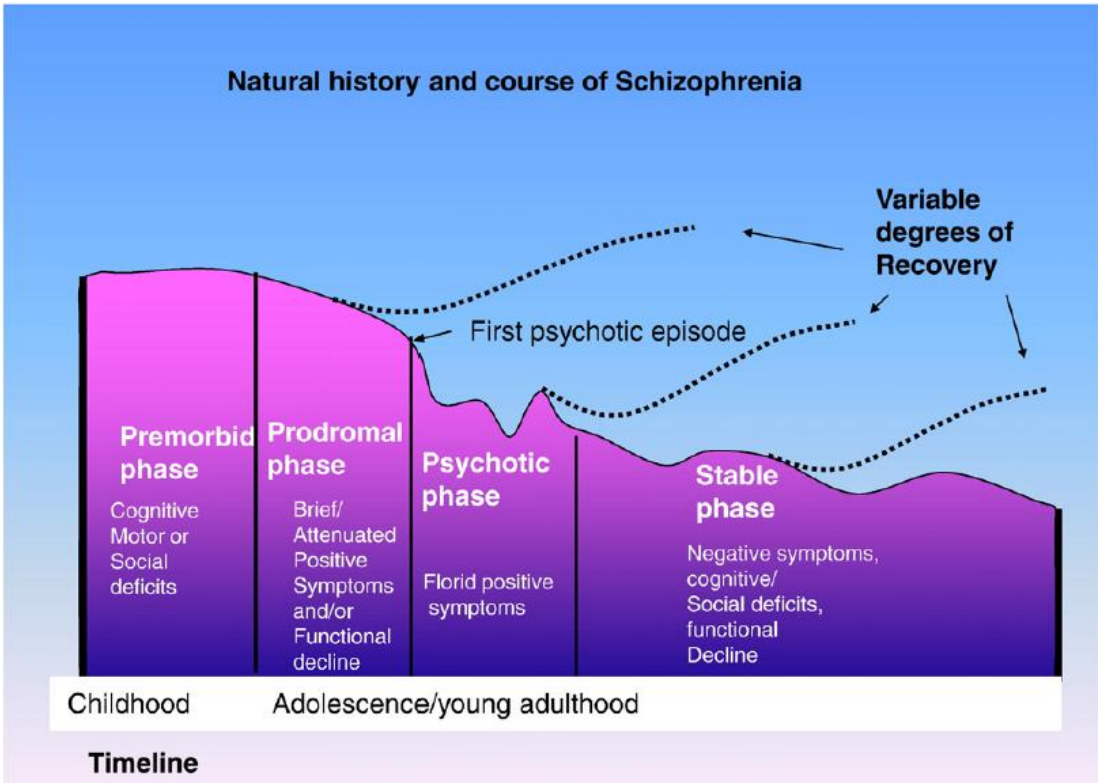

Figure 1.1 The clinical course of schizophrenia, taken from Tandon *et al*, 2009.

1.1.3 *The aetiology of psychiatric illness*

The aetiology of neuropsychiatric disorders is highly complex and still poorly understood. Many common psychiatric conditions are thought to result from the interplay between genetic susceptibility factors and damaging environmental

exposures (Uher, 2008; Uher, 2011; van Os *et al*, 2008). Our current understanding of the genetic and environmental components of the risk of major psychiatric illness is summarised below.

1.1.3.1 *Genetic factors*

Family, twin and adoption studies clearly demonstrated that many psychiatric disorders, including schizophrenia (Craddock *et al*, 2005; Gottesman *et al*, 1987; Sullivan *et al*, 2003), bipolar disorder (Craddock *et al*, 2005; Smoller & Finn, 2003) and depression (Kendler *et al*, 2006; Sullivan *et al*, 2000) are familial disorders, and that their tendency to aggregate in families is mainly due to shared genetic risk factors. The significant genetic component of these disorders is evidenced by the high concordance of diagnosis between monozygotic (MZ) twins compared to dizygotic (DZ) twins. This is estimated at ~50% for schizophrenia, ~80% for bipolar disorder, and 23-67% for major depression (Craddock & Jones, 1999; Craddock *et al*, 2005; Sullivan *et al*, 2000). The observation that the risk of developing schizophrenia, bipolar disorder or depression decreases as the genetic relatedness to a proband diminishes (Craddock & Jones, 1999; Gottesman *et al*, 1987; Kendler *et al*, 2006; Sullivan *et al*, 2000) constitutes further evidence that these diseases are determined, in part, by genetic factors. Accordingly, the risk of being diagnosed with schizophrenia or bipolar disorder is markedly increased among the offspring of couples in which one parent is affected, and it further increases if both parents are affected (Gottesman *et al*, 2010). Estimates of heritability, that is, the proportion of phenotypic variation that can be attributed to genetic variation, are particularly high for schizophrenia (80-90%) and bipolar disorder (70-80%), and average at 35% for depression (Craddock *et al*, 2005) (Sullivan *et al*, 2000). While genetic epidemiology of major psychiatric illness has revealed the importance of genes in determining the risk of disease, it has also highlighted a significant contribution of environmental factors, since the concordance of diagnosis between MZ twins and the disease heritability are both below 100% (Sullivan *et al*, 2003).

By exposing the genetic component of mental illness, family, twin and adoption studies have led to a long series of investigations aimed at identifying the

predisposing genetic loci. However, the search for candidate genes has been hindered by the particularly complex genetic architecture and pattern of inheritance of common psychiatric disorders (Hyman, 2008). Polygenicity and heterogeneity have emerged as the characterising genetic features of these disorders: no single causative gene has been identified for any common psychiatric illness to date, but instead it has become clear that many distinct combinations of multiple genetic risk factors can determine the same condition (Craddock *et al*, 2005). On the other hand, the same genetic risk factor can be associated with multiple psychiatric diagnoses (Blackwood *et al*, 2001; Craddock *et al*, 2005), suggesting that the underlying biological alterations may be at least partially shared. Further evidence for the existence of common causative biological processes for schizophrenia, bipolar disorder and major depression came from several family studies that detected increased risk of depression or schizophrenia within first-degree relatives of bipolar probands and vice versa (Berrettini, 2000; Cardno *et al*, 2002; Craddock & Owen, 2005; Gottesman *et al*, 2010; Lichtenstein *et al*, 2009; McGuffin & Katz, 1989; McGuffin *et al*, 2003).

Two non-mutually exclusive hypotheses have been adopted to explain the high degree of genetic heterogeneity that characterises psychiatric illnesses. The "common disease-common variant" (CD-CV) hypothesis states that common complex diseases such as schizophrenia result from the combination of several low-penetrance common risk-conferring alleles acting cumulatively in the individual (Chakravarti, 1999; Lander, 1996). This hypothesis forms the conceptual basis of genome-wide association studies (GWAS), used to investigate genetic causality in common diseases through high-density genotyping of single nucleotide polymorphisms (SNPs) in large sets of cases and controls (Cichon *et al*, 2009). Some of the susceptibility chromosomal regions identified in whole genome scans are shared between schizophrenia, bipolar disorder and major depression, providing further evidence for the existence of common underlying biological alterations (Green *et al*, 2010).

The second hypothesis states that psychiatric diseases are caused by one of several possible rare and highly penetrant mutations, with different mutations often segregating in different families (McClellan *et al*, 2007; Mitchell & Porteous, 2011;

Pritchard, 2001). The identification of rare disease-causing mutations has traditionally relied on linkage, association and cytogenetic studies in large families with a high recurrence of psychiatric illness. One such example is the discovery of a t(1;11) translocation that disrupts the *Disrupted-in-Schizophrenia 1* (*DISC1*) gene in a large Scottish family with a heavy burden of severe psychiatric disease (Blackwood *et al*, 2001), which will be described in detail later in this chapter. Despite the wealth of evidence gathered from family-based studies, the overall contribution of rare genetic variants to psychiatric illness was initially considered marginal because of their low frequency in the general population. However, the advent of new high-resolution methods of genetic analysis confirmed the importance of rare genetic variants in the aetiology of psychiatric illness. Indeed, the study of rare copy number variants (CNVs) revealed that these structural variants, which can be found at many loci dispersed throughout the genome, are highly enriched in psychiatric patients, with some degree of overlap observed between different disorders (Pickard, 2011; Sebat *et al*, 2009). Some of these rare CNVs are recurrent, but the majority are detected in single patients (Sebat *et al*, 2009). Similarly, deep sequencing methods are revealing an increased load of putatively damaging exonic de-novo (i.e. not inherited, but spontaneously occurring) point mutations in subjects with sporadic schizophrenia (Girard *et al*, 2011).

Two main conclusions can be drawn from the genetic studies conducted thus far on common psychiatric disorders. The first is that they are highly genetically heterogeneous, with both common variants of low penetrance and rare, highly penetrant variants significantly contributing to the risk of disease. The second conclusion is that genetic susceptibility to different mental disorders is conferred by partially overlapping sets of loci. This implies the existence of common biological underpinnings across psychiatric disorders, and suggests that they may be better conceptualised as a continuum or spectrum of clinical phenotypes, rather than nosologically distinct entities (Craddock & Owen, 2005).

1.1.3.2 *Environmental factors*

Twin, family and adoption studies strongly support a major influence of genes on the risk of developing severe mental illness, but also highlight a significant proportion of

variability in the risk of disease that cannot be explained by genetic factors (Lichtenstein *et al*, 2009). Several environmental factors acting at different stages of development have been proposed to influence the risk of developing psychotic or depressive disorders, accounting for a proportion of the "missing genetic variability" in the risk of disease (Markham & Koenig, 2011).

Brain development involves a finely-timed series of cellular and molecular events that guarantee that neurons are born, migrate and mature in the correct spatial and temporal order, resulting in correct wiring and function of the brain. Evidence for defective neurodevelopment has been found in post-mortem brains from patients with neuropsychiatric disorders, including schizophrenia, bipolar disorder and depression (Fatemi & Folsom, 2009; Jaaro-Peled *et al*, 2009; Lewis & Levitt, 2002; Weinberger *et al*, 1983). According to the neurodevelopmental hypothesis of schizophrenia, the disease originates from altered trajectories of neurodevelopment caused by both genetic factors and environmental insults acting before the brain reaches its maturity, and as early as the gestational period (Fatemi & Folsom, 2009; Insel, 2010). Several studies have investigated the influence of defined environmental exposures during foetal life on the risk of developing mental illness later in life. One of the most replicated environmental risk factors acting prenatally is maternal infection during pregnancy, which has been found to significantly increase the risk of schizophrenia, but not major depression or bipolar disorder, in the offspring (Brown, 2011; Mortensen *et al*, 2011; Pang *et al*, 2009). Given the diversity of the prenatal infections for which the association with schizophrenia has been observed, the most plausible proposed mediating mechanism is the activation of the maternal immune response, which in turn releases pro-inflammatory cytokines that interfere with foetal neuronal development (Brown, 2011). Another well-established environmental risk factor acting prenatally is maternal malnutrition (Brown, 2011). Retrospective studies based on data collected during major famines that occurred in The Netherlands and China during the 40s and 50s revealed an increased risk of schizophrenia, bipolar disorder and depression in the children of mothers who starved while pregnant (Brown & Susser, 2008; Brown *et al*, 2000; St Clair *et al*, 2005; Susser *et al*, 1996; Susser & Lin, 1992; Xu *et al*, 2009). It is still not clear, based on clinical studies, whether these associations are due to deficiencies

of specific nutrients or exposure to excess maternal glucocorticoids released as a consequence of malnutrition (Markham & Koenig, 2011). Other factors, such as advanced paternal age, maternal psychological stress exposure during gestation and obstetric complications, can contribute to the risk of psychotic and depressive disorders in the offspring (Brown, 2002; Field & Diego, 2008; Miller *et al*, 2011; Rice *et al*, 2010; Rice *et al*, 2007).

Other environmental risk factors for psychotic disorders act later in life, during childhood and adolescence (Brown, 2011). Psychological trauma (abuse or neglect) during childhood, urbanicity and migrant status are all well-replicated risk factors for schizophrenia. Adolescent cannabis use is also a proposed risk factor for psychotic disorders (Brown, 2011). A dose-response relationship has been observed between cannabis consumption in adolescence and risk of schizophrenia, with heavy users having up to six-fold increased risk of disease (Brown, 2011). Cannabis is also the most common drug of abuse among bipolar subjects, in which it induces manic symptoms (Leweke & Koethe, 2008), and heavy cannabis use has been shown to be associated with earlier onset of bipolar disorder (Lagerberg *et al*, 2011). Despite the clear association between these and other environmental exposures during peri-adolescence and risk of psychosis, the direction of cause and effect is still under debate (Brown, 2011).

One important implication of our improving understanding of the influence of environmental factors on the risk of mental illness is that relatively simple prevention approaches such as vaccination, if implemented at the population level, have the potential to significantly reduce the disease incidence (Brown, 2011).

1.2 DISC1 as a candidate gene for psychiatric illness

1.2.1 *Discovery of DISC1*

In 1968, a survey was conducted in Scotland to search for cytogenetic abnormalities in boys that had been admitted to juvenile detention centres. This led to the identification of one individual carrying a balanced translocation between chromosome 1 and one of chromosomes 6 to 12, which was subsequently detected in

members of the proband's family spanning four generations (Jacobs *et al*, 1970). At the time, no further investigations were carried out, and the pedigree was deposited in the cytogenetic registry of the Medical Research Council (MRC) Clinical and Population Cytogenetics Unit (now Human Genetics Unit) in Edinburgh, which was updated annually with clinical information collected by general practitioners.

Twenty years later, the MRC cytogenetic registry was screened in search of pedigrees with associated psychiatric illness, and it emerged that in the intervening years several members of the family originally described by Jacobs and colleagues (Jacobs *et al*, 1970) had been diagnosed with severe mental illness, including schizophrenia, bipolar disorder and major depression (St Clair *et al*, 1990). A more detailed cytogenetic analysis defined that the chromosomal rearrangement segregating in this family was a balanced t(1;11) (q43,q21) translocation, which was found to be significantly linked with psychiatric illness within this family (St Clair *et al*, 1990).

A systematic in-depth clinical examination of 87 members of this Scottish family, 37 of whom carried the t(1;11) translocation, was carried out ten years later (Blackwood *et al*, 2001). This study revealed that of the 29 translocation carriers for whom clinical data are available, 18 have been diagnosed with a form of major mental illness, including schizophrenia, bipolar disorder and major depression, whereas none of the 38 examined individuals who do not carry the translocation have major psychiatric illness (Blackwood *et al*, 2001). In this family, the t(1;11) translocation is significantly associated with schizophrenia with a LOD score of 3.6, and the strength of association increases further when the broader diagnosis of major psychiatric illness is considered, reaching a LOD score of 7.1 (Blackwood *et al*, 2001). This evidence supports a causative link between the t(1;11) translocation and psychiatric illness. Blackwood and colleagues also reported that all tested translocation carriers (affected and unaffected) present with altered measures of event related potential (ERP) P300, which quantifies the speed and efficiency of information processing and is characteristically abnormal in schizophrenia patients (Blackwood *et al*, 2001; Blackwood & Muir, 2004), indicating that the t(1;11) translocation is most likely associated with functional brain deficits in all carriers.

In the years preceding the original reports linking the t(1;11) translocation with mental illness (Blackwood *et al*, 2001; St Clair *et al*, 1990), a considerable amount of effort had been directed towards the fine-mapping of the translocation breakpoints in search of genes that might be directly affected by this chromosomal rearrangement (Devon *et al*, 1997; Evans *et al*, 1995; Fletcher *et al*, 1993; Millar *et al*, 1998; Millar *et al*, 2000b; Muir *et al*, 1995; Semple *et al*, 2001). As a result of this concerted effort, the translocation breakpoints were located at 1q42.1 and 11q14.3, and two genes on chromosome 1 were found to be directly disrupted by the translocation: *Distrupted-in-Schizophrenia 1* (*DISC1*) and *Distrupted-in-Schizophrenia 2* (*DISC2*) (Millar *et al*, 2000b). *DISC1* consists of 13 major exons, and the translocation breakpoint lies between exons 8 and 9 (Millar *et al*, 2000b), whereas *DISC2* is located antisense to *DISC1*, in a region spanning *DISC1* exon 9, and has no protein coding potential, which led to the hypothesis that this gene may be involved in the regulation of *DISC1* expression (Millar *et al*, 2001; Millar *et al*, 2000b). No genes were initially identified in the 11q14.3 region (Devon *et al*, 1997; Millar *et al*, 1998), but later examinations of this breakpoint revealed the presence of a novel gene, named *DISC1 Fusion Partner 1* (*DISC1FP1*) (Eykelenboom *et al*, 2012) or *Boymaw* (Zhou *et al*, 2010; Zhou *et al*, 2008b). *DISC1FP1* forms aberrant fusion transcripts with *DISC1* exons 9-13 as a consequence of the t(1;11) translocation, and the abnormal chimeric proteins encoded by these fusion transcripts induce mitochondrial deficiencies in transfected cells, suggesting that they may have similar deleterious effects in the brains of translocation carriers (Eykelenboom *et al*, 2012). Another gene located 150-250 kb upstream of *DISC1* has been suggested as being potentially affected by the t(1;11) translocation: *Translin-Associated factor X* (*TRAX*) (Millar *et al*, 2000a). *TRAX* and *DISC1* form fusion transcripts of as yet unknown function that are directly distrupted by the translocation, and may therefore play a role in psychopathogenesis in t(1;11) carriers (Millar *et al*, 2000a). However, no changes in TRAX protein expression levels were detected in lymphoblastoid cell lines generated from the blood of t(1;11) carriers (Millar *et al*, 2005b), shifting the focus to the functional characterisation of *DISC1*.

Biochemical studies conducted on lymphoblastoid cell lines carrying the t(1;11) translocation showed a ~50% decrease in DISC1 protein levels compared to non-

translocation cells from healthy family members, originating the hypothesis that the translocation completely prevents the expression of DISC1 from the affected chromosome 1, leading to disease via haploinsufficiency (Millar *et al*, 2005b). Other researchers have advanced the alternative hypothesis that a truncated from of DISC1 consisting of the first 597 amino acids may be produced from the derived chromosome 1, and that this mutant protein may both interfere with the function of the normal full-length protein and exert detrimental effects per-se. In support of this hypothesis, artificially expressed C-terminally truncated DISC1 was found to interfere with neuronal function in a dominant-negative fashion in several cell (Kamiya *et al*, 2005; Ozeki *et al*, 2003; Pletnikov *et al*, 2007; Taya *et al*, 2007) and mouse (Abazyan *et al*, 2011; Ayhan *et al*, 2011; Hikida *et al*, 2007; Pletnikov *et al*, 2008a; Pletnikov *et al*, 2008b; Shen *et al*, 2008) models. However, no transcripts encoding this putative truncated form of DISC1 have been identified in t(1;11) lymphoblastoid cell lines (Eykelenboom *et al*, 2012), and attempts to detect DISC1 (1-597) in these patient-derived cells have so far been usuccessful (Millar *et al*, 2005b). Since it has not yet been possible to analyse post-mortem brain samples from t(1;11) carriers, the existence of DISC1 (1-597) in neurons remains unproven.

1.2.2 *DISC1 linkage and association studies*

Despite the strong linkage detected between the t(1;11) translocation and psychiatric illness in the Scottish family, the uniqueness of this chromosomal rearrangement meant that it was initially unclear whether the *DISC1* locus should be considered a genetic susceptibility factor for major mental illness in the general population. However, soon after the discovery of *DISC1*, several independent studies provided a wealth of evidence for the wider involvement of this gene in a range of psychiatric disorders including schizophrenia, bipolar disorder, major depression, schizoaffective disorder and autism (Bradshaw & Porteous, 2012; Chubb *et al*, 2008).

Linkage of the *DISC1* locus with major psychiatric illness was first independently detected in the Finnish population, in which the 1q32.2-q41 region was linked to schizophrenia and schizoaffective disorder, and more detailed analyses determined that the strongest linkage signal was from a *DISC1* intragenic marker located in

intron 9 (Ekelund *et al*, 2004; Ekelund *et al*, 2001; Ekelund *et al*, 2000; Hovatta *et al*, 1999). These findings were subsequently replicated in studies conducted in other populations, including Taiwanese, Scottish, British and Icelandic, in which the 1q32-42 chromosome region was linked to major psychiatric illness (Curtis *et al*, 2003; Detera-Wadleigh *et al*, 1999; Hamshere *et al*, 2005; Hwu *et al*, 2003; Macgregor *et al*, 2004).

In agreement with the evidence from linkage, a large number of studies found genetic association between single nucleotide polymorphisms (SNPs) and/or haplotypes within *DISC1* and both major psychiatric illness and autism spectrum disorders, as well as with altered brain structure, cognition and behavioural phenotypes in healthy subjects (Bradshaw & Porteous, 2012; Chubb *et al*, 2008; Johnstone *et al*, 2011; Zheng *et al*, 2011). In addition, a recent study has found association of *DISC1* with agenesis of the corpus callosum, a congenital brain malformation (Osbun *et al*, 2011). A number of reports of negative association have also been published (Bradshaw & Porteous, 2012; Chubb *et al*, 2008; Mathieson *et al*, 2011), and a trend towards positive association with psychiatric illness has emerged for *DISC1* in some (Sullivan *et al*, 2008) but not other (O'Donovan *et al*, 2009; Richards *et al*, 2012; Sanders *et al*, 2008) GWAS studies of schizophrenia, bipolar disorder and depression.

Two common non-synonymous exonic SNPs of *DISC1* have been studied in particular detail in association studies: rs821616 (Ser704Cys) and rs6675281 (Leu607Phe) (Bradshaw & Porteous, 2012; Chubb *et al*, 2008). The Serine to Cysteine substitution at amino acid position 704 (Ser704Cys or S704C), is associated with schizophrenia and impaired declarative memory in schizophrenia patients (Callicott *et al*, 2005; Lepagnol-Bestel *et al*, 2010; Qu *et al*, 2007; Song *et al*, 2008; Takahashi *et al*, 2009), major depression (Hashimoto *et al*, 2006), and chronic fatigue syndrome (Fukuda *et al*, 2010a). A recent study found association between a *DISC1* haplotype containing rs821616 and P300 amplitude and latency in patients with schizophrenia or bipolar disorder (Shaikh *et al*, 2011), confirming the previously reported association of DISC1 with P300 deficits (Blackwood *et al*, 2001; Blackwood & Muir, 2004). Some studies found negative association of S704C with

schizophrenia (Hotta *et al*, 2011; Kim *et al*, 2008) or bipolar disorder (Song *et al*, 2010), but one of these detected significant association with poor concentration in schizophrenia patients (Kim *et al*, 2008). Magnetic Resonance Imaging (MRI) and functional MRI (fMRI) studies found associations between S704C and brain structural and functional changes in normal subjects. For example, Callicott and colleagues and Di Giorgio and colleagues reported reduced hippocampal gray matter volume and abnormal activation of the hippocampus during memory-related tasks in Ser704 carriers, recapitulating observations commonly made in schizophrenia patients (Callicott *et al*, 2005; Di Giorgio *et al*, 2008). In addition, in verbal fluency tests designed to measure the function of the prefrontal cortex (PFC), Ser704 homozygotes showed greater activation of the PFC, which is indicative of prefrontal hypofunction, a typical feature of schizophrenia (Prata *et al*, 2008). Ser704 homozygotes also showed an accelerated rate of cortical thinning during development in the left anterior cingulated and temporal cortices (Raznahan *et al*, 2011). By contrast, the Cys704 allele was associated with reduced gray matter volume in the cingulate cortex, cingulate gyrus and posterior gyrus, larger volume of the medial superior frontal gyrus and short insular cortex and reduced integrity and fractional anisotropy in prefrontal white matter (Hashimoto *et al*, 2006; Sprooten *et al*, 2011; Takahashi *et al*, 2009). Finally, Thomson and colleagues reported a positive association between the Cys704 allele and accelerated age-related cognitive decline in healthy women (Thomson *et al*, 2005).

The Leucine to Phenylalanine substitution at DISC1 amino acid 607 (Leu607Phe or L607F) is associated with schizoaffective disorder, schizophrenia and higher negative symptom scores in schizophrenia patients (Hodgkinson *et al*, 2004; Rastogi *et al*, 2009) (Lepagnol-Bestel *et al*, 2010), although lack of association with schizophrenia and bipolar disorder has also been reported for this SNP (Song *et al*, 2008; Song *et al*, 2010). In both schizophrenia patients and healthy controls, the Phe607 allele was associated with significantly reduced grey matter volumes in the superior prefrontal gyrus and anterior cingulated gyrus (Szeszko *et al*, 2008). A more recent structural and functional MRI study found association between the Phe607 allele and both reduced cortical thickness in the left supramarginal gyrus and increased neural activity in the left dorsolateral prefrontal cortex during working

memory tests in healthy volunteers (Brauns *et al*, 2011). In addition, schizophrenia patients carrying Phe607 were found to experience significantly more severe positive symptoms (hallucinations) (Szeszko *et al*, 2008). Like the S704C substitution, L607F has been associated with the rate of cortical thinning during development, with the Phe607 allele determining slower rates of thinning in the bilateral superior frontal and left angular cortical giri (Raznahan *et al*, 2011).

A third common exonic missense SNP (rs3738401) that determines the Arginine to Glutamine substitution at DISC1 amino acid position 264 (Arg264Gln or R264Q) has been associated with psychiatric illness and/or cognitive impairment in most (Hennah *et al*, 2005; Hennah *et al*, 2003; Mouaffak *et al*, 2011; Palo *et al*, 2007; Song *et al*, 2008; Zhang *et al*, 2006) but not all (Hotta *et al*, 2011; Kim *et al*, 2008) reported studies. In structural MRI studies, the R264Q polymorphism has been associated with altered cortical thickness in the lateral occipital gyrus and cingulate cortex (Brauns *et al*, 2011; Carless *et al*, 2011). Additionally, together with SNP rs821616 (S704C), rs3738401 (R264Q) was associated with altered amplitude and latency of P300 (Shaikh *et al*, 2011).

DISC1 sequencing in patients with schizophrenia and bipolar disorder led to the identification of novel ultra-rare missense point mutations associated with disease (Song *et al*, 2008; Song *et al*, 2010). In their first study, Song and colleagues sequenced *DISC1* exons and splice junctions in 288 patients with schizophrenia and an equal number of healthy controls, identifying seven novel missense mutations that were initially only seen in heterozygosis in schizophrenia patients: G14A, R37W, S90L, R418H, T603I, A83V and P432L (Song *et al*, 2008). Further screening of an additional 10,000 control alleles revealed that two of these mutations (A83V and P432L) were present in the gene pool at a frequency of ~1 in 200, whereas none of the other five were detected in the control alleles, leading to the conclusion that they may be schizophrenia-specific, with an estimated attributable risk of 2% (Song *et al*, 2008). Using a similar approach in 504 patients with bipolar disorder and 576 controls plus an additional 10,000 control alleles, Song and colleagues found four protein structural variants in four different patients that were absent from the controls: R338Q, R418H, T754S, S209R (Song *et al*, 2010). One of these variants

(R418H) had been previously detected in a schizophrenia patient (Song *et al*, 2008). The estimated attributable risk for bipolar disorder was 0.5% for these mutations (Song *et al*, 2010). Although a potential functional role has been hypothesised for some of the above novel ultra-rare mutations (Soares *et al*, 2011), no biological studies have been reported to date.

A more recent sequencing study investigated the contribution to schizophrenia susceptibility of genetic variation within *DISC1* and ten of its interacting proteins, and revealed a significantly increased burden of rare missense mutations in schizophrenia patients compared to healthy controls (Moens *et al*, 2011), adding to the evidence in support of the important contribution of rare mutations to the risk of psychiatric illness.

Two ultra-rare CNVs (a 2 Mb duplication and a 2 Mb deletion) spanning the *DISC1* locus were reported in subjects with autism and mental retardation, adding to the evidence that suggests the involvement of *DISC1* in a wide spectrum of mental illnesses (Crepel *et al*, 2010; Williams *et al*, 2009).

The current hypothesis that schizophrenia and other major psychiatric illnesses are highly genetically heterogeneous disorders originating from the combination of multiple susceptibility alleles, prompted combinatorial studies testing for genetic interplay within and between candidate genes. One such study detected a variable effect (either protective or risk-conferring) of *DISC1* SNP rs821633 in combined European cohorts of schizophrenia and bipolar disorder depending on whether this SNP was present on its own or in combination with either *DISC1* SNP rs821577 or rs1538789 (Hennah *et al*, 2009). Similarly, *DISC1* SNP rs1538789 was found to increase the risk of psychiatric illness only when combined with *DISC1* SNP rs821633 (Hennah *et al*, 2009).

Other genetic studies focused on well-characterised DISC1 binding proteins: NDE1, NDEL1 and CIT. The first of these studies detected positive association of schizophrenia with a marker located close to the *NDE1* locus only in the presence of a previously reported schizophrenia-associated *DISC1* haplotype (HEP3) (Hennah *et al*, 2007). In a subsequent case-control study, association with schizophrenia of the *NDEL1* haplotype identified by the tagging SNP rs1391768 was evident only on the

background of Ser/Ser at DISC1 position 704 (Burdick *et al*, 2008). On the other hand, *NDE1* SNP rs3784859 conferred risk of schizophrenia only when combined with the Cys704 DISC1 background (Burdick *et al*, 2008). A more recent schizophrenia case-control study detected epistatic interactions between SNPs within *DISC1* and *CIT*, and within *NDEL1* and *CIT*, but only the latter survived Bonferroni correction (Nicodemus *et al*, 2010). However, epistasis between *CIT* and both *DISC1* and *NDEL1* was subsequently validated in fMRI measures of hippocampal and prefrontal cortical efficiency (Nicodemus *et al*, 2010).

In summary, the numerous linkage and association studies conducted over the last decade strongly implicate *DISC1* in the pathogenesis of psychiatric conditions ranging from schizophrenia to autism, but do not concertedly point towards one or a few risk-conferring variants. These observations reinforce the blurring of the genetic and aetiological boundaries between conditions such as schizophrenia and bipolar disorder, and confirm the highly genetically heterogeneous nature of psychiatric illness.

1.2.3 *The structure and biology of DISC1*

1.2.3.1 *DISC1 splice variants*

The human *DISC1* gene comprises a total of 13 exons, producing a full-length transcript of around 7.5 kb (Millar *et al*, 2001; Millar *et al*, 2000a). *DISC1* mRNA processing is highly complex, and many alternative transcripts have been described to date, although their relative usage and respective functions remain unclear (Millar *et al*, 2001; Nakata *et al*, 2009; Taylor *et al*, 2003). Four alternatively spliced *DISC1* mRNA isoforms were originally described and confirmed, namely the Long (L), Long variant (Lv), Short (S) and Extremely short (Es) isoform (Chubb *et al*, 2008). The L isoform, or full-length transcript, contains all 13 exons, the Lv isoform lacks the 66 nucleotides at the end of exon 11, the S variant utilises an alternate 3' untranslated region (UTR) in intron 9 (exon 9a), whereas the Es form arises from an alternatively spliced exon 1a in *DISC1*, terminating two codons after the end of exon 3 (Chubb *et al*, 2008). Rare intergenic splicing events have been reported to occur between *DISC1* and the neighbouring *TSNAX* gene, producing low-abundance fusion

transcripts whose translation has not been detected yet (Millar *et al*, 2000a; Taylor *et al*, 2003). A more recent report that used a combination of PCR and 5' and 3' RACE on human hippocampal mRNA, confirmed the expression of the previously described *DISC1* splice variants, and documented several novel transcripts, bringing the total of known *DISC1* splice isoforms to 54 (Nakata *et al*, 2009). Comparison of the expression profiles of the many *DISC1* splice variants at different developmental stages of the human brain revealed that the shorter mRNA isoforms, predicted to produce a truncated form of the protein, are expressed at higher levels in the foetal brain (Nakata *et al*, 2009). Interestingly, the same short isoforms are also expressed at higher levels in schizophrenic brains compared to normal controls, hinting at aberrant *DISC1* expression as a potential disease mechanism (Nakata *et al*, 2009). Consistent with this hypothesis, the same study found that the expression of a specific *DISC1* mRNA isoform lacking exons 8 and 9 was significantly increased in post-mortem brains from Phe607 carriers and Cys704 homozygotes, two *DISC1* SNPs that had been previously associated with psychiatric illness (Nakata *et al*, 2009). It has to be noted though, that many of the novel *DISC1* splice variants described by Nakata and colleagues possess premature stop codons, and it remains uncertain whether they are translated into functional proteins in the brain (Nakata *et al*, 2009).

1.2.3.2 *DISC1 protein structure*

Of the many *DISC1* splice isoforms detected to date, only L can be confidently assigned to the corresponding translated product, an 854 amino acid protein of about 100 kDa (Chubb *et al*, 2008). Using antibodies directed against different regions of the protein, several other human DISC1 isoforms have been detected by western blotting, including species of ~75, 95-100, 150 and 200 kDa (James *et al*, 2004; Ogawa *et al*, 2005; Sawamura *et al*, 2005; Soares *et al*, 2011). The smaller ~75 kDa DISC1 isoform may arise from the S transcript, whereas DISC1 species running at 150 and 200 kDa may likely represent dimers of shorter forms, given DISC1's demonstrated ability to self-associate (Brandon *et al*, 2004; Kamiya *et al*, 2005; Leliveld *et al*, 2008; Leliveld *et al*, 2009). Assignment of different DISC1 protein

species to the corresponding transcript isoform can be further complicated by secondary modifications, such as protein phosphorylation (Ishizuka *et al*, 2011).

The full-length 854 amino acid DISC1 protein has no similarity to any other known protein, making it a completely novel protein species (Millar *et al*, 2000b). Generally, DISC1 is poorly conserved between species, although orthologues have been found both in vertebrates, including mammals, birds and fish (Chubb *et al*, 2008; Taylor *et al*, 2003) and invertebrates (Sanchez-Pulido & Ponting, 2011). To date, a detailed 3D characterisation of DISC1 protein structure is lacking, and the current structural information has been gained from biophysical studies on purified protein fragments and *in silico* analyses (Chubb *et al*, 2008; Soares *et al*, 2011). According to structure prediction programs, DISC1 can be grossly subdivided into two distinct structural domains: a disordered N-terminal "head" region spanning the first ~350 amino acids, and a more structured C-terminal region comprising amino acids ~351-854 (Millar *et al*, 2000b; Soares *et al*, 2011) (Figure 1.2, adapted from Soares *et al*, 2011). The head region of DISC1, also often referred to as the "globular domain" lacks any predicted complex secondary structures and is poorly conserved, except for a few stretches of amino acids (Millar *et al*, 2000b; Soares *et al*, 2011; Taylor *et al*, 2003). These include a tetra-arginine nuclear localisation signal spanning amino acids 35-44 and a serine/phenylalanine (SF) rich motif of unknown function at amino acids 206-217 (Taylor *et al*, 2003) (Figure 1.2). By contrast, the C-terminus of DISC1 contains several predicted alpha-helices and coiled-coil regions, as well as three predicted leucine zipper motifs at amino acids 458-486, 607-628 and 808-829 (Chubb *et al*, 2008; Soares *et al*, 2011), and it is considerably more conserved compared to the N-terminus region (Taylor *et al*, 2003) (Figure 1.2). Given the known involvement of coiled-coil domains in mediating protein-protein interactions, the high density of these structural motifs in the C-terminus of DISC1 was the earliest clue suggesting that DISC1 may be able to bind multiple protein partners (Taylor *et al*, 2003). Since disordered proteins can assume a more structured organisation upon binding to other proteins (Fink, 2005), it has been recently suggested that the low structural complexity of the head domain of DISC1 may be a necessary feature to mediate more dynamic and reversible protein-protein

interactions, such as the one existing between DISC1 and PDE4, which will be described in more detail later in this chapter (Soares *et al*, 2011).

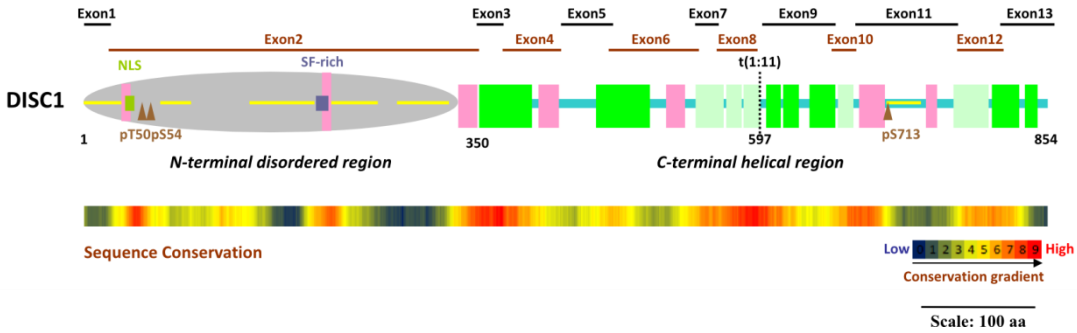

Figure 1.2 DISC1 protein structure and conservation, adapted from Soares *et al,* 2011. The figure summarises the predicted secondary structure of DISC1, with the vertical rectangles representing regular or ambiguous α-helices (pink and light green, respectively, and coiled-coils (green). The horizontal yellow lines represent disordered regions. The position of the nuclear localisation signal (NLS) and SF-rich region is also indicated, along with that of the phosphorylation sites (brown triangles). The vertical dashed line marks the position of the t(1;11) translocation breakpoint, corresponding to amino acid 597. Ortholog sequence conservation is shown below the DISC1 protein schematic.

Initial experiments carried out using recombinant tagged proteins expressed in transfected cell lines demonstrated that DISC1 is capable of self-associating, and identified the region spanning amino acids 403-504 as a self-association domain (Brandon *et al*, 2004; Kamiya *et al*, 2005). A more detailed biophysical characterisation of DISC1 protein fragments spanning the C-terminal region was carried out recently by Leliveld and colleagues (Leliveld *et al*, 2008; Leliveld *et al*, 2009). In their first study, they found DISC1 fragment 598-854 to exist in the form of dimers, octamers, multimers and insoluble aggregates under physiological conditions, and established that only DISC1 octamers are capable of binding NDEL1 (Leliveld *et al*, 2008). Additionally, they showed that DISC1 can be detected in the form of insoluble aggregates in 20% of post-mortem brains of subjects with major

psychiatric illness, but not in healthy controls (Leliveld *et al*, 2008). In two separate studies, octamer-dependent DISC1 binding to NDEL1 was confirmed, and it was shown that the assembly of DISC1 into octamers occurs through the formation of dimeric intermediates (Leliveld *et al*, 2009; Narayanan *et al*, 2011). The oligomeric state-dependency of the DISC1-NDEL1 interaction was corroborated by the observation that insoluble aggregates of full-length DISC1 fail to bind NDEL1 (Leliveld *et al*, 2009). The same study identified two additional regions involved in DISC1 self-association: the 668-747 region, necessary for oligomerisation, and the 765-854 region, which mediates dimerisation (Leliveld *et al*, 2009). A further report from the same group showed co-aggregation of DISC1 and Dysbindin, the product of another candidate gene for mental illness, in post-mortem brains of psychiatric patients, but not healthy controls (Ottis *et al*, 2011). Altogether, these findings indicate controlled self-assembly as a possible form of DISC1 regulation, and suggest that DISC1 aggregation in the brain, with consequent loss of binding or aberrant recruitment of interacting partners, may be a potential disease mechanism acting in a subset of psychiatric patients.

1.2.3.3 *DISC1 tissue expression and subcellular protein distribution*

Expression of *DISC1* at the mRNA and protein level has been detected in multiple tissues (Chubb *et al*, 2008). Studies on foetal and adult human tissues revealed *DISC1* mRNA expression in the brain, heart, placenta, kidney and pancreas, with the first three showing the strongest expression (James *et al*, 2004; Millar *et al*, 2000b). *DISC1* expression in foetal brain, heart, limbs, kidney, liver and lungs has also been documented at the protein level, with highest expression in the kidney (James *et al*, 2004). A more detailed investigation of *DISC1* mRNA expression in adult human brain detected widespread expression in several regions, including, but not limited to, the amygdala, caudate nucleus, corpus callosum, hippocampus, substantia nigra, thalamus, cerebellum, cerebral cortex, medulla, spinal cord and frontal lobe (Millar *et al*, 2000b). Human DISC1 expression is particularly high in the dentate gyrus of the hippocampus (James *et al*, 2004; Lipska *et al*, 2006), where it is strongly expressed in a subset of granule cells (James *et al*, 2004). In the adult hippocampus, DISC1 is also expressed in the pyramidal cells in layers CA1-3 (James *et al*, 2004).

Comparable observations have been reported in rodents, where *Disc1* is expressed mostly in the heart, but also in the brain, kidney, liver and testis (Ma *et al*, 2002a; Ozeki *et al*, 2003). In the rodent brain, *Disc1* has been detected in the dentate gyrus of the hippocampus, where expression is particularly high, and in many other regions, including the cerebellum, olfactory bulbs, cerebral cortex, hypothalamus, amygdala and corpus callosum (Ma *et al*, 2002a; Miyoshi *et al*, 2003; Osbun *et al*, 2011; Schurov *et al*, 2004). *Disc1* is expressed in the developing rodent hippocampus from as early as embryonic day (E) 14, the stage at which this structure becomes discernible, with strong expression in the granule cell progenitors and in the dentate gyrus, an area where adult neurogenesis occurs (Austin *et al*, 2004; Meyer & Morris, 2008). Here, DISC1 co-localises with Ki67, a marker of proliferating cells in the subgranular zone (Meyer & Morris, 2008). Additionally, DISC1 expression has been observed in the subventricular zone, another area of adult neurogenesis, where it co-localises with the neural progenitor markers nestin and Sox2 (Mao *et al*, 2009).

Limited studies of *DISC1* expression have also been conducted in primates, where *DISC1* mRNA and protein expression was similarly detected in multiple brain regions, including the dentate gyrus of the hippocampus, cerebral cortex, amygdala, cerebellum and hypothalamus (Austin *et al*, 2004; Bord *et al*, 2006).

Collectively, *DISC1* expression studies have consistently shown that it is a widely expressed gene, with particularly prominent expression in the hippocampus, a region of adult neurogenesis that has been strongly implicated in schizophrenia (Harrison, 2004).

At the subcellular level, DISC1 distributes to multiple compartments, as thoroughly reviewed by Chubb and colleaguses and Soares and colleagues (Chubb *et al*, 2008; Soares *et al*, 2011), and summarised in Table 1.1, adapted from Soares *et al*, 2011. This multicompartmentalisation is consistent with the current view that DISC1 is involved in a diverse range of cellular processes, and that it attends to its functions through the establishment of multiple interactions with different partner proteins in distinct cell compartments (Bradshaw & Porteous, 2012; Brandon *et al*, 2009; Porteous, 2008) (Table 1.1).

Localisation of DISC1 to its target subcellular regions is thought to be mediated both by signal peptides located within the protein, and by its interaction with specific partner proteins (Soares *et al*, 2011). For example, targeting of DISC1 to the centrosome has been proposed to be mediated by binding of kendrin, a protein specifically localised to the centrosome (Miyoshi *et al*, 2004). Similarly, DISC1 interaction with kinesin is necessary for it transportation along microtubules to the growth cones (Shinoda *et al*, 2007; Taya *et al*, 2007). Additionally, different DISC1 protein isoforms may be preferentially targeted to distinct subcellular compartments (Chubb *et al*, 2008).

Cellular location	Details and associated functions of DISC1	References
Centrosome	Involved in the recruitment of kendrin, dynein and dynactin subunits, LIS1, NDEL1, PCM1, ninein and CAMDI to the centrosome. Also interacts here with PDE4B, PDE4D, NDE1 and BBS4. These interactions include those important for microtubule aster formation, neurite outgrowth and neuronal migration.	(Bradshaw *et al*, 2009; Bradshaw *et al*, 2008; Fukuda *et al*, 2010b; Kamiya *et al*, 2005; Kamiya *et al*, 2008; Kamiya *et al*, 2006; Miyoshi *et al*, 2004; Morris *et al*, 2003; Shimizu *et al*, 2008)
Cilia	Found at the base of primary cilia and appears to regulate their formation and/or maintenance. Knock-down of endogenous DISC1 leads to marked reduction of primary cilia. Other DISC1 interactors seen at the base of primary cilia include BBS4, PCM1.	(Marley & von Zastrow, 2010)
Cytoskeleton	Seen along both actin filaments and microtubules. Expression of truncated DISC1 leads to a disorganized microtubule network.	(Kamiya *et al*, 2005; Miyoshi *et al*, 2003; Morris *et al*, 2003)
Golgi apparatus	Seen in association with the membrane structures of the Golgi apparatus in hippocampal neurons and astrocytes. May participate in vescicle movement from the Golgi apparatus.	(Kuroda *et al*, 2011)
Growth cones	Found here in the hippocampus and is involved in recruiting proteins including LIS1, NDEL1, 14-3-3ε and girdin via kinesin-based transport along the cytoskeleton. Also important for axonal elongation.	(Enomoto *et al*, 2009; Miyoshi *et al*, 2003; Shinoda *et al*, 2007; Taya *et al*, 2007)
Membranes	Found in membrane fractions, where it interacts with APP, which is important in cortical precursor formation.	(Brandon *et al*, 2005; Ozeki *et al*, 2003; Young-Pearse *et al*, 2010)

Mitochondria	Found at mitochondria present on microtubules and regulates their trafficking. Can cause mitochondria to form "ring" structures. Interacts with mitofilin within the mitochondria and is required for correct electron transport chain, monoamine oxidase and Ca^{2+} activity.	(Atkin *et al*, 2011; Brandon *et al*, 2005; James *et al*, 2004; Millar *et al*, 2005a; Ozeki *et al*, 2003; Park *et al*, 2010)
Nucleus	Found at the chromatin, promyelocytic leukemia (PML) bodies and outer layers of nuclear membrane. Represses ATF4 transcriptional activity and transcription of N-cadherin and alters sleep homeostasis in *Drosophila*.	(Hattori *et al*, 2010; James *et al*, 2004; Kirkpatrick *et al*, 2006; Sawamura *et al*, 2008)
Synapse	Seen at the post-synaptic density along with PDE4 and NDE1. Interacts with and inhibits TNIK here, leading to degradation of key synaptic proteins. Also affects spine formation through modulation of PSD-95/Kal-7/Rac1 complexes here.	(Bradshaw *et al*, 2008; Clapcote *et al*, 2007; Hayashi-Takagi *et al*, 2010; Kirkpatrick *et al*, 2006; Wang *et al*,2010c)

Table 1.1 DISC1 subcellular distribution, adapted from Soares *et al,* 2011. The cell compartments to which DISC1 has been demonstrated to localise are listed, along with the respective observed or proposed associated DISC1 functions.

Unlike other subcellular compartments, DISC1 targeting to the nucleus is known to be dependent on cis-acting motifs found within the protein, although the existence of additional regulatory mechanisms cannot be excluded (Soares *et al*, 2011). Several *in silico* analyses have identified putative nuclear localisation signals (NLS) and nuclear export signals (NES) within DISC1 protein sequence, and these have been subsequently investigated in-vitro (Brandon *et al*, 2005; Ma *et al*, 2002a; Sawamura *et al*, 2008; Taylor *et al*, 2003). A detailed description of these studies will be provided in the introduction to chapter three of this thesis.

1.2.3.4 *DISC1 binding partners*

Due to the lack of known human paralogs or sequence similarity with any other known protein, no prediction could be made on the function of DISC1 at the time of its discovery (Millar *et al*, 2000b), but the presence of several coiled-coil domains in its C-terminal region suggested that DISC1 could potentially establish multiple protein-protein interactions (Taylor *et al*, 2003). A series of large-scale screens based on yeast-two-hybrid assays or other methods have been successfully carried out to shed light on the function of DISC1 via the identification of its interacting proteins (Brandon *et al*, 2004; Camargo *et al*, 2007; Millar *et al*, 2003; Miyoshi *et al*, 2004; Morris *et al*, 2003; Ozeki *et al*, 2003; Shinoda *et al*, 2007; Taya *et al*, 2007). Over 200 candidate DISC1 interactors have been so far identified, and for several of these the interaction with DISC1 has been confirmed by co-localisation, co-immunoprecipitation or GST pull-downs. For some binding proteins, the interacting regions on DISC1 have been mapped using deletion mutants or peptide arrays, as recently reviewed by Soares and colleagues (Soares *et al*, 2011). Based on their gene ontology, the many DISC1 interactors can be grouped into several broad functional categories, including cell cycle regulation, RNA processing, transcription regulation, vescicle transport, cytoskeleton organisation and function, mitochondrial function and energy metabolism, signal transduction and neural migration (Camargo *et al*, 2007). The discovery of its vast number of binding partners, together with its widespread tissue and cell expression, led to the conceptualisation of DISC1 as a "scaffold" or "hub" protein to denote its high degree of connectivity, and inspired a staggering number of studies designed to dissect its cellular and molecular functions,

in search of novel intracellular therapeutic targets for psychiatric illness. Importantly, several DISC1 interactors have been independently associated with psychiatric illness, emphasising the relevance of DISC1-connected pathways for psychopathology (Bradshaw & Porteous, 2012; Moens *et al*, 2011). Well over 300 research articles have been published on DISC1 up to January 2012, which puts a thorough review of its protein interactions and biological functions beyond the remit of this thesis. In the following section, I will thus provide an overview of the most promising and best documented roles of DISC1 in neurodevelopment, signalling and synaptic function, which are biological aspects of particular interest for psychiatric illness. Some of the best-characterised molecular interactions involving DISC1, and their roles in neuronal development and function are summarised in figure 1.3, taken from Brandon & Sawa, 2011.

1.2.3.5 *DISC1 in neurodevelopment, plasticity and signalling*

In animal cells, the centrosome is the main microtubule-organising centre (MTOC), and plays a central role in cell division and migration (Nigg & Raff, 2009). The correct organisation of the centrosome and connected microtubule network is essential for proper brain development, as fundamental processes depend upon it, such as neurogenesis, neuronal migration and differentiation (Higginbotham & Gleeson, 2007).

DISC1 localises to the centrosome, where it complexes with proteins of known importance in centrosomal-dependent aspects of neurodevelopment, including lissencephaly 1 (LIS1), nuclear distribution element-like 1 (NDEL1), kendrin (or pericentrin), pericentriolar material 1 (PCM1), and Bardet-Biedl syndrome 4 protein (BBS4) (Bradshaw *et al*, 2009; Brandon *et al*, 2004; Kamiya *et al*, 2008; Millar *et al*, 2003; Miyoshi *et al*, 2004; Morris *et al*, 2003; Ozeki *et al*, 2003; Shinoda *et al*, 2007) (Figure 1.3). DISC1 has been shown to anchor several of these proteins to the centrosome, thus allowing their correct functioning. For example, recruitment of kendrin to the centrosome and its binding to DISC1 are essential for correct microtubule network formation (Shimizu *et al*, 2008). In addition, DISC1 and its interactor BBS4 cooperatively recruit PCM1 to the centrosome (Kamiya *et al*, 2008), where it is necessary for correct axon morphology and neurogenesis (de Anda *et al*,

2010; Ge *et al*, 2010). In turn, PCM1 facilitates the centrosomal recruitment of kendrin (Kamiya *et al*, 2008).

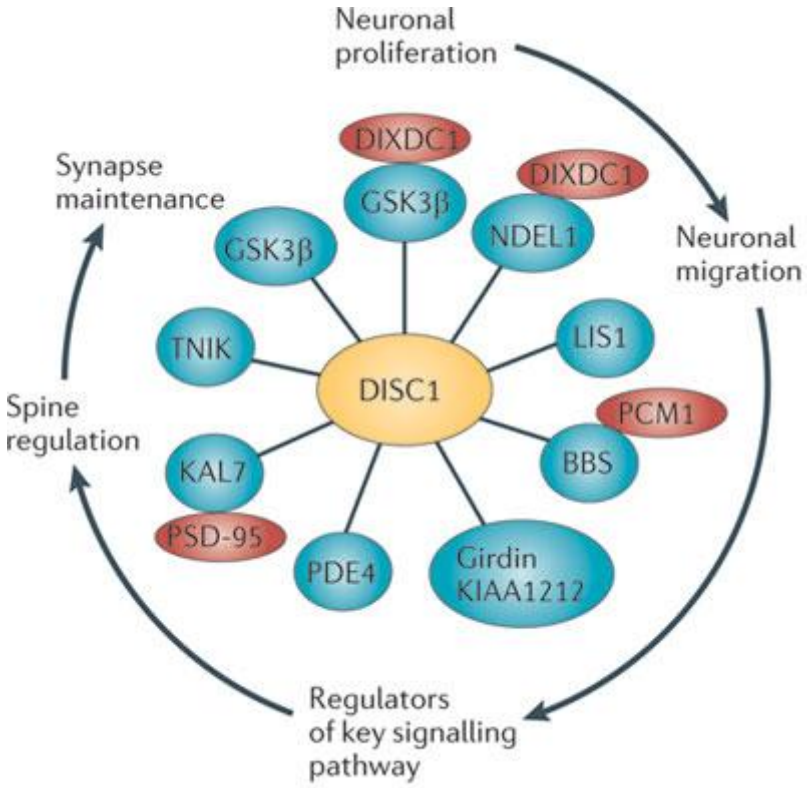

Figure 1.3 Summary of the best-characterised interactions established by DISC1, and their functional role in neuronal biology, taken form Brandon & Sawa, 2011. The known functions of the various DISC1 complexes are shown in the perimeter of the figure, and the direction of the arrows indicates their chronological order during neuronal development. BBS, Bardet–Biedl syndrome protein; DIXDC1, dishevelled axin domain containing 1; GSK3β, glycogen synthase kinase 3β; KAL7, kalirin 7; LIS1, lissencephaly protein 1; NDEL1, nuclear distribution protein nudE-like 1; PCM1, pericentriolar material 1; PDE4, phosphodiesterase type 4; PSD95, postsynaptic density protein 95; TNIK, TRAF2- and NCK-interacting protein kinase.

DISC1 is also part of the dynein microtubule motor complex, which is involved in retrograde transport along microtubules, and it is necessary for its localisation to the centrosome along with LIS1 and NDEL1, hence contributing to normal microtubule dynamics (Kamiya *et al*, 2005). Moreover, through its interaction with the

anterograde motor protein kinesin-1 and the adaptor protein growth factor bound protein 2 (Grb2), DISC1 is involved in transport of cargoes including LIS1, NDEL1 and 14-3-3ε to the distal parts of axons, a process important for neurite outgrowth (Shinoda *et al*, 2007; Taya *et al*, 2007). Consistently, many independent studies that used gene silencing or overexpression techniques *in vitro* and *in vivo* have shown that DISC1 is necessary for correct neuronal migration and neurite outgrowth, both during development and postnatally (Drerup *et al*, 2009; Duan *et al*, 2007; Enomoto *et al*, 2009; Kamiya *et al*, 2005; Kamiya *et al*, 2008; Kamiya *et al*, 2006; Kim *et al*, 2009; Kubo *et al*, 2010; Young-Pearse *et al*, 2010).

Defects of neuronal migration can also be induced by knock-down of the DISC1 binding partner DIX domain containing 1 (dixdc1), or by inhibition of the interaction between the two proteins (Singh *et al*, 2010). Dixdc1 also binds to NDEL1, and this interaction is necessary for correct neuronal migration, raising the possibility that the three proteins may interact in the same pathway (Singh *et al*, 2010) (Figure 1.3).

DISC1 and dixdc1 were recently reported to co-regulate neuronal progenitor proliferation via concerted inhibition of glycogen synthase kinase 3β (GSK3β) (Mao *et al*, 2009; Singh *et al*, 2010) (Figure 1.3). This particular aspect of DISC1 biology is of special interest in the field of psychiatric research given that Lithium Chloride, a commonly used mood stabiliser and current elective treatment for bipolar disorder, is an inhibitor of GSK3 (Beaulieu & Caron, 2008). The synergistic inhibition of GSK3β by DISC1 and dixdc1 results in increased proliferation of neural progenitors via the activation of β-catenin-mediated transcription, which is normally repressed by GSK3β (Singh *et al*, 2010). Additionally, DISC1 has been shown to inhibit the kinase activity of GSK3β by directly binding to the enzyme and blocking its activating autophosphorylation (Mao *et al*, 2009).

DISC1 has also been linked to the Akt-mTOR signalling pathway, which is involved in the modulation of several processes important for neuronal development and synaptic plasticity, and has been previously implicated in schizophrenia (Arguello & Gogos, 2008; Enomoto *et al*, 2009; Kim *et al*, 2009). Indeed, Kim and colleagues showed that by directly interacting with girdin (or KIAA1212) (Figure 1.3), a protein known to bind to and activate the serine-threonine kinase Akt, DISC1 prevents the

activation of Akt signalling, and suggested that this mechanism underlies the maturation defects they observed in adult-born neurons in the dentate gyrus of the hippocampus upon DISC1 silencing (Kim *et al*, 2009). This conclusion was supported by their observation that the maturation defects induced by DISC1 suppression could be rescued by rapamycin, an inhibitor of the Akt effector mTOR (Kim *et al*, 2009). In a parallel study, Enomoto and colleagues confirmed the DISC1-girdin interaction and its importance for the maturation of adult-born neurons in the dentate gyrus, but did not observe any rescuing effect of Akt on the maturation defects induced by girdin suppression, suggesting that girdin acts downstream of Akt (Enomoto *et al*, 2009).

Besides playing a central role in the regulation of neural progenitor proliferation, differentiation and maturation, DISC1 has been implicated in synaptic transmission and plasticity, which are processes at the basis of learning and memory (Hayashi-Takagi *et al*, 2010; Wang *et al*, 2010c). In human and rodent neurons, DISC1 is enriched in the post-synaptic density (PSD), a complex network of proteins forming an electron-dense thickening at the tip of dendritic spines, which are the post-synaptic compartments of the cell (Bradshaw *et al*, 2008; Hayashi-Takagi *et al*, 2010; Kirkpatrick *et al*, 2006; Wang *et al*, 2010c). Here, DISC1 interacts with and inhibits Traf2- and Nck-interacting kinase (TNIK) (Figure 1.3), an enzyme involved in the regulation of the actin cytoskeleton, inducing the degradation of several synaptic proteins and reducing the surface expression of the AMPA receptor subunit GluR1 (Wang *et al*, 2010c). In mature rat neurons, DISC1 inhibits the formation of spines and GluR1 expression through its interaction with kalirin-7 (Kal7) (Hayashi-Takagi *et al*, 2010), a GDP/GTP exchange factor for Rac1 and known regulator of spine morphogenesis (Xie *et al*, 2007). Activation of glutamate signalling via the N-Methyl D-Aspartate (NMDA) receptor induces dissociation of the DISC1-Kal-7 complex, releasing the inhibition on Kal-7, which is then free to regulate spine structure through activation of Rac1 (Hayashi-Takagi *et al*, 2010). These findings linking DISC1 to the modulation of glutamate signalling are particularly intriguing, given that the glutamate system is reportedly hypofunctional in schizophrenia (Coyle, 2006).

Also of particular relevance for psychiatric illness is DISC1 involvement in dopamine signalling, whose deregulation has been prominently implicated in the pathogenesis of schizophrenia (Howes & Kapur, 2009). DISC1 knock-down in mice results in reduction of extracellular dopamine in the PFC, maturation defects in dopaminergic axon terminals and increased sensitivity to metamphetamine (Niwa *et al*, 2010), a dopamine enhancing agent that can induce psychosis (Abi-Dargham, 2005). Moreover, DISC1 knock-down in NIH3T3 cells and primary striatal neurons decreases the number of primary cilia, where dopamine receptors D_1, D_2 and D_5 are prominently expressed (Marley & von Zastrow, 2010). In "schizophrenia-like" Disc1 L100P mutant mice, the dopamine-enhancing agent amphetamine has a greater psychostimulant effect compared to wild-type littermates, and this can be blocked by the D_2 recepor antagonist haloperidol, a typical antipsychotic (Lipina *et al*, 2010).

1.2.3.6 *Regulation of cAMP signalling by DISC1*

DISC1 has been implicated in the regulation of cyclic adenosine monophosphate (cAMP) signalling through its interaction with members of the family of type 4 phosphodiesterases (PDE4) (Millar *et al*, 2005b; Murdoch *et al*, 2007) (Figure 1.3). Phosphodiesterases are the sole means of cAMP inactivation in the cell, and thus represent an essential component of the system that regulates intracellular cAMP levels (Alberini *et al*, 1995; Duman, 2002). The PDE4 family consists of a large number of protein isoforms encoded by four distinct genes (PDE4A-D) (Smith & Scott, 2006). Their modular structure allows different PDE4 isoforms to be preferentially targeted to different subcellular compartments, where feed-back mechanisms regulate their activity based on the local cAMP levels (Houslay, 2010; Houslay & Adams, 2003). This system forms the basis of compartmentalised cAMP signalling, which is of central importance for the functioning of the central nervous system.

Several lines of evidence suggest PDE4s as genetic and biological candidates for mental illness. The PDE4B gene is disrupted by a chromosomal translocation found in one schizophrenia patient and a cousin with psychosis (Millar *et al*, 2005b), and multiple independent studies have found association between SNPs in this gene and either schizophrenia or depression, although some negative studies have also been

reported (Bradshaw & Porteous, 2012). There is also some genetic evidence involving PDE4D in schizophrenia in the Finnish population, suggesting a wider implication of PDE4s in mental illness (Tomppo *et al*, 2009). In *Drosophila melanogaster*, the PDE4 othologue *dunce* plays an important role in neuronal function, synaptic plasticity and memory through the regulation of cAMP hydrolysis in neurons, and it is also involved in axonal growth cone motility (Davis, 1996; Delgado *et al*, 1998; Kim & Wu, 1996; Zhao & Wu, 1997). Several PDE4 inhibitors, including the selective inhibitor rolipram, influence memory and cognition via modulation of the NMDA receptor activity (Mackie *et al*, 2007), and rolipram has an antidepressant and antipsychotic-like effect in rodent models (Kanes *et al*, 2007; Maxwell *et al*, 2004; O'Donnell & Zhang, 2004). Consistently, mice with genetic deletion of PDE4B or PDE4D display the same behaviour as wild-type mice treated with antidepressants (O'Donnell & Zhang, 2004; Zhang *et al*, 2002).

PDE4 isoforms are classified as long, short or super-short depending on their upstream conserved region (UCR) regulatory domains, which control access of the substrate to the catalytic domain (Houslay & Adams, 2003) (Figure 1.4, taken from Millar *et al,* 2005b). The UCR1 domain is exclusively found in the long isoforms, and PKA phosphorylation at this site determines a conformational change that increases the catalytic activity of the enzymes, triggering a feed-back mechanism that restores basal cAMP levels (Houslay & Adams, 2003).

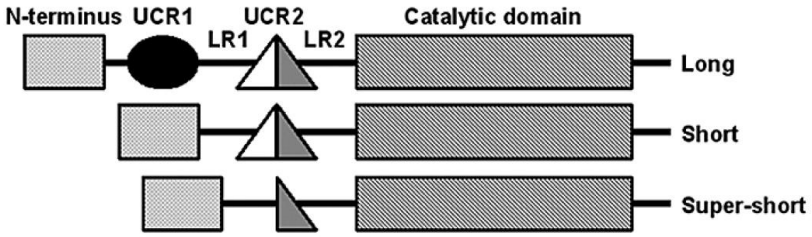

Figure 1.4 Schematic representation of long, short and super-short PDE4 isoforms, adapted from Millar *et al, 2005b*. All PDE4 isoforms possess a unique N-terminus, which mediates their differential subcellular targeting, and a conserved catalytic domain in the C-terminus. Long isoforms, but not short or super-short isoforms,

possess both the UCR1 and UCR2 regulatory domains. Short and super-short isoforms contain a complete or partial UCR2 domain, respectively.

Exogenously expressed full-length 100 kDa DISC1 is able to bind all four isoforms (A-D) of PDE4 through their UCR2 domain, and the interaction sites on both proteins have been mapped using deletion constructs and peptide arrays (Millar *et al*, 2005b; Murdoch *et al*, 2007). There are three PDE4B-specific interaction sites, located in the N-terminal region of DISC1 (amino acids 31-65, 101-135 and 266-290), and two general PDE4 binding sites; one in the N-terminal region (amino acids 190-230) and one in the C-terminal region (amino acids 611-650) (Murdoch *et al*, 2007). Interaction between endogenous 71 and 100 kDa DISC1 isoforms has also been detected by co-immunoprecipitation in human neuronal SH-SY5Y cells (Bradshaw *et al*, 2008; Millar *et al*, 2005b).

Millar and colleagues originally reported that the interaction between DISC1 and PDE4B is dynamically regulated by intracellular cAMP levels through the action of PKA (Millar *et al*, 2005b). Upon cell treatment with the adenylyl cyclase inhibitor forskolin and the general PDE inhibitor IBMX, which results in intracellular accumulation of cAMP, the interaction between endogenous 71 kDa DISC1 and PDE4B is markedly reduced, as evidenced by decreased co-immunoprecipitation, and the catalytic activity of PDE4B is increased (Millar *et al*, 2005b). This effect can be prevented by concomitant treatment with the PKA-specific inhibitor H89 (Millar *et al*, 2005b). These observations suggested a model whereby DISC1 binding maintains PDE4B in a state of low catalytic activity until cAMP-PKA signalling is activated, releasing PDE4B from DISC1 and boosting its catalytic activity (Millar *et al*, 2005b). A later study added more facets to this model by showing that the cAMP-dependent release of PDE4 from DISC1 is isoform-specific (Murdoch *et al*, 2007). In co-immunoprecipitation assays performed with exogenously expressed proteins, increased cAMP levels reduce the interaction between full-length 100 kDa DISC1 and both long and short PDE4 isoforms D and C, but not B and A (Murdoch *et al*, 2007). Additionally, this study showed that the cAMP-dependent release of PDE4D3 from DISC1 is PKA-dependent, but it is not mediated by PKA phosphorylation of

PDE4D3 or DISC1 (Murdoch *et al*, 2007). This complicates the initial observations made by Millar and colleagues, and shows that the DISC1-PDE4 interaction is affected by isoform variability in both proteins (Murdoch *et al*, 2007). Since a N-terminally truncated form of DISC1 that lacks the three PDE4B-specific binding sites fails to retain interaction with PDE4B upon increased cAMP levels, Murdoch and colleagues proposed that deletion of DISC1 N-terminus might mimic the 71 kDa isoform described by Millar and colleagues (Murdoch *et al*, 2007). However, the mechanisms mediating cAMP-dependent release of PDE4D and C from DISC1 remain unclear (Murdoch *et al*, 2007).

Recent studies suggested that interactions between PDE4, DISC1 and GSK3 may be finely interregulated, and that perturbations of this complex may lead to psychiatric illness. PKA is both an activator of PDE4 (MacKenzie *et al*, 2002) and a substrate of GSK3 (Hemmings *et al*, 1982), and in turn cAMP signalling has been shown to affect the activity of GSK3β (Goessling *et al*, 2009), suggesting the possible existence of complex feed-back control mechanisms. This is substantiated by studies *in vivo* and *in vitro*. For example, a Disc1 mouse model characterised by the L100P missense mutation, which will be described in more detail in the next section, presents behavioural abnormalities mimicking certain characteristics of schizophrenia that can be partially rescued by combined inhibition of PDE4 and GSK3, but not of either enzyme individually (Lipina *et al*, 2011a; Lipina *et al*, 2011b). In SH-SY5Y cells, both DISC1 overexpression and GSK3β inhibition attenuate the increase of PDE4 activity in response to increased cAMP levels (Carlyle *et al*, 2011). Additionally, GSK3β inhibition reduces the activity of PDE4 at basal cAMP levels, indicating that GSK3β has a tonic activating effect on the enzyme (Carlyle *et al*, 2011).

1.2.3.7 *Disc1 mouse models*

Although it is obviously not possible to accurately model complex human diseases such as schizophrenia or depression in a much simpler organism like a mouse, some of the clinical features of these illnesses have measurable behavioural, cognitive and anatomical correlates in rodents that can be analysed after genetic and/or

pharmacologic manipulations (Arguello & Gogos, 2006). Under this premise, several mouse models have been generated to investigate the effect of *Disc1* mutations or altered *Disc1* expression levels on brain development, behaviour and cognition, and shed light on their molecular consequences.

The first Disc1 mouse model was inspired by the serendipitous observation that all 129 mouse strains carry a frame-shift mutation in *Disc1* exon 6 that is predicted to result in the production of a truncated protein (Clapcote & Roder, 2006; Koike *et al*, 2006). Koike and colleagues introduced this novel mutation in the C57BL/6J background, along with two premature stop codons (one in exon 7 and one in exon 8) and a premature polyadenylation site in intron 8. Interestingly, the resulting Disc1 mutant line presented working memory defects and neurodevelopmental and brain structural abnormalities (Koike *et al*, 2006; Kvajo *et al*, 2008).

Using N-nitroso-N-ethylurea (ENU) mutagenesis, a method that can be used to introduce a single point mutation at a random locus, Clapcote and colleagues generated two mutant mouse lines carrying distinct missense mutations in *Disc1* exon 2, resulting in amino acid substitutions Q31L and L100P, respectively (Clapcote *et al*, 2007). Similarly to the *Disc1* mutation mentioned above, the Q31L and L100P amino acid substitutions resulted in working memory deficits, a commonly observed clinical feature of schizophrenia patients (Clapcote *et al*, 2007). The two ENU-induced *Disc1* mutant mouse lines displayed additional behavioural abnormalities that had not been observed in the previously described deletion mutant mice. Similarly to psychotic patients, both the Q31L and L100P mutants had prepulse inhibition (PPI) and latent inhibition (LI) deficits, which reflect abnormal sensory information processing (Clapcote *et al*, 2007). Interestingly, these deficits could be rescued by typical and atypical antipsychotics (haloperidol and clozapine, respectively) or by the PDE4 inhibitor rolipram in L100P but not in Q31L mutants, whereas the antidepressant bupropion normalised the PPI deficits in Q31L mice only (Clapcote *et al*, 2007). This suggested that the information processing deficits observed in the two *Disc1* mutant lines originated through distinct mechanisms. Further behavioural testing highlighted a net distinction between the two mutant lines: Q31L, but not L100P mice exhibited increased immobility in the forced swim

test as well as reduced sociability and reward responsiveness, which all together delineate a depression-like phenotype (Clapcote *et al*, 2007). Consistently, the antidepressant bupropion, but not the PDE4 inhibitor rolipram, significantly reduced the immobility of Q31L mice in the forced swim test (Clapcote *et al*, 2007). The distinct behavioural and pharmacological profiles of Q31L and L100P *Disc1* mutants led to the conceptualisation of the first as a model of depression and the second as a model of schizophrenia (Clapcote *et al*, 2007). Of interest, neuroanatomical abnormalities consistent with those observed in patients with schizophrenia, bipolar disorder or depression were documented in both Q31L and L100P mice, which display reduced brain volume and contraction of the cortex, thalamus and cerebellum, as well as defective neuronal proliferation, distribution and maturation in the cerebral cortex and hippocampus (Clapcote *et al*, 2007; Lee *et al*, 2011). In a recent study, Shoji and colleagues performed a battery of behavioural tests on homozygous *Disc1* Q31L and L100P mice that had been backcrossed to the C57BL/6JJcl strain (the same strain utilised in the study by Clapcote and colleagues (Clapcote *et al*, 2007)) for two more generations (Shoji *et al*, 2012). The results of the behavioural analyses conducted by Shoji and colleagues on these two *Disc1* mutant lines (Shoji *et al*, 2012) show gross inconsistencies with those previously reported by Clapcote and colleagues (Clapcote *et al*, 2007). Indeed, except for increased locomotor activity in L100P *Disc1* mutants, which had also been reported by Clapcote and colleagues (Clapcote *et al*, 2007), neither the Q31L nor the L100P mutants performed differently from wild-type controls in the study conducted by Shoji and colleagues (Shoji *et al*, 2012). These discrepancies might reflect differences in genetic background between the *Disc1* mutants analysed in the two studies, but might also be due to differences in the housing/laboratory environment and/or testing conditions (Shoji *et al*, 2012).

Several groups have generated Disc1 mouse models expressing a N- or C-terminally truncated protein in an attempt to mimic the functional consequences of the t(1;11) translocation disrupting *DISC1* in the original Scottish family. In regard to this, it is important to emphasise that although the production of a C-terminally truncated form of DISC1 in carriers of the t(1;11) translocation is theoretically possible, no evidence in support of the existence of such mutant protein has been produced to date (Millar

et al, 2005b). Nevertheless, Disc1 mouse models mimicking the t(1;11) translocation have provided valuable information on the role of Disc1 in neurodevelopment and neurosignalling. Slightly different approaches have been taken in the generation of mouse lines expressing truncated DISC1, and a vast spectrum of neuroanatomical and behavioural abnormalities have been observed in these mouse models, with some recurring features. Several models used a N- or C-terminally truncated *DISC1* cDNA expressed constitutively or inducibly under control of the promoter for αCaMKII, which is expressed in forebrain regions only (Ayhan *et al*, 2011; Hikida *et al*, 2007; Li *et al*, 2007a; Pletnikov *et al*, 2008a; Pletnikov *et al*, 2008b). An alternative approach was adopted by Shen and colleagues, who used a bacterial artificial chromosome (BAC) vector containing *Disc1* exons 1-9 and its entire upstream promoter sequence to generate mice that constitutively express truncated and endogenous full-length Disc1 at comparable levels (Shen *et al*, 2008). The observed phenotypes include macroscopic brain structural changes that have also been reported in schizophrenia patients, such as enlargement of the lateral ventricles and decreased thickness of the cerebral cortex (Ayhan *et al*, 2011; Hikida *et al*, 2007; Pletnikov *et al*, 2008b; Shen *et al*, 2008). Microscopic neuroarchitectural abnormalities have also been commonly observed in mice expressing truncated DISC1. These include decreased dendritic complexity (Li *et al*, 2007a; Pletnikov *et al*, 2008a; Shen *et al*, 2008), decreased neurite outgrowth (Pletnikov *et al*, 2008a; Shen *et al*, 2008) and reduced number of parvalbumin-positive cells in the prefrontal cortex (Ayhan *et al*, 2011; Hikida *et al*, 2007; Shen *et al*, 2008), the latter being a strongly replicated observation in post-mortem analyses of schizophrenic brains (Lewis *et al*, 2005). At the cognitive and behavioural level, expression of truncated DISC1 was found to correlate with reduced sociability (Li *et al*, 2007a; Pletnikov *et al*, 2008a), working memory deficits (Li *et al*, 2007a), defects of LI or PPI (Li *et al*, 2007a; Shen *et al*, 2008) and increased immobility in depression-related tests (Ayhan *et al*, 2011; Hikida *et al*, 2007; Li *et al*, 2007a; Shen *et al*, 2008). Only some of the histological and behavioural findings are consistent across the different mouse models expressing truncated DISC1, a discrepancy that could result from differences in the temporal and spatial expression of mutant DISC1. Indeed, a recent study revealed that many of the phenotypic alterations reported in DISC1 mutant mice are

dependent on the stage at which transgene expression is switched on (Ayhan *et al*, 2011).

Other models are based on electroporation- or retroviral-mediated delivery of *Disc1*-targeting short hairpin RNAs (shRNAs) to knock-down endogenous *Disc1* expression in the mouse brain. Knock-down of *Disc1* expression by *in utero* electroporation results in delayed neuronal migration and aberrant dendritic arborisation in the cerebral cortex (Kamiya *et al*, 2005). Using a similar approach in adult animals, Duan and colleagues demonstrated that *Disc1* suppression in neural progenitors of the dentate gyrus of the hippocampus results in overextended migration, accelerated integration and misfiring of these cells (Duan *et al*, 2007). A separate study showed that *Disc1* knock-down in the embryonic brain inhibits the proliferation and promotes the premature differentiation of neural progenitors in the cortex, and that this arises from aberrant Wnt-GSK3β-β-catenin signalling (Mao *et al*, 2009). Similar defects to those reported by Duan, Kamiya and Mao were observed after transient knock-down of *Disc1* in the PFC during early development, and resulted in defective maturation of dopaminergic neurons and behavioural alterations in adulthood (Niwa *et al*, 2010).

Due to its transcriptional complexity, complete knock-out of *Disc1* expression has proven particularly difficult to achieve (Chubb *et al*, 2008). Recently, the generation of a novel mouse line lacking *Disc1* exons 2 and 3 (Disc1 Δ2-3) has been reported (Kuroda *et al*, 2011). These mice do not express full-length Disc1, but transcripts containing *Disc1* exons 7-9 were detected in mice homozygous for the Δ2-3 mutation, indicating that shorter Disc1 isoforms lacking exons 2 and 3 may still be produced (Kuroda *et al*, 2011). Surprisingly, no structural or histological brain abnormalities were observed in these mice (Kuroda *et al*, 2011). Despite having a higher threshold for long term potentiation (LTP) induction, *Disc1* Δ2-3 mice did not display any deficits in various learning and memory-related tests (Kuroda *et al*, 2011). Further behavioural testing revealed increased impulsivity, reduced PPI and increased responsiveness to the dopaminergic agonist methamphetamine in *Disc1* Δ2-3 mice. The *Disc1* mutants also spent a significantly longer time in the open arms of the elevated plus maze, which indicates reduced anxiety, and this behaviour was

normalised by the administration of the antipsychotic clozapine (Kuroda *et al*, 2011). The discrepancy between the neuroanatomical abnormalities seen in the studies that used transient *Disc1* knock-down and the normal brain morphology in *Disc1* Δ2-3 mice may arise from compensatory mechanisms induced by chronic *Disc1* depletion, and might be resolved by the study of mice with conditional knock-out of full-length Disc1 (Kuroda *et al*, 2011).

Recent studies have investigated the impact of maternal immune activation on behavioural and neuroanatomical outcomes in mice expressing C-terminally truncated DISC1. Epidemiological studies have found a consistent association between maternal infection by various infective agents during gestation and increased risk of schizophrenia in the offspring (Brown & Derkits, 2010). Gestational infections are thought to interfere with foetal brain development through the activation of the maternal immune system and consequent production of pro-inflammatory cytokines, some of which cross the placenta (Brown, 2011). The double-stranded RNA synthetic analogue Polyribosinic-polyribocytidilic acid (PolyI:C) is commonly used to mimic infection in rodents as it induces the release of pro-inflammatory cytokines through the activation of Toll-like receptors in mammals (Nagai *et al*, 2011a). Administration of PolyI:C to pregnant dams or neonate mice has often been used as a model to study the cognitive, behavioural and anatomical consequences of infection during development (Nagai *et al*, 2011a). Despite the important limitations arising from the difficulty of matching pregnancy stages in humans and rodents, PolyI:C models have been useful in showing how maternal or neonatal immune activation can impact on a wide spectrum of cognitive and behavioural phenotypes that correlate with schizophrenia (Nagai *et al*, 2011a).

A recent study investigated the effects of neonatal administration of PolyI:C to mice expressing C-terminally truncated dominant-negative DISC1 (DN-DISC1) on cognitive and behavioural correlates of schizophrenia assessed during adolescence (Ibi *et al*, 2010). This study found synergistic detrimental effects of PolyI:C treatment and DN-DISC1 expression on short-term, object recognition and fear memory during adolescence (Ibi *et al*, 2010). Additionally, PolyI:C-treated DN-DISC1 mice display a significant social impairment and an increased response to the

NMDA receptor antagonist MK-801, which is commonly used to model psychosis (Ibi *et al*, 2010). A significant treatment x genotype interaction was also observed in relation to the number of parvalbumin-positive interneurons in the PFC, with PolyI:C-treated DN-DISC1 mice showing the most marked decrease when compared to both treated and untreated wild-type littermates and untreated mutants (Ibi *et al*, 2010). The recorded phenotypes in PolyI:C-treated DN-DISC1 mice could be differentially rescued by the antipsychotics clozapine and haloperidol, with the memory deficits responding to clozapine only, the exacerbated response to MK-801 responding to both drugs, and the social impairments responding to neither (Nagai *et al*, 2011b).

A separate study focused on the interaction between DN-DISC1 expression and PolyI:C treatment during gestation, a model considered more relevant to human psychopathology, based on epidemiological studies (Abazyan *et al*, 2011). Prenatal interaction produced markedly increased anxiety and depression-like behaviours, as well as altered social interaction, but had no effect on cognitive measures (Abazyan *et al*, 2011). These behavioural abnormalities were accompanied by reduced reactivity of the hypothalamus-pituitary-adrenal (HPA) axis, reduced serotonin neurotransmission and altered brain morphology (Abazyan *et al*, 2011).

Collectively, these studies support PolyI:C treatment in DN-DISC1 mice as a valuable tool to study the interaction between two well established genetic and environmental susceptibility factors for schizophrenia, and highlight important differences between the cognitive and behavoiral consequences of pre- and post-natal immune activation.

1.3 The interaction of DISC1 with ATF4

1.3.1 *The identification of ATF4 as a DISC1 binding partner*

Activating Transcription Factor 4 (ATF4), also known as cAMP Response Element Binding Protein 2 (CREB2), was first identified as a DISC1 binding protein in two of the three yeast-two-hybrid (Y2H) screens that shortly followed the discovery of DISC1 (Millar *et al*, 2003; Morris *et al*, 2003; Ozeki *et al*, 2003). Screens of both

foetal and adult human brain (Millar *et al*, 2003; Morris *et al*, 2003) and heart (Morris *et al*, 2003) cDNA libraries with full-length DISC1, identified several positive clones for ATF4 in the brain, but none in the heart. In the screen performed by Millar and colleagues, ATF4 was the only DISC1 interacting protein identified in both foetal and adult brain libraries (Millar *et al*, 2003). ATF4 is not the only nuclear protein identified in Y2H for DISC1 interactors, as the highly related Activating Transcription Factor 5 (ATF5) and the chromatin remodelling protein SWI/SNF related matrix associated actin dependent regulator of chromatin (SMARCE1) were also positive hits (Millar *et al*, 2003; Morris *et al*, 2003). DISC1 binding to ATF4 was first confirmed by mammalian-two-hybrid (M2H) assays (Morris *et al*, 2003) and later by co-immunoprecipitation (co-IP) of both endogenous (Bradshaw *et al*, 2008) and exogenous (Sawamura *et al*, 2008) proteins. The identification of ATF4 and other nuclear interactors provided the first clue on the potential functions of nuclear DISC1. However, to date only one study, which will be described in detail later in this thesis, has focused on the functional implications of the DISC1-ATF4 interaction in the nucleus, and how this may relate to psychiatric illness (Sawamura *et al*, 2008).

Limited evidence from linkage and association studies implicates *ATF4* in schizophrenia, but not bipolar disorder. *ATF4* is one of the genes located in the schizophrenia-linked chromosomal region 22q13, and has thus been suggested as a positional candidate gene for schizophrenia (Lewis *et al*, 2003; Mowry *et al*, 2004; Williams *et al*, 2003). A single study found association of two SNPs within *ATF4* with schizophrenia in male patients from the Han Chinese population (Qu *et al*, 2008). However, no association between *ATF4* and bipolar disorder was found in a Japanese population (Kakiuchi *et al*, 2007). No firm conclusions can be drawn from the genetic data collected so far, and further studies are needed to elucidate the potential role of *ATF4* as a candidate gene for psychiatric illness.

1.3.2 *ATF4 is a ubiquitous and multifunctional protein*

ATF4 belongs to the ATF/CREB family of basic region-leucine zipper (bZIP) transcription factors, which share the ability to bind to the cAMP response element (CRE) (Ameri & Harris, 2008; Vinson *et al*, 2002). *ATF4* is a ubiquitously expressed

gene (Karpinski *et al*, 1992; Vallejo *et al*, 1993) involved in a plethora of developmental and homeostatic processes, but its best characterised functions, which will be described in detail later in this chapter, are the control of the cellular response to stress and the modulation of long-term potentiation and long-term memory (Ameri & Harris, 2008). Consistent with its prominent role in memory formation, *ATF4* expression has been detected in the mouse hippocampal regions CA1-3 and dentate gyrus, as well as other brain regions, including the amygdala, caudate nucleus, corpus callosum, thalamus, subthalamic nuclei and substantia nigra (Yukawa *et al*, 1999).

Several *ATF4* knock-out (KO) mice have been independently generated and characterised (Hettmann *et al*, 2000; Masuoka & Townes, 2002; Tanaka *et al*, 1998). These are generally viable, but present with multiple severe defects that highlight the importance of ATF4 in the development of different tissues (Ameri & Harris, 2008). For example, *ATF4* inactivation results in defective lens development, leading to severe microphthalmia and blindness in the adult animals (Hettmann *et al*, 2000; Tanaka *et al*, 1998). Other phenotypes observed in *ATF4* KO mice include severe foetal anaemia, delayed growth and smaller size, reduced fibroblast proliferation, subfertility, lower fat mass and glucose levels, and defective skeletal development (Fischer *et al*, 2004; Masuoka & Townes, 2002; Muir *et al*, 2008; Dobreva *et al*, 2006; Yang *et al*, 2004; Yoshizawa *et al*, 2009). Consistent with a role of ATF4 in development, mutations in the *Drosophila melanogaster ATF4* homolog *cryptocephal* result in larval moulting and metamorphosis defects (Hewes *et al*, 2000).

A recent study demonstrated for the first time that ATF4 is also involved in neurodevelopment through its role in cell cycle control (Frank *et al*, 2010). Experiments in cultured cells demonstrated that ATF4 protein levels normally oscillate during the cell cycle, and that proteasome-dependent ATF4 degradation is necessary for correct cell cycle progression (Frank *et al*, 2010). Analysis of the developing mouse brain by in-situ hybridization and western blotting revealed that ATF4 expression is highest at the early stages of brain development, when progenitor proliferation predominates, and gradually decreases as neurogenesis progresses, to be

then reactivated in mature neurons (Frank *et al*, 2010). Electroporation of a proteasome-resistant mutant form of ATF4 in the embryonic mouse brain caused accumulation of neural progenitors in the ventricular zone due to cell cycle arrest in early G1, indicating that correctly timed ATF4 degradation is necessary for neurogenesis *in vivo* (Frank *et al*, 2010).

Further studies that focused on the role of ATF4 in bone morphogenesis revealed that it is essential for the maturation of osteoblasts, the cells responsible for bone formation (Hartmann, 2009). In these cells, selective accumulation of ATF4, which is otherwise present at very low levels, occurs through the inhibition of its proteasomal degradation (Hartmann, 2009). The transcriptional activity of ATF4 in osteoblasts is further activated through phosphorylation by ribosomal S6 protein kinase 2 (RSK2), and it has been proposed that the lack of ATF4 phosphorylation by RSK2 may contribute to the skeletal displasia that characterises Coffin-Lowry syndrome (Yang *et al*, 2004). Through its expression in osteoblasts, ATF4 also regulates the differentiation of osteoclasts, the cells responsible for bone resorption (Elefteriou *et al*, 2005). In osteoblasts, ATF4 activates the expression of the receptor activator of nuclear factor-KappaB ligand (RankL) gene, which encodes a secreted factor that promotes osteoclast differentiation (Elefteriou *et al*, 2005). Accordingly, *ATF4* KO mice have decreased osteoclast numbers due to reduced RankL expression (Cao *et al*, 2010).

Expression of ATF4 in osteoblasts has also been demonstrated to be responsible for the endocrine function of these cells, and in particular for their role in the control of glucose metabolism (Yoshizawa *et al*, 2009). Indeed, osteoblast-expressed ATF4 negatively regulates insulin secretion and reduces the insulin sensitivity of liver, muscle and fat tissue (Yoshizawa *et al*, 2009). As discussed later, ATF4 promotes the expression of genes involved in amino acid uptake and protein synthesis, and this particular function contributes to the anabolic and catabolic actions of insulin and glucocorticoids, respectively (Adams, 2007). Under anabolic conditions, when nutrients are abundant, insulin induces ATF4 expression through activation of mammalian target of rapamycin complex 1 (mTORC1), whereas under catabolic conditions, such as fasting, glucocorticoids reduce ATF4 expression (Adams, 2007).

ATF4 is also involved in the regulation of thermogenesis and lipid metabolism, as demonstrated by the observation that *ATF4* KO mice are leaner, they have increased energy expenditure, increased lipolysis, reduced fat accumulation and increased resistance to diabetes under high-feeding conditions (Seo *et al*, 2009; Wang *et al*, 2010a). Its multiple functions in the regulation of lipid and glucose metabolism, energy homeostasis, insulin secretion, and sensitivity, suggest that ATF4 is a central regulator of metabolism.

Tumour biology is an additional area of research in which much attention has been devoted to ATF4, by virtue of its role as a mediator of the cellular stress responses (Rzymski *et al*, 2009). Expanding solid tumours have to adapt to the adverse conditions generated by the lack of efficient vascularisation, namely the defective supply of oxygen and nutrients and the accumulation of toxic waste products. To cope with these stressful conditions, the cells activate the integrated stress response (ISR), a coordinated program of gene expression whose primary purpose is to restore homeostasis through the upregulation of pro-survival genes, but that can ultimately divert towards apoptosis if the cell damage is too advanced (Harding *et al*, 2003; Haynes *et al*, 2004). ATF4 is the master regulator of the ISR, and fibroblasts lacking ATF4 show a markedly increased sensitivity to hypoxia, nutrient deprivation and oxidative stress, which are the typical conditions present in the tumour microenvironment (Harding *et al*, 2003). By contrast, ATF4 overexpression is often detected in tumour cells (Bi *et al*, 2005), especially in the regions of more severe hypoxia (Ameri *et al*, 2004; Bi *et al*, 2005), and has been positively correlated with the degree of tumour aggressiveness (Ameri *et al*, 2010; Daibata *et al*, 2004) and with resistance to anti-cancer drugs (Rzymski *et al*, 2009). For these reasons, it has been suggested that ATF4 overexpression represents a key adaptive mechanism that promotes tumour progression and malignancy, and that hinders the effectiveness of current chemotherapeutic approaches (Rzymski *et al*, 2009). As a consequence, innovative anti-cancer strategies based on ATF4 inhibition are currently under consideration (Ameri & Harris, 2008; Rzymski *et al*, 2009; Wang *et al*, 2010a; Ye & Koumenis, 2009).

1.3.3 *ATF4 protein structure, dimerisation partners and DNA binding properties*

The human ATF4 protein is 351 amino acids long, and is organised in several domains that mediate its homo and heterodimerisation, DNA binding, transcriptional activation and protein degradation (Ameri & Harris, 2008) (Figure 1.5, taken from Ameri *et al*, 2008). *ATF4* is ubiquitously expressed at the mRNA level, but, with the exception of osteoblasts, ATF4 protein levels are very low under basal (non-stressed) conditions due to its inefficient translation and short half-life (Rzymski *et al*, 2009). As described later in this chapter, several mechanisms contribute to the regulation of ATF4 protein levels in response to stress, one of these being its proteasomal degradation (Ameri & Harris, 2008). Three domains in ATF4 are involved in the regulation of the protein stability: the histone acetyltransferase (HAT) P300-binding domain at amino acids (1-85), the oxygen-dependent degradation domain (ODDD) at amino acids (154-181), and the βTrCP recognition motif at amino acids (218-224) (Koditz *et al*, 2007; Lassot *et al*, 2005; Lassot *et al*, 2001) (Figure 1.5). Binding of HAT P300 stabilises ATF4 by inhibiting its ubiquitination (Lassot *et al*, 2005). The ODDD is recognised by the oxygen sensor prolyl-4-hydroxylase 3 (PHD3), which mediates the proteasomal degradation of ATF4 under normoxic conditions (Koditz *et al*, 2007). Finally, the βTrCP recognition motif mediates the phosphorylation-dependent degradation of ATF4 through its binding to the $SCF^{\beta TrCP}$ E3 ubiquitin ligase (Lassot *et al*, 2001).

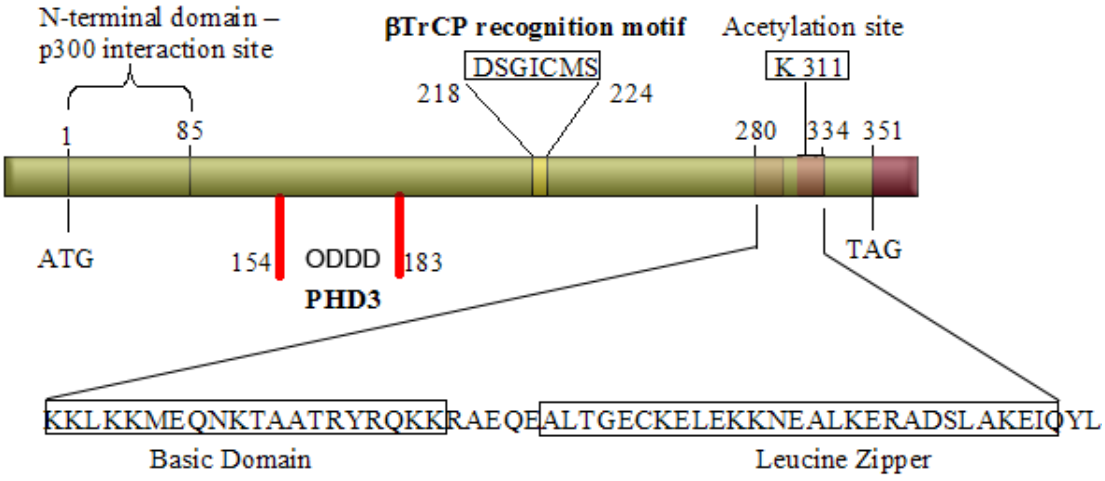

Figure 1.5 Adapted from Ameri *et al,* 2008. Schematic representation of ATF4 protein structure and modulatory domains. The position of the P300 interaction site and modulatory acetylation site (Lassot *et al*, 2005) are indicated, along with the PHD3 binding domain and ODDD. The βTrCP binding site and C-terminal bZip domain are also shown.

The initial characterisation of the protein upon cloning of its cDNA revealed the presence of a basic leucine-zipper motif and adjacent basic region in the C-terminus of ATF4, between amino acids (280-334) (Karpinski *et al*, 1992) (Figure 1.5). This motif, which is commonly referred to as the bZip motif, is shared by a variety of transcription factors, including CREB, CREM, FOS and JUN, which are thus collectively called bZip transcription factors, and is essential for their function (Vinson *et al*, 2002). Within the bZip domain, the leucine zipper mediates the homo or heterodimerisation of these transcription factors, whereas the basic region is necessary for their binding to DNA (Karpinski *et al*, 1992). ATF4 is evolutionary conserved, with the human and mouse proteins sharing 80% similarity overall, and the sequence conservation is particularly high in the bZIP region, which is 98.6% identical between human and mouse, denoting its functional importance (Mielnicki & Pruitt, 1991).

ATF4 possesses an additional conserved leucine zipper (zipper II) spanning amino acids (91-126) (Liang & Hai, 1997). Zipper II mediates the interaction of ATF4 with regulatory proteins such as PHD3 and neuronal cell death-inducible putative kinase (NIPK), and is thus involved in the control of ATF4 protein stability and transcriptional activity (Koditz *et al*, 2007; Ord & Ord, 2003).

ATF4 was originally isolated based on its ability to bind to the palindromic ATF/CRE consensus site (TGAGCTCA) (Hai *et al*, 1989). The study of the dimerisation partners of ATF4 revealed that not only can it form homodimers, but it can also heterodimerise with members of the AP-1 family of bZip transcription factors, which preferentially bind to the AP-1 consensus site (TGACTCA) (Hai & Curran, 1991), and with other bZip transcription factors belonging to the CCAAT/enhancer-binding protein (C/EBP) family (Gombart *et al*, 2007; Vallejo *et al*, 1993; Vinson *et al*, 2002). In contrast, despite being able to homodimerise, ATF4

has not been reported to heterodimerise with other ATF/CRE transcription factors (Hai & Hartman, 2001; Vinson *et al*, 2002). While ATF4 homodimers preferentially bind to the ATF4/CRE site, the DNA binding affinity of ATF4 heterodimers is dependent on the heterodimerisation partner, and in some cases it differs from that of each parental homodimer (Hai & Curran, 1991; Vallejo *et al*, 1993; Vinson *et al*, 1993). For example, ATF4-C/EBPβ heterodimers bind to a subclass of asymmetric CREs that are not recognised by either parental homodimer (Vallejo *et al*, 1993). Thus, the relative abundance of the different ATF4-binding transcription factors in a particular system and at a particular time is likely to be one of the factors controlling its transcriptional activity (Vallejo *et al*, 1993).

The N-terminus and, albeit more weakly, the C-terminal bZip domain of ATF4 have been reported to function as transactivator domains in transcriptional reporter assays (Liang & Hai, 1997; Schoch *et al*, 2001), whereas no transferrable repressor domains have been identified within the ATF4 protein sequence (Schoch *et al*, 2001). However, ATF4 has been initially described to act as a transcriptional repressor (Cibelli *et al*, 1996; Jungling *et al*, 1994; Karpinski *et al*, 1992), and this observation is at the basis of its proposed role as a repressor of long-term memory formation (Bartsch *et al*, 1995). A possible explanation for this apparent discrepancy may be provided by the reported ability of ATF4 to bind the transcriptional co-activator CREB-binding protein (CBP), as well as several components of the basic transcriptional machinery, including TATA binding protein (TBP) and transcription factors IIB (TFIIB) and IIF (TFIIF) (Liang & Hai, 1997). It has been suggested that, by binding to these factors and sequestering them away from the promoter, overexpressed ATF4 may compete with other transcription factors (Hai & Hartman, 2001; Liang & Hai, 1997; Schoch *et al*, 2001). This hypothesis is supported by titration experiments with exogenous ATF4, which showed that the protein inhibits its own transcriptional activity when expressed at high concentrations (Liang & Hai, 1997).

ATF4 has several additional interacting proteins, the variety of which reflects its multifunctionality (Ameri & Harris, 2008). A non exhaustive list of ATF4 binding proteins includes the nuclear matrix proteins Satb2 (Dobreva *et al*, 2006) and

mitosin/CENPF (Zhou *et al*, 2005), the centrosomal protein CEP290 (Sayer *et al*, 2006), the bZip protein Zhangfei, which potentiates ATF4 transcriptional activity on CRE-containing promoters (Hogan *et al*, 2006), the C/EBP homologous protein CHOP (Gachon *et al*, 2001), the transcription factor Nrf2, which regulates the expression of antioxidant genes (He *et al*, 2001), and the two subunits of the metabotropic $GABA_B$ receptor (Nehring *et al*, 2000; Ritter *et al*, 2004; Vernon *et al*, 2001; White *et al*, 2000). The last of these is a particularly intriguing interaction, given the proposed role for dysfunctional GABA signalling in schizophrenia (Coyle, 2004) and the recently reported interplay between DISC1 and GABA signalling in the regulation of neurogenesis (Kim *et al*, 2012), but it has not been investigated beyond the initial reports that proposed a functional link between $GABA_B$ receptor signalling and ATF4 transcriptional activity in neurons (Vernon *et al*, 2001; White *et al*, 2000).

Consistent with its role in transcriptional control, ATF4 is highly enriched in the nucleus, although its presence has been reported in other subcellular compartments (Lai *et al*, 2008; Nehring *et al*, 2000; White *et al*, 2000). Nuclear targeting of ATF4 is mediated by a signal sequence located within its C-terminal basic region, at amino acids (280-300). Single point mutations of basic amino acids within this region identified the sequence 280-KKLKK-284 as necessary for ATF4 nuclear targeting (Cibelli *et al*, 1999).

1.3.4 *Regulation of ATF4 transcriptional activity*

In most cell types, the main function of ATF4 is to orchestrate the transcriptional response to a range of damaging external stimuli, including oxygen deprivation, amino acid limitation, oxidative stress, viral infections and endoplasmic reticulum stress (Ameri & Harris, 2008). Consistently, ATF4 protein levels are normally very low, and often undetetectable, in the majority of non-stressed cells (Ameri & Harris, 2008). The transcriptional activation of ATF4 in response to stress is necessary to induce the expression of genes that allow the cell to successfully cope with the stressful stimulus and hence adapt and survive (Harding *et al*, 2003). However, ATF4 target genes also include pro-apoptotic factors such as CHOP, and protracted ATF4 activation can result in cell death (Lange *et al*, 2008; Ord *et al*, 2007;

Rutkowski *et al*, 2006). For these reasons, several regulatory mechanisms are normally in place to keep ATF4 transcriptional activity under strict control. As detailed below, these include the regulation of ATF4 protein dosage at the transcriptional, translational and post-translational level, as well as the direct modulation of ATF4 transcriptional activity by its interaction with partner proteins (Ameri & Harris, 2008).

1.3.4.1 *Transcriptional regulation of ATF4*

As described below, the main mechanism responsible for the increase in ATF4 protein levels in response to stress is the selective enhancement of its translation. However, some studies have reported changes in *ATF4* mRNA levels in response to certain types of stress, although the specific factors responsible for this stress-dependent transcriptional control of *ATF4* are still unknown (Dey *et al*, 2010). Like the ATF4 protein, *ATF4* mRNA is short-lived, with a half-life of only ~3 hours, which allows for rapid regulation of its levels (Dey *et al*, 2010). The changes in *ATF4* mRNA levels in response to stress do not seem to be mediated by regulation of its stability, but instead involve activation or repression of mRNA synthesis (Dey *et al*, 2010). Most, but not all studies reported increased *ATF4* mRNA synthesis in response to stress. For example, in primary rat fibroblasts, anoxia was reported to increase *ATF4* mRNA expression (Estes *et al*, 1995), but hypoxia had no effect on *ATF4* mRNA levels in HeLa cells (Blais *et al*, 2004). This may suggest that the induction of *ATF4* transcription only occurs under conditions of severe oxygen deprivation. Additionally, *ATF4* mRNA is induced by amino acid and glucose deprivation (Siu *et al*, 2002), endoplasmic reticulum stress (Adachi *et al*, 2008; Harding *et al*, 2000; Lu *et al*, 2004) and by oxidative stress (Lange *et al*, 2008). A recent study based on reporter constructs confirmed that *ATF4* transcription is activated in response to endoplasmic reticulum stress, and also found that it is inhibited by UV irradiation (Dey *et al*, 2010). Given the reportedly detrimental effect of ATF4 activation in response to some stressors, including UV irradiation, it has been proposed that the differential regulation of ATF4 expression depending on the particular stress condition may be central to cell survival (Dey *et al*, 2010).

1.3.4.2 *Translational regulation of ATF4*

In mammalian cells, multiple stress-responsive pathways converge on the phosphorylation of the eukaryotic initiation factor 2α (eIF2α) at serine 51. In turn, this results in the inhibition of general translation, which allows the cell to save resources while reconfiguring gene expression to adapt to the new conditions (Wek *et al*, 2006). There are four known eIF2α kinases, each preferentially responding to a different type of stress: RNA-dependent protein kinase-like endoplasmic reticulum kinase (PERK) is activated by endoplasmic reticulum (ER) stress, which is determined by the saturation of the protein folding capacity of the ER; protein kinase RNA-activated (PKR) responds to double-stranded RNA and is involved in the antiviral response; general control nonrepressed 2 (GCN2) is activated by uncharged tRNAs, which accumulate in the cell when the availability of amino acids is reduced, and finally, heme-regulated eIF2α kinase (HRI), which is predominantly expressed in erythroid cells and responds to decreased availability of heme, as well as oxidative stress and heat-shock (Dever, 2002).

In unstressed cells, dephosphorylated GTP-bound eIF2α binds to the initiator Met-$tRNA_i^{Met}$ and transfers it to the 40S ribosomal subunit, forming the 43S pre-initiation complex. This complex binds the 5' end of the capped mRNA chain and scans it in the 5'-3' direction until it recognises the start codon. This induces eIF2α to hydrolyse its GTP-bound molecule and dissociate from the pre-initiation complex, thus allowing the 60S ribosomal subunit to join the complex and form the 80S initiation complex (Dever, 2002). Phosphorylation of serine 51 of eIF2α by one of the four stress-responsive kinases prevents the exchange of its GDP-bound molecule with GTP, thus inhibiting the formation of the pre-initiation complex and suppressing general translation (Dever, 2002). By contrast, under these circumstances the efficiency of ATF4 mRNA translation is greatly enhanced, thus inducing a rapid increase of its protein levels. The preferential translation of ATF4 mRNA under stress conditions is due to the particular sequence of it 5' untranslated region (UTR), which includes two short upstream open reading frames (uORF). The 5' proximal and positive-acting uORF1 consists of a strong start codon surrounded by a Kozak sequence and followed by only two additional codons. Located 3' to uORF1 is the

inhibitory uORF2, which possesses a weaker start codon and overlaps with the first 83 nucleotides of the ATF4 ORF, but produces a polypeptide of only 59 amino acids. Under non-stressed conditions, the scanning ribosome initiates translation at uORF1, and retains the ability to rapidly re-initiate at the inhibitory uORF2, thus preventing translation of the ATF4 ORF. Under stressed conditions, the lack of eIF2α-GTP means that the time necessary for the 40S ribosomal subunit to acquire the Met-$tRNA_i^{Met}$ is increased, allowing it to scan through uORF2 and initiate translation at the ATF4 start codon (Harding *et al*, 2000; Lu *et al*, 2004; Vattem & Wek, 2004).

1.3.4.3 *Regulation of ATF4 protein stability*

Besides being subjected to translational inhibition, ATF4 protein is also selectively targeted to the proteasome for degradation under normal conditions. As a result, ATF4 is a very unstable protein, with a half-life of only 30 minutes (Lassot *et al*, 2001). The proteasomal degradation of ATF4 is dependent on its interaction with a specific subtype of Skp1/cullin/F-box protein (SCF) E3 ubiquitin ligase complex in which the F-box protein is beta-transducin repeat-containing protein (βTrCP) (Lassot *et al*, 2001). The function of βTrCP is to recognise the target protein (in this case ATF4) and anchor it to the SCF complex. SCF-bound ATF4 is then recognised by the E2 ubiquitin conjugating enzyme, which mediates its polyubiquitination. Deletion and single amino acid mutation analyses established that the degron motif 218-DSGICMS-224 on ATF4 mediates βTrCP binding, and that this requires phosphorylation of serine 219 located within thin motif (Lassot *et al*, 2001; Pons *et al*, 2007) (Figure 1.5). A recent study demonstrated that ATF4 interaction with βTrCP, and hence its stability, is additionally modulated by a gradient of phosphorylation at five other sites (T212, S223, S230, S234 and S247) located outside the originally identified degron (Frank *et al*, 2010). The degree of serine 219 phosphorylation and βTrCP binding depends on which and how many of these additional sites are phosphorylated, allowing for fine-tuning of ATF4 protein stability (Frank *et al*, 2010). The identity of the serine 219 kinase(s) is still under investigation. Frank and colleagues showed that exogenous ATF4 is stabilised by the inhibition of casein kinase 1 (CK1), and that this coincides with reduced S219 phosphorylation and ubiquitination (Frank *et al*, 2010). On the other hand, Wang and

colleagues demonstrated that ribosomal protein L41 (RPL41) is a strong activator of ATF4 proteasomal degradation, and that mutation of ATF4 S219 confers resistance to RPL41-induced degradation, but the effect of RPL41 is not blocked by CK1 inhibition, suggesting that alternative and yet unidentified kinases may be recruited on ATF4 through the action of RPL41 (Wang *et al*, 2011). Unlike RPL41, binding of the acetyltransferase P300 to the N-terminus of ATF4, at amino acids (1-85), protects it from proteasomal degradation and favours its accumulation in the cell (Lassot *et al*, 2005). P300 acetylates ATF4 in its bZIP domain, but this modification is not responsible for the P300-dependent stabilisation of ATF4, and might be instead involved in the regulation of its transcriptional activity (Lassot *et al*, 2005).

A specific mechanism of ATF4 protein control in response to hypoxia has been described to involve binding of the hypoxia-induced oxygen sensor PHD3 to its ODDD (Koditz *et al*, 2007). PHD3 binding to the ODDD on ATF4 promotes its degradation via the proteasome under normoxic conditions (Koditz *et al*, 2007). During hypoxia, both proteins are upregulated, and PHD3 binding accelerates the degradation of ATF4 once the oxygen levels have normalised (Koditz *et al*, 2007). This mechanism assures that ATF4 induction by hypoxia is transient and rapidly counteracted as soon as the stressful stimulus is removed.

1.3.4.4 *Regulation of ATF4 by protein-protein interactions*

Several proteins are able to bind ATF4 and regulate its transcriptional activity without interfering with the protein stability, thus providing an additional level of control. Among these, DISC1 was shown to strengthen the ATF4-mediated inhibition of the CRE at elevated intracellular cAMP levels (Sawamura *et al*, 2008). By contrast, dimerisation of ATF4 with the bZIP transcription factor Zhangfei markedly enhances its transactivation potential on CRE/ATF4-containing promoters in response to activation of the mitogen-activated protein kinase (MAPK) pathway (Hogan *et al*, 2006). Other examples of binding partners that potentiate ATF4 transcriptional transactivation include the nuclear matrix protein SATB2, whose activating effect on ATF4 promotes normal skeletal development (Dobreva *et al*, 2006) and the CREB-binding protein CBP, a transcriptional co-activator implicated in memory formation (Gachon *et al*, 2002; Liang & Hai, 1997; Yukawa *et al*, 1999).

Several interacting proteins that inhibit the transcriptional activity of ATF4 have also been described, including the anti-apoptotic factor NIPK, which is also known as tribbles homolog 3 (TRB3) (Jousse *et al*, 2007; Ohoka *et al*, 2005; Ord *et al*, 2007; Ord & Ord, 2003), the pro-apoptotic transcription factor CHOP (Gachon *et al*, 2001), and the nuclear matrix protein mitosin/CENP-F, which is involved in the regulation of cell proliferation (Zhou *et al*, 2005).

1.3.5 *ATF4 as a memory suppressor gene*

While short-term memory only requires covalent modifications of pre-existing proteins, the establishment of long-term memory, an essential component of cognition, is dependent on new protein synthesis (Kandel, 2001). At the cellular level, the process of memory consolidation is modelled by a stable increase in synaptic strength termed long-term potentiation (LTP) in vertebrates and long-term facilitation (LTF) in invertebrates, which is coupled to the establishment of new synaptic connections (Kandel, 2001). In both invertebrates and vertebrates, the transition from short- to long-term memory requires the activation of the Ca^{+2} and cAMP-responsive transcription factor CREB via phosphorylation, which in turn drives the expression of several target genes necessary for the establishment of LTP by binding to the CRE in their promoter (Kandel, 2001). Early experiments carried out in the sea snail *Aplysia* and in cultured mammalian cells revealed that ATF4 and its *Aplysia* paralog ApCREB2 inhibit the transcriptional activity of CREB (or its *Aplysia* paralog ApCREB1) on the CRE, and that the selective inhibition of ApCREB2 in neurons lowers the number of serotonin pulses required for the establishment of LTF and the growth of new synaptic connections (Bartsch *et al*, 1995; Karpinski *et al*, 1992; Lee *et al*, 2003). This led to the suggestion that ApCREB2 inhibits LTF though its repressive effect on CREB-dependent transcription, implying that LTF requires both the activation of ApCREB1 and the release of ApCREB2-mediated inhibition (Bartsch *et al*, 1995).

A later study provided evidence for a similar role of ATF4 in mammalian neurons (Chen *et al*, 2003). Following on from previous work that suggested a role of C/EBP transcription factors in LTP and memory storage (Alberini *et al*, 1994; Sterneck *et al*, 1998; Taubenfeld *et al*, 2001a; Taubenfeld *et al*, 2001b; Yukawa *et al*, 1998), Chen

and colleagues expressed a broad dominant-negative inhibitor of C/EBPs (termed AZIP) in the mouse forebrain to elucidate the function of these proteins in synaptic plasticity (Chen *et al*, 2003). AZIP was shown to preferentially interact with and inhibit several repressive isoforms of C/EBP as well as ATF4, and to result in the specific downregulation of ATF4 protein, but not mRNA levels. Importantly, AZIP transgenic mice had enhanced hippocampal-based spatial memory and LTP, and this was due to enhanced cAMP/PKA dependent transcription and translation (Chen *et al*, 2003). These findings are in line with those of previous studies conducted in the invertebrate *Aplysia* (Bartsch *et al*, 1995), and strongly suggest that the repressive role of ATF4 in long-term memory formation is conserved in mammals.

Two further studies collectively provided compelling evidence for the translational control of ATF4 acting as a key molecular switch that regulates the transition from short- to long-term memory (Costa-Mattioli *et al*, 2007; Costa-Mattioli & Sonenberg, 2006). The first study focused on the electrophysiological and behavioural characterisation of mice with a homozygous deletion of *GCN2*, encoding one of the four eIF2α kinases. Consistent with the decreased phosphorylation of eIF2α, ATF4 expression was reduced in the hippocampus of *GCN2* KO animals, and this was paralleled by increased CREB activity. In *GCN2* KO hippocampal slices, a short electrical stimulation was sufficient to elicit LTP, whereas sustained electrical stimulation or treatment with the cAMP-enhancing drug forskolin, which activates CREB, induced LTP in wild-type but not in *GCN2* KO slices. The anomalous response of *GCN2* KO neurons to LTP-inducing stimuli was reflected in the performance of the animals in the Morris water maze test, which is used to assess spatial memory. In this test, *GCN2* KO mice performed better than wild-types after short training, but worse after prolonged training. GCN2 was thus suggested to modulate synaptic plasticity via translational control of ATF4 protein levels (Costa-Mattioli & Sonenberg, 2006). A follow-up study from the same laboratory examined mice with a heterozygous S51A mutation in eIF2α, which prevents phosphorylation of the protein by all four eIF2α kinases. As expected, this mutation was found to result in decreased ATF4 protein levels, and this corresponded with a lower threshold for LTP induction, consistent with what previously seen in *GCN2* KO mice. However, eIF2α S51A animals displayed enhanced memory in a battery of tests,

including the Morris water maze, where they needed fewer trials than wild-types to achieve the same degree of learning. Again, this suggested that although the magnitude of long-term memory was unchanged in eIF2α S51A animals, they could achieve it more readily than wild-types. Consistently, the pharmacological inhibition of eIF2α dephosphorylation, which represents a reciprocal model of the eIF2α S51A mutation, inhibited the acquisition of long-term memory in wild-type animals. In addition, it increased the translation of ATF4 and blocked the induction of LTP in wild-type hippocampal slices, but strikingly it did not affect LTP induction in *ATF4* KO hippocampal slices (Costa-Mattioli *et al*, 2007). This strongly suggests that the blockage of LTP induction by eIF2α dephosphorylation inhibitors is specifically mediated by increased ATF4 translation and provides further confirmation of the role of ATF4 as a memory suppressor.

In light of its prominent regulatory role in learning and memory, it is tempting to speculate that ATF4 may be directly involved in the biological alterations underlying the cognitive and behavioural abnormalities that characterise schizophrenia. A recent study by Trinh and colleagues provided intriguing preliminary evidence supporting this hypothesis (Trinh *et al*, 2012). In mice, forebrain-specific KO of the eIF2α kinase PERK determines decresed levels of eIF2α phosphorylation and reduced ATF4 expression in the prefrontal cortex (PFC) (Trinh *et al*, 2012). These changes are associated with reduced prepulse inhibition, reduced behavioural flexibility, increased behavioural perseveration and reduced fear extincton, which are consistent with the alterations commonly observed in schizophrenia (Trinh *et al*, 2012). Chronic treatment with SSR504734, a glycine transporter inhibitor that is known to improve behavioural flexibility by enhancing the function of the N-Methyl D-Aspartate Receptor (NMDAR), rescues the cognitive impairment in PERK KO mice, and normalises the expression of phosphorylated eIF2α and ATF4 in the PFC (Trinh *et al*, 2012). Additionally, and in agreement with the cognitive and behavioural effects of PERK KO in mice, expression levels of PERK and ATF4 are reduced in the PFC of post-mortem brains from schizophrenia patients, suggesting that these alterations may contribute to the pathophysiology of schizophrenia (Trinh *et al*, 2012).

1.3.6 *ATF4 as a mediator of the cellular stress response*

While the induction of ATF4 in response to a variety of stressors has been consistently reported in numerous studies based on both *in vitro* and *in vivo* models, the observed effects of ATF4 activation are more variable, and seem to be dependent on the cell type and the particular experimental conditions. Perhaps this is not surprising, given the extensive variety of regulatory mechanisms that converge on ATF4, some of which are likely to be cell type- and/or stressor-specific. For example, as mentioned earlier, the elevated and protracted expression of ATF4 in cancer cells is thought to contribute to their survival and resistance to anti-cancer drugs through the induction of genes that confer protection from hypoxia, oxidative stress and apoptosis while promoting autophagy (Rzymski *et al*, 2009). On the other hand, most but not all studies based in neurons established a clear connection between ATF4 induction after stress exposure and increased apoptosis. Here, I will provide an overview of the studies that investigated the function of ATF4 in neurons or in pathways relevant for neuronal biology.

ER stress and impairment of ER function has been implicated in the pathogenesis of many neurological and neurodegenerative diseases, including stroke and Alzheimer's, Parkinson's and Huntington's diseases (Yang & Paschen, 2009). Activation of PERK and increased phosphorylation of eIF2α have been observed in stroke, Alzheimer's, Parkinson's and amyotrophic lateral sclerosis (Yang & Paschen, 2009). Given that ATF4 is a direct mediator of the ER stress response, several studies have investigated the effect of ATF4 induction in animal and cell models of the above neurological disorders. In a recent study, Kim and colleagues mimicked the characteristic pathological alterations of Alzheimer's disease by treating cultured neurons with the protein phosphatase-2A (PP2A) inhibitor okadaic acid (OA), which induces tau phosphorylation and deposition of amyloid-β (Aβ), resulting in cell death (Kim *et al*, 2010). In neurons treated with OA, phosphorylation of eIF2α was increased, and this resulted in ATF4 accumulation in neurites first and its migration to the nucleus later, suggesting that activation of ATF4-mediated transcription may contribute to neuronal loss in Alzheimer's (Kim *et al*, 2010).

Besides ER stress, defective autophagy has also been suggested to play a role in the pathogenesis of Alzheimer's and other neurodegenerative diseases, but the mediating mechanisms are still unclear (Hara *et al*, 2006; Komatsu *et al*, 2006; Pickford *et al*, 2008; Tsuzuki *et al*, 1994). Intriguingly, ATF4 has been reported to directly upregulate the expression of presenilin-1 (PS1) (a component of the γ-secretase enzyme responsible for the generation of Aβ) in response to reduced autophagic activity, amino acid depletion, and ER stress (Mitsuda *et al*, 2007; Ohta *et al*, 2011; Ohta *et al*, 2010). Accordingly, the ATF4-dependent upregulation of PS1 expression results in increased γ-secretase activity and secretion of Aβ, thus suggesting that the increased expression of ATF4 in Alzheimer's may actively contribute to the progression of the disease (Mitsuda *et al*, 2007; Ohta *et al*, 2011; Ohta *et al*, 2010).

While investigating the mechanisms of ER stress-induced cell death, Galehdar and colleagues found that ATF4 overexpression increases the sensitivity of neurons to ER stress-induced apoptosis, while ATF4 suppression has the opposite effect (Galehdar *et al*, 2010). They went on to show that ER stress-induced neuronal apoptosis is mediated by the activation of p53-upregulated modulator of apoptosis (Puma), but this activation occurs independently of p53 expression. On the other hand, ATF4 was found to be necessary for the induction of Puma in response to ER stress, although it did not do so directly, but through the intermediate action of its target gene CHOP, a pro-apoptotic transcription factor (Galehdar *et al*, 2010). Prolonged, but not short-term ATF4 overexpression was also reported to induce apoptosis in the absence of stressful stimuli in postmitotic neuronally differentiated PC12 cells, an effect that was blocked by co-expression of the ATF4 inhibitor NIPK (TRIB3) (Ord *et al*, 2007). This latter experiment highlights the relevance of timing in ATF4-dependent cellular events. As discussed earlier, transient ATF4 induction is necessary to promote adaptation to stress, but prolonged stress and/or persistently elevated levels of ATF4 activate the expression of pro-apoptotic genes (Rutkowski *et al*, 2006).

Other studies investigated the role of ATF4 in the cellular response to hypoxia and/or oxidative stress, two paradigms commonly used to model cerebral ischemia and stroke. The response of ATF4 to oxidative stress is also of particular interest in

relation to neurodegeneration, because oxidative stress has been implicated in the initiation or propagation of neuronal damage in several neurodegenerative diseases (Beal, 2000; Lin & Beal, 2006). Cultured cortical neurons from *ATF4* KO mice displayed increased resistance to oxidative stress compared to wild-type neurons (Lange *et al*, 2008). This effect was not caused by long-term compensatory mechanisms established in consequence of chronic ATF4 depletion, because expression of a dominant-negative mutant version of ATF4 in wild-type neurons also conferred resistance to oxidative stress. Consistently, ATF4 overexpression restored sensitivity to oxidative stress in *ATF4* KO neurons and conferred increased sensitivity to oxidative stress in wild-type neurons. In addition, and consistent with previous findings in PC12 cells (Ord *et al*, 2007), ATF4 overexpression in wild-type neurons was able to induce apoptosis on its own (Lange *et al*, 2008). Transcriptional profiling of *ATF4* KO and wild-type neurons that had been exposed or not to oxidative stress revealed that ATF4 is normally induced by oxidative stress, and that in turn it is responsible for the expression of a large number of oxidative stress-responsive genes, including those involved in glutathione metabolism (Lange *et al*, 2008). However, two independent studies reported a negative effect of ATF4 on the intracellular concentration of glutathione in neurons (Lange *et al*, 2008; Ord *et al*, 2007). Importantly, the pro-death effect of ATF4 under conditions of oxidative stress was not limited to cultured neurons, but could also be detected in vivo, as *ATF4* KO animals were found to be more resistant to neuronal loss after cerebral ischemia (Lange *et al*, 2008). A separate study used cultured mouse neurons to study the temporal patterning of gene expression after exposure to hypoxia. As expected, hypoxia determined increased eIF2α phosphorylation and ATF4 expression. The number of neurons expressing high levels of ATF4 gradually increased with prolonged exposure to hypoxia, and in the majority of neurons ATF4 expression overlapped with markers of apoptosis (Halterman *et al*, 2010). Consistent with this, induction of ATF4 was determined to coincide with the switch from adaptive to pro-apoptotic signalling in response to hypoxia (Halterman *et al*, 2008).

In contrast with the above studies, which generally observed a positive correlation between ATF4 expression and susceptibility to oxidative stress or hypoxia, ATF4 depletion in mouse embryonic fibroblasts resulted in increased cell death from

several stressors, including oxidative stress (Harding *et al*, 2003). Accordingly, elevated ATF4 expression determined the upregulation of the cysteine/glutamate antiporter system X_c^- , which is essential for the maintenance of normal glutathione levels in the cell, and resulted in increased resistance to oxidative stress, an effect that could be observed in different cell lines as well as in immature primary cortical neurons (Lewerenz & Maher, 2009; Lewerenz *et al*, 2012). Moreover, this study reported activation of eIF2α/ATF4 signalling in the brains of Alzheimer's patients (Lewerenz & Maher, 2009). The latter, which had been previously observed and interpreted as a sign of neurodegeneration (Chang *et al*, 2002; Kim *et al*, 2007; Page *et al*, 2006; Unterberger *et al*, 2006), was instead proposed to be an adaptive pro-survival response in the light of the above findings (Lewerenz & Maher, 2009; Lewerenz *et al*, 2012).

The reasons for the discrepancy between the studies that described ATF4 as a pro-death or pro-survival factor in response to oxidative stress are not clear, but may be related to the proliferative and/or maturation status of the tested cell model. Indeed, ATF4 expression appears to be detrimental in postmitotic and differentiated cells (Halterman *et al*, 2008; Halterman *et al*, 2010; Lange *et al*, 2008; Ord *et al*, 2007), but protective in proliferating cell lines and immature neurons (Harding *et al*, 2003; Lange *et al*, 2008; Lewerenz & Maher, 2009; Lewerenz *et al*, 2012). Given that oscillating ATF4 expression in proliferating non-stressed cells is involved in the regulation of cell cycle progression and neurogenesis (Frank *et al*, 2010), it is likely that additional control mechanisms are in place in these cells to prevent the activation of apoptotic genes when ATF4 protein levels peak. Further studies are needed to clarify the multiple implications of changes in ATF4 expression levels in stressed and non-stressed cells.

1.4 Aims of this PhD

A wealth of genetic and biological evidence has firmly established DISC1 as one of the most promising tools to dissect the molecular pathogenesis of psychiatric illness and identify new therapeutic targets. It is now clear that DISC1 is involved in the regulation of many pathways and cellular processes that are key to the correct

development and functioning of the brain. The next task will then be to understand if and how the deregulation of each of these DISC1-modulated pathways and processes can lead to psychiatric illness. This refinement process can be greatly aided by the study of the structural and functional impact of DISC1 mutations or variants that are known to increase the risk of mental illness. Besides the original t(1;11) translocation, whose impact on the nature and relative abundance of DISC1 protein isoforms is still uncertain, several *DISC1* missense variants have been associated with increased risk of psychiatric illness and altered brain structure or cognition in healthy subjects, but the underlying mechanisms are still largely unknown.

Thus, the first aim of this PhD is to investigate the potential effect of a selected subset of these variants on the subcellular distribution of DISC1, the disruption of which is likely to impact on its molecular interactions and ultimately interfere with its normal function. In particular, I will focus on two subcellular compartments in which DISC1 normally resides: the nucleus and the centrosome. Many of the neurodevelopmental functions of DISC1 depend on its ability to establish interactions with key centrosomal partners, and any mutation that prevents its correct targeting to the centrosome is likely to have negative consequences for brain development. On the other hand, nuclear DISC1 has been involved in the regulation of sleep homeostasis and CRE-dependent transcription, and the nuclear distribution of DISC1 is altered in schizophrenic brains, suggesting that mutations that disturb the targeting and/or function of nuclear DISC1 may contribute to psychopathogenesis.

The interaction of DISC1 with the transcription factor ATF4 has been reported by several groups but has scarcely been investigated, yet it is of potential relevance for our understanding of mental illness, since ATF4 is a key regulator of cognition, which is severely impaired in schizophrenia, and a master controller of stress responses to environmental insults that increase the risk of schizophrenia.

Thus, the second aim of this PhD is to better characterise the functional implications of the DISC1-ATF4 interaction at the molecular level, with a particular focus on the role of DISC1 as a regulator of ATF4-mediated transcription and on the functional implications of this interaction with respect to molecular and cellular phenotypes

related to stress. The potential impact of risk-conferring DISC1 amino acid substitutions on its ability to bind to and regulate ATF4 will also be investigated.

2 Materials and Methods

2.1 Bioinformatics

2.1.1 *DNA sequence analysis*

All the reporter plasmids and expression plasmids used in this study were validated by direct sequencing. Plasmid DNA sequences were obtained using the method described in 2.6.4 and aligned to the reference sequences using the Standard Nucleotide BLAST algorithm: http://blast.ncbi.nlm.nih.gov/Blast.cgi?PROGRAM=blastn&BLAST_PROGRAMS=megaBlast&PAGE_TYPE=BlastSearch&DATABASE=wgs

2.2 Reagents

The chemical reagents used in this thesis, along with the name of their supplier and, where appropriate, the vehicle in which they were dissolved, are listed below.

10x TGS (BioRad), diluted with dH_2O

30% Acrylamide/Bis solution (BioRad)

Acetic acid (Fischer)

Agar (BD Bioscience)

Agarose (Invitrogen), made up in TAE buffer

Ammonium persulphate (Sigma), made up in dH_2O

Ampicillin (Sigma), made up in dH2O

ATP solution, PCR grade (Sigma)

Boric acid (Sigma)

Bromophenol blue (Sigma)

BSA (Sigma), made up in PBS

CHAPS (Sigma)

DABCO (Sigma)

DAPI (Sigma), made up in mowiol mounting solution

DMSO (Sigma)

D-PBS (Invitrogen)

DTT (Sigma), made up in dH_2O

EDTA (Sigma), made up in dH_2O

Ethanol (Fischer), diluted with dH_2O where appropriate

Forskolin (Sigma), made up in DMSO

Glycerol (Promega)

Glycine (Sigma)

Glycogen (Sigma)

GTP solution, PCR grade (Sigma)

H_2O_2 (Sigma)

Hydrochloric acid (Fischer)

IBMX (Sigma), made up in absolute ethanol

Instant milk powder (Marvel), made up in PBS

IPTG (Melford) in dH2O

Isobutanol (Fischer)

Isopropanol (Fischer)

Magnesium chloride solution, PCR grade (Invitrogen)

Methanol (Fischer)

Mowiol (Sigma)

NP-40 (Sigma)

Orange G (Sigma)

Paraformaldehyde (Sigma), made up in PBS

PBS (Sigma), made up in dH_2O often as a 10x solution

PFA (Sigma)

Phenol/chlorophorm/isoamyl alcohol (Invitrogen)

Phosphatase inhibitor cocktail II (Calbiochem)

Poly-D-lysine (Sigma)

Ponceau S (Sigma)

Protease inhibitor cocktail (Roche)

Rolipram (Sigma)

SDS (Fischer) made up in dH_2O

Sodium acetate (BDH Laboratory Supplies), made up in dH_2O and pH adjusted using hydrochloric acid and/or sodium hydroxide

Sodium chloride (Fischer), made up in dH_2O

Sodium deoxycholate (Fischer), made up in dH_2O

Sodium hydroxide (Fischer), made up in dH_2O

TEMED (Sigma)

Thapsigargin (Sigma)

Tris (Fischer), made up in dH_2O and pH adjusted using hydrochloric acid and/or sodium hydroxide

Tris-HCl (Fischer), made up in dH_2O and pH adjusted using hydrochloric acid and/or sodium hydroxide

Triton X-100 (Sigma), made up in dH_2O

Tryptone (BD Biosciences)

TWEEN-20 (Sigma)

2.3 Solutions and buffers

The recipes of the solutions and buffers used in this thesis are listed below.

1% Triton lysis buffer

0.5 ml Triton X-100

Up to 50 ml with PBS

1 tablet Complete Protease Inhibitor Cocktail (Roche)

Stored at -20°C

2x (0.3M) Borate buffer

9.2745 g Boric acid

Up to 500 ml with dH_2O

Adjust pH to 8.5 with 1M Sodium Hydroxide.

4% PFA

Used to fix cultured mammalian cells.

2 g PFA

Up to 50 ml with PBS

Heat to 50 °C

Add 1M Sodium Hydroxide dropwise and mix until PFA is completely dissolved.

Dissection buffer

Used to dissect foetal mouse brains for primary neuron production. All the reagents are from Invitrogen.

500 ml HBSS with $CaCl_2$ and $MgCl_2$

5 ml 200 mM L-Glutamate

3.5 ml 1M HEPES (cell culture standard, pH 7.3-7.5)

DNA loading buffer (6x)

Used to load DNA on agarose gels

4.5 ml glycerol

1.875 ml 2% Xylene Cyanol FF

1.875 ml 2% Orange G

dNTP

An equal mix of PCR-grade ATP, CTP, GTP and TTP diluted appropriately in dH_2O. Stored at -20°C.

Freezing medium

Used to freeze mammalian cells for long-term storage in liquid N_2.

5 ml DMSO

45 ml FBS (Invitrogen)

Stored in 15 ml aliquots at -20°C.

L Agar/ampicillin

50 g Tryptone

25 g Yeast Extract

50 g Sodium chloride

Up to 5 litres with dH_2O

Adjust pH to 7.2. Pour into a bottle and add 1.5 g Agar per 100 ml medium. Stored at 4°C. Before use, melt in a microwave and then stand at room temperature until cool enough to touch with gloved hands and add ampicillin to a final concentration of 100 ng/ml. Used immediately.

L Broth/ampicillin

50 g Tryptone

25 g Yeast Extract

25 g Sodium chloride

Up to 5 litres with dH_2O

Adjust pH to 7.2. Solution stored at 4°C. Before use add ampicillin to a final concentration of 50 ng/ml.

Membrane blocking buffer

Used for pre-stain blocking of PDVF membranes.

2.5 g Instant milk powder

5 ml 10x PBS

100 µl TWEEN-20

Up to 50 ml dH_2O

Solution was made up immediately before use.

Membrane probing buffer

Used to incubate PDVF membrane with antibodies.

0.5 g Instant milk powder

5 ml 10x PBS

100 µl Tween-20

Up to 50 ml dH_2O

Membrane washing buffer

Used to wash PDVF membranes after incubation with antibodies.

100 ml 10x PBS

20 ml TWEEN-20

Up to 1 litre with dH_2O

Stored at room temperature.

Mowiol mounting solution

7.5 g Mowiol

10 ml Glycerol

25 ml dH_2O

Solution was then incubated overnight at room temperature

50 ml 0.2 M Tris-HCl (pH 8.5)

Solution was then heated at 100°C for 20 minutes and allowed to cool

1.75 g DABCO

Solution was stored at -20°C, with working aliquots stored at 4°C.

Poly-D-lysine solution

Used for coating coverslips prior to cell seeding.

25 ml 2x Borate buffer

2.5 ml 500 μg/ml Poly-D-Lysine

Up to 50 ml with dH_2O.

Ponceau S stain

1 g Ponceau S

4 ml Acetic acid

Up to 200 ml dH_2O

Solution was stored at room temperature and was recovered after each stain for reuse.

Protein sample buffer

1 ml 1M Tris pH 6.8

2 ml Glycerol

2 ml 20% SDS

2 ml 1M DTT

2 ml dH_2O

1ml 0.1% Bromophenol blue

Solution was stored at -20°C.

RIPA buffer

2.5 ml 1M Tris-HCl pH 7.5

1.5 ml 5M Sodium chloride

0.5 ml NP-40

2.5 ml 10% Sodium deoxycholate

250 μl 20% SDS

Up to 50ml dH_2O

1 tablet Protease inhibitor cocktail

Buffer was stored at -20°C

TAE buffer

24.2 g Tris

5.71 ml Acetic acid

10 ml 0.5 M EDTA

Make up to 5 litres with dH_2O

Buffer was stored at room temperature.

TE buffer

10 ml 1M Tris-HCl pH 7.5

2 ml 500mM EDTA

Make up to 1 litre with dH_2O

The pH of the buffer was adjusted using hydrochloric acid and/or sodium hydroxide.

Buffer was stored at room temperature.

Transfer buffer

Used to transfer protein from acrylamide gels to PDVF membranes with the BioRad system.

2.9 g Glycine

5.8 g Tris base

0.37 g SDS

200 ml methanol

Up to 1 litre with dH_2O

Trypsinisation buffer

Used to dissociate brain tissue for primary neuron preparation.

20 ml TrypLE Express (Invitrogen)

30 ml dissection buffer

2.4 Cell culture

2.4.1 *Maintenance of cell lines*

The cell lines used in this thesis, along with their source, are listed in table 2.1. Cells were grown in T25, T75, or T175 CellStar flasks (Greiner Bio-one) and maintained in a Galaxy 170 incubator (Scientific Laboratory Supplies) at 37°C in a humidified atmosphere containing 5% CO_2. Unless otherwise specified, all the buffers and media used for cell culture were from Gibco, Invitrogen. Live cells were manipulated aseptically in an Envair Bio2+ Class II Safety Cabinet under containment level 1. Cells were grown in DMEM (catalogue number 41965) supplemented with 10% FBS (DMEM/FBS) until they had reached the desired confluence. To harvest the cells, the culture medium was replaced with the minimum volume of Tryple Express that completely and evenly covered the cells. After incubation at 37°C for 2-5 minutes, the flask was gently tapped or rocked to aid detachment of the cells from the plastic surface, then 5 volumes of DMEM/FBS were added and the cell suspension was repeatedly pipetted to insure dissociation of cell clusters. The cell suspension was then transferred to a 50 ml Falcon tube and centrifuged at 1000 RPM in a 5804R centrifuge (Eppendorf) for 5 minutes. After centrifugation, the supernatant was discarded and the cell pellet resuspended in an adequate volume of DMEM/FBS, which was adjusted depending on the size of the pellet. If necessary for subsequent applications, the cell concentration of the resulting cell suspension was determined as described in 2.4.2. If the cells were to be maintained for future use, they were passaged by diluting the cell suspension 1:2 or more in a new flask containing fresh DMEM/FBS, then transferred back to the incubator.

Cell line	Source
COS7	ECACC
HEK293	Mark Bradley, Bradley research group, University of Edinburgh
HeLa	ECACC
MO3.13	Novartis Institute for Biomedical Research, Basel

NSC-34	Cathy Abbott, Abbott research group, University of Edinburgh
SH-SY5Y	Organon and ECACC

Table 2.1 List of cell lines used in this thesis. ECACC is the European Collection of Cell Culture.

2.4.1.1 *Preparation of the cell culture medium used in the amino acid deprivation experiments*

The cell culture media used in the amino acid deprivation experiments described in section 4.5.1 of this thesis ware prepared as follows. 7.4 g of HAM's F12 medium powder (Sigma D9785) were dissolved in deionised H_2O to a final volume of 50 ml to generate a 10X stock medium solution, which was sterilised by filtration through a 0.22 µm filter and stored at 4 °C until further use. In a sterile 50 ml tube, 4 ml of 10X HAM's F12 medium were supplemented with 50 µl each of the following salt solutions, which had been previously sterilised by filtration through a 0.22 µm filter: $MgSO_4$ (Sigma M2643) (48.84 g/l, final concentration 0.04884 g/l); $MgCl_2$ x $6H_2O$ (Sigma M2393) (61.2 g/l, final concentration 0.0612 g/l); $CaCl_2$ x $2H_2O$ (Sigma C2536) (154.5 g/l, final concentration 0.1545 g/l), plus 640 µl of a 7.5% solution of Sodium Bicarbonate (Gibco 25080)(final concentration 0.12%). The medium was then supplemented with the following amino acid solutions: 400 µL of GlutaMAX-1 (200 mM; final concentration 2 mM); 40 µL of L-lysine monochloryde (Sigma L8662) (450 mM; final concentration 450 µM); 40 µl of L-methionine (Sigma M5308) (115.549 mM; final concentration 115,549 µM); 400 µl of L-leucine (Sigma L8912) (45 mM; final concentration 450 µM). To induce amino-acid starvation, the medium was prepared as above, but without adding leucine and lysine. After adding the amino acids, the medium was supplemented with 160 µl of a 250X solution of Phenol red, then 30 ml of deionised H_2O was added, and the pH adjusted to 7.4 using a 0.5M solution of NaOH. Finally, the volume was adjusted to 40 ml by adding deionised H_2O, and the medium was supplemented with 4 ml of dialised foetal bovine serum (Sigma F0392) before being passed through a 0.22 µm filter.

2.4.2 *Cell counting*

If the cells were to be plated for subsequent applications, they were harvested as described in 2.4.1, then the concentration of the cell suspension was measured using an Improved Neubauer haemocytometer. First, the haemocytometer and coverslip were washed in tap water, rinsed with 70% ethanol and wiped dry with a paper tissue, then the coverslip was humidified and applied to the haemocytometer. The cell suspension was mixed gently using a thin bore plastic Pastette, and a small amount of cell suspension was loaded on one of the two chambers of the haemocytometer. The same process was repeated to fill the second chamber of the haemocytometer. The cells were counted in a 0.1 mm^3 area in each chamber, then the average cell count was calculated from readings made in the two chambers and multiplied by 10^4 to obtain the cell concentration in the original cell suspension, expressed in cells/ml.

2.4.3 *Cell plating*

If the cells were to be transfected and/or subjected to drug treatments, they were seeded in sterile cell dishes (Iwaki) or multi-well plates (Corning) of different sizes, depending on the particular downstream application. The cells were first harvested and counted as described in 2.4.1 and 2.4.2, respectively. For plating in 6, 12, 24 or 96 well plates, cells were first diluted to the desired final concentration and then equal volumes of cell suspension were dispensed in each well. For plating in 6 or 10 cm dishes, a fixed volume of cell suspension corresponding to the desired cell number was dispensed in each dish, and, if necessary, the total volume of medium was adjusted by adding DMEM/FBS. If the cells were to be analysed by immunocytochemistry (see 2.5.7) they were plated on dry heat sterilised glass coverslips in 12 well plates. In the case of primary neurons, the coverslips were treated with ethanol before sterilisation (see 2.4.5). Cells were plated ~16 hours before transfection/treatment, and the cell density was adjusted so that would reach at least 70-80% confluence at the time of transfection/treatment.

2.4.4 *Freezing and recovery of cell lines*

To generate stocks for long-term storage in liquid N_2, the cells were grown in T75 flasks until they had reached 70-80% confluence, then they were harvested as described in 2.4.1. The cell pellet obtained from each T75 flask was resuspended in 3 ml of freezing medium (see section 2.3), then 1 ml aliquots were dispensed in individual cryovials (Nunc) that had been previously labelled with cell line name and passage number and the date. The cryovials were then placed in a "Mr. Frosty" (Nalgene) pre-filled with isopropanol at room temperature and transferred to -70°C for at least 16 hours. This procedure guarantees a steady cooling rate of -1°C/minute, allowing successful cryopreservation and efficient recovery. Once frozen, the cells were rapidly transferred from the "Mr. Frosty" to storage boxes in a liquid N_2 tank. To recover cryopreserved cells, the desired cryovials were rapidly transferred from liquid N_2 to dry ice and transported to the laboratory. The vials were sprayed with 70% ethanol and transferred to a safety cabinet, where the lid was slightly unscrewed to release any residues of N_2 that could have remained trapped inside the tube, so to prevent explosion of the vial during the subsequent heating stage. Next, the vial was held upright in a 37°C water bath until only one small ice crystal was left in the cell suspension, using particular care to insure that the water level was constantly below the lid, so to avoid contamination by microorganisms. Once thawed, the cells were transferred to a T25 flask pre-filled with DMEM/FBS and grown to confluence, then harvested as described in 2.4.1. After harvesting, the cell pellett was resuspended in fresh DMEM/FBS, the entire cell suspension was transferred to a T75 flask and the cells were allowed to grow to confluence, then passaged as described in 2.4.1.

2.4.5 *Establishment and maintenance of cultures of primary neurons*

Primary neurons were seeded on glass coverslips to allow for subsequent analysis by immunocytochemistry. The coverslips were incubated overnight (O/N) in methanol at 4°C with end-over-end agitation, washed twice with fresh methanol to remove any debris and dry heat sterilised. To allow neurons to adhere, the coverslips were coated with Poly-D-Lysine as described below. One day before use, individual sterile coverslips were placed in the wells of 12 well tissue culture plates, covered with 500

μl of Poly-D-Lysine solution, and incubated O/N at 37°C. Immediately before use, the coverslips were washed 4 times with sterile distilled water (Gibco, Invitrogen).

All the buffers, media and supplements used for the establishment and culture of primary neurons were from Gibco, Invitrogen. Eighteen days post fertilisation (DPF), pregnant CD1 mice were sacrificed by a schedule 1 procedure performed by experienced animal facility technicians, then handed to me for dissection. Embryonic day 18 (E18) foetuses were extracted from the mother's uterus and immediately placed in tissue culture grade ice-cold PBS. Using sterile surgical tools, the brains were removed from the embryos, transferred to ice-cold dissection buffer and dissected under a Leica MZ6 microscope with a Fiber-Lite MI-150 high intensity illuminator. After removal of the meninges, the cortices and hippocampi were isolated and stored separately in ice-cold dissection buffer until all the brains had been dissected, then they were finely triturated with a sterile scalpel and processed as described below.

2.4.5.1 *Hippocampal neurons*

The triturated hippocampal tissue obtained from an individual litter (10-13 foetuses) was placed in a 15 ml Falcon tube with 10 ml of tripsinisation buffer and incubated at 37°C for 45 minutes, manually inverting the tube every 15 minutes. After tripsinisation, the tissue was centrifuged for 5 minutes at 1500 revolutions per minute (RPM) in a MSE Mistral 1000 centrifuge and the supernatant carefully removed with a thin bore pastette. The pellet was then resuspended in 10 ml DMEM/FBS by repeatedly pipetting with a wide bore pastette, and centrifuged as before. The pellet was thoroughly resuspended in 5 ml DMEM/FBS using a P1000 Gilson pipette set at 1 ml, then 5 ml DMEM/FBS were added, and the sample was centrifuged as above. The pellet was resuspended in 2 ml DMEM/FBS as before, then 8 ml DMEM/FBS were added.

2.4.5.2 *Cortical neurons*

The triturated cortical tissue obtained from an individual litter was placed in a 50 ml Falcon tube with 15 ml of tripsinisation buffer and incubated as described in 2.4.5.1,

then passed through a wide bore Pastette 10-15 times. The resulting suspension was centrifuged as described in 2.4.5.1, resuspended in 20 ml DMEM/FBS and passed through a wide bore pastette 10-15 times. After a second centrifugation, the pellet was resuspended in 10 ml DMEM/FBS by 20 passages through a wide bore Pastette followed by 10 passages through a thin bore Pastette, then centrifuged again and resuspended in 20 ml DMEM/FBS.

The resulting cell suspention of hippocampal or cortical neurons was passed through a 40 μm cell strainer, collected in a 50 ml Falcon tube and counted as described in 2.4.2, then centrifuged as before. The cell pellet was resuspended in Neurobasal medium supplemented with 200 mM GlutaMAX-1, 100 μg/ml of penicillin and streptomycin and 20% (vol/vol) of B-27 supplement, and plated in 12 well plates at a final concentration of $2x10^5$ cells/well and in a total volume of 2 ml. Primary neurons were maintained at 37°C in a humidified atmosphere containing 5% CO_2 in a Galaxy 170 incubator.

After 7 days in vitro, and every 7 days thereafter, 1 ml of the culture medium was replaced with fresh medium. Neurons were maintained in vitro for up to 24 days.

2.4.6 *Transfection of cell lines and primary neurons*

Different transfection methods were used to express one or more exogenous proteins, luciferase reporter constructs or small interfering RNAs (siRNAs) in cell lines and primary neurons. The pre-existing protein expression constructs and luciferase reporters used in this study, along with their source, are listed in Table 2.2.

Plasmid name	Encoded protein	Tag	Source
CREB1α	Human CREB1α	none	Richard Killick[1]
p5HuSH-GFP	GFP Turbo	none	Origene
pCDNA3.1(+)	Empty vector	none	Invitrogen
pcDNA3.1-Myc DISC1-WT	Human DISC1	N-terminal Myc	Fumiaki Ogawa[2]
pcDNA3.1-Myc DISC1-37A	Human DISC1	N-terminal Myc	Fumiaki Ogawa[2]
pcDNA3.1-Myc DISC1-37W	Human DISC1	N-terminal Myc	Fumiaki Ogawa[2]
pcDNA3-PDE4D3	PDE4D3	none	Miles Houslay[3] (Bolger *et al*, 1997)
pcDNA4/TO	Empty vector	none	Invitrogen
pcDNA4/TO-Flag DISC1	Human DISC1	N-terminal Flag	Shaun Mackie[2]
pcDNA6/myc-HIS B	Empty vector	C-terminal Myc	Invitrogen
pCG-ATF4	Human ATF4	none	Adrian Harris[4] (Liang & Hai, 1997)
pDEST53-ATF4	Human ATF4	N-terminal GFP	Kirsty Millar and Sheila Christie[2] (Bradshaw *et al*, 2009)
pEE7-PDE4B1	PDE4B1	none	Miles Houslay[3] (Huston *et al*, 1997)
pGL4.23[luc2/minP]	Firefly Luciferae	none	Promega
pGL4.29[luc2P/CRE/Hygro]	Firefly Luciferase	none	Promega, donated by Richard Killick[1]
PKIα-mCherry	PKIα	mCherry	Jin Zhang[5] (Herbst *et al*, 2009)

pRK5-HA Disc1 100P	Mouse Disc1-100P mutant	N-terminal HA	Akira Sawa[5]
pRK5-HA Disc1 31L	Mouse Disc1-31L mutant	N-terminal HA	Shaun Mackie[2]
pRK5-HA Disc1 WT	Mouse Disc1-wild type	N-terminal HA	Shaun Mackie[2]
pRK7	Empty vector	none	Pamela Maher[6] (Lewerenz & Maher, 2009)
pRK7-ATF4	Mouse ATF4	none	Pamela Maher[6] (Lewerenz & Maher, 2009)
SomCRE-Luc	Firefly Luciferase	none	Stratagene, donated by Richard Killick[1]
TK-Renilla	Renilla Luciferase	none	Richard Killick[1]
SV40-Renilla	Renilla Luciferase	none	Richard Killick[1]

Table 2.2 Pre-existing protein expression constructs and luciferase reporters used in this study. [1]King's College, London, UK. [2]University of Edinburgh, UK. [3]University of Glasgow, UK. [4]University of Oxford, UK. [5]Johns Hopkins University, MA. [6]Salk Institute for Biological Studies, La Jolla, CA.

2.4.6.1 *Lipofectamine 2000*

Transfection with the liposome-based reagent Lipofectamine 2000 (Invitrogen) was used to express exogenous proteins and/or luciferase reporter vectors in primary neurons, HEK293, COS7 and MO3.13 cells, and to deliver siRNAs to HEK293 and MO3.13 cells. For transfection of cell lines, on the evening of the day before transfection, cells were plated in dishes or multi-well plates of different sizes as described in 2.4.3, and the cell density was adjusted so that cells would be 70-80% confluent the following morning. For luciferase assays, HEK293 and MO3.13 cells were plated in black-walled 96 well plates (Corning) at a cell density of $6x10^4$ and $2.5x10^4$/well, respectively, in a total volume of 100 μl DMEM/FBS. Cells were transfected the following morning using Lipofectamine:DNA complexes formed in warm OptiMEM (Gibco, Invitrogen), according to the manufacturer's instructions. The cell plating volume, amount of Lipofectamine 2000 and DNA, and volume of transfection mix were adjusted to the dish/plate format as suggested by the manufacturer. Primary neurons were transfected after 21 DIV, and the Lipofectamine:DNA complexes were assembled in 200 μl of warm Neurobasal medium supplemented with GlutaMAX-1, using 4 μl of Lipofectamine 2000 and 3-4 μg of DNA. Not sooner than 1 hour before transfection, the old medium was removed from the wells and replaced with 1 ml of fresh Neurobasal supplemented with GlutaMAX-1. Neurons were transfected for 3-4 hours, then the transfection medium was removed and replaced with the old preconditioned medium.

2.4.6.2 *Fugene HD*

Fugene HD Tranfection Reagent (Roche) was used to express exogenous proteins in SH-SY5Y cells, and to transfect HEK293, NSC-34 and MO3.13 for luciferase reporter assays. Cells were plated on the evening before transfection so that they could reach 90-100% confluence by the following morning, when they were transfected. Fugene HD:DNA complexes were formed in warm OptiMEM following the manufactures's directions. SH-SY5Y cells were transfected in 6 or 10 cm dishes, following the protocol summarised in Table 2.3.

Dish ø (cm)	Cell density (cells/dish)	Volume of plating medium (ml)	Fugene HD (μl)	OptiMEM (μl)	DNA (μg)
6	$1.5x10^5$	5	30	300	7.5
10	$3.5x10^6$	11.6	58	580	11.6

Table 2.3 Summary of SH-SY5Y transfection conditions with Fugene HD

For luciferase reporter assays, HEK293 and MO3.13 cells were plated in black-walled 96 well plates (Corning) at a cell density of $6x10^4$/well and $2.5x10^4$/well, respectively, in a total volume of 100 μl of medium. Fugene HD:DNA complexes were assembled as follows: 4 μl of Fugene HD were mixed with 300 ng of Firefly luciferase reporter vector, 30 ng of Thymidine Kinase (TK) Renilla Luciferase reporter vector, and up to 670 ng of the relevant expression plasmids. If necessary, the total amount of DNA was brought to 1 μg by adding an appropriate empty vector. The total volume of transfection mix was adjusted to 40 μl by varying the volume of OptiMEM. Cells were transfected with 12 μl/well of transfection mix for 48 hours. The day after transfection, 200 μl/well of fresh DMEM/FBS were added to the cells.

2.4.6.3 *Nucleofection*

Nucleofection was used to transfect SH-SY5Y cells for luciferase reporter assays, and was performed with the Amaxa Nucleofector device (Lonza) according to the manufacturer's instructions, which are summarised below. Cells were grown to ~80% confluence in a T75 flask. The medium was removed from the flask, and the cells were washed twice with 3 ml of Tryple Express, leaving ~200 μl of solution in the flask after the second wash, and then incubated at 37°C without tapping or rocking until the cells had completely detached. After adding 4 ml DMEM/FBS, the cell suspension was pipetted several times to break most cell clusters then transferred to a 15 ml Falcon tube, and the cell density was measured as described in 2.4.2. A

volume of cell suspension corresponding to $2x10^6$ cells was transferred to a 1.5 ml tube and centrifuged at 2000 rpm for 10 minutes at RT in a table top microcentrifuge (Heraeus). During the centrifugation step, 100 μl of RT Nucleofector solution V (Amaxa) were mixed in a 1.5 ml tube with 3 μg of DNA containing the luciferase reporters (900 ng of Firefly luciferase reporter and 90 ng of TK-Renilla luciferase reporter) and the appropriate expression constructs or empty vector. The dried cell pellet was thoroughly resuspended in the Nucleofector solution V:DNA mix before being transferred to a Nucleofector cuvette. The cuvette was placed in the Nucleofector device and a built-in program optimised for SH-SY5Y transfection (A-023) was applied. After nucleofection, the cell mix was rapidly transferred from the cuvette to a 1.5 ml tube pre-filled with 900 μl of warm DMEM/FBS, then 250 μl of this suspension (~$5x10^5$ cells) were plated in each well of a black walled 96 well plate.

2.4.6.4 *Assessment of transfection efficiency*

When new tranfection protocols were tested, their efficacy was assessed by replacing the luciferase reporters or protein expression constructs with the GFP Turbo expressing vector P5HuSH. At regular time intervals after transfection (typically 24, 48, 72 hours), live cells were examined under an inverted microscope equipped with a Mercury lamp and the appropriate light filter for GPF excitation (~480 nm). Both cell viability and transfection rate (proportion of GFP-expressing cells) were estimated by visual examination of cells transfected in parallel using different transfection protocols.

2.4.7 *Drug treatments*

2.4.7.1 *Mitotracker Red*

Mitotracker Red (Molecular Probes, Invitrogen), is a cell-permeant red-fluorescent probe that accumulates in active mitochondria, where it is retained after cell fixation, allowing the visualisation of mitochondria by fluorescent or confocal microscopy. Mitotracker Red was used to label mitochondria in cells that had been transfected with protein expression contructs or an empty vector. Approximately 24 hours after

transfection, the cells were exposed to fresh DMEM/FBS containing 50 nM Mitotracker Red for 30 minutes at 37°C and 5% CO_2 in a humidified incubator. Next, the cells were washed twice with warm PBS before being processed for immunocytochemistry as described in 2.5.7.

2.4.7.2 *Other drug treatments*

Forskolin treatment was used to increase the intracellular cAMP concentration by stimulating adenylyl cyclase, and Rolipram was used to specifically inhibit the activity of endogenous PDE4s. To induce the expression of endogenous ATF4 trough the activation of stress-responsive pathways, the cells were exposed to the endoplasmic reticulum (ER) stress-inducer Thapsigargin or to the oxidative stress inducers H_2O_2 or DL-Homocysteine. All the above drugs were sourced from Sigma except for DL-Homocysteine, which was purchased from Santa Cruz Biotechnology. Unless otherwise specified, the drugs or an equal volume of the respective vehicles were diluted in warm DMEM/FBS and administered to the cells as detailed in table 2.4. When DMSO (Sigma) was used as vehicle, its final concentration in the medium was 0.1% or lower, and it did not affect cell viability or morphology.

Drug	**Final concentration (μM)**	**vehicle**	**Treatment time (hours)**
Forskolin	10 or 1	DMSO	4
Rolipram	10	DMSO	4
Thapsigargin	1	DMSO	16 or 24
H_2O_2	200	H_2O	16 or 24
DL-Homocysteine	500	H_2O	24

Table 2.4 Details of the drug treatments used in this thesis.

2.5 Protein biochemistry

2.5.1 *Preparation of cell lysates*

Cell lysates were produced for subsequent protein analysis by western blotting (WB) or immunoprecipitation (IP). Unless otherwise specified, cell lysates were prepared in RIPA buffer for western blotting and in PBS 1% Triton X-100 for IP. After removal of the culture medium the cells were rinsed once in ice-cold PBS, then lysed in the appropriate volume of ice-cold lysis buffer, which was adjusted to the size of the tissue culture plate or well. For 10 cm dishes, the volume of lysis buffer was 600-700 μl, with slight adjustments made depending on the cell density. For 6, 24 and 96 well plates, the volume of lysis buffer was 200, 100 and 30 μl/well, respectively. Immediately after addition of the lysis buffer, the cell dish or plate was placed on ice, and the cell lysates were harvested with the aid of a cell scraper or, in the case of 24 and 96 well plates, by pipetting repeatedly. For cells grown in 96 well plates, the lysates obtained from 6 wells that had received identical treatment were pooled to give a final volume of ~180 μl. The crude lysates were transferred to appropriately labelled pre-chilled 1.5 ml tubes and incubated for one hour at 4°C on a rotary wheel before being centrifuged for 30 minutes at 13,000 RPM in a table-top microcentrifuge (Heraeus) to sediment the cell debris. The resulting cleared supernatant was transferred to a clean pre-labelled 1.5 ml tube. If they were not processed immediately, cell lysates were stored at -70°C until use.

2.5.2 *Measurement of protein concentration*

The protein concentration in cell lysate to be analysed by western blotting and in subcellular protein extracts was measured using the DC Protein Assay (Biorad). The DC Protein Assay is a colorimetric assay based on a two-step chemical reaction. First, proteins react with Copper tartrate in an alkaline solution, then Folin is reduced by the Copper-treated proteins, resulting in the production of coloured products that turn the solution blue. The assay was performed in 96 well flat-bottomed clear microtiter plates following the manufacturer's instructions. Briefly, Bovine Serum Albumin (BSA) protein standards with concentrations ranging between 0 and 2 mg/ml were prepared from a stock solution of BSA (2 mg/ml) (Biorad).

Alternatively, commercially available pre-diluted BSA protein standards were used (Biorad). Cell lysates were diluted 4 times in H_2O, then 5 μl/well of each BSA standard and protein sample were loaded in the microtiter plate, in triplicate. Reagent A' was prepared by mixing reagents A and S, and 25 μl were added to each well, followed by 200 μl of reagent B. After incubation at room temperature for 10 minutes, the absorbance was read at 750 nm using a Synergy HT Multi-detection Microplate Reader and bespoke Gen 5 software (Bio Tek). The Prism GraphPad software was used to calculate the equation of the regression line from the plotted mean absorbance values of the BSA standards, and the concentration of the protein samples was then calculated by interpolation from this regression line.

2.5.3 *Subcellular protein fractionation*

Subcellular protein fractionation was used to analyse the distribution of exogenous and endogenous DISC1 and ATF4 in different cell compartments in HEK293 and SH-SY5Y cells. HEK293 and SH-SY5Y cells were tranfected for 24 and 72 hours, respectively, then harvested in Tryple Express and diluted in fresh DMEM/FBS in a 15 ml Falcon tube. The cell suspension was pelleted by centrifugation at 500 g for 5 minutes in an Eppendorf 5804 R centrifuge, then resuspended in 0.5-1 ml of ice-cold PBS and transferred to a pre-chilled 1.5 ml tube. If subcellular fractions were to be prepared from transfected cells, a small proportion of this cell suspension (~50 μl) was transferred to a new 1.5 ml tube, then both tubes were centrifuged at 500 g for 3 minutes at 4°C in a table-top microcentrifuge (Heraeus), and the supernatant was carefully removed. The larger cell pellet was used to produce subcellular fractions, while the smaller cell pellet was lysed in 50 μl of RIPA buffer to produce a whole cell lysate. Subcellular fractions were generated using two different commercial kits from Pierce. The Subcellular Protein Fractionation kit was used to extract cytoplasmic, membrane-bound, soluble nuclear, cytoskeletal and chromatin-bound proteins from SH-SH5Y cells. The NE-PER Nuclear and Cytoplasmic Extraction Reagents were used to isolate nuclear and cytoplasmic proteins from SH-SY5Y and HEK293 cells. The protein concentration of each subcellular extract was measured as described in 2.5.2. The fractions were stored at -70°C until use.

2.5.4 *Antibodies*

Details of the antibodies used in this thesis for protein immunoprecipitation or immunodetection, along with the conditions at which they were used, can be found in Table 2.5.

Name in text	Specificity	Species	Supplier (Catalogue number)	Conditions (WB)	Conditions (ICC)	Amount for IP	Notes
α-DISC1	DISC1	Rabbit	Tetsu Akiyama[1]	1:10,000 O/N 1:1,000 3hours	1:250	0.5 μg	(Ogawa *et al*, 2005) Raised against the 669-832 fragment of Lv DISC1. Used for WB at 1:10,000 and 1:1,000 to detect the exogenous and endogenous protein, respectively
β-actin	β-actin	Mouse	Sigma	1:50,000	_	_	
γ-tubulin M	γ-tubulin	Mouse	Sigma (T6557)	_	1:3,000	_	
γ-tubulin R	γ-tubulin	Rabbit	AbCam (ab11317)	_	1:2000	_	
ATF4 MMC	ATF4	Mouse	Sigma (WH0000468M1)	1:1,000 3 hours	1:2,500 1:100	1 μg	Used for ICC at 1:2,500 or 1:100 to detect the exogenous and endogenous protein, respectively
ATF4 RPC	ATF4	Rabbit	Santa Cruz (sc-200)	1:1000 3 hours	1:100 1:4000	1 μg	Unless otherwise stated, this ATF4 antibody was used
Calreticulin	Calreticulin	Mouse	AbCam (ab22683)	1:100,000 1 hour	_	_	
c-myc	c-myc tag	Mouse	Santa Cruz (sc-40)	1:1000 1 hour	1:500		
Flag MMC	Flag tag	Mouse	Sigma (F3165)	1:10,000 O/N	1:10,000	1 μg	Unless otherwise stated, this Flag antibody was used for WB
Flag RPC	Flag tag	Rabbit	Sigma (F7425)	1:10,000 O/N	1:2000		Unless otherwise stated, this Flag antibody was used for ICC
GAPDH	GAPDH	Mouse	Chemicon (MAB347)	1:100,000 1 hour	_	_	
H3	H3	Rabbit	AbCam (ab1791)	1:10,000 1 hour	_	_	

HA Y-11	HA tag	Rabbit	Santa Cruz (sc-805)	–	1:2000	–	
HA.11	HA tag	Mouse	Covance MMS-101P	–	1:3,000	–	
HSP90	HSP90	Mouse	AbCam (ab13492)	1:100,000 1 hour	–	–	
N-16	DISC1	Goat	Santa Cruz (sc-47990)	–	1:100		Requires PFA fixation
p84	p84	Mouse	AbCam (ab487)	1:100,000 1 hour	–	–	
PSD95	PSD95	Mouse	ABR (MAI-046)		1:1000	–	
Synaptophysin	Synaptophysin	Mouse	Sigma (S5758)	1:5,000 O/N	1:50,000	–	
V5	V5 tag	Mouse	Invitrogen (R96025)	1:1,000 1 hour	1:5,000		
Vimentin	Vimentin	Mouse	AbCam (ab8978)	1:100,000 1 hour	–	–	
Goat anti rabbit	Rabbit IgG	Goat	Dako (P0448)	1:2,000 30 minutes	–	–	HRP-conjugated secondary antibody
Goat anti mouse	Mouse IgG	Goat	Dako (P0447)	1:1,000 30 minutes	–	–	HRP-conjugated secondary antibody
Goat anti rabbit	Rabbit IgG	Goat	Invitrogen (A11008)	–	1:1,000	–	Fluorescent secondary antibody (488 nm)
Goat anti rabbit	Rabbit IgG	Goat	Invitrogen (A11012)	–	1:1,000	–	Fluorescent secondary antibody (594 nm)
Goat anti mouse	Mouse IgG	Goat	Invitrogen (A11029)	–	1:1,000	–	Fluorescent secondary antibody (488 nm)
Goat anti mouse	Mouse IgG	Goat	Invitrogen (A11005)	–	1:1,000	–	Fluorescent secondary antibody (594 nm)

Table 2.5 Details of the antibodies used in this study, and the conditions at which they were used for western blotting (WB), immunocytochemistry (ICC) and immunoprecipitation (IP) in 600 μl of cell lysate. All the antibodies detect human antigens. Species refers to the species in which the antibody was raised. O/N indicates overnight incubation at 4°C on a horizontal shaker. The probing conditions reported in the table refer to typical experiments, and may have been adjusted depending on the particular nature of the experiment. [1]Laboratory of Molecular and Genetic Information, University of Tokyo, Japan.

2.5.5 *Immunoprecipitation*

Immunoprecipitation allows to concentrate a target protein from a cell lysate or a similar protein mixture by exploiting a specific antibody. In this study, immunoprecipitation was used to compare the ability of the target protein to complex with different interactors that were present in the original cell lysates. This was done by semiquantitative detection of the different interactors that had co-immunoprecipitated with the target protein. Cells were grown in 10 cm tissue culture dishes (Iwaki) and either transfected for 24 hours as described in 2.4.6.1 or left untransfected. Cell lysates were prepared as detailed in 2.5.1 and processed immediately, without freezing. Unless otherwise stated, cell lysates were prepared in PBS 1% Triton X-100. The precipitating antibody was added to 600-700 μl of lysate in a 1.5 ml tube at the concentration detailed in table 2.5, and incubated for 1 hour at 4°C on a rotary wheel. This step allows the antibody to complex with its target protein, if this is present in the lysate. The protein concentration was measured in the remaining lysate (100-200 μl) as detailed in 2.5.2, and this was subsequently stored at -70°C until further use. At the end of the first hour of incubation with the precipitating antibody, 50 μl of protein G-coated Sepharose beads diluted in PBS (Sigma) were added to the lysate, and incubated as above for 2 hours. This allows the establishment of a stable interaction between protein G and the immunoglobulins present in the lysate. At the end of this stage, thus, the antigen-antibody complexes should be captured on the surface of the G Sepharose beads. Next, the lysate was

transferred to the column of a spin cup equipped with a paper filter (Pierce) and rapidly centrifuged in a table-top microcentrifuge set at 4°C until the speed of ~10,000 RPM had been reached. This allows the G Separose-bound antigen-antibody complexes to sediment on the paper filter, while the unbound proteins are collected in the collection tube below, along with the rest of the lysate, which was discarded. The beads were washed by adding 500 μl of the same buffer used to produce the lysate to the column, followed by incubation for 5 minutes at 4°C on a rotary wheel. The spin cups were then centrifuged as before, the flow-through was discarded and the process was reapeated 3 more times. After the final wash, the collection tube was carefully dried, the column placed back in the collection tube and 50 μl of protein sample buffer were added to the bead slurry in the column to elute the antigen-antibody complexes from the beads. The spin cups were then heated to either 40°C for 10 minutes or 100°C for 5 minutes, depending on the downstream application, then quickly centrifuged as above to transfer the eluate to the collection tube. The column was discarded, and the protein eluate was either processed immediately for western blotting or stored at -70°C until use.

2.5.6 *SDS-PAGE and western blotting*

2.5.6.1 *Sample preparation*

The protein concentration of cell lysates and subcellular protein fractions was measured as described in 2.5.2, and used to calculate the volume of protein sample corresponding to the desired total amount of protein to be analysed by western blotting (WB). This volume of protein sample was transferred to a clean 1.5 ml tube and mixed with an equal volume of protein sample buffer, then heated at 100°C to denature the proteins and disrupt protein complexes. Protein samples obtained by immunoprecipitation were prepared as detailed in 2.5.5, and 10μl/sample were analysed by WB, unless otherwise specified.

2.5.6.2 *BioRad system*

The BioRad system was used when it was necessary to achieve satisfactory resolution of proteins of similar molecular weight. High density resolving gels containing 12% acrylamide were prepared following the recipe detailed below.

2.672 ml	dH_2O
3.2 ml	30% acrylamide/bisacrylamide solution
2 ml	1.5M Tris pH 8.8
40 µl	20% SDS
80 µl	10% APS
8 µl	TEMED
8 ml	Total volume

Once mixed, the gel solution was poured between two glass plates separated by a 1 mm spacer, to produce a gel with a thickness of 1 mm, and an empty space of about ~2 cm was left at the top. This empty space was filled with isobutanol, and the gel was allowed to polymerise for ~1 hour, after which the isobutanol was replaced with a 4% stacking gel prepared as described below.

3.0 ml	dH_2O
670 µl	30% acrylamide/bisacrylamide solution
1.25 ml	1.5M Tris pH 8.8
50 µl	20% SDS
50 µl	10% APS
5 µl	TEMED
5 ml	Total volume

A 1 mm-thick comb was placed inside the stacking gel to produce either 10 or 15 wells, and the gel was allowed to polymerise for ~1 hour. Once polymerisation was complete, the glass plates containing the gel were placed in Mini TransBlot Cell

(BioRad), which was then filled with enough 1 x TGS buffer to completely cover the gel. After removing the comb, the wells were gently flushed with 1 x TGS buffer, and the protein samples that had been prepared as detailed in 2.5.6.1 were loaded in the wells using a thin bore gel loading tip (Fisher). A prestained protein size marker (BioRad All Blue Precision Plus Protein Standard) was loaded next to the protein samples. The gel tank was connected to a Power Pac 3000 (BioRad) and a 150V current was applied for 60-90 minutes to achieve separation of the proteins by molecular weight. Once the desired degree of protein resolution had been achieved, as judged by the spacing between the protein marker bands, the current was switched off, and the proteins were transferred to a PDVF membrane as follows.

A 6 cm by 8 cm rectangle was cut out from a sheet of Hybond-P PDVF membrane (Amersham) and briefly soaked in methanol, then rinsed in dH_2O and equilibrated in transfer buffer for at least 5 minutes. Meanwhile, 2 rectangles of 6 cm by 8 cm were cut out from a sheet of blotting paper (Whatman) and briefly soaked in transfer buffer. The protein gel was carefully removed from the glass plates and laid flat on one of the 2 pre-wetted rectangles of blotting paper. The PDVF membrane was then placed on top of the gel, making sure that no air bubbles were trapped between the gel and the membrane, and covered with the second rectangle of blotting paper. Once stacked as described, the gel, membrane and blotting paper were placed in a TransBlot Gel Holder Cassette (BioRad), between 2 fibre pads soaked in transfer buffer. A TransBlot modular electrode (BioRad) was placed in a TransBlot Cell pre-filled with transfer buffer, and the Gel Holder Cassette was then inserted in the TransBlot electrode. Finally, a current of 30V was applied for 90-120 minutes to induce the transfer of the proteins, including the pre-stained marker, from the gel to the PDVF membrane. Once the transfer was complete, the PDVF membrane was rinsed once in PBS, and stored in PBS at 4°C until staining.

2.5.6.3 *Invitrogen system*

The Invitrogen protein electrophoresis system (Novex NuPAGE SDS-PAGE Gel System) was used in combination with NuPAGE 7% Tris-Acetate or NuPAGE 4-12% Bis-Tris precast gels (Invitrogen). One or two gels were removed from their plastic pouches and rinsed with dH_2O before being placed in the gel tank (XCell

SureLock Mini-Cell) (Invitrogen). The gel tank was filled with the appropriate 1x running buffer (NuPAGE Tris-Acetate SDS Running Buffer for Tris-Acetate gels, or NuPAGE MES SDS Running Buffer for Bis-Tris gels), then the gel(s) was loaded as described in 2.5.6.2 and electrophoresis was performed on a Power Pac 3000 (BioRad) at 150V for 60-90 minutes at 4°C to separate the proteins by molecular weight. Meanwhile, one or two Invitrolon PDVF membranes (Invitrogen) were briefly soaked in methanol, then rinsed in dH_2O and equilibrated for at least 5 minutes in the transfer buffer (1x NuPAGE Transfer Buffer containing 20% methanol). Once electrophoresis was complete, the gel(s) were removed from the gel tank and laid flat on the 3 MM filter paper supplied with the Invitrolon PDVF membrane, which had been quickly soaked in transfer buffer. The Invitrolon PDVF membrane(s) was then placed on the gel(s), and covered with a second sheet of pre-soaked 3 MM paper. Maintaining the same orientation, the gel, membrane and paper stack was placed inside an XCell II Blot Module, between two layers of sponges soaked in transfer buffer. If two gels were transferred simultaneously, a soaked sponge was placed between them. The blotting module was then filled with transfer buffer and a 30V current was applied for 2 hours to allow the protein to transfer from the gel(s) to the PDVF membrane(s). Once the transfer was complete, the membrane(s) was extracted from the blotting module, washed once in PBS and stored in PBS at 4°C until staining.

2.5.6.4 *Staining of protein blots*

Staining of total protein on PDVF membranes was used to confirm efficient protein transfer after western blotting and, in some instances, to verify equal protein loading between samples. Three different total protein staining methods were employed to visualise proteins on PDVF membranes after western blotting and before immunostaining, as detailed below.

2.5.6.4.1 Ponceau-S

Ponceau-S is a reversible red-coloured protein dye. Proteins on PDVF membranes were stained by incubation in Ponceau-S for ~5 minutes at room temperature with constant agitation. At the end of this incubation time, proteins were visualised by eye

as red bands on the PDVF membrane, and the dye was recycled for future use. The dye was subsequently removed from the membrane by washing repeatedly with dH_2O.

2.5.6.4.2 SimplyBlue

SimplyBlue SafeStain is a Coomassie-based reversible protein dye with a higher sensitivity than Ponceau-S. Dry PDVF membranes were soaked in SimplyBlue for 2 minutes with gentle shaking, then the dye was discarded and the membrane washed 3 times for 1 minute in dH_2O to remove the background staining. After the washes, proteins were visualised by eye as blue bands on the PDVF membrane. De-staining of PDVF membranes was achieved by repeated washes with dH_2O.

2.5.6.4.3 SYPRO Ruby

SYPRO Ruby Protein Blot Stain (Invitrogen) is a sensitive orange/red-fluorescent protein dye that can be visualised using UV illumination. All the staining steps were performed at room temperature with gentle agitation. Dry PDVF membranes were floated face-down in a solution containing 7% acetic acid and 10% methanol for 15 minutes, then rinsed 4 times for 5 minutes in dH_2O before being floated face-down on SYPRO Ruby for 15 minutes. The membranes were then washed 3 times for 1 minute in dH_2O to remove the excess dye, after which they were ready to visualise. Protein bands stained with SYPRO Ruby were visualised and photographed under UV illumination using a Gene Genius Bioimaging System (Syngene).

2.5.6.5 *Immunostaining of protein blots*

To block non-specific binding of the antibodies, PDVF membranes were incubated in blocking buffer for 30 minutes. The primary antibody was diluted in 10 ml of probing buffer as detailed in Table 2.5, then incubated with the PDVF membrane for the appropriate time. After incubation with the primary antibody, the membrane was washed 3 times for 5 minutes with washing buffer, then incubated with the appropriate HRP-conjugated secondary antibody diluted in probing buffer (see Table 2.5). The membrane was then washed as before and transferred to PBS. All the steps described above were performed at room temperature and under constant agitation.

To visualise the protein bands, the membranes were incubated with SuperSignal West Dura Extended Duration Substrate (Pierce), a highly sensitive chemiluminescent substrate for HRP detection on western blots. The chemiluminescent signal was detected using a CCD camera (GeneGnome Imaging System, Syngene), and the exposure time was adjusted depending on the intensity of the signal in order to obtain the best signal/noise ratio.

Alternatively, the membranes were incubated with ECL Plus solution (Amesham) for 5 minutes, then the excess substrate was removed from the membrane by holding it upright and touching a piece of blotting paper with the bottom edge of the membrane. The drained membrane was tightly wrapped in a single layer of cling film, then exposed to photographic film (Scientific Laboratory Supplies) for a between 1 second and 16 hours. To visualise the protein bands, the film was developed using an Amersham Hyperprocessor.

2.5.6.6 *Band densitometry*

For relative quantification of protein band intensities on western blots, images acquired with the GeneGnome Imaging System, as detailed in 2.5.6.5, were analysed with the GeneTools software (Syngene). To quantify the signal intensity of bands on photographic film, a digital image of the film was acquired using an office scanner, then analysed with the software ImageJ, downloaded from http://rsbweb.nih.gov/ij/download. Band density measurements obtained from different samples were then analysed and compared statistically.

2.5.6.7 *Stripping PDVF membranes*

In some cases, PDVF membranes had to be probed for immunodetection of two distinct proteins of the same or very similar size, or probed for the same protein using two different antibodies. In these cases, the membranes were probed with the first set of antibodies and imaged as described in 2.5.6.5, then the antibodies were removed chemically from the membrane and the second set of antibodies was applied. Removal of the antibodies bound to proteins on a PDVF membrane (or membrane stripping) was achieved by incubating the membrane for a period of time

between 1 hour and 16 hours in Restore Western Blot Stripping Buffer (Perbio Science) at room temperature with constant agitation. The incubation time varied depending on the intensity of the signal recorded after probing with the first set of antibodies, with stronger signals requiring longer incubation times. After stripping, the membrane was washed 3 or 4 times with PBS to completely remove the stripping buffer. To verify complete removal of both the primary and secondary antibodies, the membrane was blocked and re-probed with the same secondary antibody as described in 2.5.6.5. If no chemiluminescent signal was detected at this stage, the membrane was washed in PBS, then probed with the second set of antibodies (see 2.5.6.5).

2.5.7 *Immunocytochemistry*

Immunocytochemistry allows the detection of one or multiple proteins in structurally intact cells, and can be used to analyse the subcellular expression pattern of the protein(s) and investigate protein-protein interactions. This technique requires adherent cells to be grown as a monolayer on the surface of glass coverslips. Cells (either transfected or untransfected) are then fixed and the protein(s) of interest are detected by sequentially incubating the cells with one or more protein-specific antibodies, followed by fluorescently labelled secondary antibodies. Stained cells can then be visualised using a light microscope equipped with the necessary excitation an emission filters.

2.5.7.1 *Cell fixation and permeabilisation*

By rapidly stopping the activity of any biomolecule, chemical fixation kills the cells while preserving their structure and preventing decay due to autolysis. Membrane permeabilisation can be achieved by treating the cells with solvents or detergents, and is necessary for immunodetection of antigens that are not exposed on the cell surface. Two different methods were used to fix and permeabilise cells in this study.

For the first method, the cells were washed once with warm PBS, then PBS was replaced with ~500 µl/well of -20°C methanol and the cells were incubated at -20°C for 5 minutes. After this, methanol was aspirated from the wells and the cells were

gently washed 3 times with ice-cold PBS. Since methanol simultaneously fixes and permabilises the cells, no further permeabilisation steps were necessary.

For the second method, cells were washed once with warm PBS, then PBS was replaced with ~500 µl/well of room temperature 4% PFA, and the cells were incubated at room temperature for 10 minutes. After removal of 4% PFA, the cells were washed 4 times with ice-cold PBS. For membrane permabilisation, the PFA-fixed cells were incubated in PBS containing 0.1% Triton X-100 for 5 minutes at room temperature, then washed 4 times with room temperature PBS to remove the detergent. This method of permabilisation was used whenever the cell nuclei were to be counterstained with TO-PRO-3 (Invitrogen).

Fixed and permeabilised cells were either immunostained immediately or wrapped in tin foil and stored in PBS at 4°C for up to 2 days before immunostaining.

2.5.7.2 *Immunostaining*

Immunostaining was performed at room temperature. To block non-specific binding sites, the cells were incubated in ~300 µl/well of PBS containing 3% BSA (w/v) (blocking buffer). Meanwhile, the primary antibody was diluted in blocking buffer as detailed in Table 2.5. If the cells were to be probed with 2 or more primary antibodies, these had to be raised in different species, and they were diluted together in blocking buffer. After blocking, the blocking buffer was removed from the wells and replaced with the primary antibody dilution, and the cells were incubated for 2 hours with gentle agitation. Cells were then subjected to 2 quick washes followed by 3 x 5 minute washes with PBS containing 0.02% BSA (w/v) (washing buffer). Meanwhile, the appropriate fluorescently labelled secondary antibody was diluted in blocking buffer (see Table 2.5). If two or more proteins were to be detected simultaneously, secondary antibodies with well resolved excitation and emission peaks were selected so that they could be visualised separately. Whenever possible, if two or more secondary antibodies were to be used together, antibodies raised in the same species were chosen so to avoid any artefact due to cross-reaction between secondary antibodies. Cells were incubated with the secondary antibody for 1 hour. If nuclei were to be stained with TO-PRO-3 (Invitrogen) the dye was diluted 500

times and added to the cells along with the secondary antibody. Once the secondary antibody had been added, the cells were protected from light at all times to prevent photobleaching of the fluorophores. After incubation with the secondary antibody, the cells were washed as before, then mounted on glass slides using mowiol mounting medium supplemented with 2 mg/ml of DAPI to counterstain the nuclei. The slides were wrapped in tin foil and kept at 4°C for at least 16 hours after mounting to allow the mounting medium to set completely.

2.5.7.3 *Confocal microscopy*

Laser scanning confocal microscopy allows the generation of images representing a thin horizontal optical section of a fluorescently stained cell or tissue, with minimal contamination from light deriving from adjacent planes. This is achieved through the utilisation of high-intensity monochromatic laser beams that can be precisely focused to excite a defined focal plane, in combination with a photomultiplier detector with a pinhole aperture that excludes the out-of-focus light. These technical characteristic render confocal microscopy the method of choice to detect co-localisation of fluorescent signals in a biological specimen, as it can be assumed that two sources of light (i.e. two fluorescently labelled proteins or structures) will generate overlapping signals only if they are located on the same plane. A further advantage of using confocal microscopy consists in the possibility of minimising colocalisation artefacts caused by spectral bleed-through. This occurs when two fluorophores with partially overlapping spectral profiles are used to stain a sample and consists in the emission of one fluorophore being detected in the photomultiplier channel or through the filter combination reserved for the second fluorophore. Bleed-through can be minimised by sequentially scanning the sample with individual lasers to excite the different fluorophores and carefully setting the width of the photomultiplier slit so that only the light emitted by one fluorophore can be detected. Sequential scanning was used in this study whenever more than one fluorophore had to be imaged in the same cell.

Confocal images were acquired using either a Zeiss LSM510 or a Nikon A1R confocal microscope, each used in combination with its bespoke software. Since the Zeiss LSM510 microscope was not equipped with a laser suitable to image DAPI,

cell nuclei were counterstained with TO-PRO-3 (Invitrogen) when using this microscope.

2.5.7.3.1 Analysis of DISC1 centrosomal distribution

For the analysis of the centrosomal distribution of DISC1 variants in transfected COS7 cells, confocal images were acquired with the Zeiss LSM510 microscope. This analysis was based on measurement of the co-localisation of exogenous DISC1 and the endogenous centrosomal protein γ-tubulin. Initially, fluorescent TetraSpeck beads (Invitrogen) were used to check the registration of the confocal microscope, i.e. the microscope's ability to resolve and co-localise two objects fluorescing at different wavelengths on the same focal plane. This was a necessary control step to verify that the microscope could correctly detect co-localisation between DISC1 puncta and the centrosome. Since the size of the centrosome varies between 0.8 and 1.5 μm, blue, red and green-fluorescing TetraSpeck microspheres with a diameter of 0.5 μm were used. A 5 μl droplet of bead suspension was spotted on a glass slide and allowed to dry, after which 5 μl of glycerol were applied on the beads and a coverslip was mounted and secured to the slide by applying nail polish along its edges. Multichannel confocal images of the fluorescent beads were acquired and inspected visually to verify perfect overlap between images of the same sphere in different channels and absence of overlap between images of adjacent spheres.

Given the relatively small size of the centrosome, particular care was taken to guarantee that the maximum possible image resolution was achieved. Image resolution is determined by two factors: the optics of the microscope and the sampling interval or pixel size. To achieve the ideal image resolution it is necessary to adjust the sampling interval (pixel size) so that it is equal or smaller than the optical resolution capacity of the microscope. The optical parameters of the microscope were entered in the Nyquist Calculator (www.svi.nl/NyquistCalculator) to compute the minimal sampling interval necessary to capture in the image all the information generated by the microscope. The image resolution, digital zoom level and thickness of the optical z plane of the microscope were adjusted to achieve the calculated pixel size. A dual channel z-stack of images (one channel for DISC1 signal and one channel for γ-tubulin signal) was acquired for each cell in randomly

selected microscope fields. Up to 7 z-sections were acquired for each cell, each with a sampling interval of 0.04 x 0.04 x 0.3 μm, to cover a total surface area of 73.1 x 73.1 μm, with a thickness of up to 2.8 μm. For comparability, all the cells were imaged using the same confocal settings.

Image analysis was performed using a bespoke IPLab script developed in collaboration with Paul Perry at the MRC HGU in Edinburgh. For each dual channel image, the script generates a maximum pixel projection of the γ-tubulin channel stack and the operator is asked to indicate, using the paintbrush tool, which area is to be analysed. The image data within this region of interest (ROI) is auto-segmented to select the actual centrosomal signal and exclude the background noise. The term "segmentation" used here refers to the selection of all pixels in the image whose intensity is above an arbitrarily set background value. A three-dimensional sequence plot is then calculated for this small ROI for all z planes. The z plane with the maximum average centrosomal pixel value is taken to be the plane of best centrosomal focus and the rest of the analysis relates to this plane only. The operator is prompted to paint an encircling ring around the cell in the contrast enhanced DISC1 channel. The outer rim of this ring delimits the ROI for the analysis. The pixels in this channel are segmented using an arbitrary pixel intensity threshold value, which is the same for all images, and detailed information on the segmented pixels is recorded. Segment analysis is similarly performed on the region of the DISC1 channel corresponding to the previously selected centrosomal ROI, and all the data is recorded in an automatically-generated table.

2.5.7.3.2 Analysis of DISC1 nuclear distribution

For the analysis of the nuclear distribution of DISC1 variants in transfected COS7 cells, images were acquired using the Zeiss LSM510 microscope. Until completion of the analysis, the operator was blinded to which DISC1 variant had been transfected in each set of cells. Cells were stained to detect exogenous DISC1 and the nucleus, as detailed in 2.5.7.2, then dual-channel single plane images of individual cells in randomly selected fields were acquired, with a pixel size of 0.14 x 0.14 μm. To insure comparability of the results, all the cells in the same experiment were imaged using identical microscope settings.

Image analysis was performed using an IPLab script developed in collaboration with Paul Perry, at MRC HGU in Edinburgh. For each dual channel image, where one channel corresponds to DISC1 signal and the other channel corresponds to the nuclear signal, the script prompts the operator to encircle the cell perimeter using the paintbrush tool on the DISC1 channel. The outer rim of this circle defines the boundaries of the region of interest (ROI) to be analysed. Within this ROI, all the DISC1 pixels whose intensity is above an arbitrarily defined background threshold, which is the same for all images, are selected. This processed is defined as pixel segmentation. The script then records detailed information on the segmented pixels in the DISC1 channel. The image corresponding to the nuclear channel is then auto-segmented to select the actual nuclear ROI and exclude the background noise. The nuclear ROI is then transferred to the DISC1 channel, and detailed information on the pixels within this ROI is recorded. At the end of the analysis of each cell, a table containing all the measured image parameters is automatically generated.

2.6 Molecular biology methods

A complete list of primers used in this thesis is shown in Tables 2.6, 2.7 and 2.8. Unless otherwise stated, all primers were supplied by Sigma and were designed manually.

Name	Sequence (5'-3')	Purpose
DISC1 Q264R F[1]	GACCCGCGATGTCTCTCTAGACCCTTCAGTCTCTTGGCTACA	Replace Q with R at position 264 in human DISC1. Introduces an XbaI restriction site
DISC1 Q264R R[1]	TGTAGCCAAGAGACTGAAGGGTCTAGAGAGACATCGCGG	
DISC1 R37W F	GCGTGCTTTCGGAGGTGGCGGCTGGCACGGAGGC	Replace R with W at position 37 in human DISC1
DISC1 R37W R	GCCTCCGTGCCAGCCGCCACCTCCGAAAGCACGC	
DISC1 T603I F	GGAAACCATTTCTGGATGGCTAAAGACCTCACCG	Replace T with I at position 603 in human DISC1
DISC1 T603I R	CGGTGAGGTCTTTAGCCATCCAGAAATGGTTTCC	
DISC1 C704S F	GGAAGCATGTCGATTGCTTATCCAGAGCCTACAGCTCCAGG	Replace C with S at position 704 in human DISC1. Removes a HindIII restriction site
DISC1 C704S R	CCTGGAGCTGTAGGCTCTGGATAAGCAATCGACATGCTTCC	
DISC1 T847A F	GCTTCCTGCATGACAGCTGGTGTCCACGAAGCACAAGCCTGA	Replace T with A at position 847 in human DISC1
DISC1 T847A R	TCAGGCTTGTGCTTCGTGGACACCAGCTGTCATGCAGGAAGC	
DISC1 P432L F	GGAGATGACACCCACACCCTACTGAGAATGGAGCC	Replace P with L at position 432 in human DISC1
DISC1 P423L R	GGCTCCATTCTCAGTAGGGTGTGGGTGTCATCTCC	
DISC1 L607F F[1]	TCTGGACGGCTAAAGACTTCACCGAGGAGATTAGA	Replace L with F at position 607 in human DISC1
DISC1 L607F R[1]	TCTAATCTCCTCGGTGAAGTCTTTAGCCGTCCAGA	
CHOPAARE F	CGCTAGCCTCGAGGAAACATTGCATCATCCCCGCAACATTGCATCATCCCCGCATCTGGCCTCG	Introduce the CHOP AARE in the pGL4.23 luciferase reporter
CHOPAARE R	CCGAGGCCAGATGCGGGGATGATGCAATGTTGCGGGGATGATGCAATGTTTCCTCGAGGCTAGG	
mutCHOPAARE F	CGCTAGCCTCGAGGAAACAATGCATCATCCCCGCAACAATGCATCATCCCCGCATCTGGCCTCG	Introduce the mutant CHOP AARE in

mutCHOPAARE R	CCGAGGCCAGATGCGGGGATGATGCATTGTTGCGGGGATGATGCATTGTTTCCTCGAGGCTAG	the pGL4.23 luciferase reporter
pcDNA4TO Flag to myc F	GGAATTCGCCGCCATGGAACAAAAGCTAATATCAGAAGAAGACCTACCAGGCGGGGGTCC	Replace the Flag tag with the Myc tag in pcDNA4/TO-Flag DISC1
pcDNA4TO Flag to myc R	GGACCCCCGCCTGGTAGGTCTTCTTCTGATATTAGCTTTTGTTCCATGGCGGCGAATTCC	Replace the Flag tag with the Myc tag in pcDNA4/TO-Flag DISC1
ATF4ΔRK F	GCAAAACAAGACAGCAGCCACTGGTTACCTGGAAGCAGCGGCCGCGGAGCAGGAGGC	Mutate the DNA binding domain of human ATF4 to generate ATF4ΔRK
ATF4ΔRK R	GCCTCCTGCTCCGCGGCCGCTGCTTCCAGGTAACCAGTGGCTGCTGTCTTGTTTTGC	
hDISC1 ΔLZ9 F	GGACGGCTAAAGACTTGGTGTTGAGTTCC	Remove the predicted Leucine zipper in exon 9 of human DISC1 to generate DISC1ΔLZ9
hDISC1 ΔLZ9 R	GGAACTCAACACCAAGTCTTTAGCCGTCC	

Table 2.6 Details of the mutagenic primers used in this study. [1]Primers designed and supplied by Shaun Mackie.

Name	Sequence (5'-3')	Purpose
BGH R	TAGAAGGCACAGTCGAGG	Reverse sequencing of plasmids from the BGH polyadenylation signal
CMV F	CGCAAATGGGCGGTAGGCGTG	Forward sequencing of plasmids from the CMV promoter
Firefly R1	ATGTGCATCTGTAAAACG	Reverse sequencing of firefly luciferase in the Som-CRE-Luc reporter
Firefly R2	AACCGAACGGACATTTCG	Reverse sequencing of firefly luciferase in the Som-CRE-Luc reporter
Promega Luc2 F	TACCCACTCGAAGACGGG	Forward sequencing of firefly luciferase in the pGL4.23 reporter

Promega Luc2 R	ATGTGCGTCGGTAAAGGC	Reverse sequencing of firefly luciferase in the pGL4.23 reporter
S1[1]	GTGAGCCACCGCGCAG	Forward sequencing of human DISC1 cDNA
S2[1]	CACTTTGGGATTCAGCTC	Forward sequencing of human DISC1 cDNA
S3[1]	ATTCGGCTCTCGCTTGGC	Forward sequencing of human DISC1 cDNA
S4[1]	GATGCCCACTCTTGGGAC	Forward sequencing of human DISC1 cDNA
S5[1]	GCCACTCAGCAGGCCAGC	Forward sequencing of human DISC1 cDNA
S6[1]	CTGGGTCAGCTGCAGGAG	Forward sequencing of human DISC1 cDNA
S7[1]	CTGGAGGGACTCCTCAGC	Forward sequencing of human DISC1 cDNA
S8[1]	GAGAGGCAGATGGATGAC	Forward sequencing of human DISC1 cDNA
SP6 F	ATTTAGGTGACACTATAG	Forward sequencing of mouse DISC1 cDNA in pRK5 vector
T7 F	TAATACGACTCACTATAGGG	Forward sequencing of plasmids from the T7 promoter

Table 2.7 Details of the sequencing primers used in this study. [1]Primers designed and provided by Fumiaki Ogawa.

Name	**Sequence (5'-3')**	**Purpose**
ATF4 F	GATCGAATTCCCACCATGACCGAAATGAGCTTCCTGAGC	ATF4 sub-cloning
ATF4 Flag R	GATCCTCGAGCTACTTGTCATCGTCGTCCTTGTAGTCACCGGGGACCCTTTTCTTCCC	

CRE mut F	TCGAGAGCCTGACGTCAGAGAGCCTGACGTCAGAGAGCCTGACGTCAGAGAGCCTGACGTCAGAGA	Insertion of 4 copies of the Somatostation CRE in pGL4.23
CRE mut R	AGCTTCTCTGACGTCAGGCTCTCTGACGTCAGGCTCTCTGACGTCAGGCTCTCTGACGTCAGGCTC	
Mouse Disc1 HA F	GATCGAATTCACCATGGGCTACCCC	Sub-cloning of mouse *Disc1* from pRK5 to pcDNA4/TO
Mouse Disc1 R	CTTAGCGGCCGCTCAGGCCTCGG	
Mouse Disc1 mut F	AATTCGCCGCCATGGATTACAAGGATGACGACGATGACAAGCAGGGCGGGG	Replacing the HA tag with the Flag tag in pcDNA4/TO-HA mouse *Disc1*
Mouse Disc1 mut R	GACCCCCGCCCTGCTTGTCATCGTCGTCATCCTTGTAATCCATGGCGGCG	
pDEST53 ATF4 F1	GATCGAATTCACCGAAATGAGCTTCCTGAGC	ATF4 sub-cloning from pDEST53 to pcDNA3.1
pDEST53 ATF4 R2	GATCCTCGAGTTAATTCGCGGGGACCCTTTTCTTCC	

Table 2.8 Details of the primers and oligonucleotides used in the cloning reactions described in this thesis.

2.6.1 *PCR*

PCR was used was used to introduce point mutations in DISC1 coding sequence (cds) cloned in pcDNA4/TO, as well as insert or remove segments of DNA from other plasmids. PCR was also used to amplify mouse DISC1 and ATF4 coding sequences from their original vectors (pRK5 and pDEST53, respectively) and insert them into a different vector. Finally, PCR was used to screen bacterial colonies after transformation with a ligation product and, in a variant form, to generate DNA fragments for automated sequencing. All PCR reactions were carried out using a PTC-225 Peltier Thermal Cycler (MJ Reasearch). Unless otherwise specified, the PCR reactions were assembled in 0.2 ml thin walled Thermowell PCR tubes (Costar).

2.6.1.1 *Basic PCR reaction*

The basic PCR reaction was used to amplify cDNAs from a vector for sub-cloning. To minimise the chance of introducing unwanted base changes in the original cDNA, a high-fidelity DNA polymerase was used. The reaction was set up as follows, and the individual components were added in the order in which they are listed:

37 μl	dH_2O
5 μl	10x reaction buffer
1 μl	5 ng/μl plasmid DNA template
2.5 μl	20 pmol/μl forward primer
2.5 μl	20 pmol/μl reverse primer
1.25 μl	10 mM dNTPs
0.75 μl	Pfu Ultra Fusion Polymerase (Stratagene)

Reaction conditions were as follows:

1. 95°C 4 minutes

2. 95°C 30 seconds
3. 60°C for 30 seconds
4. 72°C for 15 seconds/kb of plasmid length
5. Repeat steps 2-4 for an additional 29 times
6. 72°C for 10 minutes
7. 4°C Holding temperature

2.6.1.2 *Site-directed mutagenesis PCR*

Site-directed mutagenesis was used to introduce point mutations, deletions or insertions in ATF4 or DISC1 coding sequences, as well as the pGL4.23 luciferase reporter vector. Site-directed mutagenesis was performed with the QuikChange II Site-Directed Mutagenesis Kit or the QuikChange Lightning Site-Directed Mutagenesis Kit, both from Stratagene. The PCR recipe shown below refers to the QuikChange II kit, when additional/different reagents or volumes were used for the QuikChange Lightning kit, these are shown in parenthesis. The reaction components were added in the order in which they are listed.

39.5 µl	dH_2O (38 µl)
5 µl	10x Reaction buffer
1 µl	25 or 100 ng/µl plasmid DNA template
1.25 µl	125 ng/µl forward primer
1.25 µl	125 ng/µl reverse primer
1 µl	10 mM dNTPs
(1.5 µl	QuikSolution Reagent)
1 µl	2.5 U/µl Pfu Ultra HF DNA polymerase (QuikChange Lightning Enzyme)

Reaction conditions were as follows:

QuikChange II

1. 95°C 30 seconds
2. 95°C 30 seconds
3. 60°C 1 minute
4. 68°C 1 minute/kb of DNA
5. Repeat steps 2-4 for an additional 17 times
6. 4°C Holding temperature

QuikChange Lightning

1. 95°C 2 minutes
2. 95°C 20 seconds
3. 60°C 10 seconds
4. 68°C 30 seconds/kb of plasmid DNA
5. Repeat steps 2-4 for an additional 17 times
6. 68°C 5 minutes
7. 4°C Holding temperature

2.6.1.3 *Pre-sequencing PCR*

Pre-sequencing PCR was used to generate DNA templates for automated sequencing and was performed in 96 well PCR plates (Sarstedt), using the Big Dye Terminator Ready Reaction Mix v3.1 system (Applied Biosystems). Reactions were assembled as follows:

5.5 μl	dH_2O
1 μl	300 ng/μl plasmid DNA template
1 μl	3.2 pmol/μl sequencing primer

1.5 μl	5x Sequencing Reaction Dilution Buffer
1 μl	Big Dye v3.1 enzyme

Reaction conditions were as follows:

1. 96°C 1 minute
2. 96°C 10 seconds
3. 50°C 5 seconds
4. 60°C 4 minutes
5. Repeat steps 2-4 an additional 24 times
6. 4°C Holding temperature

2.6.1.4 *Colony PCR*

To screen colonies of *E.coli* transformed with DNA ligation products, the following protocol was used. Fifty microliters of dH_2O were added to the wells of a 96 well PCR plate. Individual bacterial colonies were numbered and picked with a sterile toothpick, which was then used to inoculate the dH_2O in individual wells of the 96 well plate. Once all the desired colonies had been picked, the plate was sealed with adhesive PCR film (Thermo Scientific) and heated at 95°C for 5 minutes in a PTC-225 Peltier Thermal Cycler (MJ Reasearch). The resulting bacterial lysate was used as substrate in the following PCR reaction, assembled in a 96 well PCR plate (Sarstedt):

10.75 μl	H_2O
1.5 μl	10x PCR reaction buffer (Sigma)
0.9 μl	25 mM Magnesium Chloride
0.75 μl	20 μM forward primer
0.75 μl	20 μM reverse primer
0.15 μl	10 mM dNTPs

0.2 μl	in-house produced Taq DNA polymerase

The reaction conditions were as detailed in 2.6.1.1.

2.6.2 *DNA sequencing*

Sequencing was used to verify all the new protein expression and luciferase reporter plasmids generated in this study, as well as plasmids that had been received as gifts from researchers from other laboratories. The plasmid to be sequenced was used as template in a pre-sequencing PCR assembled in a 96 well PCR plate, as detailed in 2.6.1.3. At completion of the PCR, the plate was briefly centrifuged in a Jouan CR422 centrifuge to remove any condensation from the lid, which was then carefully removed. 2.5 μl of 125 mM EDTA (Sigma) were added to each sample in the plate, followed by 30 μl of 100% ethanol (Fisher). The plate was sealed with a Hybaid rubber sealing mat and inverted 4 times to mix the samples, then incubated at room temperature for 15 minutes. Immediately after this, the plate was centrifuged at 3000 RPM for 30 minutes at 8°C to precipitate DNA. After spinning, the sealing mat was removed and the plate was inverted over a paper towel, gently tapped and quickly centrifuged up to 1000 RPM to completely dry the DNA pellet. After adding 30 μl/sample of 70% ethanol to wash the DNA pellet, the plate was centrifuged again at 3000 RPM for 15 minutes at 8°C, then the ethanol was completely removed as before. Next, the plate was sealed with a sheet of adhesive PCR film (Thermo Scientific), appropriately labelled and stored at -20°C until analysis.

The DNA sequence was determined by the technical staff at the DNA Sequencing Facility of the MRC HGU in Edinburgh, who then forwarded the results to me for analysis. DNA sequences were viewed and analysed using FinchTV version 1.4.0 (Geospiza).

2.6.3 *DNA electrophoresis*

DNA electrophoresis was used to assess the size of DNA fragments generated by PCR, verify the effectiveness of DNA restriction reactions and isolate DNA fragments after restriction.

2.6.3.1 *Preparation and running of agarose gels*

To prepare agarose gels for DNA electrophoresis, agarose (Invitrogen) was added to room temperature TAE buffer to a final concentration of 1%. This suspension was heated in a microwave to completely dissolve the agarose, after which SYBR Safe DNA Gel Stain (Invitrogen) was added to a final concentration of 0.02% v/v. The melted agarose solution was then gently poured in a plastic gel mould of the appropriate size (Bioscience Service), which had been previously prepared by inserting one or more combs to create wells in the gel. The agarose solution was allowed to cool and solidify into a gel. Once set, the gel was placed in an electrophoresis tank (Bioscience Service) filled with TAE buffer and completely submerged, then the comb was carefully removed. The DNA samples and DNA marker (1 Kb DNA Ladder, Invitrogen) were diluted 5 times in DNA loading buffer, then loaded into the wells of the gel. To run the DNA gel, a current of 90V was applied to the electrodes of the tank for the time necessary to achieve good resolution of the DNA fragments of interest. The DNA fragments in the gel were visualised by UV light illumination using an Uvidoc Lightbox (Uvitec) and photographed with the built-in camera.

2.6.3.2 *Purification of DNA fragments from agarose gels*

To isolate DNA fragments after restriction digest, the DNA samples were ran on an agarose gel as described in 2.6.3.1. The gel was then placed on a Safe Imager Box UV transilluminator (Invitrogen) to visualise the DNA bands. Next, using a sterile scalpel, the gel was cut around the DNA band of interest, then the fragment of gel containig the DNA was excised from the rest of the gel and placed in a sterile 1.5 ml tube. The DNA fragment was then extracted from the gel and purified using the QIAquick Gel Extraction Kit (QIAGEN), following the manufacturer's protocol.

2.6.4 *Isolation, amplification and purification of plasmids*

DNA plasmids carrying one or more genes conferring resistance to antibiotics were isolated and amplified by transformation of different strains of the bacterium *Escherichia coli* (*E.coli*), followed by selection of the transformants with the

appropriate antibiotic and expansion of the transformant clones. The plasmids were then extracted and purified from the transformed bacterial cells.

2.6.4.1 *Transformation and expansion of E.coli*

Strains of *E.coli* with different transformation efficiencies were used in this thesis. DH5α Competent Cells (Invitrogen) were used to amplify existing purified plasmids and to isolate new plasmids generated by cloning. XL1-Blue and XL10-Gold Ultracompetent Cells (Statagene) were used to isolate new plasmids generated by site-directed mutagenesis using the QuikChange II and QuikChange Lightning Mutagenesis Kits, respectively. The general transformation protocol is described below, and the specific conditions applied to each strain of *E.coli* are detailed in Table 2.9.

After thawing on ice, an aliquot of cell suspension was transferred to a pre-chilled sterile tube and kept on ice. 1-5 μl of plasmid DNA was added to the cells and gently stirred by swirling the pipette tip. The cells were incubated on ice for 30 minutes before being heat shocked by incubation at 42°C followed by 2 minutes on ice. S.O.C. medium (Invitrogen) preheated at 37 °C was added to the cells, which were then incubated for 1-2 hours at 37°C with shaking at 250 RPM in an Innova 4300 incubator shaker (New Brunswick Scientific). After this, 50-200 μl of bacterial culture was evenly spread on LB Agar supplemented with the appropriate antibiotic in a Petri dish and incubated at 37°C in a Plus II incubator (Gallencamp) until bacterial colonies were visible (typically 16-22 hours). To expand the clones of transformants, individual colonies were picked from the plate using a sterile toothpick or loop and used to inoculate either 5 ml or 200 ml of LB Broth supplemented with the appropriate antibiotic. The cultures were then incubated at 37° with shaking at 250 RPM for 14-16 hours.

***E.coli* strain**	**Tube type**	**Cell volume**	**Incubation time at 42°C**	**Notes**
DH5α	1.5 ml Eppendorf	50 μl	20 seconds	
XL1-Blue	15 ml Falcon	50 μl	45 seconds	

XL10-Gold	15 ml Falcon	45 μl	30 seconds	2 μl of β-mercaptoethanol were added to the cells before the heat shock

Table 2.9 Conditions used to transform the different strains of *E.coli* used in this thesis.

2.6.4.2 *Purification of plasmids from E.coli*

Plasmids were extracted and purified from expanded clones of transformed *E.coli* using commercial kits supplied by QIAGEN. These kits are based on the alkaline lysis of bacterial cells followed by binding of DNA to a resin under appropriate salt conditions. Once all the unwanted cell components have been washed off the resin under low-salt conditions, DNA is eluted using a high-salt solution, then desalted and concentrated by isopropanol precipitation. If plasmid DNA was to be used to transfect particularly delicate cells, like primary neurons, it was purified from bacterial endotoxin using the EndoFree Maxi Prep kit.

Bacterial cultures grown in 5 ml of LB broth were centrifuged in 1.5 ml tubes. 1.5 ml of culture was transferred to the tube and spun at 13,000 RPM for 1 minute at room temperature in a table-top microcentrifuge (Eppendorf). The supernatant was discarded by tipping the tube, then 1.5 ml of culture was added to the tube and centrifuged again as before. The supernatant was carefully removed using a pipette to completely dry the cell pellet. Plasmid DNA was purified from the cell pellet using the Spin Miniprep Kit (QIAGEN), according to the manufacturer's directions. To produce larger amounts of Plasmid DNA, bacterial cultures grown in 200 ml of L Broth were centrifuged at 6,000 RPM for 15 minutes at 4°C in an Avanti J-201 centrifuge (Beckman Coulter). The supernatant was discarded and the plasmid DNA was extracted and purified from the cells using a standard or EndoFree Plasmid Maxiprep Kit (QIAGEN).

2.6.5 *Measurement of DNA concentration*

The DNA concentration of purified plasmid solutions was determined using the Nanodrop 2000 spectrophotometer (Thermo Scientific). After cleaning the pedestal of the instrument with dH_2O, 1.5 μl of undiluted DNA solution was placed on the pedestal and the absorbance measured at 230, 260 and 280 nm. The instrument automatically calculates the concentration of the DNA solution based on its absorbance, and also returns the 260/280 nm and 260/230 nm absorbance ratios. These are good indicators of potential contamination of the DNA solution with proteins or carbohydrates, respectively. The purity of the DNA solution was considered satisfactory when the 260/280 nm ratio was above 1.8 and the 260/230 ratio was above 2.2.

2.6.6 *Cloning methods*

2.6.6.1 *Site-directed mutagenesis*

Site-directed mutagenesis was used to introduce specific mutations such as single amino acid substitutions or larger amino acid insertions and deletions in ATF4 and DISC1 expression constructs, as well as to insert the appropriate Response Element in the promoter region of the pGL4.23 luciferase reporter. Site-directed mutagenesis was performed using the QuikChange II or QuikChange Lightning Site-Directed Mutagenesis kit (Stratagene).

The DNA plasmid to be modified by site-directed mutagenesis was used as template in a PCR reaction carried out as described in 2.6.1.2, using appropriate mutagenic primers designed to introduce the desired mutation (see Table 2.6). The PCR product was treated with DpnI to digest the parental methylated and hemimethylated DNA. Treatment conditions were 1 μl of enzyme for 1 hour (QuikChange II kit) or 2 μl of enzyme for 5 minutes (QuikChange Lightning kit) at 37°C. After DpnI treatment the PCR product was used to transform ultracompetent bacterial cells as detailed in 2.6.4.1. The transformant colonies were expanded in 5 ml of LB broth (2.6.4.1) and the plasmid DNA was extracted and purified (2.6.4.2) before being analysed by

sequencing (2.6.1.3 and 2.6.2) to confirm that only the desired mutation had been inserted.

2.6.6.2 *Purification of PCR products*

PCR products obtained with the method described in 2.6.1.1 were purified using the QIAquick PCR purification kit (QIAGEN), according to the manufacturer's instructions. Briefly, DNA is absorbed on a silica column under high-salt condition, and all impurities are washed off the column and discarded. After this, the purified DNA is eluted from the column using a low-salt buffer like Tris, or dH2O.

2.6.6.3 *Restriction digests*

Restriction digests were used to cleave DNA fragments generated by PCR, along with the desired destination vectors, to generate compatible overhangs. In turn, this allowed DNA fragments to be easily inserted in the destination vectors in the desired orientation. Restriction digests were also used to analyse plasmid DNA obtained from bacteria transformed with ligation products after sub-cloning reactions. Prior to restriction, PCR products were purified as described in 2.6.6.2 and eluted in 35 μl of dH_2O. 30 μl of purified PCR product or 3 μg of vector DNA were mixed with 5 μl of the appropriate 10x restriction buffer and 1 μl of each restriction enzyme, and the final volume of the mix was brought to 50 μl by adding dH_2O. The reactions were incubated at 37°C for 2-16 hours. The restriction products were then analysed by electrophoresis on agarose gel (2.6.3.1). When a relatively large fragment was removed from a DNA vector by restriction digest, the linearised vector was subsequently purified as described in 2.6.3.2. Table 2.10 shows the restriction enzymes used in this thesis, along with their corresponding buffers.

Enzyme	Target site (5'-3')	Buffer	Source
EcoRI	$G^{>}AATT_{<}C$	H	Roche
XhoI	$C^{>}TCGA_{<}G$	H	Roche

PpuMI	RG$^{>}$GWC$_{<}$CY	4	New England Biolabs
HindIII	A$^{>}$AGCT$_{<}$T	B	Roche
NotI	G$^{>}$CGGCCG$_{<}$C	H	Roche

Table 2.10 Details of the restriction enzymes used in this thesis. The position of the cleavage sites on the top ($^{>}$) and bottom ($_{<}$) strand are shown. R: A or G; W: A or T; Y: C or T.

2.6.6.4 *Purification of DNA fragments*

DNA fragments generated by restriction digest were purified by phenol-chlorophorm extraction followed by ethanol precipitation before being used in ligation reactions. The volume of the DNA solution to be purified was brought to 100 μl by adding the appropriate volume of TE buffer, then 100 μl of phenol/clorophorm/isoamyl alcohol mix (Sigma) was added. The sample was vortexed for 10 seconds, then centrifuged at 13,000 RPM for 2 minutes at 4°C in a table-top microcentrifuge (Heareus) to separate the phases. 75 μl of the aqueous (top) phase, containing the DNA, was transferred to a fresh tube and 50 μl of TE was added to the remaining mixture, which was then vortexed and spun again as before. A further 70-80 μl was removed from the aqueous phase and pooled with the 50 μl extracted before, and the rest of the tube contents were discarded. 1 μl of a 2 mg/ml glycogen solution (Sigma) was added to the extracted DNA, along with a volume of 3 M pH 5.2 Sodium Acetate solution corresponding to one tenth of the DNA solution. After this, a volume of 100% ethanol (Sigma) corresponding to the original volume of the DNA solution was added, the mix was vortexed and incubated at -20°C for 15 minutes to facilitate DNA precipitation. DNA was then pelleted by centrifugation at 13,000 RPM for 30 minutes at 4°C, the supernatant discarded and an equal volume of 80% ethanol was added to wash the pellet. After spinning as before for 5 minutes, the ethanol was removed thoroughly and the pellet was allowed to air dry before being resuspended in 30 μl (vector DNA) or 10 μl (insert DNA) or dH_2O.

2.6.6.5 *SAP phosphatase treatment*

Shrimp Alkaline Phosphatase (SAP) treatment was performed on linearised DNA vectors after purification (2.6.6.5) and before ligation with the appropriate inserts. By dephosphorylating DNA ends, this step prevents religation of vector DNA, thus favouring the ligation of insert and vector. 10 μl of purified DNA vector was mixed with 8.5 μl of SAP buffer and 1.5 μl of SAP enzyme, both from USB. The reaction mix was incubated at 37°C for 1 hour, then heated at 65°C for 15 minutes to inactivate the enzyme

2.6.6.6 *DNA ligation*

DNA ligation was used to insert either purified DNA fragments generated by PCR or chemically synthesised oligonucleotydes (see Table 2.8), in purified linearised vectors with complementary ends. DNA ligation was performed using the Rapid DNA Ligation Kit (Roche). A reaction mix was assembled containing 2 μl DNA dilution buffer, 2-5 μl of insert, 1 μl of vector and dH_2O to a final volume of 10 μl. 10 μ of T4 DNA ligation buffer was added to the mix, followed by 1 μl of T4 DNA ligase. The reaction was gently mixed and incubated at room temperature for 5 minutes or longer, then transformed into competent DH5α cells as described in 2.6.4.1.

2.6.7 *Gene silencing by RNA interference*

Small interfering RNA oligonucleotides (siRNAs) were used in this study to knock-down the expression of endogenous DISC1 and ATF4 in human cell lines. Detailed information on the siRNA oligonucleotides used in this thesis is shown in table 2.11. siRNAs were transfected into cells using Lipofectamine 2000 (Invitrogen) as described in 2.4.6.1, and cells were lysed 48 hours after transfection. Ambion and Qiagen siRNAs were used at the final concentration of 6 nM and 5 nM, respectively. Unless otherwise specified, when drug treatments were performed on cells transfected with siRNAs, these were started ~34 hours after transfection and lasted 16 hours. At the end of the drug treatments, the cells were either lysed (2.5.1), fractionated (2.5.3), or subjected to cell viability assays (2.7.2).

Name in text	Full name	Target	Source	Sequence (5'-3')	Notes
DISC1 #2	Silencer Select siRNA DISC1_2	Exon 13 of DISC1	Ambion	Sense: GGAUUUGAGAAUAGUUUCAtt Antisense: UGAAACUAUUCUCAAAUCCtt	Pre-designed, HPLC purified and annealed by the supplier.
DISC1 #5	Silencer Select siRNa DISC1_5	Exon 2 of DISC1	Ambion	Sense: GCGUGACAUGCAUUCUUUAtt Antisense: UAAAGAAUGCAUGUCACGCtt	Pre-designed, HPLC purified and annealed by the supplier.
Q ATF4	Hs_ATF4_5 FlexiTube siRNA (SI03019345)	5' UTR of ATF4	Qiagen	Sense: GCGUUGCUGUAACCGACAAtt Antisense: UUGUCGGUUACAGCAACGCtg	Pre-designed and annealed by the supplier. The siRNA sequence is proprietary.
A ATF4	Silencer Select siRNA ATF4	Exon 3 of ATF4	Ambion	Sense: GCCUAGGUCUCUUAGAUGAtt Antisense: UCAUCUAAGAGACCUAGGCtt	HPLC purified and annealed by the supplier. The siRNA sequence was designed by (Averous *et al*, 2004).
Q NC	AllStars Negative Control siRNA	None in mammalian transcriptome.	Qiagen	Proprietary, not disclosed by the supplier.	Pre-designed and annealed by the supplier.
A NC	Silencer Select Negative Control #1 siRNA	None in human, mouse and rat transcriptome.	Ambion	Proprietary, not disclosed by the supplier.	Pre-designed by Ambion. HPLC purified and annealed by the supplier.

Table 2.11 Details of the siRNA oligonucleotides used in this study. All siRNAs target human genes. UTR: untranslated region. The final concentration of siRNA used for transfection was 6 nM for Ambion siRNAs and 5 nM for Qiagen siRNAs.

2.7 Functional assays

2.7.1 *Luciferase reporter assays*

Luciferase reporter assays were used to measure the effect of ATF4 and DISC1 on transcription driven by the cyclic AMP Response Element (CRE) or the C/EBP homologous protein (CHOP) Amino Acid Response Element (AARE). Luciferase activity was measured in transiently transfected cells using the Dual-Glo Luciferase Assay System (Promega), as directed by the manufacturer. This system is based on the use of two reagents that are added step-wise to the cells to be analysed. First, the Dual-Glo Luciferase Reagent induces cell lysis and provides the substrate for Firefly luciferase. Next, the Dual-Glo Stop & Glow Reagent quenches the Firefly luminescence and provides the substrate for Renilla luciferase. In the present study, transcription of Firefly luciferase was driven by the CRE or CHOP AARE regulatory elements, while transcription of Renilla luciferase was driven by the constitutively active Thymidine Kinase (TK) promoter, and served as an internal control to correct for differences in transfection efficiency between samples.

To minimise signal interference between adjacent well, cells were plated and assayed in black-walled 96 well plates (Corning). HEK293 and MO3.13 cells were transfected with Fugene HD (2.4.6.2), whereas SH-SY5Y cells were transfected by Nucleofection (2.4.6.3). In each experiment, cells transfected with an appropriate empty vector were used to measure the background luminescence. Each transfection was performed in triplicate.

If drug treatments were to be performed, these were started 48 hours after transfection. Unless otherwise specified, the appropriate drugs and vehicles were diluted in 37°C DMEM/FBS (2.4.7.2 and Table 2.4), then the transfection medium was carefully aspirated from the wells and replaced with either 50 μl/well (for treatments that lasted up to 8 hours) or 200 μl/well (for treatments that lasted longer than 8 hours) of drug dilution.

If the volume of DMEM/FBS in each well was higher than 50 μl, this was adjusted to 50 μl/well before adding the luciferase reagents. To do this, the old medium was

completely aspirated and replaced with 50 μl/well of fresh DMEM/FBS at 37°C, and the plate was allowed to equilibrate at room temperature for 5-10 minutes. After adding 50 μl/well of room temperature Dual-Glo Luciferase Reagent, the plate was incubated at room temperature for 10 minutes and gently tapped to facilitate cell lysis. Firefly luminescence was then measured using a Synergy HT Multi-detection Microplate Reader with bespoke Gen 5 software (Bio Tek). Next, 50 μl/well of room temperature Dual-Glo Stop & Glo Reagent was added and the plate was incubated as above before reading Renilla luminescence.

For each sample, the mean Firefly and Renilla luminescence was calculated from the 3 technical replicates. Next, the mean background luminescence was subtracted from these values, and the ratio between Firefly and Renilla luminescence was calculated. Measurements obtained from a minimum of 3 independent experiments were then analysed and compared statistically.

2.7.2 *Cell viability assay*

The cell viability assay described below was used to assess the effect of ATF4 or DISC1 knock-down and overexpression on survival of MO3.13 oligodendrocytes after exposure to environmental stress. Cell viability was measured using the CellTiter-Glo Luminescent Cell Viability Assay (Promega), according to the manufacturer's directions. This assay exploits a bioluminescent reaction to quantify the amount of ATP present in each well, which is in turn directly proportional to the number of metabolically active cells.

Cells were plated in black-walled 96 well plates (Corning) in a total volume of 100 μl of DMEM/FBS/well (2.4.3). Cell density was $1x10^4$/well for siRNA transfections and $2x10^4$/well for DNA transfections. Cells were transfected with Lipofectamine 2000 (2.4.6.1), using 50 μl/well of transfection mix containing 0.5 μl Lipofectamine 2000, 15 nM or 18 nM of Qiagen or Ambion siRNA, respectively, or 200 ng of the appropriate protein expression plasmid. Each transfection was performed in duplicate. 24 hours after transfection, the medium was replaced with 200 μl/well of DMEM/FBS containing the appropriate drug/vehicle, and the cells were incubated for 24 hours at 37°C, 5% CO_2. At the end of the drug treatment, the medium was

replaced with 50 μl/well of fresh 37°C DMEM/FBS, and the plate was allowed to equilibrate at room temperature for 10 minutes. After adding 50 μl/well of room temperature CellTiter-Glo Reagent, the plate was incubated for 10 minutes at room temperature on an orbital shaker to induce cell lysis, then luminescence was recorded from individual wells using a Synergy HT Multi-detection Microplate Reader with bespoke Gen 5 software (Bio Tek). For each sample, the mean luminescence was calculated from the 2 technical replicates. Mean readings obtained from 3 independent experiments were analysed and compared statistically.

3 The effect of missense variants on the subcellular distribution of DISC1

3.1 Introduction

Besides the originally described t(1;11) translocation, several common and rare *DISC1* missense point mutations are associated with increased risk of psychiatric illness and/or brain and cognitive abnormalities in healthy carriers (Chubb *et al*, 2008; Soares *et al*, 2011). The three common polymorphisms resulting in amino acid substitutions R264Q, L607F and S704C appear to increase the risk of psychiatric illness in at least some studies and are associated with brain structural and cognitive defects, as detailed in the introduction of this thesis (Chubb *et al*, 2008; Soares *et al*, 2011). In addition, several rare or ultra-rare amino acid substitutions are associated with schizophrenia or schizoaffective spectrum disorders (G14A, R37W, S90L, T603I and P758R), bipolar disorder (S209L, R338Q and T754S) or both (R418H) (Green *et al*, 2011; Song *et al*, 2008; Song *et al*, 2010).

In vitro studies have provided biological evidence suggesting that amino acid substitutions R264Q, L607F and S704C negatively impact on specific functions of DISC1 at the cellular and molecular level. In particular, L607F and S704C are associated with specific alterations in DISC1 expression profiles observed in schizophrenia patients (Nakata *et al*, 2009), and both have been shown to interfere with the recruitment of PCM1 to the centrosome in neuronal cells and glia (Eastwood *et al*, 2009; Eastwood *et al*, 2010). L607F additionally interferes with neurotransmitter release from cultured neuronal cells (Eastwood *et al*, 2009) and induces mitochondrial trafficking defects when expressed in neurons (Atkin *et al*, 2011). Both R264Q and L607F dampen the inhibitory effect of DISC1 on GSK3β, resulting in defects in Wnt signalling, neural progenitor proliferation and brain development (Singh *et al*, 2011). Finally, S704C reduces the kinase activity of Extracellular signal-regulated kinase 1 (ERK1) and Akt1 (Takahashi *et al*, 2009), alters DISC1 binding affinity to NDE1 and NDEL1 (Burdick *et al*, 2008; Kamiya *et al*, 2006), interferes with DISC1 oligomerisation (Leliveld *et al*, 2009) and impairs neuronal migration in the developing cortex (Singh *et al*, 2011). These findings are

consistent with the evidence from association and imaging studies, and support the hypothesis that R264Q, L607F and S704C may be functional variants that increase the risk of psychiatric illness by impacting on multiple aspects of DISC1 biology. On the other hand, no biological effects have been reported to date for any of the rare *DISC1* missense mutations associated with psychiatric illness, but ongoing research indicates that R37W enhances the mitochondrial localisation of DISC1 and induces perinuclear mitochondrial clustering when expressed in cell lines (Ogawa F., unpublished data) (Brandon *et al*, 2009). Despite the growing biological evidence supporting a functional role of risk-conferring DISC1 amino acid substitutions, the mechanisms linking them to the observed clinical phenotypes still need to be elucidated.

Predictions based on sequence conservation across species, location within protein structural motifs and likelihood of introducing detrimental structural changes in the protein suggest that human DISC1 amino acid substitutions R37W, R264Q, P432L, T603I, L607F and S704C are likely to affect the protein function ((Soares *et al*, 2011) and Soares D., unpublished observations) (Table 3.1 and Figure 3.1, adapted from Soares *et al*, 2011). Mouse DISC1 mutations Q31L and L100P, which are associated with abnormal cognitive and behavioural phenotypes in mice, are similarly predicted to negatively impact on the protein structure and function (Clapcote *et al*, 2007; Soares *et al*, 2011) (Table 3.2 and Figure 3.1). As a consequence of their potential for structural disruption, any of the above amino acid substitutions might interfere with the correct subcellular targeting of DISC1, which is inextricably linked with its function. Thus, to better elucidate their biological effects, I tested their ability to disrupt the subcellular distribution of the protein using *in vitro* models. Any such effect may provide valuable insight on the particular DISC1 functions and/or protein-protein interactions that could be affected by these amino acid substitutions. In particular, I focused on two subcellular compartments in which DISC1 is normally enriched and where it is thought to play important roles for brain development and function: the centrosome and the nucleus.

Sequence variant in DISC1	Sequence conservation and location on structure	Notes, motifs and potential effects on structure and function
Human common variants		
R264Q (Q264 minor allele frequency 0.2599)	R in *hs, pt, ma;* Not well conserved, Q not seen in any ortholog; loop	Lies close to peptide region in DISC1 266-290 mapped as PDE4B1 binding. Loss or gain of charge alters-interaction propensity?
L607F (F607 minor allele frequency 0.0986)	*hs, pt, ma, bt, cf, rn, mm, tr, dr;* strictly conserved; coiled coil helix	Located directly within a leucine zipper motif, within a heptad repeat at position 'd'. Change to Phe could alter the intricate Leu-Leu packing between adjacent helices. The presence of repeating leucine residues at position 'd' in leucine zippers is critical for modulating coiled-coil stability, maintaining oligomeric state, partner selection, and orientation of coiled coil helices. L607F is likely to impact on the structure of the protein.
S704C (C704 minor allele frequency 0.2472)	*hs, pt, ma, bt, rn, mm*; largely conserved amino acid position: G in *cf, tr, dr*; alpha-helix	S704C lies close (context amino acid) to a predicted nuclear export signal (NES4). The context around the leucine residues in the nuclear export signal has been suggested to play an important role (la Cour *et al*, 2004).
Human rare and ultra-rare mutations		
R37W	*hs, pt, ma, cf, rn, mm, tr, dr;* strictly conserved; alpha-helix	Proximal residue in mouse Q31L mutation (equivalent human residue R35) causes reduced binding to PDE4B1. Hence, R37W might also affect PDE4B binding (since it lies within binding peptide mapped to 31-65). It also lies close to Kal-7 binding site (41-100). R37W lies within tetra-arginine nuclear localization signal motif (R35-R38) (NLS1).

P432L	*hs, rn, mm*; low conservation; loop	Could alter DISC1 structure/conformation. May impact on DISC1 oligomerisation as it is located within a self-association domain (region 403-504). Located within a potential proline-directed kinase recognition site (T431-P432-L433-A434).
T603I	*hs, pt, ma, bt, cf, rn, mo*; highly conserved (S in *tr, dr*); coiled coil helix	Potential to disrupt a predicted phosphorylation site. Also close to ATF4 binding region 606-628 and near PDE4 (general) binding region 611-650.
Mouse missense mutations		
Q31L	*mm, rn*; Q31 is not conserved; in humans the equivalent amino acid is R35; boundary of loop and α-helix	Part of peptide region in DISC1 31-65 mapped as important for PDE4B1 binding. However, outside known GSK3β-binding regions. These have however been incompletely mapped. Clapcote and colleagues (Clapcote *et al*, 2007) suggested likely effects of the mouse mutations based upon the physicochemical properties of amino acids; that is, glutamine is hydrophilic and would normally be found surface exposed. This is probably true in the case of Q31, as it is immediately adjacent to the nuclear localization signal NES1. Q31 replaced by leucine, a hydrophobic amino acid, would be unfavourable at this position.
L100P	*mm, rn*; L100P is not conserved; in humans the equivalent amino acid is S100; loop	Adjacent to the peptide region 101-135 shown to bind PDE4B. However, outside known GSK3β binding regions. As mentioned above, these have been incompletely mapped. However, a change from a Leu to a Pro could have structural consequences, since Pro is a conformationally important amino acid.

Table 3.1 Sequence conservation and predicted structural effects of DISC1 sequence variants, adapted from Soares *et al,* 2011. *hs: Homo sapiens, pt: Pan*

troglodytes, ma: Macaca mulatta, bt: Bos taurus, cf: Canis familiaris, rn: Rattus norvegicus, mm: Mus musculus, tr: Takifugu rubripes, dr: Danio rerio.

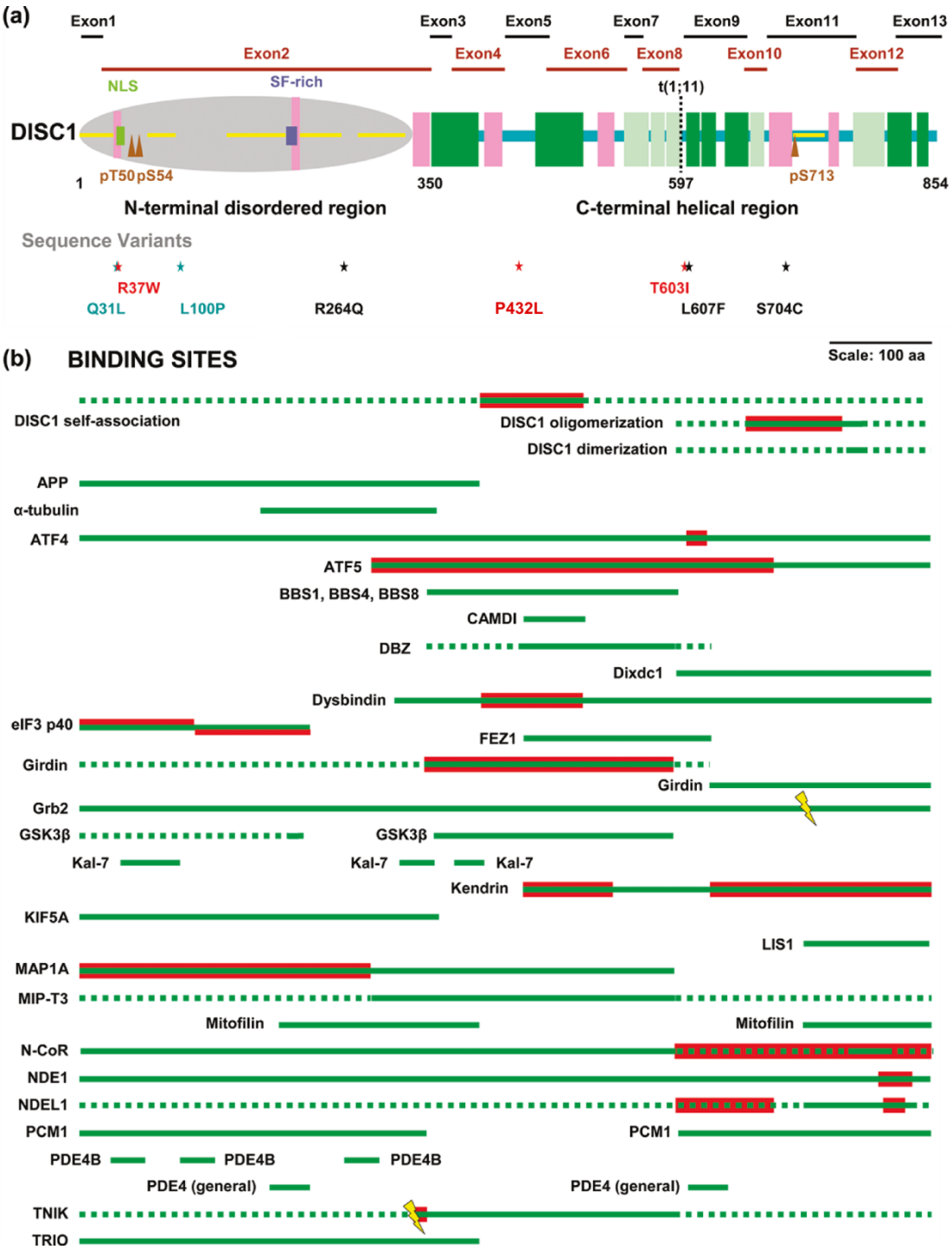

Figure 3.1 Position of DISC1 sequence variants in relation to the predicted structural motifs and known protein binding sites, adapted from Soares *et al,* 2011.

(A) Predicted secondary structure of DISC1 and position of sequence variants. The vertical rectangles represent regular or ambiguous α-helices (pink and light green, respectively, and coiled-coils (green). The horizontal yellow lines represent disordered regions. The position of the nuclear localisation signal (NLS) and SF-rich region is also indicated, along with that of the phosphorylation sites (brown triangles). The vertical dashed line marks the position of the t(1;11) translocation breakpoint, corresponding to amino acid 597. Common and rare/ultra rare human amino acid substitutions are indicated in black and red, respectively, whereas mouse mutations are in turquoise. (B) DISC1 regions that are known to be involved in self-association or protein binding. Regions that are sufficient for protein binding are in green; if two or more regions are sufficient for binding, the overlapping sections are indicated with a solid line and the rest with a dotted line. Regions that are essential for binding are in red. The bolts indicate short stretches of amino acids that abolish binding when mutated.

In actively dividing animal cells, microtubules nucleate from the centrosome, which functions as the main microtubule-organising center (MTOC) (Nigg & Raff, 2009). The centrosome consists of a pair of microtubule-based structures, the centrioles, embedded in an amorphous protein matrix, the pericentriolar matrix (PCM) (Nigg & Raff, 2009). As well as being essential for the process of cell division, it is well established that the centrosome plays important roles throughout neurodevelopment. In proliferating neural progenitors, the centrosome regulates asymmetrical distribution of cell fate factors to daughter cells, thus determining whether they will continue dividing, or begin differentiating (Higginbotham & Gleeson, 2007). Moreover, correct positioning of the centrosome is necessary for the establishment of cell polarity in newborn neurons, and for the correct migration of developing neurons to their final destinations in the brain (Kuijpers & Hoogenraad, 2011). As discussed in the introduction of this thesis, the correct centrosomal function of DISC1 is known to be important for proper brain development in animal models. Indeed, centrosomal DISC1 is involved in the recruitment of several proteins, including kendrin, dynein, dynactin, LIS1, NDEL1 and PCM1 to the centrosome (Soares *et al*, 2011) and in the regulation of fundamental processes such as neuronal migration and neurite

outgrowth (Kamiya *et al*, 2005; Kamiya *et al*, 2008; Miyoshi *et al*, 2004; Shimizu *et al*, 2008). Thus, DISC1 variants that prevent the correct positioning of DISC1 at the centrosome may have detrimental effects on brain structure and function.

Although the nuclear function of DISC1 has not been investigated as extensively as its roles at the centrosome, some studies provided intriguing clues suggesting that nuclear DISC1 may also be important for correct brain functioning. A particular example is represented by a study conducted on autopsied brains, which revealed aberrant nuclear distribution of DISC1 in psychiatric patients. In particular, a 75-85 kDa DISC1 protein isoform was found to be specifically enriched in nuclear extracts obtained from the orbitofrontal cortex of patients with schizophrenia and major depression. While this effect was correlated with drug abuse in patients with major depression, none of the common brain-associated confounding factors explained the nuclear enrichment of DISC1 in schizophrenic brains, suggesting aberrant DISC1 nuclear targeting as a potential pathogenetic mechanism (Sawamura *et al*, 2005). Another study examined the effects of brain-specific human DISC1 overexpression in the fruit fly *Drosophyla melanogaster* (Sawamura *et al*, 2008). In transgenic flies, expression of full-length DISC1 was limited to the nucleus, where the protein formed distinct puncta or speckles, whereas C-terminally truncated DISC1 ((DISC1(1-597)) assumed a diffuse distribution in both the nucleus and cytoplasm. Intriguingly, in male flies only, expression of full-length but not truncated DISC1 induced disturbances of sleep homeostasis, suggesting a potential role for nuclear DISC1 in the regulation of sleep/wake cycles (Sawamura *et al*, 2008). However, it is important to point out that invertebrates are not known to express endogenous DISC1 (Chubb *et al*, 2008). This represents a major limitation of this study, whose results should therefore be interpreted with caution. Nevertheless, the findings of Sawamura and colleagues are of particular relevance as they highlight the potential involvement of DISC1 in the regulation of sleep homeostasis, a process that is often disturbed in psychiatric patients (Schulz & Steimer, 2009; Wulff *et al*, 2009) and that is partly regulated by cAMP signalling (Zimmerman *et al*, 2008), a pathway in which DISC1 is involved by virtue of its modulatory interaction with PDE4 (Millar *et al*, 2005b; Murdoch *et al*, 2007).

DISC1 targeting to the nucleus is mediated by well-conserved cis-acting elements in the protein (Soares *et al*, 2011). The high degree of conservation of these nuclear targeting elements suggests that DISC1 may have important functions in the nucleus. *In silico* analyses originally identified two putative nuclear localisation signals (NLS) within DISC1 protein sequence (Brandon *et al*, 2005; Ma *et al*, 2002a; Taylor *et al*, 2003). The first is a classical tetra-arginine NLS motif (Kalderon *et al*, 1984; Nakai & Horton, 1999) at positions 35-RRRR-38 (NLS1), and the second is a bipartite motif (Nakai & Horton, 1999; Robbins *et al*, 1991) at positions 331-RKWEPVLRDCLLRNRRQ-347 (NLS2). Additionally, two putative nuclear export signals (NES) were identified at positions 504-513 (NES1) and 621-631 (NES2) (Brandon *et al*, 2005).

Two studies, whose results are detailed in the text below and summarised in Table 3.2, investigated the NLSs and NESs within DISC1 (Brandon *et al*, 2005; Sawamura *et al*, 2008). To better assess the role of the putative NLSs and NESs in DISC1, Brandon and colleagues expressed different mutant forms of GFP-tagged DISC1 in HeLa cells, and analysed their subcellular distribution by immunofluorescence (Brandon *et al*, 2005). Deletion of the tetra-arginine motif within NLS1 did not affect DISC1 localisation, nor did amino acid substitutions in NLS2, NES1 and NES2 that had previously been shown to block the function of similar motifs in other proteins, indicating that none of these motifs are functional (Brandon *et al*, 2005).

Domain mutated	**Details of the mutation**	**Effect on DISC1 nuclear localisation**	**References**
NLS1	31-AACFRRRRLARR-42 31-AACF********LARR-42	NONE	(Brandon *et al*, 2005)
NLS1	Deletion of amino acids 1-45	Impaired (not quantified)	(Sawamura *et al*, 2008)
NLS1	35-RRRRLARRP-43 35-AAAALARRP-43	Impaired by ~60%	(Sawamura *et al*, 2008)
NLS2	331-RKWEPVLRDCLLRNRRQ-347 331-NQWEPVLRDCLLRNQNQ-347	NONE	(Brandon *et al*, 2005)

NES1	502-CDLTPLVGQLSLGQ-515 502-CDATPAVGQASAGQ-515	NONE	(Brandon *et al*, 2005)
NES2	619-EGLEGLLSKLLVLSS-633 619-EGAEGAASKAAVVASS-633	NONE	(Brandon *et al*, 2005)
LZ	607-LTEEIRSLTSEREGLEGLLSKL-628 607-LTEEIRSPTSEREGPEGLLSKL-628	Impaired (not quantified)	(Sawamura *et al*, 2008)
NES2, NES4, LZ	Deletion of amino acids 598-854	Impaired by ~50%	(Sawamura *et al*, 2008)
NES3	546-LQERIKSLNL-555 546-LQERIKSSNL-555	Rescues nuclear targeting of DISC1 (1-597)	(Sawamura *et al*, 2008)

Table 3.2 Summary of the mutation analyses conducted on the putative NLSs and NESs in DISC1. The asterisks indicate deletion of the corresponding amino acids. The mutated amino acids are underlined.

The putative NLSs and NESs in DISC1 were further analysed in a subsequent study that adopted a similar strategy, but used the HA epitope instead of GFP to tag DISC1 (Sawamura *et al*, 2008). A DISC1 (46-854) deletion construct lacking NES1 displayed defective nuclear targeting, and so did a mutant DISC1 form in which the tetra-arginine motif within NES1 had been replaced by a stretch of four alanines (Sawamura *et al*, 2008). Consistently, an eGPF-NLS1 chimera was efficiently targeted to the nucleus, whereas its counterpart containing a mutated NLS1 was not (Sawamura *et al*, 2008). This is in contrast with the findings of Brandon and colleagues, who saw no effect of deletion or mutation of NES1 (Brandon *et al*, 2005). This discrepancy is likely caused by technical differences between the studies, and in particular by the use of different DISC1 tagging epitopes. Indeed, GFP tagging is known to interfere with DISC1 subcellular targeting (Kirsty Millar, personal communication), and might have masked the effect of NLS1 mutation in the experiments described by Brandon and colleagues (Brandon *et al*, 2005). By contrast, and in agreement with the findings of Brandon and colleagues, an eGFP-NLS2 chimera did not localise to the nucleus, suggesting that NLS1, but not NLS2,

is an active NLS within DISC1 (Sawamura *et al*, 2008). Sawamura and collegues also identified an additional putative NES at DISC1 positions 546-555 (NES3), and showed that a leucine to serine substitution at position 553 within NES3 results in redistribution of DISC1 (1-597) from the cytoplasm to the nucleus, while an eGFP-NES3 chimera was localised entirely to the nucleus (Sawamura *et al*, 2008). This led the authors to conclude that NES3 is a functional NES, although reservations based on the structural conformation of this region were raised recently (Soares *et al*, 2011). Finally, Sawamura and colleagues reported that the introduction of leucine to proline substitutions at positions 614 and 621, within the putative leucine zipper spanning residues 607-628, results in cytoplasmic distribution of DISC1 (Sawamura *et al*, 2008). Consistently, DISC1 (1-597) showed defective nuclear localisation (Sawamura *et al*, 2008). A more recent bioinformatic investigation led to the identification of a further putative NES (NES4) within DISC1, at positions 607-709, which has not been experimentally investigated yet (Soares *et al*, 2011).

3.2 Generation of DISC1 expression constructs

3.2.1 *Human DISC1 expression constructs*

The construct pcDNA4/TO-Flag DISC1 (Table 2.2), encoding N-terminally Flag-tagged full-length human DISC1 (isoform L) was used as template in a series of site-directed mutagenesis reactions to generate a selected panel of DISC1 amino acid variants. The resulting expression constructs (n=20) carried either a rare or ultra-rare DISC1 mutation (37W, 432L or 603I) or the common variant 607F in all possible combinations with the common polymorphisms R264Q and S704C (Figure 3.2). With the exception of R264Q and P432L, all of the above DISC1 variants are at highly conserved amino acid positions, and all have the potential to influence the subcellular distribution of DISC1, either because they are predicted to disrupt critical structural motifs, or because they occur in regions of DISC1 that mediate binding to key partner proteins (Soares *et al*, 2011) (Table 3.1 and Figure 3.1). Variant P432L is predicted to impact on the structure/function of DISC1 but does not increase the risk of schizophrenia (Song *et al*, 2008), thus it might provide useful information on the relation between altered protein distribution and risk of disease. By combining

common and rare DISC1 amino acid substitutions, the expression constructs generated here offer the possibility to test for potential functional interactions between distinct risk-conferring *DISC1* missense variants.

The expression constructs encoding N-terminally Myc-tagged wild-type, 37W or 607F DISC1 as well as the DISC1ΔLZ9 mutant, which lacks the leucine zipper spanning amino acids 607-628 in exon 9, were all generated from the corresponding pcDNA4/TO-Flag DISC1 constructs by site-directed mutagenesis.

Partially overlapping sequences spanning the entire DISC1 coding sequence were obtained for each construct to verify that only the desired nucleotide substitutions had been introduced. The details of the mutagenic and sequencing primers used to generate the human DISC1 expression constructs used in this thesis are reported in tables 2.6 and 2.7, respectively.

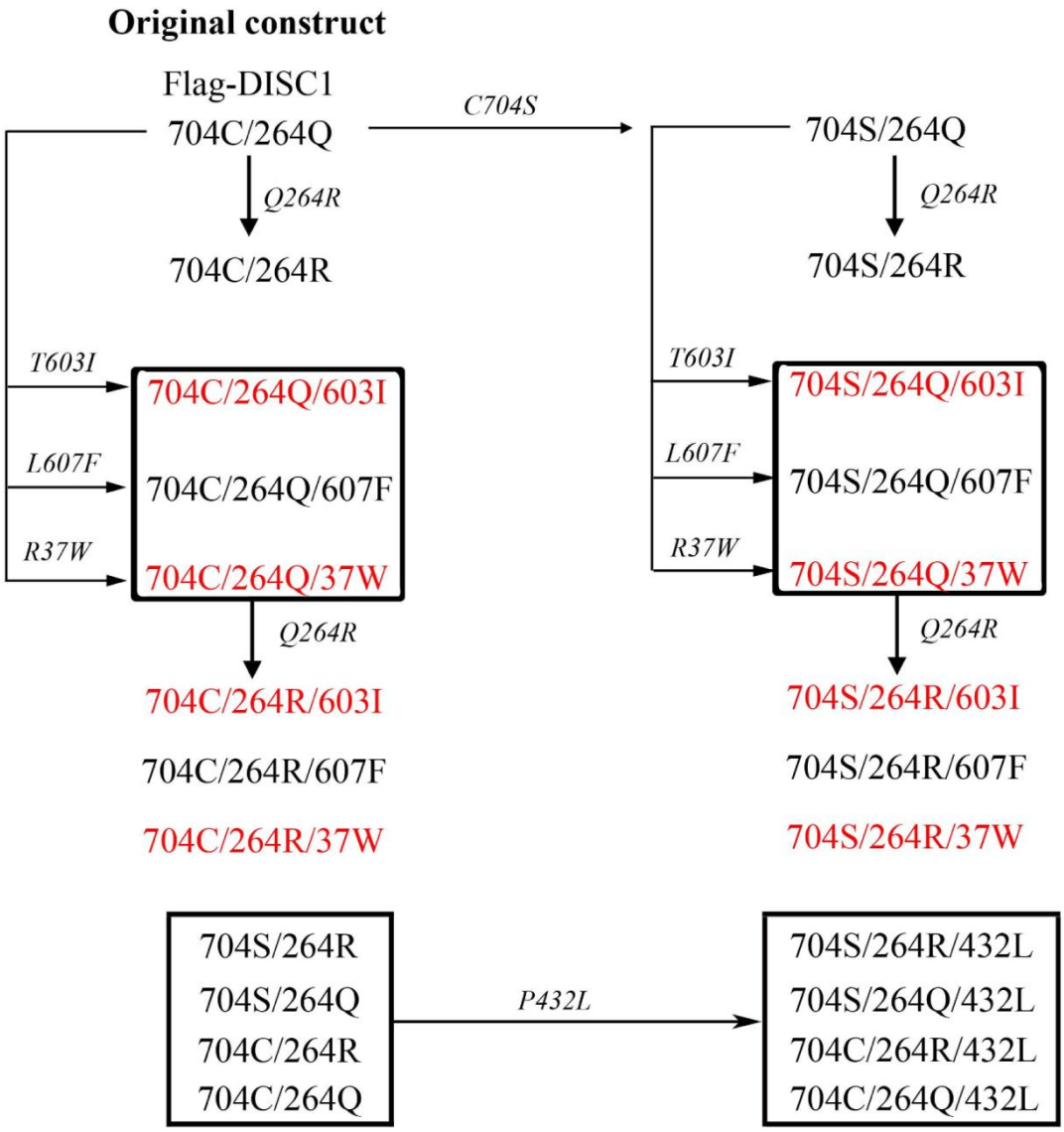

Figure 3.2 Generation of human DISC1 expression constructs by site-directed mutagenesis. The diagram represents the mutagenic reactions used to generate the human DISC1 variant expression constructs used in this thesis. DISC1 constructs are named according to the amino acid substitution(s) carried by the respective encoded protein. The constructs carrying common variants only are in black, whereas the ones carrying rare or ultra-rare mutations are in red. The arrows represent individual mutagenic reactions, and the resulting amino acid substitution is reported above each arrow in italics.

3.2.2 *Mouse Disc1 expression constructs*

The constructs pcDNA4/TO-Flag mDisc1, encoding N-terminally tagged wild-type, 31L or 100P mouse Disc1 were generated from the corresponding pRK5-HA Disc1 plasmids (Table 2.2). The Disc1 coding sequences in pRK5 were amplified by PCR using primers Mouse Disc1 HA F and Mouse Disc1 R (Table 2.8) and sub-cloned between the EcoRI and NotI sites of pcDNA4/TO (Table 2.2). After sub-cloning in pcDNA4/TO, the HA tag was replaced with the Flag tag by restriction with EcoRI and PpuMI followed by religation with the chemically synthesised oligonucleotides Mouse Disc1 mut F and Mouse Disc1 mut R (Table 2.8). The resulting expression constructs were verified by direct sequencing using primers SP6 F and BGH R (Table 2.7).

3.3 Analysis of the subcellular distribution of DISC1 variants by immunocytochemistry

3.3.1 *Human DISC1 variants*

3.3.1.1 *Analysis of the centrosomal abundance of DISC1 variants*

To determine the relative abundance of human DISC1 variants at the centrosome, COS7 cells were transfected with equal amounts of the 20 Flag-DISC1 expression constructs individually and subsequently double-stained with an anti-Flag and an anti-γ-tubulin antibody (Table 2.5) to detect exogenous DISC1 and the centrosome, respectively (Figure 3.3).

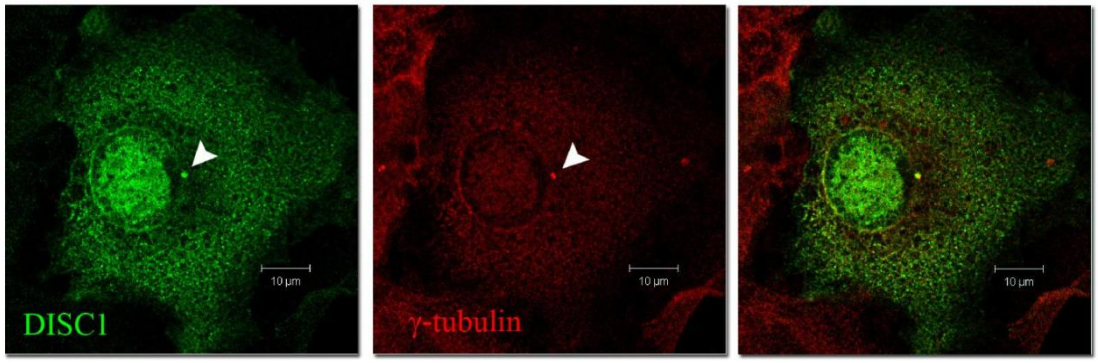

Figure 3.3 Confocal image of a representative COS7 cell expressing exogenous Flag-DISC1 and stained with the Flag RPC and the γ-tubulin M antibodies. The arrowheads indicate the centrosome.

Confocal images of at least 20 transfected cells for each DISC1 variant were acquired and analysed as described in detail in the methods chapter of this thesis (paragraphs 2.5.7.3 and 2.5.7.3.1). For each DISC1 variant analysed, the proportion of exogenous DISC1 localising at the centrosome was calculated as the ratio between the total pixel intensity of DISC1 staining at the centrosome and the total pixel intensity of DISC1 staining in the whole cell, and was used as an estimate of the efficiency of DISC1 centrosomal targeting (Figure 3.4). The common variant of DISC1, or wild-type DISC1, was the reference against which all other variants were compared. No statistically significant difference between the variants was detected using two-way ANOVA, probably due to the high variability of the centrosomal distribution observed for some DISC1 variants. However, it is interesting to note that although neither of the common amino acid substitutions 264R and 704C alone seems to produce any effect on DISC1 centrosomal targeting, the centrosomal abundance of both mutants 432L and 603I appears to be influenced by the concomitant presence of the 704C substitution, albeit with opposing effects (Figure 3.4). Similarly, while the common 607F variant is efficiently targeted to the centrosome, its combination with either 264Q or 704C appears to be detrimental for DISC1 centrosomal abundance, which is particularly decreased when all three variants are present together (Figure 3.4). Although no firm conclusions can be drawn from this experiment, it appears possible that different combinations of amino

acid substitutions may have substantially different effects on the centrosomal localisation of DISC1. In particular, two neutral substitutions may become detrimental when combined and, on the other hand, the effects of a deleterious substitution may be rescued by the simultaneous presence of a second substitution. Further analyses will be needed to accept or reject these preliminary observations.

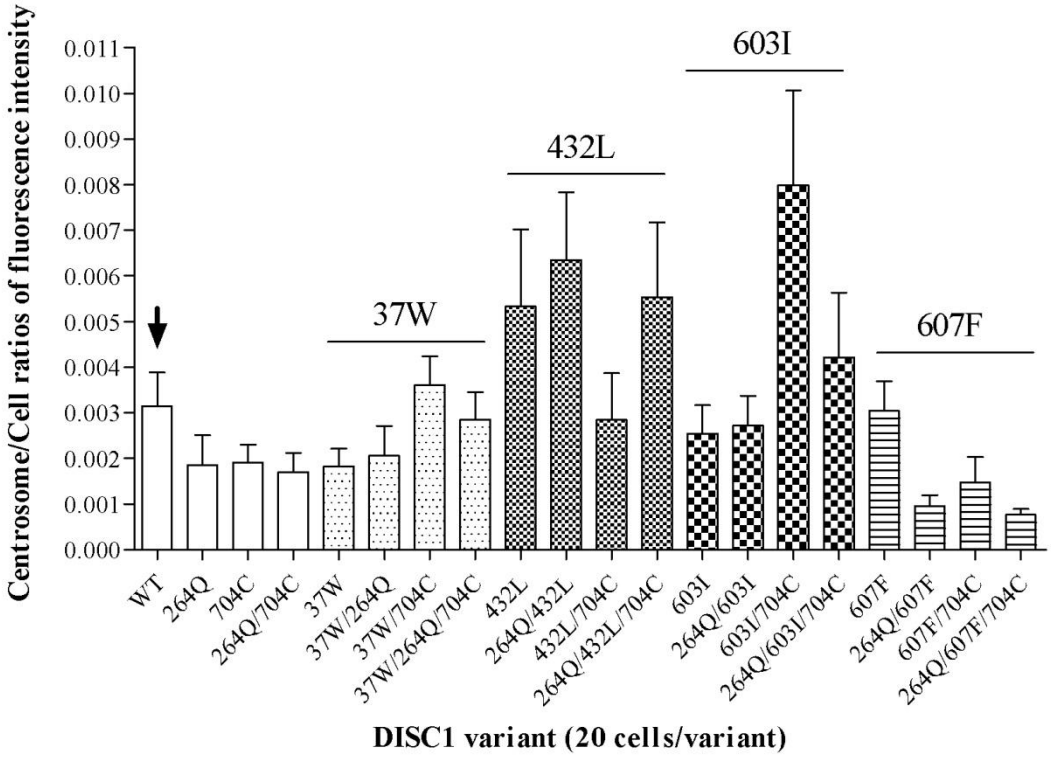

Figure 3.4 Centrosomal distribution of DISC1 variants. Relative centrosomal abundance of exogenous DISC1 in transfected COS7 cells. The arrow indicates the reference wild-type DISC1 variant, to which all other variants were compared. The bars represent the average of 20 cells/variant analysed in a single experiment.

3.3.1.2 *Analysis of the nuclear abundance of DISC1 variants*

To assess the potential effect of common and rare DISC1 amino acid substitutions on the nuclear targeting of the protein, COS7 cells were transfected with either one of

the 20 Flag-DISC1 expression constructs and subsequently stained with an anti-Flag antibody and the nuclear dye TO-PRO-3. Single-plane confocal images of individual transfected cells were then acquired and analysed as detailed in paragraphs 2.5.7.3 and 2.5.7.3.2. As for the centrosome, the relative nuclear abundance of each DISC1 variant was calculated as the ratio between the total pixel intensity of DISC1 staining in the nucleus and the total pixel intensity of DISC1 staining in the whole cell. A pilot experiment in which at least 20 cells/variant were analysed demonstrated that sequence changes at positions 264, 432, 603 or 704 do not interfere with the nuclear targeting of DISC1 (Figures 3.5 and 3.6), nor do they grossly alter the overall subcellular distribution of DISC1 (Figure 3.6). However, it cannot be excluded that these variants might have subtle and/or cell type-specific effects on DISC1 targeting, whose detection requires more sensitive and specific methods. On the other hand, the R to W, and L to F substitutions at positions 37 and 607, respectively, result in partial depletion of exogenous DISC1 from the nucleus (Figures 3.5 and 3.6). Additional variation at positions 264 and 704 does not modify the effect of 37W or 607F on the nuclear abundance of DISC1 (Figure 3.5).

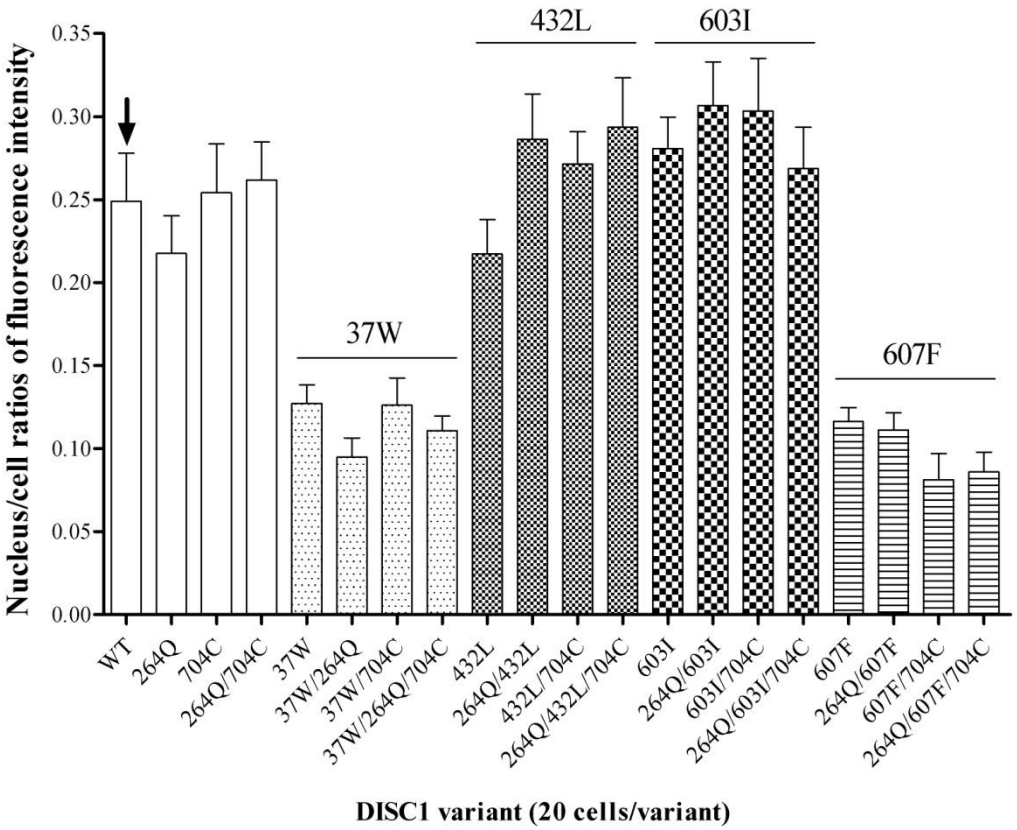

Figure 3.5 Nuclear distribution of DISC1 variants. Relative abundance of DISC1 variants in the nucleus of transfected COS7 cells, calculated as the ratio between the total pixel intensity of DISC1 staining in the nucleus and the total pixel intensity of DISC1 staining in the whole cell. The bars represent mean measurements of 20 cells/variant carried out in a single experiment. The arrow indicates the common variant of DISC1 (WT), to which all other variants are compared.

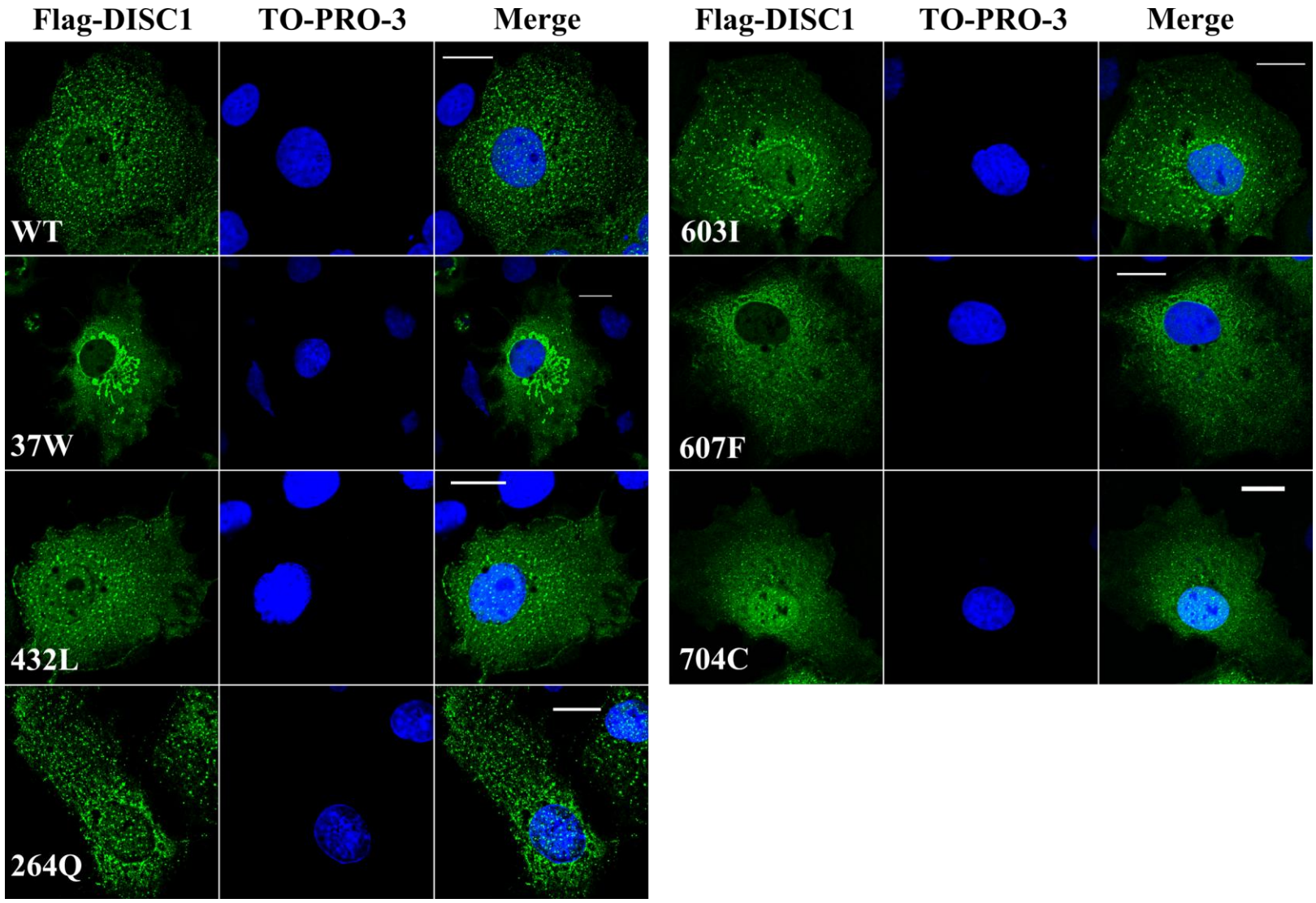
Flag-DISC1
TO-PRO-3
Merge
Flag-DISC1
TO-PRO-3
Merge
WT
603I
37W
607F
432L
704C
264Q

Figure 3.6 Subcellular distribution of DISC1 variants. Representative COS7 cells expressing the indicated DISC1 variants and stained with the Flag RPC antibody to detect the exogenous protein. Nuclei were counterstained with TO-PRO-3. Scale bars are 20 µm.

These preliminary observations on the effect of 37W and 607F on the nuclear distribution of DISC1 were confirmed by further immunocytochemistry experiments in which a larger sample of cells was analysed (Figures 3.7). Both sequence variants reduce the nuclear expression of DISC1 by approximately 50% ($P<0.01$).

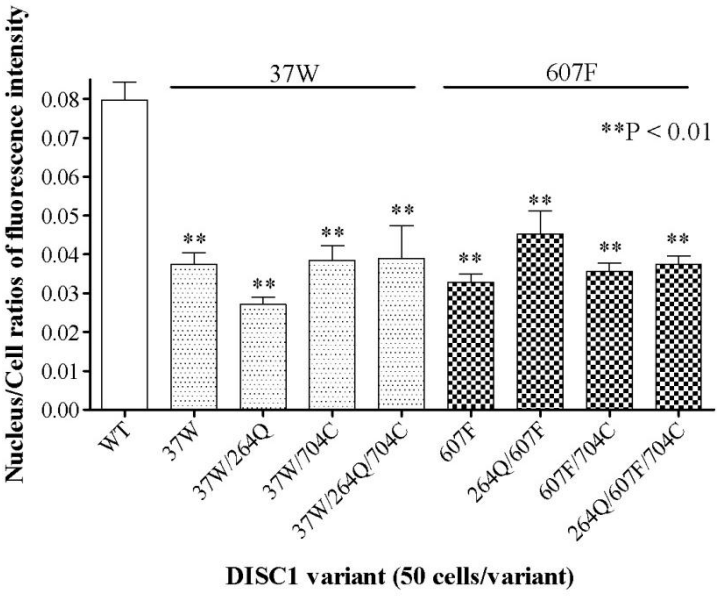

Figure 3.7 Nuclear distribution of DISC1 variants. Relative abundance of DISC1 variants in the nucleus of transfected COS7 cells calculated as the ratio between the total pixel intensity of DISC1 staining in the nucleus and the total pixel intensity of DISC1 staining in the whole cell. The bars represent the mean values measured in 3 independent experiments in which 50 cells/variant were analysed, for a total of 150 cells/variant. Data were analysed by one-way ANOVA followed by Dunnett's Multiple Comparisons Test.

The observed decrease in nuclear expression of DISC1-37W or DISC1-607F is not due to decreased overall expression of these DISC1 variants (Figure 3.8), which confirms that DISC1 carrying R or L at positions 37 and 607, respectively, is targeted to the nucleus more efficiently.

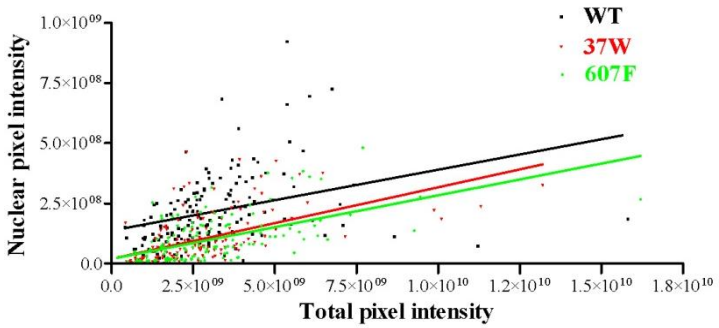

Figure 3.8 Scatterplot and regression lines of total pixel intensity of DISC1 staining in the whole cell (x-axis, independent variable) vs. nucleus (y-axis, dependent variable) in individual COS7 cells transfected with wild-type DISC1, DISC1-37W or DISC1-607F. The graph was generated by pooling measurements obtained from 50 cells/variant in 3 independent experiments (150 cells/variant in total). Pearson r (95% confidence interval) = 0.3337, P<0.0001 (wild-type DISC1); 0.5648, P<0.0001 (DISC1-37W); 0.5760, P<0.0001 (DISC1-607F).

Since there is no evidence for an effect of amino acid variation at positions 264 and 704 on the subcellular distribution of DISC1, all the subsequent experiments were performed using DISC1 constructs encoding the common variants at these positions (264R and 704S). The common DISC1 variant, to which all other variants analysed here are compared, will henceforth be referred to in the text as "wild-type (WT) DISC1"

The defective nuclear targeting of DISC1-37W and DISC1-607F is not limited to COS7 cells, as the same effect can be observed upon expression of these variants in SH-SY5Y human neuroblastoma cells (Figure 3.9). Consistently, when expressed in

primary mouse hippocampal neurons, DISC1-WT, but not DISC1-37W is efficiently targeted to the nucleus (Figure 3.10).

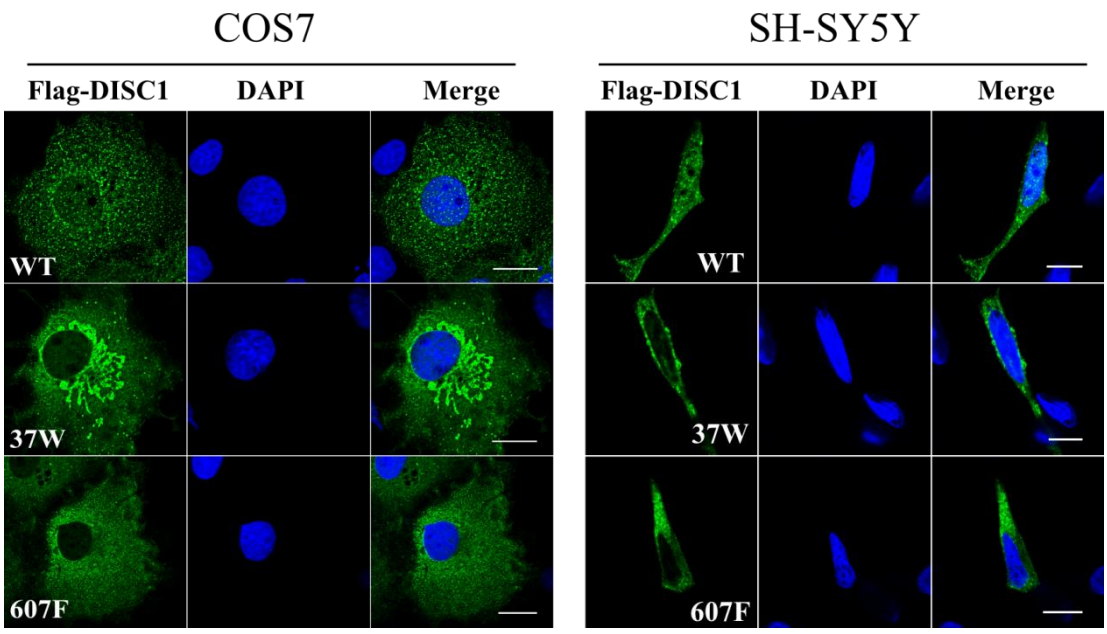

Figure 3.9 Subcellular distribution of DISC1 variants in COS7 and SH-SY5Y cells. Confocal images of representative COS7 and SH-SY5Y cells expressing DISC1-WT, DISC1-37W or DISC1-607F and stained with the Flag RPC antibody (green). Nuclei (blue) are counterstained with DAPI. Scale bars are 20 µm (COS7 cells) and 10 µm (SH-SY5Y cells).

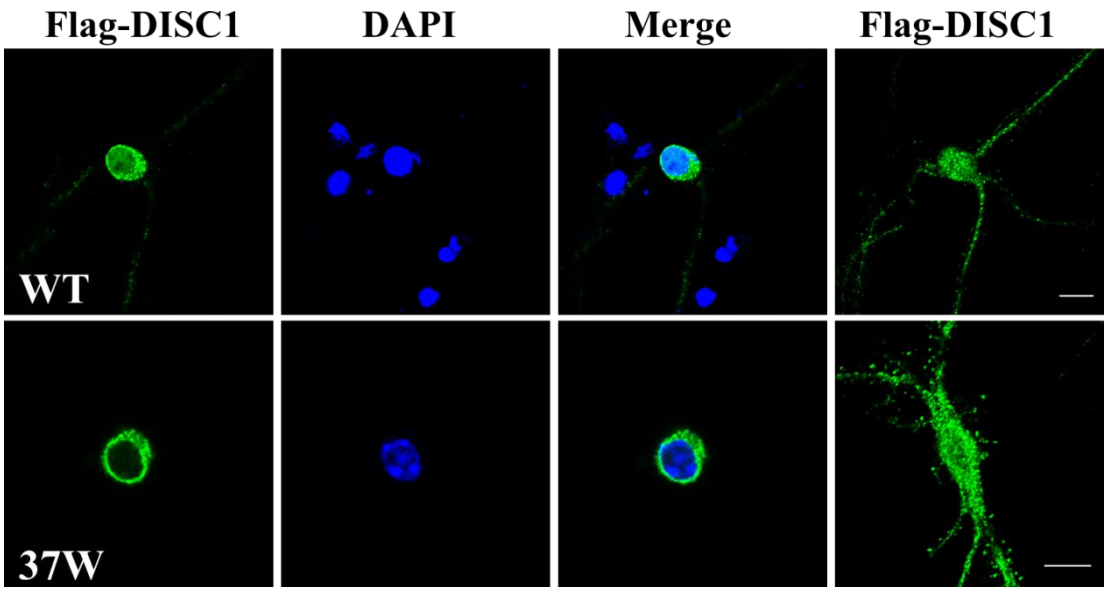

Figure 3.10 Distribution of DISC1 variants in hippocampal neurons. Primary mouse hippocampal neurons were transfected with pcDNA4/TO-FLAG DISC1-wild-type or pcDNA4/TO-Flag DISC1-37W after 21 days in vitro and stained with the Flag RPC antibody to detect exogenous DISC1 (green). Confocal images of individual transfected neurons were acquired focusing on the nucleus (left hand panels) or on the neurites (far-right panels). Nuclei (blue) are counterstained with DAPI. Scale bars are 10µm.

When expressed in cell lines, DISC1-37W is recruited to the mitochondria, and it induces the formation of perinuclear mitochondrial clusters (Figures 3.6 and 3.9), which is the subject of a separate study (Ogawa F., unpublished data). To establish whether the defective nuclear targeting of DISC1-37W is related to its increased recruitment to mitochondria, COS7 cells were transfected with a construct expressing the mutant DISC1-37A, which was kindly provided by Fumiaki Ogawa. Independent investigations have established that like 37W, the artificial mutation 37A elevates DISC1 mitochondrial targeting and induces mitochondrial aggregation, but it does so to a much lesser extent than 37W (Ogawa F., unpublished data). Thus, if the defective nuclear targeting of DISC1-37W is related to its aberrant recruitment to the mitochondria, this phenotype should be markedly attenuated in cells expressing DISC1-37A.

However, when expressed in COS7 cells, the nuclear distribution of DISC1-37A is indistinguishable from that of DISC1-37W, indicating that both mutants are equally excluded from the nucleus (Figure 3.11). This suggests that the defective nuclear targeting of DISC1-37W is likely a direct consequence of the disruption of NSL1 by this mutation and it is not caused indirectly by its preferential accumulation at the mitochondria.

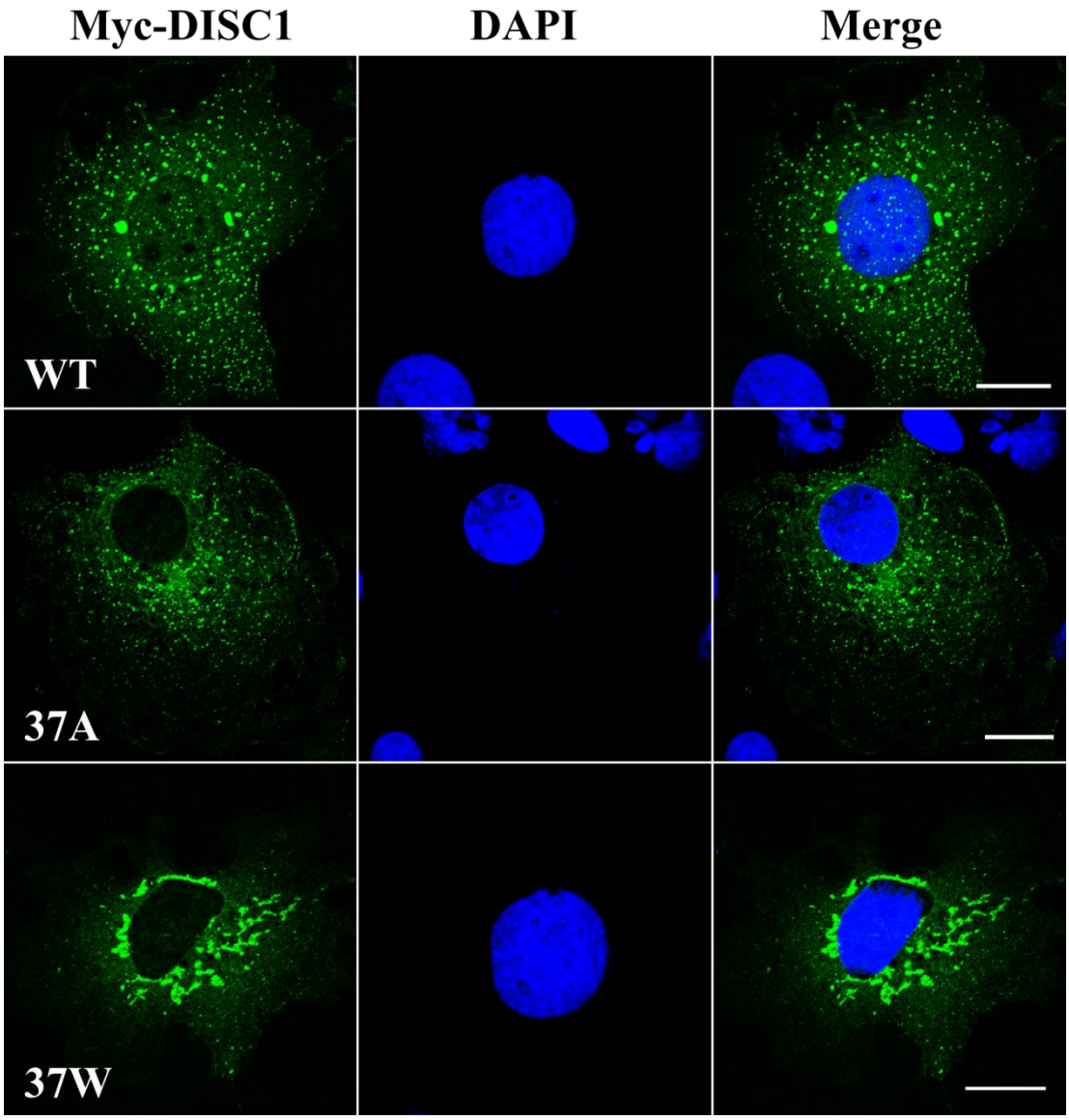

Figure 3.11 Subcellular distribution of DISC1-37A. Representative COS7 cells transfected with either pcDNA3.1-Myc DISC1-WT, pcDNA3.1-Myc DISC1-37W or pcDNA3.1-Myc DISC1-37A (Table 2.2), which were provided by Fumiaki Ogawa.

Exogenous DISC1 was detected with the c-myc antibody (Table 2.5). Nuclei (blue) are stained with DAPI. Scale bars are 20 µm.

Leucine 607 is part of a predicted leucine zipper located in DISC1 exon 9 (DISC1LZ9), spanning amino acids 607-628. This putative leucine zipper is thought to be important for the correct nuclear targeting of DISC1, as alanine substitutions at positions 614 and 621 result in exclusion of DISC1 from the nucleus (Sawamura *et al*, 2008) (Table 3.2). To confirm that DISC1LZ9 is indeed an important cis-acting element that controls the nuclear distribution of DISC1, the subcellular distribution of a mutant form of DISC1 lacking LZ9 (DISC1ΔLZ9) was analysed in transfected COS7 cells. As expected, deletion of LZ9 prevents the nuclear accumulation of DISC1, suggesting that the defective nuclear targeting of DISC1-607F may arise from its disruption of this important structural motif (Figure 3.12).

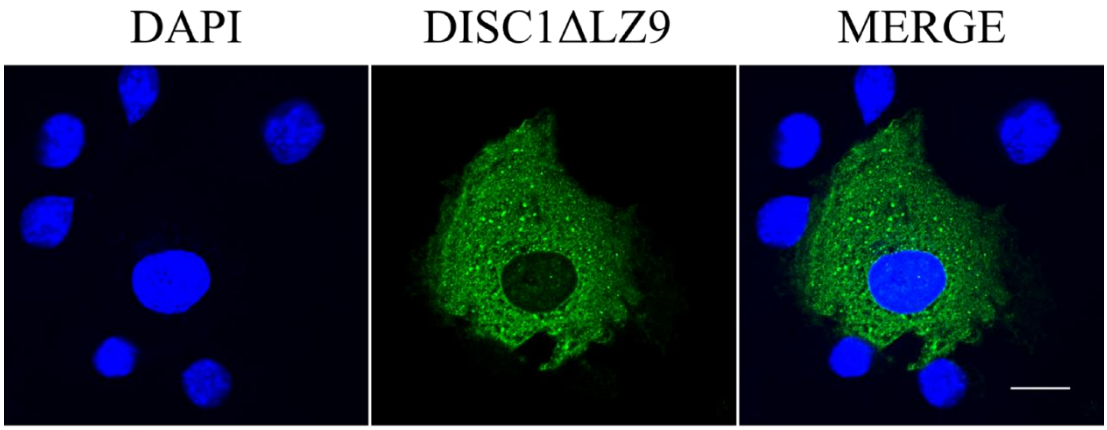

Figure 3.12 Subcellular distribution of DISC1ΔLZ9. Confocal images of a representative COS7 cell expressing DISC1ΔLZ9 and stained with the Flag RPC antibody (green). Nuclei (blue) are stained with DAPI. The scale bar is 20 µm.

Interestingly, besides interfering with the nuclear targeting of DISC1, 607F additionally promotes a more diffuse cytoplasmic distribution of the protein, with

fewer large punctate cytoplasmic structures evidenced by immunocytochemistry (Figure 3.13).

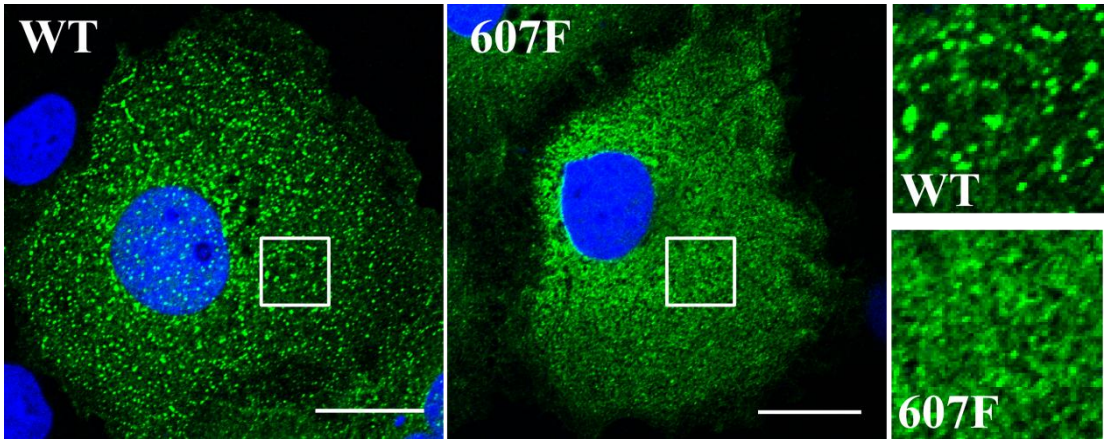

Figure 3.13 Subcellular distribution of DISC1-607F. Confocal images of representative COS7 cells expressing either DISC1-WT or DISC1-607F and stained with the Flag RPC antibody (green). Nuclei (blue) are stained with DAPI. The cytoplasmic regions delimited by the white squares are magnified in the panels on the right. Scale bars are 20 μm.

Due to the propensity of DISC1 to oligomerise (Leliveld *et al*, 2008; Leliveld *et al*, 2009; Narayanan *et al*, 2011; Ottis *et al*, 2011), I hypothesised that risk-conferring DISC1 variants 37W and 607F might affect the nuclear targeting of wild-type DISC1 in a dominant-negative fashion. To further examine this, DISC1-37W or DISC1-607F were co-expressed with wild-type DISC1 in COS7 and SH-SY5Y cells and the subcellular distribution of each variant was analysed by immunocytochemistry, using cells transfected with wild-type DISC1 only as a control. As expected, when wild-type DISC1 is expressed alone it translocates to the nucleus, where it is detectable as numerous bright puncta on a more diffuse background (Figure 3.14). As predicted, both DISC1-37W and DISC1-607F reduce the formation of wild-type DISC1 puncta in the nucleus and, as observed in a separate study (Ogawa F., unpublished data), DISC1-37W recruits wild-type DISC1 to large perinuclear mitochondrial aggregates (Figure 3.14).

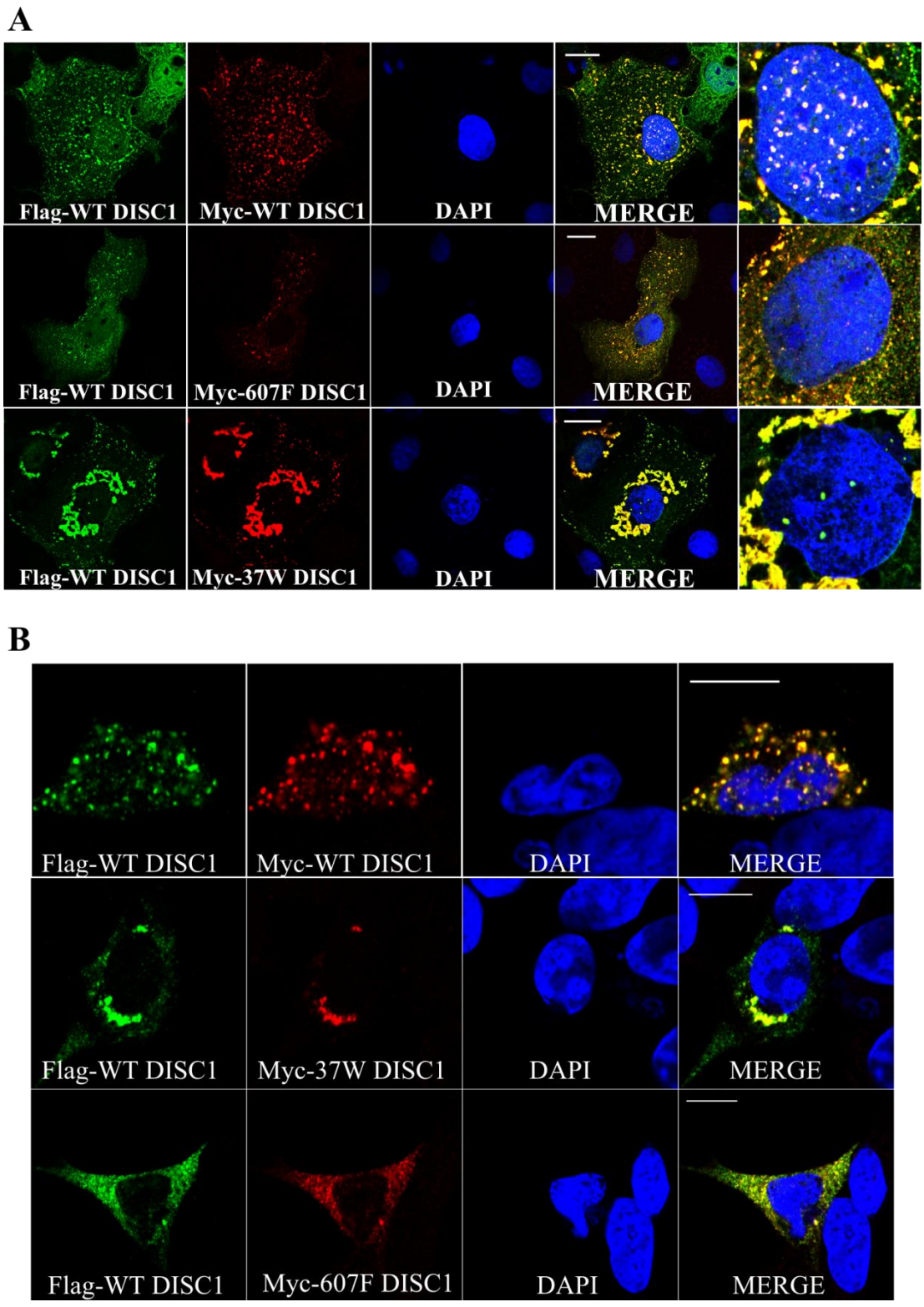

Figure 3.14 Dominant-negative effect of DISC1-37W and DISC1-607F. Subcellular distribution of Flag-DISC1 (green) and Myc-DISC1 (red) in representative COS7 (A) or SH-SY5Y cells (B) transfected with pcDNA4/TO-Flag DISC1-WT in combination

with an equal amount of either pcDNA4/TO-Myc DISC1-WT (top), pcDNA4/TO-Myc DISC1-37W (middle) or pcDNA4/TO-Myc DISC1-607F (bottom). Flag-DISC1 and Myc-DISC1 were detected using the Flag RPC and c-myc antibodies, respectively. Magnifications of the nuclei are shown in the far-right panels in (A). Nuclei (blue) are stained with DAPI. Scale bars are 20µm (A) and 10µm (B).

3.3.1.3 *Analysis of the mitochondrial distribution of DISC1 variants*

A pool of DISC1 normally localises to mitochondria and is involved in mitochondrial function (Atkin *et al*, 2011; Brandon *et al*, 2005; James *et al*, 2004; Millar *et al*, 2005a; Ozeki *et al*, 2003; Park *et al*, 2010). Given that 37W has been shown to both enhance the recruitment of DISC1 to this organelle and induce mitochondrial clustering in the perinuclear region (Ogawa F. unpublished data), the potential effect of other DISC1 amino acid substitutions on the mitochondrial targeting of the protein and/or mitochondrial morphology was examined by immunocytochemistry. As shown in figure 3.15, amino acid substitutions 264Q, 432L, 603I, 607F and 704C do not appear to interfere with DISC1 mitochondrial targeting, nor do they grossly alter mitochondrial morphology. However, since a precise quantification of the mitochondrial pool of DISC1 was not carried out in this thesis, it is not possible to exclude that the above variants may have more subtle influences on the mitochondrial targeting of the protein.

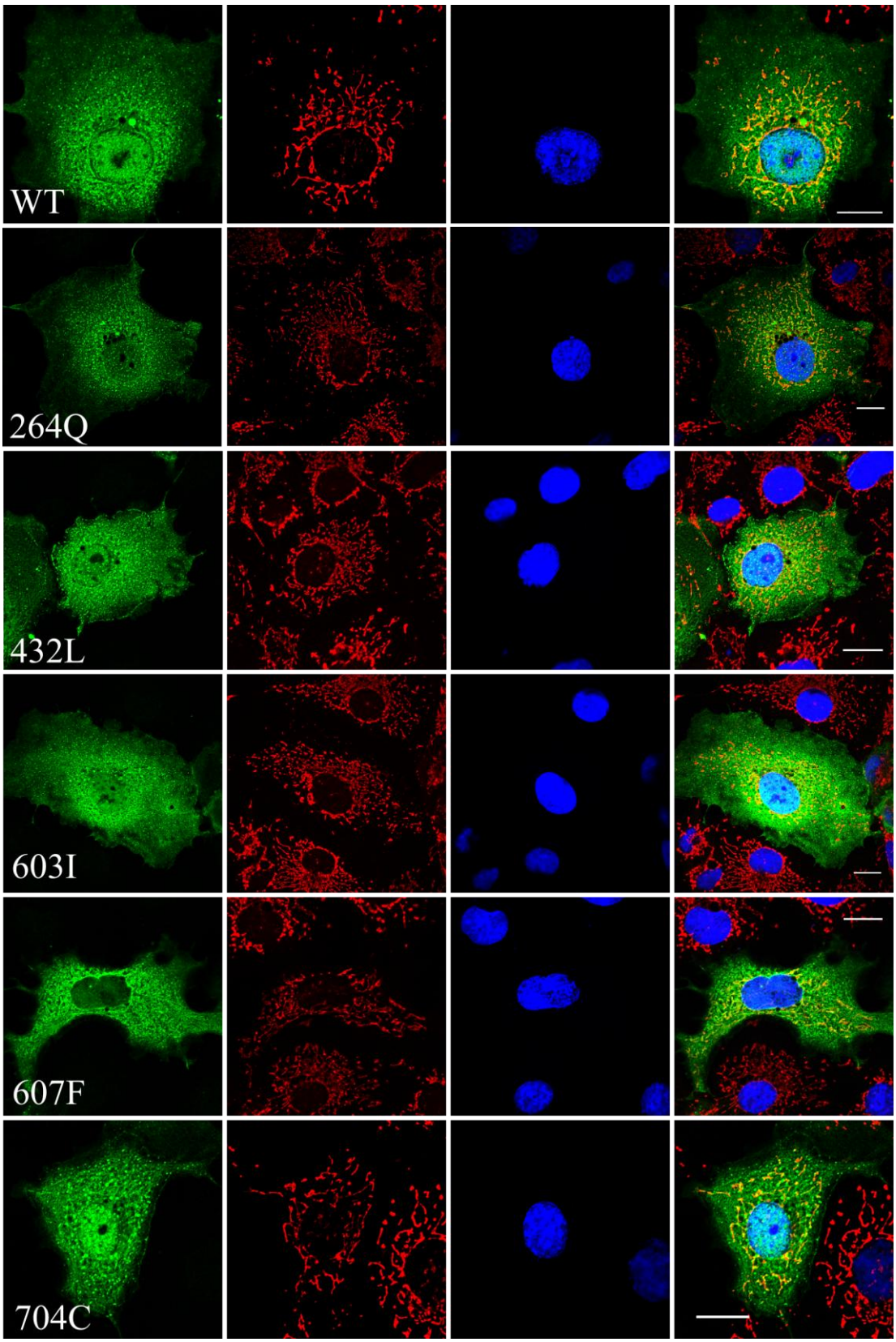

Figure 3.15 Mitochondrial distribution of DISC1 variants. COS7 cells expressing the indicated Flag-DISC1 variant were stained with the Flag RPC antibody (green) and

the fluorescent mitochondrial dye Mitotracker (red) and analysed by confocal microscopy. Nuclei (blue) are stained with DAPI. Scale bars are 20 µm.

3.3.2 *Mouse Disc1 variants*

The ENU-induced amino acid substitutions Q31L and L100P determine depression-like and schizophrenia-like behavioural phenotypes in mice, respectively (Clapcote *et al*, 2007). Both mutations reduce Disc1 interaction with PDE4B and GSK3β (Clapcote *et al*, 2007; Lipina *et al*, 2011a; Lipina *et al*, 2011b). Additionally, 31L inhibits the activity of PDE4 and enhances that of GSK3β, while 100P affects dopamine function (Clapcote *et al*, 2007; Lipina *et al*, 2011a; Lipina *et al*, 2010; Lipina *et al*, 2011b). Amino acid positions 31 and 100 are not conserved between human and mouse, and nor 31L or 100P correspond to known clinical mutations (Table 3.1, Figure 3.1) (Soares *et al*, 2011). However, since they both occur in the proximity of functional domains or protein binding regions within Disc1 and they both have the potential to introduce deleterious structural changes, these amino acid substitutions might affect the subcellular distribution of the protein, and could provide useful clues on the relation between altered DISC1 distribution and function (Table 3.1, Figure 3.1) (Soares *et al*, 2011). In particular, 31L may interfere with the nuclear targeting of Disc1 as it is located in close proximity to NLS1 (Table 3.1, Figure 3.1) (Soares *et al*, 2011). To test for possible effects of 31L and 100P on Disc1 localisation, the distribution of mDisc1-WT, 31L and 100P was analysed by immunocytochemistry in transfected COS7 cells (Figure 3.16). Overall, the distribution of mouse Disc1 is very similar to that of the human protein, the only exception being that the nuclear staining is slightly less prominent for the former (Figure 3.16). Qualitative comparison of transfected cell images did not reveal any gross abnormalities in the subcellular distribution of Disc1 mutants 31L and 100P (Figure 3.16). In particular, the nuclear distribution of Disc1-31L was indistinguishable from that of the wild-type protein (Figure 3.16). However, these observations do not exclude the possibility that either Disc1 mutant may have more subtle and/or cell type-specific affects on Disc1 targeting.

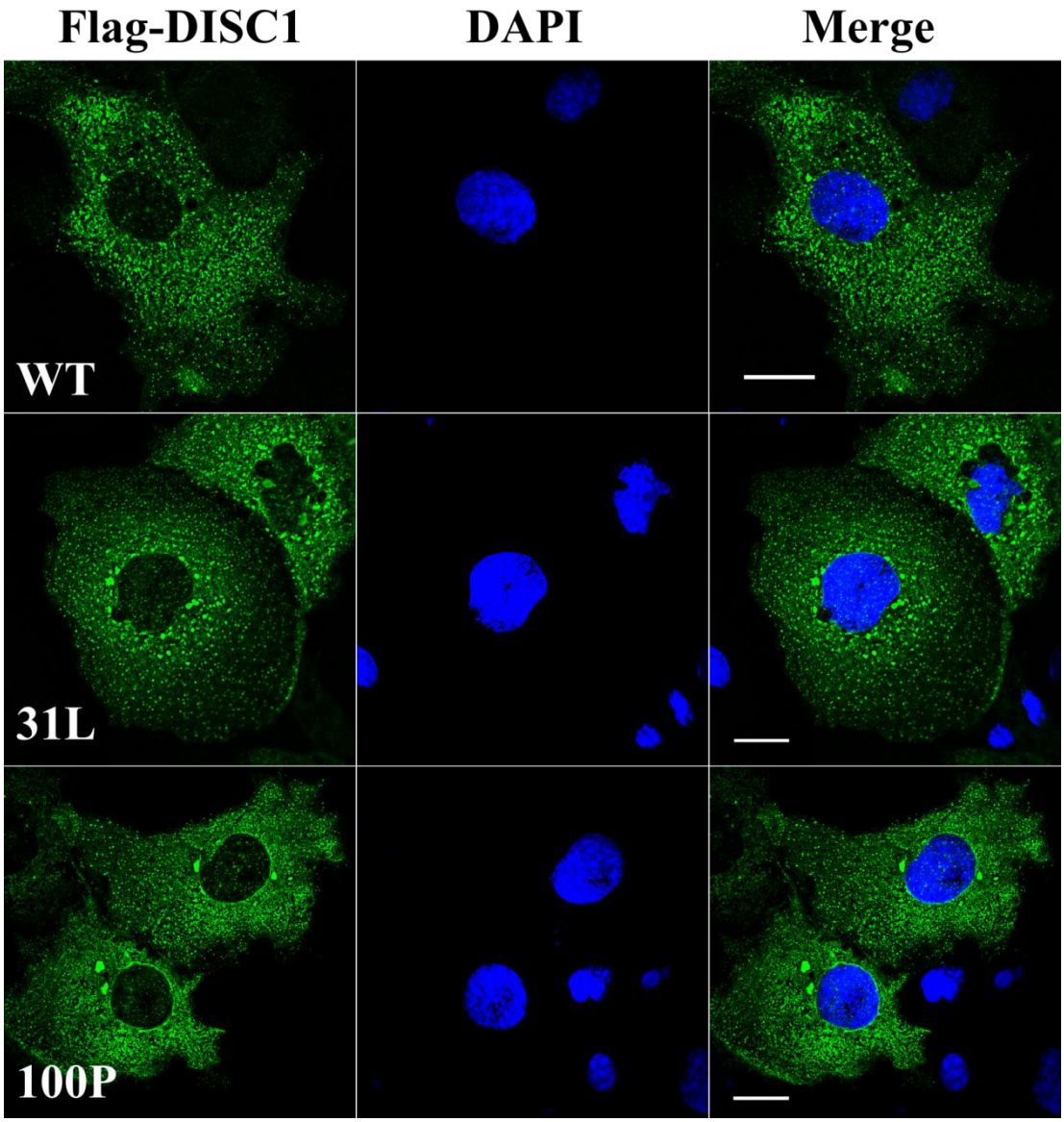

Figure 3.16 Subcellular distribution of Disc1 mutants 31L and 100P. Representative COS7 cells expressing mDisc1-WT, 31L or 100P and stained with the Flag RPC antibody (green). Nuclei (blue) are stained with DAPI. Scale bars are 20 µm.

3.4 Analysis of the subcellular distribution of DISC1 variants by subcellular fractionation

To further examine the impact of risk-conferring amino acid substitutions 37W and 607F on the subcellular distribution of DISC1, whole cell lysates and subcellular protein fractions were prepared from transfected and untransfected SH-SY5Y cells as described in paragraph 2.5.3, and analysed by western blotting. Cellular proteins were fractionated into cytoplasmic extract (CE), membrane-bound extract (ME), soluble nuclear extract (SNE), chromatin-bound nuclear extract (CBNE) and cytoskeletal extract (CSKE). To verify the purity of the individual subcellular protein fractions, a mock-transfected cell sample was included in each fractionation experiment, and the resulting fractions were analysed in parallel by western blotting using specific antibodies to detect fraction-specific proteins, which were used as fraction markers (Figure 3.17). As expected, heat shock protein 90 (HSP90) was highly enriched in the CE, whereas the nuclear matrix protein p84 was predominantly found in the SNE (Figure 3.17). Similarly, the cytoskeletal protein Vimentin was enriched in the CSKE, and Calreticulin in the ME (Figure 3.17). On the other hand, chromatin-bound histone 3 (H3) was detected both in the CBNE and in the CSKE, indicating that the latter fraction is contaminated by chromatin-associated proteins (Figure 3.17). A similar distribution profile of the above fraction markers was detected in all sets of fractions examined, which guarantees the comparability of the subcellular expression profiles of exogenous DISC1 observed in the different fractionation experiments.

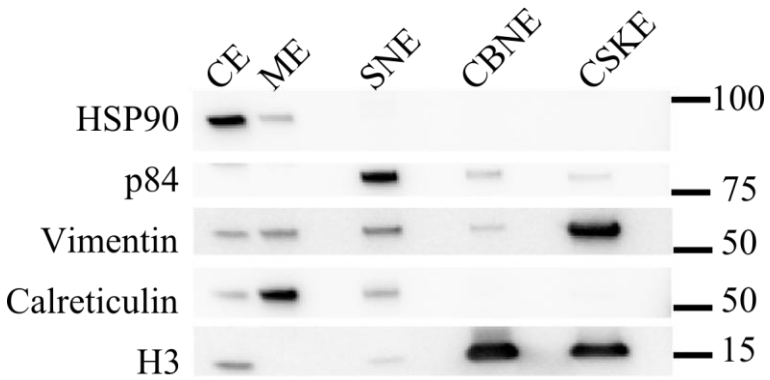

Figure 3.17 Purity control of subcellular protein fractions. Mock-transfected SH-SY5Y cells were subjected to subcellular fractionation, and equal amounts of protein for each fraction were analysed in parallel by western blotting using antibodies to detect proteins that are known to be enriched in either one of the fractions. ME: membrane exctract, CE: cytoplasmic extract, CSKE: cytoskeletal extract, SNE: soluble nuclear extract, CBNE: chromatin-bound nuclear extract. The size (kDa) and position of the protein markers is indicated.

3.4.1 *Distribution of endogenous and exogenous DISC1*

To compare the subcellular distribution of endogenous and exogenous DISC1, subcellular fractions were prepared from SH-SY5Y cells that had been either transfected with pcDNA4/TO-Flag DISC1-WT or left untransfected (Figure 3.18). Both the exogenous and the endogenous full-length 100 kDa DISC1 isoform can be detected in the membrane-bound, cytoplasmic, soluble nuclear and cytoskeletal extracts, but not in the chromatin-bound nuclear extract (Figure 3.18). However, while exogenous DISC1 is predominantly enriched in the cytoskeletal fraction, which contains most of the protein, endogenous DISC1 mainly distributes to the cytoplasmic and membrane-bound fractions, and it is scarcely represented in the cytoskeletal extract (Figure 3.18). The absence of DISC1 from the chromatin-bound nuclear extract implies that the contamination of the cytoskeletal extract with proteins from this fraction does not prevent the accurate quantification of cytoskeletal DISC1. Overall, the relative distribution of exogenous DISC1 reflects

that of the endogenous protein except for the cytoskeletal fraction, where the vast majority of the overexpressed protein accumulates.

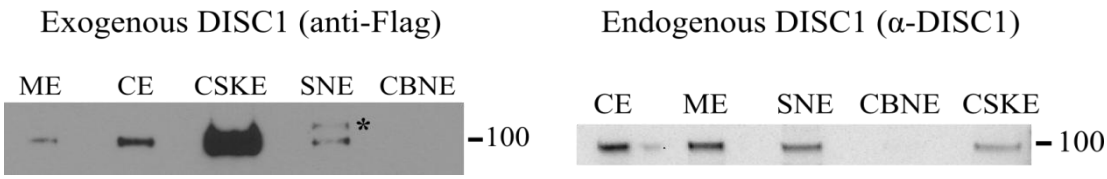

Figure 3.18 Distribution of exogenous and endogenous DISC1 in subcellular fractions. Equal amounts of subcellular protein exctracts obtained from SH-SY5Y cells that were either transfected with pcDNA4/TO-Flag DISC1-WT (left) or untransfected (right) were analysed by western blotting to detect exogenous and endogenous DISC1, respectively. Exogenous DISC1 was detected with the Flag MMC antibody, whereas endogenous DISC1 was detected with and antibody raised against the C-terminus of the protein that specifically recognises the 100 kDa isoform of DISC1 (α-DISC1). ME: membrane exctract, CE: cytoplasmic extract, CSKE: cytoskeletal extract, SNE: soluble nuclear extract, CBNE: chromatin-bound nuclear extract. The position and size (kDa) of the protein marker is indicated.

3.4.2 *Distribution of DISC1 variants 37W and 607F*

To compare the subellular distribution of DISC1-WT, DISC-37W and DISC1-607F, SH-SY5Y cells were transfected with equal amounts of the respective pcDNA4/TO-Flag DISC1 expression constructs before being subjected to subcellular fractionation. Before fractionation, a small aliquot of transfected cells were lysed in RIPA buffer, which contains particularly strong detergents, and the resulting whole cell lysate was later used to determine the total expression level of exogenous DISC1 (Figure 3.19). For each DISC1 variant, equal amounts of each subcellular protein extract were analysed in parallel by western blotting, and the respective DISC1 band intensities were corrected using appropriate loading controls (p84 for nuclear extracts, GAPDH for cytoplasmic extracts, Calreticulin for membrane-bound extracts and Vimentin for cytoskeletal extracts). In each experiment, all the fractions were analysed in

duplicate, and the mean relative DISC1 band density was taken as one technical replicate. To correct for variation in DISC1 total expression levels, the relative protein abundance of DISC1 variants in each fraction was divided by the respective GAPDH-corrected protein abundance in whole cell lysates.

While the total expression levels of exogenous DISC1-WT, DISC1-37W and DISC1-607F do not differ significantly, the relative nuclear abundance of DISC1-37W and DISC1-607F is decreased by ~50% compared to DISC1-WT ($P<0.01$, Figure 3.19). This is equivalent to the reduction in nuclear expression of DISC-37W and DISC1-607F observed in COS7 cells by immunocytochemistry (Figures 3.6 and 3.6). In addition, while the relative protein abundance of DISC1-WT, DISC1-37W and DISC1-607F is comparable in the cytoplasmic and membrane-associated fractions, DISC1-607F is strongly depleted from the cytoskeletal extract ($P<0.01$, Figure 3.19), consistent with its aberrant cytoplasmic distribution (Figure 3.12).

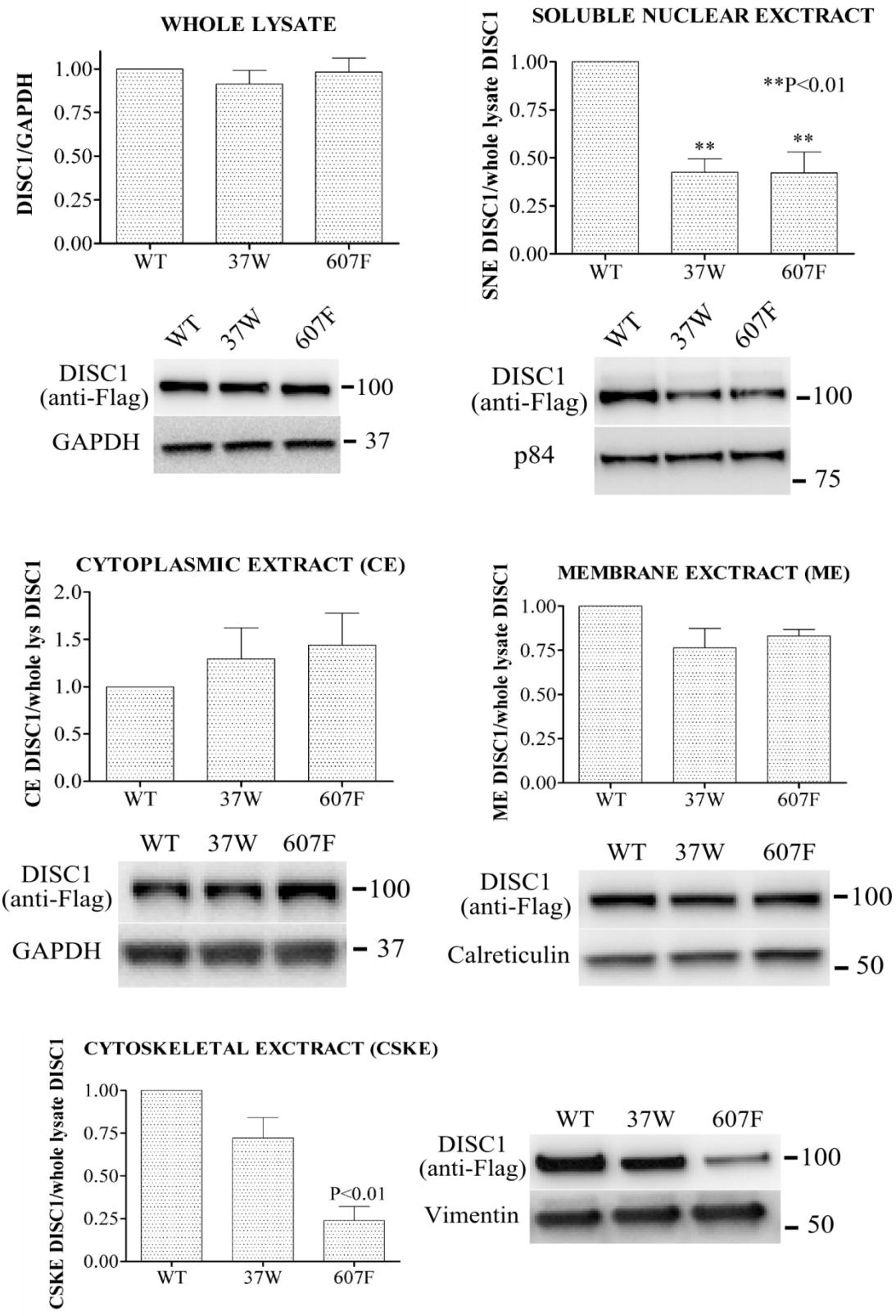

Figure 3.19 Subcellular distribution of DISC1 variants 37W and 607F. Distribution of DISC1-WT, DISC1-37W and DISC1-607F in whole cell lysates and subcellular

protein fractions obtained from transfected SH-SY5Y cells. The loading controls are proteins known to be preferentially enriched in either of the different subcellular fractions analysed. The bars represent the average of four independent experiments. All the densitometry data are normalised to the relative band intensity of DISC1-WT. The position and size (kDa) of the protein markers is indicated. Data were analysed by one-way ANOVA followed by Dunnett's Multiple Comparisons Test.

3.4.3 *Dominant-negative effect of DISC1 variants 37W and 607F*

To further test if DISC1-37W and DISC1-607F can disrupt the nuclear targeting of DISC1-WT in a dominant-negative fashion, whole cell lysates and nuclear protein extracts from SH-SY5Y cells expressing wild-type DISC1 alone or in combination with either DISC1-37W or DISC1-607F were analysed by western blotting. The different DISC1 expression constructs used in this experiment achieved comparable levels of protein expression, as confirmed by western blotting analysis of lysates from transfected SH-SY5Y cells (Figure 3.20).

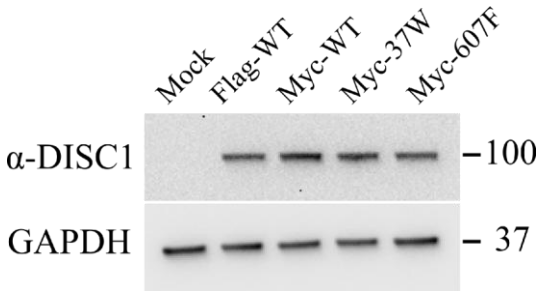

Figure 3.20 Testing of DISC1 expression constructs. Whole cell lysates were obtained from SH-SY5Y cells that were either mock transfected or transfected with equal amounts of the indicated pcDNA4/TO-DISC1 expression constructs, and analysed by western blotting. DISC1 expression was assessed using the α-DISC1 antibody (Table 2.5) to ensure that comparable total exogenous DISC1 expression was achieved, and the antibody concentration was adjusted so that only exogenous DISC1 could be detected. The position and size (kDa) of the protein markers is shown.

As shown in Figure 3.21, co-expression of DISC1-37W or DISC1-607F results in a significant decrease in nuclear abundance of wild-type DISC1 ($P<0.01$), with this effect being particularly pronounced for the 37W variant when compared to 607F ($P<0.05$). This finding is in agreement with the impaired nuclear localisation of DISC1-WT upon co-expression of DISC1-37W or DISC1-607F observed by immunocytochemistry in both COS7 and SH-SY5Y cells (Figure 3.14). Collectively, the results obtained by immunocytochemistry and subcellular fractionation predict that 37W or 607F carriers may have reduced nuclear DISC1 expression, and that 607F homozygotes may be similar to 607F heterozygotes in this particular respect.

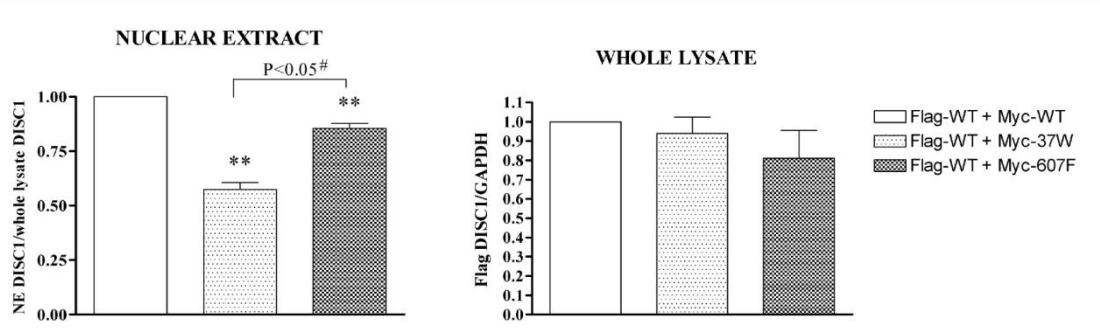

Figure 3.21 SH-SY5Y cells were transfected with Flag-WT DISC1 and an equal amount of either Myc-DISC1-WT, Myc-DISC1-37W or Myc-DISC1-607F. The relative abundance of Flag-WT DISC1 was then quantified by western blotting in whole cell lysates and nuclear extracts (NE) prepared from the transfected cells. The bars represent the average of 3 independent experiments. The data are normalised to the relative band density of Flag-DISC1 in samples expressing WT DISC1 only and were analysed by one-way ANOVA followed by Dunnett's multiple comparison test, except where indicated. **P<0.01; # paired two-tailed student's t-test.

3.5 Discussion

Growing evidence indicates that by establishing dynamic interactions with multiple binding partners, DISC1 functions as a hub protein whose principal role is to modulate various cellular processes in a space- and time-regulated manner. Sequence changes in DISC1 that disrupt its normal compartmentalisation and/or protein

interactions are therefore likely to have functional consequences, and may highlight biological processes involved in psychopathology.

In this chapter, I have demonstrated that both the ultra-rare, putatively causal mutation 37W, observed in a patient diagnosed with schizophrenia and not in 10.000 control alleles (Song *et al*, 2008), and the common polymorphism 607F induce a ~50% depletion of the nuclear pool of DISC1, and perturb the nuclear targeting of wild-type DISC1 in a dominant-negative fashion.

The 37W mutation disrupts a highly conserved tetra-arginine nuclear localisation signal, which I have previously referred to as NLS1, in the otherwise poorly conserved head region of DISC1 (Sawamura *et al*, 2008). There is contrasting evidence regarding the importance of NLS1 for DISC1 nuclear targeting (Brandon *et al*, 2005; Sawamura *et al*, 2008) (Table 3.2), but the detrimental effect of 37W suggests that the integrity of NLS1 is indeed necessary for the correct nuclear localisation of DISC1. However, 37W additionally dramatically increases the recruitment of DISC1 to perinuclear mitochondrial aggregates (Ogawa F., unpublished data), an effect that may in itself obstruct DISC1 translocation to the nucleus. Here, I have provided evidence that the defective nuclear targeting of DISC1-37W and its increased recruitment to the mitochondria are likely two independent consequences of the 37W mutation. Thus, although additional mechanisms cannot be excluded, my results strongly suggest that 37W impairs DISC1 nuclear targeting by directly disrupting NSL1, providing further confirmation that this is a functional NLS within DISC1.

The common polymorphism 607F is located in a conserved predicted leucine zipper (DISC1LZ9) which was previously shown to contribute to DISC1 nuclear targeting (Sawamura *et al*, 2008) (Table 3.2). Here, I confirmed that DISC1LZ9 in indeed essential for the correct nuclear localisation of DISC1. Thus, the predicted disruption of this leucine zipper structural feature by 607F (Soares *et al*, 2011) likely explains the reduced DISC1 nuclear targeting induced by this amino acid substitution.

Depending on the construct tested, DISC1 is capable of forming dimers, octamers and other oligomers and multimers (Brandon *et al*, 2004; Kamiya *et al*, 2005; Leliveld *et al*, 2008; Leliveld *et al*, 2009; Narayanan *et al*, 2011). Hence, in co-

transfected cells expressing wild-type and variant DISC1, hetero/oligomerisation will likely occur, accounting for the dominant-negative effects reported here. Indeed, DISC1-37W recruits wild-type DISC1 to perinuclear mitochondrial aggregates (Ogawa F., unpublished data). It is therefore possible that the dominant-negative effect exerted by DISC1-37W on the nuclear targeting of wild-type DISC1 results from redistribution of wild-type DISC1 to mitochondria. I have observed a significant, but milder reduction in nuclear abundance of wild-type DISC1 upon co-expression of DISC1-607F. 607F is located close to a region of DISC1 (668-747) identified as essential for oligomerisation (Leliveld *et al*, 2009), and it resides within a predicted leucine zipper, a structural motif generally known to promote protein oligomerisation (Soares *et al*, 2011). Thus, the dominant-negative effect of DISC1-607F may be related to the potentially altered oligomerisation propensity of this variant form of DISC1, which may interfere with the normal oligomerisation of wild-type DISC1 by establishing partial interactions with it. Formal testing of this hypothesis will only be possible once the structural effects of 607F have been established experimentally. Collectively, these observations indicate that nuclear expression of wild-type and variant DISC1 will likely be reduced in 37W or 607F carriers, with consequent impairment of the nuclear function of DISC1. In this respect, it is important to remark that the average population frequency of 607L/607F heterozygotes and 607F/607F homozygotes is 23% and 2.2%, respectively, implying that, on average, ~25% of the population carries at least one 607F allele (http://www.ncbi.nlm.nih.gov/SNP/snp_ref.cgi?rs=rs6675281). Hence, while the data presented here suggest that the 607F allele might profoundly affect DISC1 nuclear localisation, this variant is not strongly associated with schizophrenia or other major mental disorders. This suggests that, consistent with the complex aetiology of these diseases, the penetrance of the 607F allele likely depends on the individual's genetic and environmental context.

Here, I showed that exogenously expressed full-length DISC1 is highly enriched in the cytoskeletal protein fraction, which is consistent with its prominent role in the regulation of cytoskeleton-dependent processes (Wang *et al*, 2010a), and that variant 607F markedly reduces the relative abundance of DISC1 in this fraction. This effect may be related to the aberrant cytoplasmic distribution of DISC1-607 observed by

immunocytochemistry, and is consistent with the predicted deleterious consequences of 607F on DISC1 structure and oligomerisation propensity (Soares *et al*, 2011). It is possible that the abnormal cytoskeletal fractionation and cytoplasmic distribution of DISC1-607F may arise from its impaired ability to assemble into functional complexes and establish proper connections with cytoskeleton-associated partners. Interestingly, 607F has been associated with impaired centrosomal recruitment of PCM1 and reduced neurotransmitter release (Eastwood *et al*, 2009; Eastwood *et al*, 2010), as well as defective mitochondrial trafficking in neurons (Atkin *et al*, 2011). It is intriguing to speculate that these reported effects of 607F may be related to its reduced association with the cytoskeleton.

Despite its aberrant cytoskeletal and cytoplasmic distribution, DISC1-607F appears to normally distribute to the centrosome. Since the analysis of the centrosomal distribution of DISC1 variants was carried out on a relatively small cell sample, it is not possible to confidently speculate on the results. However, it appears that DISC1 centrosomal targeting might be differentially perturbed by distinct amino acid substitutions, and that 607F might become deleterious only when present in combination with 264Q or 704C. If confirmed, this observation would be consistent with the reported cumulative effect of 607F and 704C on the centrosomal immunoreactivity of PCM1 in glial cells in post-mortem human brains (Eastwood *et al*, 2010). Here, PCM1 immunoreactity is lower in 704C carriers that are also 607F homozygotes compared to 704C carriers that are 607F heterozygotes or 607L homozygotes (Eastwood *et al*, 2010).

Finally, since 37W is known to profoundly impact on DISC1 mitochondrial recruitment and morphology, which may contribute to its putative pathogenic role (Ogawa F., unpublished data), I tested whether any of DISC1 variants 264Q, 432L, 603I, 607F and 704C produces a similar effect. My findings indicate that none of the above amino acids substitutions grossly disturb mitochondrial morphology and/or DISC1 recruitment to this organelle. It appears then that different DISC1 amino acid substitutions might increase the risk of psychiatric illness by impacting on distinct functions of the protein.

4 The effect of DISC1 on transcriptional regulation

4.1 Introduction

In the nucleus, DISC1 interacts with two members of the ATF4 sub-family of bZIP transcription factors: ATF4 and ATF5 (Millar *et al*, 2003; Morris *et al*, 2003; Sawamura *et al*, 2008). Both ATF4 and ATF5 are stress-inducible transcription factors that are preferentially translated in response to many different cellular stressors, including amino acid limitation, endoplasmic reticulum stress and oxidative stress (Ameri & Harris, 2008; Watatani *et al*, 2008; Zhou *et al*, 2008a). By using reporter-based assays in human cell lines, Sawamura and colleagues demonstrated that DISC1 regulates the transcriptional activity of ATF4 (Sawamura *et al*, 2008). In particular, DISC1 co-expression significantly represses Gal4 promoter transactivation by a Gal4-ATF4 chimera and strengthens the ATF4-mediated repression of cAMP-induced CRE-dependent transcription (Sawamura *et al*, 2008). The same study also showed that DISC1 interaction with ATF4 is mediated by a putative leucine zipper motif located in DISC1 exon 9 (DISC1LZ9), between amino acids 607 and 628. Indeed, deletion of DISC1LZ9 completely abolishes ATF4 binding and, accordingly, it suppresses DISC1-dependent regulation of ATF4 transcriptional activity (Sawamura *et al*, 2008). Since a region in the C-terminus of DISC1 also mediates binding to the nuclear receptor co-repressor N-CoR, a transcriptional co-repressor that recruits histone deacetylase to the transcriptional machinery (Jepsen & Rosenfeld, 2002), it was hypothesised that DISC1 may act by recruiting this factor to the ATF4-containing complex (Sawamura *et al*, 2008).

The transcriptional targets of ATF4 are not limited to CRE-containing genes. Indeed, ATF4 homo- or heterodimers are known to bind other response elements, including the composite C/EBP-ATF4 response elements (CARE), which mediate the ATF4-dependent activation of several stress-responsive genes (Kilberg *et al*, 2009). ATF4-responsive CARE-containing targets include, but are not limited to, genes involved in the response to amino acid limitation, such as asparagine synthetase (*ASNS*), System A neutral amino acid transporter 2 (*SNAT2*), sodium-independent

aspartate/glutamate/cystine transporter (*SLC7A11*), and genes with pro- or antiapoptotic functions, such as C/EBP homology protein (*CHOP*) and Tribbles 3 (*TRB3*) (Kilberg *et al*, 2009). In particular, ATF4 activates the transcription of *CHOP* by binding to a specific type of CARE in its promoter, known as the Amino Acid Response Element (AARE) (Fawcett *et al*, 1999; Ma *et al*, 2002b; Shan *et al*, 2009). Although ATF4 is not the only transcription factor to be preferentially translated in response to cellular stress, ectopic expression of ATF4 alone is sufficient to induce transcriptional activation of CARE-containing genes in the absence of stress, but it does so at a relatively lower efficiency compared to stress-induced endogenous ATF4 (Shan *et al*, 2009). This suggests that, although ATF4 is able to independently activate the stress response, other stress-responsive factors normally modulate its activity (Shan *et al*, 2009).

In chapter 3 of this thesis I demonstrated that risk-conferring DISC1 amino acid substitutions 37W and 607F result in defective nuclear targeting of the protein in cell lines and primary neurons. This implies that both 37W and 607F may potentially impair the nuclear functions of DISC1, and that this mechanism may contribute to the increased risk of psychiatric illness associated with these variants. Thus, in this chapter I investigate the potential effects of these and other schizophrenia-associated variants on the ability of DISC1 to regulate ATF4-dependent transcription on CRE- and CARE-containing reporters.

4.2 Generation of luciferase reporter constructs

Most of the experiments described in this chapter were performed using the reporter vector SomCRE-Luc (Table 2.2), which drives the expression of Firefly luciferase under the control of four multimerised copies of the palindromic Somatostatin CRE 5'-(AGCC[TGACGTCA]GAG)-3′ (CRE denoted in brackets) located immediately upstream of a minimal promoter (TATA box).

The luciferase reporter vector pGL4.23-CRE was used to perform experiments in hard-to-transfect cells, since it carries a codon-optimised Firefly luciferase cDNA that guarantees very efficient protein expression in mammalian cells. The reporter pGL4.23-CRE was generated by ligating the pre-annealed oligonucleotides CRE mut

F and CRE mut R (Table 2.8) between the XhoI and HindIII restriction sites of the vector pGL4.23[luc2/minP] (Table 2.2), which contains a minimal promoter (TATA box) upstream of the Firefly luciferase cDNA. To guarantee comparability between experiments carried out using the SomCRE-Luc and pGL4.23-CRE reporters, the sequence, number and spacing of the CREs in the resulting vector was identical to that of the SomCRE-luc reporter.

The reporter vector pGL4.23-CHOP AARE and its mutant, non responsive version pGL4.23-mutCHOP AARE were generated by site-directed mutagenesis from pGL4.23[luc2/minP], using mutagenic primers CHOP AARE F and R and mutCHOP AARE F and R, respectively (Table 2.6). Mutagenic primers contained two copies of the core CHOP Amino Acid Response Element (AARE) (underlined) and its flanking regions: CHOP AARE, 5' AAC<u>A**T**TGCATCA</u>TCCCCGC 3' and mut CHOP AARE, 5' AAC<u>A**A**TGCATCA</u>TCCCCGC 3' (Bruhat *et al*, 2002), which only differed from each other by the base in bold.

4.3 Design and optimisation of luciferase reporter assays

Several preliminary experiments were carried out to determine the transfection conditions that achieved the best possible signal-to-noise ratio in luciferase reporter assays without producing cell toxicity. Different transfection methods and conditions were tested and compared in SH-SY5Y, HEK293 and HeLa cells.

4.3.1 *SH-SY5Y cells*

For luciferase reporter assays, SH-SY5Y cells were initially transfected with Fugene HD transfection reagent, which is designed to achieve good transfection rates in hard-to-transfect cells forming a high-density monolayer. To determine the optimal cell density and Fugene HD:DNA ratio, cells were seeded in 12 well plates and transfected with the P5HuSH-GFP expression plasmid (Table 2.2) as detailed in Figure 4.1, then the transfection efficiency was visually assessed at 24 hour intervals using an inverted fluorescence microscope. The transfection rate gradually increased with the Fugene HD:DNA ratio, up to a maximum of 20-30%, and was not affected by cell density. However, higher Fugene HD:DNA ratios produced signs of cell

toxicity at lower cell densities. Higher numbers of transfected cells were obtained when cells were harvested 48 or 72 hours post-transfection compared to 24 hours post-transfection (not shown).

In a second experiment, higher Fugene HD:DNA ratios were tested in the same way, but only on cells seeded at high density, as shown in Figure 4.2, and the transfection efficiency was assessed as before. This identified 4:0.8 as the optimal Fugene HD:DNA ratio, and 72 hours as the best incubation time post-transfection. These conditions achieved a transfection rate of 30-40% (not shown).

Next, cells were seeded in 96 well plates, and the optimised cell density was proportionately scaled down to $2x10^4$/well. To determine the minimum amount of transfected reporter DNA/well necessary to achieve a good signal-to-noise ratio in luciferase assays, four transfection mixes containing reporter DNA and the empty vector pRK7 (Table 2.2) mixed in different proportions were assembled in OptiMEM as detailed in Table 4.1.

A

$1.2x10^5$ / 1.2/0.8	$1.2x10^5$ / 1.6/0.8	$1.2x10^5$ / 2/0.8	$1.2x10^5$ / 2.4/0.8
$1.2x10^5$ / 2.8/0.8	$1.2x10^5$ / 3.2/0.8	$1.6x10^5$ / 1.2/0.8	$1.6x10^5$ / 1.6/0.8
$1.6x10^5$ / 2/0.8	$1.6x10^5$ / 2.4/0.8	$1.6x10^5$ / 2.8/0.8	$1.6x10^5$ / 3.2/0.8

B

$2x10^5$ / 1.2/0.8	$2x10^5$ / 1.6/0.8	$2x10^5$ / 2/0.8	$2x10^5$ / 2.4/0.8
$2x10^5$ / 2.8/0.8	$2x10^5$ / 3.2/0.8	$2.4x10^5$ / 1.2/0.8	$2.4x10^5$ / 1.6/0.8
$2.4x10^5$ / 2/0.8	$2.4x10^5$ / 2.4/0.8	$2.4x10^5$ / 2.8/0.8	$2.4x10^5$ / 3.2/0.8

C

$1.2x10^5$ / 3.2/0.8	$1.6x10^5$ / 3.2/0.8	$2x10^5$ / 3.2/0.8	$2.4x10^5$ / 3.2/0.8
$1.2x10^5$ / 3.2/0.8	$1.6x10^5$ / 3.2/0.8	$2x10^5$ / 3.2/0.8	$2.4x10^5$ / 3.2/0.8
$1.2x10^5$ / x	$1.6x10^5$ / x	$2x10^5$ / x	$2.4x10^5$ / x

Figure 4.1 SH-SY5Y transfection scheme. The three rectangles in A, B and C represent 12 well tissue culture plates, and are subdivided in 12 smaller rectangles, each representing an individual well. Each well is further divided in two triangles; the number in the upper triangle indicates the corresponding plating cell density (cells/well), and the number in the lower triangle indicates the Fugene HD:DNA ratio

(µl:µg) used to transfect cells in each well. To control for potential toxic effects of GFP overexpression, cells in plate 3, row 1, were transfected with the empty vector pcDNA3.1+. The “X” indicates that cells in the corresponding well were not transfected.

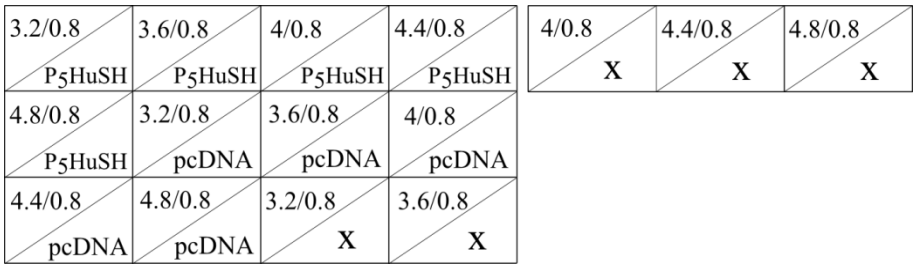

Figure 4.2 SH-SY5Y transfection scheme. The smaller rectangles represent individual wells of a 12 well plate. The corresponding Fugene HD:DNA ratios and plasmid DNA are indicated in the upper and lower triangles, respectively. The “X” indicates that cells in the corresponding well were not transfected.

In 40 µl mix: 1 µg DNA, 4µl Fugene HD			
Mix	SomCRE-Luc (ng)	TK-Renilla (ng)	pRK7 (ng)
A	50	5	945
B	100	10	890
C	200	20	780
D	/	/	1000

Table 4.1 Transfection mixes for luciferase assay. The indicated amounts of CRE (SomCRE-Luc) and internal control (TK-Renilla) reporter vectors were mixed with the empty vector pRK7, Fugene HD and OptiMEM to obtain a total volume of transfection mix of 40 µl. For ease of calculation, the Fugene HD:DNA ratio was decreased to 4:1. The total volume of transfection mix was scaled up as necessary.

Cells were transfected in triplicate with increasing volumes of each transfection mix, as shown in Figure 4.3. To activate CRE-dependent transcription, cells were treated for 4 hours with either 100 µM forskolin or vehicle (DMSO) starting from 24, 48 or 72 hours after transfection, then the luciferase activity was measured as described in paragraph 2.7.1. None of the tested conditions produced luminescence readings significantly above the background value, which corresponded to the readings in cells transfected with the empty vector only (mix D) (not shown).

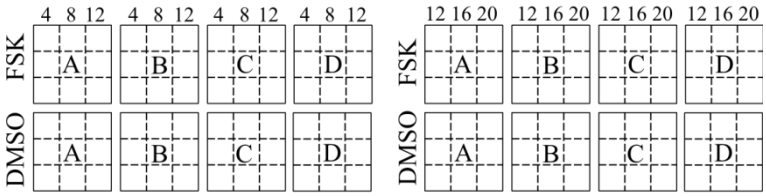

Figure 4.3 SH-SY5Y transfection and assay scheme. The small squares delimited by dashed lines represent individual wells of a 96 well plate. The letters (A, B, C and D) indicate the transfection mix that was added to the cells in the respective wells, and the numbers indicate the volume of transfection mix that was added to the wells in the respective columns. In each plate, the wells in the top half were treated with forskolin (FSK) and the wells in the bottom half were treated with vehicle (DMSO).

In an attempt to improve the transfection efficiency achieved with the selected protocol, cells seeded in 96 well plates were transfected with the P5HuSH-GFP vector and pRK7 mixed in different proportions, as shown in Table 4.2. The transfection mixes were incubated at room temperature for either 15 or 40 minutes, and then increasing volumes (4, 8, 12, 16 and 20 µl) of each mix were added to the cells. The best proportion of GPF-expressing cells (~40-50%) with the least signs of cell toxicity were achieved with transfection mix D added to the cells at 12 µl/well and incubated for 48 hours (not shown).

40 µl mix		
Mix	P5HuSH (ng)	pRK7(ng)
A (4:1)	50	950
B (4:1)	100	900
C (4:1)	200	800
D (4:1)	400	600
E (4:1.6)	400	1200
F (12:8)	1600	6400
G (16:4)	800	3200
Mock (4:1)	/	1000
Mock (4:1.6)	/	1600
Mock (12:8)	/	8000

Table 4.2 SH-SY5Y transfection mixes for GFP expression test in 96 well plates. The indicated amounts of plasmids were mixed in OptiMEM, to achieve a total volume of 40 µl. The Fugene HD:DNA ratios used in each mix are in brackets.

Next, the newly optimised transfection conditions were further tested in a luciferase reporter assay in 96 well plates. The transfection mixes were assembled as described in Table 4.3, and added to the cells at 12 µl/well. 48 hours after transfection, the cells were treated for 4 hours with 100 µM forskolin or DMSO, as described before, before being assayed for luciferase activity. However, even with the improved transfection conditions, the luminescence signal-to-noise ratio achieved was not satisfactory (not shown).

In 40 µl mix: 1µg DNA, 4µl Fugene HD			
Mix	SomCRE-Luc (ng)	TK-Renilla (ng)	pRK7 (ng)
D	400	40	560
D2	600	60	340
D3	800	80	120
Mock	/	/	1000

Table 4.3 SH-SY5Y transfection mixes for luciferase assay.

Next, nucleofection was tested as an alternative transfection method to perform luciferase reporter assays in SH-SY5Y cells (see paragraph 2.4.6.3). Cells were transfected with either pGL4.29[luc2P/CRE/Hygro] (Table 2.2), a commercially available CRE-luciferase reporter optimised to achieve high luciferase expression levels in mammalian cells, or SomCRE-Luc, as shown in Table 4.4. 24 hours after transfection, cells were treated with 10 µM forskolin for 4 hours before being assayed. The reporter pGL4.29[luc2P/CRE/Hygro], but not SomCRE-Luc, produced a good luminescence signal (not shown). However, the signal generated by Renilla luciferase was extremely low. This was resolved by replacing the TK-Renilla internal control with the SV40-Renilla reporter (Table 2.2), which expressed luciferase at higher levels in SH-SY5Y cells (not shown).

Mix	**pGL4.29 (ng)**	**SomCRE-Luc (ng)**	**TK-Renilla (ng)**	**pRK7 (ng)**
A	600	/	60	1340
B	/	600	60	1340

Table 4.4 Amounts of DNA used to transfect SH-SY5Y cells by nucleofection. Detailed methods are described in paragraph 2.4.6.3.

4.3.2 *HEK293 cells*

Fugene HD was also tested in HEK293 cells, which normally achieve very high transfection rates. Cells were plated in 96 well plates in 100 µl/well of medium, at densities of 1, 2, 3, 4 or $5x10^4$ cells/well, and transfected with 4 µl/well of a mix containing either the pRK7 vector alone or in combination with P5HuSH-GFP (Table 4.5). The following Fugene HD:DNA ratios were tested: 1.5:1, 2:1, 2.5:1, 3:1, 3.5:1 and 4:1, and the proportion of GFP-expressing cells was assessed visually after 24 and 48 hours. The highest transfection rate (70-80%) and lowest toxicity was achieved in cells seeded at $5x10^4$ cells/well and transfected for 48 hours with a mix containing Fugene HD and DNA in a 4:1 ratio (not shown).

In 40 µl mix: 1 µg DNA and 1.5, 2, 2.5, 3, 3.5 or 4 µl Fugene HD		
Mix	P5HuSH (ng)	pRK7 (ng)
A	300	700
B	/	1000

Table 4.5 HEK293 transfection mixes for GFP expression test in 96 well plates.

In a similar experiment, cells were transfected with increasing volumes of transfection mix to identify the volume that achieved the best transfection rate without inducing cell toxicity. As expected, higher volumes of mix achieved higher transfection rates, and volumes of 12 or 20 µl/well achieved similar results after 48 hours, thus both these conditions were further tested in luciferase reporter assays. Trasfection mixes assembled as shown in Table 4.6 were added to the cells at 12 or

20 µl/well. 48 or 72 hours after transfection, the cells were treated with either 10 or 100 µM forskolin, 1 mM 8-Br-cAMP or vehicle, and assayed for luciferase activity. Overall, the strongest relative luminescence signal was observed in cells that had been transfected with 20 µl of mix for 48 hours, and then treated with 10 µM forskolin (Figure 4.4). However, in this experiment transfection with 20 µl of mix produced evidence of apoptosis (i.e. cells appeared rounded and partially detached) (not shown). Therefore, in the following assays the cells were transfected with 12 µl of mix for 48 hours and treated with 10 µM forskolin.

In 40 µl mix: 1 µg DNA, 4 µl Fugene HD			
Mix	SomCRE-luc (ng)	TK-Renilla (ng)	pRK7 (ng)
A	300	30	670
B	/	/	1000

Table 4.6 Composition of the mixes used to transfect HEK293 cells for luciferase assay optimisation.

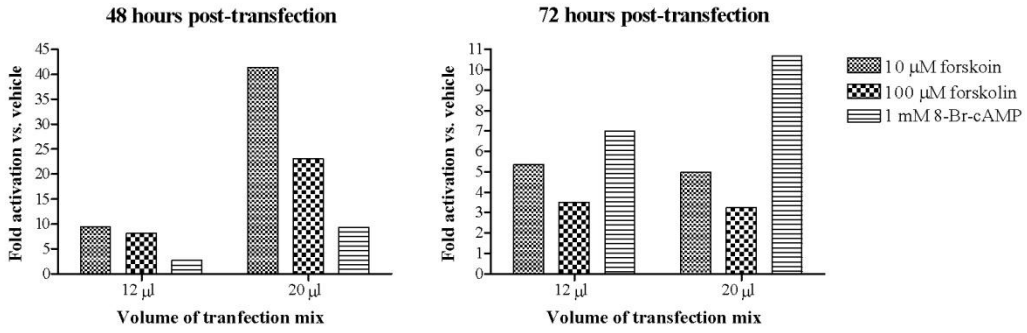

Figure 4.4 Pilot luciferase assay in HEK293 cells. Cells were transfected with 12 or 20 µl of the transfection mixes detailed in table 4.6 for either 48 or 72 hours, then treated for 4 hours with the indicated drugs and assayed for luciferase activity.

4.3.3 *HeLa cells*

Initially, cells seeded in 96 well plates at a cell density of 2 or $5x10^4$/well were transfected with mixes assembled as described in Table 4.5, using a Fugene HD:DNA ratio of 4:1. The mixes were added to the cells at 12, 16 or 20 µl/well and the proportion of GFP-expressing cells was visually assessed after 24 and 48 hours. The highest transfection rate (30-40%) and lowest toxicity was achieved in cells seeded at $5x10^4$/well and transfected with 12 µl/well of mix for 48 hours (not shown). Since the best transfection rate obtained with Fugene HD in HeLa cells was markedly lower that that achieved in HEK293 cells, a further optimisation experiment was performed in which the optimised Fugene HD transfection protocol was compared to Lipofectamine 2000 transfection. The Lipofectamine 2000 transfection mixes were assembled in OptiMEM using 1 µg of DNA (300 ng P5HuSH + 700 ng pRK7) and 2 (mix 1), 3 (mix 2) or 4 (mix 3) µl of Lipofectamine 2000 in a total volume of 50 µl, and added to the cells at 50, 30 or 15 µl/well, as summarised in Table 4.7. Overall, Lipofectamine 2000 performed better than Fugene HD, and the highest transfection rate (50-60%) was observed after 48 hours in cells seeded at $2x10^4$/well and transfected with 15 µl/well of mix (not shown). Thus, these transfection conditions were tested in a luciferase reporter assay using mixes assembled as shown in Table 4.8. However, the luminescence signal observed after 4 hour incubation with 10 µM forskolin was not significantly above background, leading to the conclusion that HeLa cells are not a suitable cell model for luciferase assays using the specified set of reporters.

Mix #	Volume of transfection mix (µl) added to $5x10^4$ cells/well			Volume of transfection mix (µl) added to $2x10^4$ cells/well		
1	50	30	15	50	30	15
2	50	30	15	50	30	15
3	50	30	15	50	30	15
4	12	12	12	12	12	12

Table 4.7 Transfection otimisation experiment in HeLa cells. The indicated volumes of transfection mixes containing Lipofectamine 2000 (1, 2 and 3) of Fugene HD (4) were added to cells seeded at 5 or $2x10^4$/well.

In 50 µl mix: 1µg DNA, 4 µl Lipofectamine 2000			
Mix	SomCRE-Luc (ng)	TK-Renilla (ng)	pcDNA4/TO (ng)
A	300	30	670
B	/	/	1000

Table 4.8 Pilot luciferase assay in HeLa cells. The composition of the mixes used to transfect the cells for a pilot luciferase assay is shown.

4.4 The effect of DISC1 on ATF4-dependent transcription

4.4.1 *DISC1 inhibits ATF4-dependent transcription at basal cAMP levels*

Sawamura and colleagues (Sawamura *et al*, 2008) showed that co-expression of DISC1 suppresses Gal4-ATF4 mediated transcription and that it enhances the ATF4-mediated inhibition of CRE-dependent transcription in response to increased intracellular cAMP levels. Since ATF4 has also been reported to activate CRE-mediated transcription under basal (low cAMP) conditions (Koyanagi *et al*, 2011; Liang & Hai, 1997; Ord & Ord, 2003; Vallejo *et al*, 1993), I initially sought to confirm the findings of Sawamura and collegues, and test whether DISC1 regulates ATF4-mediated activation of the CRE at basal cAMP levels.

HEK293 cells were initially chosen to perform luciferase reporter assays because in the optimisation tests they yielded a satisfactory transfection rate and luminescence signal-to-noise ratio (see paragraph 4.3). Furthermore, HEK293 cells are an established model to study the transcriptional effects of ATF4 (Ord *et al*, 2007; Sayer

et al, 2006; Shan *et al*, 2009; Zhou *et al*, 2005). Cells were transfected as described in paragraph 2.7.1, using the SomCRE-Luc reporter vector and the TK-Renilla internal control alone or in combination with different amounts of pRK7-ATF4 (mouse ATF4, Table 2.2), pcDNA4/TO-Flag DISC1-WT (human DISC1) or both. As shown in Figure 4.5 A, at basal cAMP levels, ATF4 activates transcription from the CRE, as previously reported (Koyanagi *et al*, 2011; Liang & Hai, 1997; Ord & Ord, 2003; Vallejo *et al*, 1993), whereas DISC1 on its own has no effect. Consistent with the reported inhibition of Gal4-ATF4 by DISC1 (Sawamura *et al*, 2008), co-expression of DISC1 significantly inhibits ATF4 transactivation of the CRE (Figure 4.5 A). As previously observed (Karpinski *et al*, 1992; Sawamura *et al*, 2008), elevation of intracellular cAMP levels by forskolin treatment strongly activates CRE-dependent transcription, and this effect is counteracted by ATF4 (Figure 4.5 A). DISC1 alone has no effect on the cAMP-dependent activation of CRE-driven transcription and, in contrast with the findings of Sawamura and colleagues (Sawamura *et al*, 2008), it does not strengthen ATF4-mediated inhibition (Figure 4.5 A). Since at the concentrations shown in figure 4.5 A ATF4 inhibits CRE transcription very strongly and might have a saturating effect, the experiment was repeated using lower, non saturating concentrations of ATF4. This experiment confirmed that DISC1 does not modify the inhibitory effect of ATF4 on cAMP-induced CRE-driven transcription, but it efficiently inhibits ATF4-mediated activation of the CRE at basal cAMP levels (Figure 4.5 B).

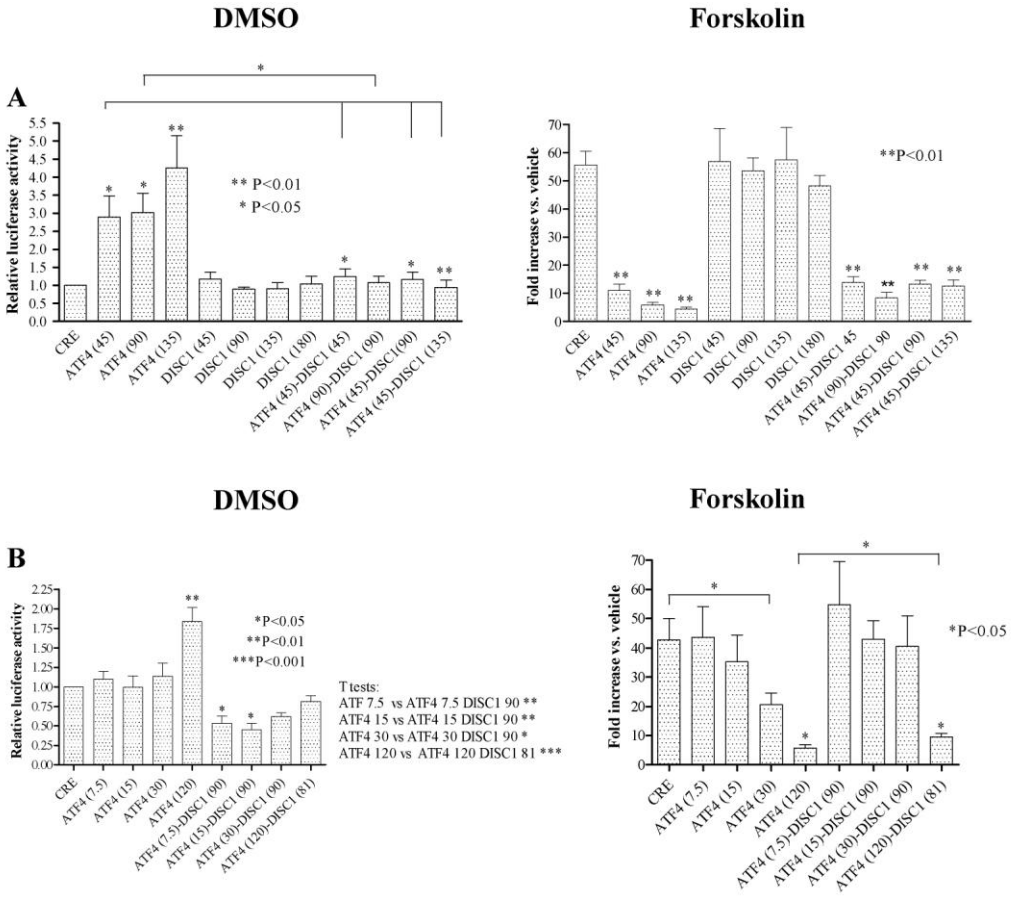

Figure 4.5 (A,B) HEK293 cells were transfected with the luciferase reporters only (CRE) or in combination with increasing amounts of pRK7-ATF4 (mouse ATF4), pcDNA4/TO-Flag DISC1-WT (human DISC1), or both. The transfected amounts of plasmid DNA are indicated in brackets as ng/well. Relative luciferase activity was measured after a 4 hour treatment with DMSO of 10 µM forskolin. The bars represent the average of at least 4 independent experiments. Data are normalised to the basal luciferase activity in DMSO-treated cells transfected with the reporters only. Data were analysed by one-way ANOVA and Dunnett's post test. Pair-wise comparisons were performed using two-tailed paired student's t-test.

As expected, and similarly to mouse ATF4 (Figure 4.5), human ATF4 efficiently activates transcription from the CRE at basal cAMP levels, and human DISC1 inhibits this effect in a dose-dependent manner, but does not modify the inhibitory effect of human ATF4 at high cAMP levels (Figure 4.6). Thus, unless otherwise

specified, all subsequent experiments were carried out using human ATF4 and human DISC1 expression constructs. The discrepancy between these results and those reported by Sawamura and colleagues (Sawamura *et al*, 2008) may arise from experimental and/or analytical differences between the two studies such as, for example, the use of different cell types. Indeed, Sawamura and colleagues performed luciferase reporter assays in HeLa cells (Sawamura *et al*, 2008). However, this was not investigated further in this thesis because initial attempts to optimise the experimental conditions to perform luciferase assays in HeLa cells were not successful (Paragraph 4.3.3).

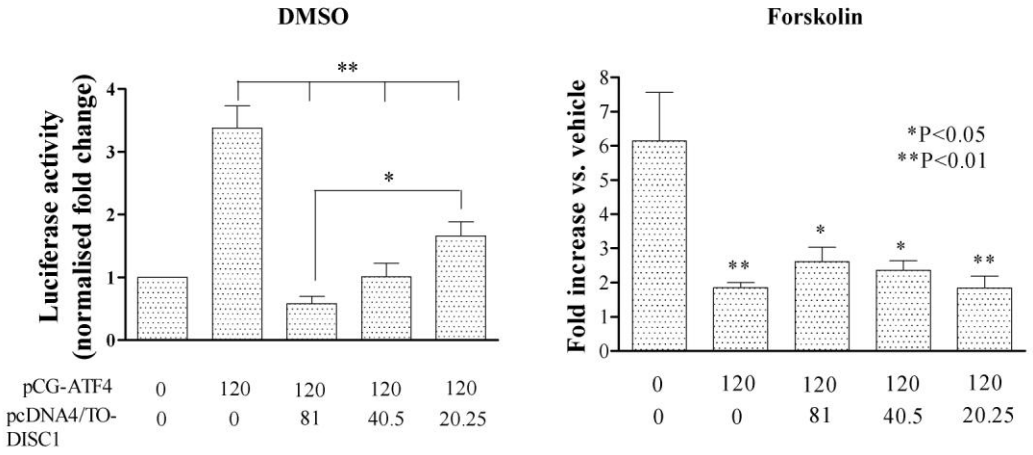

Figure 4.6 Relative CRE-dependent luciferase activity in HEK293 cells transfected with a fixed amount of pCG-ATF4 (human ATF4, Table 2.2) and decreasing amounts of human DISC1-WT. Transfected cells were treated for 4 hours with DMSO or 10 µM forskolin before being assayed for luciferase activity. The numbers indicate the amount (ng/well) of plasmid DNA used for transfection. The bars represent the average of at least 5 independent experiments. Data are normalised to the basal luciferase activity in DMSO-treated cells transfected with the reporters only, and were analysed by one-way ANOVA and Dunnett's post test.

Attempts to replicate my findings were also carried out in SH-SY5Y cells, using two distinct CRE reporters (pGL4.29[luc2P/CRE/Hygro] and pGL4.23-CRE). These

reporters have been codon-optimised to efficiently drive firefly luciferase expression in mammalian cells, and were chosen for these experiments because the non codon-optimised SomCRE-Luc reporter did not produce a detectable signal in SH-SY5Y cells (see paragraph 4.2). Moreover, since the Fugene HD transfection protocol adopted for HEK293 cells did not achieve a satisfactory signal-to-noise ratio in luciferase assays performed in SH-SY5Y cells (see paragraph 4.3.1), these cells were transfected by nucleofection, as described in paragraph 2.4.6.3. As shown in Figure 4.7 A, ATF4 does not significantly activate transcription from the pGL4.29[luc2P/CRE/Hygro] reporter in these cells, and it was therefore not possible to test for modifying effects of DISC1 using this reporter (Figure 4.7 A). On the other hand, ATF4 significantly activates transcription from the pGL4.23-CRE reporter in SH-SY5Y cells, and this effect is not modified by DISC1 co-expression (Figure 4.7 B). Similar discrepancies between the effects of ATF4 on different CRE reporters have been observed before (Bartsch *et al*, 1995), and may be caused by differences in the number of CRE repeats and/or the nature of the flanking sequence. The lack of effect of DISC1 co-expression on ATF4 transactivation activity in SH-SY5Y cells is in clear contrast with what was observed in HEK293 cells (Figure 4.6). However, this discrepancy may be explained by several important experimental differences. First, the two experiments were performed using different sets of reporter constructs (SomCRE-Luc and TK-Renilla for HEK293 and pGL4.29[luc2P/CRE/Hygro] or pGL4.23-CRE and SV40-Renilla in SH-SY5Y), and different transfection methods. Secondly, luminescence was assayed 48 hours after transfection in HEK293 cells and 24 hours after transfection in SH-SY5Y cells. A shorter transfection time was adopted in SH-SY5Y cells because the luminescence signal from the internal control (SV40 Renilla) drops below background 48 hours after transfection in these cells (not shown). The shorter incubation time post transfection may have significantly affected the expression levels of ATF4 and DISC1 in SH-SY5Y cells. Additionally, despite the improved luminescence signal achieved by nucleofection in SH-SY5Y cells, the luminescence generated by the internal control plasmid (SV40-Renilla luciferase) remains very low, and only slightly exceeds the background luminescence recorded in untransfected cells. All the above factors, combined with the markedly lower transfection efficiency

achieved in SH-SY5Y cells compared to HEK293 cells, question the validity of the results obtained in the former, and preclude any direct comparison between reporter assays carried out in the two cell lines.

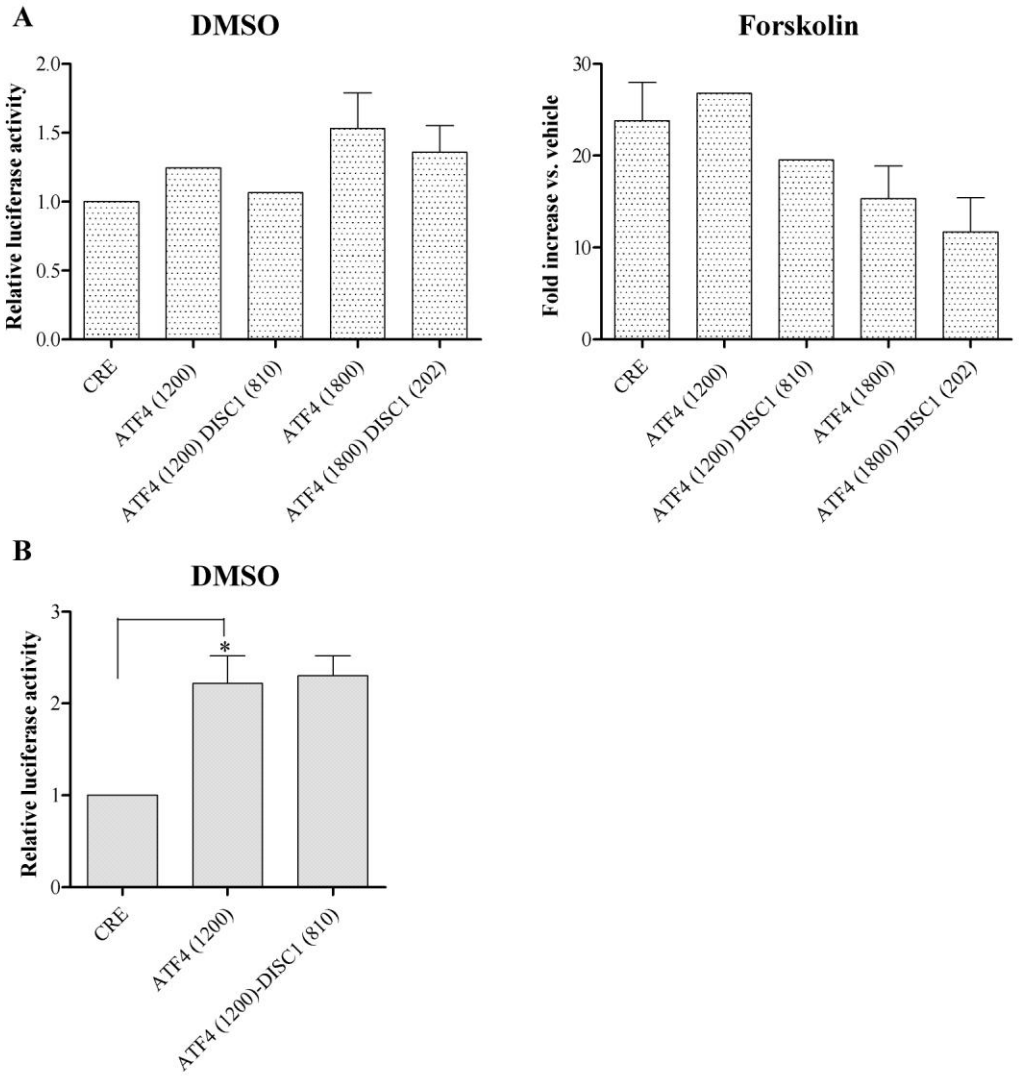

Figure 4.7 (A, B) SH-SY5Y cells were transfected by nucleofection with the reporters only (CRE) or in combination with the indicated amounts (ng) of human ATF4 and human DISC1. CRE reporters were pGL4.29[luc2P/CRE/Hygro (A) or pGL4.23-CRE (B). The internal control was SV40-Renilla. Relative luciferase activity was measured after treatment with DMSO or 10 µM forskolin for 4 hours. The indicated amounts of expression plasmid DNA were tested in one (no error bars) or four (error bars) independent experiments. Data are normalised to the basal

luciferase activity in DMSO-treated cells transfected with the reporters only, and were analysed by one way ANOVA followed by Dunnett's multiple comparisons test.

To test for the specificity of the activating and repressive effects of ATF4 on SomCRE-Luc, the experiment was repeated using a dominant-negative mutant form of ATF4 (ATF4ΔRK), which lacks the DNA binding domain (He *et al*, 2001; Siu *et al*, 2002). The ATF4ΔRK expression plasmid pCG-ATF4ΔRK was obtained by mutating the DNA binding domain of human ATF4 (^{294}RYRQKKR^{300} to ^{294}GYLEAAA^{300}) in pCG-ATF4 (Table 2.2) by site-directed mutagenesis, using mutagenic primers ATF4ΔRK F and R (Table 2.6). As expected, at basal cAMP levels ATF4, but not ATF4ΔRK, significantly activates transcription from SomCRE-Luc in HEK293 cells, and DISC1 has no effect on ATF4ΔRK (Figure 4.8). At high cAMP levels, ATF4ΔRK still significantly inhibits activation of the CRE, albeit to a lesser extent compared to ATF4, and DISC1 does not modify this effect (Figure 4.8). The latter observation is consistent with the current hypothesis that at high cAMP levels ATF4 inhibits CRE-dependent transcription by competing with CREB for transcriptional co-factors such as CBP (Thiel *et al*, 2005), a mechanism that does not require DNA binding.

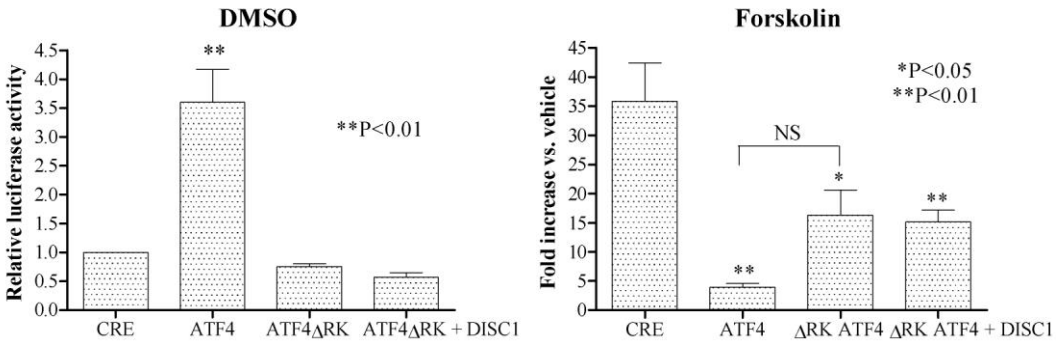

Figure 4.8 HEK293 cells were transfected with the reporters only (CRE) or in combination with ATF4, ATF4ΔRK and DISC1, as indicated. Relative luciferase activity was measured after a 4 hour treatment with DMSO or 10 μM forskolin. The bars represent the average of 4 independent experiments. Data are normalised to

the basal luciferase activity in cells transfected with the reporters only, and were analysed by one-way ANOVA and Dunnett's post test.

4.4.2 *The differential effect of DISC1 variants on ATF4-dependent transcription*

4.4.2.1 *Effects on CRE-driven transcription*

In chapter 3 of this thesis I demonstrated that risk-conferring amino acid substitutions 37W and 607F, but not 264R, 432L, 603I and 704C, significantly reduce DISC1 nuclear expression, and might thus potentially interfere with the nuclear functions of the protein. Having observed that DISC1 represses the ATF4-dependent activation of CRE-driven transcription at basal cAMP levels, an effect that might be conceivably mediated by nuclear DISC1, I next sought to test whether any of the above amino acid substitutions affect this particular DISC1 function. Initially, all 20 DISC1 variants were simultaneously compared for their ability to inhibit mouse ATF4, but no statistically significant effects were observed (Figure 4.9). As shown in Figure 4.9, this experiment produced highly variable results, probably reflecting technical inconsistencies due to the simultaneous handling of a large number of samples. Thus, the following analysis was focused on a selected subset of DISC1 variants, which were compared for their ability to inhibit human ATF4. All transfections were performed with 120 ng/well of pGC-ATF4, while the amount of transfected DISC1 DNA was either 81 (Figure 4.10 A, C) or 20.25 ng/well (Figure 4.10, B). At basal cAMP levels, all the analysed DISC1 variants retain the ability to significantly inhibit ATF4 ($P<0.05$ for DISC1-704C, $P<0.01$ for all other variants, Figure 4.10 A and B), but the inhibitory effect of DISC1-37W and DISC1-607F is significantly weaker compared to DISC1-WT ($P<0.05$ for 37W, $P<0.01$ for 607F, Figure 4.10 A). As expected, overexpression of the PKA-dependent transcription factor CREB1α (Table 2.2), either alone or in combination with DISC1, has no effect at basal cAMP levels, when PKA activity is low (Figure 4.10 A). In addition, at high cAMP levels, none of the analysed DISC1 variants significantly modifies the inhibitory effect of ATF4 on CRE-driven transcription (Figure 4.10). These results

are consistent with the detrimental effect of 37W and 607F, but not 432L, 603I and 704C, on DISC1 nuclear targeting described in chapter 3 of this thesis.

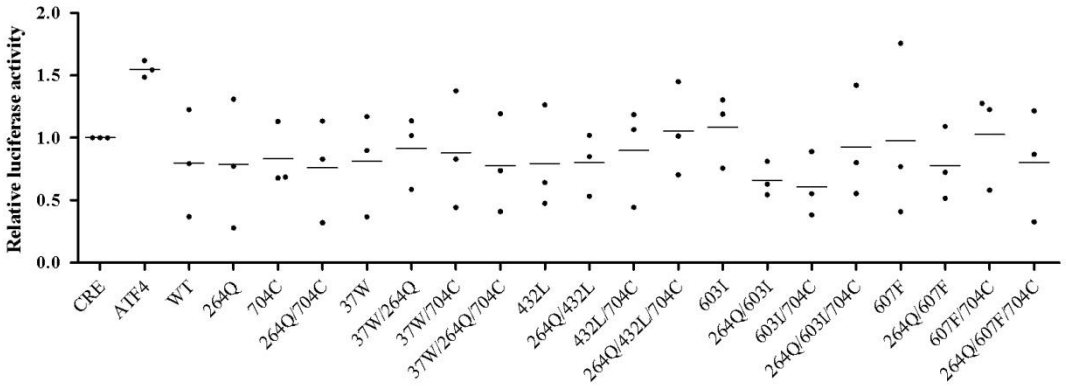

Figure 4.9 Relative luciferase activity in HEK293 cells transfected with the reporters only (CRE) or in combination with mouse ATF4, with or without the indicated DISC1 variants. Dots indicate the relative luminescence readings in individual experiments, and the mean value for each sample is indicated by a horizontal bar. Data are normalised to the basal luciferase activity in cells transfected with the reporters only, and were analysed by one-way ANOVA.

To further investigate the likely relationship between the decreased ability of DISC1 variants 37W and 607F to inhibit the transcriptional activity of ATF4 and their defective nuclear targeting, I tested the effect of DISC1ΔLZ9, a mutant form of DISC1 that fails to accumulate in the nucleus (Figure 3.12). Consistent with its exclusion from the nucleus, DISC1ΔLZ9 does not significantly inhibit ATF4-mediated activation of CRE-dependent transcription ($P<0.05$, paired student's t-test, Figure 4.10 C). In contrast with my previous observations, in this particular experiment DISC1-WT, but not DISC1ΔLZ9, significantly dampened ATF4-mediated inhibition of CRE-driven transcription at high cAMP levels (Figure 4.10 C).

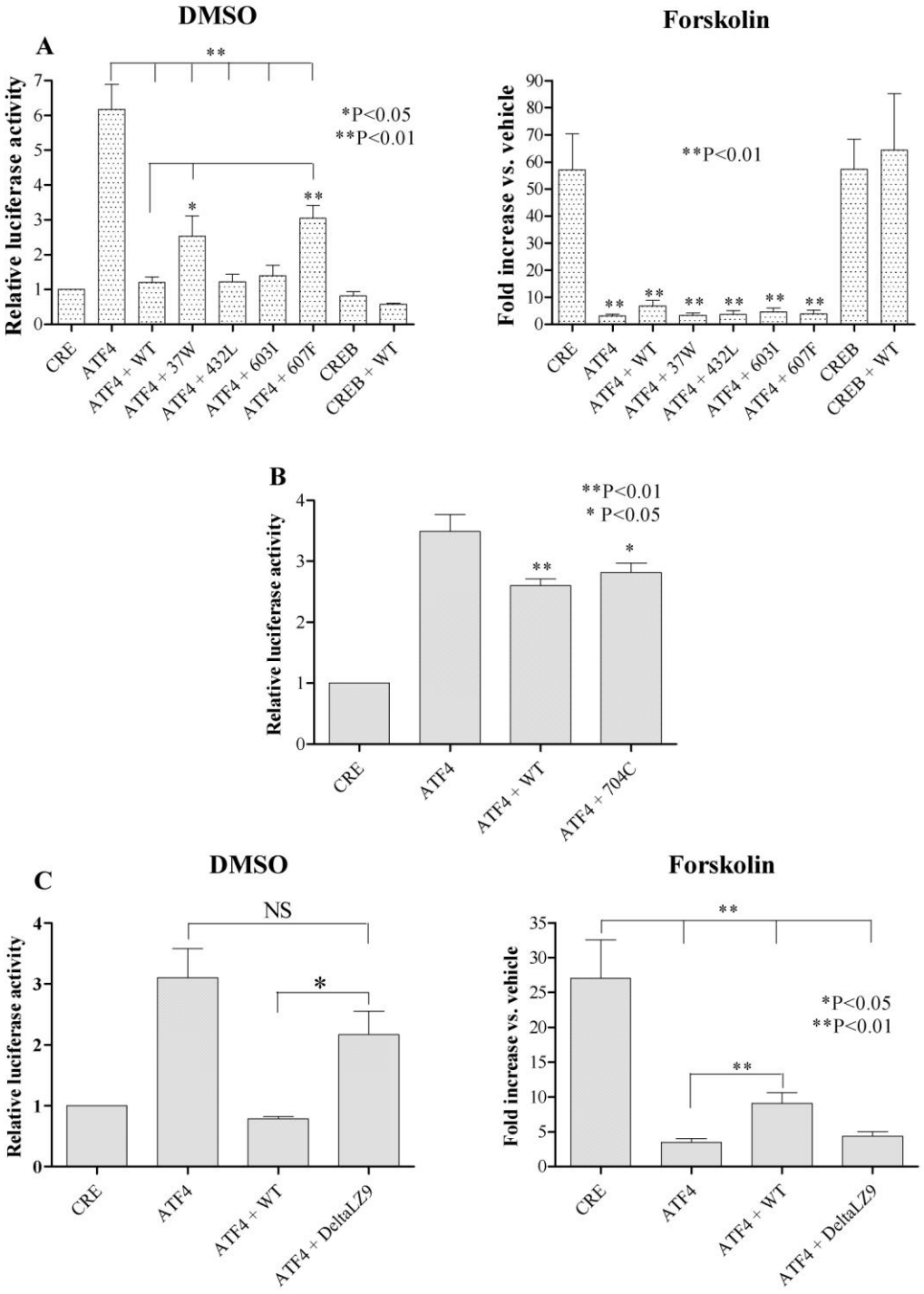

Figure 4.10 (A, B and C) HEK293 cells were transfected with the reporters only (CRE) or in combination with human ATF4 or CREB1α (A), with our without the indicated DISC1 variant. (A, C) Relative luciferase activity was measured after a 4 hour treatment with DMSO or 10 μM forskolin. Transfected cells analysed in (B) were untreated. Bars represent the average of at least 3 independent experiments.

Data are normalised to the basal luciferase activity in cells transfected with the reporters only, and were analysed by one-way ANOVA followed by Dunnett's multiple comparisons test and paired student's t-test.

The differential effect of DISC1-WT, DISC1-37W and DISC1-607 on ATF4-mediated transcription is not caused by differences in expression levels (Figure 4.11). Next, to test if the differential effect of DISC1 variants is limited to HEK293 cells, their inhibitory effect on ATF4-dependent transcription was compared in MO3.13 human oligodendrocytes. In these cells, the SomCRE-Luc reporter does not respond to ATF4, and produces a very weak response to increased cAMP levels, probably due to lower transfection efficiency compared to HEK293 cells (Figure 4.12 A). To overcome this, the SomCRE-Luc reporter was replaced with the codon-optimised reporter pGL4.23-CRE, which is designed to efficiently drive luciferase expression in mammalian cells (see paragraph 4.2). As shown in figure 4.12 B, pGL4.23-CRE responds to ATF4 when transfected in MO3.13 cells, and this transcriptional activation is significantly inhibited by DISC1-WT, but not DISC1-37W or DISC1-607F, replicating the findings in HEK293 cells. However, similarly to SomCRE-Luc, pGL4.23-CRE responds very weakly to forskolin treatment in MO3.13 cells (Figure 4.12). The reasons for this are not clear, but it is possible that MO3.13 cells have a reduced sensitivity to forskolin, or that they respond differently to increased cAMP levels compared to HEK293 cells. Additionally, it cannot be excluded that the pGL4.23-CRE reporter has an intrinsically lower capacity to respond to cAMP, possibly due to long-range effects of sequences surrounding the CREs in this construct.

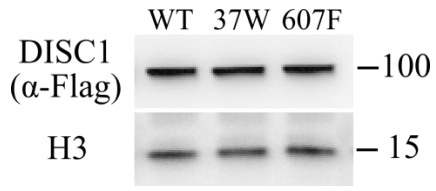

Figure 4.11 To compare the expression levels of DISC1-WT, DISC1-37W and DISC1-607F, whole cell lysates were obtained from HEK293 cells transfected with

equal amounts of the indicated pcDNA4/TO-Flag DISC1 expression constructs, and analysed by western blotting. The loading control is histone 3 (H3) (Table 2.5). The position and size (kDa) of the protein markers is shown.

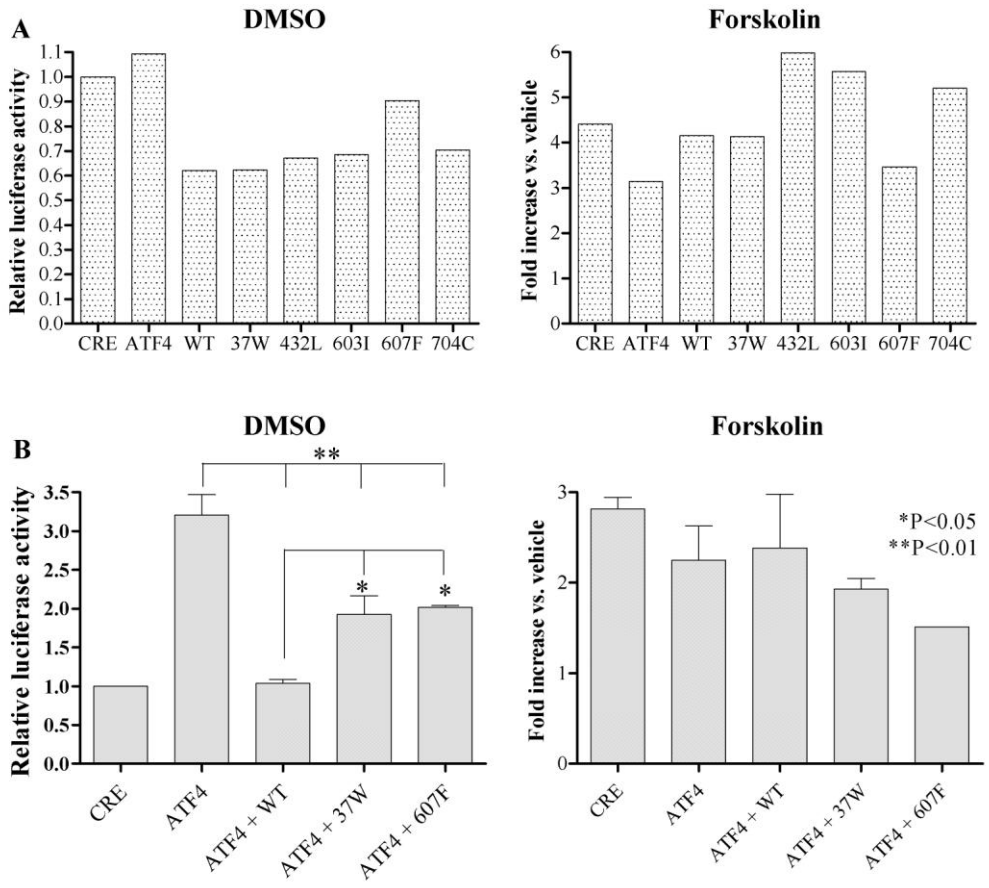

Figure 4.12 Relative luciferase activity in MO3.13 cells transfected with the reporters only (CRE) or in combination with ATF4 alone, with or without the indicated DISC1 variant. Cells were transfected with the SomCRE-Luc (A) or pGL4.23-CRE (B) luciferase reporter and treated for 4 hours with DMSO or 10 µM forskolin before being assayed for luciferase activity. The bars represent the average of one (A) or 3 (B) independent experiments. Data are normalised to the basal luciferase activity in DMSO-treated cells transfected with the reporters only, and were analysed by one-way ANOVA followed by Dunnett's post test.

Next, I asked whether the ENU-induced mouse mutations Q31L and L100P, which are associated with depression- and schizophrenia-like behaviours in mice, respectively (Clapcote *et al*, 2007), affect Disc1's inhibitory effect on ATF4. In HEK293 cells transfected with pRK7-ATF4, encoding mouse ATF4, and either pcDNA4/TO-Flag mouse Disc1-WT, 31L or 100P (paragraph 3.2), ATF4 weakly activates CRE-driven transcription at basal cAMP levels, although this effect does not reach statistical significance in this particular experiment, and DISC1 has no effect on ATF4 (Figure 4.13 A). Similarly, mouse Disc1 does not affect the magnitude of the ATF4-dependent inhibition of cAMP-induced CRE activity (Figure 4.13 A). Although I have never compared them directly, I have noticed that mouse ATF4 has, on average, a weaker activating effect on the basal CRE activity in HEK293 cells compared to human ATF4, which may be explained by differential expression levels due to their different vector backbone (pRK7 and pCG, respectively, Table 2.2). Alternatively, it is conceivable that the expression, stability and/or function of mouse ATF4 may be sub-optimal in human HEK293 cells. Thus, to better test their potential effect on ATF4-dependent transcription, mouse Disc1-WT, 31L and 100P where co-expressed with human ATF4 in HEK293 cells. In this experiment, human ATF4 clearly activates CRE-dependent transcription, but mouse Disc1 does not inhibit this, nor does it interfere with the inhibitory effect of ATF4 at high cAMP levels (Figure 4.13 B).

The lack of effect of mouse Disc1 on the transcriptional activity human ATF4 is in contrast with the strong inhibitory effect of human DISC1 on human ATF4 (Figure 4.6). This discrepancy may reflect the substantial sequence differences between human and mouse Disc1 proteins (Taylor *et al*, 2003). To test this possibility, mouse ATF4 was co-expressed with either human DISC1 or mouse Disc1 in the mouse neuronal cell line NSC-34 (Cashman *et al*, 1992), and their transcriptional effects were tested in parallel on the pGL4.23-CRE reporter. NSC-34 cells were chosen for this particular experiment to rule out any potential detrimental effect of species context on the expression of exogenous ATF4 and DISC1. In NSC-34 cells, mouse ATF4 significantly activates transcription from the CRE at basal cAMP levels and human, but not mouse, DISC1 significantly inhibits this (Figure 4.13 C). Additionally, this experiment shows no effect of mouse mutants Disc1-31L and

Disc1-100P (Figure 4.13 C). As observed in MO3.13 cells (Figure 4.12 B), pGL4.23-CRE responds very weakly to forskolin treatment in NSC-34 cells, reinforcing the possibility that this reporter might be intrinsically unable to respond to cAMP (Figure 4.13 C). As confirmed by western blotting analysis, the differential effect of mouse and human DISC1 on ATF4-dependent transcription cannot be explained by different expression levels, at least in HEK293 cells, nor it is likely to arise from relatively weaker interaction between mouse ATF4 and mouse Disc1 (Figures 4.14 and 4.15). In fact, in a co-immunoprecipitation assay performed in HEK293 cells, the relative amount of mouse ATF4 that co-precipitated with mouse Disc1 was higher compared to human DISC1 (Figure 4.15). Interestingly, the same assay also showed potentially reduced interaction of mouse ATF4 with Disc1-31L and Disc1-100P, although this would need to be confirmed by further experimental replicates (Figure 4.15).

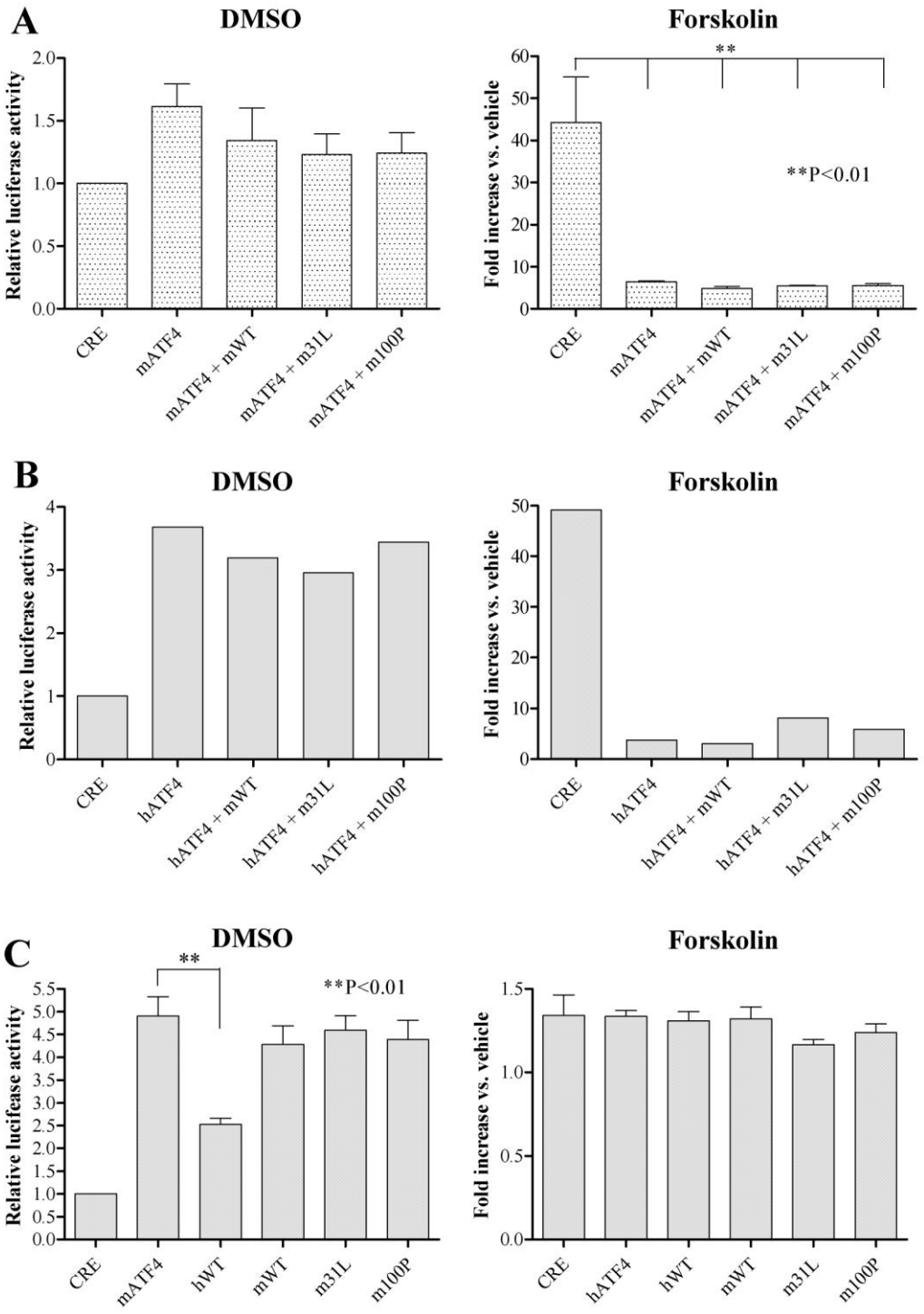

Figure 4.13 HEK293 (A, B) or NSC-34 (C) cells were transfected with the reporters only (CRE) or in combination with human (h) or mouse (m) ATF4, with or without the indicated human or mouse Disc1 variant. Cells were transfected with the SomCRE-Luc (A,B) or pGL4.23-CRE (C) luciferase reporter and treated for 4 hours with DMSO or 10 µM forskolin before being assayed for luciferase activity. The bars

represent the average of one (B) or 4 (A, C) experiment(s). Data are normalised to the basal luciferase activity in cells transfected with the reporters only, and were analysed by one-way ANOVA followed by Dunnett's post test.

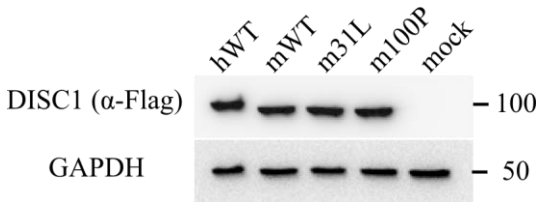

Figure 4.14 To compare the expression levels of the indicated variants of human (h) and mouse (m) DISC1, whole cell lysates were obtained from HEK293 cells transfected with equal amounts of the respective pcDNA4/TO-Flag DISC1 expression constructs (see paragraph 3.2), and analysed by western blotting using the Flag MMC antibody (Table 2.5). The position and size (kDa) of the protein markers is shown.

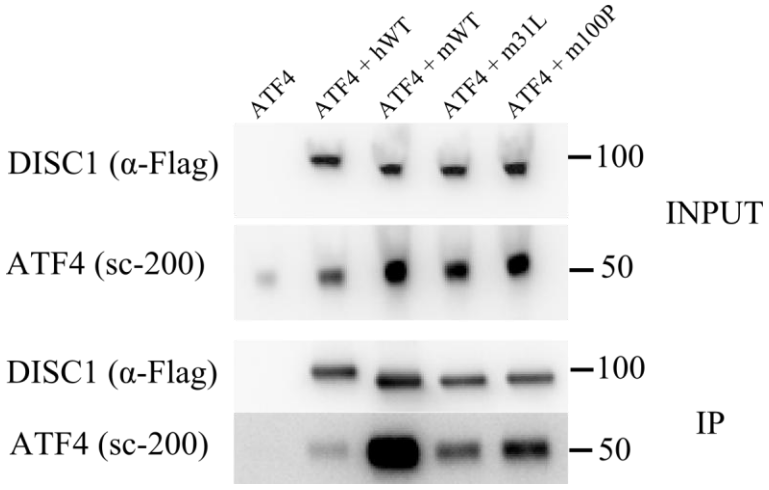

Figure 4.15 HEK293 cells were transfected with pRK7-ATF4 (encoding mouse ATF4) alone or in combination with the indicated human (h) or mouse (m) DISC1 variants. Exogenous DISC1 was immunoprecipitated using the Flag MMC antibody and detected using the Flag RPC antibody. Co-precipitating ATF4 was detected with the ATF4 RPC antibody (sc-200) (Table 2.5). The position and size (kDa) of the protein markers is indicated.

When expressed in COS7 cells, mouse Disc1 appears to translocate to the nucleus less efficiently compared to human DISC1 (Figure 3.16). This effect might reflect sequence differences between human and mouse DISC1 in regions of the protein that are known to be important for nuclear localisation, such as NLS1 and LZ9 (Table 3.2). Indeed, while the distribution of repeating leucines in LZ9 is highly conserved between human and mouse DISC1, suggesting that the structure and hence functionality of this motif is likely preserved, NLS1 shows a lower degree of conservation between the two species (Figure 4.16). The classic NLS motif is composed of four consecutive basic residues (Kalderon *et al*, 1984), and these are strictly conserved in NLS1 from human to dog in a multiple sequence alignment (Chubb *et al*, 2008). However, in mouse Disc1, NLS1 only has three consecutive basic residues (Figure 4.16). All DISC1 orthologues, including mouse Disc1, have a "loose" bipartite NLS motif (two clusters of basic amino acids separated by a short linker sequence) in the region spanning NLS1, which could also favour importin binding and nuclear translocation (Chubb *et al*, 2008; Robbins *et al*, 1991) (Figure 4.16). However, the classic tetra-arginine NLS motif is likely to be the key driver of DISC1 nuclear import, implying that mouse Disc1 NLS1 might function less efficiently than human DISC1 NLS1 (Dinesh Soares, personal communication). Thus, it is conceivable that the lack of repressive activity of mouse Disc1 on ATF4 may be related to its intrinsically reduced nuclear localisation compared to human DISC1, similarly to what observed for human DISC1 variants 37W and 607F.

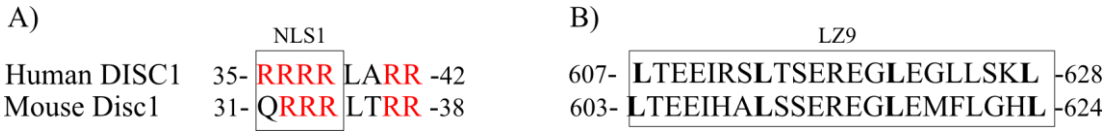

Figure 4.16 Sequence alignment of the NLS1 (A) and LZ9 (B) regions in human and mouse DISC1. (A) Basic residues are shown in red. (B) The leucine residues involved in the formation of the predicted leucine zipper are shown in bold.

Hence, to test the hypothesis that the differential effect of human and mouse DISC1 on ATF4-dependent transcription may reflect differences in their respective nuclear

targeting efficiencies, nuclear and cytoplasmic fractions were obtained from NSC-34 cells transfected with equal amounts of human or mouse Disc1, and analysed by western blotting. Contrary to what was seen in HEK293 cells (Figure 4.14), mouse Disc1 is expressed at higher levels than human DISC1 in NSC-34 cells ($P<0.05$, Figure 4.17). Accordingly, the relative nuclear abundance of mouse Disc1 is higher compared to human DISC1, although this does not reach statistical significance (Figure 4.17). Collectively, these data indicate that the differential ability of human and mouse Disc1 to repress the transcriptional activity of ATF4 cannot be explained by differences in nuclear targeting or ATF4 binding, and might thus reflect a functional divergence between the two proteins. Further experiments will be needed to test this possibility.

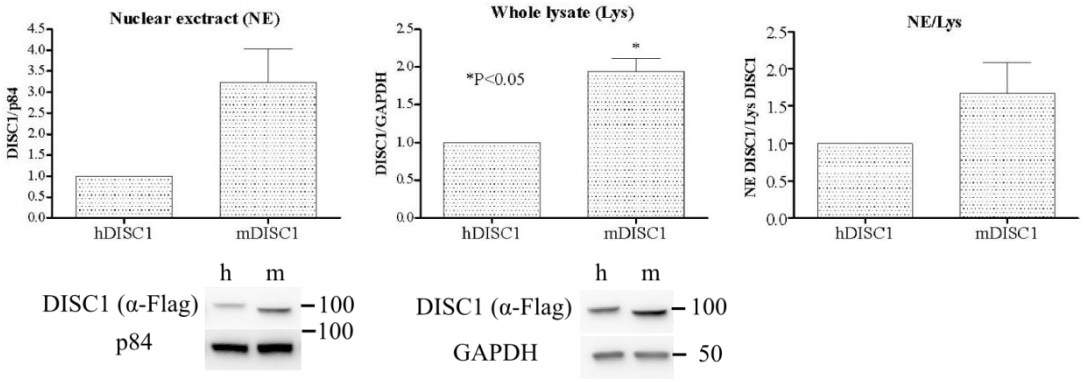

Figure 4.17 The indicated subcellular protein extracts were obtained from NSC-34 cells transfected with equal amounts of human (h) or mouse (m) Flag DISC1-WT in pcDNA4/TO and analysed by western blotting using the Flag MMC antibody to detect exogenous DISC1, followed by band densitometry. The loading controls (p84 and GAPDH) are proteins known to be preferentially enriched in either of the different subcellular fractions analysed. The bars represent the average of 3 independent experiments. All the densitometry data are normalised to the relative band intensity of human DISC1. Data were analysed by one sample two-tailed student's t-test. The position and size (kDa) of the protein markers is indicated.

4.4.3 *Testing for a dominant-negative effect of DISC1 variants 37W and 607F*

In chapter 3 of this thesis I demonstrated that DISC1 variants 37W and 607F disrupt the nuclear targeting of wild-type DISC1 in a dominant-negative fashion, and here I showed that these variants also significantly reduce the inhibitory effect of DISC1 on ATF4 transcriptional activity. Altogether, these observations suggest that the proper nuclear expression of DISC1 may be necessary for its regulation of ATF4 activity. If true, this would in turn imply that, by exerting a dominant-negative effect on the nuclear targeting of DISC1-WT, DISC1 variants 37W and 607F might also reduce its repressive activity on ATF4 in a dominant-negative fashion. Thus, I asked whether DISC1-37W and DISC1-607F affect the ability of DISC1-WT to inhibit the transcriptional activity of ATF4 on the CRE at basal cAMP levels. My previous experiments established that, in HEK293 cells, transfection of 81 ng/well of DISC1-WT completely abolishes the transcriptional activation induced by 120 ng/well of ATF4 (Figures 4.5, 4.6 and 4.10 A and C). Thus, to produce partial inhibition of ATF4, HEK293 cells were transfected with 120 ng/well of ATF4 and 40.5 ng/well of DISC1-WT. As expected, this lower amount of DISC1-WT alone produces a milder (~65%) inhibition of ATF4 ($P<0.01$, Figure 4.18) and, consistent with my previous observations, the same amount of DISC1-37W or DISC1-607F alone inhibits ATF4 to a lesser extent compared to DISC1-WT (~47% and ~45%, respectively) ($P<0.05$, Figure 4.18). Combining 40.5 ng/well of DISC1-WT with the same amount of either DISC1-37W or DISC1-607F produces an apparently stronger (~85%) inhibition of ATF4 compared to 40.5 ng/well of DISC1-WT alone (Figure 4.18). However, the degree of inhibition produced by 40.5 ng/well of DISC1-WT plus 40.5 ng/well of DISC1/37W or DISC1-607F is not significantly different from the inhibitory effect produced by 40.5 ng/well of DISC1-WT alone (two tailed paired student's t-test, Figure 4.18). These results suggest that DISC1's potential to inhibit ATF4 may be reduced in subjects that are heterozygous for either 37W or 607F. However, due to the technical limitations of this reporter assay, it was not possible to determine whether these amino acid substitutions impair the inhibitory effect of DISC1-WT in a dominant-negative fashion. Indeed, although a previous experiment established that the degree of ATF4 inhibition increases with the amount of transfected DISC1-WT

DNA (Figure 4.6), it was not possible to accurately determine the relationship between these two variables in the co-expression experiment (Figure 4.18). As a consequence, this experiment does not allow to accurately predict the degree of ATF4 inhibition based on the amount of transfected DISC1 DNA.

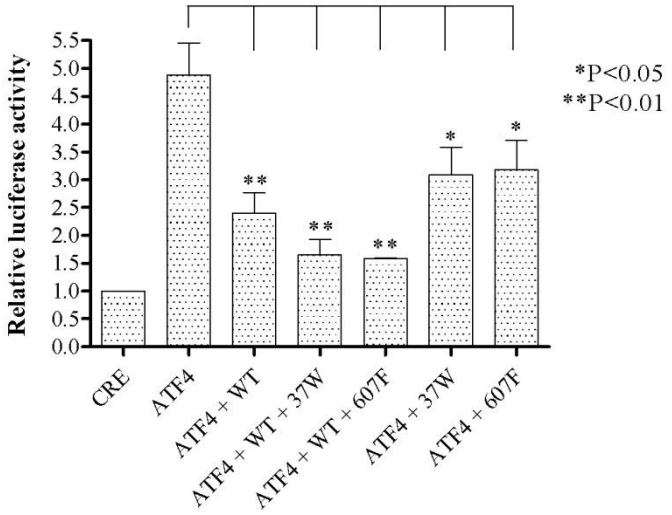

Figure 4.18 Relative luciferase activity in HEK293 cells transfected with the reporters alone (CRE) or in combination with ATF4, with or without equal amounts (40.5 ng/well) of each of the indicated DISC1 variants. Bars represent the average of 3 independent experiments. Data are normalised to the basal luciferase activity in cells transfected with the reporters only, and were analysed by one-way ANOVA followed by Dunnett's post test.

4.4.4 *Effect of DISC1 variants on AARE-driven transcription*

To test whether DISC1 is capable of modulating the transcriptional activity of other response elements regulated by ATF4, I generated a novel reporter that drives the expression of Firefly luciferase under control of two copies of the amino acid response element (AARE) found in the promoter of *CHOP*, one of ATF4 target genes (Kilberg *et al*, 2009; Shan *et al*, 2009; Siu *et al*, 2002) (Paragraph 4.2). The

AARE is a particular type of CARE that preferentially drives the transcriptional response to amino acid limitation (Bruhat *et al*, 2002; Kilberg *et al*, 2009), and ATF4 overexpression alone is sufficient to activate the expression of *CHOP* and other CARE-containing genes (Shan *et al*, 2009). Accordingly, ectopic ATF4 activates transcription from the CHOP AARE, but not its mutant, non-responsive form (mutCHOP AARE), and this effect is not influenced by cAMP levels (Figure 4.19). As seen on the CRE promoter (Figure 4.5), DISC1-WT alone does not affect transcription from the CHOP AARE, but it significantly inhibits ATF4-mediated transactivation ($P<0.05$, Figure 4.19). However, DISC1-mediated inhibition of ATF4 transcriptional activity on the CHOP AARE is not affected by 37W or 607F, as both DISC1-37W and DISC1-607F produce the same degree of inhibition as DISC1-WT ($P<0.05$ for 37W, $P<0.01$ for 607F, Figure 4.19). Interestingly, although the transactivation potential of ATF4 on the CHOP AARE remains unchanged at high cAMP levels, co-expression of either DISC1 variant has no effect on ATF4 under these conditions, suggesting that the interaction between the two proteins may be regulated by cAMP (Figure 4.19). Overall, these results indicate that the regulatory effect of DISC1 on ATF4 extends to the CHOP AARE, and may be influenced by cAMP levels. Additionally, they indicate that under the same experimental conditions, ATF4 has a markedly stronger transactivation activity on the CHOP AARE (10-11 fold activation) compared to the CRE (3-5 fold activation), and that the inhibitory effect of DISC1-WT is relatively milder on the CHOP AARE (~20%) compared to the CRE (90-100%). Since for both 37W and 607F the loss of function observed on the CRE is partial (~30% for 37W and ~40% for 607F), the above observations may explain why no differential effects of DISC1-37W and DISC1-607F were apparent in this particular experiment.

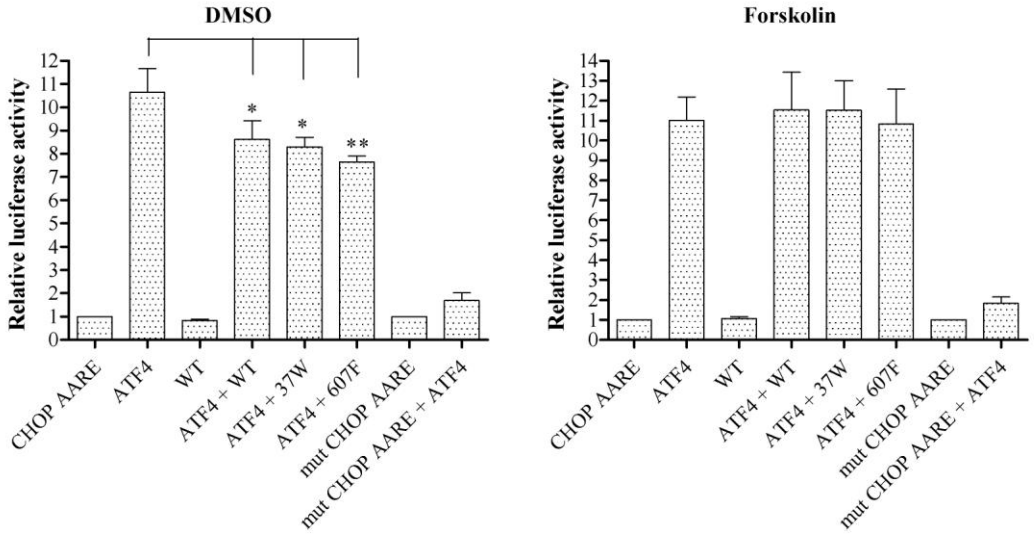

Figure 4.19 HEK293 cells were transfected with the reporters only (CHOP AARE or mut CHOP AARE) or in combination with ATF4, DISC1-WT or both ATF4 and the indicated DISC1 variant. Luciferase activity was measured after a 4 hour treatment with DMSO or 10 μM forskolin. Bars represent the average of at least 4 independent experiments. Data are normalised to the basal luciferase activity in cells transfected with the reporters only, and were analysed by one-way ANOVA followed by Dunnett's post test. *P<0.05; **P<0.001.

Next, I hypothesised that, since the transactivation activity of ATF4 on the CHOP AARE is much stronger compared to the CRE, the amount of exogenous ATF4 that fully activates the CRE may over-saturate the CHOP AARE, thus partially masking the inhibitory effect of DISC1. As shown in figure 4.20, the CHOP AARE activation induced by 90 ng/well of ATF4 is the same as that previously seen with 120 ng/well of ATF4 (Figure 4.19), suggesting that the latter ATF4 concentration is indeed over-saturating on this particular reporter. Consistently, the inhibitory effect of DISC1 is generally stronger (up to 40-50%) in the presence of lower concentrations of ATF4 (Figure 4.20).

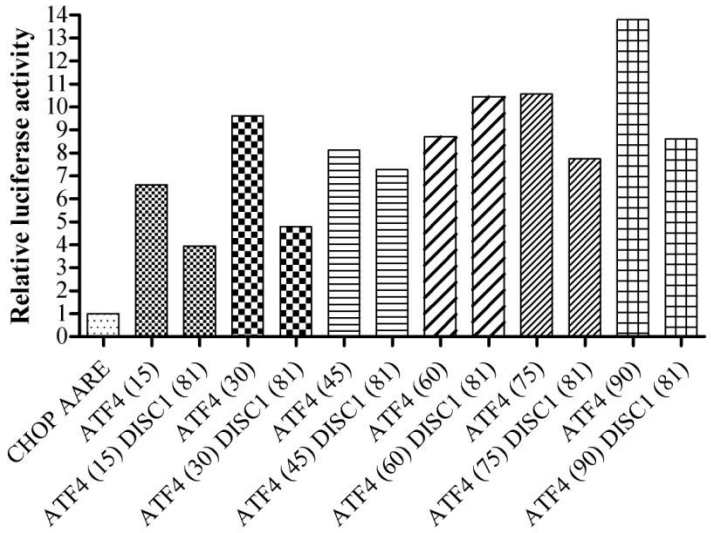

Figure 4.20 HEK293 cells were transfected with the reporters only (CHOP AARE) or in combination with different concentrations of ATF4, with or without a fixed amount of DISC1-WT (reported in brackets as ng/well of expression plasmid). 48 hours after transfection, the cells were lysed and assayed for luciferase activity. Bars represent mean luciferase activities measured in a single experiment. Data are normalised to the luciferase activity in cells transfected with the reporters only.

In the next experiment, equal amounts of DISC1-WT, 37W or 607F (81 ng/well) were co-expressed with a non-saturating concentration of ATF4 that still produces a strong activation of CHOP AARE-driven transcription (15 ng/well) (Figure 4.20). These optimised experimental conditions revealed that DISC1-WT and DISC1 -607F significantly repress the ATF4-dependent transactivation of the CHOP AARE ($P<0.01$ for DISC1-WT and $P<0.05$ for DISC1-607F, Figure 4.21). On the other hand, DISC1-37W does not affect ATF4 transactivation of the CHOP AARE (Figure 4.21). Importantly, and consistent with what I previously observed on the CRE (Figures 4.10 and 4.12), the inhibitory effect of both DISC1-37W and DISC1-607F is significantly weaker compared to DISC1-WT ($P<0.05$, Figure 4.21).

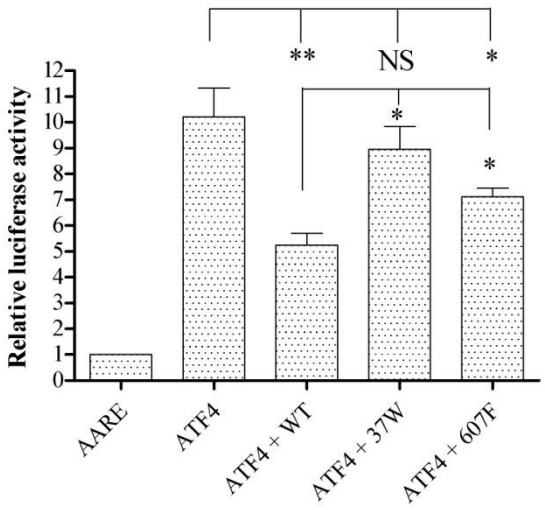

Figure 4.21 HEK293 cells were transfected with the reporters only (CHOP AARE) or in combination with ATF4 (15 ng/well), with or without the indicated DISC1 variants (81 ng/well). 48 hours after transfection, the cells were lysed and assayed for luciferase activity. Bars represent the average of at least 4 independent experiments. Data are normalised to the luciferase activity in cells transfected with the reporters only, and were analysed by one-way ANOVA followed by Dunnett's post test. *P<0.05; **P<0.01.

4.5 The effect of DISC1 variants on the transcriptional response to stress

In the previous sections of this chapter I demonstrated that DISC1 inhibits the transcriptional activity of ectopically expressed ATF4, and that this effect is significantly impaired by amino acid substitutions 37W and 607F. Following on from these findings, I asked whether DISC1 similarly regulates the activity of endogenous stress-induced ATF4, and I investigated the effect of 37W and 607F on stress-related transcriptional events.

4.5.1 *Testing different stress paradigms to induce endogenous ATF4*

Preliminary experiments were designed to identify suitable experimental conditions to activate CRE- and/or CHOP AARE-driven transcription from the respective

reporter plasmids through induction of endogenous ATF4. The different stress paradigms tested in these experiments and the respective transcriptional responses they elicited are summarised in Figure 4.22. All the different drugs or treatments used here are known to induce expression of endogenous ATF4 by perturbing cellular homeostasis through different mechanisms. For example, the histidinyl tRNA synthetase inhibitor histidinol (HisOH) simulates amino acid deprivation and activates the amino acid deprivation response through the induction of ATF4 (Hansen *et al*, 1972; Shan *et al*, 2009; Su & Kilberg, 2008), an effect that can also be induced by selective removal of leucine and/or lysine from the culture medium (Ohta *et al*, 2010). However, I could not detect activation of the CRE or CHOP AARE reporters upon treatment with 2 mM HisOH, nor after leucine and/or lysine deprivation (Figure 4.22) (for the composition of the media used in the leucine/lysine deprivation experiment, see section 2.4.1.1 of this thesis). Thapsigargin is a non-competitive inhibitor of the sarco/endoplasmic reticulum Ca^{2+} ATPase and causes release of Ca^{2+} from the endoplasmic reticulum (ER) into the cytoplasm, whereas tunicamycin selectively inhibits N-linked glycosylation (Samali *et al*, 2010). Both drugs interfere with the normal function of the ER and induce accumulation of misfolded protein in the ER, triggering the unfolded protein response, which in turn results in the activation of ATF4 (Armstrong *et al*, 2010; Galehdar *et al*, 2010; Milani *et al*, 2009; Yamaguchi *et al*, 2008). At both concentrations (2 and 4 µg/ml) and incubation times (8 and 16 hours) tested, tunicamycin did not activate transcription from either reporter (Figure 4.22), possibly because it is highly toxic to the cells, many of which had become apoptotic during the treatment (data not shown). On the other hand, when used at the concentration of 1 µM for 16 hours, thapsigargin is well tolerated by the cells, and induces a ~2-fold activation of CRE-driven transcription but has no effect on the CHOP AARE reporter (Figure 4.22). As expected, the above thapsigargin treatment strongly induces endogenous ATF4 expression in HEK293 cells (Figure 4.23). Importantly, the thapsigargin-induced activation of CRE-driven transcription is significantly inhibited by DISC1 ($P<0.01$, Figure 4.22). The selective activation of the CRE by thapsigargin is not surprising given that the CHOP AARE has been shown to preferentially respond to amino acid limitation (Bruhat *et al*, 2002). On the other hand, it is not clear why the CHOP

AARE reporter did not respond to amino acid starvation, as the same response element induces a five-fold reporter activation in leucine starved HeLa cells (Bruhat *et al*, 2002). As other studies used different reporters, it is possible that the context in which the response element is placed may influence the binding of transcription factors.

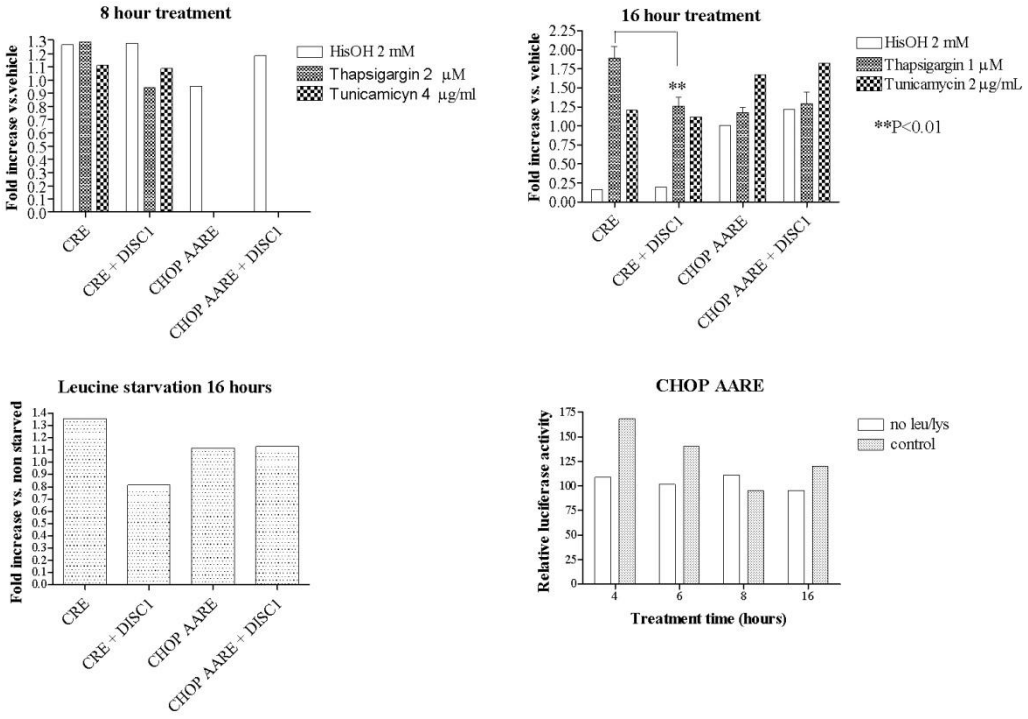

Figure 4.22 HEK293 cells transfected with the indicated reporter plasmids alone or in combination with DISC1 were subjected to the indicated treatments before being assayed for luciferase activity. Where error bars are absent, bars represent the results of a single experiment. Where error bars are present, bars represent the average of 3 independent experiments. Data were analysed by two-tailed paired student's t-test.

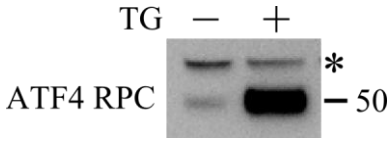

Figure 4.23 HEK293 cells were treated with 1 μM thapsigargin (TG) for 16 hours. At the end of the drug treatment, nuclear protein extracts were prepared from the transfected cells and analysed by western blotting. Endogenous ATF4 was detected with the ATF4 RPC antibody. The position and size (kDa) of the protein markers is indicated. * Non specific band.

4.5.2 *DISC1 variants differentially affect the transcriptional response to endoplasmic reticulum stress*

In HEK293 cells, the thapsigargin-induced activation of the CRE is significantly inhibited by DISC1-WT, but not by DISC1-37W, DISC1-607F or DISC1ΔLZ9 ($P<0.01$, Figure 4.24), consistent with their differential nuclear targeting and impaired ability to inhibit exogenous ATF4. However, these findings could not be confirmed in MO3.13 cells, since thapsigargin had no effect on CRE-driven transcription in these cells (Figure 4.24). Due to time limitations, it was not possible to replicate this experiment in neuronal cells, such as SH-SY5Y and NSC-34.

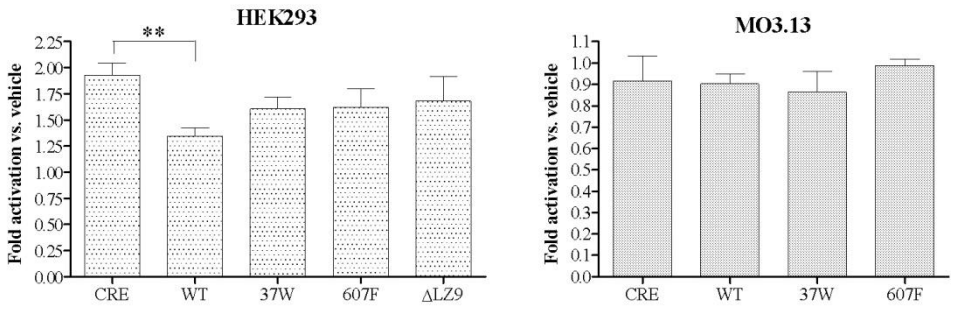

Figure 4.24 Relative luciferase activity in HEK293 (left) or MO3.13 cells (right) transfected for 32 hours with SomCRE-luc and pGL4.23-CRE, respectively, with or without the indicated DISC1 variants, then treated with 1 μM thapsigargin for 16

hours. Bars represent the average of at least 3 independent experiments. Data were analysed by one-way ANOVA followed by Dunnett's post test.

4.6 Discussion

In this chapter, I demonstrated that DISC1 is capable of inhibiting the ATF4-dependent transactivation of CRE- and CHOP AARE-driven transcription at basal cAMP levels in different neuronal and non-neuronal cell models. In addition, I showed that both risk-conferring amino acid substitutions 37W and 607F significantly reduce the inhibitory effect of DISC1 on the ATF4-dependent transactivation of the CRE and CHOP AARE. The partial loss of function induced by 37W and 607F is likely related to the detrimental effect of these amino acid substitutions on the nuclear targeting of DISC1. Indeed, amino acid substitutions that do not affect the nuclear targeting of DISC1 also have no effect on its ability to inhibit ATF4 and, on the other hand, the mutant DISC1ΔLZ9, which is not properly targeted to the nucleus, has no effect on the transcriptional activity of ATF4. However, it is important to remark that the loss-of-function phenotype observed for DISC1-607F and DISC1ΔLZ9 may also be determined by partial or complete loss of ATF4 binding. Indeed, DISC1LZ9 was previously shown to be essential for DISC1 interaction with ATF4 (Sawamura *et al*, 2008), and 607F has the potential to disrupt this ATF4 binding region by removing the first leucine in DISC1LZ9 and hence disrupting the leucine-leucine packing in this putative leucine zipper (Soares *et al*, 2011). Since ATF4 mainly resides in the nucleus, the effects of DISC1 amino acid substitutions on DISC1 nuclear targeting, ATF4 binding and ATF4 repression are likely interconnected.

As demonstrated in chapter 3 of this thesis, both DISC1-37W and DISC1-607F reduce the nuclear expression of DISC1-WT in a dominant-negative fashion, which potentially represents an additional mechanism of ATF4 deregulation by these variants. Although it was not possible to produce conclusive evidence that DISC1-37W and DISC1-607F exert a dominant-negative effect on ATF4 inhibition by

DISC1-WT, co-expression of DISC1-37W or DISC1-607F does not significantly strengthen the inhibitory effect induced by a non-saturating dose of DISC1-WT alone. Put differently, one dose of DISC1-WT alone produces the same degree of ATF4 inhibition as one dose of DISC1-WT plus one dose of DISC1-37W or DISC1-607F, and this degree of inhibition is lower than that achieved with two doses of DISC1-WT. This suggests that, overall, the ability of DISC1 to regulate ATF4 may be impaired in 37W and 607F carriers.

As discussed in the introduction of this thesis, ATF4 transcriptional activity is modulated at multiple levels, including transcription and translation, post-translational modification, regulation of protein stability and repression of its transcriptional activity through protein-protein interactions (Ameri & Harris, 2008; Dey *et al*, 2010; Elefteriou *et al*, 2005; Lassot *et al*, 2005; Lassot *et al*, 2001; Ord & Ord, 2003; Pons *et al*, 2007; Yang *et al*, 2004). The existence of multiple mechanisms controlling the production, persistence and activity of ATF4 indicates the critical importance of tight regulation of ATF4-mediated gene transcription. Given that I and others (Sawamura *et al*, 2008) have clearly demonstrated that DISC1 is capable of regulating the transcriptional activity of ATF4 *in vitro*, it is reasonable to speculate that DISC1 may be one of the many essential modulators of ATF4-mediated transcription in the brain. My observations suggest that the repressive activity of DISC1 on ATF4 may be weakened by sequence variants that influence the risk of mental illness, implying that the dysregulation of ATF4-mediated transcription might be a contributing factor to the overall risk of disease.

The activation of CRE-dependent transcription by CREB and the release of ATF4-mediated transcriptional repression are essential for learning and memory consolidation in both invertebrates and mammals (Kandel, 2001). Therefore, through its modulatory effect on ATF4, DISC1 might be involved in the regulation of the transcriptional events that mediate synaptic plasticity. This in turn implies that DISC1 variants 37W and 607F may deregulate synaptic plasticity and cognitive processes through their defective modulation of ATF4 transcriptional activity. Since cognitive impairment is a core feature of schizophrenia, this is a potential route by which these DISC1 variants influence risk of mental illness.

A recent study demonstrated that ATF4 expression is controlled by key components of the circadian clock, and showed that its protein levels exhibit circadian oscillation in several mouse tissues, including the suprachiasmatic nucleus (SCN), the main controller of the mammalian circadian clock (Koyanagi *et al*, 2011). In the SCN, ATF4 is essential for the circadian expression of the *Period2* gene, a central component of the circadian clock, and regulates its transcription by directly binding to the CRE in its promoter (Koyanagi *et al*, 2011). Thus, through its regulation of CRE-driven transcription, ATF4 is involved in the control of circadian pathways. That ATF4 is a direct target of Clock, a transcription factor that mediates the periodical expression of several genes controlling hormone release and sleep-wake cycles, constitutes further evidence for the importance of ATF4 in circadian control (Igarashi *et al*, 2007). Intriguingly, overexpression of human DISC1 in fruit flies induces alterations of sleep homeostasis, a process known to be regulated by CRE-dependent transcription (Sawamura *et al*, 2008). If confirmed, the proposed role of DISC1 in sleep homeostasis would be of particular relevance to psychiatric illness, because sleep disturbances are common among psychiatric patients (Schulz & Steimer, 2009; Trbovic, 2010; Wulff *et al*, 2012; Wulff *et al*, 2009), and a recent study demonstrated that circadian rhythms are deregulated in a mouse model of schizophrenia (Oliver *et al*, 2012). Intriguingly, in *Drosophyla melanogaster*, mutation of the PDE4 orthologue *dunce* is associated with increased cAMP concentration and reduced sleep (Hendricks *et al*, 2001). In light of these observations, it is intriguing to speculate that the effect of DISC1 on sleep homeostasis might be mediated by its concomitant regulation of ATF4 and PDE4, both of which converge on the modulation of CRE-driven transcription. If true, this would in turn imply that 37W and 607F might negatively impact on DISC1-mediated regulation of sleep homeostasis.

Both DISC1 and ATF4 are implicated in the regulation of emotional behaviour in rodent models (Ayhan *et al*, 2011; Clapcote *et al*, 2007; Green *et al*, 2008; Hikida *et al*, 2007; Li *et al*, 2007a; Mao *et al*, 2009; Shen *et al*, 2008). Expression of endogenous ATF4 in the nucleus accumbens (NA), a key reward region in the brain, is induced by amphetamine administration or restraint stress, and ATF4 overexpression in this region decreases the behavioural responsiveness to

amphetamine (Green *et al*, 2008). Like its related transcription factor CREB, ATF4 attenuates emotional reactivity and induces depression-like behaviours when overexpressed in the NA, strongly suggesting that ATF4 functions as an activator of CRE-driven transcription in this brain area (Green *et al*, 2008). Like ATF4, DISC1 modulates the behavioural responsiveness to amphetamine in rodent models (Ayhan *et al*, 2011; Lipina *et al*, 2010; Niwa *et al*, 2010), and both DISC1 mutations and altered DISC1 expression are associated with depression-like behaviours in several mouse models (Ayhan *et al*, 2011; Clapcote *et al*, 2007; Hikida *et al*, 2007; Li *et al*, 2007a; Mao *et al*, 2009; Shen *et al*, 2008). Thus, it is tempting to speculate that DISC1 regulation of ATF4 transcriptional activity on the CRE might contribute to its effects on emotional behaviour. If true, this would imply that DISC1 variants that interfere with this particular function of DISC1, such as 37W and 607F, may directly impact on the regulation of emotional behaviour.

ATF4 is also a key mediator of the Integrated Stress Response, and its transcription and translation are strongly upregulated in response to a range of stressors, including amino acid deprivation, oxidative stress, hypoxia, viral infections, endoplasmic reticulum stress and mitochondrial dysfunction (Badiola *et al*, 2011; Granberg *et al*, 2006; Kilberg *et al*, 2009; Lange *et al*, 2008; Silva *et al*, 2009). Stress-induced ATF4 can activate the transcription of target genes by binding to the CRE in their promoter. For example, ATF4 activates the expression of the anti-apoptotic gene *Grp78* in response to endoplasmic reticulum stress by interacting with a CRE element in its promoter (Luo *et al*, 2003). However, induction of most of the stress-responsive ATF4 target genes that have been studied so far is mediated by CARE composite sites, of which the CHOP AARE is a very well characterised example (Bruhat *et al*, 2002; Ma *et al*, 2002b; Oyadomari & Mori, 2004). In this chapter, I showed that, besides regulating the activity of ATF4 on the CRE, DISC1 is also capable of inhibiting the transactivation of the CHOP AARE by ATF4, and this effect is significantly weakened by amino acid substitutions 37W and 607F. The contribution of damaging environmental exposures to the risk of developing schizophrenia is well established, but still mechanistically unclear. Maternal starvation, viral infections and perinatal hypoxia are among the best supported risk factors for schizophrenia (Brown, 2011), and each of these exposures could potentially activate the stress

responses mediated by ATF4. It is intriguing to speculate that, by modulating ATF4-dependent stress-induced transcriptional events, DISC1 might contribute to the regulation of cellular responses to stress, tipping the balance towards adaptation or apoptosis. In this scenario, 37W and 607F substitutions in DISC1 could increase the risk of mental illness by rendering the brain more susceptible to stress (Figure 4.25).

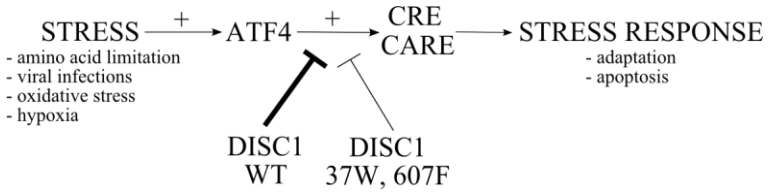

Figure 4.25 Hypothetical role of DISC1 in the regulation of ATF4-mediated stress responses. Several types of microenvironmental stress induce the expression of ATF4, which in turn regulates the transcription of target genes by binding to CRE or CARE elements in their promoters. ATF4 target genes can promote the cell's adaptation to stress, but they also include pro-apoptotic factors, thus protracted ATF4 activation can result in cell death (Harding *et al*, 2003; Lange *et al*, 2008; Ord *et al*, 2007; Rutkowski & Kaufman, 2003). DISC1 might inhibit ATF4 transcriptional activity in response to stess, thus contributing to the regulation of the cell's response to stress. Hence, by reducing DISC1's ability to repress ATF4, amino acid substitutions 37W and 607F might alter the cell's susceptibility to stress.

5 Testing the effect of cAMP on DISC1-mediated regulation of ATF4

5.1 Introduction

Post-translational modification, and in particular phosphorylation, contributes to the regulation of ATF4 transcriptional activity (Elefteriou *et al*, 2005; Yang *et al*, 2004). As previously discussed, ATF4 possesses a strong and constitutively active transactivation domain, and unlike its related factor CREB, ATF4 activity does not depend on PKA-mediated phosphorylation (Schoch *et al*, 2001). However, both RSK2 and PKA protein kinases are known to modulate ATF4 transactivation capacity in bone cells by direct phosphorylation (Elefteriou *et al*, 2005; Yang *et al*, 2004).

DISC1 is known to bind to all four isoforms (A,B,C,D) of type 4 phosphodiesterases (PDE4s) in a cAMP-regulated fashion (Millar *et al*, 2005b; Murdoch *et al*, 2007) and to inhibit induction of PDE4 cAMP hydrolysis activity in response to elevated cAMP levels (Millar *et al*, 2005b; Murdoch *et al*, 2007). In turn, PDE4s contribute to the modulation of intracellular cAMP levels and PKA activity in a compartmentalised fashion (Houslay, 2010). Interestingly, through its interaction with PDE4, DISC1 has been shown to regulate PKA-dependent phosphorylation of its binding partner NDE1, which in turn controls its association with NDEL1 and LIS1 and regulates neurite extension (Bradshaw *et al*, 2009; Bradshaw *et al*, 2011). I therefore hypothesised that a similar mechanism might be in place to regulate the PKA-mediated phosphorylation of ATF4, and that the inhibitory effect of DISC1 on ATF4-dependent transcription may occur, at least partially, through the regulation of PKA-dependent phosphorylation of ATF4 by DISC1-bound PDE4 (Figure 5.1). Thus, in this chapter I investigate the potential involvement of PKA and PDE4 in the regulation of ATF4 transcriptional activity on the CRE, and test whether these proteins contribute to its DISC1-mediated inhibition.

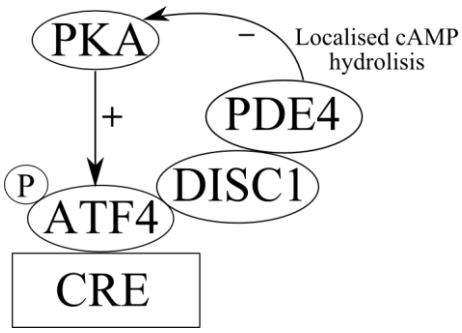

Figure 5.1 Hypothetical mechanism of DISC1-mediated inhibition of ATF4 transcriptional activity. PKA phosphorylation of ATF4 might increase its transactivation activity on the CRE element. By linking PDE4 to the ATF4 complex, DISC1 might favour a localised reduction of cAMP levels, which would in turn inhibit PKA activity, thus inhibiting ATF4 phosphorylation.

5.2 The effect of PKA inhibition on ATF4-dependent transcription

First, to test for the potential involvement of PKA in the regulation of ATF4 transactivation of the CRE, the luciferase reporter assay was performed in the presence of a selective PKA inhibitor. As detailed in the following sections, three different PKA inhibitors were tested. The results obtained with the first two, KT5720 and mPKI, were largely inconclusive or negative under the tested experimental conditions, and are included only for completeness. More emphasis is placed on the findings obtained with PKIα, which yielded interesting results.

5.2.1 *KT5720*

KT5720 is a membrane-permeant selective and potent PKA inhibitor (IC_{50}=56nM) that works by blocking the catalytic ATP sites on PKA (Cabell & Audesirk, 1993; Gadbois *et al*, 1992; Kase *et al*, 1987). In the first pilot experiment, KT5720 (0.1, 5 or 10 µM) was added to the cells 24 hours after transfection and incubated for 24 hours before performing the luciferase assay. The tested concentrations correspond to the KT5720 concentration range commonly used in cell-based assays (Herbst *et al*, 2009). When used at 0.1 or 10 µM, KT5720 partially inhibited the ATF4-induced activation of CRE-driven transcription, but surprisingly, it had the opposite effect at 5 µM (Figure 5.2). These incongruent results prompted me to perform further

experiments to test whether KT5720 efficiently inhibits PKA under the tested experimental conditions.

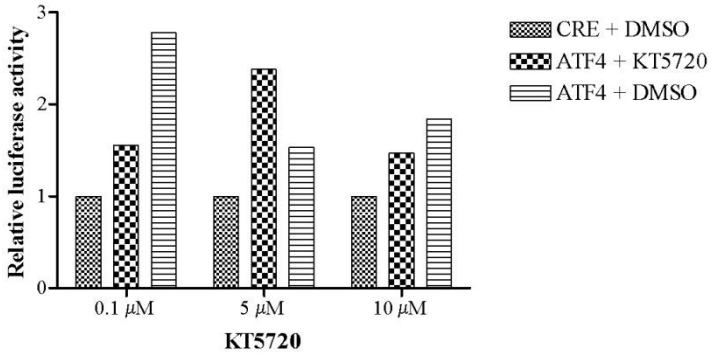

Figure 5.2 HEK293 cells were transfected with the reporters only (CRE) or in combination with ATF4 (ATF4). 24 hours later, the transfection medium was replaced with fresh medium supplemented with the indicated concentrations of KT5720, and the cells were incubated for further 24 hours before being assayed for luciferase activity. The bars represent the results of a single experiment. Data were normalised to the relative luciferase activity in DMSO-treated cells transfected with the reporters only.

The adenylate cyclase activator forskolin is commonly used as a tool to raise intracellular cAMP levels (Insel & Ostrom, 2003). In turn, cAMP induces the phosphorylation of CREB at Serine 133, thus activating CRE-driven transcription (Delghandi *et al*, 2005). In cells treated with forskolin, the activation of CREB and CRE-driven transcription is largely mediated by the cAMP-dependent activation of PKA, the main CREB kinase (Delghandi *et al*, 2005). Indeed, the forskolin-induced activation of the CRE is almost entirely blocked by specific PKA inhibitors (Delghandi *et al*, 2005). Thus, to control for the ability of KT5720 to efficiently inhibit PKA activity under the tested conditions, transfected HEK293 cells were treated for 4 hours with KT5720 only (0.1, 5 or 10 µM) or in combination with 10 µM forskolin before being assayed for CRE-driven luciferase expression. In the absence of forskolin, 10 and 5 µM KT5720 prevented ATF4 transactivation of the

CRE, but 0.1 µM KT5720 had no effect on ATF4 (Figure 5.3 A). In addition, under the same conditions, KT5720 did not prevent DISC1-mediated inhibition of ATF4 trancriptional activity (Figure 5.3 A). Furthermore, KT5720 had virtually no effect on the ATF4-induced suppression of cAMP-dependent CRE activity, either in the presence or absence of DISC1 (Figure 5.3 A). Surprisingly, KT5720 not only did not prevent the forskolin-induced activation of CRE-driven transcription, but it had the opposite effect at all tested concentrations (Figure 5.3 A, B). This latter observation suggests that, under these particular experimental conditions, KT5720 might not effectively inhibit PKA activity. Thus, no conclusions can be drawn on the potential effect of PKA on ATF4 transactivation of the CRE from this particular experiment.

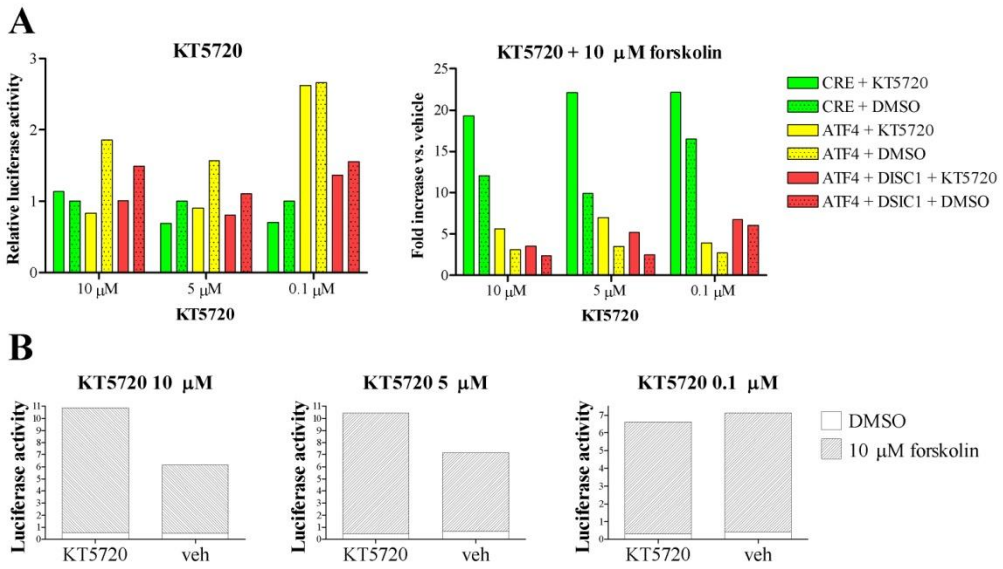

Figure 5.3 (A) HEK293 cells were transfected with the reporters only (CRE) or in combination with ATF4, with or without DISC1. 48 hours later, cells were treated for 4 hours with the indicated concentrations of KT5720 alone or in combination with 10 µM forskolin, and then assayed for luciferase activity. Data are normalised to the luciferase activity in cells transfected with the reporters only and treated with vehicle (DMSO). (B) Effect of forskolin and KT5720 on cells transfected with the reporters only. The graphs in (A) and (B) were generated from the same experimental data set. The bars represent the results of a single experiment.

The following experiment was designed to test the activity of KT5720 at different time points, as the apparent inactivity of the drug in the previous experiments might have been caused by gradual loss of activity with prolonged incubation times. To do this, HEK293 cells transfected with the SomCRE-Luc and TK-Renilla reporters were treated with either 10 µM KT5720, 10 µM forskolin or both drugs together for 30, 60, 90, 120 and 240 minutes before being assayed for luciferase activity. As expected, the luminescence signal gradually increased over time in cells treated with forskolin alone, but this increase was only partially counteracted by co-treatment with KT5720 (Figure 5.4). Even at the earlier time points, when the activity of the drug should be intact, KT5720 only partially inhibited the accumulation of luciferase in HEK293 cells treated with forskolin (Figure 5.4). Again, this result suggests that KT5720 might not efficiently inhibit PKA activity in this particular test system. However, it is important to remark that in this particular set of experiments the activity of PKA was not measured directly, but was evinced indirectly from the activity of the CRE element. This was based on the assumption that the activation of CRE-driven transcription in response to increased cAMP levels is largely mediated by PKA-dependent phosphorylation of CREB, as demonstrated in other cell systems (Delghandi *et al*, 2005). However, based on the data presented here, it is not possible to formally exclude that in this particular test system the activation on CRE in response to increased cAMP levels might be mediated by PKA-independent mechanisms. Thus, the data shown here do not allow to conclusively establish whether KT5720 efficiently inhibits PKA phosphorylation in the tested system.

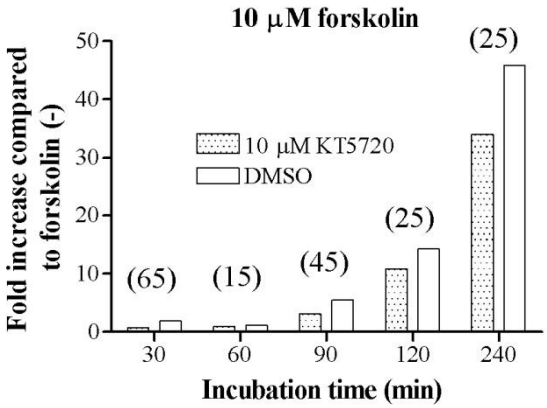

Figure 5.4 HEK293 cells were transfected with the reporters only (SomCRE-Luc and TK-Renilla) for 48 hours, and then treated for the indicated times with 10 μM forskolin alone or in combination with 10 μM KT5720 before being assayed for luciferase activity. The bars represent the results of a single experiment. The numbers in brackets indicate the % inhibition of the forskolin-induced activation of the CRE by KT5720.

5.2.2 *mPKI*

Next, the PKA inhibitor mPKI was tested. This is a synthetic peptide corresponding to amino acids 14-22 of protein kinase inhibitor peptide (PKI) whose N-terminus is myristoylated to increase cell membrane permeability (Glass *et al*, 1989a; Glass *et al*, 1989b). PKI is a family of endogenous neuropeptides (PKIα, β and γ) that inhibit PKA activity by binding to the free catalytic subunits of the enzyme and blocking the phosphorylation of its substrates (Dalton & Dewey, 2006). The effect of mPKI on ATF4-mediated activation of CRE-driven transcription was tested under two different experimental conditions, as shown in Figure 5.5. The tested mPKI concentrations are within the range commonly used in cell-based assays (Gong *et al*, 2010; Nedvetsky *et al*, 2010). Under the tested conditions, mPKI did not inhibit the ATF4-induced activation of CRE-driven transcription at basal cAMP levels, nor did it prevent the forkolin-induced activation of CRE-driven transcription, suggesting

that it may not have a substantial inhibitory effect on PKA activity (Figure 5.5). Thus, like KT5720, in this particular test system mPKI may not be suitable to test the potential influence of PKA phosphorylation on ATF4 transactivation of the CRE.

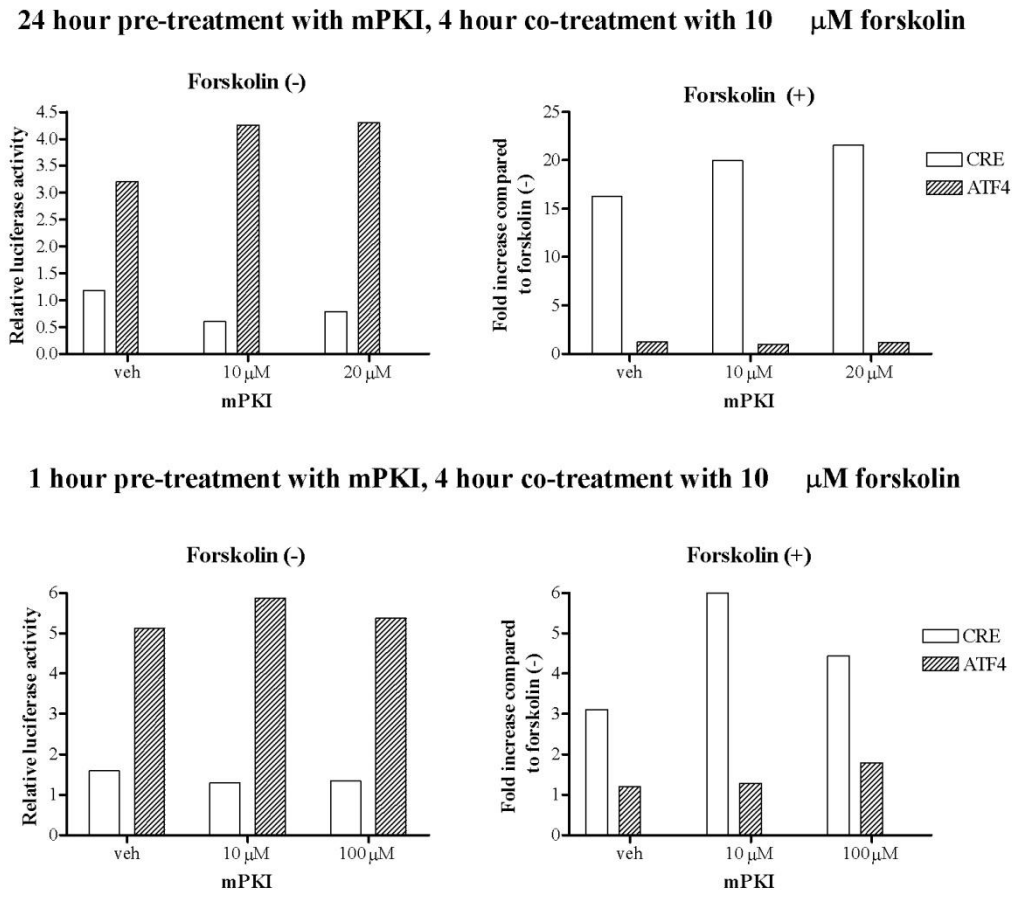

Figure 5.5 HEK293 cells were transfected with the reporters only (CRE) or in combination with ATF4. 24 (top) or 48 (bottom) hours later, cells were treated for the indicated times with mPKI alone or in combination with 10 μM forskolin, as shown, and then assayed for luciferase activity. The bars represent the results of a single experiment. Data were normalised to the relative luciferase activity in DMSO-treated cells transfected with the reporters only.

5.2.3 *PKIα*

Overexpression of the PKA inhibitor PKIα (see Paragraph 5.2.2 and Table 2.2) was tested as a possible alternative method to efficiently inhibit PKA activity in HEK293 cells. Unlike other PKI isoforms, which inhibit both the cGMP-dependent protein kinase (PKG) and PKA, PKIα is a totally specific PKA inhibitor (Glass *et al*, 1986; Kumar & Walsh, 2002). At basal cAMP levels, PKIα expression does not affect the activity of the CRE, but it almost completely prevents the forskolin-induced activation of CRE-driven transcription ($P<0.01$, Figure 5.6). This result confirms that, as observed in other cell models (Delghandi *et al*, 2005), the forskolin-induced activation of the CRE in this particular test system is indeed mediated by PKA, and it indicates that PKIα, but not KT5720 or mPKI, is an effective inhibitor of PKA in these cells. Interestingly, PKIα co-expression partially inhibits the ATF4-induced transactivation of the CRE at basal cAMP levels ($P<0.05$, Figure 5.6). These results are consistent with the reported modulatory effect of direct PKA phosphorylation on the transcriptional activity of ATF4 (Elefteriou *et al*, 2005), and indicate that, in the tested cell model, ATF4 transactivation of the SomCRE-Luc reporter is positively regulated by PKA at basal cAMP levels (Figure 5.7). However, this experiment does not establish whether this modulatory effect involves direct phosphorylation of ATF4 by PKA. PKIα additionally strengthens the inhibitory effect of ATF4 on the forskolin-induced activation of CRE-driven transcription ($P<0.01$, Figure 5.6). This might reflect a direct or indirect inhibitory effect of PKA on ATF4 at high cAMP levels, but it most likely arises from the concerted inhibition of CREB by ATF4 and PKIα, the former competing with CREB for Basic Transcription Factors (BTF), and the latter directly blocking PKA-dependent CREB phosphorylation (Figure 5.7). Further experiments will be needed to test these alternative possibilities.

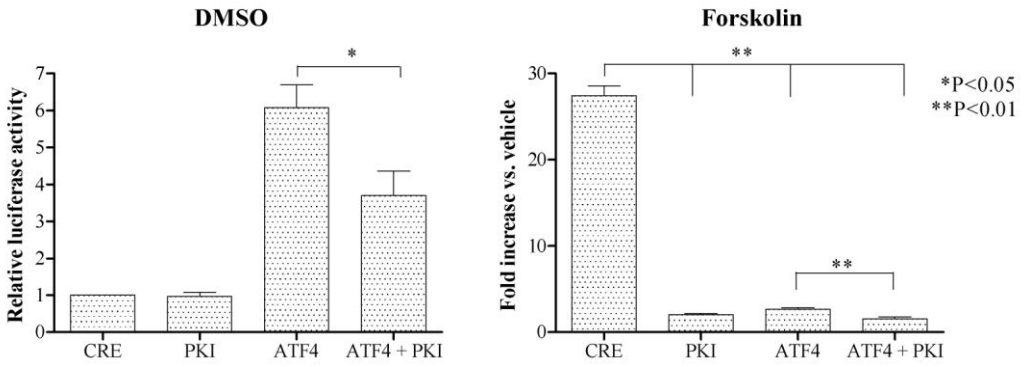

Figure 5.6 Relative luciferase activity in HEK293 cells transfected with the reporters only (CRE) or in combination with PKIα, ATF4 or both. Transfected cells were treated for 4 hours with DMSO or 10 μM forskolin before being assayed for luciferase activity. Bars represent the average of 4 independent experiments. Data were normalised to the relative luciferase activity in DMSO-treated cells transfected with the reporters only and were analysed by one-way ANOVA and Dunnett's multiple comparisons test, except for datasets "ATF4" and "ATF4 + PKI", which were compared using two-tailed paired student's t-test.

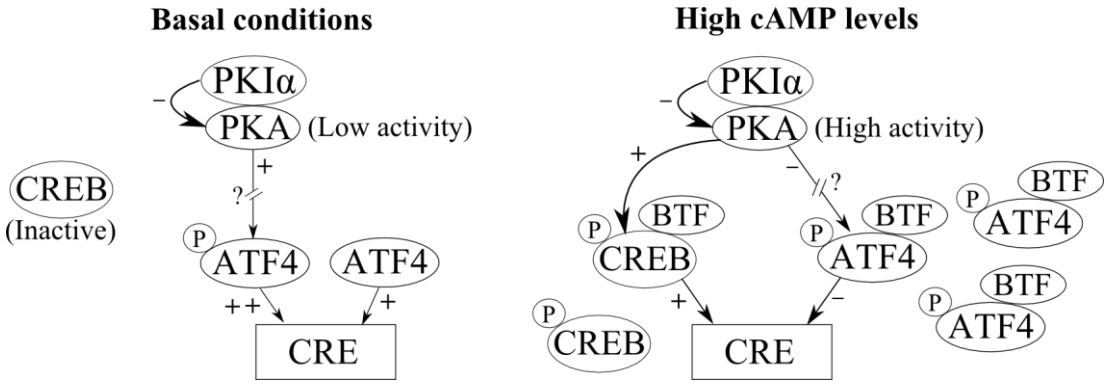

Figure 5.7 Proposed molecular model of interaction between ATF4, PKA and CREB. At basal cAMP levels, PKA activity is low. ATF4 positively regulates CRE activity, and PKA-mediated phosphorylation directly or indirectly strengthens ATF4 transactivation of the CRE. Consequently, by inhibiting PKA activity, PKIα weakens ATF4 transactivation of the CRE. Under these conditions, CREB is either completely unphosphorylated (and thus inactive) or has a low level of activity that is below the sensitivity limit of the detection system used here. At high cAMP levels, PKA is fully active and phosphorylates CREB, which consequently activates CRE-driven

transcription. PKIα expression prevents the rise in CRE activity by inhibiting CREB phosphoryation by PKA. ATF4 strongly represses CRE activity, possibly by sequestering basic transcription factors (BTF) from CREB, and PKIα strengthens the inhibitory effect of ATF4 on the CRE. This latter effect may be due to the concomitant inhibition of CREB phosphorylation by PKIα and sequestration of BTF by ATF4. Alternatively, it is possible that PKA phosphorylation (direct or indirect) inhibits the repressive activity of ATF4 on the CRE.

5.2.4 *The effect of PDE4 overexpression and inhibition*

Having established that PKA enhances the transcriptional activity of ATF4 on the CRE at basal cAMP levels, I sought to test whether PDE4 activity, which regulates PKA by controlling intracellular cAMP concentration gradients (Houslay, 2010), is also implicated in the regulation of ATF4. A potential regulatory role of PDE4 on ATF4 is also supported by the fact that interaction between endogenous PDE4 and ATF4 has been detected by co-immunoprecipitation in SH-SY5Y cells (Bradshaw *et al*, 2008). As shown in Figure 5.8, co-expression of two distinct PDE4 isoforms (B1 and D3) inhibits ATF4 transactivation of the CRE at basal cAMP levels to a similar extent as PKIα co-expression ($P<0.05$ for PDE4B1 and $P<0.01$ for PDE4D3). On the other hand, PDE4 co-expression has no effect on ATF4-mediated inhibition of the forskolin-induced activation of the CRE (Figure 5.8). This indicates that, at basal cAMP levels, PDE4s might modulate CRE-dependent transcription via ATF4, possibly by inhibiting its PKA phosphorylation.

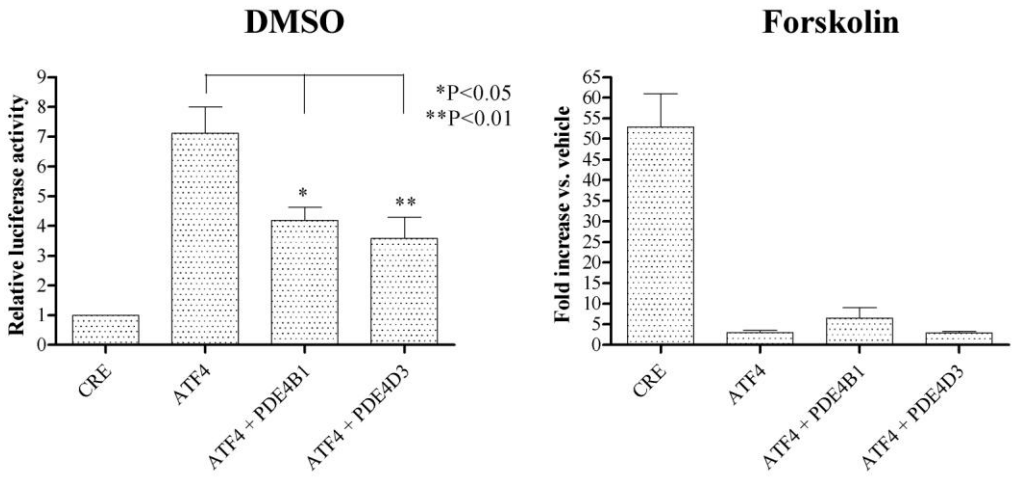

Figure 5.8 HEK293 cells were transfected for 48 hours with the reporters only (CRE) or in combination with the indicated constructs, then subjected to a 4 hour treatment with either DMSO or 10 μM forskolin before being assayed for luciferase activity. The bars represent the average of 3 independent experiments. Data were normalised to the relative luciferase activity in DMSO-treated cells transfected with the reporters only and were analysed by one-way ANOVA and Dunnett's multiple comparisons test.

Next, to test whether the inhibitory effect of DISC1 on ATF4-dependent transcription is partially mediated by PDE4, endogenous PDE4 activity was blocked using the specific PDE4 inhibitor rolipram. Rolipram treatment does not induce CRE-driven transcription from the SomCRE-luc reporter under basal cAMP levels (Figure 5.9 A and C), but significantly strengthens the forskolin-induced activation of the CRE (Figure 5.9 B and C), which confirms the effectiveness of the drug in this particular test system at the concentration used (10 μM), and is consistent with the previously established role of endogenous PDE4s in the regulation of CREB phosphorylation (Li *et al*, 2011; Li *et al*, 2009; MacKenzie & Houslay, 2000) and CRE-mediated transcription (Xia *et al*, 2009a; Xia *et al*, 2009b). At basal cAMP levels, the activity of ATF4 is not affected by rolipram treatment (Figure 5.9 A), which is in contrast with the inhibitory effect of PDE4 overexpression (Figure 5.8). The reasons for this discrepancy are not clear, but may arise from the fact that the first experiment evaluates the effects of overexpressed PDE4s, whereas the second is

focused on the endogenous proteins. As shown in Figure 5.9 A, the inhibitory effect of DISC1 on ATF4-mediated transcription at basal cAMP levels is entirely preserved in the presence of rolipram. Thus, while PDE4 appears to modulate ATF4-mediated transcription at basal, but not high cAMP levels (Figure 5.8), it is not required for the inhibitory effect of DISC1 at basal cAMP levels.

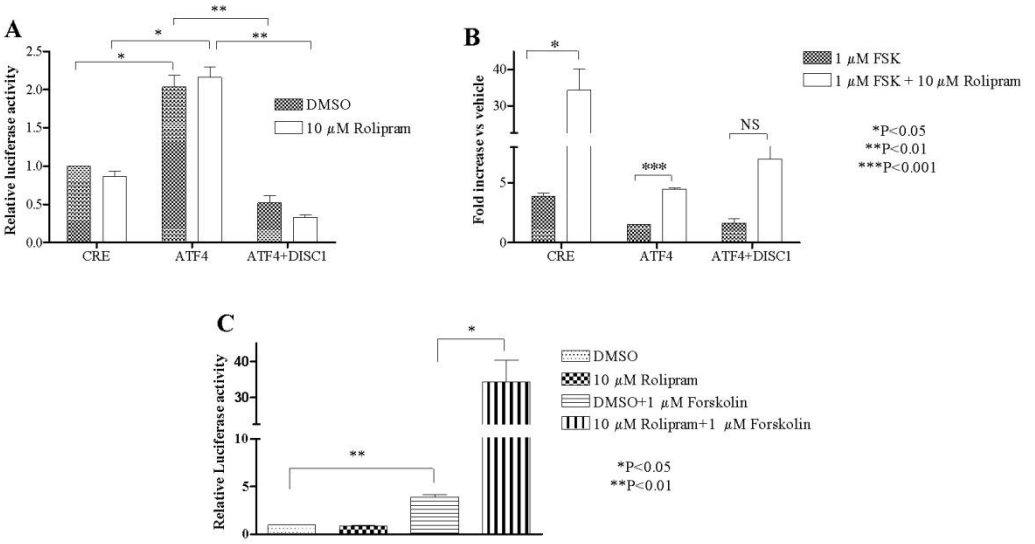

Figure 5.9 HEK293 cells were transfected with the reporters only (CRE) (C) or in combination with the indicated constructs (A, B). 48 hours after transfection, the cells were simultaneously subjected to either one of the following drug treatments: vehicle (DMSO) or 10 μM rolipram for 4 hours (A, C); 30 minute pre-treatment with DMSO followed by 3.5 hour treatment with 1 μM forskolin; 30 minute pre-treatment with 10 μM rolipram followed by 3.5 hour treatment with 1 μM forskolin and 10 μM rolipram (B, C). (C) Represents the same data from cells transfected with the reporters only plotted in (A) and (B). Relative CRE-dependent luciferase activity was measured at the end of the drug treatments. Data were normalised to the relative luciferase activity in vehicle-treated cells transfected with the reporters only, and analysed by two-tailed paired student's t-test. The bars represent the average of 3 independent experiments.

As shown in figure 5.9 B, rolipram has virtually no effect on the ability of ATF4 to inhibit the forskolin-induced activation of the CRE (~82% inhibition with 1 µM forskolin, ~89% inhibition with 1 µM forkolin + 10 µM rolipram). This is consistent with the lack of effect of PDE4 co-expression on the ATF4-mediated repression of CRE-driven transcription at high cAMP levels (Figure 5.8). Furthermore, at high cAMP levels, the net CRE activity in cells transfected with ATF4 is higher in the presence of rolipram ($P<0.001$, Figure 5.9 B), which is consistent with the reduction of CRE activity seen in ATF4-epressing cells upon co-expression of PKIα (Figure 5.6). Altogether, these data suggest that at high cAMP levels ATF4 is not directly regulated by PDE4, and that the opposing effects of PKIα and rolipram on the net CRE activity in ATF4-expressing cells most likely arise from their opposing effects on CREB. Similarly, and in line with my previous observations, the repressive activity of ATF4 at high cAMP levels is not influenced by DISC1 co-expression, either in the presence or absence of rolipram (~78% inhibition with 1 µM forskolin, ~82% inhibition with 1 µM forkolin + 10 µM rolipram) (Figure 5.9 B).

5.3 Discussion

In osteoblasts, the Adrenergic beta-agonist isoproterenol increases ATF4 transactivation activity on the Rankl promoter CRE by inducing its PKA-dependent phosphorylation at serine 254 (Elefteriou *et al*, 2005). Consistently, the inhibitory effect of PKIα on ATF4 observed here suggests that, under basal conditions, PKA contributes to the regulation of the transcriptional activity of ATF4 on the Somatostatin CRE element used in this study, either directly or indirectly. It is not known whether ATF4 is phosphorylated by PKA in response to forskolin treatment, but the ATF4-dependent repression of forskolin-induced activation of the CRE is thought to be mainly mediated by competition with CREB for access to basic transcription factors (BTF) (Thiel *et al*, 2005). Thus, as illustrated in the diagram in Figure 5.10, the stronger inhibition of cAMP-induced CRE activation observed in cells co-expressing ATF4 and PKIα compared to cells expressing ATF4 alone might be caused by concomitant sequestration of basic transcription factors by ATF4 and

inhibition of PKA-dependent CREB phosphorylation by PKIα. However, it cannot be excluded that PKA might inhibit the repressive activity of ATF4 at high cAMP levels by direct phosphorylation.

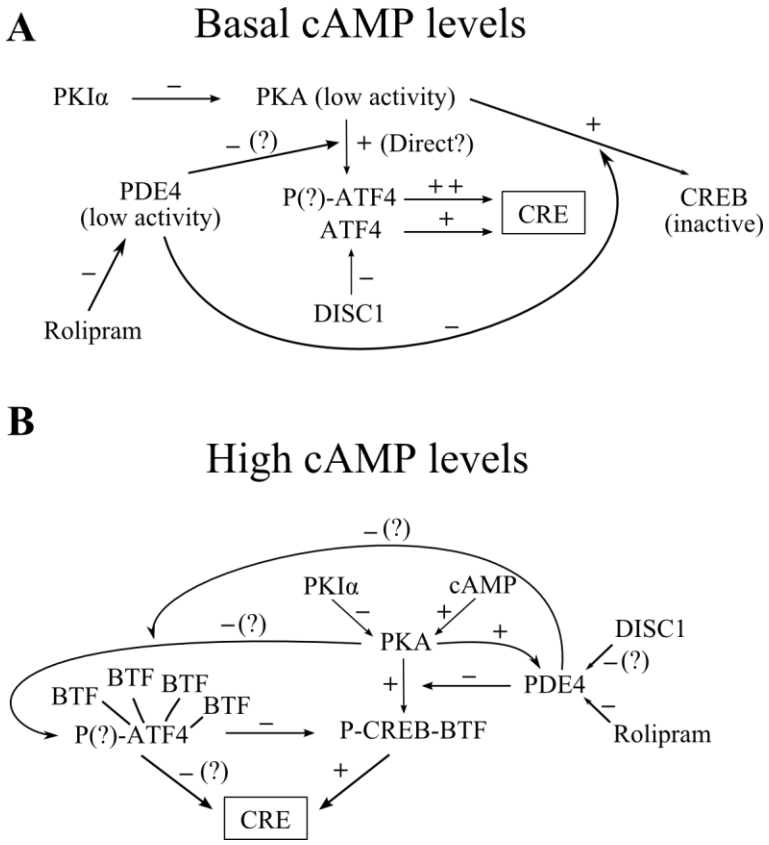

Figure 5.10 Proposed model of interaction between PKA, PDE4, ATF4 and DISC1. (A) At basal cAMP levels, PKA and PDE4 are in a low-activity state. PDE4 inhibits the PKA-mediated phosphorylation of CREB, thus preventing its activation. Rolipram inhibition of PDE4 removes the PDE4-dependent repression of CREB, thus activating CRE-driven transcription (Li *et al*, 2011; Li *et al*, 2009; MacKenzie & Houslay, 2000; Xia *et al*, 2009a; Xia *et al*, 2009b). ATF4 might be present in both phosphorylated and unphosphorylated forms. Both forms of ATF4 are capable of binding to and activating the CRE, but phosphorylated ATF4 has a stronger transactivating effect on this promoter. ATF4 is inhibited by DISC1 via an unknown mechanism that does not appear to involve PDE4. PKA strengthens ATF4 transactivation of the CRE, potentially via direct phosphorylation of ATF4, a mechanism that has been demonstrated in osteoblasts (Elefteriou *et al*, 2005). PDE4 and PKIα inhibit ATF4 transactivation of the CRE, perhaps by inhibiting its

PKA-dependent phosphorylation. (B) At high cAMP levels, PKA is fully active, and can thus phosphorylate and activate CREB. PKA also activates PDE4 (MacKenzie *et al*, 2002), which in turn inhibits the PKA-dependent phosphorylation of CREB, providing a negative feedback mechanism. Rolipram inhibition of PDE4 removes the PDE4-dependent inhibition of CREB, thus resulting in higher CRE activity. DISC1 might potentially have a similar, albeit milder, effect as rolipram, as it has been shown to attenuate the rise in PDE4 activity in response to increased cAMP levels (Carlyle *et al*, 2011). However, no evidence for a regulatory role of DISC1 on CRE activity at high cAMP levels has been found in this thesis. ATF4 overexpression inhibits the forskolin-induced activation of the CRE, probably by competing with endogenous CREB for interaction with basic transcription factors (BTF) (Hai & Hartman, 2001; Liang & Hai, 1997; Schoch *et al*, 2001), although a direct repressive effect of ATF4 on the CRE cannot be excluded. CRE-driven transcription is lower in cells co-expressing ATF4 and PKIα compared to cells expressing ATF4 alone, and it is higher in ATF4-expressing cells exposed to rolipram compared to vehicle-treated cells. This may suggest that, by phosphorylating ATF4, PKA might inhibit its repressive effect on the CRE, and PDE4 might counteract this. Alternatively (or additionally) it is possible that the effect of PKIα reflects a further inhibition of CREB due to blockage of its PKA-dependent phosphorylation. Similarly, the effect of rolipram may be due to removal of the PDE4-dependent inhibition of CREB phosphorylation. The overall conclusion is that the regulation of CRE-driven transcription is complex, context- and mutation/variant-dependent with DISC1, PDE4, ATF4, PKA and potentially other untested components interacting directly and/or indirectly to regulate cAMP signalling.

The inhibitory effect of PDE4 co-expression on the ATF4 transactivation of the CRE is consistent with the observed inhibitory effect of PKIα, and suggests the involvement of PDE4-regulated pathways in the control of ATF4 transcription at basal cAMP levels (Figure 5.10). However, this is in contrast with the lack of effect of rolipram on the transactivating effect of ATF4 at basal cAMP levels. In this respect, it is important to notice that, when used at the concentration of 10 μM, rolipram does not induce a sufficient increase in cAMP levels to activate the SomCRE-Luc reporter used in this set of experiments. In contrast, in a previous

study, rolipram determined a significant activation of a CRE-β-lactamase reporter in CHO cells, with an EC_{50} of 200 nM (Xia *et al*, 2009b). This suggests that the SomCRE-Luc reporter used in this study might not be sensitive enough to reveal activation of the PKA-CREB pathway in response to rolipram treatment at basal cAMP levels. Moreover, at basal cAMP levels, PDE4 is in a low-activity state (Houslay & Adams, 2003), thus under these conditions, PDE4 inhibition is unlikely to produce a large rise in cAMP levels. On the other hand, the effect produced by PDE4 overexpression at basal cAMP levels may derive from cumulative contributions from a high number of low-activity molecules.

At high cAMP levels, PDE4 is fully active and could potentially counteract the effect of forskolin on CRE-driven transcription (Houslay & Adams, 2003). However, unlike PKIα, PDE4 co-expression does not strengthen the repressive effect of ATF4 on the forskolin-induced activation of the CRE. This apparent lack of effect of PDE4 is likely due to experimental limitations. Although I have not performed a thorough titration experiment, forskolin is likely to induce saturation of the SomCRE-Luc reporter in my particular experimental system when used at a concentration of 10 µM. Indeed, increasing the forskolin concentration to 100 µM does not produce a comparatively stronger activation of SomCRE-Luc in HEK293 cells (Figure 4.4). Thus, it is possible that the exogenous PDE4 expression levels achieved in this particular experiment are not sufficiently high to effectively counteract the strong activation of the CRE induced by 10 µM forskolin. My observation that rolipram strongly enhances CRE-driven transcription when used in combination with a non-saturating dose of forskolin (1 µM) clearly indicates that PDE4 is indeed involved in the regulation of cAMP-induced CRE-driven transcription in the tested system (Figure 5.10). Thus, to better elucidate the role of different PDE4 isoforms in the regulation of cAMP-induced CRE-driven transcription, it would be necessary to test the effect of different amounts of PDE4s on the activity of the SomCRE-Luc reporter in the presence of non-saturating forskolin concentrations.

Consistent with the effect of PKIα, the forskolin-stimulated activity of the SomCRE-Luc reporter in cells expressing ATF4 is higher in the presence of rolipram. At first, this might be interpreted as a direct antagonising effect of rolipram on the repressive

activity of ATF4. However, the relative ability of ATF4 to repress the forskolin-induced activation of the CRE is virtually unaffected by rolipram, suggesting that, at least in the tested system, PDE4 is not involved in the regulation of ATF4 at high cAMP levels. Thus, as for PKIα, the increase in forskolin-induced CRE activity observed in ATF4-transfected cells in the presence of rolipram likely results from the independent activating effect of rolipram on CREB activity (Figure 5.10).

In conclusion, this limited set of experiments suggests that, although PDE4s are potentially involved in the regulation of ATF4 at basal cAMP levels, they do not mediate the repressive activity of DISC1 under the tested experimental conditions. Moreover, while PDE4s do not appear to influence the repressive activity of ATF4 at high cAMP levels, they are potentially involved in the regulation of CRE-driven transcription under these conditions. Further experiments will be needed to elucidate the mechanism by which DISC1 and PDE4s, either independently or in concert, participate in the regulation of ATF4 activity and CRE-driven transcription.

6 Testing the effect of DISC1 on the cell's response to oxidative stress

6.1 Introduction

There is increasing evidence supporting a role of oxidative stress in the pathogenesis of psychiatric conditions including depression, bipolar disorder and schizophrenia (Berk *et al*, 2011; Bitanihirwe & Woo, 2011; Do *et al*, 2009; Fendri *et al*, 2006; Ng *et al*, 2008; Wood *et al*, 2009b; Yao *et al*, 2001; Zhang *et al*, 2010). Oxidative stress results from the accumulation of reactive oxygen and nitrogen species (ROS and RNS, respectively) in the cell as a result of their increased production and/or defective elimination by the cells' antioxidant defence system (Berg *et al*, 2004; Kohen & Nyska, 2002). ROS and RNS are highly toxic to the cell as they directly damage multiple essential cell components, including proteins, DNA and lipids (Avery, 2011; Lockwood, 2000; Stadtman & Levine, 2003). The brain is particularly susceptible to oxidative damage because of its high metabolic rate and high content of oxidisable molecules such as polyunsaturated fatty acids, coupled with its relatively low content of antioxidants (Bitanihirwe & Woo, 2011). Indeed, oxidative damage is implicated in the pathogenesis of several neurodegenerative diseases, including Alzheimer's and Parkinson's (Roberts *et al*, 2009). Several studies found that the expression of enzymes involved in ROS detoxification is reduced in schizophrenic and bipolar brains, including first-episode drug-naive patients, suggesting that this is not a side-effect of medication (Do *et al*, 2000; Gawryluk *et al*, 2011; Yao *et al*, 2006). Accordingly, markers of oxidative stress are reportedly increased in the brain, blood and urine of schizophrenia and bipolar disorder patients, and their concentration correlates with the degree of psychotic symptoms (Dietrich-Muszalska *et al*, 2009; Golse *et al*, 1978; Mico *et al*, 2011; Owe-Larsson *et al*, 2011; Wang *et al*, 2009; Yao *et al*, 2006; Yao *et al*, 1999; Zhang *et al*, 2009). However, it is important to point out that, although the majority of studies observed an impairment of antioxidant defence in psychiatric patients, some reported the opposite (Boskovic *et al*, 2011). These discrepancies may be caused by multiple factors, including, but not limited to, medication status, ethnicity, lifestyle and disease stage

(Boskovic *et al*, 2011). Intriguingly, a number of pre-clinical studies showed that perturbations of the antioxidant defence system result in cognitive deficits as well as behavioural and histological alterations relevant to schizophrenia (Cabungcal *et al*, 2007; Dean *et al*, 2009; Steullet *et al*, 2010). Moreover, studies in humans and rodents demonstrated that many of the established environmental risk factors for schizophrenia, such as maternal malnutrition, obstetric complications, prenatal infection and psychosocial stress, increase ROS production and compromise the antioxidant defence system in the brain (Do *et al*, 2009). Despite the mounting evidence linking oxidative stress to psychopathogenesis, the role of the antioxidant defence system in the onset and progression of mental illness still needs to be elucidated (Bitanihirwe & Woo, 2011).

Oxidative stress has been directly linked to two processes of central relevance for schizophrenia: NMDAR hypofunction and myelination defects (Do *et al*, 2009). Multiple lines of evidence suggest that NMDAR hypofunction likely contributes to the pathogenesis of schizophrenia (Coyle, 2006; Kantrowitz & Javitt, 2010; Olney *et al*, 1999). Administration of NMDAR antagonists exacerbates positive symptoms in schizophrenia patients, and in healthy individuals it induces disturbances typical of schizophrenia, such as psychosis and cognitive impairment (Coyle, 2006; Kantrowitz & Javitt, 2010; Olney *et al*, 1999). Additionally, post-mortem analysis of brains from schizophrenia, bipolar disorder and depression patients showed reduced expression of NMDAR subunits (Beneyto *et al*, 2007; Beneyto & Meador-Woodruff, 2008; Clinton *et al*, 2003; Gao *et al*, 2000; McCullumsmith *et al*, 2007; Meador-Woodruff *et al*, 2003; Nudmamud-Thanoi & Reynolds, 2004; Vrajova *et al*, 2010). By inhibiting the function of NMDARs, oxidative stress negatively impacts on the maintenance and function of parvalbumin (PV) interneurons, a cell population that plays a critical role in the synchronisation of brain activity, and that is reportedly depleted in schizophrenic brains (Do *et al*, 2009). Intriguingly, the environmental schizophrenia risk factors linked to increased oxidative stress in the brain were recently shown to decrease the number of PV interneurons in the hippocampus and prefrontal cortex in rodent models, and to induce behavioural and cognitive alterations compatible with schizophrenia (Powell *et al*, 2012). Thus, it has been suggested that schizophrenia may result from oxidative damage to PV interneurons

during development (Behrens & Sejnowski, 2009; Powell *et al*, 2012). Of relevance, several DISC1 mouse models display reduced PV expression in the cortex, although a potential functional link with increased oxidative stress has not been investigated yet (Ayhan *et al*, 2011; Hikida *et al*, 2007; Shen *et al*, 2008).

Growing evidence from imaging, gene expression and post-mortem studies indicates that oligodendrocyte function and myelination are impaired in schizophrenia and bipolar disorder (Davis *et al*, 2003; Dracheva *et al*, 2006; Haroutunian & Davis, 2007; McIntosh *et al*, 2009; Sussmann *et al*, 2009; Takahashi *et al*, 2011; Tkachev *et al*, 2003; Uranova *et al*, 2004; Uranova *et al*, 2007). White matter (WM) volume reductions, reduced fractional anisotropy (a measure of WM integrity), reduced expression of oligodendrocyte-specific genes and oligodendrocyte abnormalities such as decreased cell density, altered morphology and increased apoptosis have all been observed in these diseases (Bernstein *et al*, 2009; Ellison-Wright & Bullmore, 2009; Hof *et al*, 2003; Martins-de-Souza, 2010; Tkachev *et al*, 2003; Uranova *et al*, 2001). The results of several studies that tested the effects of typical and atypical antipsychotics on oligodendrocyte viability, proliferation, differentiation and morphology *in vitro* or *in vivo* support the conclusion that the oligodendrocyte abnormalities associated with schizophrenia are not side-effects of antipsychotic medication, and may therefore be inherent to the pathogenetic mechanism (Garver *et al*, 2008; Hakak *et al*, 2001; Konopaske *et al*, 2008; Steiner *et al*, 2011; Wang *et al*, 2010b; Xiao *et al*, 2008). According to the connectivity hypothesis, schizophrenia and bipolar disorder arise from defects in wiring and communication within and between different brain regions, which in turn lead to altered behaviour, perception and thought process (Harrison & Weinberger, 2005; Stewart & Davis, 2004). Since axon myelination is essential for the normal propagation of electric signals between neurons, it has been proposed that the WM abnormalities seen in schizophrenia and bipolar disorder may contribute to the aberrant connectivity characterising these disorders (Davis *et al*, 2003; Hulshoff Pol *et al*, 2004; Takahashi *et al*, 2011). Interestingly, the risk-conferring DISC1 polymorphism resulting in amino acid substitution S704C is associated with reduced fractional anisotropy (FA) in healthy carriers (Hashimoto *et al*, 2006; Sprooten *et al*, 2011). FA measures the directional selectivity of the motion of water molecules within a tissue. Highly myelinated WM

fibres are associated with high FA values, because the structure and chemical composition of this tissue prevents water diffusion in any direction other than along the fibres, and decreasing FA is thought to reflect structural degeneration of WM tracts (Kochunov *et al*, 2007). Thus, the findings reported by Hashimoto and colleagues and Spooten and colleagues establish a direct link between genetic variation in DISC1 and WM abnormalities in humans (Hashimoto *et al*, 2006; Sprooten *et al*, 2011). Due to their high iron content and reduced antioxidant capacity, both mature oligodendrocytes and their progenitor cells are particularly sensitive to oxidative stress-induced cell damage (Bitanihirwe & Woo, 2011). Moreover, oxidative stress was shown to inhibit the proliferation and promote the differentiation of oligodendrocyte progenitors (Li *et al*, 2007b; Smith *et al*, 2000) and to cause direct damage to myelin sheaths (Halliwell, 1992), providing a potential functional link between increased oxidative stress and defective myelination in schizophrenia (Bitanihirwe & Woo, 2011).

ATF4 is activated by oxidative stress, and in turn regulates the expression of target genes involved in the regulation of redox metabolism (Fung *et al*, 2007; Harding *et al*, 2003; Igarashi *et al*, 2007; Jin *et al*, 2009a; Lange *et al*, 2008; Lewerenz & Maher, 2009; Lewerenz *et al*, 2012; Ogawa *et al*, 2008; Tagawa *et al*, 2011). Interestingly, aberrant ATF4 expression has been linked to the oligodendrocyte abnormalities that characterise Vanishing White Matter Disease (VWM) (Kantor *et al*, 2008; van der Voorn *et al*, 2005). VWM is caused by inactivating mutations of the ubiquitously expressed eukaryotic initiation factor 2B (EIF2B), which result in selective loss of oligodendrocytes and consequent loss of white matter and neurodegeneration (Bugiani *et al*, 2010). The progression of VWM is accelerated by physiological stresses such as fever, head trauma and fright (Bugiani *et al*, 2010). Intriguingly, cultured primary fibroblasts from VWM patients are hypersensitive to endoplasmic reticulum stress, as demonstrated by the hyperactivation of ATF4 in response to the ER stress inducer thapsigargin (Kantor *et al*, 2008). Consistently, immunohystochemical and biochemical analysis of post-mortem VWM brains revealed abnormal activation of *ATF4* and its target gene *CHOP* in glial cells. Thus, it has been proposed that the increased stress response and ATF4 activation in oligodendrocytes might contribute to the apoptotic loss of these cells in VWM (van

der Voorn *et al*, 2005). It is therefore intriguing to speculate that excessive and/or prolonged ATF4 activation in response to oxidative stress may similarly contribute to oligodendrocyte loss in schizophrenia and bipolar disorder.

Recent studies conducted in zebrafish and mouse provided evidence for the involvement of DISC1 in oligodendrocyte proliferation, differentiation and function in the developing brain, and suggested a potential functional interaction between DISC1 and Neuregulin 1 (NRG1), a gene of known importance for oligodendrocyte development and function (Katsel *et al*, 2011; Wood *et al*, 2009a). However, the mechanisms underlying the reported effects of DISC1 on oligodendrocyte physiology are currently unknown.

In chapter 4 of this thesis I demonstrated that DISC1 inhibits the transcriptional activity of ATF4 and represses the thapsigargin-induced activation of CRE-driven transcription, suggesting that it may be involved in the regulation of the transcriptional response to cellular stress. Thus, in this chapter I test the hypothesis that, through its regulation of ATF4, DISC1 modulates the cell's ability to adapt and survive to stressful stimuli that activate ATF4. I additionally test the hypothesis that DISC1 amino acid substitutions 37W and 607F, which negatively impact on the repressive activity of DISC1 on ATF4, may similarly perturb any potential effect of DISC1 on cell viability after stress exposure. Given the proposed involvement of oxidative stress in the pathogenesis of schizophrenia, and the well-established role of ATF4 in the transcriptional response to oxidative stress, I chose this particular paradigm to investigate the putative effects of DISC1 on the cell's adaptation to stress. Since oxidative damage to oligodendrocytes has been suggested to underlie the WM abnormalities seen in schizophrenia (Bitanihirwe & Woo, 2011), I chose the MO3.13 human oligodendroglial cell line (McLaurin *et al*, 1995) as my experimental model. The MO3.13 cell line was established by McLaurin and colleagues (McLaurin *et al*, 1995) by fusing primary human oligodendrocytes with a human rhabdomyosarcoma cell line. MO3.13 cells express the glial cell markers myelin basic protein (MBP), glial fibrillary acidic protein (GFAP), galactosylceramide (GalC), myelin-associated glycoprotein (MAG) and proteolipid protein (PLP) (McLaurin *et al*, 1995), and exhibit strong phenotypical similarity to primary human

oligodendrocytes (Buntinx *et al*, 2003), thus representing a suitable model to study oxidative stress-mediated injury in these cells.

6.2 The effect of oxidative stress on endogenous DISC1 and ATF4 expression

To determine the optimal experimental conditions for the induction of endogenous ATF4 in response to oxidative stress, MO3.13 cells were incubated with increasing concentrations of hydrogen peroxide (H_2O_2) for 4, 8, 16 or 24 hours before being lysed and analysed by western blotting. The H_2O_2 concentrations tested here reflect the range of concentrations that have been previously used to induce oxidative stress in cell models (Papadia *et al*, 2008; Qin *et al*, 2008; Wei *et al*, 2003; Zhang *et al*, 2005). As shown in Figure 6.1, H_2O_2 induces ATF4 expression when used at the concentration of 100 or 200 μM, whereas lower concentrations have no detectable effect. ATF4 induction appears stronger after 8 hours of treatment compared to 4 hours, but does not increase further with prolonged incubation times (Figure 6.1).

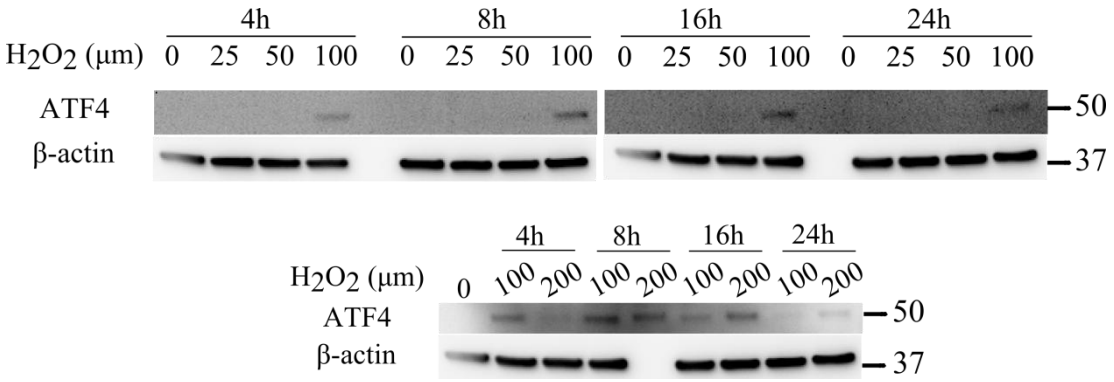

Figure 6.1 MO3.13 cells were treated with the indicated concentrations of H_2O_2 for 4, 8, 16 or 24 hours. After treatment, the cells were lysed and analysed by western blotting to detect endogenous ATF4, using β-actin as a loading control. ATF4 was detected with the ATF4 RPC antibody. The position and size (kDa) of the protein markers is indicated.

Next, to compare the effect of H_2O_2 on ATF4 and DISC1 nuclear expression, MO3.13 cells were treated with 100 or 200 µM H_2O_2 for 24 hours, then fractionated to obtain nuclear protein extracts, which were subsequently analysed by western blotting. ATF4 nuclear expression is strongly increased after treatment with 200, but not 100 µM H_2O_2 (Figure 6.2). On the other hand, H_2O_2 treatment reduces DISC1 nuclear expression in a concentration-dependent manner, with 200 µM H_2O_2 having a stronger effect compared to 100 µM H_2O_2 (Figure 6.2).

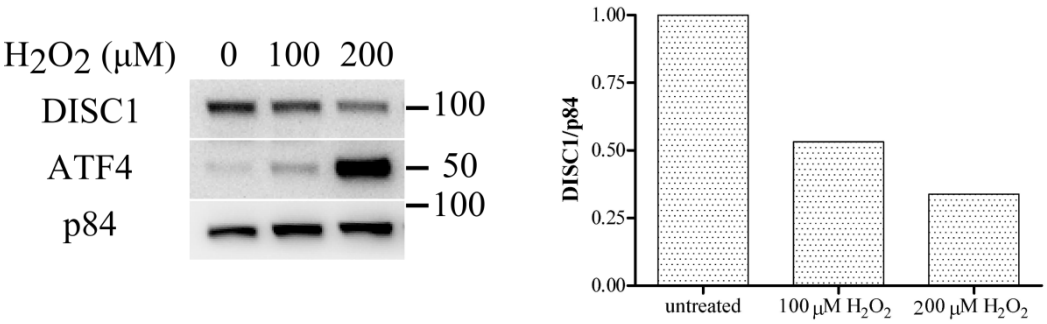

Figure 6.2 Western blotting analysis of nuclear extracts prepared from MO3.13 cells that had been treated for 24 hours with the indicated concentrations of H_2O_2. Endogenous DISC1 and ATF4 were detected using the α-DISC1 and ATF4 RPC antibodies, respectively, and the normalised relative DISC1 band densities are shown in the graph on the right. Nuclear matrix protein p84 was used as loading control. The position and size (kDa) of the protein markers is shown.

To further investigate the effect of H_2O_2 treatment on DISC1 expression in MO3.13 cells, nuclear and cytoplasmic extracts were prepared from cells treated with 200 µM H_2O_2 for 24 hours, and analysed by western blotting. As shown in Figure 6.3, DISC1 protein levels are significantly reduced both in the nuclear and cytoplasmic fractions obtained from cells exposed to H_2O_2, confirming the initial observations reported in Figure 6.2. The differential effect of H_2O_2 treatment on the expression of endogenous DISC1 and ATF4 in MO3.13 cells was further confirmed by immunocytochemistry (Figure 6.4).

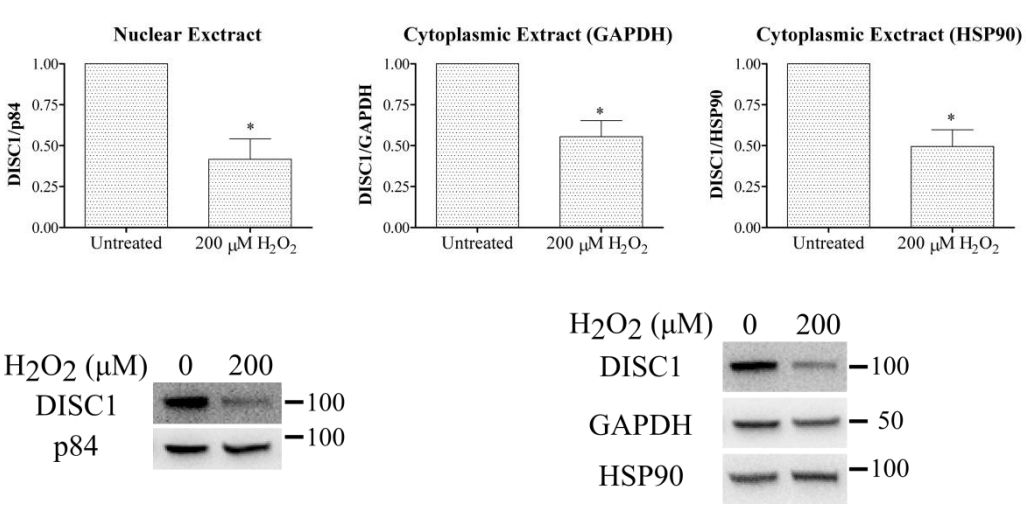

Figure 6.3 Western blotting analysis of nuclear and cytoplasmic extracts prepared from MO3.13 cells after a 24 hour treatment with either vehicle (H_2O) or 200 µM H_2O_2. Endogenous DISC1 was detected with the α-DISC1 antibody. The relative abundance of DISC1 in the cytoplasmic extracts was measured using two distinct loading controls (GAPDH or HSP90), which produced comparable results. The position and size (kDa) of the protein markers is indicated. The bars represent the average of three independent experiments. Normalised data were analysed by two-tailed one sample student's t-test. *P<0.05.

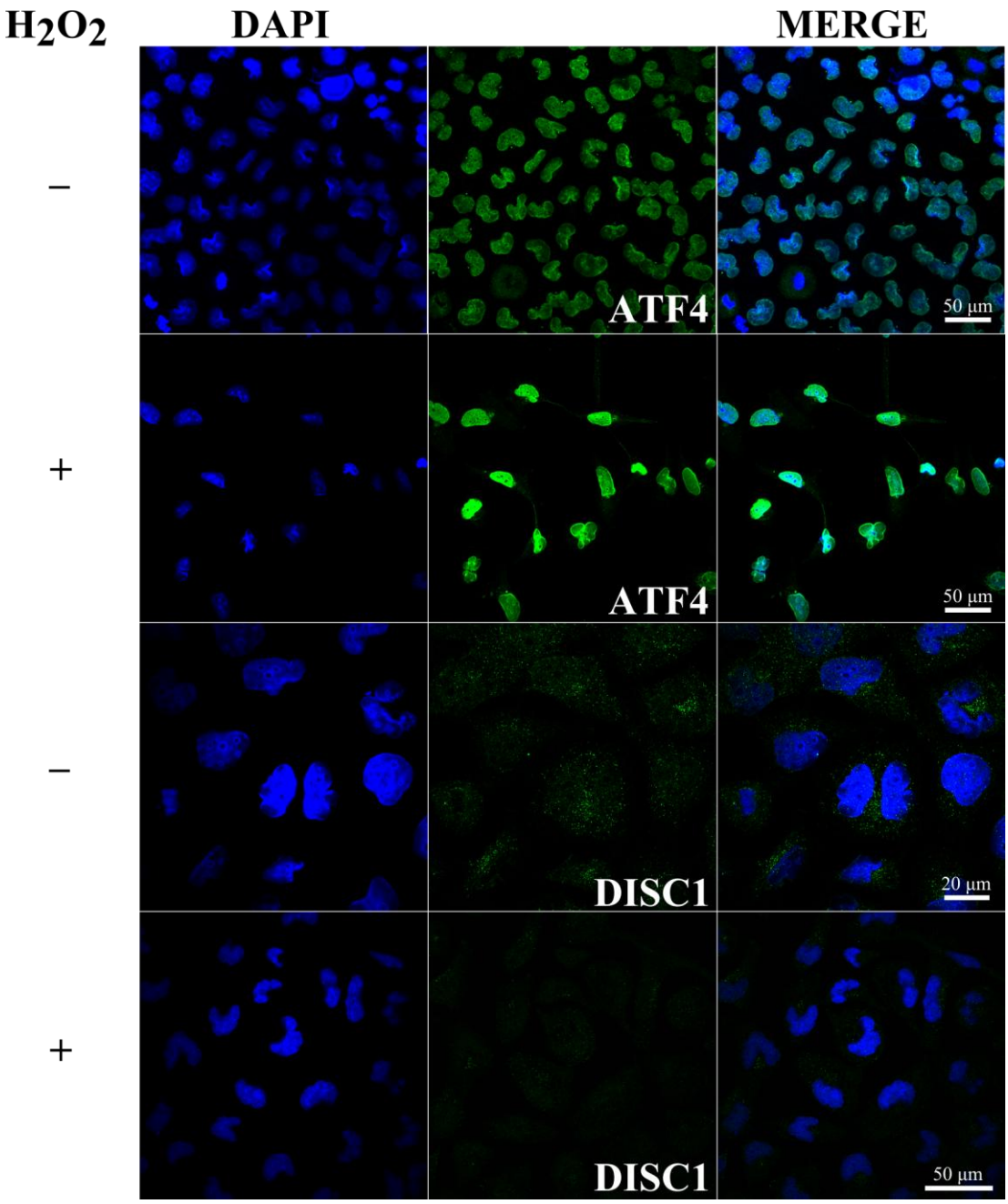

Figure 6.4 Endogenous ATF4 (top two rows) and DISC1 (bottom two rows) in MO3.13 cells treated for 24 hours with either 200 µM H_2O_2 or vehicle (H_2O). ATF4 and DISC1 were detected with the α-DISC1 and ATF4 MMC antibodies, respectively. For comparability, images of treated and untreated cells were acquired using the same confocal settings. Nuclei (blue) were stained with DAPI.

6.3 Testing the effect of ATF4 and DISC1 on MO3.13 cell viability in response to oxidative stress

Initially, I verified that the expression of endogenous ATF4 and DISC1 can be successfully silenced using specific siRNA oligonucleotides in MO3.13 cells. The cells were transfected with siRNA oligonucleotydes for 48 hours, as detailed in paragraph 2.6.7, before being lysed and analysed by western blotting. As expected, DISC1 expression is efficiently knocked-down by two distinct DISC1-targeting siRNAs (DISC1 #2 and DISC1 #5, Table 2.11), but not by the negative control siRNA (A NC siRNA, Table 2.11) (Figure 6.5 A). Similarly, the ATF4 targeting siRNAs obtained from Qiagen (Q ATF4, Table 2.11) and Ambion (A ATF4, Table 2.11), but not the respective negative controls (Q NC and A NC, Table 2.11), entirely prevented the H_2O_2-induced accumulation of ATF4 in the nucleus, confirming the efficiency of the siRNA transfection protocol in MO3.13 cells (Figure 6.5 B).

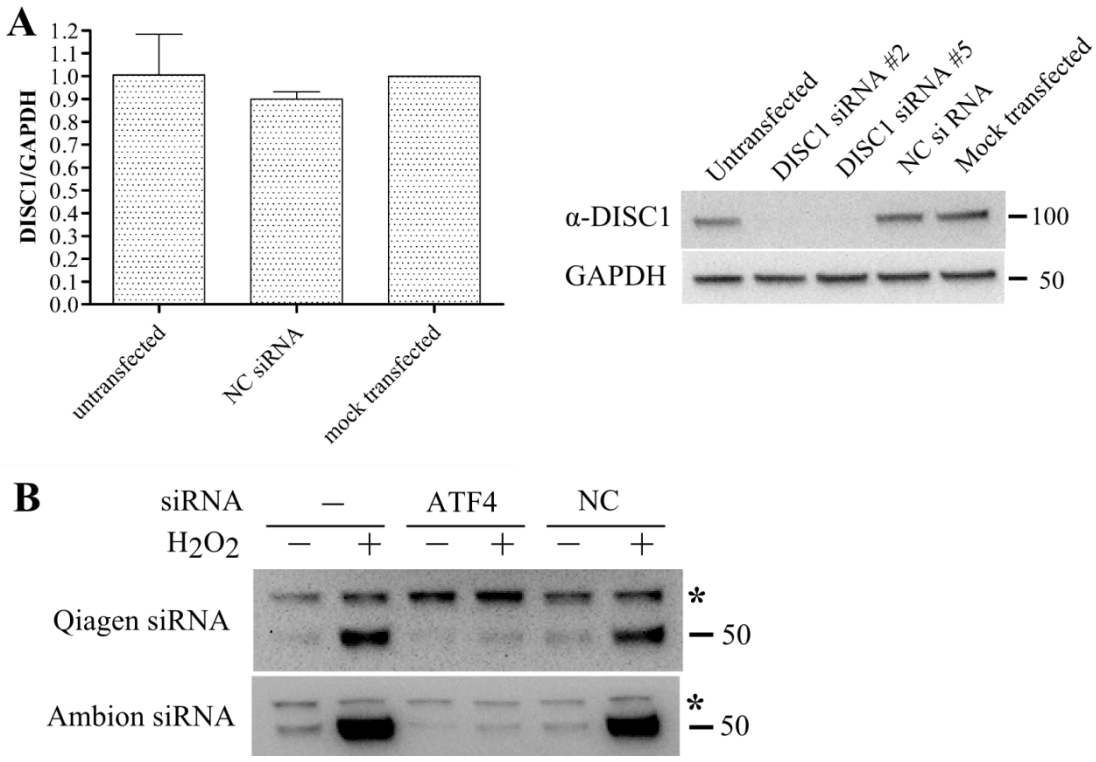

Figure 6.5 (A) DISC1 expression in whole cell lysates from MO3.13 that were either left untransfected, mock transfected, or transfected for 48 hours with the indicated siRNAs. The bars represent the mean relative DISC1 band densities measured in

three independent experiments. DISC1 protein expression was not quantified in the two DISC1 siRNA samples as no bands were visible, even after a prolonged exposure time (>30 minutes). (B) MO3.13 cells were either mock transfected or transfected with Qiagen or Ambion ATF4-targeting siRNA or the respective negative controls. Starting from 32 hours after transfection, the cells were treated with 200 µM H_2O_2 for 16 hours, then nuclear protein extracts were prepared and analysed by western blotting. DISC1 and ATF4 were detected using the α-DISC1 and ATF4 RPC antibodies, respectively. NC: negative control. The position and size (kDa) of the protein markers is indicated. * non-specific bands.

To investigate the potential effects of ATF4 and DISC1 on MO3.13 survival under conditions of oxidative stress, the cells were treated for 24 hours with either 200 µM H_2O_2 or 5 mM DL-Homocysteine (HCY) after ATF4 or DISC1 knock-down or overexpression, as detailed in paragraph 2.7.2. HCY is a non-essential sulphur-containing amino acid generated by demethylation from methionine (Bouaziz *et al*, 2010). When HCY plasma levels are abnormally elevated, it can cause oxidative stress by increasing the generation of ROS (Heinecke *et al*, 1987; Yan *et al*, 2006), by inducing lipid peroxidation (Jones *et al*, 1994) and by inhibiting the synthesis of glutathione peroxidase (Handy *et al*, 2005; Pasca *et al*, 2006; Upchurch *et al*, 1997). Accordingly, HCY treatment induces ATF4 expression in cultured cells (Jin *et al*, 2009b; Outinen *et al*, 1999; Roybal *et al*, 2004), and a number of studies suggest that increased HCY plasma levels may be a risk factor for schizophrenia (Applebaum *et al*, 2004; Bouaziz *et al*, 2010; Brown & Susser, 2005; Levine *et al*, 2002; Levine *et al*, 2006; Muntjewerff *et al*, 2005; Muntjewerff *et al*, 2006; Regland, 2005; Susser *et al*, 1998). Following on from my finding that the endoplasmic reticulum stress inducer thapsigargin (TG) elicits a CRE-driven transcriptional response that is differentially regulated by DISC1 variants 37W and 607F, I tested whether DISC1 and its variants affect MO3.13 viability in response to TG treatment.

Initially, for each different siRNA transfection, the cell viability at the end of each drug treatment was compared to the cell viability in untreated cells using paired student's t-tests. In this set of experiments, cell viability was determined indirectly

by using a bioluminescent reaction to quantify the amount of ATP present in each well, which is in turn proportional to the number of metabolically active cells (see paragraph 2.7.2 for a detailed method description). As expected, all drug treatments significantly reduce MO3.13 cell viability in siRNA-transfected cells (Figure 6.6 A, B, C and D). HCY treatment (5mM) produces the strongest cell toxicity, and consistently reduces the number of viable cells by ~60% (Figure 6.6 A, B, C and D). The effect of 200 µM H_2O_2 is comparable to that of HCY, whereas 1 µM TG determines a milder reduction of cell viability (30-40%) (Figure 6.6 A, B, C and D). Next, the same data were plotted differently for ease of comparison between different siRNA transfections (Figure 6.6 C and D). For each drug treatment, the viability of cells transfected with ATF4- or DISC1-targeting siRNAs was compared to the viability of cells transfected with the respective negative control siRNAs, using paired student's t-tests. Surprisingly, when compared to the appropriate negative controls, ATF4-targeting siRNAs do not significantly affect MO3.13 cell viability after stress exposure (Figure 6.6 A and C). On the other hand, ATF4 silencing mildly affects viability in untreated MO3.13 cells (Figure 6.6 E). However, since two distinct ATF4-targeting siRNAs produce opposing effects when compared to the respective negative controls, this observation is likely artifactual (Figure 6.6 E). Very similar results were obtained after DISC1 silencing: neither DISC1-targeting siRNA affects cell viability in stressed cells (Figure 6.6 B, D), but the two distinct DISC1 siRNAs have opposing effects in untreated cells (Figure 6.6 F). Overall, then, these data indicate that transient knock-down of ATF4 or DISC1 has no effect upon MO3.13 cell viability in response to the tested cellular stressors.

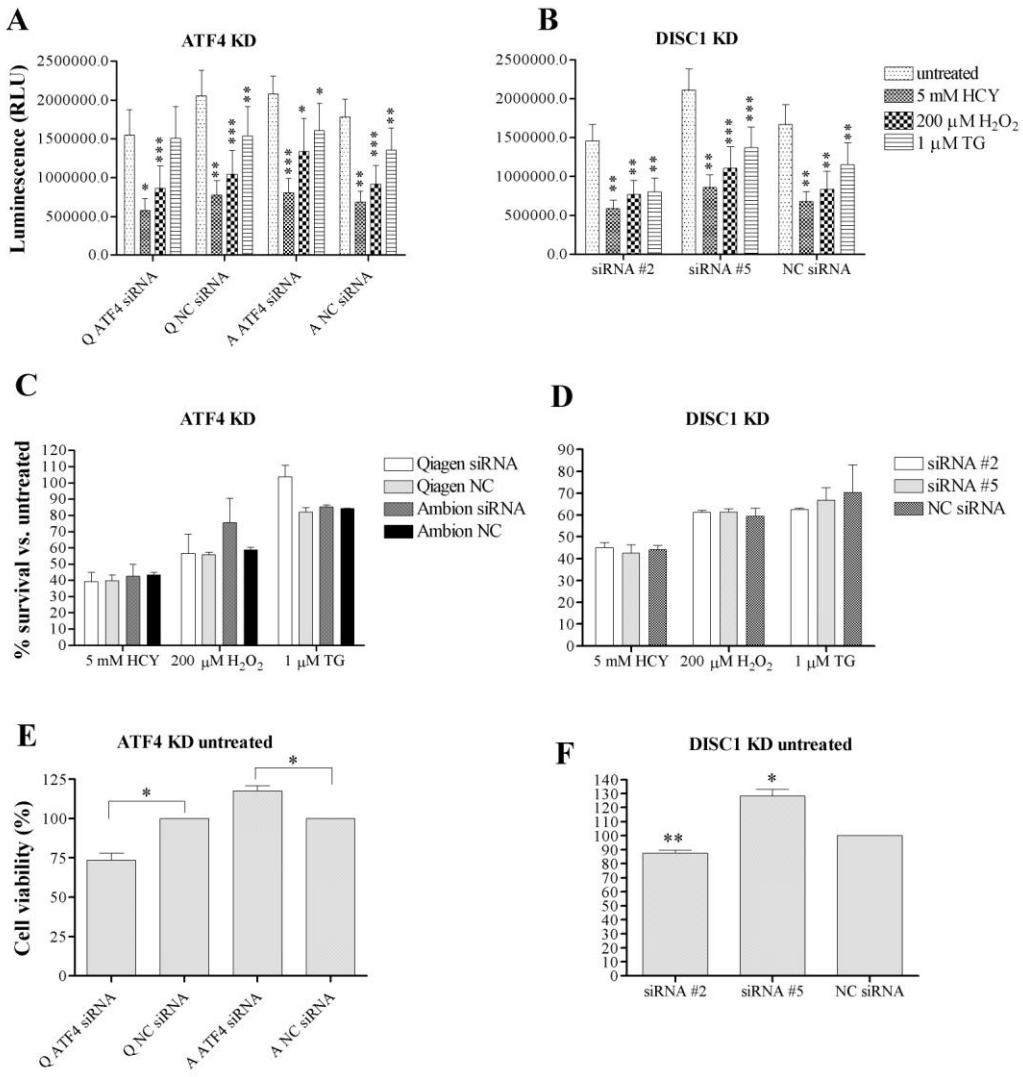

Figure 6.6 MO3.13 cells were transfected with the indicated siRNAs for 24 hours before being subjected to the specified drug treatments for 24 hours, and then assayed for total cell viability. Figures A and B report the actual luminescence readings, which are directly proportional to the number of viable cells in each sample. In A and B, for each siRNA tested, the readings obtained after drug exposure were compared to the readings in non-drug-treated cells. The same data is plotted differently in C and D, to show the proportion of viable cells in each sample normalised to the viability of non-drug-treated cells, which was assumed to be 100%. In C and D, for each drug treatment condition, the readings obtained from cells transfected with ATF4 or DISC1-targeting siRNAs were compared to the readings from cells transfected with the respective negative control siRNA. Figures E and F show the proportion of viable cells in non-drug treated samples. In Figures

E and F, the viability of cells transfected with ATF4- or DISC1-targeting siRNAs is normalised to the viability of the respective negative control-transfected cells, which was assumed to be 100%. The bars represent the average of 4 independent experiments. Data were analysed by two-tailed paired student's t-test. *P<0.05; **P<0.01; ***P<0.001. Q ATF4 siRNA: Qiagen ATF4 siRNA; Q NC siRNA: Qiagen negative control siRNA; A ATF4 siRNA: Ambion ATF4 siRNA; A NC siRNA: Ambion NC siRNA.

Next, the same analysis was applied to cells transfected with ATF4 or DISC1 expression plasmids (Figure 6.7). Unlike siRNA-transfected cells, in ATF4-, ATF4ΔRK- or mock-transfected cells, HCY or H_2O_2 treatment only mildly, and non-significantly, reduces cell viability (~30% and ~20% reduction, respectively), whereas TG has no effect (Figure 6.7 A and C). Overexpression of ATF4 or its dominant-negative mutant ATF4ΔRK produces no effect on cell viability when compared to mock-transfected cells, both under stressed and unstressed conditions (Figure 6.7 A, C and E). However, since in this particular experiment no significant effect of stress exposure could be detected in the control, mock-transfected cells (Figure 6.7 A), no firm conclusions can be drawn about the putative effect of ATF4 overexpression on cell viability. In the absence of drug treatment, the viability of DISC1-transfected cells does not differ from that of mock-transfected cells (Figure 6.7 F), indicating that DISC1 overexpression alone does not affect cell viability. Similarly to ATF4-transfected cells, DISC1- or mock-transfected cells are not significantly affected by H_2O_2 or TG treatment (Figure 6.7 B and D). On the other hand, HCY significantly reduces cell viability in wild-type DISC1- and mock-transfected cells (P<0.05, Figure 6.7 A), but not in cells expressing DISC1-37W or DISC1-607F (Figure 6.7 A). This suggests that DISC1-37W- and DISC1-607F-, but not DISC1-WT expressing cells might be protected from cell death induced by HCY. However, this is in contrast with the observation that, when compared to mock-transfected cells, cells expressing DISC1-WT show a small, but statistically significant increase in viability after exposure to HCY (P<0.05, Figure 6.7 D), whereas cells expressing DISC-37W and DISC1-607F do not significantly differ

from mock-transfected cells (Figure 6.7 D). The latter observation suggests that cells overexpressing DISC1-WT might be better protected from HCY-induced cell death compared to cells expressing DISC1-37W or DISC1-607F. The discrepancy between these two observations, which likely arises from the higher experimental error associated with viability measurements in cells expressing DISC1-WT or DISC1-607F compared to cells expressing DISC1-WT and mock-transfected cells (Figure 6.7 B and D), prevents any firm conclusions about the potential differential effect of DISC1 variants on MO3.13 cell survival after HCY exposure.

As detailed in chapter 2 of this thesis, MO3.13 cells were plated at a cell density of $1x10^4$/well for the silencing experiments and $2x10^4$/well for the overexpression experiments (Paragraph 2.7.2). This was done because while DNA transfection caused cell death at cell densities below $2x10^4$/well, siRNA transfection was well tolerated by cells seeded at $1x10^4$/well. The reason for this difference is not clear, as it does not depend on the transfection protocol, nor on the type of transfected DNA. Indeed, transfection of protein expression plasmids or empty vector produced similar degrees of cell toxicity (not shown). A titration experiment carried out using HCY established that increased cell density increases cell survival after stress exposure (Figure 6.8). For this reason, and to achieve the strongest possible response to stress, each set of experiments was performed using the lowest cell density that allows transfection without toxicity (i.e. $1x10^4$ for siRNA transfection and $2x10^4$ for DNA transfection). Thus, the reduced cell toxicity of H_2O_2, HCY and TG in DNA-transfected cells (Figure 6.7 A) compared to siRNA-transfected cells (Figure 6.6 A) likely reflects the substantially higher plating cell density of the former.

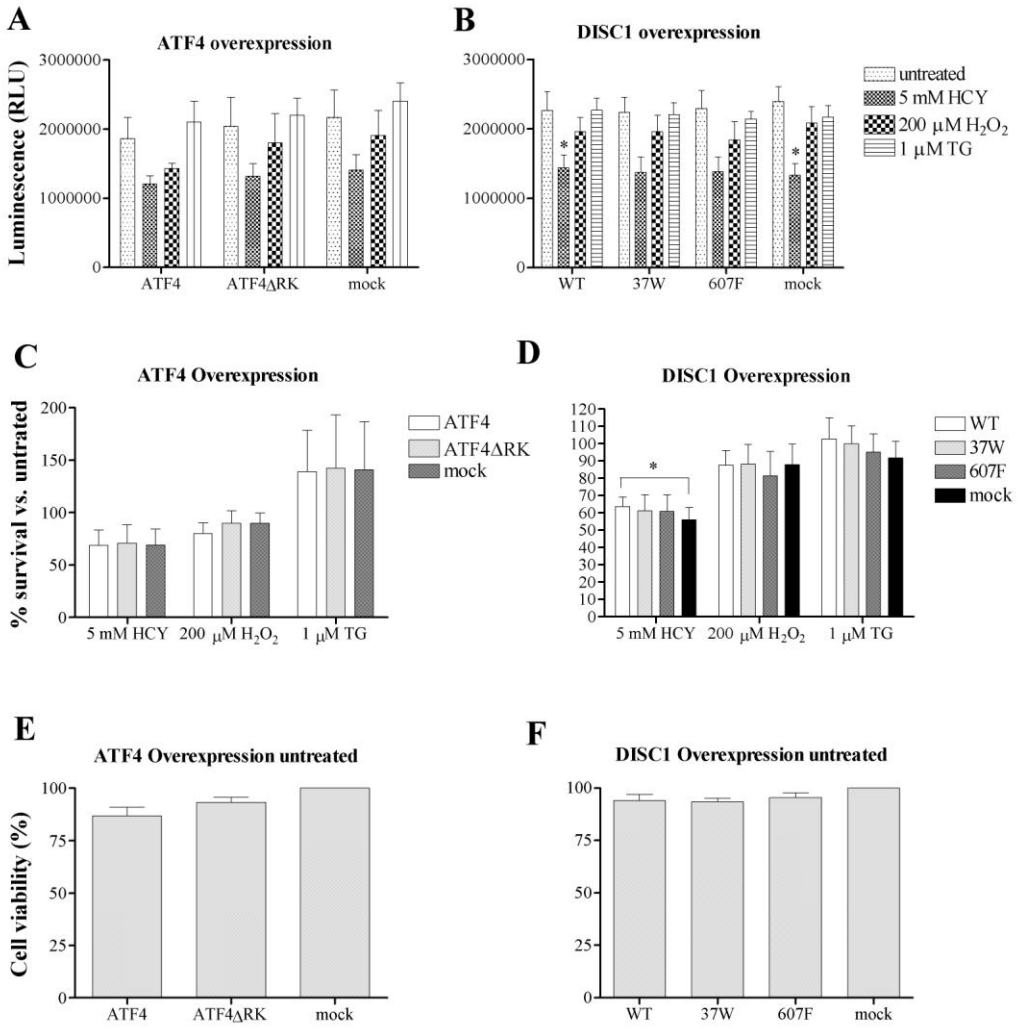

Figure 6.7 MO3.13 cells were transfected with the indicated expression plasmids before being subjected to the specified drug treatments for 24 hours, and then assayed for total cell viability. Figures A and B report the actual luminescence readings, which are directly proportional to the number of viable cells in each sample. In A and B, for each DNA construct tested, the readings obtained after drug exposure were compared to the readings in untreated cells. The same data is plotted differently in C and D, to show the proportion of viable cells in each sample normalised to the viability of untreated cells, which was assumed to be 100%. In C and D, for each treatment condition, the readings obtained from cells transfected with ATF4 or DISC1 expression plasmids were compared to the readings from mock-transfected cells. Figures E and F show the proportion of viable cells in untreated samples, and each data set is normalised to the viability of mock-transfected cells, which was set at 100%. The bars represent the average of 3

independent experiments. Data were analysed by two-tailed paired student's t-test. *P<0.05.

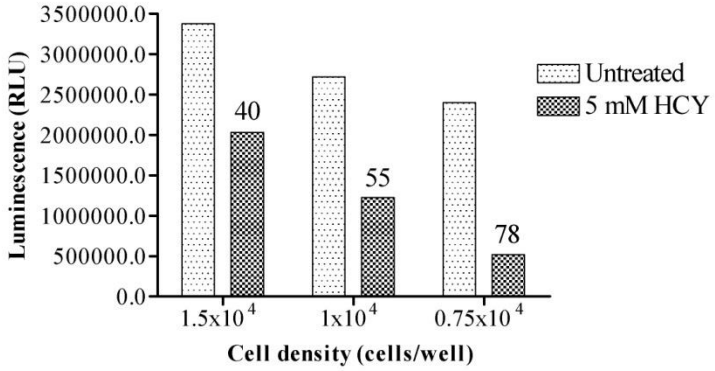

Figure 6.8 MO3.13 cells seeded in 96 well plates at the indicated cell densities were either treated with 5 mM HCY for 24 hours or left untreated before being assayed for cell viability. The luminescence readings for each sample are directly proportional to the number of viable cells. The bars represent the readings obtained in a single experiment. The numbers above the bars indicate the reduction in cell viability, expressed as percentage.

6.4 Discussion

In this chapter, I investigated the effect of oxidative stress on ATF4 and DISC1 protein expression in MO3.13 human oligodendrocytes, and tested for potential effects of both proteins on MO3.13 cell survival under conditions of oxidative and endoplasmic reticulum stress. As previously observed in other cell types (Jin *et al*, 2009a; Miyamoto *et al*, 2011), H_2O_2 treatment robustly induces ATF4 nuclear expression in MO3.13 cells. Interestingly, the same treatment produces the opposite effect on DISC1 protein levels. A recent study showed that exposure of primary mouse cortical neurons to H_2O_2 promotes the accumulation of endogenous DISC1 aggregates (containing both full-length and 72 kDa isoforms) in the sarkosyl-insoluble subcellular protein fraction (Atkin *et al*, 2012), an effect that may be potentially related to the H_2O_2-induced reduction of DISC1 expression in the soluble

nuclear and cytoplasmic fractions described here. However, in contrast with my findings, the above study found no evidence for a concomitant reduction of soluble DISC1 protein levels upon H_2O_2 treatment (Atkin *et al*, 2012). This discrepancy may be explained by experimental differences, as my experiments were performed using a 10-fold higher H_2O_2 concentration (200 µM instead of 20 µM) and a significantly longer treatment time (16 hours instead of 2 hours). The immunocytochemical analysis described in this chapter confirmed reduced DISC1 expression levels in MO3.13 cells exposed to 200 µM H_2O_2, but provided no evidence suggesting that this may result from the formation of insoluble endogenous DISC1 aggregates, the visualisation of which may require a higher resolution technique, such as electron microscopy. H_2O_2-induced insoluble DISC1 aggregation in neurons is enhanced by disruption of the autophagy pathway, indicating that these aggregates are normally degraded by autophagy (Atkin *et al*, 2012). Since stress-induced ATF4 is known to activate the autophagic pathway (Avivar-Valderas *et al*, 2011; Milani *et al*, 2009; Rouschop *et al*, 2010; Rzymski *et al*, 2010; Rzymski *et al*, 2009), it is intriguing to speculate that H_2O_2 concentrations that induce ATF4 expression may also promote the degradation of insoluble DISC1 aggregates by autophagocytosis. It would therefore be interesting to test whether inhibiting ATF4 expression promotes the accumulation of insoluble DISC1 aggregates in H_2O_2-treated cells. It is also possible that, besides promoting DISC1 aggregation, H_2O_2 treatment, and perhaps other cellular stressors, may control DISC1 expression by indirectly regulating its transcription and/or translation. Indeed, the recently characterised human DISC1 promoter (Walker *et al*, 2012) contains one copy of the AP-1 consensus binding site (5' TGAGTCA 3') (Rosie Walker, personal communication). Consistently, ChIP-seq experiments performed as part of the ENCODE project (http://www.genome.gov/10005107) identified binding of AP-1 family members JunD and c-Jun to the DISC1 promoter region. The AP-1 family of transcription factors, which is composed by Fos, Jun and ATF homo- and heterodimers, is implicated in the transcriptional response to a variety of physiological and pathological stimuli, including stress signals (Hess *et al*, 2004). In the light of these observations, it would be particularly interesting to test for potential regulatory effects of cellular stress on DISC1 promoter activity.

ATF4 has been shown to affect cell viability in response to oxidative stress in different cell models (Dickhout *et al*, 2012; Fung *et al*, 2007; Harding *et al*, 2003; Lange *et al*, 2008; Ogawa *et al*, 2008; Ord *et al*, 2007). It is therefore surprising that ATF4 silencing does not affect MO3.13 cell survival after exposure to toxic concentrations of H_2O_2 or HCY. The reasons for this discrepancy are not clear, but may be related to methodological problems. For example, all previous studies were performed in *ATF4* KO cell lines or primary neurons, as opposed to cells in which ATF4 expression has been silenced by transient siRNA transfection, and may have reflected long-term changes arising from chronic ATF4 depletion. Moreover, in the present study both ATF4- and DISC1-targeting siRNAs were shown to efficiently knock-down protein expression 48 hours after transfection, but the drug treatments were started 24 hours after transfection. Thus, it cannot be excluded that ATF4 and DISC1 expression were only partially silenced at the start of the drug treatments, which may have affected the results. The choice of method used to evaluate cell viability may also have contributed to the discrepancy between my observations and what has previously been reported in the literature. Indeed, while in the present study cell viability was estimated on the basis of cellular ATP content, other studies used the 3-(4,5-Dimethylthiazol-2-yl)-2,5-diphenyltetrazolium (MTT) assay (Lange *et al*, 2008). MTT assay can overestimate cell toxicity as it measures cellular NAD(P)H-dependent reducing activity, which can be decreased by sub-toxic stress through a reduction of intracellular NAD(P)H levels (Bell *et al*, 2011). Since knocking down ATF4, which is a key mediator of the cellular response to stress, does not show any effect upon MO3.13 cell survival to H_2O_2- and HCY-induced toxicity in this set of experiments, it is not surprising that DISC1 silencing also has no consequence on stress survival under the same conditions. Thus, based on this particular experimental model, it is not possible to draw any conclusions on the putative direct involvement of DISC1 in stress adaptation.

The ATF4/DISC1 overexpression model described here is affected by a major technical limitation, as the minimal cell density that guarantees cell survival after transfection also protects the cells from death after exposure to the subsequent drug treatments. As a result of this, I could not detect a statistically significant decrease in cell viability upon drug exposure, except for wild-type DISC1 or mock-transfected

cells exposed to HCY. Moreover, since transfection methods based on liposome DNA carriers, like the one used in this study, can induce cellular stress responses and thus alter the gene expression profile in transfected cells (Fiszer-Kierzkowska *et al*, 2011), it is likely that stress-inducible pathways were already active in MO3.13 cells before the start of the drug treatments, which may have blunted the observed effects. Interestingly, cells expressing wild-type DISC1, but not 37W- or 607F-DISC1, show slightly but significantly improved stress survival compared to mock-transfected cells. However, given the very small size of this protective effect, coupled with the lack of effect of DISC1 silencing, this result must be interpreted with caution, and cannot be taken as direct evidence supporting a role of DISC1 in the regulation of the cell's adaptation to stress. Nevertheless, this is a potentially relevant observation that would deserve further investigation, especially in the light of the differential effects of DISC1 variants on ATF4-dependent transcription reported in chapter four of this thesis. Future experiments focused on alternative and more relevant cell models, such as primary oligodendrocytes or neurons, and exploiting efficient DNA delivery methods, such as adenoviral-mediated overexpression or gene silencing, may provide a better experimental approach to explore the potential role of DISC1 in the regulation of stress-survival pathways in the brain.

7 Molecular characterisation of the DISC1-ATF4 interaction

7.1 Introduction

In the previous chapters of this thesis I demonstrated that amino acid substitutions 37W and 607F significantly decrease the nuclear abundance of exogenously expressed full-length DISC1. I additionally demonstrated that at basal cAMP levels DISC1 inhibits the transcriptional activity of ATF4, and that this particular DISC1 function is impaired by amino acid substitutions 37W and 607F. Since the partial loss of function phenotype observed for DISC1-37W and DISC1-607F in luciferease reporter assays is coupled with their reduced nuclear targeting, I hypothesised that a causal relationship might exist between these two observations, whereby reduced DISC1 nuclear expression results in, or contributes to its decreased ability to repress ATF4 activity. In support of this, as shown in chapters 3 and 4 of this thesis, the repressive effect of DISC1 on ATF4 function is not affected by the ultra-rare mutation 603I, which does not impair DISC1 nuclear expression. On the other hand, the artificial mutant DISC1ΔLZ9, which is not expressed in the nucleus, is unable to repress ATF4 transcriptional activity. I additionally postulated that amino acid substitutions 37W and 607F, both of which are predicted to introduce structural changes in DISC1 (Soares *et al*, 2011), might either directly or indirectly destabilise its physical interaction with ATF4, which in turn may contribute to their observed detrimental effect on the functional interaction between DISC1 and ATF4. Thus, this chapter aims to investigate the mechanism(s) by which DISC1 represses ATF4 transcriptional activity, and shed light on the molecular basis for the differential effects of DISC1 variants on the functional interaction with ATF4. In particular, I investigate the effect of amino acid substitutions 37W, 607F and 603I on DISC1's ability to interact with ATF4 in intact cells, and ask if and how the impact of such DISC1 amino acid changes on ATF4 binding may relate to their differential effect on ATF4 regulation. In addition, having previously established that DISC1 represses ATF4-dependent transcription at basal cAMP levels, but has no effect on ATF4 transactivation at high cAMP levels, I test for potential effects of cAMP levels on

ATF4 and DISC1 subcellular distribution and binding. Finally, to test the hypothesis that the ATF4-DISC1 interaction may not be restricted to the cell nucleus, I analyse the subcellular distribution of both exogenous and endogenous ATF4 and DISC1 in two distinct human cell lines.

7.2 Generation of novel ATF4 expression constructs

To generate expression constructs pcDNA3.1-ATF4-Flag, coding for C-terminally Flag-tagged human ATF4, and pcDNA6-ATF4-Myc, coding for C-terminally Myc-tagged human ATF4, the ATF4 coding sequence was amplified from construct pDEST53-ATF4 (Table 2.2), using primer couples ATF4 F plus ATF4 Flag R and pDEST ATF4 F1 plus pDEST ATF4 R2, respectively (Table 2.8). The PCR reactions were performed as detailed in paragraph 2.6.1.1. The purified PCR products were ligated between the EcoRI and XhoI sites of destination vector pcDNA3.1(+) (Table 2.2), to generate pcDNA3.1-ATF4-Flag, or pcDNA6/myc-HIS B (Table 2.2), to generate pcDNA6-ATF4-Myc, according to the methods described in paragraphs 2.6.6.2 to 2.6.6.6. The new ATF4 expression constructs were validated by direct sequencing, using primers T7 F, CMV F and BGH R (Table 2.7).

7.3 The effect of DISC1 on ATF4 expression and nuclear targeting

In chapter 4 of this thesis I demonstrated that DISC1 co-expression inhibits the transactivation activity of ATF4 on the CRE and CHOP AARE promoters at basal cAMP levels. Interestingly, a previous study by Morris and colleagues showed that co-expression of full-length DISC1 inhibits the nuclear targeting of its interactor ATF5, a transcription factor that is both structurally and functionally related to ATF4 (Morris *et al*, 2003). Thus, I sought to test whether DISC1 co-expression exerts a similar effect on the nuclear distribution and/or total protein expression levels of ATF4, which may contribute to its repressive effect on ATF4 transcriptional activity. Initially, COS7 cells were transfected using the same ATF4/DISC1 DNA ratio used in luciferase assays (i.e. 1/0.67) and analysed by immunocytochemistry to detect ATF4 and DISC1, using cells transfected with ATF4 only as controls. As shown in Figure 7.1, co-expression of DISC1 does not grossly interfere with ATF4 nuclear

expression in COS7 cells. Interestingly, in transfected COS7 cells, ATF4 expression is not restricted to the nucleus, but can also be detected in the cytoplasm in a pattern closely resembling the typical morphology of mitochondria (Figure 7.1), an organelle where DISC1 is known to localise (James *et al*, 2004; Millar *et al*, 2005a; Park *et al*, 2010). Notably, exogenous ATF4 and DISC1 partially co-localise both in the nucleus and cytoplasm, and particularly in the perinuclear region (Figure 7.1). To further test for potential effects of DISC1 on the overall protein expression and/or nuclear targeting of exogenous ATF4, whole cell lysates, nuclear extracts and cytoplasmic extracts were obtained from HEK293 cells expressing ATF4 alone or in combination with DISC1, and analysed by western blotting. Consistent with what was observed by immunofluorescence in COS7 cells, DISC1 co-expression does not reduce ATF4 expression in the nucleus or cytoplasm, nor does it reduce its total expression levels in HEK293 cells (Figure 7.2). Instead, and contrary to my expectations, DISC1 co-expression appears to moderately increase ATF4 expression both in the nucleus and cytoplasm, although this effect is not statistically significant (Figure 7.2). Thus, on the basis of these results, the hypothesis that DISC1 may inhibit ATF4-mediated transcription by reducing its nuclear expression can be confidently rejected.

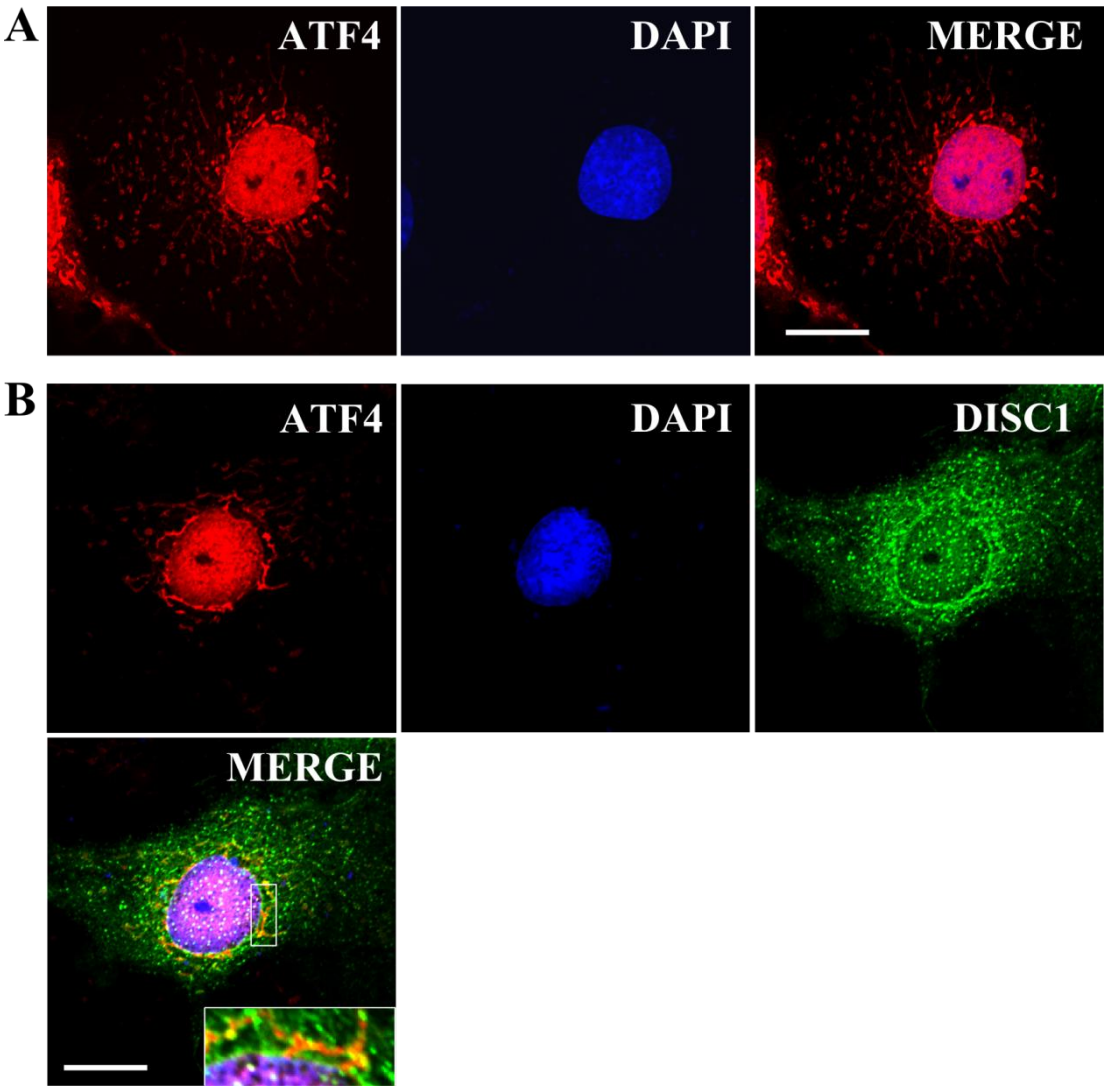

Figure 7.1 COS7 cells transfected with pCG-ATF4 and either the empty vector pcDNA4/TO (A) or pcDNA4/TO-Flag DISC1 WT (B) at a 1/0.67 ratio were double stained with the ATF4 RPC and Flag MMC antibodies to detect exogenous ATF4 and DISC1, respectively, then analysed by confocal microscopy. The area delimited by a white rectangle is magnified in the inset. Nuclei are stained with DAPI (blue). Scale bars are 20 µm.

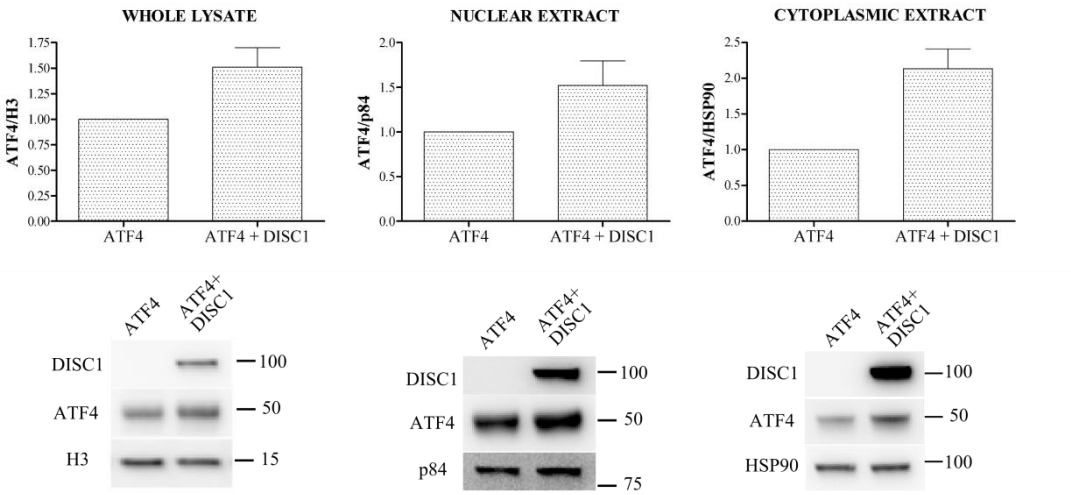

Figure 7.2 HEK293 cells were transfected with pCG-ATF4 and either pcDNA4/TO-Flag DISC1 WT or the empty vector pcDNA4/TO. The ATF4/DISC1 transfected DNA ratio was 1/0.67, reflecting the transfection conditions used for luciferase reporter assays. 24 hours after transfection, the cells were subjected to subcellular fractionation, and the resulting nuclear and cytoplamic extracts were analysed by western blotting, along with the corresponding whole cell lysates. Loading controls are histone 3 (H3) for whole cell lysates, nuclear matrix protein p84 for nuclear extracts and heat shock protein 90 (HSP90) for cytoplasmic extracts. Bars represent the average of 3 independent experiments. The position and size (kDa) of the protein markers is indicated. Data are normalised to ATF4 protein levels in cells transfected with ATF4 alone, and were analysed by one sample student's t test.

7.4 Distribution of DISC1 and ATF4 in human cell lines

Although exogenous ATF4 is highly enriched in the nucleus, it is also expressed in the cytoplasm, in a pattern resembling the typical conformation of mitochondria (Figure 7.1). Hence, to better test whether exogenous ATF4 partially distributes to mitochondria, I used four different antibodies to detect the protein (both tagged and untagged) in transfected COS7 cells. In each case, I observed partial co-localisation of ATF4 with mitochondria, particularly in the perinuclear region (Figure 7.3). This confirms my previous observations, and suggests that ATF4 may potentially interact with mitochondrial DISC1.

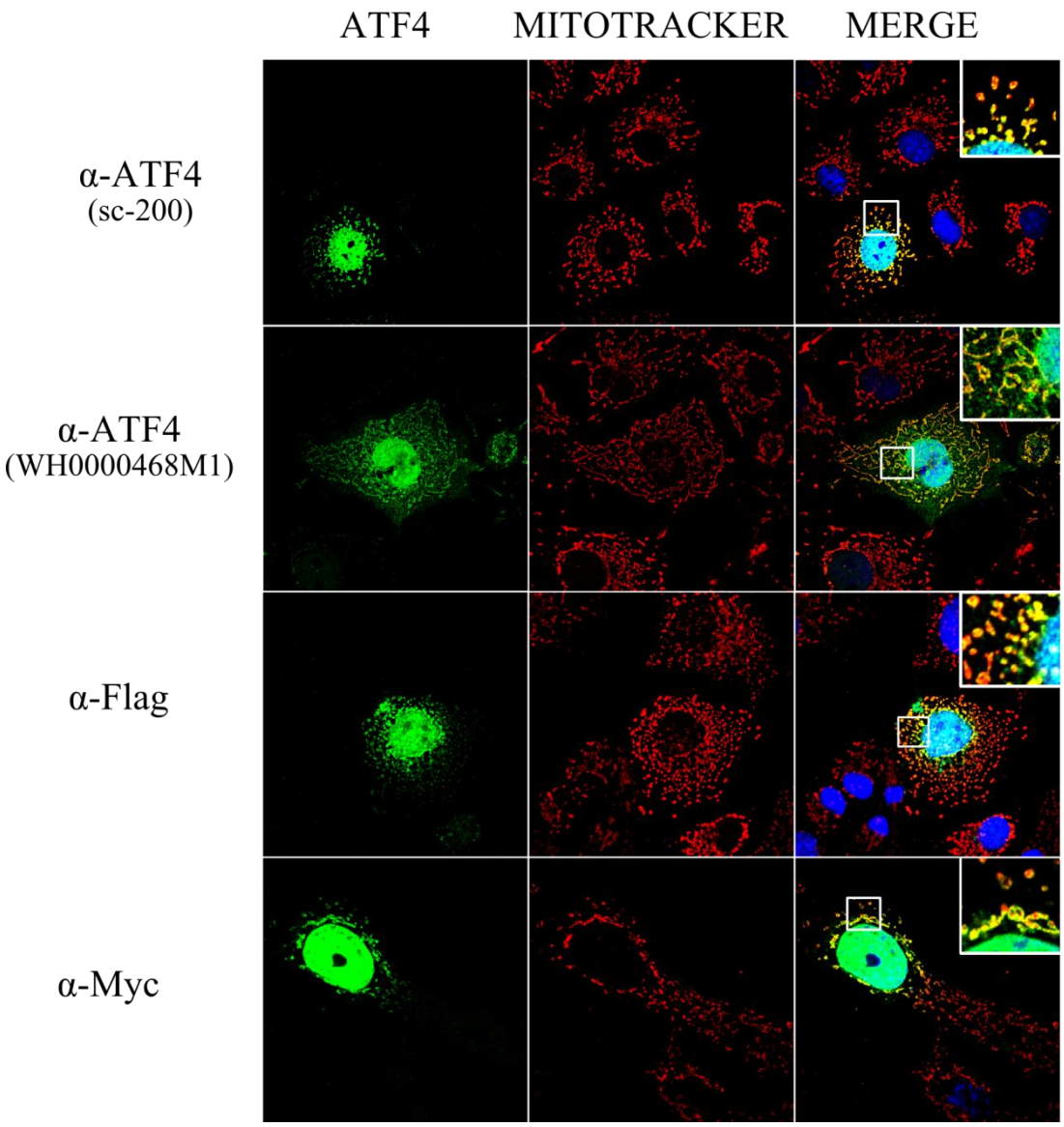

Figure 7.3 COS7 cells were transfected with pCG-ATF4 (top two rows), pcDNA3.1-ATF4-Flag (third row) or pcDNA6-ATF4-Myc (bottom row). Exogenous ATF4 was detected using the following antibodies: ATF4 RPC (sc-200, top row), ATF4 MMC (WH000048M1, second row), Flag RPC (third row) or Myc MMC (bottom row). Mitochondria were stained with Mitotracker Red. The areas delimited by a white square are magnified in the insets.

Next, I asked whether endogenous ATF4 also localises at mitochondria. As expected, two distinct ATF4 antibodies reveal that endogenous ATF4 is prominently nuclear in

both HEK293 and SH-SY5Y human cell lines (Figure 7.4 A and B, respectively). In addition, like the exogenous protein, endogenous ATF4 is also detectable in the cytoplasmic region, where it assumes a punctate distribution (Figure 7.4 A and B). Consistent with my previous observations, endogenous cytoplasmic ATF4 partially overlaps with mitochondria, and here its distribution is strikingly similar to that independently observed for endogenous mitochondrial DISC1 (Figure 7.4 A and B). These data indicate that both endogenous full-length DISC1 and ATF4 partially localise at mitochondria in HEK293 and SHSY5Y cells. However, due to technical limitations concerning the staining protocol, it was not possible to determine with confidence whether endogenous ATF4 and DISC1 co-localise at mitochondria in these cells. In the future, this could be tested by using triple staining to detect ATF4, DISC1 and mitochondria, or by combining mitotracker staining with Proximity Ligation Assay (see Paragraph 8.6) to visualise ATF4 and DISC1.

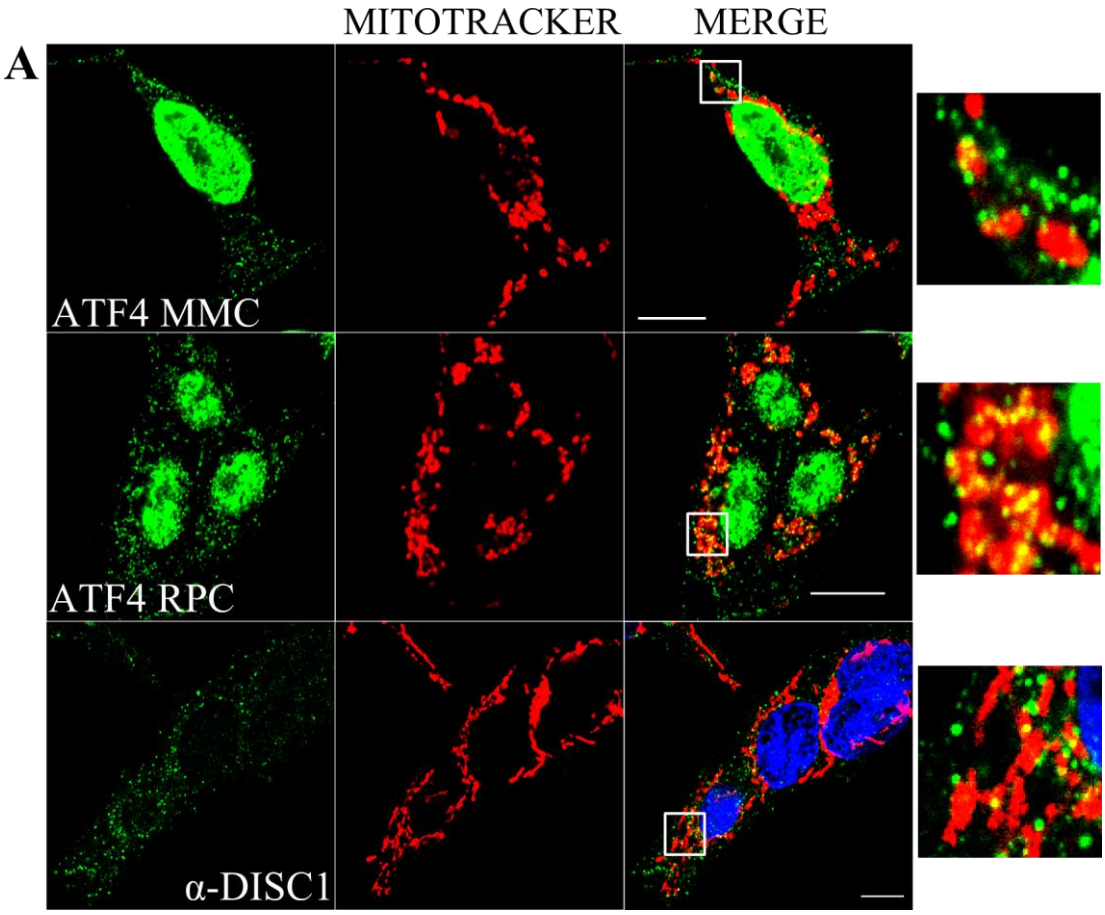

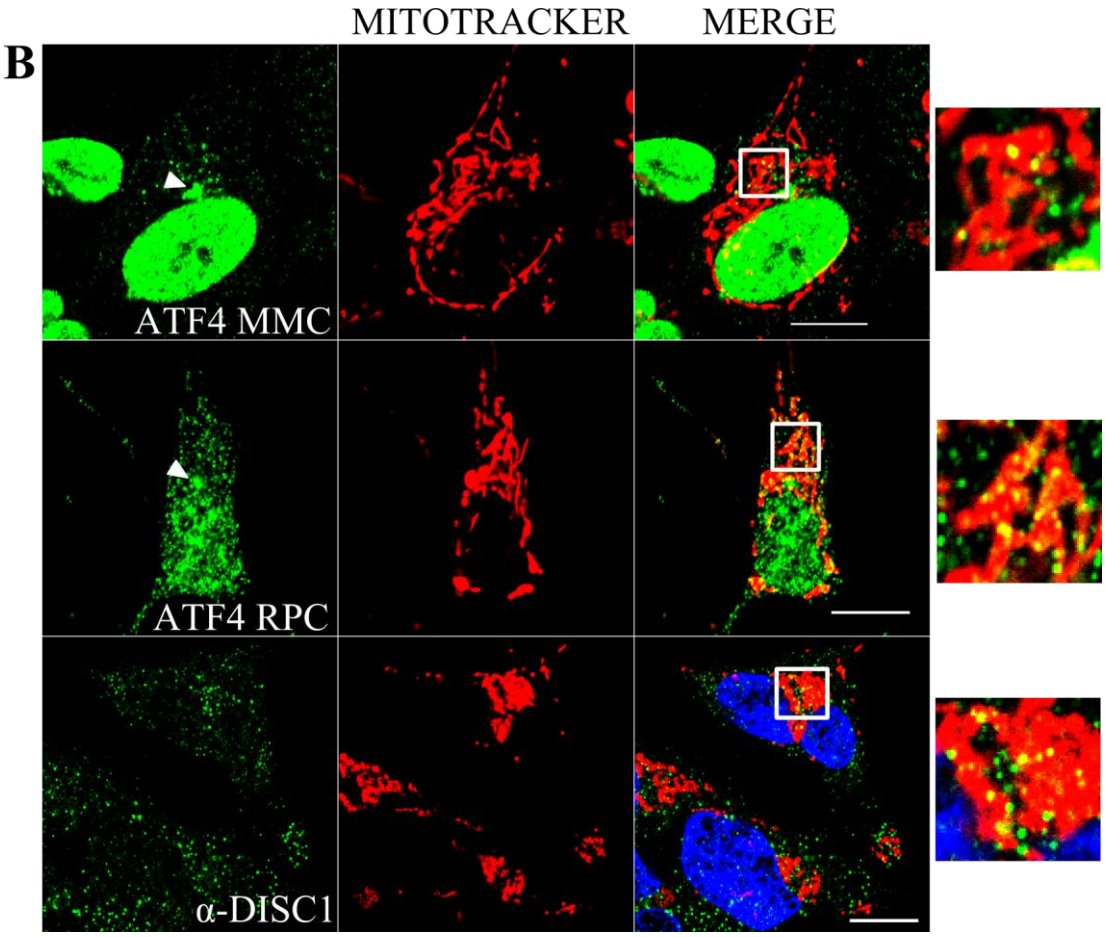

Figure 7.4 Distribution of endogenous ATF4 and DISC1 in HEK293 (A) and SH-SY5Y (B) cells analysed by confocal microscopy. ATF4 was detected with either the ATF4 MMC or ATF4 RPC antibody, whereas DISC1 was detected with the α-DISC1 antibody. Mitochondria were stained with Mito Tracker Red. In cells stained with the α-DISC1 antibody, nuclei were visualised using DAPI (blue). The regions delimited by a white square are magnified in the far-right panels. The white arrowheads in (B) indicate juxtanuclear ATF4 speckles (see text). Scale bars are 10 µm.

While analysing endogenous ATF4 distribution in cell lines, I noticed that ATF4 can often be seen in dense juxtanuclear speckles or puncta, which are particularly evident in cells stained with the ATF4 MMC antibody (Figure 7.4 B). Each cell typically shows one or two juxtanuclear ATF4 speckles (Figure 7.4 B). Intriguingly, the subcellular location of these ATF4 speckles is compatible with the position of the centrosome, another organelle in which DISC1 is enriched, and where it is known to

play important roles for neurite outgrowth and neuronal migration (Bradshaw *et al*, 2009; Bradshaw *et al*, 2008; Kamiya *et al*, 2005; Kamiya *et al*, 2008; Miyoshi *et al*, 2004; Morris *et al*, 2003; Shimizu *et al*, 2008). Indeed, centrosomal localisation of endogenous ATF4 in HEK293 cells has been observed before (Vaz Meirelles *et al*, 2010). This prompted me to test whether endogenous ATF4 and DISC1 co-localise at the centrosome in human cells. As shown in Figure 7.5, in both HEK293 and SH-SY5Y cells, ATF4 juxtanuclear puncta clearly co-localise with the centrosomal protein γ-tubulin, which is commonly used as a centrosomal marker (Bradshaw *et al*, 2009; Bradshaw *et al*, 2008; Kamiya *et al*, 2005; Morris *et al*, 2003). Co-localisation of ATF4 with γ-tubulin is evidenced by two distinct anti-ATF4 antibodies in two different cell types (Figure 7.5 A and B), indicating that it is unlikely to be artefactual, and confirming previous findings (Vaz Meirelles *et al*, 2010). Thus, these data indicate that ATF4 juxtanuclear puncta correspond to the centrosomal pool of ATF4. As expected, endogenous DISC1 also partially localises at the centrosome (Figure 7.5 A and B) and, intriguingly, ATF4 and DISC1 clearly co-localise in juxtanuclear puncta both in HEK293 and SH-SY5Y cells (Figure 7.5 A and B). Due to time limitations, it was not possible to confirm that the juxtanuclear puncta where DISC1 and ATF4 co-localise correspond to the centrosome. In the future, this could be achieved by using a triple staining protocol that employs anti-ATF4, anti-DISC1 and anti-γ-tubulin antibodies raised in different species. Collectively, these data demonstrate that ATF4 expression is not restricted to the nucleus, but can also be observed at the mitochondria and centrosome, and suggest that DISC1 may be able to interact with ATF4 at these additional subcellular locations.

A

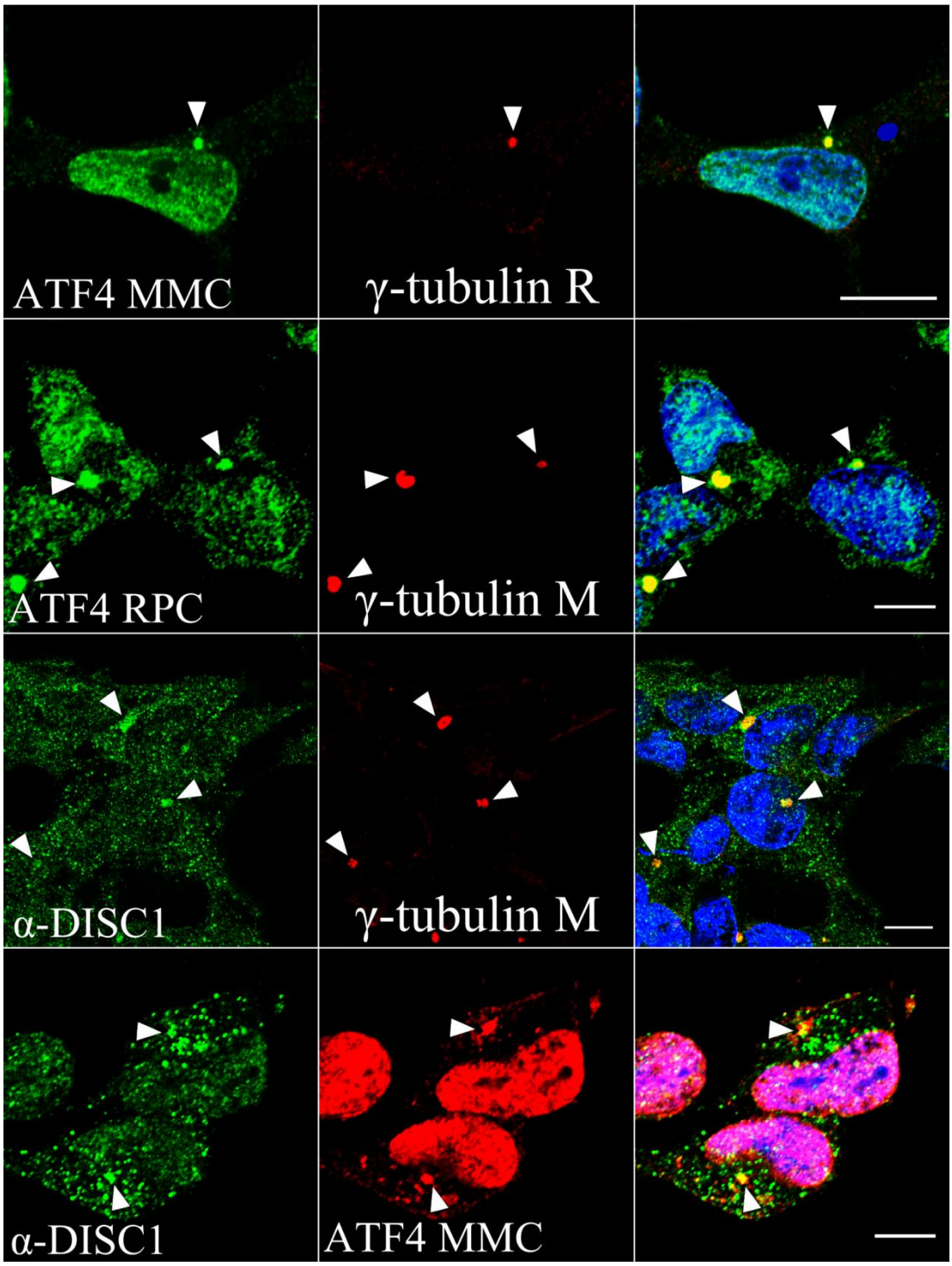
ATF4 MMC
γ-tubulin R
ATF4 RPC
γ-tubulin M
α-DISC1
γ-tubulin M
α-DISC1
ATF4 MMC

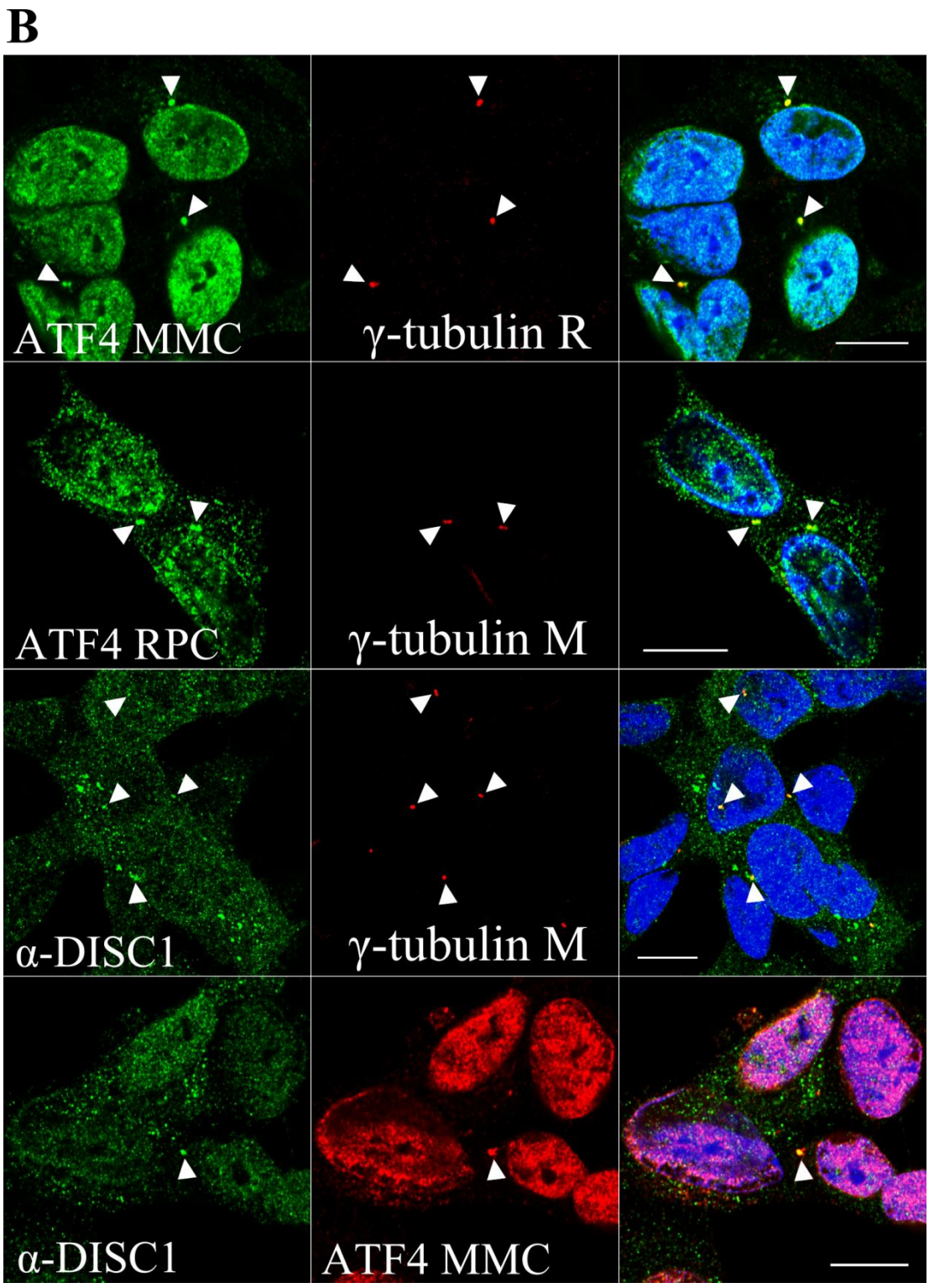

Figure 7.5 Distribution of endogenous ATF4 and DISC1 in HEK293 (A) and SH-SY5Y (B) cells analysed by confocal microscopy. ATF4 was detected with either the ATF4 MMC or ATF4 RPC antibody, whereas DISC1 was detected with the α-DISC1 antibody. Centrosomes were stained with the γ-tubulin M or the γ-tubulin R antibody,

raised in mouse and rabbit, respectively. Nuclei were visualised using DAPI (blue). The white arrowheads indicate the position of the centrosomes. Scale bars are 10 μm.

7.5 Effect of DISC1 variants on the interaction with ATF4

In chapters 3 and 4 of this thesis I demonstrated that amino acid substitutions 37W and 607F significantly reduce DISC1 distribution to the nucleus, and impair its ability to repress ATF4 transcriptional activity at basal cAMP levels. Since ATF4, both exogenous and endogenous, is predominantly expressed in the nucleus (Figures 7.3, 7.4 and 7.5), these observations imply that amino acid substitutions 37W and 607F may reduce the inhibitory effect of DISC1 on ATF4 by promoting the physical segregation of the two proteins inside the cell. Additionally, both 37W and 607F may introduce structural changes in DISC1 protein that destabilise its interaction with ATF4, either directly or indirectly. This is particularly likely for amino acid substitution 607F, as it occurs in a region of DISC1 that was previously shown to be important for ATF4 binding (Sawamura *et al*, 2008). Thus, to investigate the potential impact of DISC1 amino acid substitutions 37W and 607F on its ability to interact with ATF4, I carried out semi-quantitative co-immunoprecipitation assays (co-IP) in transfected HEK293 cells. These were performed as described in detail in paragraph 2.5.5. First, to determine the optimal conditions for co-IP of exogenous DISC1 and ATF4, the assay was performed in parallel using two different cell lysis buffers: Triton X-100 and RIPA. Triton X-100 is a relatively mild lysis buffer that contains a non-ionic detergent (Triton X-100). On the other hand, RIPA lysis buffer contains a mixture of non-ionic detergents and Sodium Dodecyl Sulphate (SDS), which is a strong anionic detergent. As shown in Figure 7.6, Flag-DISC1 is successfully immunoprecipitated both in the presence of Triton X-100 and RIPA, but while ATF4 does not co-precipitate with DISC1 in RIPA buffer, it clearly does in Triton X-100 buffer. Consequently, the following co-IP assay was performed using Triton X-100 lysis buffer. In this assay, DISC1-WT was directly compared with DISC1-37W, DISC1-603I and DISC1-607F for its ability to co-precipitate ATF4. The ultra-rare, putatively causal DISC1 mutation 603I was included in this analysis

because it occurs in proximity to the ATF4 binding region in DISC1 (amino acids 607-628) (Sawamura *et al*, 2008), and might therefore affect DISC1-ATF4 interaction.

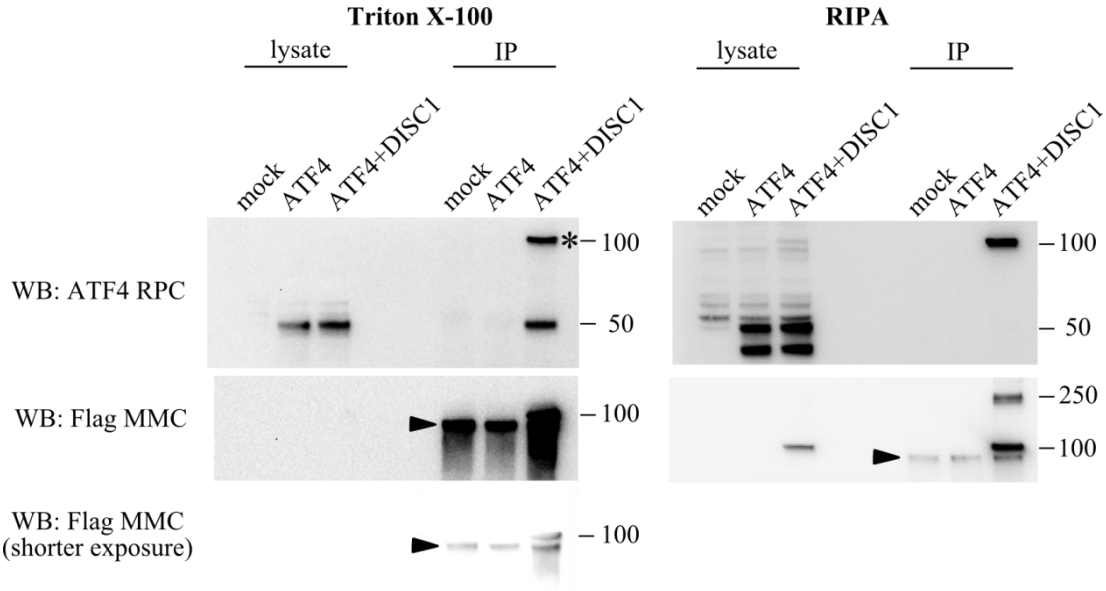

Figure 7.6 HEK293 cells were transfected with the empty vector pcDNA4/TO (mock) or with pCG-ATF4 (human ATF4) in combination with either pcDNA4/TO or pcDNA4/TO-Flag DISC1 WT. 24 hours after transfection the cells were lysed in Triton X-100 or RIPA lysis buffer, then Flag-DISC1 was immunoprecipitated using the Flag MMC antibody. The immunoprecipitates, along with the corresponding whole cell lysates, were then analysed by western blotting using the indicated antibodies. The asterisk indicates a non-specific band due to cross-reaction of the ATF4 RPC antibody with exogenous DISC1. The black arrowheads indicate non-specific bands due to reaction of the secondary HRP-labelled antibody with the heavy chains of the precipitating anti-Flag antibody.

Compared to DISC1-WT, ATF4 binding to DISC1-607F and DISC1-603I is reduced by ~50% and ~65%, respectively ($P<0.01$, Figure 7.7). By contrast, 37W does not significantly affect DISC1-ATF4 binding (Figure 7.7).

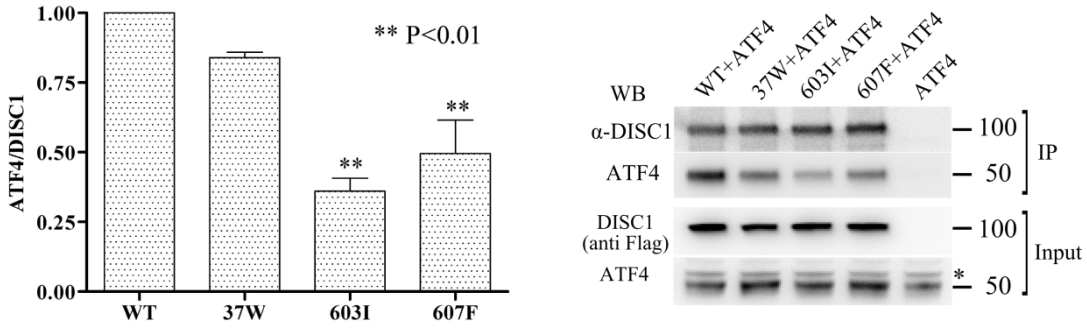

Figure 7.7 HEK293 cells were transfected with pCG-ATF4 alone or in combination with the indicated human DISC1 variants. Exogenous DISC1 was immunoprecipitated using the Flag MMC antibody and detected using an anti-DISC1 antibody (α-DISC1). Co-precipitating ATF4 was detected with the ATF4 RPC antibody. The bars represent the average of 3 independent experiments. Data are normalised to the average ATF4/DISC1 band intensity ratio measured for DISC1-WT, and were analysed by one-way ANOVA and Dunnett's multiple comparisons test. * Non-specific band. The position and size (kDa) of the protein markers is indicated

As discussed earlier in this chapter, by virtue of their inhibitory effect on DISC1 nuclear targeting, amino acid substitutions 37W and 607F might reduce DISC1 binding to ATF4 by promoting a partial physical segregation of the two proteins in different cell compartments. However, there is an obvious discrepancy between the defective nuclear targeting of DISC1-37W (Figures 3.6 to 3.10) and its largely preserved interaction with ATF4 (Figure 7.7). This led me to hypothesise that 37W might favour DISC1 binding to ATF4 outside the nucleus, thus compensating for their reduced interaction in the nucleus. To test this, I co-expressed ATF4 with DISC1-WT, -37W, -607F or -603I in COS7 cells and analysed the subcellular distribution of the two proteins by immunocytochemistry. Interestingly, all DISC1 variants analysed here showed partial co-localisation with ATF4 at mitochondria, providing further evidence in support of a possible interaction between the two proteins at this site (Figure 7.8). Of relevance, although the degree of mitochondrial co-localisation between DISC1 and ATF4 was not formally quantified here, this

appears strikingly higher for DISC1-37W compared to all other tested DISC1 variants (Figure 7.8). The latter observation raises the possibility that amino acid substitution 37W might increase ATF4-DISC1 binding at mitochondria, providing a potential explanation for its overall lack of effect on ATF4 binding.

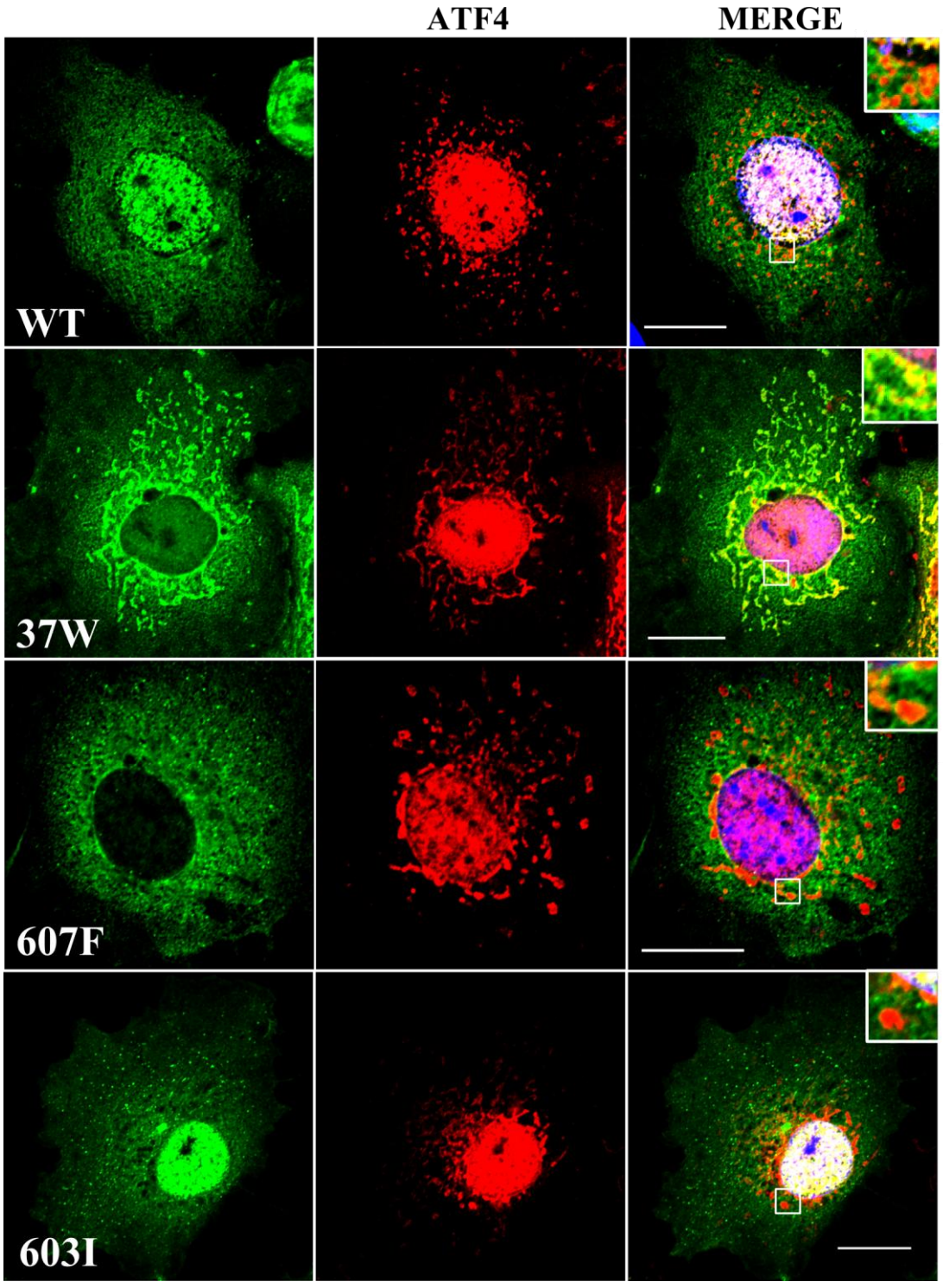

Figure 7.8 COS7 cells transfected with the indicated variants of DISC1 (green) and ATF4 (red). The right hand panels represent the corresponding merged images. The areas delimited by a white square are magnified in the insets. Scalebars are 20 μm.

The observed inhibitory effect of amino acid substitution 603I on DISC1 binding to ATF4 (Figure 7.7) is in contrast with my previous observations that 603I does not perturb DISC1 nuclear targeting, and that the ability of DISC1-603I to inhibit the transcriptional activity of ATF4 is entirely preserved (Figure 4.10). Thus, to better elucidate the relationship between the inhibitory effect of DISC1 on ATF4-mediated transcription and its interaction with ATF4, I exploited a mutant form of DISC1 lacking the leucine zipper in exon 9 (DISC1ΔLZ9). This artificial DISC1 mutant, which was originally generated by Sawamura and colleagues to map ATF4 binding regions on DISC1, reportedly results in complete loss of ATF4 binding (Sawamura *et al*, 2008). On the basis of this finding, Sawamura and colleagues concluded that the leucine zipper in DISC1 exon 9 is essential for ATF4 binding (Sawamura *et al*, 2008). Accordingly, I demonstrated that DISC1ΔLZ9 does not significantly affect ATF4 transcriptional activity (Figure 4.10). In an initial attempt to partially replicate the experimental conditions described by Sawamura and collegues (Sawamura *et al*, 2008), I transfected HEK293 cells with ATF4 and DISC1-WT or DISC1ΔLZ9, followed by immunoprecipitation of ATF4 with the ATF4 RPC antibody. The co-IP protocol adopted here does not accurately reflect the experimental conditions described by Sawamura and colleagues, who used a different cell line (HeLa) and different ATF4 and DISC1 expression constructs (Sawamura *et al*, 2008). However, the anti-ATF4 precipitating antibody (ATF4 RPC), and the co-IP buffer (RIPA) used in this thesis are the same used by Sawamura and colleagues (Sawamura *et al*, 2008). As shown in Figure 7.9 A, ATF4 is successfully immunoprecipitated by the ATF4 RPC antibody. Surprisingly though, both DISC1-WT and DISC1ΔLZ9 co-precipitate with ATF4 (Figure 7.9 A). However, this experiment was invalidated by the fact that the ATF4 RPC antibody strongly cross-reacted with exogenous DISC1, as evidenced by the presence of DISC1 immunoreactivity in control samples transfected with DISC1 only (Figure 7.9 A). The same cross-reactivity problem was observed in a subsequent experiment that used a five-time lower concentration of ATF4 RPC antibody (0.2 µg instead of 1 µg per co-IP, Figure 7.9 B), leading to the conclusion that the low specificity of this antibody renders it unsuitable for use in this particular co-IP experiment.

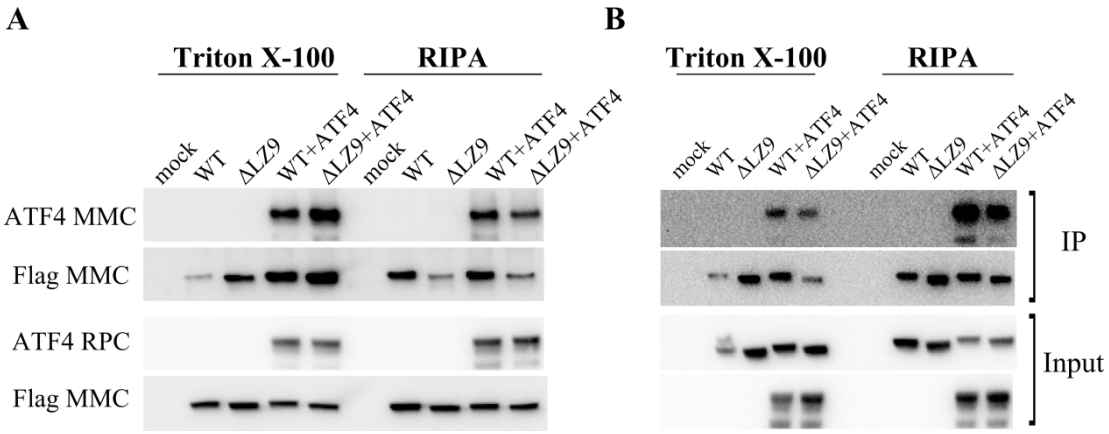

Figure 7.9 HEK293 cells were transfected with pCG-ATF4 alone or in combination with DISC1 WT (WT) or DISC1ΔLZ9 (ΔLZ9). Cells were lysed in Triton X-100 or RIPA lysis buffer, then ATF4 was immunoprecipitated using 1 µg (A) or 0.2 µg (B) of ATF4 RPC antibody. The resulting immunoprecipitates (IP), along with the corresponding whole cell lysates (Input) were analysed by western blotting, using the indicated antibodies.

Next, I performed a similar co-IP assay using either the ATF4 MMC or the Flag MMC antibody to immunoprecipitate ATF4 or DISC1, respectively. Unlike the ATF4 RPC antibody, both these antibodies successfully and specifically precipitate their target proteins (Figure 7.10). The co-IP experiment performed with the Flag MMC antibody was thus replicated, and the results were quantified by band densitometry (Figure 7.10). Surprisingly, and in contrast with the findings of Sawamura and colleagues, this experiment indicates that DISC1-WT and DISC1ΔLZ9 do not significantly differ in their ability to bind ATF4. Collectively, these results suggest that the inhibitory effect of DISC1 on ATF4 transcriptional activity is affected by DISC1 nuclear expression levels, but not by its ability to bind ATF4.

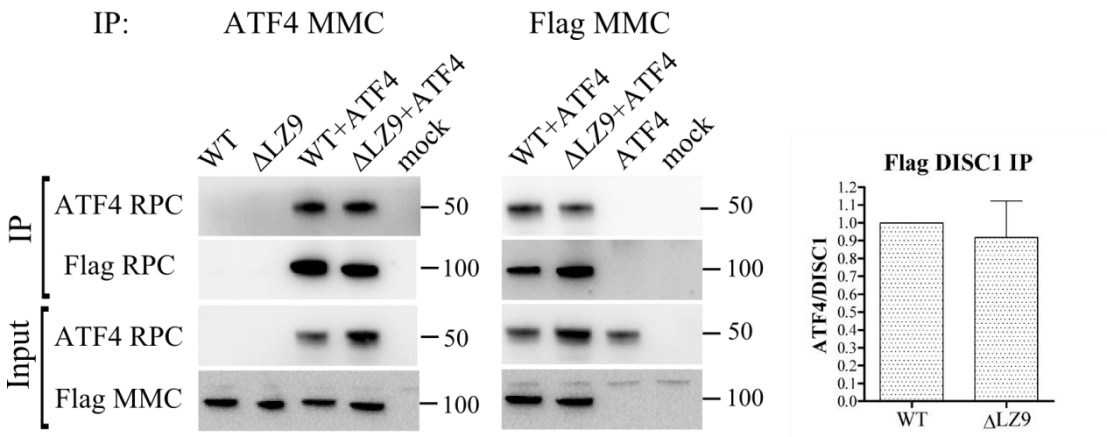

Figure 7.10 HEK293 cells transfected with ATF4 and DISC1, as indicated, were lysed in Triton X-100 lysis buffer, then subjected to immunoprecipitation (IP) using the ATF4 MMC or the Flag MMC antibody. The resulting immunoprecipitates (IP), along with the corresponding whole cell lysates (Input), were analysed by western blotting, using the indicated antibodies. The position and size (kDa) of the protein markers is indicated. The bars represent the average of 3 independent experiments. Data were normalised to the average ATF4/DISC1 band intensity measured for DISC1-WT, and were analysed by one-sample student's t-test. WT: DISC1-WT; ΔLZ9: DISC1ΔLZ9.

7.6 Effect of high cAMP levels on the interaction and subcellular distribution of DISC1 and ATF4

In chapter 4 of this thesis, I provided evidence suggesting that the functional interaction between DISC1 and ATF4 is regulated by cAMP levels. Indeed, while DISC1 efficiently inhibits ATF4 transactivation of the CRE and CHOP AARE promoters at basal cAMP levels, it has no effect on ATF4 function at high cAMP levels. On the basis of this observation, I hypothesised that cAMP levels might regulate DISC1 physical interaction with ATF4. The second messenger cAMP, either directly or indirectly, regulates the activity of several protein kinases, including PKA (Delghandi *et al*, 2005), which in turn is capable of phosphorylating both ATF4 (Elefteriou *et al*, 2005) and DISC1 (Ishizuka *et al*, 2011). Thus, cAMP has the potential to regulate DISC1-ATF4 binding by controlling the phosphorylation status of these proteins. To test whether cAMP regulates the DISC1-ATF4 interaction, I

performed co-IP assays in transfected HEK293 cells after exposure to the adenylate cyclase activator forskolin, using DMSO-treated cells as controls. The drug treatment conditions adopted in this set of experiments reflect those used in the luciferase assays described in chapter 4 of this thesis. Given the potential relevance of ATF4 and DISC1 phosphorylation status in this context, this particular set of co-IP experiments was performed using Triton X-100 lysis buffer supplemented with phosphatase inhibitors (Phosphatase inhibitor cocktail set II (Calbiochem), 10 μM β-glycerophosphate, 100 nM okadaic acid). As shown in Figure 7.11, forskolin treatment dramatically increases ATF4 protein levels in whole cell lysates ($P<0.001$, Figure 7.11), but has no significant effects on DISC1 total protein expression levels (Figure 7.11). As a result, the ATF4/DISC1 protein ratio is increased by almost 10-fold in cells exposed to forskolin ($P<0.01$, Figure 7.11). In contrast with the lack of effect of DISC1 on ATF4 transcriptional activity at high cAMP levels observed in chapter 4 of this thesis, ATF4 binding to DISC1 is significantly increased by forskolin treatment (Figure 7.11).

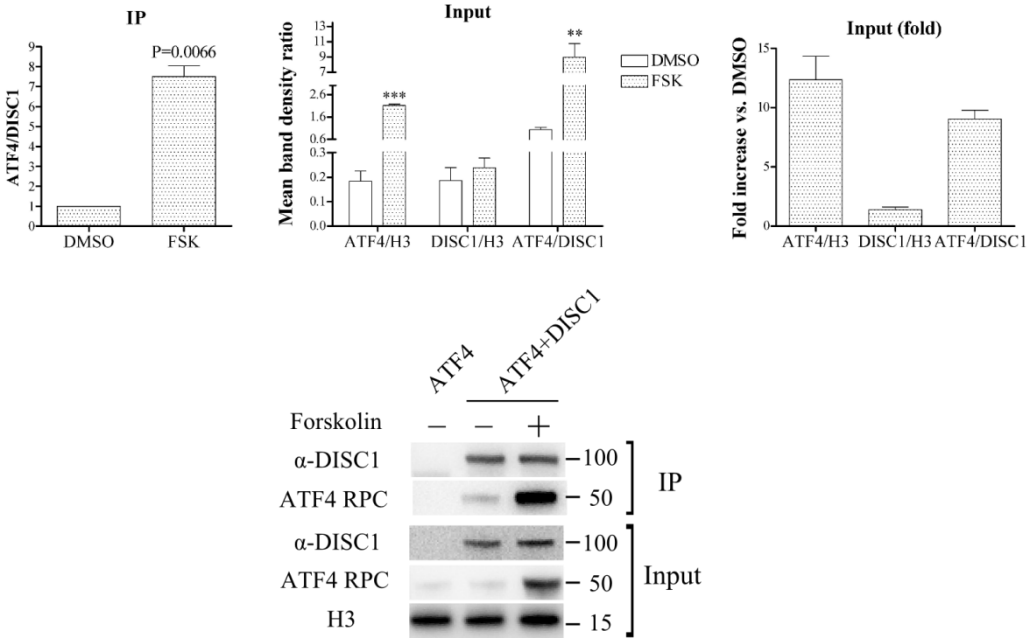

Figure 7.11 HEK293 cells were transfected with pCG-ATF4 (human ATF4) in combination with an equal amount of the empty vector pcDNA4/TO or pcDNA4/TO-Flag-DISC1 WT (human DISC1), as indicated. 24 hours after transfection, the cells

were treated for 4 hours with 10 μM forskolin or vehicle (DMSO), to reflect the treatment conditions used in luciferase reporter assays, then lysed in Triton X-100 lysis buffer and subjected to immunoprecipitation using the Flag MMC antibody. The resulting immunoprecipitates (IP), along with the corresponding whole cell lysates (Input), were analysed by western blotting, using the indicated antibodies. The position and size (kDa) of the protein markers is indicated. The bars represent the average of 3 independent experiments. Data were analysed by one-sample student's t test (IP) or paired two-tailed student's t test (Input). ***P<0.001; **P<0.01.

To further investigate the effect of increased cAMP levels on ATF4 and DISC1 protein levels and subcellular distribution, I prepared whole cell lysates, nuclear extracts and cytoplasmic extracts from transfected and untransfected HEK293 cells treated with forskolin, and analysed them by western blotting. Consistent with my previous observations (Figure 7.11), forskolin treatment results in a marked increase in ATF4 protein levels in whole cell lysates ($P<0.01$, Figure 7.12). A similar increase in ATF4 protein levels (~4 to 5-fold) is observed in nuclear and cytoplasmic extracts ($P<0.01$, Figure 7.12), indicating that forskolin does not promote the preferential accumulation of ATF4 in either of these subcellular compartments. In contrast with my previous findings (Figure 7.11), DISC1 protein expression is significantly increased in whole cell lysates and nuclear extracts, but not cytoplasmic extracts, prepared from forskolin-treated HEK293 cells ($P<0.05$, Figure 7.12). Consequently, the ATF4/DISC1 protein ratio is not significantly increased by forskolin in this experiment (Figure 7.12). The reasons for the discrepancy between the lack of effect of forskolin on DISC1 protein levels seen in the co-IP experiment and the preferential increase in nuclear DISC1 expression observed by subcellular fractionation are not clear. However, this inconsistency may be related to the substantial technical differences between the two experimental approaches. For example, unlike the co-IP experiment, subcellular fractionation was performed using commercially available pre-made buffers that do not contain phosphatase inhibitors, which may have potentially affected DISC1 protein stability after cell lysis. In addition, DISC1 was detected using two different antibodies in the two experiments:

α-DISC1 for the co-IP experiment and Flag MMC in the subcellular fractionation experiment, which may have contributed to the observed discrepancy in DISC1 protein levels.

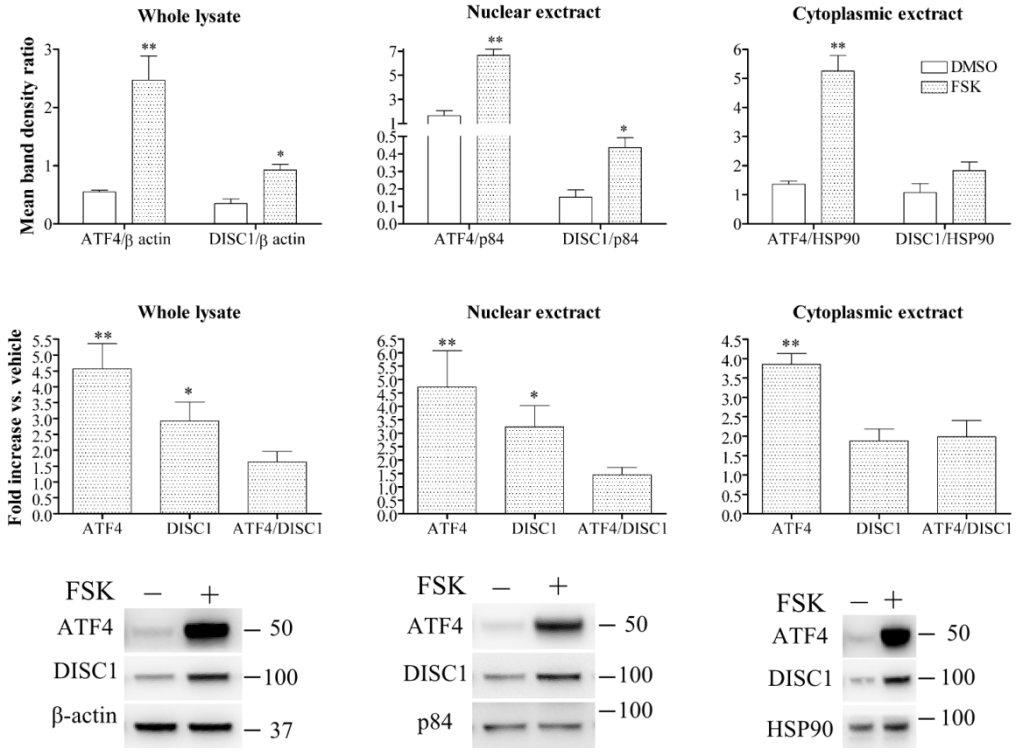

Figure 7.12 HEK293 cells co-transfected for 24 hours with equal amounts of pCG-ATF4 (human ATF4) and pCDNA4/TO-Flag DISC1 WT (human DISC1) were treated for 4 hours with 10 μM forskolin (FSK) or vehicle (DMSO) before being subjected to subcellular fractionation. The resulting nuclear and cytoplasmic extracts, along with the corresponding whole cell lysates, were analysed by western blotting, using nuclear matrix protein p84, heat-shock protein HSP90 and β-actin, respectively, as loading controls. ATF4 and DISC1 were detected using the ATF4 RPC antibody and the Flag MMC antibody, respectively. The position and size (kDa) of the protein markers is indicated. The bars represent the average of 3 independent experiments. Data were analysed by paired two-tailed student's t test. **P<0.01, *P<0.05.

To test whether forskolin similarly affects expression of endogenous ATF4 and DISC1 proteins, the same subcellular fractionation experiment was carried out using untransfected HEK293 cells. Surprisingly, forskolin treatment significantly reduces total ATF4 protein expression levels ($P<0.01$, Figure 7.13), but does not affect the nuclear expression of endogenous ATF4 in these cells (Figure 7.13). In this set of experiments, endogenous ATF4 protein expression could not be quantified in the cytoplasmic extracts because it was below the antibody's detection limit (data not shown). As observed for ATF4, the total expression level of endogenous 100 kDa DISC1 is mildly but significantly reduced by forskolin treatment ($P<0.05$, Figure 7.13). Quantification of endogenous 100 kDa DISC1 protein levels is limited to whole cell lysates as the protein could not be detected in the nuclear and cytoplasmic extracts prepared from HEK293 cells (data not shown). Collectively, these results indicate that forkolin exerts distinct effects on the expression of exogenous and endogenous ATF4 and DISC1 in HEK293 cells.

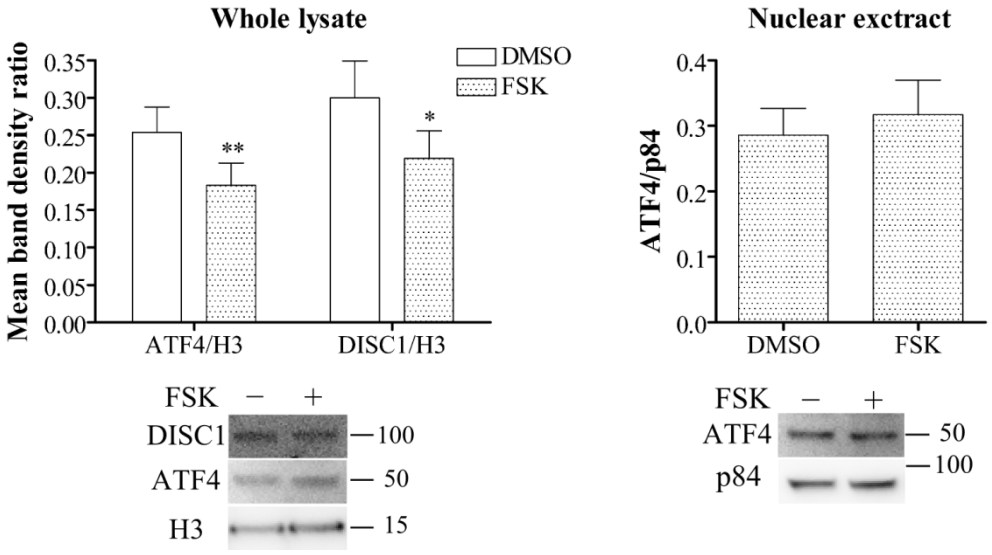

Figure 7.13 Untransfected HEK293 cells were subjected to subcellular fractionation after a 4 hour treatment with 10 µM forskolin (FSK) of vehicle (DMSO). The resulting nuclear extracts and the corresponding whole cell lysates were analysed by western blotting, using the nuclear matrix protein p84 and histone 3 (H3) as loading controls, respectively. Endogenous ATF4 and DISC1 were detected using the ATF4 RPC and the α-DISC1 antibody, respectively. The position and size (kDa) of the protein

markers is indicated. The bars represent the average of 3 independent experiments. Data were analysed by paired two-tailed student's t test. **P<0.01, *P<0.05.

7.7 Discussion

Like most transcription factors, ATF4 is predominantly enriched in the cell nucleus. Consequently, amino acid substitutions that reduce DISC1 nuclear expression might prevent its interaction with ATF4, even if they do not directly impact on their binding potential. Under the above assumption, both amino acid substitutions 37W and 607F are predicted to reduce DISC1 binding to ATF4 in intact cells. However, in the co-IP assays described here, DISC1-607F, but not DISC1-37W, shows reduced binding to ATF4. This apparent contradiction may be resolved by the observed increased co-localisation between DISC1-37W and ATF4 at mitochondria. Based on this observation, it is plausible to speculate that the increased mitochondrial recruitment of DISC1-37W (Ogawa F., in preparation) may facilitate its interaction with mitochondrial ATF4, thereby compensating for the presumed reduced interaction between ATF4 and DISC1-37W in the nucleus. If true, this would in turn imply that the 37W mutation reduces DISC1's ability to suppress ATF4 transcriptional activity indirectly, by preventing DISC1 translocation to the nucleus, but has no direct effect on DISC1-ATF4 binding. On the other hand, amino acid substitution L607F reduces both DISC1 nuclear expression and ATF4 binding, but has no obvious effects on DISC1 co-localisation with ATF4 outside the nucleus. However, based on the currently available data, it is not possible to speculate whether 607F inhibits the DISC1-ATF4 interaction directly, by destabilising protein-protein bonds, indirectly, by preventing DISC1 translocation to the nucleus, or both. Further experiments will be needed to test these possibilities.

The conserved predicted leucine zipper located in DISC1 exon 9 (here referred to as DISC1LZ9) was previously shown to contribute to DISC1 nuclear targeting and to be essential for its interaction with ATF4 (Sawamura *et al*, 2008). Consistently, in chapter 4 of this thesis I demonstrated that the artificial mutant DISC1ΔLZ9, which lacks DISC1LZ9, is not expressed in the nucleus and does not inhibit ATF4 transcriptional activity. It is therefore surprising that in the co-IP assays described

here, which were initially designed to partially replicate the experimental conditions described by Sawamura and colleagues (Sawamura *et al*, 2008), DISC1ΔLZ9 does not differ from DISC1 WT in its ability to interact with ATF4. While the discrepancy between the results reported by Sawamura and colleagues (Sawamura *et al*, 2008) and the findings described here might be explained by experimental differences (e.g. different ATF4 and DISC1 expression constructs, different batch of immunoprecipitating ATF4 RPC antibody, different DISC1 tag, different cell line etc.), it is difficult to reconcile the lack of effect of DISC1ΔLZ9 on ATF4 transcriptional activity and its exclusion from the nucleus with its intact ATF4 binding capacity. Since the subcellular distribution of ATF4 and DISC1ΔLZ9 in co-transfected cells was not analysed here, it cannot be excluded that, like 37W, ΔLZ9 might favour DISC1 interaction with ATF4 outside the nucleus. However, based on my previous observation that the subcellular distribution of DISC1ΔLZ9 is strikingly similar to that of DISC1-607F, which does not show increased interaction with cytoplasmic ATF4, this seems unlikely. The lack of effect of ΔLZ9 on DISC1 binding to ATF4 is also in contrast with the detrimental effect of 607F on the DISC1-ATF4 interaction. Indeed, leucine 607 is located within DISC1LZ9, and the L607F amino acid substitution is predicted to disrupt the leucine packing within DISC1LZ9 (Soares *et al*, 2011). In this respect, it is important to emphasise that, since DISC1 protein structure has not yet been experimentally resolved, the available structural information is largely based on bioinformatic predictions, and hence may not be completely accurate. However, it is surprising that, while the disruption of a predicted DISC1 leucine zipper by 607F reduces ATF4 binding, its complete removal has no apparent effect on DISC1-ATF4 binding. Assuming that, as my results suggest, DISC1LZ9 is not directly involved in ATF4 binding, one might hypothesise that the effect of 607F on DISC1 binding to ATF4 arises indirectly, as a consequence of its detrimental effect upon DISC1 nuclear localisation. However, this hypothetical scenario is incongruent with the observed effect of ΔLZ9, which, like 607F, inhibits DISC1 nuclear expression. An alternative, albeit highly hypothetical possibility is that 607F, but not ΔLZ9, might indirectly introduce deleterious structural changes in other yet unknown ATF4 binding sites on DISC1. Moreover, it cannot be excluded that some of the effects observed here might be artifactual and

may not accurately reflect the interactions taking place inside the cell. For example, it is possible that the results of the co-IP experiments described here reflect, at least in part, protein-protein interactions that are established after cell disruption and that were not present in the intact cells. Finally, one may speculate that the differential effects of DISC1-WT, -37W, -603I, -607F and -ΔLZ9 on ATF4 transcriptional activity might be mediated by differential binding to other yet unknown regulatory proteins that might potentially be present in the ATF4/DISC1 complex.

In contrast with the observed lack of effect of ΔLZ9 on DISC1 binding to ATF4, the ultra-rare DISC1 mutation T603I significantly reduces interaction between the two proteins. Since 603I does not grossly affect DISC1 subcellular distribution, its effect on ATF4 binding might arise from direct or indirect disruption of an ATF4 binding site on DISC1. This suggests that additional contact sites may exist between DISC1 and ATF4, besides the originally mapped DISC1LZ9, the evidence for which is now contrasting. Intriguingly, despite its detrimental effect on ATF4 binding, 603I does not impair DISC1-mediated repression of ATF4, as shown in chapter 4 of this thesis. This observation, in combination with the preserved ATF4 binding of DISC1ΔLZ9 and DISC1-37W, indicates that DISC1 nuclear expression, but not its ability to co-precipitate ATF4, is a good predictor of its ability to repress ATF4 activity. In turn, this suggests that nuclear DISC1 may inhibit ATF4 via an indirect mechanism that does not involve establishment of a direct protein-protein interaction with ATF4. For example, DISC1 may act by sequestering transcriptional co-factors and preventing their binding to ATF4. Collectively, this set of experiments suggests that DISC1LZ9 may not be directly involved in ATF4 binding, which may be instead at least partially mediated by the DISC1 region spanning threonine 603. Further experiments will be needed to determine the mechanism by which nuclear DISC1 inhibits ATF4 and, in particular, whether this functional interaction requires a physical interaction between the two proteins in the nucleus. Cell-free techniques such as in-vitro binding assays or surface plasmon resonance may be exploited to clarify the role of DISC1LZ9 on the interaction with ATF4 and further test the effect of amino acid substitutions 37W, 607F and 603I, eliminating their differential nuclear expression as a confounding factor.

In contrast with the findings of Sawamura and colleagues, and as detailed in chapter 4 of this thesis, I detected no effect of DISC1 co-expression on the transcriptional activity of ATF4 on the CRE and CHOP AARE at high cAMP levels. This observation suggested that DISC1's ability to bind to and regulate ATF4 transcriptional activity might be reduced at high cAMP levels. However, the co-IP experiment described here indicates that the DISC1-ATF4 interaction is instead strengthened by cAMP. Once again, this observation indicates that DISC1's ability to co-precipitate ATF4 does not directly correlate with its ability to regulate ATF4 transcriptional activity, supporting the existence of indirect regulatory mechanisms. Nevertheless, the dramatic effect of forskolin on DISC1-ATF4 binding suggests that this interaction might be important in mediating some of the effects of increased cAMP levels. If the DISC1-ATF4 complex is indeed involved in transcriptional regulation in response to cAMP, it is possible that its effects may be context-, cell-type- or target gene-dependent, and may not be evidenced by the reporter assays described in this thesis. Besides strengthening the DISC1-ATF4 interaction, forskolin increases ATF4 expression levels, both in the nucleus and cytoplasm, and might also regulate DISC1 protein levels, although different experimental approaches provided contradictory evidence in this particular respect. In particular, it is surprising that forskolin dramatically enhances expression of exogenous ATF4 while having the opposite effect on the endogenous protein expressed in the same cell type. Perhaps this could be an artefact due to the ATF4 expression vector used in these experiments, although no known cAMP-responsive elements are present in the pCG plasmid. Alternatively, it is possible that the effect of cAMP on ATF4 protein stability may be somehow dependent on ATF4 expression levels. The effects of cAMP on endogenous ATF4 expression levels have been previously investigated in a study by Yukawa and colleagues (Yukawa *et al*, 1999). In cultured mouse hippocampal neurons, forskolin treatment for 3-4 hours strongly induces ATF4 protein expression in the nucleus, but has no effect on ATF4 mRNA levels (Yukawa *et al*, 1998). This is consistent with the enhancing effects of forskolin on exogenous ATF4 expression observed here, and indicates that cAMP regulates ATF4 protein abundance at the post-transcriptional level. Human ATF4 can be phosphorylated by PKA at serine 254, and phosphorylation at this residue enhances its transactivation of

the Rankl promoter CRE site (Elefteriou *et al*, 2005). It is therefore possible that cAMP-dependent phosphorylation of ATF4 serine 254 might increase ATF4 protein stability. Alternatively, cAMP might up-regulate ATF4 translation, although this latter possibility seems less likely, given that forskolin enhances ATF4 expression from the pCG-ATF4 construct, which does not contain the ATF4 mRNA 5' UTR regulatory region that is known to modulate ATF4 mRNA translation. Interestingly, DISC1 is also a PKA target (Ishizuka *et al*, 2011), and some of the experiments described here suggest that cAMP might regulate DISC1 expression levels, raising the possibility that PKA phosphorylation could similarly regulate DISC1 protein stability. Further experiments will be needed to test the potential effects of PKA-dependent phosphorylation on ATF4 and DISC1 protein expression and functional interaction.

Although ATF4 is predominantly expressed in the nucleus, it has been observed at other subcellular locations, including the cytoplasm and neuritis of mouse neurons, and the dendrites of Aplysia sensory neurons (Lai *et al*, 2008; Vernon *et al*, 2001; White *et al*, 2000). Here, I observed for the first time that ATF4 partially localises to the mitochondria in human cell lines, although the function of this mitochondrial pool of ATF4 remains to be elucidated. Of relevance, a previous study showed that in cultured human oligodendroglial cells, mitochondrial dysfunction induced by the respiratory chain Complex I inhibitor rotenone activates ATF4 protein expression (Silva *et al*, 2009). Interestingly, different studies showed that external stimuli can induce the translocation of ATF4 from the cytoplasm to the nucleus (Lai *et al*, 2008; White *et al*, 2000). In cultured mouse hippocampal neurons, LTD-, but not LTP-inducing stimuli promote the retrograde translocation of ATF4 from distal neuritis to the nucleus (Lai *et al*, 2008) and, similarly, $GABA_B$ receptor activation in primary cortical neurons was shown to trigger the translocation of endogenous ATF4 from the cytoplasm to the nucleus (White *et al*, 2000). It is therefore tempting to speculate that mitochondrial ATF4 might be involved in retrograde signalling to the nucleus in response to mitochondrial dysfunction. Additionally, since I showed that endogenous full-length DISC1 also partially localises to mitochondria, it is possible that ATF4 and DISC1 might interact at this location. Future experiments should investigate this,

and test for potential functional implications of DISC1-ATF4 binding at mitochondria.

In this chapter I showed that endogenous ATF4 partially localises at the centrosome in human cells. Since DISC1 is also expressed at the centrosome (Bradshaw *et al*, 2009; Bradshaw *et al*, 2008; Kamiya *et al*, 2005; Kamiya *et al*, 2008; Miyoshi *et al*, 2004; Morris *et al*, 2003; Shimizu *et al*, 2008), this observation suggests that the two proteins might interact at this additional location. Indeed, in a preliminary immunocytochemistry experiment, I detected co-localisation of endogenous ATF4 and DISC1 in juxtanuclear puncta that are consistent with the morphology and location of the centrosome. However, due to time limitations, I could not confirm that these juxtanuclear puncta correspond to the centrosome. Interestingly, ATF4 reportedly directly interacts with two structurally related centrosomal proteins, Nephronophthisis 6 (NPHP6, also known as CENP290) (Sayer *et al*, 2006) and Mitosin/CENP-F (Zhou *et al*, 2005). NPHP6 is implicated in the pathogenesis of Joubert syndrome, which is characterised by kidney failure, retinal degeneration, cerebellar aplasia and mental retardation, and of Senior-Loken syndrome, characterised by kidney dysfunction and retinal degeneration (Sayer *et al*, 2006). Consistently, NPHP6-targeting morpholinos cause defects in eye, kidney, and cerebellum development in zebrafish (Sayer *et al*, 2006). On the other hand, Mitosin/CENP-F is implicated in cell cycle progression and myoblast differentiation (Zhou *et al*, 2005). Like DISC1, both NPHP6 and Mitosin/CENP-F regulate ATF4 transactivation of the CRE in luciferase reporter assays, the first acting as an activator and the second as a repressor (Sayer *et al*, 2006; Zhou *et al*, 2005). These findings suggest that the regulation of ATF4 transcriptional activity may be important for centrosomal function. Consistently, ATF4 KO mice exhibit severe growth and development defects, which may arise from underlying defects in cell division (Dobreva *et al*, 2006; Fischer *et al*, 2004; Hettmann *et al*, 2000; Masuoka & Townes, 2002; Muir *et al*, 2008; Tanaka *et al*, 1998; Yang *et al*, 2004; Yoshizawa *et al*, 2009). The observed co-localisation of endogenous ATF4 and DISC1 at the centrosome is particularly intriguing, given that both proteins have been implicated in centrosome-dependent processes such as neuronal progenitor proliferation and migration (Duan *et al*, 2007; Frank *et al*, 2010; Ishizuka *et al*, 2011; Kamiya *et al*,

2005; Kim *et al*, 2009; Mao *et al*, 2009; Meyer & Morris, 2009). Future experiments should aim to elucidate the function of centrosomal ATF4, and investigate the potential regulatory role of DISC1, as well as other centrosomal DISC1 binding partners, like NDE1, LIS1 and PDE4 (Bradshaw *et al*, 2008).

8 Conclusions

Over ten years after its discovery, *DISC1* remains one of the best supported genetic candidates for major psychiatric illness. In addition to the compelling genetic evidence implicating *DISC1* in mental illness, a wealth of biological evidence has now firmly established DISC1 as a key player in processes such as neurodevelopment, plasticity and signalling (Brandon & Sawa, 2011; Chubb *et al*, 2008; Porteous *et al*, 2011), the disturbance of which is thought to contribute to major psychiatric illness (Fatemi & Folsom, 2009; Insel, 2010). However, despite our greatly increased knowledge of the multiple biological functions of DISC1, the mechanisms linking impaired DISC1 function to increased risk of mental illness remain elusive.

One widely used, and in many cases successful approach to dissect disease mechanism is to analyse the functional impact of causal genetic mutations by artificially introducing them in model organisms or in-vitro systems. In the case of *DISC1*, the only definitively causal mutation discovered to date is the t(1;11) translocation. However, the very complex nature of this mutation renders it particularly hard, if not impossible, to accurately reproduce in model systems. On the other hand, risk-conferring SNPs and point mutations in *DISC1* are comparatively easy to model, but their genetic contribution to disease is less well defined, and their biological effects are likely to be more subtle. Nevertheless, understanding the effects of multiple risk-conferring SNPs and point mutations can provide valuable clues as to which of the many DISC1 functions might be affected in the carriers, and help generate testable hypotheses about the mechanisms linking genetics and environment to clinical outcomes.

In this thesis, the impact of a subset of common and rare risk-conferring DISC1 amino acid substitutions was investigated. More specifically, two main objectives were set out in chapter one. The first was to analyse the potential effects of such risk-conferring structural variants on the subcellular distribution of DISC1, with a particular focus on the nucleus and centrosome. The second was to better

characterise the functional implications of DISC1's interaction with the transcription factor ATF4, and to analyse the potential impact of DISC1 amino acid substitutions on this particular interaction. Table 8.1 lists the DISC1 amino acid substitutions examined in this thesis, and summarises their observed effects in the limited set of assays described in the previous chapters. Figure 8.1 summarises the known regulators and biological functions of ATF4, and illustrates the potential influence of DISC1 on ATF4-regulated pathways. In the following sections I will recapitulate the experimental observations described in this thesis and their potential implications, discuss the outstanding questions and propose future experiments to address them.

8.1 Effect of risk-conferring amino acid substitutions on the subcellular distribution of DISC1

In chapter 3 of this thesis, I analysed the effect of a selected subset of human and mouse DISC1 amino acid substitutions on the subcellular distribution of the protein. This was done by overexpressing the selected DISC1 variants in different cell lines and primary neurons and quantifying their relative subcellular distribution by immunocytochemistry and subcellular fractionation. The main finding reported in this chapter is that human DISC1 amino acid substitutions 37W and 607F, but not 264R, 432L, 603I and 704C, reduce the nuclear expression of the protein by approximately 50%, and also exert a dominant-negative effect on the nuclear distribution of exogenous wild-type DISC1. Additionally, 607F reduces DISC1 association with the cytoskeleton by ~75% and reduces the formation of DISC1 cytoplasmic puncta. These observations suggest that DISC1 nuclear expression might be significantly reduced in 37W and 607F carriers, with potential detrimental effects on the nuclear functions of the protein. 607F might additionally impair the cytoskeletal functions of DISC1, with potential repercussions for neuronal development.

8.2 Effect of DISC1 amino acid substitutions on the functional interaction with ATF4

In chapter 4 of this thesis, to test the hypothesis that amino acid substitutions that reduce DISC1 nuclear expression may also compromise its nuclear function, I

designed luciferase reporter assays to investigate the potential impact of selected risk-conferring DISC1 missense mutations on the transcriptional activity of its interactor ATF4. These experiments, which were carried out in different transfected human and mouse cell lines, demonstrated that DISC1 represses ATF4 transcriptional activity on CRE and AARE promoter elements at basal, but not elevated, cAMP levels.

The luciferase reporter assays described in this thesis additionally showed that amino acid substitutions 37W and 607F, but not 432L, 603I and 704C significantly reduce DISC1's ability to repress the transactivation activity of exogenously expressed ATF4. Accordingly, while wild-type DISC1 significantly inhibits the transcriptional activation of the CRE in response to the ATF4 inducer thapsigargin, DISC1-37W and DISC1-607F have no effect. Unexpectedly, despite being efficiently expressed in the nucleus in the tested cell model and being able to interact with ATF4, mouse Disc1 does not affect ATF4 activity in the particular CRE reporter assays described in this thesis. This suggests that mouse and human DISC1 might have functionally diverged in this particular respect, and that perhaps mouse Disc1 regulates ATF4 activity on a different and/or more restricted set of promoters and/or cell types.

Collectively, these observations support the hypothesis that amino acid substitutions 37W and 607F might compromise the nuclear function of DISC1 by preventing its proper nuclear expression, implying that the former might be impaired in 37W and 607F carriers, with potential repercussions on the regulation of ATF4 transcriptional activity. Since ATF4 is implicated in the regulation of several processes that have been linked to psychiatric illness, including stress responses (Ameri & Harris, 2008), emotional behaviour (Green *et al*, 2008), learning and memory consolidation (Chen *et al*, 2003; Costa-Mattioli *et al*, 2007; Costa-Mattioli & Sonenberg, 2006) and circadian rhythms (Koyanagi *et al*, 2011; Ushijima *et al*, 2012), it is conceivable that DISC1 amino acid substitutions 37W and 607F might impact on all of the above processes, which might potentially contribute to their risk-conferring effect.

	Observed Effects on DISC1 subcellular distribution/function (compared to human DISC1-WT)						
DISC1 variant	**Nuclear expression**	**Cytoplasmic distribution**	**Mitochondrial distribution**	**Inhibitory effect on ATF4 transcriptional activity**	**Inhibitory effect on TG-induced CRE activation**	**MO3.13 cell survival to oxidative stress (5 mM HCY)**	**ATF4 binding (measured by Co-IP)**
37W	↓ (~50%) DN	Concentrated at mitochondria[1]	↑[1]	↓ (~34% on CRE#; ~74% on CHOP AARE)	LOF	? (inconclusive results)	=
264R	=	Punctate	= (NQ)	NT	NT	NT	NT
432L	=	Punctate	= (NQ)	= (tested on CRE only)	NT	NT	NT
603I	=	Punctate	= (NQ)	= (tested on CRE only)	NT	NT	↓ (~65%)
607F	↓ (~50%) DN	Diffuse; ↓ CKSE expression (~75%)	= (NQ)	↓ (~41% on CRE#; 38% on CHOP AARE)	LOF	? (inconclusive results)	↓ (~50%)
704C	=	Punctate	= (NQ)	= (tested on CRE only)	NT	NT	NT
ΔLZ9	↓ (NQ)	Diffuse	NT	LOF	LOF	NT	=
Mouse WT	↓ (NQ)	Punctate	NT	Null*	NT	NT	↑ (NQ)
Mouse 31L	↓ (NQ)	Punctate	NT	Null*	NT	NT	↑ (NQ); ↓ compared to mouse Disc1 WT (NQ)

	Observed Effects on DISC1 subcellular distribution/function (compared to human DISC1-WT)						
DISC1 variant	**Nuclear expression**	**Cytoplasmic distribution**	**Mitochondrial distribution**	**Inhibitory effect on ATF4 transcriptional activity**	**Inhibitory effect on TG-induced CRE activation**	**MO3.13 cell survival to oxidative stress (5 mM HCY)**	**ATF4 binding (measured by Co-IP)**
Mouse 100P	↓ (NQ)	Punctate	NT	Null*	NT	NT	↑ (NQ); ↓ compared to mouse Disc1 WT (NQ)

Table 8.1 Summary of the observed effects of DISC1 amino acid substitutions/mutations on the protein's subcellular distribution and function. TG: thapsigargin; HCY: homocysteine; Co-IP: co-immunoprecipitation; ↑: increased; ↓: decreased; =: not affected; NQ: Not Quantified; NT: Not Tested; LOF: Loss of Function; CSKE: cytoskeletal extract. The numbers in brackets indicate the percent change in the specified phenotype/function introduced by the DISC1 variant/mutation. DN indicates that the specified DISC1 variant affects DISC1-WT in a dominant-negative fashion. [1]Fumiaki Ogawa, unpublished data. [#]Average between the effects measured in HEK293 and MO3.13 cells. [*]These DISC1 variants have no effect on ATF4 transactivation of the CRE.

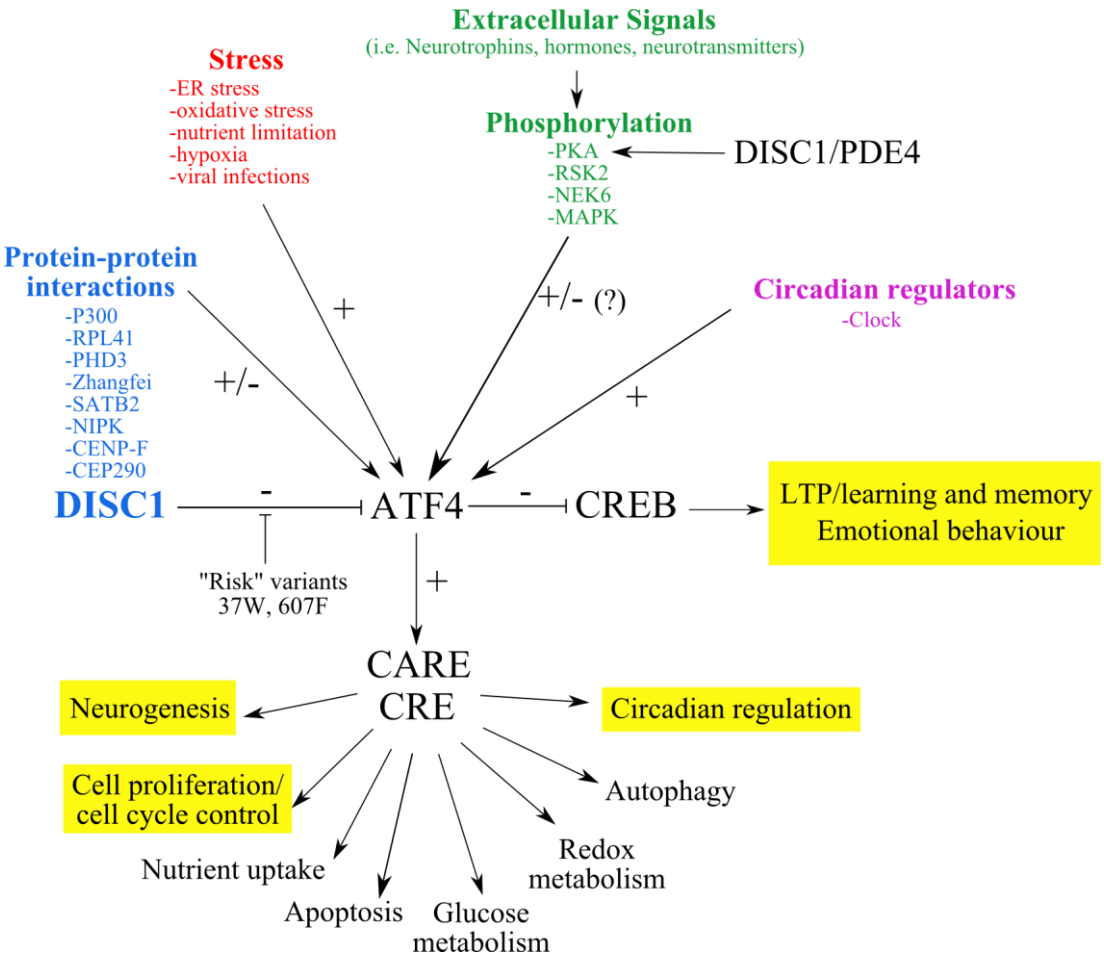

Figure 8.1 Regulators and biological functions of ATF4, and potential role of DISC1. Multiple mechanisms contribute to the regulation of *ATF4* transcription, translation, protein stability and transcriptional activity. Microenvironmental stressors, including endoplasmic reticulum (ER) stress, oxidative stress, nutrient limitation, hypoxia and viral infections upregulate ATF4 transcription and translation (see section 1.3.4 of this thesis). ATF4 can also be regulated by direct phosphorylation by kinases that respond to various extracellular stimuli. Examples of kinases that can directly phosphorylate ATF4 *in vitro* include PKA (Elefteriou *et al*, 2005), RSK2 (Yang *et al*, 2004), NEK6 (Vaz Meirelles *et al*, 2010) and MAPK (Bartsch *et al*, 1995). While PKA and RSK2 have been shown to positively regulate ATF4 activity (Elefteriou *et al*, 2005; Yang *et al*, 2004), the effects of NEK6- and MAPK-dependent phosphorylation on ATF4 transactivation activity have not been directly investigated yet. *ATF4* expression is also controlled by circadian regulators, such as Clock (Igarashi *et al*, 2007). Besides being controlled by direct phosphorylation, the

transcriptional activity of ATF4 can also be modulated (either activated or repressed) by its interaction with several binding partners, some examples of which are listed in the figure (see section 1.3 of this thesis). By binding to CRE and CARE elements in the promoters of its target genes, ATF4 can activate a plethora of biological pathways involved in cell proliferation, cell survival and apoptosis. Additionally, through its repressive effect on CREB, ATF4 is involved in the regulation of Long-Term Potentiation (LTP), the process underlying learning and memory, as well as emotional behaviour. DISC1 can bind to ATF4 and inhibit its activity on both CRE and CARE elements, and by doing so it could potentially impact on the function of all/any ATF4-regulated genes and pathways. Intriguingly, ATF4 and DISC1 converge on the regulation of several biological processes of known relevance for psychiatric illness (highlighted in yellow), and it is conceivable that this functional convergence arises, at least in part, from their biological interaction. Under this assumption, DISC1 variants that modify its functional interaction with ATF4, like 37W and 607F, might impact on multiple transcriptional events governing neurogenesis, stress responses, cognition, and circadian rhythms, all of which are implicated in psychiatric illness. DISC1 might additionally regulate ATF4 indirectly, by controlling its PKA-dependent phosphorylation through the establishment of dynamic interactions with PDE4. PKA: Protein kinase A; RSK2: Ribosomal protein S6 kinase, 90 kDa, polypeptide 3; NEK6: NIMA-related kinase 6; MAPK: Mitogen-activated protein kinase; PDE4: Phosphodiesterase 4; RPL41: Ribosomal protein L41; PHD3: Prolyl-4-hydroxylase 3; SATB2: Special AT-rich sequence-binding homeobox 2; NIPK: Neuronal cell death-inducible putative kinase; CENP-F: Centromere protein F, 350/400 kDa; CEP290: Centrosomal protein, 290 kDa.

8.3 Effect of cAMP on DISC1-mediated transcriptional regulation

In chapter 5 of this thesis I used luciferase assays to investigate the potential involvement of cAMP, its regulator PDE4 and its effector PKA on DISC1-mediated regulation of ATF4 transactivation activity. At basal cAMP levels, ATF4 activity on the CRE is positively regulated by PKA, as demonstrated by the repressive effect of the specific PKA inhibitor PKIα. Since PKA phosphorylation of ATF4 at serine 254 was previously shown to enhance its activity on the RankL promoter CRE site, it is possible that the effect observed here might be similarly mediated by direct

phosphorylation of ATF4 by PKA. By contrast, at high cAMP levels, PKA inhibits the repressive effect of ATF4 on CRE-driven transcription. Again, this may be due to a direct inhibitory effect of PKA on ATF4, but it may also arise indirectly through the activation of endogenous CREB by PKA.

At basal, but not at high cAMP levels, ATF4 activity on the CRE is inhibited by co-expression of PDE4B and D. This suggests that PDE4 might be involved in the regulation of ATF4 activity at basal cAMP levels, perhaps via the control of local PKA activity. However, this is in contrast with the observed lack of effect of the PDE4 inhibitor rolipram on ATF4 activity at basal cAMP. As discussed in chapter 5 of this thesis, this inconsistency might be related to the technical limitations of the particular reporter assay adopted here, and further experiments will be required to better elucidate the potential role of PDE4 and PKA in the regulation of ATF4. Some proposed experimental approaches will be described later in this chapter.

Despite the potential regulatory role of PDE4 on ATF4 activity, the observed repressive effect of DISC1 on ATF4 does not appear to require the contribution of endogenous PDE4, as indicated by the fact that it is entirely preserved in the presence of a concentration of rolipram that efficiently inhibits PDE4 activity in the tested cell model. However, based on the limited experiments described here, it is not possible to rule out that PDE4 might contribute to the repressive effect of DISC1 on ATF4 on different promoters/cell types.

8.4 The role of DISC1 in the cellular response to stress

Given the well-established role of ATF4 in the regulation of the cellular response to stress, in chapter 6 of this thesis I hypothesised that DISC1 variants that impair its repressive effect on ATF4 might consequently impact on the cell's ability to adapt and survive to stress. As expected, under conditions of oxidative stress induced by H_2O_2 treatment, endogenous ATF4 nuclear expression is greatly enhanced. On the other hand, the same experimental conditions determine a significant reduction of endogenous DISC1 expression in the particular tested cell line (MO3.13 human oligodendrocytes). Although highly preliminary, this observation suggests that cellular stress might specifically regulate DISC1 expression, perhaps as a way of

tuning its repressive effect on ATF4. Alternatively, it is possible that the particular drug treatment adopted here destabilises DISC1 protein structure, hence promoting its misfolding, aggregation and consequent degradation in autophagosomes.

The limited set of experiments performed in MO3.13 cells provided no conclusive evidence for a role of ATF4 or DISC1 in survival of these cells after exposure to oxidative or endoplasmic reticulum stress. This is in contrast with the well-characterised function of ATF4 in the cell's adaptation to stress. However, as discussed in chapter 6 of this thesis, the experimental approach adopted here is flawed by technical limitations that might explain these unexpected results. Potential alternative and improved experimental approaches that might be used to investigate the role of DISC1 in stress regulation are described later in this chapter.

8.5 Characterisation of the molecular interaction between DISC1 and ATF4

The final results chapter of this thesis investigates whether the factors that influence the functional interaction between DISC1 and ATF4 (i.e. DISC1 amino acid substitutions 37W and 607F and cAMP levels) also affect the physical interaction between the two proteins in the cell, which may potentially explain their functional impact. In addition, the distribution of endogenous and exogenous ATF4 and DISC1 was analysed by immunocytochemistry in HEK293 and SHSY5Y cells. Interestingly, in these cells ATF4 is not confined to the nucleus but, like DISC1, it can also be detected at the mitochondria and centrosome, suggesting that ATF4 and DISC1 might interact at these additional locations. If confirmed, this possibility would open new lines of enquiry about the potential role of the DISC1-ATF4 complex in the regulation of cell cycle progression and energy homeostasis.

Consistent with its partial exclusion from the nucleus and decreased inhibitory effect on ATF4, DISC1-607F shows reduced interaction with ATF4. This effect may also arise from direct and/or indirect disruption of ATF4 binding sites on DISC1 by 607F. Unlike 607F, the artificial DISC1 mutation ΔLZ9, which removes DISC1 amino acids 607-628 and ablates DISC1's repressive effect on ATF4, has no apparent effect on ATF4 binding. Similarly, and in contrast with its exclusion from the nucleus and

reduced inhibitory effect on ATF4, no effect upon ATF4 binding was detected for DISC1 mutation 37W. Finally, DISC1 mutation 603I significantly decreases ATF4 binding despite having no effect upon DISC1's inhibitory effect on ATF4 transactivation. Although the lack of effect of 37W on DISC1-ATF4 binding might be partially explained by potentially increased interaction of DISC1-37W with mitochondrial ATF4, these results are largely incongruent. As discussed in chapter 7 of this thesis, this incongruence may reflect experimental artefacts, and suggests a requirement for adoption of alternative experimental approaches to clarify the relationship between the physical and functional interaction between DISC1 and ATF4.

Forskolin treatment dramatically enhances binding of exogenous ATF4 and DISC1, suggesting that this protein-protein interaction may be strengthened by cAMP, perhaps via PKA-dependent phosphorylation. Although this observation is in contrast with the lack of effect of DISC1 on ATF4 transactivation of the CRE and CHOP AARE at high cAMP levels observed here, it cannot be excluded that the effects of cAMP-dependent modulation of DISC1-ATF4 binding might be evident in different contexts (e.g. different cell types and/or different promoters). In addition, the effect of forskolin on ATF4 and DISC1 protein levels was investigated, but this produced contrasting results. Indeed, while forskolin appears to increase ATF4 protein levels in ATF4-overexpressing cells, it has the opposite effect in untransfected cells. Similarly, forskolin appears to increase DISC1 expression in some but not other experiments based on DISC1-overexpressing cells, but it reduces expression of endogenous DISC1 in untransfected cells. Although tantalising, these observations raise more questions than they answer about the potential regulatory role of cAMP on the physical and functional interaction between DISC1 and ATF4. Possible future experimental approaches to clarify the potential role of cAMP in the regulation of the DISC1-ATF4 interaction will be discussed in the next session.

8.6 Future experiments

The experiments described in this thesis provided intriguing preliminary evidence suggesting that nuclear human DISC1 might be involved in the regulation of ATF4

transcriptional activity at multiple promoters. In addition, they suggest that DISC1 amino acid substitutions 37W and 607F may compromise DISC1 nuclear targeting and ATF4 regulation in brain cells, which in turn may contribute to their risk-conferring effect, perhaps by introducing subtle changes in the way the brain responds to stressful and emotional stimuli, learns, and regulates its sleep/wake cycles. Although the present study was undoubtedly useful as it generated an array of interesting testable hypotheses, the fact that it is almost entirely based on overexpression of exogenous proteins represents an important limitation. This is a particularly relevant point especially in light of a recent study that proposed that, at least in the mouse brain, DISC1 expression levels are relatively low (Kuroda *et al*, 2011). Thus, more work will be required to determine if and how endogenous DISC1 regulates ATF4 transcriptional activity, and establish whether amino acid substitutions 37W and 607F impact on this particular DISC1 function in neurons.

Below I propose some potential experimental approaches that might be adopted to expand and validate (or reject) the observations presented in this thesis.

- It would be particularly important to establish whether amino acid substitutions 37W and 607F significantly impair the nuclear expression of endogenous DISC1 in neurons. This could be achieved by introducing these mutations in the DISC1 gene in a human neural cell line, such as SH-SY5Y. A more rigorous, albeit considerably more expensive and technically challenging approach, would be to analyse nuclear DISC1 expression in neurons derived from 607F and 37W carriers, and compare it with that of non-carriers. Such neurons could be differentiated from induced pluripontent stem cells (iPS cells) generated in vitro from skin biopsies. For the common 607F substitution, it might also be possible to analyse DISC1 protein expression in post-mortem brains using immunohistochemistry and/or subcellular fractionation. Finally, since the t(1;11) translocation results in ~50% decreased DISC1 expression in patient-derived lymphoblastoid cell lines (Millar *et al*, 2005b), it would be particularly interesting to test whether nuclear DISC1 expression is decreased in iPS cell-derived neurons from t(1;11) carriers.

– Several approaches of increasing complexity could be adopted to confirm that DISC1 regulates ATF4 transcriptional activity. Initially, this could be tested using overexpessed proteins in luciferase assays in which the entire promoters of selected well-characterised ATF4 target genes could be used, instead of isolated CRE or AARE elements. Examples of potential ATF4 target promoters that could be tested in this way are Grp78 (containing a CRE element) and CHOP (containing an AARE element). This system could also be used to further examine the effect of increased cAMP levels on the regulatory effect of DISC1, and to test whether these ATF4-targeted promoters can be regulated by exogenous DISC1 when activated by stress.

  Another relatively simple way to further test DISC1's potential to regulate ATF4 would be to test for co-localisation of both proteins with PML nuclear bodies, sites of active transcription in which exogenous DISC1 has been previously described to localise (Sawamura *et al*, 2008).

  Next, it would be important to determine whether DISC1 regulates ATF4 in neuronal cells. This experiment has been attempted in this thesis using SH-SY5Y cells, but failed due to the insufficient transfection rate achieved in these cells, which are notoriously hard to transfect. Thus, to circumvent this problem it would be necessary to engineer a human neuronal cell line, such as SH-SY5Y, in which ATF4 and DISC1 can be induced either separately or together. Alternatively, one might use lentiviral transfection to express ATF4 and/or DISC1 in cultured primary neurons. These cell models could be used to answer multiple questions. For example, one might quantify the expression of selected ATF4 target genes using Q-PCR before and after ATF4 expression, and test whether this changes when DISC1 is co-expressed. In addition, it would be possible to use gene microarrays to analyse the transcriptional effect of ATF4 or DISC1 expression, and compare it to effects of ATF4-DISC1 co-expression. This might lead to the discovery of novel ATF4 and/or DISC1 regulated genes. These cells could also be exposed to cAMP-increasing drugs such as forskolin and/or IBMX before analysing gene expression to test whether any potential functional interaction between DISC1 and ATF4 is modulated by cAMP levels. To further test whether

DISC1 modulates the transcription of ATF4-target genes in response to stress, as suggested by the thapsigargin experiment described in chapter 4 of this thesis, it would be possible to expose these cells to stress to induce endogenous ATF4, and then evaluate the effect of DISC1 co-expression on the mRNA levels of ATF4 target genes. These cells could also be engineered to express DISC1-37W or DISC1-607F instead of DISC1-WT, so to compare any potential transcriptional effects of these variants. Moreover, the transcriptional effects of ATF4 and DISC1 might be analysed and compared in undifferentiated/proliferating vs. differentiated/post-mitotic neural cells. Finally, to control for potential artefacts due to protein overexpression, one might perform complementary experiments in neuronal cells or primary neurons that express ATF4 and/or DISC1 short hairpin RNAs (shRNAs) to knock-down the endogenous proteins. If this approach leads to the identification of specific DISC1-regulated genes, it would then be possible to compare their expression in SH-SY5Y cells in which endogenous DISC1 has been mutated to encode the 607F or 37W variants, or, ideally, in iPS cells-derived neurons from 37W, 607F and t(1;11) carriers.

– Next, it would be interesting to understand how DISC1 regulates ATF4 activity. In this thesis I showed that, at least in the tested system, DISC1-mediated repression of ATF4 is not mediated by sequestration of ATF4 by DISC1 outside the nucleus, and that DISC1 does not act via PDE4. Again, different experimental approaches of increasing complexity could be used to test this. Initially, the Elecrophoretic Mobility Shift Assay (EMSA) could be employed to ask whether ATF4 and DISC1 bind together to promoter elements such as the CRE or AARE, or instead DISC1 prevents or inhibits ATF4 binding to its target DNA. If DISC1 and ATF4 bind DNA as a complex, the same experimental approach could also be used to test whether DISC1 prevents recruitment of basic transcription factors to the ATF4-DNA complex. If it were demonstrated that ATF4 and DISC1 bind DNA as a complex, it would also be interesting to identify the genes that are directly targeted by this complex, as a complementary approach to the gene

expression profiling studies proposed above. This could be done using neural cells with inducible ATF4/DISC1 expression, or neural/glial cells that have been exposed to stress to induce endogenous ATF4. A sequential chromatin immunoprecipitation (chIP) experiment (e.g. ATF4 chIP followed by DISC1 chIP) could be performed to enrich for promoters that are bound by both proteins. These promoters could be subsequently identified by sequencing of the immunoprecipitated chromatin.

– The results presented in chapter 5 of this thesis suggest that the activity of ATF4 on the CRE might be regulated by PDE4 and PKA. However, because of time limitations, it was not possible to investigate this further in this thesis. In the future, it would be interesting to test whether the activating effect of PKA on ATF4 transactivation of the CRE is mediated by direct PKA-dependent phosphorylation of ATF4 at serine 254. This could be done by performing CRE-reporter assays with ATF4 serine 254 phospho-resistant and phospho-mimic mutants. Indeed, if PKA directly regulates ATF4 both at basal and elevated cAMP levels, the ATF4 serine 254 phospho-resistant mutant should be less active at basal cAMP levels and more active at high cAMP levels, whereas the serine 254 phospho-mimic mutant should have the opposite effect. However, if the repressive effect of PKA on ATF4 at high cAMP levels is not due to direct phosphorylation of ATF4, but to concomitant activation of CREB, mutating ATF4 serine 254 should not affect this. As a complementary approach, it would also be interesting to test whether the phosphoryation status of ATF4 is affected by forskolin treatment and/or PDE4 overexpression, which could be done by mass spectrometry. Given the observed effect of PDE4 on ATF4 activity, the interaction between these two proteins, which was previously reported (Bradshaw *et al*, 2008), should be analysed further. For example, immunocytochemistry could be used to ask whether ATF4 and PDE4 co-localise in the nucleus and/or centrosome. In addition, the effect of PDE4 on CRE activity, both in the presence and absence of ATF4, should be tested after exposure to non-saturating concentrations of forskolin.

- In the light of the intriguing preliminary findings described in chapter 6 of this thesis, the potential involvement of DISC1 in the regulation of the cellular response to stress should be investigated further. It would be of particular interest to establish whether DISC1 protein expression can be modulated by other types of cellular stressors besides H_2O_2 and in other cell types, and test whether this occurs at the transcriptional or post-transcriptional level, or both. To test this, one may ask whether the effect of stress on DISC1 protein levels can be rescued by proteasome inhibitors, or inhibitors of autophagocytosis. Moreover, since the DISC1 promoter has already been cloned (Walker *et al*, 2012), luciferase reporter assays could be easily used to investigate the potential effect of various stressors on DISC1 promoter activity in different cell types. Because of technical and time limitations, it was not possible to conclusively assess the role of ATF4 and DISC1 in MO3.13 cell survival after stress in this thesis. However, if the regulatory effect of DISC1 on ATF4-dependent transcription will be confirmed using the methods described above, the study of the potential effects of DISC1 on cellular stress survival would definitely be a line of enquiry worth pursuing. The neuronal cell models with inducible overexpression or silencing of ATF4 and DISC1 proposed above might be a more suited system in which to investigate this further. Additional stress paradigms relevant to schizophrenia (e.g. exposure to pro-inflammatory cytokines, nutrient deprivation, exposure to cortisol) should be tested in this model, and their effects on cell survival should be assessed both in undifferentiated and differentiated cells. Ultimately, it would be also necessary to analyse the stress response in DISC1-WT, -37W, -607F mutant cells and iPS cell-derived neurons.

- In chapter 7 of this thesis, I showed that forskolin increases binding of exogenous ATF4 and DISC1. To confirm this observation, it would be useful to test the effect of forskolin on the interaction between the endogenous proteins. As an additional control, alternative methods could be used to raise intracellular cAMP levels, such as IBMX, rolipram or caffeine treatment, and

additional cell types should be tested. To test the hypothesis that this effect is mediated by direct phosphorylation of ATF4 and/or DISC1 by PKA, co-IP experiments could be performed using phospho-mimic and phospho-resistant ATF4 and DISC1 mutants for each known PKA site. In addition, the observed effects of forskolin on the expression levels and subcellular distribution of ATF4 and DISC1, both exogenous and endogenous, should be confirmed in other cell types, and complemented by immunocytochemistry.

– The effects of DISC1 amino acid substitutions 37W, 607F and 603I and mutation ΔLZ9 on ATF4 binding could be further investigated using in-vitro binding assays or surface plasmon resonance (SPR). Very briefly, SPR is based on the measurement of the angle by which incident light is reflected off a thin metal film. Such measure is influenced, among other things, by the presence of biomolecules (e.g. protein) on the metal film. Thus, once a bait protein (e.g. ATF4) is immobilised on a metal surface through a chemical linker, SPR can measure the change in refractive index that occurs when a solution containing the purified prey protein (e.g. DISC1) is allowed to flow on this surface. Since the degree of change in the SPR signal is proportional to the mass of protein bound to the metal surface, this methods allows to measure the stoichiometry of the interaction between the bait and prey proteins and compare different prey proteins (e.g. DISC1 variants) for their ability to bind to the immobilised bait.

– Finally, it would be necessary to determine whether ATF4 and DISC1 interact at the mitochondria and centrosome. This could be initially tested by developing a triple immunostaining technique to simultaneously detect ATF4, DISC1 and the mitochondria or centrosome. A more sensitive and specific follow-up experiment could be based on Proximity Ligation Assay (PLA) (Soderberg *et al*, 2006). This in-situ detection method exploits secondary antibodies bound to specific DNA strands. If the two secondary antibodies used to detect the two target proteins in the cell (ATF4 and DISC1, in this case) are in close proximity, as it should be if the proteins are interacting, the

DNA strands linked to the antibodies will both anneal with subsequently added circle-forming DNA oligonucleotides. Next, a DNA polymerase is added to amplify these oligonucleotides in-situ via the formation of a rolling circle. Finally, addition of fluorescently labelled oligonucleotide probes allows the detection of the amplified DNA, which can be visualised as a bright spot under a fluorescence microscope. The potential presence of other DISC1 binding partners, such as PDE4, NDE1 and NDEL1, in mitochondrial and centrosomal ATF4-DISC1 complexes, should also be investigated.

In conclusion, this thesis provided interesting insights on the potential role of nuclear DISC1, and proposed a novel mechanism by which amino acid substitutions 37W and 607F might contribute to the risk of mental illness, thus opening new avenues of research for the future.

References

Abazyan B, Nomura J, Kannan G, Ishizuka K, Tamashiro KL, Nucifora F, Pogorelov V, Ladenheim B, Yang C, Krasnova IN, Cadet JL, Pardo C, Mori S, Kamiya A, Vogel MW, Sawa A, Ross CA, Pletnikov MV (2011) Prenatal interaction of mutant DISC1 and immune activation produces adult psychopathology. *Biol Psychiatry* **68**(12): 1172-1181

Abi-Dargham A (2005) The Dopamine Hypothesis of Schizophrenia. *Current Hypotheses IN FORUM* **S.R. (Ed.)**

Adachi Y, Yamamoto K, Okada T, Yoshida H, Harada A, Mori K (2008) ATF6 is a transcription factor specializing in the regulation of quality control proteins in the endoplasmic reticulum. *Cell Struct Funct* **33**(1): 75-89

Adams CM (2007) Role of the transcription factor ATF4 in the anabolic actions of insulin and the anti-anabolic actions of glucocorticoids. *J Biol Chem* **282**(23): 16744-16753

Alberini CM, Ghirardi M, Huang YY, Nguyen PV, Kandel ER (1995) A molecular switch for the consolidation of long-term memory: cAMP-inducible gene expression. *Ann N Y Acad Sci* **758**: 261-286

Alberini CM, Ghirardi M, Metz R, Kandel ER (1994) C/EBP is an immediate-early gene required for the consolidation of long-term facilitation in Aplysia. *Cell* **76**(6): 1099-1114

Ameri K, Harris AL (2008) Activating transcription factor 4. *Int J Biochem Cell Biol* **40**(1): 14-21

Ameri K, Lewis CE, Raida M, Sowter H, Hai T, Harris AL (2004) Anoxic induction of ATF-4 through HIF-1-independent pathways of protein stabilization in human cancer cells. *Blood* **103**(5): 1876-1882

Ameri K, Luong R, Zhang H, Powell AA, Montgomery KD, Espinosa I, Bouley DM, Harris AL, Jeffrey SS (2010) Circulating tumour cells demonstrate an altered response to hypoxia and an aggressive phenotype. *Br J Cancer* **102**(3): 561-569

Applebaum J, Shimon H, Sela BA, Belmaker RH, Levine J (2004) Homocysteine levels in newly admitted schizophrenic patients. *J Psychiatr Res* **38**(4): 413-416

Arguello PA, Gogos JA (2006) Modeling madness in mice: one piece at a time. *Neuron* **52**(1): 179-196

Arguello PA, Gogos JA (2008) A signaling pathway AKTing up in schizophrenia. *J Clin Invest* **118**(6): 2018-2021

Armstrong JL, Flockhart R, Veal GJ, Lovat PE, Redfern CP (2010) Regulation of endoplasmic reticulum stress-induced cell death by ATF4 in neuroectodermal tumor cells. *J Biol Chem* **285**(9): 6091-6100

Atkin TA, Brandon NJ, Kittler JT (2012) Disrupted in Schizophrenia 1 forms pathological aggresomes that disrupt its function in intracellular transport. *Hum Mol Genet* **21**(9): 2017-2028

Atkin TA, MacAskill AF, Brandon NJ, Kittler JT (2011) Disrupted in Schizophrenia-1 regulates intracellular trafficking of mitochondria in neurons. *Mol Psychiatry* **16**(2): 122-124

Austin CP, Ky B, Ma L, Morris JA, Shughrue PJ (2004) Expression of Disrupted-In-Schizophrenia-1, a schizophrenia-associated gene, is prominent in the mouse hippocampus throughout brain development. *Neuroscience* **124**(1): 3-10

Averous J, Bruhat A, Jousse C, Carraro V, Thiel G, Fafournoux P (2004) Induction of CHOP expression by amino acid limitation requires both ATF4 expression and ATF2 phosphorylation. *J Biol Chem* **279**(7): 5288-5297

Avery SV (2011) Molecular targets of oxidative stress. *Biochem J* **434**(2): 201-210

Avivar-Valderas A, Salas E, Bobrovnikova-Marjon E, Diehl JA, Nagi C, Debnath J, Aguirre-Ghiso JA (2011) PERK integrates autophagy and oxidative stress responses to promote survival during extracellular matrix detachment. *Mol Cell Biol* **31**(17): 3616-3629

Ayhan Y, Abazyan B, Nomura J, Kim R, Ladenheim B, Krasnova IN, Sawa A, Margolis RL, Cadet JL, Mori S, Vogel MW, Ross CA, Pletnikov MV (2011) Differential effects of prenatal and postnatal expressions of mutant human DISC1 on neurobehavioral phenotypes in transgenic mice: evidence for neurodevelopmental origin of major psychiatric disorders. *Mol Psychiatry* **16**(3): 293-306

Badiola N, Penas C, Minano-Molina A, Barneda-Zahonero B, Fado R, Sanchez-Opazo G, Comella JX, Sabria J, Zhu C, Blomgren K, Casas C, Rodriguez-Alvarez J (2011) Induction of ER stress in response to oxygen-glucose deprivation of cortical cultures involves the activation of the PERK and IRE-1 pathways and of caspase-12. *Cell Death Dis* **2**(e149)

Bartsch D, Ghirardi M, Skehel PA, Karl KA, Herder SP, Chen M, Bailey CH, Kandel ER (1995) Aplysia CREB2 represses long-term facilitation: relief of repression converts transient facilitation into long-term functional and structural change. *Cell* **83**(6): 979-992

Beal MF (2000) Oxidative metabolism. *Ann N Y Acad Sci* **924**: 164-169

Beaulieu JM, Caron MG (2008) Looking at lithium: molecular moods and complex behaviour. *Mol Interv* **8**(5): 230-241

Behrens MM, Sejnowski TJ (2009) Does schizophrenia arise from oxidative dysregulation of parvalbumin-interneurons in the developing cortex? *Neuropharmacology* **57**(3): 193-200

Bell KF, Al-Mubarak B, Fowler JH, Baxter PS, Gupta K, Tsujita T, Chowdhry S, Patani R, Chandran S, Horsburgh K, Hayes JD, Hardingham GE (2011) Mild oxidative stress activates Nrf2 in astrocytes, which contributes to neuroprotective ischemic preconditioning. *Proc Natl Acad Sci U S A* **108**(1): E1-2; author reply E3-4

Beneyto M, Kristiansen LV, Oni-Orisan A, McCullumsmith RE, Meador-Woodruff JH (2007) Abnormal glutamate receptor expression in the medial temporal lobe in schizophrenia and mood disorders. *Neuropsychopharmacology* **32**(9): 1888-1902

Beneyto M, Meador-Woodruff JH (2008) Lamina-specific abnormalities of NMDA receptor-associated postsynaptic protein transcripts in the prefrontal cortex in schizophrenia and bipolar disorder. *Neuropsychopharmacology* **33**(9): 2175-2186

Berg D, Youdim MB, Riederer P (2004) Redox imbalance. *Cell Tissue Res* **318**(1): 201-213

Berk M, Kapczinski F, Andreazza AC, Dean OM, Giorlando F, Maes M, Yucel M, Gama CS, Dodd S, Dean B, Magalhaes PV, Amminger P, McGorry P, Malhi GS (2011) Pathways underlying neuroprogression in bipolar disorder: focus on inflammation, oxidative stress and neurotrophic factors. *Neurosci Biobehav Rev* **35**(3): 804-817

Bernstein HG, Steiner J, Bogerts B (2009) Glial cells in schizophrenia: pathophysiological significance and possible consequences for therapy. *Expert Rev Neurother* **9**(7): 1059-1071

Berrettini WH (2000) Are schizophrenic and bipolar disorders related? A review of family and molecular studies. *Biol Psychiatry* **48**(6): 531-538

Bi M, Naczki C, Koritzinsky M, Fels D, Blais J, Hu N, Harding H, Novoa I, Varia M, Raleigh J, Scheuner D, Kaufman RJ, Bell J, Ron D, Wouters BG, Koumenis C (2005) ER stress-regulated translation increases tolerance to extreme hypoxia and promotes tumor growth. *Embo J* **24**(19): 3470-3481

Bitanihirwe BK, Woo TU (2011) Oxidative stress in schizophrenia: an integrated approach. *Neurosci Biobehav Rev* **35**(3): 878-893

Blackwood DH, Fordyce A, Walker MT, St Clair DM, Porteous DJ, Muir WJ (2001) Schizophrenia and affective disorders--cosegregation with a translocation at chromosome 1q42 that directly disrupts brain-expressed genes: clinical and P300 findings in a family. *Am J Hum Genet* **69**(2): 428-433

Blackwood DH, Muir WJ (2004) Clinical phenotypes associated with DISC1, a candidate gene for schizophrenia. *Neurotox Res* **6**(1): 35-41

Blais JD, Filipenko V, Bi M, Harding HP, Ron D, Koumenis C, Wouters BG, Bell JC (2004) Activating transcription factor 4 is translationally regulated by hypoxic stress. *Mol Cell Biol* **24**(17): 7469-7482

Bolger GB, Erdogan S, Jones RE, Loughney K, Scotland G, Hoffmann R, Wilkinson I, Farrell C, Houslay MD (1997) Characterization of five different proteins produced by alternatively spliced mRNAs from the human cAMP-specific phosphodiesterase PDE4D gene. *Biochem J* **328 (Pt 2)**(539-548)

Bord L, Wheeler J, Paek M, Saleh M, Lyons-Warren A, Ross CA, Sawamura N, Sawa A (2006) Primate disrupted-in-schizophrenia-1 (DISC1): high divergence of a gene for major mental illnesses in recent evolutionary history. *Neurosci Res* **56**(3): 286-293

Boskovic M, Vovk T, Kores Plesnicar B, Grabnar I (2011) Oxidative stress in schizophrenia. *Curr Neuropharmacol* **9**(2): 301-312

Bouaziz N, Ayedi I, Sidhom O, Kallel A, Rafrafi R, Jomaa R, Melki W, Feki M, Kaabechi N, El Hechmi Z (2010) Plasma homocysteine in schizophrenia: determinants and clinical correlations in Tunisian patients free from antipsychotics. *Psychiatry Res* **179**(1): 24-29

Bradshaw NJ, Christie S, Soares DC, Carlyle BC, Porteous DJ, Millar JK (2009) NDE1 and NDEL1: multimerisation, alternate splicing and DISC1 interaction. *Neurosci Lett* **449**(3): 228-233

Bradshaw NJ, Ogawa F, Antolin-Fontes B, Chubb JE, Carlyle BC, Christie S, Claessens A, Porteous DJ, Millar JK (2008) DISC1, PDE4B, and NDE1 at the centrosome and synapse. *Biochem Biophys Res Commun* **377**(4): 1091-1096

Bradshaw NJ, Porteous DJ (2012) DISC1-binding proteins in neural development, signalling and schizophrenia. *Neuropharmacology* **62**(3): 1230-1241

Bradshaw NJ, Soares DC, Carlyle BC, Ogawa F, Davidson-Smith H, Christie S, Mackie S, Thomson PA, Porteous DJ, Millar JK (2011) PKA phosphorylation of NDE1 is DISC1/PDE4 dependent and modulates its interaction with LIS1 and NDEL1. *J Neurosci* **31**(24): 9043-9054

Brandon NJ, Handford EJ, Schurov I, Rain JC, Pelling M, Duran-Jimeniz B, Camargo LM, Oliver KR, Beher D, Shearman MS, Whiting PJ (2004) Disrupted in Schizophrenia 1 and Nudel form a neurodevelopmentally regulated protein complex: implications for schizophrenia and other major neurological disorders. *Mol Cell Neurosci* **25**(1): 42-55

Brandon NJ, Millar JK, Korth C, Sive H, Singh KK, Sawa A (2009) Understanding the role of DISC1 in psychiatric disease and during normal development. *J Neurosci* **29**(41): 12768-12775

Brandon NJ, Sawa A (2011) Linking neurodevelopmental and synaptic theories of mental illness through DISC1. *Nat Rev Neurosci* **12**(12): 707-722

Brandon NJ, Schurov I, Camargo LM, Handford EJ, Duran-Jimeniz B, Hunt P, Millar JK, Porteous DJ, Shearman MS, Whiting PJ (2005) Subcellular targeting of DISC1 is dependent on a domain independent from the Nudel binding site. *Mol Cell Neurosci* **28**(4): 613-624

Brauns S, Gollub RL, Roffman JL, Yendiki A, Ho BC, Wassink TH, Heinz A, Ehrlich S (2011) DISC1 is associated with cortical thickness and neural efficiency. *Neuroimage* **57**(4): 1591-1600

Brown AS (2002) Prenatal risk factors and schizophrenia. *Expert Rev Neurother* **2**(1): 53-60

Brown AS (2011) The environment and susceptibility to schizophrenia. *Prog Neurobiol* **93**(1): 23-58

Brown AS, Derkits EJ (2010) Prenatal infection and schizophrenia: a review of epidemiologic and translational studies. *Am J Psychiatry* **167**(3): 261-280

Brown AS, Susser ES (2005) Homocysteine and schizophrenia: from prenatal to adult life. *Prog Neuropsychopharmacol Biol Psychiatry* **29**(7): 1175-1180

Brown AS, Susser ES (2008) Prenatal nutritional deficiency and risk of adult schizophrenia. *Schizophr Bull* **34**(6): 1054-1063

Brown AS, van Os J, Driessens C, Hoek HW, Susser ES (2000) Further evidence of relation between prenatal famine and major affective disorder. *Am J Psychiatry* **157**(2): 190-195

Bruhat A, Averous J, Carraro V, Zhong C, Reimold AM, Kilberg MS, Fafournoux P (2002) Differences in the molecular mechanisms involved in the transcriptional activation of the CHOP and asparagine synthetase genes in response to amino acid deprivation or activation of the unfolded protein response. *J Biol Chem* **277**(50): 48107-48114

Bugiani M, Boor I, Powers JM, Scheper GC, van der Knaap MS (2010) Leukoencephalopathy with vanishing white matter: a review. *J Neuropathol Exp Neurol* **69**(10): 987-996

Buntinx M, Vanderlocht J, Hellings N, Vandenabeele F, Lambrichts I, Raus J, Ameloot M, Stinissen P, Steels P (2003) Characterization of three human oligodendroglial cell

lines as a model to study oligodendrocyte injury: morphology and oligodendrocyte-specific gene expression. *J Neurocytol* **32**(1): 25-38

Burdick KE, Kamiya A, Hodgkinson CA, Lencz T, DeRosse P, Ishizuka K, Elashvili S, Arai H, Goldman D, Sawa A, Malhotra AK (2008) Elucidating the relationship between DISC1, NDEL1 and NDE1 and the risk for schizophrenia: evidence of epistasis and competitive binding. *Hum Mol Genet* **17**(16): 2462-2473

Cabell L, Audesirk G (1993) Effects of selective inhibition of protein kinase C, cyclic AMP-dependent protein kinase, and Ca(2+)-calmodulin-dependent protein kinase on neurite development in cultured rat hippocampal neurons. *Int J Dev Neurosci* **11**(3): 357-368

Cabungcal JH, Preissmann D, Delseth C, Cuenod M, Do KQ, Schenk F (2007) Transitory glutathione deficit during brain development induces cognitive impairment in juvenile and adult rats: relevance to schizophrenia. *Neurobiol Dis* **26**(3): 634-645

Callicott JH, Straub RE, Pezawas L, Egan MF, Mattay VS, Hariri AR, Verchinski BA, Meyer-Lindenberg A, Balkissoon R, Kolachana B, Goldberg TE, Weinberger DR (2005) Variation in DISC1 affects hippocampal structure and function and increases risk for schizophrenia. *Proc Natl Acad Sci U S A* **102**(24): 8627-8632

Camargo LM, Collura V, Rain JC, Mizuguchi K, Hermjakob H, Kerrien S, Bonnert TP, Whiting PJ, Brandon NJ (2007) Disrupted in Schizophrenia 1 Interactome: evidence for the close connectivity of risk genes and a potential synaptic basis for schizophrenia. *Mol Psychiatry* **12**(1): 74-86

Cao H, Yu S, Yao Z, Galson DL, Jiang Y, Zhang X, Fan J, Lu B, Guan Y, Luo M, Lai Y, Zhu Y, Kurihara N, Patrene K, Roodman GD, Xiao G (2010) Activating transcription factor 4 regulates osteoclast differentiation in mice. *J Clin Invest* **120**(8): 2755-2766

Cardno AG, Rijsdijk FV, Sham PC, Murray RM, McGuffin P (2002) A twin study of genetic relationships between psychotic symptoms. *Am J Psychiatry* **159**(4): 539-545

Carless MA, Glahn DC, Johnson MP, Curran JE, Bozaoglu K, Dyer TD, Winkler AM, Cole SA, Almasy L, MacCluer JW, Duggirala R, Moses EK, Goring HH, Blangero J (2011) Impact of DISC1 variation on neuroanatomical and neurocognitive phenotypes. *Mol Psychiatry* **16**(11): 1096-1104

Carlyle BC, Mackie S, Christie S, Millar JK, Porteous DJ (2011) Co-ordinated action of DISC1, PDE4B and GSK3beta in modulation of cAMP signalling. *Mol Psychiatry* **16**(7): 693-694

Cashman NR, Durham HD, Blusztajn JK, Oda K, Tabira T, Shaw IT, Dahrouge S, Antel JP (1992) Neuroblastoma x spinal cord (NSC) hybrid cell lines resemble developing motor neurons. *Dev Dyn* **194**(3): 209-221

Chakravarti A (1999) Population genetics--making sense out of sequence. *Nat Genet* **21**(1 Suppl): 56-60

Chang RC, Wong AK, Ng HK, Hugon J (2002) Phosphorylation of eukaryotic initiation factor-2alpha (eIF2alpha) is associated with neuronal degeneration in Alzheimer's disease. *Neuroreport* **13**(18): 2429-2432

Chen A, Muzzio IA, Malleret G, Bartsch D, Verbitsky M, Pavlidis P, Yonan AL, Vronskaya S, Grody MB, Cepeda I, Gilliam TC, Kandel ER (2003) Inducible enhancement of memory storage and synaptic plasticity in transgenic mice expressing an inhibitor of ATF4 (CREB-2) and C/EBP proteins. *Neuron* **39**(4): 655-669

Chubb JE, Bradshaw NJ, Soares DC, Porteous DJ, Millar JK (2008) The DISC locus in psychiatric illness. *Mol Psychiatry* **13**(1): 36-64

Cibelli G, Jungling S, Schoch S, Gerdes HH, Thiel G (1996) Identification of a functional cAMP response element in the secretogranin II gene. *Eur J Biochem* **236**(1): 171-179

Cibelli G, Schoch S, Thiel G (1999) Nuclear targeting of cAMP response element binding protein 2 (CREB2). *Eur J Cell Biol* **78**(9): 642-649

Cichon S, Craddock N, Daly M, Faraone SV, Gejman PV, Kelsoe J, Lehner T, Levinson DF, Moran A, Sklar P, Sullivan PF (2009) Genomewide association studies: history, rationale, and prospects for psychiatric disorders. *Am J Psychiatry* **166**(5): 540-556

Clapcote SJ, Lipina TV, Millar JK, Mackie S, Christie S, Ogawa F, Lerch JP, Trimble K, Uchiyama M, Sakuraba Y, Kaneda H, Shiroishi T, Houslay MD, Henkelman RM, Sled JG, Gondo Y, Porteous DJ, Roder JC (2007) Behavioral phenotypes of Disc1 missense mutations in mice. *Neuron* **54**(3): 387-402

Clapcote SJ, Roder JC (2006) Deletion polymorphism of Disc1 is common to all 129 mouse substrains: implications for gene-targeting studies of brain function. *Genetics* **173**(4): 2407-2410

Clinton SM, Haroutunian V, Davis KL, Meador-Woodruff JH (2003) Altered transcript expression of NMDA receptor-associated postsynaptic proteins in the thalamus of subjects with schizophrenia. *Am J Psychiatry* **160**(6): 1100-1109

Cornblatt B, Obuchowski M, Roberts S, Pollack S, Erlenmeyer-Kimling L (1999) Cognitive and behavioral precursors of schizophrenia. *Dev Psychopathol* **11**(3): 487-508

Costa-Mattioli M, Gobert D, Stern E, Gamache K, Colina R, Cuello C, Sossin W, Kaufman R, Pelletier J, Rosenblum K, Krnjevic K, Lacaille JC, Nader K, Sonenberg

N (2007) eIF2alpha phosphorylation bidirectionally regulates the switch from short- to long-term synaptic plasticity and memory. *Cell* **129**(1): 195-206

Costa-Mattioli M, Sonenberg N (2006) Translational control of long-term synaptic plasticity and memory storage by eIF2alpha. *Crit Rev Neurobiol* **18**(1-2): 187-195

Coyle JT (2004) The GABA-glutamate connection in schizophrenia: which is the proximate cause? *Biochem Pharmacol* **68**(8): 1507-1514

Coyle JT (2006) Glutamate and schizophrenia: beyond the dopamine hypothesis. *Cell Mol Neurobiol* **26**(4-6): 365-384

Craddock N, Jones I (1999) Genetics of bipolar disorder. *J Med Genet* **36**(8): 585-594

Craddock N, O'Donovan MC, Owen MJ (2005) The genetics of schizophrenia and bipolar disorder: dissecting psychosis. *J Med Genet* **42**(3): 193-204

Craddock N, Owen MJ (2005) The beginning of the end for the Kraepelinian dichotomy. *Br J Psychiatry* **186**: 364-366

Crepel A, Breckpot J, Fryns JP, De la Marche W, Steyaert J, Devriendt K, Peeters H (2010) DISC1 duplication in two brothers with autism and mild mental retardation. *Clin Genet* **77**(4): 389-394

Curtis D, Kalsi G, Brynjolfsson J, McInnis M, O'Neill J, Smyth C, Moloney E, Murphy P, McQuillin A, Petursson H, Gurling H (2003) Genome scan of pedigrees multiply affected with bipolar disorder provides further support for the presence of a susceptibility locus on chromosome 12q23-q24, and suggests the presence of additional loci on 1p and 1q. *Psychiatr Genet* **13**(2): 77-84

Daibata M, Matsuo Y, Machida H, Taguchi T, Ohtsuki Y, Taguchi H (2004) Differential gene-expression profiling in the leukemia cell lines derived from indolent and aggressive phases of CD56+ T-cell large granular lymphocyte leukemia. *Int J Cancer* **108**(6): 845-851

Dalton GD, Dewey WL (2006) Protein kinase inhibitor peptide (PKI): a family of endogenous neuropeptides that modulate neuronal cAMP-dependent protein kinase function. *Neuropeptides* **40**(1): 23-34

Davis KL, Stewart DG, Friedman JI, Buchsbaum M, Harvey PD, Hof PR, Buxbaum J, Haroutunian V (2003) White matter changes in schizophrenia: evidence for myelin-related dysfunction. *Arch Gen Psychiatry* **60**(5): 443-456

Davis RL (1996) Physiology and biochemistry of Drosophila learning mutants. *Physiol Rev* **76**(2): 299-317

de Anda FC, Meletis K, Ge X, Rei D, Tsai LH (2010) Centrosome motility is essential for initial axon formation in the neocortex. *J Neurosci* **30**(31): 10391-10406

Dean O, Bush AI, Berk M, Copolov DL, van den Buuse M (2009) Glutathione depletion in the brain disrupts short-term spatial memory in the Y-maze in rats and mice. *Behav Brain Res* **198**(1): 258-262

Delgado R, Davis R, Bono MR, Latorre R, Labarca P (1998) Outward currents in Drosophila larval neurons: dunce lacks a maintained outward current component downregulated by cAMP. *J Neurosci* **18**(4): 1399-1407

Delghandi MP, Johannessen M, Moens U (2005) The cAMP signalling pathway activates CREB through PKA, p38 and MSK1 in NIH 3T3 cells. *Cell Signal* **17**(11): 1343-1351

Detera-Wadleigh SD, Badner JA, Berrettini WH, Yoshikawa T, Goldin LR, Turner G, Rollins DY, Moses T, Sanders AR, Karkera JD, Esterling LE, Zeng J, Ferraro TN, Guroff JJ, Kazuba D, Maxwell ME, Nurnberger JI, Jr., Gershon ES (1999) A high-density genome scan detects evidence for a bipolar-disorder susceptibility locus on 13q32 and other potential loci on 1q32 and 18p11.2. *Proc Natl Acad Sci U S A* **96**(10): 5604-5609

Dever TE (2002) Gene-specific regulation by general translation factors. *Cell* **108**(4): 545-556

Devon RS, Evans KL, Maule JC, Christie S, Anderson S, Brown J, Shibasaki Y, Porteous DJ, Brookes AJ (1997) Novel transcribed sequences neighbouring a translocation breakpoint associated with schizophrenia. *Am J Med Genet* **74**(1): 82-90

Dey S, Baird TD, Zhou D, Palam LR, Spandau DF, Wek RC (2010) Both transcriptional regulation and translational control of ATF4 are central to the integrated stress response. *J Biol Chem* **285**(43): 33165-33174

Di Giorgio A, Blasi G, Sambataro F, Rampino A, Papazacharias A, Gambi F, Romano R, Caforio G, Rizzo M, Latorre V, Popolizio T, Kolachana B, Callicott JH, Nardini M, Weinberger DR, Bertolino A (2008) Association of the SerCys DISC1 polymorphism with human hippocampal formation gray matter and function during memory encoding. *Eur J Neurosci* **28**(10): 2129-2136

Dickhout JG, Carlisle RE, Jerome DE, Mohammed-Ali Z, Jiang H, Yang G, Mani S, Garg SK, Banerjee R, Kaufman RJ, Maclean KN, Wang R, Austin RC (2012) Integrated Stress Response Modulates Cellular Redox State via Induction of Cystathionine gamma-Lyase: CROSS-TALK BETWEEN INTEGRATED STRESS RESPONSE AND THIOL METABOLISM. *J Biol Chem* **287**(10): 7603-7614

Dietrich-Muszalska A, Olas B, Glowacki R, Bald E (2009) Oxidative/nitrative modifications of plasma proteins and thiols from patients with schizophrenia. *Neuropsychobiology* **59**(1): 1-7

Do KQ, Cabungcal JH, Frank A, Steullet P, Cuenod M (2009) Redox dysregulation, neurodevelopment, and schizophrenia. *Curr Opin Neurobiol* **19**(2): 220-230

Do KQ, Trabesinger AH, Kirsten-Kruger M, Lauer CJ, Dydak U, Hell D, Holsboer F, Boesiger P, Cuenod M (2000) Schizophrenia: glutathione deficit in cerebrospinal fluid and prefrontal cortex in vivo. *Eur J Neurosci* **12**(10): 3721-3728

Dobreva G, Chahrour M, Dautzenberg M, Chirivella L, Kanzler B, Farinas I, Karsenty G, Grosschedl R (2006) SATB2 is a multifunctional determinant of craniofacial patterning and osteoblast differentiation. *Cell* **125**(5): 971-986

Dracheva S, Davis KL, Chin B, Woo DA, Schmeidler J, Haroutunian V (2006) Myelin-associated mRNA and protein expression deficits in the anterior cingulate cortex and hippocampus in elderly schizophrenia patients. *Neurobiol Dis* **21**(3): 531-540

Drerup CM, Wiora HM, Topczewski J, Morris JA (2009) Disc1 regulates foxd3 and sox10 expression, affecting neural crest migration and differentiation. *Development* **136**(15): 2623-2632

Duan X, Chang JH, Ge S, Faulkner RL, Kim JY, Kitabatake Y, Liu XB, Yang CH, Jordan JD, Ma DK, Liu CY, Ganesan S, Cheng HJ, Ming GL, Lu B, Song H (2007) Disrupted-In-Schizophrenia 1 regulates integration of newly generated neurons in the adult brain. *Cell* **130**(6): 1146-1158

Duman RS (2002) Synaptic plasticity and mood disorders. *Mol Psychiatry* **7** (Suppl 1): S29-34

Eastwood SL, Hodgkinson CA, Harrison PJ (2009) DISC-1 Leu607Phe alleles differentially affect centrosomal PCM1 localization and neurotransmitter release. *Mol Psychiatry* **14**(6): 556-557

Eastwood SL, Walker M, Hyde TM, Kleinman JE, Harrison PJ (2010) The DISC1 Ser704Cys substitution affects centrosomal localization of its binding partner PCM1 in glia in human brain. *Hum Mol Genet* **19**(12): 2487-2496

Ekelund J, Hennah W, Hiekkalinna T, Parker A, Meyer J, Lonnqvist J, Peltonen L (2004) Replication of 1q42 linkage in Finnish schizophrenia pedigrees. *Mol Psychiatry* **9**(11): 1037-1041

Ekelund J, Hovatta I, Parker A, Paunio T, Varilo T, Martin R, Suhonen J, Ellonen P, Chan G, Sinsheimer JS, Sobel E, Juvonen H, Arajarvi R, Partonen T, Suvisaari J, Lonnqvist J, Meyer J, Peltonen L (2001) Chromosome 1 loci in Finnish schizophrenia families. *Hum Mol Genet* **10**(15): 1611-1617

Ekelund J, Lichtermann D, Hovatta I, Ellonen P, Suvisaari J, Terwilliger JD, Juvonen H, Varilo T, Arajarvi R, Kokko-Sahin ML, Lonnqvist J, Peltonen L (2000) Genome-wide scan for schizophrenia in the Finnish population: evidence for a locus on chromosome 7q22. *Hum Mol Genet* **9**(7): 1049-1057

Elefteriou F, Ahn JD, Takeda S, Starbuck M, Yang X, Liu X, Kondo H, Richards WG, Bannon TW, Noda M, Clement K, Vaisse C, Karsenty G (2005) Leptin regulation of bone resorption by the sympathetic nervous system and CART. *Nature* **434**(7032): 514-520

Ellison-Wright I, Bullmore E (2009) Meta-analysis of diffusion tensor imaging studies in schizophrenia. *Schizophr Res* **108**(1-3): 3-10

Enomoto A, Asai N, Namba T, Wang Y, Kato T, Tanaka M, Tatsumi H, Taya S, Tsuboi D, Kuroda K, Kaneko N, Sawamoto K, Miyamoto R, Jijiwa M, Murakumo Y, Sokabe M, Seki T, Kaibuchi K, Takahashi M (2009) Roles of disrupted-in-schizophrenia 1-interacting protein girdin in postnatal development of the dentate gyrus. *Neuron* **63**(6): 774-787

Estes SD, Stoler DL, Anderson GR (1995) Normal fibroblasts induce the C/EBP beta and ATF-4 bZIP transcription factors in response to anoxia. *Exp Cell Res* **220**(1): 47-54

Evans KL, Brown J, Shibasaki Y, Devon RS, He L, Arveiler B, Christie S, Maule JC, Baillie D, Slorach EM, et al. (1995) A contiguous clone map over 3 Mb on the long arm of chromosome 11 across a balanced translocation associated with schizophrenia. *Genomics* **28**(3): 420-428

Eykelenboom JE, Briggs GJ, Bradshaw NJ, Soares DC, Ogawa F, Christie S, Malavasi EL, Makedonopoulou P, Mackie S, Malloy MP, Wear MA, Blackburn EA, Bramham J, McIntosh AM, Blackwood DH, Muir WJ, Porteous DJ, Millar JK (2012) A t(1;11) translocation linked to schizophrenia and affective disorders gives rise to aberrant chimeric DISC1 transcripts that encode structurally altered, deleterious mitochondrial proteins. *Hum Mol Genet* **21**(15): 3374-3386

Fatemi SH, Folsom TD (2009) The neurodevelopmental hypothesis of schizophrenia, revisited. *Schizophr Bull* **35**(3): 528-548

Fawcett TW, Martindale JL, Guyton KZ, Hai T, Holbrook NJ (1999) Complexes containing activating transcription factor (ATF)/cAMP-responsive-element-binding protein (CREB) interact with the CCAAT/enhancer-binding protein (C/EBP)-ATF composite site to regulate Gadd153 expression during the stress response. *Biochem J* **339** (Pt 1): 135-141

Fendri C, Mechri A, Khiari G, Othman A, Kerkeni A, Gaha L (2006) [Oxidative stress involvement in schizophrenia pathophysiology: a review]. *Encephale* **32**(2 Pt 1): 244-252

Field T, Diego M (2008) Cortisol: the culprit prenatal stress variable. *Int J Neurosci* **118**(8): 1181

Fink AL (2005) Natively unfolded proteins. *Curr Opin Struct Biol* **15**(1): 35-41

Fischer C, Johnson J, Stillwell B, Conner J, Cerovac Z, Wilson-Rawls J, Rawls A (2004) Activating transcription factor 4 is required for the differentiation of the lamina propria layer of the vas deferens. *Biol Reprod* **70**(2): 371-378

Fiszer-Kierzkowska A, Vydra N, Wysocka-Wycisk A, Kronekova Z, Jarzab M, Lisowska KM, Krawczyk Z (2011) Liposome-based DNA carriers may induce cellular stress response and change gene expression pattern in transfected cells. *BMC Mol Biol* **12**: 27

Fletcher JM, Evans K, Baillie D, Byrd P, Hanratty D, Leach S, Julier C, Gosden JR, Muir W, Porteous DJ, et al. (1993) Schizophrenia-associated chromosome 11q21 translocation: identification of flanking markers and development of chromosome 11q fragment hybrids as cloning and mapping resources. *Am J Hum Genet* **52**(3): 478-490

Frank CL, Ge X, Xie Z, Zhou Y, Tsai LH (2010) Control of activating transcription factor 4 (ATF4) persistence by multisite phosphorylation impacts cell cycle progression and neurogenesis. *J Biol Chem* **285**(43): 33324-33337

Fukuda S, Hashimoto R, Ohi K, Yamaguti K, Nakatomi Y, Yasuda Y, Kamino K, Takeda M, Tajima S, Kuratsune H, Nishizawa Y, Watanabe Y (2010a) A functional polymorphism in the disrupted-in schizophrenia 1 gene is associated with chronic fatigue syndrome. *Life Sci* **86**(19-20): 722-725

Fukuda T, Sugita S, Inatome R, Yanagi S (2010b) CAMDI, a novel disrupted in schizophrenia 1 (DISC1)-binding protein, is required for radial migration. *J Biol Chem* **285**(52): 40554-40561

Fung H, Liu P, Demple B (2007) ATF4-dependent oxidative induction of the DNA repair enzyme Ape1 counteracts arsenite cytotoxicity and suppresses arsenite-mediated mutagenesis. *Mol Cell Biol* **27**(24): 8834-8847

Gachon F, Devaux C, Mesnard JM (2002) Activation of HTLV-I transcription in the presence of Tax is independent of the acetylation of CREB-2 (ATF-4). *Virology* **299**(2): 271-278

Gachon F, Gaudray G, Thebault S, Basbous J, Koffi JA, Devaux C, Mesnard J (2001) The cAMP response element binding protein-2 (CREB-2) can interact with the C/EBP-homologous protein (CHOP). *FEBS Lett* **502**(1-2): 57-62

Gadbois DM, Crissman HA, Tobey RA, Bradbury EM (1992) Multiple kinase arrest points in the G1 phase of nontransformed mammalian cells are absent in transformed cells. *Proc Natl Acad Sci U S A* **89**(18): 8626-8630

Galehdar Z, Swan P, Fuerth B, Callaghan SM, Park DS, Cregan SP (2010) Neuronal apoptosis induced by endoplasmic reticulum stress is regulated by ATF4-CHOP-

mediated induction of the Bcl-2 homology 3-only member PUMA. *J Neurosci* **30**(50): 16938-16948

Gao XM, Sakai K, Roberts RC, Conley RR, Dean B, Tamminga CA (2000) Ionotropic glutamate receptors and expression of N-methyl-D-aspartate receptor subunits in subregions of human hippocampus: effects of schizophrenia. *Am J Psychiatry* **157**(7): 1141-1149

Garver DL, Holcomb JA, Christensen JD (2008) Compromised myelin integrity during psychosis with repair during remission in drug-responding schizophrenia. *Int J Neuropsychopharmacol* **11**(1): 49-61

Gawryluk JW, Wang JF, Andreazza AC, Shao L, Young LT (2011) Decreased levels of glutathione, the major brain antioxidant, in post-mortem prefrontal cortex from patients with psychiatric disorders. *Int J Neuropsychopharmacol* **14**(1): 123-130

Ge X, Frank CL, Calderon de Anda F, Tsai LH (2010) Hook3 interacts with PCM1 to regulate pericentriolar material assembly and the timing of neurogenesis. *Neuron* **65**(2): 191-203

Girard SL, Gauthier J, Noreau A, Xiong L, Zhou S, Jouan L, Dionne-Laporte A, Spiegelman D, Henrion E, Diallo O, Thibodeau P, Bachand I, Bao JY, Tong AH, Lin CH, Millet B, Jaafari N, Joober R, Dion PA, Lok S, Krebs MO, Rouleau GA (2011) Increased exonic de novo mutation rate in individuals with schizophrenia. *Nat Genet* **43**(9): 860-863

Glass DB, Cheng HC, Kemp BE, Walsh DA (1986) Differential and common recognition of the catalytic sites of the cGMP-dependent and cAMP-dependent protein kinases by inhibitory peptides derived from the heat-stable inhibitor protein. *J Biol Chem* **261**(26): 12166-12171

Glass DB, Cheng HC, Mende-Mueller L, Reed J, Walsh DA (1989a) Primary structural determinants essential for potent inhibition of cAMP-dependent protein kinase by inhibitory peptides corresponding to the active portion of the heat-stable inhibitor protein. *J Biol Chem* **264**(15): 8802-8810

Glass DB, Lundquist LJ, Katz BM, Walsh DA (1989b) Protein kinase inhibitor-(6-22)-amide peptide analogs with standard and nonstandard amino acid substitutions for phenylalanine 10. Inhibition of cAMP-dependent protein kinase. *J Biol Chem* **264**(24): 14579-14584

Goessling W, North TE, Loewer S, Lord AM, Lee S, Stoick-Cooper CL, Weidinger G, Puder M, Daley GQ, Moon RT, Zon LI (2009) Genetic interaction of PGE2 and Wnt signaling regulates developmental specification of stem cells and regeneration. *Cell* **136**(6): 1136-1147

Golse B, Debray Q, Puget K, Michelson AM (1978) [Superoxide dismutase 1 and glutathione peroxidase levels in erythrocytes of adult schizophrenics]. *Nouv Presse Med* **7**(23): 2070-2071

Gombart AF, Grewal J, Koeffler HP (2007) ATF4 differentially regulates transcriptional activation of myeloid-specific genes by C/EBPepsilon and C/EBPalpha. *J Leukoc Biol* **81**(6): 1535-1547

Gong F, Alzamora R, Smolak C, Li H, Naveed S, Neumann D, Hallows KR, Pastor-Soler NM (2010) VACUOLAR H+-ATPase APICAL ACCUMULATION IN KIDNEY INTERCALATED CELLS IS REGULATED BY PKA AND AMP-ACTIVATED PROTEIN KINASE. *Am J Physiol Renal Physiol* **298**(5): F1162-F1169

Gottesman, II, Laursen TM, Bertelsen A, Mortensen PB (2010) Severe mental disorders in offspring with 2 psychiatrically ill parents. *Arch Gen Psychiatry* **67**(3): 252-257

Gottesman, II, McGuffin P, Farmer AE (1987) Clinical genetics as clues to the "real" genetics of schizophrenia (a decade of modest gains while playing for time). *Schizophr Bull* **13**(1): 23-47

Granberg F, Svensson C, Pettersson U, Zhao H (2006) Adenovirus-induced alterations in host cell gene expression prior to the onset of viral gene expression. *Virology* **353**(1): 1-5

Green EK, Grozeva D, Jones I, Jones L, Kirov G, Caesar S, Gordon-Smith K, Fraser C, Forty L, Russell E, Hamshere ML, Moskvina V, Nikolov I, Farmer A, McGuffin P, Holmans PA, Owen MJ, O'Donovan MC, Craddock N (2010) The bipolar disorder risk allele at CACNA1C also confers risk of recurrent major depression and of schizophrenia. *Mol Psychiatry* **15**(10): 1016-1022

Green EK, Grozeva D, Sims R, Raybould R, Forty L, Gordon-Smith K, Russell E, St Clair D, Young AH, Ferrier IN, Kirov G, Jones I, Jones L, Owen MJ, O'Donovan MC, Craddock N (2011) DISC1 exon 11 rare variants found more commonly in schizoaffective spectrum cases than controls. *Am J Med Genet B Neuropsychiatr Genet* **156B**(4): 490-492

Green TA, Alibhai IN, Unterberg S, Neve RL, Ghose S, Tamminga CA, Nestler EJ (2008) Induction of activating transcription factors (ATFs) ATF2, ATF3, and ATF4 in the nucleus accumbens and their regulation of emotional behavior. *J Neurosci* **28**(9): 2025-2032

Gustavsson A, Svensson M, Jacobi F, Allgulander C, Alonso J, Beghi E, Dodel R, Ekman M, Faravelli C, Fratiglioni L, Gannon B, Jones DH, Jennum P, Jordanova A, Jonsson L, Karampampa K, Knapp M, Kobelt G, Kurth T, Lieb R, Linde M, Ljungcrantz C, Maercker A, Melin B, Moscarelli M, Musayev A, Norwood F, Preisig M, Pugliatti M, Rehm J, Salvador-Carulla L, Schlehofer B, Simon R, Steinhausen HC, Stovner LJ, Vallat JM, den Bergh PV, van Os J, Vos P, Xu W,

Wittchen HU, Jonsson B, Olesen J (2011) Cost of disorders of the brain in Europe 2010. *Eur Neuropsychopharmacol* **21**(10): 718-779

Hai T, Curran T (1991) Cross-family dimerization of transcription factors Fos/Jun and ATF/CREB alters DNA binding specificity. *Proc Natl Acad Sci U S A* **88**(9): 3720-3724

Hai T, Hartman MG (2001) The molecular biology and nomenclature of the activating transcription factor/cAMP responsive element binding family of transcription factors: activating transcription factor proteins and homeostasis. *Gene* **273**(1): 1-11

Hai TW, Liu F, Coukos WJ, Green MR (1989) Transcription factor ATF cDNA clones: an extensive family of leucine zipper proteins able to selectively form DNA-binding heterodimers. *Genes Dev* **3**(12B): 2083-2090

Hakak Y, Walker JR, Li C, Wong WH, Davis KL, Buxbaum JD, Haroutunian V, Fienberg AA (2001) Genome-wide expression analysis reveals dysregulation of myelination-related genes in chronic schizophrenia. *Proc Natl Acad Sci U S A* **98**(8): 4746-4751

Halliwell B (1992) Reactive oxygen species and the central nervous system. *J Neurochem* **59**(5): 1609-1623

Halterman MW, De Jesus C, Rempe DA, Schor NF, Federoff HJ (2008) Loss of c/EBP-beta activity promotes the adaptive to apoptotic switch in hypoxic cortical neurons. *Mol Cell Neurosci* **38**(2): 125-137

Halterman MW, Gill M, DeJesus C, Ogihara M, Schor NF, Federoff HJ (2010) The endoplasmic reticulum stress response factor CHOP-10 protects against hypoxia-induced neuronal death. *J Biol Chem* **285**(28): 21329-21340

Hamshere ML, Bennett P, Williams N, Segurado R, Cardno A, Norton N, Lambert D, Williams H, Kirov G, Corvin A, Holmans P, Jones L, Jones I, Gill M, O'Donovan MC, Owen MJ, Craddock N (2005) Genomewide linkage scan in schizoaffective disorder: significant evidence for linkage at 1q42 close to DISC1, and suggestive evidence at 22q11 and 19p13. *Arch Gen Psychiatry* **62**(10): 1081-1088

Handy DE, Zhang Y, Loscalzo J (2005) Homocysteine down-regulates cellular glutathione peroxidase (GPx1) by decreasing translation. *J Biol Chem* **280**(16): 15518-15525

Hansen BS, Vaughan MH, Wang L (1972) Reversible inhibition by histidinol of protein synthesis in human cells at the activation of histidine. *J Biol Chem* **247**(12): 3854-3857

Hara T, Nakamura K, Matsui M, Yamamoto A, Nakahara Y, Suzuki-Migishima R, Yokoyama M, Mishima K, Saito I, Okano H, Mizushima N (2006) Suppression of

basal autophagy in neural cells causes neurodegenerative disease in mice. *Nature* **441**(7095): 885-889

Harding HP, Novoa I, Zhang Y, Zeng H, Wek R, Schapira M, Ron D (2000) Regulated translation initiation controls stress-induced gene expression in mammalian cells. *Mol Cell* **6**(5): 1099-1108

Harding HP, Zhang Y, Zeng H, Novoa I, Lu PD, Calfon M, Sadri N, Yun C, Popko B, Paules R, Stojdl DF, Bell JC, Hettmann T, Leiden JM, Ron D (2003) An integrated stress response regulates amino acid metabolism and resistance to oxidative stress. *Mol Cell* **11**(3): 619-633

Haro JM, Novick D, Suarez D, Ochoa S, Roca M (2008) Predictors of the course of illness in outpatients with schizophrenia: a prospective three year study. *Prog Neuropsychopharmacol Biol Psychiatry* **32**(5): 1287-1292

Haroutunian V, Davis KL (2007) Introduction to the special section: Myelin and oligodendrocyte abnormalities in schizophrenia. *Int J Neuropsychopharmacol* **10**(4): 499-502

Harrison PJ (2004) The hippocampus in schizophrenia: a review of the neuropathological evidence and its pathophysiological implications. *Psychopharmacology (Berl)* **174**(1): 151-162

Harrison PJ, Weinberger DR (2005) Schizophrenia genes, gene expression, and neuropathology: on the matter of their convergence. *Mol Psychiatry* **10**(1): 40-68

Hartmann C (2009) Transcriptional networks controlling skeletal development. *Curr Opin Genet Dev* **19**(5): 437-443

Hashimoto R, Numakawa T, Ohnishi T, Kumamaru E, Yagasaki Y, Ishimoto T, Mori T, Nemoto K, Adachi N, Izumi A, Chiba S, Noguchi H, Suzuki T, Iwata N, Ozaki N, Taguchi T, Kamiya A, Kosuga A, Tatsumi M, Kamijima K, Weinberger DR, Sawa A, Kunugi H (2006) Impact of the DISC1 Ser704Cys polymorphism on risk for major depression, brain morphology and ERK signaling. *Hum Mol Genet* **15**(20): 3024-3033

Hattori T, Shimizu S, Koyama Y, Yamada K, Kuwahara R, Kumamoto N, Matsuzaki S, Ito A, Katayama T, Tohyama M (2010) DISC1 regulates cell-cell adhesion, cell-matrix adhesion and neurite outgrowth. *Mol Psychiatry* **15**(8): 778, 798-809

Hayashi-Takagi A, Takaki M, Graziane N, Seshadri S, Murdoch H, Dunlop AJ, Makino Y, Seshadri AJ, Ishizuka K, Srivastava DP, Xie Z, Baraban JM, Houslay MD, Tomoda T, Brandon NJ, Kamiya A, Yan Z, Penzes P, Sawa A (2010) Disrupted-in-Schizophrenia 1 (DISC1) regulates spines of the glutamate synapse via Rac1. *Nat Neurosci* **13**(3): 327-332

Haynes CM, Titus EA, Cooper AA (2004) Degradation of misfolded proteins prevents ER-derived oxidative stress and cell death. *Mol Cell* **15**(5): 767-776

He CH, Gong P, Hu B, Stewart D, Choi ME, Choi AM, Alam J (2001) Identification of activating transcription factor 4 (ATF4) as an Nrf2-interacting protein. Implication for heme oxygenase-1 gene regulation. *J Biol Chem* **276**(24): 20858-20865

Heinecke JW, Rosen H, Suzuki LA, Chait A (1987) The role of sulfur-containing amino acids in superoxide production and modification of low density lipoprotein by arterial smooth muscle cells. *J Biol Chem* **262**(21): 10098-10103

Hemmings BA, Aitken A, Cohen P, Rymond M, Hofmann F (1982) Phosphorylation of the type-II regulatory subunit of cyclic-AMP-dependent protein kinase by glycogen synthase kinase 3 and glycogen synthase kinase 5. *Eur J Biochem* **127**(3): 473-481

Hendricks JC, Williams JA, Panckeri K, Kirk D, Tello M, Yin JC, Sehgal A (2001) A non-circadian role for cAMP signaling and CREB activity in Drosophila rest homeostasis. *Nat Neurosci* **4**(11): 1108-1115

Hennah W, Thomson P, McQuillin A, Bass N, Loukola A, Anjorin A, Blackwood D, Curtis D, Deary IJ, Harris SE, Isometsa ET, Lawrence J, Lonnqvist J, Muir W, Palotie A, Partonen T, Paunio T, Pylkko E, Robinson M, Soronen P, Suominen K, Suvisaari J, Thirumalai S, St Clair D, Gurling H, Peltonen L, Porteous D (2009) DISC1 association, heterogeneity and interplay in schizophrenia and bipolar disorder. *Mol Psychiatry* **14**(9): 865-873

Hennah W, Tomppo L, Hiekkalinna T, Palo OM, Kilpinen H, Ekelund J, Tuulio-Henriksson A, Silander K, Partonen T, Paunio T, Terwilliger JD, Lonnqvist J, Peltonen L (2007) Families with the risk allele of DISC1 reveal a link between schizophrenia and another component of the same molecular pathway, NDE1. *Hum Mol Genet* **16**(5): 453-462

Hennah W, Tuulio-Henriksson A, Paunio T, Ekelund J, Varilo T, Partonen T, Cannon TD, Lonnqvist J, Peltonen L (2005) A haplotype within the DISC1 gene is associated with visual memory functions in families with a high density of schizophrenia. *Mol Psychiatry* **10**(12): 1097-1103

Hennah W, Varilo T, Kestila M, Paunio T, Arajarvi R, Haukka J, Parker A, Martin R, Levitzky S, Partonen T, Meyer J, Lonnqvist J, Peltonen L, Ekelund J (2003) Haplotype transmission analysis provides evidence of association for DISC1 to schizophrenia and suggests sex-dependent effects. *Hum Mol Genet* **12**(23): 3151-3159

Herbst KJ, Allen MD, Zhang J (2009) The cAMP-dependent protein kinase inhibitor H-89 attenuates the bioluminescence signal produced by Renilla Luciferase. *PLoS One* **4**(5): e5642

Hess J, Angel P, Schorpp-Kistner M (2004) AP-1 subunits: quarrel and harmony among siblings. *J Cell Sci* **117**(Pt 25): 5965-5973

Hettmann T, Barton K, Leiden JM (2000) Microphthalmia due to p53-mediated apoptosis of anterior lens epithelial cells in mice lacking the CREB-2 transcription factor. *Dev Biol* **222**(1): 110-123

Hewes RS, Schaefer AM, Taghert PH (2000) The cryptocephal gene (ATF4) encodes multiple basic-leucine zipper proteins controlling molting and metamorphosis in Drosophila. *Genetics* **155**(4): 1711-1723

Higginbotham HR, Gleeson JG (2007) The centrosome in neuronal development. *Trends Neurosci* **30**(6): 276-283

Hikida T, Jaaro-Peled H, Seshadri S, Oishi K, Hookway C, Kong S, Wu D, Xue R, Andrade M, Tankou S, Mori S, Gallagher M, Ishizuka K, Pletnikov M, Kida S, Sawa A (2007) Dominant-negative DISC1 transgenic mice display schizophrenia-associated phenotypes detected by measures translatable to humans. *Proc Natl Acad Sci U S A* **104**(36): 14501-14506

Hodgkinson CA, Goldman D, Jaeger J, Persaud S, Kane JM, Lipsky RH, Malhotra AK (2004) Disrupted in schizophrenia 1 (DISC1): association with schizophrenia, schizoaffective disorder, and bipolar disorder. *Am J Hum Genet* **75**(5): 862-872

Hof PR, Haroutunian V, Friedrich VL, Jr., Byne W, Buitron C, Perl DP, Davis KL (2003) Loss and altered spatial distribution of oligodendrocytes in the superior frontal gyrus in schizophrenia. *Biol Psychiatry* **53**(12): 1075-1085

Hogan MR, Cockram GP, Lu R (2006) Cooperative interaction of Zhangfei and ATF4 in transactivation of the cyclic AMP response element. *FEBS Lett* **580**(1): 58-62

Hotta Y, Ohnuma T, Hanzawa R, Shibata N, Maeshima H, Baba H, Hatano T, Takebayashi Y, Kitazawa M, Higa M, Suzuki T, Arai H (2011) Association study between Disrupted-in-Schizophrenia-1 (DISC1) and Japanese patients with treatment-resistant schizophrenia (TRS). *Prog Neuropsychopharmacol Biol Psychiatry* **35**(2): 636-639

Houslay MD, (2010) Underpinning compartmentalised cAMP signalling through targeted cAMP breakdown. *Trends Biochem Sci* **35**(2): 91-100

Houslay MD, Adams DR (2003) PDE4 cAMP phosphodiesterases: modular enzymes that orchestrate signalling cross-talk, desensitization and compartmentalization. *Biochem J* **370**(Pt 1): 1-18

Hovatta I, Varilo T, Suvisaari J, Terwilliger JD, Ollikainen V, Arajarvi R, Juvonen H, Kokko-Sahin ML, Vaisanen L, Mannila H, Lonnqvist J, Peltonen L (1999) A genomewide screen for schizophrenia genes in an isolated Finnish subpopulation, suggesting multiple susceptibility loci. *Am J Hum Genet* **65**(4): 1114-1124

Howes OD, Kapur S (2009) The dopamine hypothesis of schizophrenia: version III--the final common pathway. *Schizophr Bull* **35**(3): 549-562

Hulshoff Pol HE, Schnack HG, Mandl RC, Cahn W, Collins DL, Evans AC, Kahn RS (2004) Focal white matter density changes in schizophrenia: reduced inter-hemispheric connectivity. *Neuroimage* **21**(1): 27-35

Huston E, Lumb S, Russell A, Catterall C, Ross AH, Steele MR, Bolger GB, Perry MJ, Owens RJ, Houslay MD (1997) Molecular cloning and transient expression in COS7 cells of a novel human PDE4B cAMP-specific phosphodiesterase, HSPDE4B3. *Biochem J* **328**(Pt 2): 549-558

Hwu HG, Liu CM, Fann CS, Ou-Yang WC, Lee SF (2003) Linkage of schizophrenia with chromosome 1q loci in Taiwanese families. *Mol Psychiatry* **8**(4): 445-452

Hyman SE (2007) Can neuroscience be integrated into the DSM-V? *Nat Rev Neurosci* **8**(9): 725-732

Hyman SE (2008) A glimmer of light for neuropsychiatric disorders. *Nature* **455**(7215): 890-893

Ibi D, Nagai T, Koike H, Kitahara Y, Mizoguchi H, Niwa M, Jaaro-Peled H, Nitta A, Yoneda Y, Nabeshima T, Sawa A, Yamada K (2010) Combined effect of neonatal immune activation and mutant DISC1 on phenotypic changes in adulthood. *Behav Brain Res* **206**(1): 32-37

Igarashi T, Izumi H, Uchiumi T, Nishio K, Arao T, Tanabe M, Uramoto H, Sugio K, Yasumoto K, Sasaguri Y, Wang KY, Otsuji Y, Kohno K (2007) Clock and ATF4 transcription system regulates drug resistance in human cancer cell lines. *Oncogene* **26**(33): 4749-4760

Insel PA, Ostrom RS (2003) Forskolin as a tool for examining adenylyl cyclase expression, regulation, and G protein signaling. *Cell Mol Neurobiol* **23**(3): 305-314

Insel TR (2010) Rethinking schizophrenia. *Nature* **468**(7321): 187-193

Ishizuka K, Kamiya A, Oh EC, Kanki H, Seshadri S, Robinson JF, Murdoch H, Dunlop AJ, Kubo K, Furukori K, Huang B, Zeledon M, Hayashi-Takagi A, Okano H, Nakajima K, Houslay MD, Katsanis N, Sawa A (2011) DISC1-dependent switch from progenitor proliferation to migration in the developing cortex. *Nature* **473**(7345): 92-96

Jaaro-Peled H, Hayashi-Takagi A, Seshadri S, Kamiya A, Brandon NJ, Sawa A (2009) Neurodevelopmental mechanisms of schizophrenia: understanding disturbed postnatal brain maturation through neuregulin-1-ErbB4 and DISC1. *Trends Neurosci* **32**(9): 485-495

Jacobs PA, Brunton M, Frackiewitcz A, Newton M, Cook PJL, Robson EB (1970) Studies on a family with three cytogenetic markers. *Ann Hum Genet* **33**(4): 325-336

James R, Adams RR, Christie S, Buchanan SR, Porteous DJ, Millar JK (2004) Disrupted in Schizophrenia 1 (DISC1) is a multicompartmentalized protein that predominantly localizes to mitochondria. *Mol Cell Neurosci* **26**(1): 112-122

Jepsen K, Rosenfeld MG (2002) Biological roles and mechanistic actions of co-repressor complexes. *J Cell Sci* **115**(Pt 4): 689-698

Jin HO, Seo SK, Woo SH, Kim ES, Lee HC, Yoo DH, An S, Choe TB, Lee SJ, Hong SI, Rhee CH, Kim JI, Park IC (2009a) Activating transcription factor 4 and CCAAT/enhancer-binding protein-beta negatively regulate the mammalian target of rapamycin via Redd1 expression in response to oxidative and endoplasmic reticulum stress. *Free Radic Biol Med* **46**(8): 1158-1167

Jin HO, Seo SK, Woo SH, Kim ES, Lee HC, Yoo DH, Choe TB, Hong SI, Kim JI, Park IC (2009b) SP600125 negatively regulates the mammalian target of rapamycin via ATF4-induced Redd1 expression. *FEBS Lett* **583**(1): 123-127

Johnstone M, Thomson PA, Hall J, McIntosh AM, Lawrie SM, Porteous DJ (2011) DISC1 in schizophrenia: genetic mouse models and human genomic imaging. *Schizophr Bull* **37**(1): 14-20

Jones BG, Rose FA, Tudball N (1994) Lipid peroxidation and homocysteine induced toxicity. *Atherosclerosis* **105**(2): 165-170

Jousse C, Deval C, Maurin AC, Parry L, Cherasse Y, Chaveroux C, Lefloch R, Lenormand P, Bruhat A, Fafournoux P (2007) TRB3 inhibits the transcriptional activation of stress-regulated genes by a negative feedback on the ATF4 pathway. *J Biol Chem* **282**(21): 15851-15861

Jungling S, Cibelli G, Czardybon M, Gerdes HH, Thiel G (1994) Differential regulation of chromogranin B and synapsin I gene promoter activity by cAMP and cAMP-dependent protein kinase. *Eur J Biochem* **226**(3): 925-935

Kakiuchi C, Ishiwata M, Nanko S, Kunugi H, Minabe Y, Nakamura K, Mori N, Fujii K, Yamada K, Yoshikawa T, Kato T (2007) Association analysis of ATF4 and ATF5, genes for interacting-proteins of DISC1, in bipolar disorder. *Neurosci Lett* **417**(3): 316-321

Kalderon D, Roberts BL, Richardson WD, Smith AE (1984) A short amino acid sequence able to specify nuclear location. *Cell* **39**(3 Pt 2): 499-509

Kamiya A, Kubo K, Tomoda T, Takaki M, Youn R, Ozeki Y, Sawamura N, Park U, Kudo C, Okawa M, Ross CA, Hatten ME, Nakajima K, Sawa A (2005) A schizophrenia-associated mutation of DISC1 perturbs cerebral cortex development. *Nat Cell Biol* **7**(12): 1167-1178

Kamiya A, Tan PL, Kubo K, Engelhard C, Ishizuka K, Kubo A, Tsukita S, Pulver AE, Nakajima K, Cascella NG, Katsanis N, Sawa A (2008) Recruitment of PCM1 to the centrosome by the cooperative action of DISC1 and BBS4: a candidate for psychiatric illnesses. *Arch Gen Psychiatry* **65**(9): 996-1006

Kamiya A, Tomoda T, Chang J, Takaki M, Zhan C, Morita M, Cascio MB, Elashvili S, Koizumi H, Takanezawa Y, Dickerson F, Yolken R, Arai H, Sawa A (2006) DISC1-NDEL1/NUDEL protein interaction, an essential component for neurite outgrowth, is modulated by genetic variations of DISC1. *Hum Mol Genet* **15**(22): 3313-3323

Kandel ER (2001) The molecular biology of memory storage: a dialogue between genes and synapses. *Science* **294**(5544): 1030-1038

Kanes SJ, Tokarczyk J, Siegel SJ, Bilker W, Abel T, Kelly MP (2007) Rolipram: a specific phosphodiesterase 4 inhibitor with potential antipsychotic activity. *Neuroscience* **144**(1): 239-246

Kantor L, Pinchasi D, Mintz M, Hathout Y, Vanderver A, Elroy-Stein O (2008) A point mutation in translation initiation factor 2B leads to a continuous hyper stress state in oligodendroglial-derived cells. *PLoS One* **3**(11): e3783

Kantrowitz JT, Javitt DC (2010) N-methyl-d-aspartate (NMDA) receptor dysfunction or dysregulation: the final common pathway on the road to schizophrenia? *Brain Res Bull* **83**(3-4): 108-121

Karpinski BA, Morle GD, Huggenvik J, Uhler MD, Leiden JM (1992) Molecular cloning of human CREB-2: an ATF/CREB transcription factor that can negatively regulate transcription from the cAMP response element. *Proc Natl Acad Sci U S A* **89**(11): 4820-4824

Kase H, Iwahashi K, Nakanishi S, Matsuda Y, Yamada K, Takahashi M, Murakata C, Sato A, Kaneko M (1987) K-252 compounds, novel and potent inhibitors of protein kinase C and cyclic nucleotide-dependent protein kinases. *Biochem Biophys Res Commun* **142**(2): 436-440

Katsel P, Tan W, Abazyan B, Davis KL, Ross C, Pletnikov MV, Haroutunian V (2011) Expression of mutant human DISC1 in mice supports abnormalities in differentiation of oligodendrocytes. *Schizophr Res* **130**(1-3): 238-249

Kendell RE, Brockington IF (1980) The identification of disease entities and the relationship between schizophrenic and affective psychoses. *Br J Psychiatry* **137**: 324-331

Kendler KS, Gatz M, Gardner CO, Pedersen NL (2006) A Swedish national twin study of lifetime major depression. *Am J Psychiatry* **163**(1): 109-114

Kessler RC, Aguilar-Gaxiola S, Alonso J, Chatterji S, Lee S, Ormel J, Ustun TB, Wang PS (2009) The global burden of mental disorders: an update from the WHO World Mental Health (WMH) surveys. *Epidemiol Psichiatr Soc* **18**(1): 23-33

Kilberg MS, Shan J, Su N (2009) ATF4-dependent transcription mediates signaling of amino acid limitation. *Trends Endocrinol Metab* **20**(9): 436-443

Kim HJ, Park HJ, Jung KH, Ban JY, Ra J, Kim JW, Park JK, Choe BK, Yim SV, Kwon YK, Chung JH (2008) Association study of polymorphisms between DISC1 and schizophrenia in a Korean population. *Neurosci Lett* **430**(1): 60-63

Kim HS, Choi Y, Shin KY, Joo Y, Lee YK, Jung SY, Suh YH, Kim JH (2007) Swedish amyloid precursor protein mutation increases phosphorylation of eIF2alpha in vitro and in vivo. *J Neurosci Res* **85**(7): 1528-1537

Kim JY, Duan X, Liu CY, Jang MH, Guo JU, Pow-anpongkul N, Kang E, Song H, Ming GL (2009) DISC1 regulates new neuron development in the adult brain via modulation of AKT-mTOR signaling through KIAA1212. *Neuron* **63**(6): 761-773

Kim JY, Liu CY, Zhang F, Duan X, Wen Z, Song J, Feighery E, Lu B, Rujescu D, St Clair D, Christian K, Callicott JH, Weinberger DR, Song H, Ming GL (2012) Interplay between DISC1 and GABA signaling regulates neurogenesis in mice and risk for schizophrenia. *Cell* **148**(5): 1051-1064

Kim SM, Yoon SY, Choi JE, Park JS, Choi JM, Nguyen T, Kim DH (2010) Activation of eukaryotic initiation factor-2 alpha-kinases in okadaic acid-treated neurons. *Neuroscience* **169**(4): 1831-1839

Kim YT, Wu CF (1996) Reduced growth cone motility in cultured neurons from Drosophila memory mutants with a defective cAMP cascade. *J Neurosci* **16**(18): 5593-5602

Kirkpatrick B, Xu L, Cascella N, Ozeki Y, Sawa A, Roberts RC (2006) DISC1 immunoreactivity at the light and ultrastructural level in the human neocortex. *J Comp Neurol* **497**(3): 436-450

Kochunov P, Thompson PM, Lancaster JL, Bartzokis G, Smith S, Coyle T, Royall DR, Laird A, Fox PT (2007) Relationship between white matter fractional anisotropy and other indices of cerebral health in normal aging: tract-based spatial statistics study of aging. *Neuroimage* **35**(2): 478-487

Koditz J, Nesper J, Wottawa M, Stiehl DP, Camenisch G, Franke C, Myllyharju J, Wenger RH, Katschinski DM (2007) Oxygen-dependent ATF-4 stability is mediated by the PHD3 oxygen sensor. *Blood* **110**(10): 3610-3617

Kohen R, Nyska A (2002) Oxidation of biological systems: oxidative stress phenomena, antioxidants, redox reactions, and methods for their quantification. *Toxicol Pathol* **30**(6): 620-650

Koike H, Arguello PA, Kvajo M, Karayiorgou M, Gogos JA (2006) Disc1 is mutated in the 129S6/SvEv strain and modulates working memory in mice. *Proc Natl Acad Sci U S A* **103**(10): 3693-3697

Komatsu M, Waguri S, Chiba T, Murata S, Iwata J, Tanida I, Ueno T, Koike M, Uchiyama Y, Kominami E, Tanaka K (2006) Loss of autophagy in the central nervous system causes neurodegeneration in mice. *Nature* **441**(7095): 880-884

Konopaske GT, Dorph-Petersen KA, Sweet RA, Pierri JN, Zhang W, Sampson AR, Lewis DA (2008) Effect of chronic antipsychotic exposure on astrocyte and oligodendrocyte numbers in macaque monkeys. *Biol Psychiatry* **63**(8): 759-765

Koyanagi S, Hamdan AM, Horiguchi M, Kusunose N, Okamoto A, Matsunaga N, Ohdo S (2011) cAMP-response element (CRE)-mediated transcription by activating transcription factor-4 (ATF4) is essential for circadian expression of the Period2 gene. *J Biol Chem* **286**(37): 32416-32423

Kubo K, Tomita K, Uto A, Kuroda K, Seshadri S, Cohen J, Kaibuchi K, Kamiya A, Nakajima K (2010) Migration defects by DISC1 knockdown in C57BL/6, 129X1/SvJ, and ICR strains via in utero gene transfer and virus-mediated RNAi. *Biochem Biophys Res Commun* **400**(4): 631-637

Kuijpers M, Hoogenraad CC (2011) Centrosomes, microtubules and neuronal development. *Mol Cell Neurosci* **48**(4): 349-358

Kumar P, Walsh DA (2002) A dual-specificity isoform of the protein kinase inhibitor PKI produced by alternate gene splicing. *Biochem J* **362**(Pt 3): 533-537

Kuroda K, Yamada S, Tanaka M, Iizuka M, Yano H, Mori D, Tsuboi D, Nishioka T, Namba T, Iizuka Y, Kubota S, Nagai T, Ibi D, Wang R, Enomoto A, Isotani-Sakakibara M, Asai N, Kimura K, Kiyonari H, Abe T, Mizoguchi A, Sokabe M, Takahashi M, Yamada K, Kaibuchi K (2011) Behavioral alterations associated with targeted disruption of exons 2 and 3 of the Disc1 gene in the mouse. *Hum Mol Genet* **20**(23): 4666-4683

Kvajo M, McKellar H, Arguello PA, Drew LJ, Moore H, MacDermott AB, Karayiorgou M, Gogos JA (2008) A mutation in mouse Disc1 that models a schizophrenia risk allele leads to specific alterations in neuronal architecture and cognition. *Proc Natl Acad Sci U S A* **105**(19): 7076-7081

la Cour T, Kiemer L, Molgaard A, Gupta R, Skriver K, Brunak S (2004) Analysis and prediction of leucine-rich nuclear export signals. *Protein Eng Des Sel* **17**(6): 527-536

Lagerberg TV, Sundet K, Aminoff SR, Berg AO, Ringen PA, Andreassen OA, Melle I (2011) Excessive cannabis use is associated with earlier age at onset in bipolar disorder. *Eur Arch Psychiatry Clin Neurosci* **261**(6): 397-405

Lai KO, Zhao Y, Ch'ng TH, Martin KC (2008) Importin-mediated retrograde transport of CREB2 from distal processes to the nucleus in neurons. *Proc Natl Acad Sci U S A* **105**(44): 17175-17180

Lander ES (1996) The new genomics: global views of biology. *Science* **274**(5287): 536-539

Lange PS, Chavez JC, Pinto JT, Coppola G, Sun CW, Townes TM, Geschwind DH, Ratan RR (2008) ATF4 is an oxidative stress-inducible, prodeath transcription factor in neurons in vitro and in vivo. *J Exp Med* **205**(5): 1227-1242

Lassot I, Estrabaud E, Emiliani S, Benkirane M, Benarous R, Margottin-Goguet F (2005) p300 modulates ATF4 stability and transcriptional activity independently of its acetyltransferase domain. *J Biol Chem* **280**(50): 41537-41545

Lassot I, Segeral E, Berlioz-Torrent C, Durand H, Groussin L, Hai T, Benarous R, Margottin-Goguet F (2001) ATF4 degradation relies on a phosphorylation-dependent interaction with the SCF(betaTrCP) ubiquitin ligase. *Mol Cell Biol* **21**(6): 2192-2202

Lee FH, Fadel MP, Preston-Maher K, Cordes SP, Clapcote SJ, Price DJ, Roder JC, Wong AH (2011) Disc1 point mutations in mice affect development of the cerebral cortex. *J Neurosci* **31**(9): 3197-3206

Lee JA, Kim H, Lee YS, Kaang BK (2003) Overexpression and RNA interference of Ap-cyclic AMP-response element binding protein-2, a repressor of long-term facilitation, in Aplysia kurodai sensory-to-motor synapses. *Neurosci Lett* **337**(1): 9-12

Leliveld SR, Bader V, Hendriks P, Prikulis I, Sajnani G, Requena JR, Korth C (2008) Insolubility of disrupted-in-schizophrenia 1 disrupts oligomer-dependent interactions with nuclear distribution element 1 and is associated with sporadic mental disease. *J Neurosci* **28**(15): 3839-3845

Leliveld SR, Hendriks P, Michel M, Sajnani G, Bader V, Trossbach S, Prikulis I, Hartmann R, Jonas E, Willbold D, Requena JR, Korth C (2009) Oligomer assembly of the C-terminal DISC1 domain (640-854) is controlled by self-association motifs and disease-associated polymorphism S704C. *Biochemistry* **48**(32): 7746-7755

Lepagnol-Bestel AM, Dubertret C, Benmessaoud D, Simonneau M, Ades J, Kacha F, Hamdani N, Gorwood P, Ramoz N (2010) Association of DISC1 gene with schizophrenia in families from two distinct French and Algerian populations. *Psychiatr Genet* **20**(6): 298-303

Levine J, Stahl Z, Sela BA, Gavendo S, Ruderman V, Belmaker RH (2002) Elevated homocysteine levels in young male patients with schizophrenia. *Am J Psychiatry* **159**(10): 1790-1792

Levine J, Stahl Z, Sela BA, Ruderman V, Shumaico O, Babushkin I, Osher Y, Bersudsky Y, Belmaker RH (2006) Homocysteine-reducing strategies improve symptoms in chronic schizophrenic patients with hyperhomocysteinemia. *Biol Psychiatry* **60**(3): 265-269

Leweke FM, Koethe D (2008) Cannabis and psychiatric disorders: it is not only addiction. *Addict Biol* **13**(2): 264-275

Lewerenz J, Maher P (2009) Basal levels of eIF2alpha phosphorylation determine cellular antioxidant status by regulating ATF4 and xCT expression. *J Biol Chem* **284**(2): 1106-1115

Lewerenz J, Sato H, Albrecht P, Henke N, Noack R, Methner A, Maher P (2012) Mutation of ATF4 mediates resistance of neuronal cell lines against oxidative stress by inducing xCT expression. *Cell Death Differ* **19**(5): 847-858

Lewis CM, Levinson DF, Wise LH, DeLisi LE, Straub RE, Hovatta I, Williams NM, Schwab SG, Pulver AE, Faraone SV, Brzustowicz LM, Kaufmann CA, Garver DL, Gurling HM, Lindholm E, Coon H, Moises HW, Byerley W, Shaw SH, Mesen A, Sherrington R, O'Neill FA, Walsh D, Kendler KS, Ekelund J, Paunio T, Lonnqvist J, Peltonen L, O'Donovan MC, Owen MJ, Wildenauer DB, Maier W, Nestadt G, Blouin JL, Antonarakis SE, Mowry BJ, Silverman JM, Crowe RR, Cloninger CR, Tsuang MT, Malaspina D, Harkavy-Friedman JM, Svrakic DM, Bassett AS, Holcomb J, Kalsi G, McQuillin A, Brynjolfson J, Sigmundsson T, Petursson H, Jazin E, Zoega T, Helgason T (2003) Genome scan meta-analysis of schizophrenia and bipolar disorder, part II: Schizophrenia. *Am J Hum Genet* **73**(1): 34-48

Lewis DA, Hashimoto T, Volk DW (2005) Cortical inhibitory neurons and schizophrenia. *Nat Rev Neurosci* **6**(4): 312-324

Lewis DA, Levitt P (2002) Schizophrenia as a disorder of neurodevelopment. *Annu Rev Neurosci* **25**: 409-432

Li W, Zhou Y, Jentsch JD, Brown RA, Tian X, Ehninger D, Hennah W, Peltonen L, Lonnqvist J, Huttunen MO, Kaprio J, Trachtenberg JT, Silva AJ, Cannon TD (2007a) Specific developmental disruption of disrupted-in-schizophrenia-1 function results in schizophrenia-related phenotypes in mice. *Proc Natl Acad Sci U S A* **104**(46): 18280-18285

Li YF, Cheng YF, Huang Y, Conti M, Wilson SP, O'Donnell JM, Zhang HT (2011) Phosphodiesterase-4D knock-out and RNA interference-mediated knock-down enhance memory and increase hippocampal neurogenesis via increased cAMP signaling. *J Neurosci* **31**(1): 172-183

Li YF, Huang Y, Amsdell SL, Xiao L, O'Donnell JM, Zhang HT (2009) Antidepressant- and anxiolytic-like effects of the phosphodiesterase-4 inhibitor rolipram on behavior depend on cyclic AMP response element binding protein-

mediated neurogenesis in the hippocampus. *Neuropsychopharmacology* **34**(11): 2404-2419

Li Z, Dong T, Proschel C, Noble M (2007b) Chemically diverse toxicants converge on Fyn and c-Cbl to disrupt precursor cell function. *PLoS Biol* **5**(2): e35

Liang G, Hai T (1997) Characterization of human activating transcription factor 4, a transcriptional activator that interacts with multiple domains of cAMP-responsive element-binding protein (CREB)-binding protein. *J Biol Chem* **272**(38): 24088-24095

Lichtenstein P, Yip BH, Bjork C, Pawitan Y, Cannon TD, Sullivan PF, Hultman CM (2009) Common genetic determinants of schizophrenia and bipolar disorder in Swedish families: a population-based study. *Lancet* **373**(9659): 234-239

Lin MT, Beal MF (2006) Mitochondrial dysfunction and oxidative stress in neurodegenerative diseases. *Nature* **443**(7113): 787-795

Lipina TV, Kaidanovich-Beilin O, Patel S, Wang M, Clapcote SJ, Liu F, Woodgett JR, Roder JC (2011a) Genetic and pharmacological evidence for schizophrenia-related Disc1 interaction with GSK-3. *Synapse* **65**(3): 234-248

Lipina TV, Niwa M, Jaaro-Peled H, Fletcher PJ, Seeman P, Sawa A, Roder JC (2010) Enhanced dopamine function in DISC1-L100P mutant mice: implications for schizophrenia. *Genes Brain Behav* **9**(7): 777-789

Lipina TV, Wang M, Liu F, Roder JC (2011b) Synergistic interactions between PDE4B and GSK-3: DISC1 mutant mice. *Neuropharmacology* **62**(3): 1252-1262

Lipska BK, Peters T, Hyde TM, Halim N, Horowitz C, Mitkus S, Weickert CS, Matsumoto M, Sawa A, Straub RE, Vakkalanka R, Herman MM, Weinberger DR, Kleinman JE (2006) Expression of DISC1 binding partners is reduced in schizophrenia and associated with DISC1 SNPs. *Hum Mol Genet* **15**(8): 1245-1258

Lockwood TD (2000) Redox control of protein degradation. *Antioxid Redox Signal* **2**(4): 851-878

Lu PD, Harding HP, Ron D (2004) Translation reinitiation at alternative open reading frames regulates gene expression in an integrated stress response. *J Cell Biol* **167**(1): 27-33

Luo S, Baumeister P, Yang S, Abcouwer SF, Lee AS (2003) Induction of Grp78/BiP by translational block: activation of the Grp78 promoter by ATF4 through and upstream ATF/CRE site independent of the endoplasmic reticulum stress elements. *J Biol Chem* **278**(39): 37375-37385

Ma L, Liu Y, Ky B, Shughrue PJ, Austin CP, Morris JA (2002a) Cloning and characterization of Disc1, the mouse ortholog of DISC1 (Disrupted-in-Schizophrenia 1). *Genomics* **80**(6): 662-672

Ma Y, Brewer JW, Diehl JA, Hendershot LM (2002b) Two distinct stress signaling pathways converge upon the CHOP promoter during the mammalian unfolded protein response. *J Mol Biol* **318**(5): 1351-1365

Macgregor S, Visscher PM, Knott SA, Thomson P, Porteous DJ, Millar JK, Devon RS, Blackwood D, Muir WJ (2004) A genome scan and follow-up study identify a bipolar disorder susceptibility locus on chromosome 1q42. *Mol Psychiatry* **9**(12): 1083-1090

MacKenzie SJ, Baillie GS, McPhee I, MacKenzie C, Seamons R, McSorley T, Millen J, Beard MB, van Heeke G, Houslay MD (2002) Long PDE4 cAMP specific phosphodiesterases are activated by protein kinase A-mediated phosphorylation of a single serine residue in Upstream Conserved Region 1 (UCR1). *Br J Pharmacol* **136**(3): 421-433

MacKenzie SJ, Houslay MD (2000) Action of rolipram on specific PDE4 cAMP phosphodiesterase isoforms and on the phosphorylation of cAMP-response-element-binding protein (CREB) and p38 mitogen-activated protein (MAP) kinase in U937 monocytic cells. *Biochem J* **347**(Pt 2): 571-578

Mackie S, Millar JK, Porteous DJ (2007) Role of DISC1 in neural development and schizophrenia. *Curr Opin Neurobiol* **17**(1): 95-102

Mao Y, Ge X, Frank CL, Madison JM, Koehler AN, Doud MK, Tassa C, Berry EM, Soda T, Singh KK, Biechele T, Petryshen TL, Moon RT, Haggarty SJ, Tsai LH (2009) Disrupted in schizophrenia 1 regulates neuronal progenitor proliferation via modulation of GSK3beta/beta-catenin signaling. *Cell* **136**(6): 1017-1031

Markham JA, Koenig JI (2011) Prenatal stress: role in psychotic and depressive diseases. *Psychopharmacology (Berl)* **214**(1): 89-106

Marley A, von Zastrow M (2010) DISC1 regulates primary cilia that display specific dopamine receptors. *PLoS One* **5**(5): e10902

Martins-de-Souza D (2010) Proteome and transcriptome analysis suggests oligodendrocyte dysfunction in schizophrenia. *J Psychiatr Res* **44**(3): 149-156

Masuoka HC, Townes TM (2002) Targeted disruption of the activating transcription factor 4 gene results in severe fetal anemia in mice. *Blood* **99**(3): 736-745

Mathieson I, Munafo MR, Flint J (2011) Meta-analysis indicates that common variants at the DISC1 locus are not associated with schizophrenia. *Mol Psychiatry*

Maxwell CR, Kanes SJ, Abel T, Siegel SJ (2004) Phosphodiesterase inhibitors: a novel mechanism for receptor-independent antipsychotic medications. *Neuroscience* **129**(1): 101-107

McClellan JM, Susser E, King MC (2007) Schizophrenia: a common disease caused by multiple rare alleles. *Br J Psychiatry* **190**: 194-199

McCullumsmith RE, Kristiansen LV, Beneyto M, Scarr E, Dean B, Meador-Woodruff JH (2007) Decreased NR1, NR2A, and SAP102 transcript expression in the hippocampus in bipolar disorder. *Brain Res* **1127**(1): 108-118

McGuffin P, Katz R (1989) The genetics of depression and manic-depressive disorder. *Br J Psychiatry* **155**: 294-304

McGuffin P, Rijsdijk F, Andrew M, Sham P, Katz R, Cardno A (2003) The heritability of bipolar affective disorder and the genetic relationship to unipolar depression. *Arch Gen Psychiatry* **60**(5): 497-502

McIntosh AM, Hall J, Lymer GK, Sussmann JE, Lawrie SM (2009) Genetic risk for white matter abnormalities in bipolar disorder. *Int Rev Psychiatry* **21**(4): 387-393

McLaurin J, Trudel GC, Shaw IT, Antel JP, Cashman NR (1995) A human glial hybrid cell line differentially expressing genes subserving oligodendrocyte and astrocyte phenotype. *J Neurobiol* **26**(2): 283-293

Meador-Woodruff JH, Clinton SM, Beneyto M, McCullumsmith RE (2003) Molecular abnormalities of the glutamate synapse in the thalamus in schizophrenia. *Ann N Y Acad Sci* **1003**: 75-93

Meyer KD, Morris JA (2008) Immunohistochemical analysis of Disc1 expression in the developing and adult hippocampus. *Gene Expr Patterns* **8**(7-8): 494-501

Meyer KD, Morris JA (2009) Disc1 regulates granule cell migration in the developing hippocampus. *Hum Mol Genet* **18**(17): 3286-3297

Mico JA, Rojas-Corrales MO, Gibert-Rahola J, Parellada M, Moreno D, Fraguas D, Graell M, Gil J, Irazusta J, Castro-Fornieles J, Soutullo C, Arango C, Otero S, Navarro A, Baeza I, Martinez-Cengotitabengoa M, Gonzalez-Pinto A (2011) Reduced antioxidant defense in early onset first-episode psychosis: a case-control study. *BMC Psychiatry* **11**: 26

Mielnicki LM, Pruitt SC (1991) Isolation and nucleotide sequence of a murine cDNA homologous to human activating transcription factor 4. *Nucleic Acids Res* **19**(22): 6332

Milani M, Rzymski T, Mellor HR, Pike L, Bottini A, Generali D, Harris AL (2009) The role of ATF4 stabilization and autophagy in resistance of breast cancer cells treated with Bortezomib. *Cancer Res* **69**(10): 4415-4423

Millar JK, Brown J, Maule JC, Shibasaki Y, Christie S, Lawson D, Anderson S, Wilson-Annan JC, Devon RS, St Clair DM, Blackwood DH, Muir WJ, Porteous DJ (1998) A long-range restriction map across 3 Mb of the chromosome 11 breakpoint region of a translocation linked to schizophrenia: localization of the breakpoint and the search for neighbouring genes. *Psychiatr Genet* **8**(3): 175-181

Millar JK, Christie S, Anderson S, Lawson D, Hsiao-Wei Loh D, Devon RS, Arveiler B, Muir WJ, Blackwood DH, Porteous DJ (2001) Genomic structure and localisation within a linkage hotspot of Disrupted In Schizophrenia 1, a gene disrupted by a translocation segregating with schizophrenia. *Mol Psychiatry* **6**(2): 173-178

Millar JK, Christie S, Porteous DJ (2003) Yeast two-hybrid screens implicate DISC1 in brain development and function. *Biochem Biophys Res Commun* **311**(4): 1019-1025

Millar JK, Christie S, Semple CA, Porteous DJ (2000a) Chromosomal location and genomic structure of the human translin-associated factor X gene (TRAX; TSNAX) revealed by intergenic splicing to DISC1, a gene disrupted by a translocation segregating with schizophrenia. *Genomics* **67**(1): 69-77

Millar JK, James R, Christie S, Porteous DJ (2005a) Disrupted in schizophrenia 1 (DISC1): subcellular targeting and induction of ring mitochondria. *Mol Cell Neurosci* **30**(4): 477-484

Millar JK, Pickard BS, Mackie S, James R, Christie S, Buchanan SR, Malloy MP, Chubb JE, Huston E, Baillie GS, Thomson PA, Hill EV, Brandon NJ, Rain JC, Camargo LM, Whiting PJ, Houslay MD, Blackwood DH, Muir WJ, Porteous DJ (2005b) DISC1 and PDE4B are interacting genetic factors in schizophrenia that regulate cAMP signaling. *Science* **310**(5751): 1187-1191

Millar JK, Wilson-Annan JC, Anderson S, Christie S, Taylor MS, Semple CA, Devon RS, Clair DM, Muir WJ, Blackwood DH, Porteous DJ (2000b) Disruption of two novel genes by a translocation co-segregating with schizophrenia. *Hum Mol Genet* **9**(9): 1415-1423

Miller B, Messias E, Miettunen J, Alaraisanen A, Jarvelin MR, Koponen H, Rasanen P, Isohanni M, Kirkpatrick B (2011) Meta-analysis of paternal age and schizophrenia risk in male versus female offspring. *Schizophr Bull* **37**(5): 1039-1047

Mitchell KJ, Porteous DJ (2011) Rethinking the genetic architecture of schizophrenia. *Psychol Med* **41**(1): 19-32

Mitsuda T, Hayakawa Y, Itoh M, Ohta K, Nakagawa T (2007) ATF4 regulates gamma-secretase activity during amino acid imbalance. *Biochem Biophys Res Commun* **352**(3): 722-727

Miyamoto N, Izumi H, Miyamoto R, Bin H, Kondo H, Tawara A, Sasaguri Y, Kohno K (2011) Transcriptional regulation of activating transcription factor 4 under oxidative

stress in retinal pigment epithelial ARPE-19/HPV-16 cells. *Invest Ophthalmol Vis Sci* **52**(3): 1226-1234

Miyoshi K, Asanuma M, Miyazaki I, Diaz-Corrales FJ, Katayama T, Tohyama M, Ogawa N (2004) DISC1 localizes to the centrosome by binding to kendrin. *Biochem Biophys Res Commun* **317**(4): 1195-1199

Miyoshi K, Honda A, Baba K, Taniguchi M, Oono K, Fujita T, Kuroda S, Katayama T, Tohyama M (2003) Disrupted-In-Schizophrenia 1, a candidate gene for schizophrenia, participates in neurite outgrowth. *Mol Psychiatry* **8**(7): 685-694

Moens LN, De Rijk P, Reumers J, Van den Bossche MJ, Glassee W, De Zutter S, Lenaerts AS, Nordin A, Nilsson LG, Medina Castello I, Norrback KF, Goossens D, Van Steen K, Adolfsson R, Del-Favero J (2011) Sequencing of DISC1 pathway genes reveals increased burden of rare missense variants in schizophrenia patients from a northern Swedish population. *PLoS One* **6**(8): e23450

Morris JA, Kandpal G, Ma L, Austin CP (2003) DISC1 (Disrupted-In-Schizophrenia 1) is a centrosome-associated protein that interacts with MAP1A, MIPT3, ATF4/5 and NUDEL: regulation and loss of interaction with mutation. *Hum Mol Genet* **12**(13): 1591-1608

Mortensen PB, Pedersen CB, McGrath JJ, Hougaard DM, Norgaard-Petersen B, Mors O, Borglum AD, Yolken RH (2011) Neonatal antibodies to infectious agents and risk of bipolar disorder: a population-based case-control study. *Bipolar Disord* **13**(7-8): 624-629

Mouaffak F, Kebir O, Chayet M, Tordjman S, Vacheron MN, Millet B, Jaafari N, Bellon A, Olie JP, Krebs MO (2011) Association of Disrupted in Schizophrenia 1 (DISC1) missense variants with ultra-resistant schizophrenia. *Pharmacogenomics J* **11**(4): 267-273

Mowry BJ, Holmans PA, Pulver AE, Gejman PV, Riley B, Williams NM, Laurent C, Schwab SG, Wildenauer DB, Bauche S, Owen MJ, Wormley B, Sanders AR, Nestadt G, Liang KY, Duan J, Ribble R, Norton N, Soubigou S, Maier W, Ewen-White KR, DeMarchi N, Carpenter B, Walsh D, Williams H, Jay M, Albus M, Nertney DA, Papadimitriou G, O'Neill A, O'Donovan MC, Deleuze JF, Lerer FB, Dikeos D, Kendler KS, Mallet J, Silverman JM, Crowe RR, Levinson DF (2004) Multicenter linkage study of schizophrenia loci on chromosome 22q. *Mol Psychiatry* **9**(8): 784-795

Muir T, Wilson-Rawls J, Stevens JD, Rawls A, Schweitzer R, Kang C, Skinner MK (2008) Integration of CREB and bHLH transcriptional signaling pathways through direct heterodimerization of the proteins: role in muscle and testis development. *Mol Reprod Dev* **75**(11): 1637-1652

Muir WJ, Gosden CM, Brookes AJ, Fantes J, Evans KL, Maguire SM, Stevenson B, Boyle S, Blackwood DH, St Clair DM, et al. (1995) Direct microdissection and

microcloning of a translocation breakpoint region, t(1;11)(q42.2;q21), associated with schizophrenia. *Cytogenet Cell Genet* **70**(1-2): 35-40

Muntjewerff JW, Hoogendoorn ML, Kahn RS, Sinke RJ, Den Heijer M, Kluijtmans LA, Blom HJ (2005) Hyperhomocysteinemia, methylenetetrahydrofolate reductase 677TT genotype, and the risk for schizophrenia: a Dutch population based case-control study. *Am J Med Genet B Neuropsychiatr Genet* **135B**(1): 69-72

Muntjewerff JW, Kahn RS, Blom HJ, den Heijer M (2006) Homocysteine, methylenetetrahydrofolate reductase and risk of schizophrenia: a meta-analysis. *Mol Psychiatry* **11**(2): 143-149

Murdoch H, Mackie S, Collins DM, Hill EV, Bolger GB, Klussmann E, Porteous DJ, Millar JK, Houslay MD (2007) Isoform-selective susceptibility of DISC1/phosphodiesterase-4 complexes to dissociation by elevated intracellular cAMP levels. *J Neurosci* **27**(35): 9513-9524

Murray CJ, Lopez AD (1996) Evidence-based health policy--lessons from the Global Burden of Disease Study. *Science* **274**(5288): 740-743

Nagai T, Ibi D, Yamada K (2011a) Animal model for schizophrenia that reflects gene-environment interactions. *Biol Pharm Bull* **34**(9): 1364-1368

Nagai T, Kitahara Y, Ibi D, Nabeshima T, Sawa A, Yamada K (2011b) Effects of antipsychotics on the behavioral deficits in human dominant-negative DISC1 transgenic mice with neonatal polyI:C treatment. *Behav Brain Res* **225**(1): 305-310

Nakai K, Horton P (1999) PSORT: a program for detecting sorting signals in proteins and predicting their subcellular localization. *Trends Biochem Sci* **24**(1): 34-36

Nakata K, Lipska BK, Hyde TM, Ye T, Newburn EN, Morita Y, Vakkalanka R, Barenboim M, Sei Y, Weinberger DR, Kleinman JE (2009) DISC1 splice variants are upregulated in schizophrenia and associated with risk polymorphisms. *Proc Natl Acad Sci U S A* **106**(37): 15873-15878

Napal O, Ojeda N, Elizagarate E, Pena J, Ezcurra J, Gutierrez M (2012) The course of the schizophrenia and its impact on cognition: a review of literature. *Actas Esp Psiquiatr* **40**(4): 198-220

Narayanan S, Arthanari H, Wolfe MS, Wagner G (2011) Molecular Characterization of Disrupted in Schizophrenia-1 Risk Variant S704C Reveals the Formation of Altered Oligomeric Assembly. *J Biol Chem* **286**(51): 44266-44276

Nedvetsky PI, Tabor V, Tamma G, Beulshausen S, Skroblin P, Kirschner A, Mutig K, Boltzen M, Petrucci O, Vossenkamper A, Wiesner B, Bachmann S, Rosenthal W, Klussmann E (2010) Reciprocal regulation of aquaporin-2 abundance and degradation by protein kinase A and p38-MAP kinase. *J Am Soc Nephrol* **21**(10): 1645-1656

Nehring RB, Horikawa HP, El Far O, Kneussel M, Brandstatter JH, Stamm S, Wischmeyer E, Betz H, Karschin A (2000) The metabotropic GABAB receptor directly interacts with the activating transcription factor 4. *J Biol Chem* **275**(45): 35185-35191

Ng F, Berk M, Dean O, Bush AI (2008) Oxidative stress in psychiatric disorders: evidence base and therapeutic implications. *Int J Neuropsychopharmacol* **11**(6): 851-876

Nicodemus KK, Callicott JH, Higier RG, Luna A, Nixon DC, Lipska BK, Vakkalanka R, Giegling I, Rujescu D, St Clair D, Muglia P, Shugart YY, Weinberger DR (2010) Evidence of statistical epistasis between DISC1, CIT and NDEL1 impacting risk for schizophrenia: biological validation with functional neuroimaging. *Hum Genet* **127**(4): 441-452

Nigg EA, Raff JW (2009) Centrioles, centrosomes, and cilia in health and disease. *Cell* **139**(4): 663-678

Niwa M, Kamiya A, Murai R, Kubo K, Gruber AJ, Tomita K, Lu L, Tomisato S, Jaaro-Peled H, Seshadri S, Hiyama H, Huang B, Kohda K, Noda Y, O'Donnell P, Nakajima K, Sawa A, Nabeshima T (2010) Knockdown of DISC1 by in utero gene transfer disturbs postnatal dopaminergic maturation in the frontal cortex and leads to adult behavioral deficits. *Neuron* **65**(4): 480-489

Nudmamud-Thanoi S, Reynolds GP (2004) The NR1 subunit of the glutamate/NMDA receptor in the superior temporal cortex in schizophrenia and affective disorders. *Neurosci Lett* **372**(1-2): 173-177

O'Donnell JM, Zhang HT (2004) Antidepressant effects of inhibitors of cAMP phosphodiesterase (PDE4). *Trends Pharmacol Sci* **25**(3): 158-163

O'Donovan MC, Craddock NJ, Owen MJ (2009) Genetics of psychosis; insights from views across the genome. *Hum Genet* **126**(1): 3-12

Ogawa F, Kasai M, Akiyama T (2005) A functional link between Disrupted-In-Schizophrenia 1 and the eukaryotic translation initiation factor 3. *Biochem Biophys Res Commun* **338**(2): 771-776

Ogawa Y, Saito Y, Nishio K, Yoshida Y, Ashida H, Niki E (2008) Gamma-tocopheryl quinone, not alpha-tocopheryl quinone, induces adaptive response through up-regulation of cellular glutathione and cysteine availability via activation of ATF4. *Free Radic Res* **42**(7): 674-687

Ohoka N, Yoshii S, Hattori T, Onozaki K, Hayashi H (2005) TRB3, a novel ER stress-inducible gene, is induced via ATF4-CHOP pathway and is involved in cell death. *Embo J* **24**(6): 1243-1255

Ohta K, Mizuno A, Li S, Itoh M, Ueda M, Ohta E, Hida Y, Wang MX, Furoi M, Tsuzuki Y, Sobajima M, Bohmoto Y, Fukushima T, Kobori M, Inuzuka T, Nakagawa T (2011) Endoplasmic reticulum stress enhances gamma-secretase activity. *Biochem Biophys Res Commun* **416**(3-4): 362-366

Ohta K, Mizuno A, Ueda M, Li S, Suzuki Y, Hida Y, Hayakawa-Yano Y, Itoh M, Ohta E, Kobori M, Nakagawa T (2010) Autophagy impairment stimulates PS1 expression and gamma-secretase activity. *Autophagy* **6**(3): 345-352

Oliver PL, Sobczyk MV, Maywood ES, Edwards B, Lee S, Livieratos A, Oster H, Butler R, Godinho SI, Wulff K, Peirson SN, Fisher SP, Chesham JE, Smith JW, Hastings MH, Davies KE, Foster RG (2012) Disrupted circadian rhythms in a mouse model of schizophrenia. *Curr Biol* **22**(4): 314-319

Olney JW, Newcomer JW, Farber NB (1999) NMDA receptor hypofunction model of schizophrenia. *J Psychiatr Res* **33**(6): 523-533

Ord D, Meerits K, Ord T (2007) TRB3 protects cells against the growth inhibitory and cytotoxic effect of ATF4. *Exp Cell Res* **313**(16): 3556-3567

Ord D, Ord T (2003) Mouse NIPK interacts with ATF4 and affects its transcriptional activity. *Exp Cell Res* **286**(2): 308-320

Ormel J, Petukhova M, Chatterji S, Aguilar-Gaxiola S, Alonso J, Angermeyer MC, Bromet EJ, Burger H, Demyttenaere K, de Girolamo G, Haro JM, Hwang I, Karam E, Kawakami N, Lepine JP, Medina-Mora ME, Posada-Villa J, Sampson N, Scott K, Ustun TB, Von Korff M, Williams DR, Zhang M, Kessler RC (2008) Disability and treatment of specific mental and physical disorders across the world. *Br J Psychiatry* **192**(5): 368-375

Osbun N, Li J, O'Driscoll MC, Strominger Z, Wakahiro M, Rider E, Bukshpun P, Boland E, Spurrell CH, Schackwitz W, Pennacchio LA, Dobyns WB, Black GC, Sherr EH (2011) Genetic and functional analyses identify DISC1 as a novel callosal agenesis candidate gene. *Am J Med Genet A* **155A**(8): 1865-1876

Ottis P, Bader V, Trossbach SV, Kretzschmar H, Michel M, Leliveld SR, Korth C (2011) Convergence of two independent mental disease genes on the protein level: recruitment of dysbindin to cell-invasive disrupted-in-schizophrenia 1 aggresomes. *Biol Psychiatry* **70**(7): 604-610

Outinen PA, Sood SK, Pfeifer SI, Pamidi S, Podor TJ, Li J, Weitz JI, Austin RC (1999) Homocysteine-induced endoplasmic reticulum stress and growth arrest leads to specific changes in gene expression in human vascular endothelial cells. *Blood* **94**(3): 959-967

Owe-Larsson B, Ekdahl K, Edbom T, Osby U, Karlsson H, Lundberg C, Lundberg M (2011) Increased plasma levels of thioredoxin-1 in patients with first episode

psychosis and long-term schizophrenia. *Prog Neuropsychopharmacol Biol Psychiatry* **35**(4): 1117-1121

Owen MJ, Craddock N, Jablensky A (2007) The genetic deconstruction of psychosis. *Schizophr Bull* **33**(4): 905-911

Oyadomari S, Mori M (2004) Roles of CHOP/GADD153 in endoplasmic reticulum stress. *Cell Death Differ* **11**(4): 381-389

Ozeki Y, Tomoda T, Kleiderlein J, Kamiya A, Bord L, Fujii K, Okawa M, Yamada N, Hatten ME, Snyder SH, Ross CA, Sawa A (2003) Disrupted-in-Schizophrenia-1 (DISC-1): mutant truncation prevents binding to NudE-like (NUDEL) and inhibits neurite outgrowth. *Proc Natl Acad Sci U S A* **100**(1): 289-294

Page G, Rioux Bilan A, Ingrand S, Lafay-Chebassier C, Pain S, Perault Pochat MC, Bouras C, Bayer T, Hugon J (2006) Activated double-stranded RNA-dependent protein kinase and neuronal death in models of Alzheimer's disease. *Neuroscience* **139**(4): 1343-1354

Palo OM, Antila M, Silander K, Hennah W, Kilpinen H, Soronen P, Tuulio-Henriksson A, Kieseppa T, Partonen T, Lonnqvist J, Peltonen L, Paunio T (2007) Association of distinct allelic haplotypes of DISC1 with psychotic and bipolar spectrum disorders and with underlying cognitive impairments. *Hum Mol Genet* **16**(20): 2517-2528

Pang D, Syed S, Fine P, Jones PB (2009) No association between prenatal viral infection and depression in later life--a long-term cohort study of 6152 subjects. *Can J Psychiatry* **54**(8): 565-570

Papadia S, Soriano FX, Leveille F, Martel MA, Dakin KA, Hansen HH, Kaindl A, Sifringer M, Fowler J, Stefovska V, McKenzie G, Craigon M, Corriveau R, Ghazal P, Horsburgh K, Yankner BA, Wyllie DJ, Ikonomidou C, Hardingham GE (2008) Synaptic NMDA receptor activity boosts intrinsic antioxidant defenses. *Nat Neurosci* **11**(4): 476-487

Park YU, Jeong J, Lee H, Mun JY, Kim JH, Lee JS, Nguyen MD, Han SS, Suh PG, Park SK (2010) Disrupted-in-schizophrenia 1 (DISC1) plays essential roles in mitochondria in collaboration with Mitofilin. *Proc Natl Acad Sci U S A* **107**(41): 17785-17790

Pasca SP, Nemes B, Vlase L, Gagyi CE, Dronca E, Miu AC, Dronca M (2006) High levels of homocysteine and low serum paraoxonase 1 arylesterase activity in children with autism. *Life Sci* **78**(19): 2244-2248

Perala J, Suvisaari J, Saarni SI, Kuoppasalmi K, Isometsa E, Pirkola S, Partonen T, Tuulio-Henriksson A, Hintikka J, Kieseppa T, Harkanen T, Koskinen S, Lonnqvist J (2007) Lifetime prevalence of psychotic and bipolar I disorders in a general population. *Arch Gen Psychiatry* **64**(1): 19-28

Peralta V, Cuesta MJ (2001) How many and which are the psychopathological dimensions in schizophrenia? Issues influencing their ascertainment. *Schizophr Res* **49**(3): 269-285

Pickard B (2011) Progress in defining the biological causes of schizophrenia. *Expert Rev Mol Med* **13**(e25)

Pickford F, Masliah E, Britschgi M, Lucin K, Narasimhan R, Jaeger PA, Small S, Spencer B, Rockenstein E, Levine B, Wyss-Coray T (2008) The autophagy-related protein beclin 1 shows reduced expression in early Alzheimer disease and regulates amyloid beta accumulation in mice. *J Clin Invest* **118**(6): 2190-2199

Pletnikov MV, Ayhan Y, Nikolskaia O, Xu Y, Ovanesov MV, Huang H, Mori S, Moran TH, Ross CA (2008a) Inducible expression of mutant human DISC1 in mice is associated with brain and behavioral abnormalities reminiscent of schizophrenia. *Mol Psychiatry* **13**(2): 173-186, 115

Pletnikov MV, Ayhan Y, Xu Y, Nikolskaia O, Ovanesov M, Huang H, Mori S, Moran TH, Ross CA (2008b) Enlargement of the lateral ventricles in mutant DISC1 transgenic mice. *Mol Psychiatry* **13**(2): 115

Pletnikov MV, Xu Y, Ovanesov MV, Kamiya A, Sawa A, Ross CA (2007) PC12 cell model of inducible expression of mutant DISC1: new evidence for a dominant-negative mechanism of abnormal neuronal differentiation. *Neurosci Res* **58**(3): 234-244

Pons J, Evrard-Todeschi N, Bertho G, Gharbi-Benarous J, Benarous R, Girault JP (2007) Phosphorylation-dependent structure of ATF4 peptides derived from a human ATF4 protein, a member of the family of transcription factors. *Peptides* **28**(12): 2253-2267

Porteous D (2008) Genetic causality in schizophrenia and bipolar disorder: out with the old and in with the new. *Curr Opin Genet Dev* **18**(3): 229-234

Porteous DJ, Millar JK, Brandon NJ, Sawa A (2011) DISC1 at 10: connecting psychiatric genetics and neuroscience. *Trends Mol Med* **17**(12): 699-706

Powell SB, Sejnowski TJ, Behrens MM (2012) Behavioral and neurochemical consequences of cortical oxidative stress on parvalbumin-interneuron maturation in rodent models of schizophrenia. *Neuropharmacology* **62**(3): 1322-1331

Prata DP, Mechelli A, Fu CH, Picchioni M, Kane F, Kalidindi S, McDonald C, Kravariti E, Toulopoulou T, Miorelli A, Murray R, Collier DA, McGuire PK (2008) The DISC1 Ser704Cys polymorphism is associated with prefrontal function in healthy individuals. *Mol Psychiatry* **13**(10): 909

Pritchard JK (2001) Are rare variants responsible for susceptibility to complex diseases? *Am J Hum Genet* **69**(1): 124-137

Qin J, Goswami R, Dawson S, Dawson G (2008) Expression of the receptor for advanced glycation end products in oligodendrocytes in response to oxidative stress. *J Neurosci Res* **86**(11): 2414-2422

Qu M, Tang F, Wang L, Yan H, Han Y, Yan J, Yue W, Zhang D (2008) Associations of ATF4 gene polymorphisms with schizophrenia in male patients. *Am J Med Genet B Neuropsychiatr Genet* **147B**(6): 732-736

Qu M, Tang F, Yue W, Ruan Y, Lu T, Liu Z, Zhang H, Han Y, Zhang D, Wang F, Zhang D (2007) Positive association of the Disrupted-in-Schizophrenia-1 gene (DISC1) with schizophrenia in the Chinese Han population. *Am J Med Genet B Neuropsychiatr Genet* **144B**(3): 266-270

Rastogi A, Zai C, Likhodi O, Kennedy JL, Wong AH (2009) Genetic association and post-mortem brain mRNA analysis of DISC1 and related genes in schizophrenia. *Schizophr Res* **114**(1-3): 39-49

Raznahan A, Lee Y, Long R, Greenstein D, Clasen L, Addington A, Rapoport JL, Giedd JN (2011) Common functional polymorphisms of DISC1 and cortical maturation in typically developing children and adolescents. *Mol Psychiatry* **16**(9): 917-926

Regland B (2005) Schizophrenia and single-carbon metabolism. *Prog Neuropsychopharmacol Biol Psychiatry* **29**(7): 1124-1132

Rice F, Harold GT, Boivin J, van den Bree M, Hay DF, Thapar A (2010) The links between prenatal stress and offspring development and psychopathology: disentangling environmental and inherited influences. *Psychol Med* **40**(2): 335-345

Rice F, Jones I, Thapar A (2007) The impact of gestational stress and prenatal growth on emotional problems in offspring: a review. *Acta Psychiatr Scand* **115**(3): 171-183

Richards AL, Jones L, Moskvina V, Kirov G, Gejman PV, Levinson DF, Sanders AR, Purcell S, Visscher PM, Craddock N, Owen MJ, Holmans P, O'Donovan MC (2012) Schizophrenia susceptibility alleles are enriched for alleles that affect gene expression in adult human brain. *Mol Psychiatry* **17**(2): 193-201

Richards D (2011) Prevalence and clinical course of depression: a review. *Clin Psychol Rev* **31**(7): 1117-1125

Ritter B, Zschuntsch J, Kvachnina E, Zhang W, Ponimaskin EG (2004) The GABA(B) receptor subunits R1 and R2 interact differentially with the activation transcription factor ATF4 in mouse brain during the postnatal development. *Brain Res Dev Brain Res* **149**(1): 73-77

Robbins J, Dilworth SM, Laskey RA, Dingwall C (1991) Two interdependent basic domains in nucleoplasmin nuclear targeting sequence: identification of a class of bipartite nuclear targeting sequence. *Cell* **64**(3): 615-623

Roberts RA, Laskin DL, Smith CV, Robertson FM, Allen EM, Doorn JA, Slikker W (2009) Nitrative and oxidative stress in toxicology and disease. *Toxicol Sci* **112**(1): 4-16

Rouschop KM, van den Beucken T, Dubois L, Niessen H, Bussink J, Savelkouls K, Keulers T, Mujcic H, Landuyt W, Voncken JW, Lambin P, van der Kogel AJ, Koritzinsky M, Wouters BG (2010) The unfolded protein response protects human tumor cells during hypoxia through regulation of the autophagy genes MAP1LC3B and ATG5. *J Clin Invest* **120**(1): 127-141

Roybal CN, Yang S, Sun CW, Hurtado D, Vander Jagt DL, Townes TM, Abcouwer SF (2004) Homocysteine increases the expression of vascular endothelial growth factor by a mechanism involving endoplasmic reticulum stress and transcription factor ATF4. *J Biol Chem* **279**(15): 14844-14852

Rutkowski DT, Arnold SM, Miller CN, Wu J, Li J, Gunnison KM, Mori K, Sadighi Akha AA, Raden D, Kaufman RJ (2006) Adaptation to ER stress is mediated by differential stabilities of pro-survival and pro-apoptotic mRNAs and proteins. *PLoS Biol* **4**(11): e374

Rutkowski DT, Kaufman RJ (2003) All roads lead to ATF4. *Dev Cell* **4**(4): 442-444

Rzymski T, Milani M, Pike L, Buffa F, Mellor HR, Winchester L, Pires I, Hammond E, Ragoussis I, Harris AL (2010) Regulation of autophagy by ATF4 in response to severe hypoxia. *Oncogene* **29**(31): 4424-4435

Rzymski T, Milani M, Singleton DC, Harris AL (2009) Role of ATF4 in regulation of autophagy and resistance to drugs and hypoxia. *Cell Cycle* **8**(23): 3838-3847

Saha S, Chant D, Welham J, McGrath J (2005) A systematic review of the prevalence of schizophrenia. *PLoS Med* **2**(5): e141

Samali A, Fitzgerald U, Deegan S, Gupta S (2010) Methods for monitoring endoplasmic reticulum stress and the unfolded protein response. *Int J Cell Biol* **2010**: 830307

Sanchez-Pulido L, Ponting CP (2011) Structure and evolutionary history of DISC1. *Hum Mol Genet* **20**(R2): R175-181

Sanders AR, Duan J, Levinson DF, Shi J, He D, Hou C, Burrell GJ, Rice JP, Nertney DA, Olincy A, Rozic P, Vinogradov S, Buccola NG, Mowry BJ, Freedman R, Amin F, Black DW, Silverman JM, Byerley WF, Crowe RR, Cloninger CR, Martinez M, Gejman PV (2008) No significant association of 14 candidate genes with

schizophrenia in a large European ancestry sample: implications for psychiatric genetics. *Am J Psychiatry* **165**(4): 497-506

Sawamura N, Ando T, Maruyama Y, Fujimuro M, Mochizuki H, Honjo K, Shimoda M, Toda H, Sawamura-Yamamoto T, Makuch LA, Hayashi A, Ishizuka K, Cascella NG, Kamiya A, Ishida N, Tomoda T, Hai T, Furukubo-Tokunaga K, Sawa A (2008) Nuclear DISC1 regulates CRE-mediated gene transcription and sleep homeostasis in the fruit fly. *Mol Psychiatry* **13**(12): 1138-1148, 1069

Sawamura N, Sawamura-Yamamoto T, Ozeki Y, Ross CA, Sawa A (2005) A form of DISC1 enriched in nucleus: altered subcellular distribution in orbitofrontal cortex in psychosis and substance/alcohol abuse. *Proc Natl Acad Sci U S A* **102**(4): 1187-1192

Sayer JA, Otto EA, O'Toole JF, Nurnberg G, Kennedy MA, Becker C, Hennies HC, Helou J, Attanasio M, Fausett BV, Utsch B, Khanna H, Liu Y, Drummond I, Kawakami I, Kusakabe T, Tsuda M, Ma L, Lee H, Larson RG, Allen SJ, Wilkinson CJ, Nigg EA, Shou C, Lillo C, Williams DS, Hoppe B, Kemper MJ, Neuhaus T, Parisi MA, Glass IA, Petry M, Kispert A, Gloy J, Ganner A, Walz G, Zhu X, Goldman D, Nurnberg P, Swaroop A, Leroux MR, Hildebrandt F (2006) The centrosomal protein nephrocystin-6 is mutated in Joubert syndrome and activates transcription factor ATF4. *Nat Genet* **38**(6): 674-681

Schenkel LS, Silverstein SM (2004) Dimensions of premorbid functioning in schizophrenia: a review of neuromotor, cognitive, social, and behavioral domains. *Genet Soc Gen Psychol Monogr* **130**(3): 241-270

Schoch S, Cibelli G, Magin A, Steinmuller L, Thiel G (2001) Modular structure of cAMP response element binding protein 2 (CREB2). *Neurochem Int* **38**(7): 601-608

Schulz P, Steimer T (2009) Neurobiology of circadian systems. *CNS Drugs* **23**(Suppl 2): 3-13

Schurov IL, Handford EJ, Brandon NJ, Whiting PJ (2004) Expression of disrupted in schizophrenia 1 (DISC1) protein in the adult and developing mouse brain indicates its role in neurodevelopment. *Mol Psychiatry* **9**(12): 1100-1110

Sebat J, Levy DL, McCarthy SE (2009) Rare structural variants in schizophrenia: one disorder, multiple mutations; one mutation, multiple disorders. *Trends Genet* **25**(12): 528-535

Semple CA, Devon RS, Le Hellard S, Porteous DJ (2001) Identification of genes from a schizophrenia-linked translocation breakpoint region. *Genomics* **73**(1): 123-126

Seo J, Fortuno ES, 3rd, Suh JM, Stenesen D, Tang W, Parks EJ, Adams CM, Townes T, Graff JM (2009) Atf4 regulates obesity, glucose homeostasis, and energy expenditure. *Diabetes* **58**(11): 2565-2573

Shaikh M, Hall MH, Schulze K, Dutt A, Li K, Williams I, Walshe M, Constante M, Broome M, Picchioni M, Toulopoulou T, Collier D, Stahl D, Rijsdijk F, Powell J, Murray RM, Arranz M, Bramon E (2011) Effect of DISC1 on the P300 Waveform in Psychosis. *Schizophr Bull* (epub ahead of print)

Shan J, Ord D, Ord T, Kilberg MS (2009) Elevated ATF4 expression, in the absence of other signals, is sufficient for transcriptional induction via CCAAT enhancer-binding protein-activating transcription factor response elements. *J Biol Chem* **284**(32): 21241-21248

Shen S, Lang B, Nakamoto C, Zhang F, Pu J, Kuan SL, Chatzi C, He S, Mackie I, Brandon NJ, Marquis KL, Day M, Hurko O, McCaig CD, Riedel G, St Clair D (2008) Schizophrenia-related neural and behavioral phenotypes in transgenic mice expressing truncated Disc1. *J Neurosci* **28**(43): 10893-10904

Shimizu S, Matsuzaki S, Hattori T, Kumamoto N, Miyoshi K, Katayama T, Tohyama M (2008) DISC1-kendrin interaction is involved in centrosomal microtubule network formation. *Biochem Biophys Res Commun* **377**(4): 1051-1056

Shinoda T, Taya S, Tsuboi D, Hikita T, Matsuzawa R, Kuroda S, Iwamatsu A, Kaibuchi K (2007) DISC1 regulates neurotrophin-induced axon elongation via interaction with Grb2. *J Neurosci* **27**(1): 4-14

Shoji H, Toyama K, Takamiya Y, Wakana S, Gondo Y, Miyakawa T (2012) Comprehensive behavioral analysis of ENU-induced Disc1-Q31L and -L100P mutant mice. *BMC Res Notes* **5**: 108

Silva JM, Wong A, Carelli V, Cortopassi GA (2009) Inhibition of mitochondrial function induces an integrated stress response in oligodendroglia. *Neurobiol Dis* **34**(2): 357-365

Singh KK, De Rienzo G, Drane L, Mao Y, Flood Z, Madison J, Ferreira M, Bergen S, King C, Sklar P, Sive H, Tsai LH (2011) Common DISC1 Polymorphisms Disrupt Wnt/GSK3beta Signaling and Brain Development. *Neuron* **72**(4): 545-558

Singh KK, Ge X, Mao Y, Drane L, Meletis K, Samuels BA, Tsai LH (2010) Dixdc1 is a critical regulator of DISC1 and embryonic cortical development. *Neuron* **67**(1): 33-48

Siu F, Bain PJ, LeBlanc-Chaffin R, Chen H, Kilberg MS (2002) ATF4 is a mediator of the nutrient-sensing response pathway that activates the human asparagine synthetase gene. *J Biol Chem* **277**(27): 24120-24127

Smith FD, Scott JD (2006) Anchored cAMP signaling: onward and upward - a short history of compartmentalized cAMP signal transduction. *Eur J Cell Biol* **85**(7): 585-592

Smith J, Ladi E, Mayer-Proschel M, Noble M (2000) Redox state is a central modulator of the balance between self-renewal and differentiation in a dividing glial precursor cell. *Proc Natl Acad Sci U S A* **97**(18): 10032-10037

Smoller JW, Finn CT (2003) Family, twin, and adoption studies of bipolar disorder. *Am J Med Genet C Semin Med Genet* **123C**(1): 48-58

Soares DC, Carlyle BC, Bradshaw NJ, Porteous DJ (2011) DISC1: Structure, Function, and Therapeutic Potential for Major Mental Illness. *ACS Chem Neurosci* **2**(11): 609-632

Soderberg O, Gullberg M, Jarvius M, Ridderstrale K, Leuchowius KJ, Jarvius J, Wester K, Hydbring P, Bahram F, Larsson LG, Landegren U (2006) Direct observation of individual endogenous protein complexes in situ by proximity ligation. *Nat Methods* **3**(12): 995-1000

Song W, Li W, Feng J, Heston LL, Scaringe WA, Sommer SS (2008) Identification of high risk DISC1 structural variants with a 2% attributable risk for schizophrenia. *Biochem Biophys Res Commun* **367**(3): 700-706

Song W, Li W, Noltner K, Yan J, Green E, Grozeva D, Jones IR, Craddock N, Longmate J, Feng J, Sommer SS (2010) Identification of high risk DISC1 protein structural variants in patients with bipolar spectrum disorder. *Neurosci Lett* **486**(3): 136-140

Sprooten E, Sussmann JE, Moorhead TW, Whalley HC, Ffrench-Constant C, Blumberg HP, Bastin ME, Hall J, Lawrie SM, McIntosh AM (2011) Association of white matter integrity with genetic variation in an exonic DISC1 SNP. *Mol Psychiatry* **16**(7): 685, 688-689

St Clair D, Blackwood D, Muir W, Carothers A, Walker M, Spowart G, Gosden C, Evans HJ (1990) Association within a family of a balanced autosomal translocation with major mental illness. *Lancet* **336**(8706): 13-16

St Clair D, Xu M, Wang P, Yu Y, Fang Y, Zhang F, Zheng X, Gu N, Feng G, Sham P, He L (2005) Rates of adult schizophrenia following prenatal exposure to the Chinese famine of 1959-1961. *Jama* **294**(5): 557-562

Stadtman ER, Levine RL (2003) Free radical-mediated oxidation of free amino acids and amino acid residues in proteins. *Amino Acids* **25**(3-4): 207-218

Steiner J, Sarnyai Z, Westphal S, Gos T, Bernstein HG, Bogerts B, Keilhoff G (2011) Protective effects of haloperidol and clozapine on energy-deprived OLN-93 oligodendrocytes. *Eur Arch Psychiatry Clin Neurosci* **261**(7): 477-482

Sterneck E, Paylor R, Jackson-Lewis V, Libbey M, Przedborski S, Tessarollo L, Crawley JN, Johnson PF (1998) Selectively enhanced contextual fear conditioning in

mice lacking the transcriptional regulator CCAAT/enhancer binding protein delta. *Proc Natl Acad Sci U S A* **95**(18): 10908-10913

Steullet P, Cabungcal JH, Kulak A, Kraftsik R, Chen Y, Dalton TP, Cuenod M, Do KQ (2010) Redox dysregulation affects the ventral but not dorsal hippocampus: impairment of parvalbumin neurons, gamma oscillations, and related behaviors. *J Neurosci* **30**(7): 2547-2558

Stewart DG, Davis KL (2004) Possible contributions of myelin and oligodendrocyte dysfunction to schizophrenia. *Int Rev Neurobiol* **59**: 381-424

Su N, Kilberg MS (2008) C/EBP homology protein (CHOP) interacts with activating transcription factor 4 (ATF4) and negatively regulates the stress-dependent induction of the asparagine synthetase gene. *J Biol Chem* **283**(50): 35106-35117

Sullivan PF, Kendler KS, Neale MC (2003) Schizophrenia as a complex trait: evidence from a meta-analysis of twin studies. *Arch Gen Psychiatry* **60**(12): 1187-1192

Sullivan PF, Lin D, Tzeng JY, van den Oord E, Perkins D, Stroup TS, Wagner M, Lee S, Wright FA, Zou F, Liu W, Downing AM, Lieberman J, Close SL (2008) Genomewide association for schizophrenia in the CATIE study: results of stage 1. *Mol Psychiatry* **13**(6): 570-584

Sullivan PF, Neale MC, Kendler KS (2000) Genetic epidemiology of major depression: review and meta-analysis. *Am J Psychiatry* **157**(10): 1552-1562

Susser E, Brown AS, Klonowski E, Allen RH, Lindenbaum J (1998) Schizophrenia and impaired homocysteine metabolism: a possible association. *Biol Psychiatry* **44**(2): 141-143

Susser E, Neugebauer R, Hoek HW, Brown AS, Lin S, Labovitz D, Gorman JM (1996) Schizophrenia after prenatal famine. Further evidence. *Arch Gen Psychiatry* **53**(1): 25-31

Susser ES, Lin SP (1992) Schizophrenia after prenatal exposure to the Dutch Hunger Winter of 1944-1945. *Arch Gen Psychiatry* **49**(12): 983-988

Sussmann JE, Lymer GK, McKirdy J, Moorhead TW, Munoz Maniega S, Job D, Hall J, Bastin ME, Johnstone EC, Lawrie SM, McIntosh AM (2009) White matter abnormalities in bipolar disorder and schizophrenia detected using diffusion tensor magnetic resonance imaging. *Bipolar Disord* **11**(1): 11-18

Szeszko PR, Hodgkinson CA, Robinson DG, Derosse P, Bilder RM, Lencz T, Burdick KE, Napolitano B, Betensky JD, Kane JM, Goldman D, Malhotra AK (2008) DISC1 is associated with prefrontal cortical gray matter and positive symptoms in schizophrenia. *Biol Psychol* **79**(1): 103-110

Tagawa Y, Hiramatsu N, Kato H, Sakoh T, Nakajima S, Hayakawa K, Saito Y, Johno H, Takahashi S, Gu L, Yao J, Kitamura M (2011) Induction of CCAAT/enhancer-binding protein-homologous protein by cigarette smoke through the superoxide anion-triggered PERK-eIF2alpha pathway. *Toxicology* **287**(1-3): 105-112

Takahashi N, Sakurai T, Davis KL, Buxbaum JD (2011) Linking oligodendrocyte and myelin dysfunction to neurocircuitry abnormalities in schizophrenia. *Prog Neurobiol* **93**(1): 13-24

Takahashi T, Suzuki M, Tsunoda M, Maeno N, Kawasaki Y, Zhou SY, Hagino H, Niu L, Tsuneki H, Kobayashi S, Sasaoka T, Seto H, Kurachi M, Ozaki N (2009) The Disrupted-in-Schizophrenia-1 Ser704Cys polymorphism and brain morphology in schizophrenia. *Psychiatry Res* **172**(2): 128-135

Tanaka T, Tsujimura T, Takeda K, Sugihara A, Maekawa A, Terada N, Yoshida N, Akira S (1998) Targeted disruption of ATF4 discloses its essential role in the formation of eye lens fibres. *Genes Cells* **3**(12): 801-810

Tandon R, Nasrallah HA, Keshavan MS (2009) Schizophrenia, "just the facts" 4. Clinical features and conceptualization. *Schizophr Res* **110**(1-3): 1-23

Taubenfeld SM, Milekic MH, Monti B, Alberini CM (2001a) The consolidation of new but not reactivated memory requires hippocampal C/EBPbeta. *Nat Neurosci* **4**(8): 813-818

Taubenfeld SM, Wiig KA, Monti B, Dolan B, Pollonini G, Alberini CM (2001b) Fornix-dependent induction of hippocampal CCAAT enhancer-binding protein [beta] and [delta] Co-localizes with phosphorylated cAMP response element-binding protein and accompanies long-term memory consolidation. *J Neurosci* **21**(1): 84-91

Taya S, Shinoda T, Tsuboi D, Asaki J, Nagai K, Hikita T, Kuroda S, Kuroda K, Shimizu M, Hirotsune S, Iwamatsu A, Kaibuchi K (2007) DISC1 regulates the transport of the NUDEL/LIS1/14-3-3epsilon complex through kinesin-1. *J Neurosci* **27**(1): 15-26

Taylor MS, Devon RS, Millar JK, Porteous DJ (2003) Evolutionary constraints on the Disrupted in Schizophrenia locus. *Genomics* **81**(1): 67-77

Thiel G, Al Sarraj J, Vinson C, Stefano L, Bach K (2005) Role of basic region leucine zipper transcription factors cyclic AMP response element binding protein (CREB), CREB2, activating transcription factor 2 and CAAT/enhancer binding protein alpha in cyclic AMP response element-mediated transcription. *J Neurochem* **92**(2): 321-336

Thomson PA, Harris SE, Starr JM, Whalley LJ, Porteous DJ, Deary IJ (2005) Association between genotype at an exonic SNP in DISC1 and normal cognitive aging. *Neurosci Lett* **389**(1): 41-45

Tkachev D, Mimmack ML, Ryan MM, Wayland M, Freeman T, Jones PB, Starkey M, Webster MJ, Yolken RH, Bahn S (2003) Oligodendrocyte dysfunction in schizophrenia and bipolar disorder. *Lancet* **362**(9386): 798-805

Tomppo L, Hennah W, Lahermo P, Loukola A, Tuulio-Henriksson A, Suvisaari J, Partonen T, Ekelund J, Lonnqvist J, Peltonen L (2009) Association between genes of Disrupted in schizophrenia 1 (DISC1) interactors and schizophrenia supports the role of the DISC1 pathway in the etiology of major mental illnesses. *Biol Psychiatry* **65**(12): 1055-1062

Trbovic SM (2010) Schizophrenia as a possible dysfunction of the suprachiasmatic nucleus. *Med Hypotheses* **74**(1): 127-131

Trinh MA, Kaphzan H, Wek RC, Pierre P, Cavener DR, Klann E (2012) Brain-Specific Disruption of the eIF2alpha Kinase PERK Decreases ATF4 Expression and Impairs Behavioral Flexibility. *Cell Rep* **1**(6): 676-688

Tsuzuki K, Fukatsu R, Takamaru Y, Kimura K, Abe M, Shima K, Fujii N, Takahata N (1994) Immunohistochemical evidence for amyloid beta in rat soleus muscle in chloroquine-induced myopathy. *Neurosci Lett* **182**(2): 151-154

Uher R (2008) The implications of gene-environment interactions in depression: will cause inform cure? *Mol Psychiatry* **13**(12): 1070-1078

Uher R (2011) Genes, environment, and individual differences in responding to treatment for depression. *Harv Rev Psychiatry* **19**(3): 109-124

Unterberger U, Hoftberger R, Gelpi E, Flicker H, Budka H, Voigtlander T (2006) Endoplasmic reticulum stress features are prominent in Alzheimer disease but not in prion diseases in vivo. *J Neuropathol Exp Neurol* **65**(4): 348-357

Upchurch GR, Jr., Welch GN, Fabian AJ, Freedman JE, Johnson JL, Keaney JF, Jr., Loscalzo J (1997) Homocyst(e)ine decreases bioavailable nitric oxide by a mechanism involving glutathione peroxidase. *J Biol Chem* **272**(27): 17012-17017

Uranova NA, Orlovskaia DD, Vikhreva OV, Zimina IS, Rakhmanova VI (2001) Morphometric study of ultrastructural changes in oligodendroglial cells in the postmortem brain in endogenous psychoses. *Vestn Ross Akad Med Nauk* **7**: 42-48

Uranova NA, Vostrikov VM, Orlovskaya DD, Rachmanova VI (2004) Oligodendroglial density in the prefrontal cortex in schizophrenia and mood disorders: a study from the Stanley Neuropathology Consortium. *Schizophr Res* **67**(2-3): 269-275

Uranova NA, Vostrikov VM, Vikhreva OV, Zimina IS, Kolomeets NS, Orlovskaya DD (2007) The role of oligodendrocyte pathology in schizophrenia. *Int J Neuropsychopharmacol* **10**(4): 537-545

Ushijima K, Koyanagi S, Sato Y, Ogata T, Matsunaga N, Fujimura A, Ohdo S (2012) Role of Activating Transcription Factor-4 in 24-hour Rhythm of Serotonin Transporter Expression in the Mouse Midbrain. *Mol Pharmacol* **82**(2):264-270

Vallejo M, Ron D, Miller CP, Habener JF (1993) C/ATF, a member of the activating transcription factor family of DNA-binding proteins, dimerizes with CAAT/enhancer-binding proteins and directs their binding to cAMP response elements. *Proc Natl Acad Sci U S A* **90**(10): 4679-4683

van der Voorn JP, van Kollenburg B, Bertrand G, Van Haren K, Scheper GC, Powers JM, van der Knaap MS (2005) The unfolded protein response in vanishing white matter disease. *J Neuropathol Exp Neurol* **64**(9): 770-775

van Os J, Rutten BP, Poulton R (2008) Gene-environment interactions in schizophrenia: review of epidemiological findings and future directions. *Schizophr Bull* **34**(6): 1066-1082

Vattem KM, Wek RC (2004) Reinitiation involving upstream ORFs regulates ATF4 mRNA translation in mammalian cells. *Proc Natl Acad Sci U S A* **101**(31): 11269-11274

Vaz Meirelles G, Ferreira Lanza DC, da Silva JC, Santana Bernachi J, Paes Leme AF, Kobarg J (2010) Characterization of hNek6 interactome reveals an important role for its short N-terminal domain and colocalization with proteins at the centrosome. *J Proteome Res* **9**(12): 6298-6316

Vernon E, Meyer G, Pickard L, Dev K, Molnar E, Collingridge GL, Henley JM (2001) GABA(B) receptors couple directly to the transcription factor ATF4. *Mol Cell Neurosci* **17**(4): 637-645

Vinson C, Myakishev M, Acharya A, Mir AA, Moll JR, Bonovich M (2002) Classification of human B-ZIP proteins based on dimerization properties. *Mol Cell Biol* **22**(18): 6321-6335

Vinson CR, Hai T, Boyd SM (1993) Dimerization specificity of the leucine zipper-containing bZIP motif on DNA binding: prediction and rational design. *Genes Dev* **7**(6): 1047-1058

Vrajova M, Stastny F, Horacek J, Lochman J, Sery O, Pekova S, Klaschka J, Hoschl C (2010) Expression of the hippocampal NMDA receptor GluN1 subunit and its splicing isoforms in schizophrenia: postmortem study. *Neurochem Res* **35**(7): 994-1002

Walker RM, Hill AE, Newman AC, Hamilton G, Torrance HS, Anderson SM, Ogawa F, Derizioti P, Nicod J, Vernes SC, Fisher SE, Thomson PA, Porteous DJ, Evans KL (2012) The DISC1 promoter: characterization and regulation by FOXP2. *Hum Mol Genet* **21**(13):2862-2872

Wang A, Xu S, Zhang X, He J, Yan D, Yang Z, Xiao S (2011) Ribosomal protein RPL41 induces rapid degradation of ATF4, a transcription factor critical for tumour cell survival in stress. *J Pathol* **225**(2): 285-292

Wang C, Huang Z, Du Y, Cheng Y, Chen S, Guo F (2010a) ATF4 regulates lipid metabolism and thermogenesis. *Cell Res* **20**(2): 174-184

Wang H, Xu H, Niu J, Mei F, Li X, Kong J, Cai W, Xiao L (2010b) Haloperidol activates quiescent oligodendroglia precursor cells in the adult mouse brain. *Schizophr Res* **119**(1-3): 164-174

Wang JF, Shao L, Sun X, Young LT (2009) Increased oxidative stress in the anterior cingulate cortex of subjects with bipolar disorder and schizophrenia. *Bipolar Disord* **11**(5): 523-529

Wang Q, Charych EI, Pulito VL, Lee JB, Graziane NM, Crozier RA, Revilla-Sanchez R, Kelly MP, Dunlop AJ, Murdoch H, Taylor N, Xie Y, Pausch M, Hayashi-Takagi A, Ishizuka K, Seshadri S, Bates B, Kariya K, Sawa A, Weinberg RJ, Moss SJ, Houslay MD, Yan Z, Brandon NJ (2010c) The psychiatric disease risk factors DISC1 and TNIK interact to regulate synapse composition and function. *Mol Psychiatry* **16**(10): 1006-1023

Watatani Y, Ichikawa K, Nakanishi N, Fujimoto M, Takeda H, Kimura N, Hirose H, Takahashi S, Takahashi Y (2008) Stress-induced translation of ATF5 mRNA is regulated by the 5'-untranslated region. *J Biol Chem* **283**(5): 2543-2553

Waters F, Allen P, Aleman A, Fernyhough C, Woodward TS, Badcock JC, Barkus E, Johns L, Varese F, Menon M, Vercammen A, Laroi F (2012) Auditory hallucinations in schizophrenia and nonschizophrenia populations: a review and integrated model of cognitive mechanisms. *Schizophr Bull* **38**(4): 683-693

Wei Z, Bai O, Richardson JS, Mousseau DD, Li XM (2003) Olanzapine protects PC12 cells from oxidative stress induced by hydrogen peroxide. *J Neurosci Res* **73**(3): 364-368

Weinberger DR, Wagner RL, Wyatt RJ (1983) Neuropathological studies of schizophrenia: a selective review. *Schizophr Bull* **9**(2): 193-212

Wek RC, Jiang HY, Anthony TG (2006) Coping with stress: eIF2 kinases and translational control. *Biochem Soc Trans* **34**(Pt 1): 7-11

White JH, McIllhinney RA, Wise A, Ciruela F, Chan WY, Emson PC, Billinton A, Marshall FH (2000) The GABAB receptor interacts directly with the related transcription factors CREB2 and ATFx. *Proc Natl Acad Sci U S A* **97**(25): 13967-13972

Williams JM, Beck TF, Pearson DM, Proud MB, Cheung SW, Scott DA (2009) A 1q42 deletion involving DISC1, DISC2, and TSNAX in an autism spectrum disorder. *Am J Med Genet A* **149A**(8): 1758-1762

Williams NM, Norton N, Williams H, Ekholm B, Hamshere ML, Lindblom Y, Chowdari KV, Cardno AG, Zammit S, Jones LA, Murphy KC, Sanders RD, McCarthy G, Gray MY, Jones G, Holmans P, Nimgaonkar V, Adolfson R, Osby U, Terenius L, Sedvall G, O'Donovan MC, Owen MJ (2003) A systematic genomewide linkage study in 353 sib pairs with schizophrenia. *Am J Hum Genet* **73**(6): 1355-1367

Wood JD, Bonath F, Kumar S, Ross CA, Cunliffe VT (2009a) Disrupted-in-schizophrenia 1 and neuregulin 1 are required for the specification of oligodendrocytes and neurones in the zebrafish brain. *Hum Mol Genet* **18**(3): 391-404

Wood SJ, Yucel M, Pantelis C, Berk M (2009b) Neurobiology of schizophrenia spectrum disorders: the role of oxidative stress. *Ann Acad Med Singapore* **38**(5): 396-396

Wulff K, Dijk DJ, Middleton B, Foster RG, Joyce EM (2012) Sleep and circadian rhythm disruption in schizophrenia. *Br J Psychiatry* **200**(4): 308-316

Wulff K, Porcheret K, Cussans E, Foster RG (2009) Sleep and circadian rhythm disturbances: multiple genes and multiple phenotypes. *Curr Opin Genet Dev* **19**(3): 237-246

Xia M, Guo V, Huang R, Inglese J, Nirenberg M, Austin CP (2009a) A Cell-based beta-Lactamase Reporter Gene Assay for the CREB Signaling Pathway. *Curr Chem Genomics* **3**(1): 7-12

Xia M, Huang R, Guo V, Southall N, Cho MH, Inglese J, Austin CP, Nirenberg M (2009b) Identification of compounds that potentiate CREB signaling as possible enhancers of long-term memory. *Proc Natl Acad Sci U S A* **106**(7): 2412-2417

Xiao L, Xu H, Zhang Y, Wei Z, He J, Jiang W, Li X, Dyck LE, Devon RM, Deng Y, Li XM (2008) Quetiapine facilitates oligodendrocyte development and prevents mice from myelin breakdown and behavioral changes. *Mol Psychiatry* **13**(7): 697-708

Xie Z, Srivastava DP, Photowala H, Kai L, Cahill ME, Woolfrey KM, Shum CY, Surmeier DJ, Penzes P (2007) Kalirin-7 controls activity-dependent structural and functional plasticity of dendritic spines. *Neuron* **56**(4): 640-656

Xu MQ, Sun WS, Liu BX, Feng GY, Yu L, Yang L, He G, Sham P, Susser E, St Clair D, He L (2009) Prenatal malnutrition and adult schizophrenia: further evidence from the 1959-1961 Chinese famine. *Schizophr Bull* **35**(3): 568-576

Yamaguchi S, Ishihara H, Yamada T, Tamura A, Usui M, Tominaga R, Munakata Y, Satake C, Katagiri H, Tashiro F, Aburatani H, Tsukiyama-Kohara K, Miyazaki J,

Sonenberg N, Oka Y (2008) ATF4-mediated induction of 4E-BP1 contributes to pancreatic beta cell survival under endoplasmic reticulum stress. *Cell Metab* **7**(3): 269-276

Yan SK, Chang T, Wang H, Wu L, Wang R, Meng QH (2006) Effects of hydrogen sulfide on homocysteine-induced oxidative stress in vascular smooth muscle cells. *Biochem Biophys Res Commun* **351**(2): 485-491

Yang W, Paschen W (2009) The endoplasmic reticulum and neurological diseases. *Exp Neurol* **219**(2): 376-381

Yang X, Matsuda K, Bialek P, Jacquot S, Masuoka HC, Schinke T, Li L, Brancorsini S, Sassone-Corsi P, Townes TM, Hanauer A, Karsenty G (2004) ATF4 is a substrate of RSK2 and an essential regulator of osteoblast biology; implication for Coffin-Lowry Syndrome. *Cell* **117**(3): 387-398

Yao JK, Leonard S, Reddy R (2006) Altered glutathione redox state in schizophrenia. *Dis Markers* **22**(1-2): 83-93

Yao JK, Reddy RD, van Kammen DP (1999) Human plasma glutathione peroxidase and symptom severity in schizophrenia. *Biol Psychiatry* **45**(11): 1512-1515

Yao JK, Reddy RD, van Kammen DP (2001) Oxidative damage and schizophrenia: an overview of the evidence and its therapeutic implications. *CNS Drugs* **15**(4): 287-310

Ye J, Koumenis C (2009) ATF4, an ER stress and hypoxia-inducible transcription factor and its potential role in hypoxia tolerance and tumorigenesis. *Curr Mol Med* **9**(4): 411-416

Yoshizawa T, Hinoi E, Jung DY, Kajimura D, Ferron M, Seo J, Graff JM, Kim JK, Karsenty G (2009) The transcription factor ATF4 regulates glucose metabolism in mice through its expression in osteoblasts. *J Clin Invest* **119**(9): 2807-2817

Young-Pearse TL, Suth S, Luth ES, Sawa A, Selkoe DJ (2010) Biochemical and functional interaction of disrupted-in-schizophrenia 1 and amyloid precursor protein regulates neuronal migration during mammalian cortical development. *J Neurosci* **30**(31): 10431-10440

Yukawa K, Tanaka T, Tsuji S, Akira S (1998) Expressions of CCAAT/Enhancer-binding proteins beta and delta and their activities are intensified by cAMP signaling as well as Ca2+/calmodulin kinases activation in hippocampal neurons. *J Biol Chem* **273**(47): 31345-31351

Yukawa K, Tanaka T, Tsuji S, Akira S (1999) Regulation of transcription factor C/ATF by the cAMP signal activation in hippocampal neurons, and molecular interaction of C/ATF with signal integrator CBP/p300. *Brain Res Mol Brain Res* **69**(1): 124-134

Zhang F, Sarginson J, Crombie C, Walker N, St Clair D, Shaw D (2006) Genetic association between schizophrenia and the DISC1 gene in the Scottish population. *Am J Med Genet B Neuropsychiatr Genet* **141B**(2): 155-159

Zhang HT, Huang Y, Jin SL, Frith SA, Suvarna N, Conti M, O'Donnell JM (2002) Antidepressant-like profile and reduced sensitivity to rolipram in mice deficient in the PDE4D phosphodiesterase enzyme. *Neuropsychopharmacology* **27**(4): 587-595

Zhang L, Zhou R, Xiang G (2005) Stepholidine protects against H2O2 neurotoxicity in rat cortical neurons by activation of Akt. *Neurosci Lett* **383**(3): 328-332

Zhang M, Zhao Z, He L, Wan C (2010) A meta-analysis of oxidative stress markers in schizophrenia. *Sci China Life Sci* **53**(1): 112-124

Zhang XY, Chen da C, Xiu MH, Wang F, Qi LY, Sun HQ, Chen S, He SC, Wu GY, Haile CN, Kosten TA, Lu L, Kosten TR (2009) The novel oxidative stress marker thioredoxin is increased in first-episode schizophrenic patients. *Schizophr Res* **113**(2-3): 151-157

Zhao ML, Wu CF (1997) Alterations in frequency coding and activity dependence of excitability in cultured neurons of Drosophila memory mutants. *J Neurosci* **17**(6): 2187-2199

Zheng F, Wang L, Jia M, Yue W, Ruan Y, Lu T, Liu J, Li J, Zhang D (2011) Evidence for association between Disrupted-in-Schizophrenia 1 (DISC1) gene polymorphisms and autism in Chinese Han population: a family-based association study. *Behav Brain Funct* **7**: 14

Zhou D, Palam LR, Jiang L, Narasimhan J, Staschke KA, Wek RC (2008a) Phosphorylation of eIF2 directs ATF5 translational control in response to diverse stress conditions. *J Biol Chem* **283**(11): 7064-7073

Zhou X, Chen Q, Schaukowitch K, Kelsoe JR, Geyer MA (2010) Insoluble DISC1-Boymaw fusion proteins generated by DISC1 translocation. *Mol Psychiatry* **15**(7): 669-672

Zhou X, Geyer MA, Kelsoe JR (2008b) Does disrupted-in-schizophrenia (DISC1) generate fusion transcripts? *Mol Psychiatry* **13**(4): 361-363

Zhou X, Wang R, Fan L, Li Y, Ma L, Yang Z, Yu W, Jing N, Zhu X (2005) Mitosin/CENP-F as a negative regulator of activating transcription factor-4. *J Biol Chem* **280**(14): 13973-13977

Zimmerman JE, Naidoo N, Raizen DM, Pack AI (2008) Conservation of sleep: insights from non-mammalian model systems. *Trends Neurosci* **31**(7): 371-376

Appendix – Relevant publications

At the time of writing, one article relevant to this thesis has been published by Oxford Journals, who grants all authors the "right to include the article in full or in part in a thesis or dissertation, provided that this is not published commercially".

The details of this publication are as follows:

"DISC1 variants 37W and 607F disrupt its nuclear targeting and regulatory role in ATF4-mediated transcription"

Elise L.V. Malavasi, Fumiaki Ogawa, David J. Porteous and J. Kirsty Millar

Hum. Mol. Genet. *(2012)* ***21****(12): 2779-2792*

This article contains work described in chapters 3, 4 and 7 of this thesis. I have designed and performed all the experimental work described in the article. The IPLab script used to analyse confocal images for DISC1 nuclear distribution measurements was developed in collaboration with Paul Perry, from the MRC HGU in Edinburgh. The article was written by me, with input from Kirsty Millar, David Porteous, Dinesh Soares and Fumiaki Ogawa. The graphics were prepared by me. The full version of the article and the corresponding supplementary online material follow.

“DISC1 variants 37W and 607F disrupt its nuclear targeting and regulatory role in ATF4-mediated transcription”

Manuscript

Human Molecular Genetics, 2012, Vol. 21, No. 12 **2779–2792**
doi:10.1093/hmg/dds106
Advance Access published on March 15, 2012

DISC1 variants 37W and 607F disrupt its nuclear targeting and regulatory role in ATF4-mediated transcription

Elise L.V. Malavasi, Fumiaki Ogawa, David J. Porteous and J. Kirsty Millar*

The Centre for Molecular Medicine at the Medical Research Council Institute of Genetics and Molecular Medicine, The University of Edinburgh, Crewe Road, Edinburgh EH4 2XU, UK

Received January 26, 2012; Revised and Accepted March 12, 2012

***Disrupted-In-Schizophrenia 1* (*DISC1*), a strong genetic candidate for psychiatric illness, encodes a multicompartmentalized molecular scaffold that regulates interacting proteins with key roles in neurodevelopment and plasticity. Missense *DISC1* variants are associated with the risk of mental illness and with brain abnormalities in healthy carriers, but the underlying mechanisms are unclear. We examined the effect of rare and common DISC1 amino acid substitutions on subcellular targeting. We report that both the rare putatively causal variant 37W and the common variant 607F independently disrupt DISC1 nuclear targeting in a dominant-negative fashion, predicting that DISC1 nuclear expression is impaired in 37W and 607F carriers. In the nucleus, DISC1 interacts with the transcription factor Activating Transcription Factor 4 (ATF4), which is involved in the regulation of cellular stress responses, emotional behaviour and memory consolidation. At basal cAMP levels, wild-type DISC1 inhibits the transcriptional activity of ATF4, an effect that is weakened by both 37W and 607F independently, most likely as a consequence of their defective nuclear targeting. The common variant 607F additionally reduces DISC1/ATF4 interaction, which likely contributes to its weakened inhibitory effect. We also demonstrate that DISC1 modulates transcriptional responses to endoplasmic reticulum stress, and that this modulatory effect is ablated by 37W and 607F. By showing that DISC1 amino acid substitutions associated with psychiatric illness affect its regulatory function in ATF4-mediated transcription, our study highlights a potential mechanism by which these variants may impact on transcriptional events mediating cognition, emotional reactivity and stress responses, all processes of direct relevance to psychiatric illness.**

INTRODUCTION

Disrupted-In-Schizophrenia 1 (*DISC1*) is a risk factor for brain disorders ranging from depression to schizophrenia (1). *DISC1* encodes a multifunctional, multicompartmentalized scaffold protein with well-established roles in several aspects of neuronal physiology, including neural progenitor proliferation, migration and differentiation, as well as neurotransmission (2).

In the nucleus, DISC1 partially co-localizes with promyelocytic leukaemia nuclear bodies, which identify sites of active transcription (3), suggesting that DISC1 might be involved in transcriptional regulation. In support of this, DISC1 can interact with two highly related stress-responsive transcription factors, Activating Transcription Factor 4 (ATF4) and Activating Transcription Factor 5 (ATF5) (3–6), as well as the transcriptional repressor nuclear receptor co-repressor (N-CoR) (3). The first direct evidence for the involvement of nuclear DISC1 in transcriptional regulation was provided in a study by Sawamura *et al*. (3), who demonstrated that DISC1 can modulate cAMP-dependent cAMP-response element (CRE)-mediated transcription by interacting with ATF4.

ATF4 belongs to the activating transcription factor/CRE binding protein (ATF/CREB) family of basic region-leucine zipper (bZIP) transcription factors, which share the ability to bind to the CRE (7). Under basal conditions, ATF4 is expressed at very low levels, but its transcription and

*To whom correspondence should be addressed at: Molecular Medicine Centre, Crewe Road, Edinburgh EH4 2XU, UK. Tel: +44 1316511044; Fax: +44 1316511059; Email: kirsty.millar@ed.ac.uk

translation are rapidly upregulated in response to a range of different stressors (8). ATF4 can function both as a transcriptional activator and a transcriptional repressor (7). Genes whose expression is activated by ATF4 include pro- and anti-apoptotic factors (9,10), as well as genes involved in amino acid metabolism, regulation of the cell's redox balance and mitochondrial function (11). Additionally, ATF4 regulates emotional behaviour, synaptic plasticity and behavioural learning (12,13). Indeed, because of its ability to repress the CREB-mediated late phase of long-term potentiation (LTP) and long-term memory (LTM) (13), ATF4 has been referred to as a 'memory suppressor gene' (14,15). It is therefore possible that through its interaction with ATF4, DISC1 might contribute to the regulation of the transcriptional response to cellular stress as well as to emotional and LTP-inducing stimuli.

A number of *DISC1* missense variants have been associated with the increased risk of psychiatric illness, altered brain morphology or cognitive deficits (1,2), but the molecular link between structural changes in DISC1 and clinical outcome has yet to be established. Several risk-conferring missense variants within *DISC1* have the potential to modify the structure, biochemical properties and subcellular targeting of the protein, lending support to their putative pathogenic role (16). In this study, we examined the effect of a spectrum of common and rare amino acid substitutions of DISC1 associated with psychiatric illness on the nuclear targeting of the protein. We found that both the rare putatively causal variant 37W and the common 607F substitution impair nuclear targeting of DISC1, exerting a dominant-negative effect on the nuclear distribution of wild-type DISC1. Furthermore, the defective nuclear targeting of DISC1 variants 37W and 607F is reflected in their decreased ability to inhibit ATF4-dependent transcription. Recently, 607F was shown to impact on neural development by abrogating DISC1-mediated activation of *wnt*-dependent transcription (17). Our findings add to the evidence for a functional role of 607F in transcriptional regulation, and provide a direct link between risk-conferring genetic variants and aberrant targeting and function of nuclear DISC1.

RESULTS

Variants 37W and 607F decrease the nuclear abundance of DISC1

Several non-synonymous *DISC1* variants have been associated with psychiatric illness and structural brain changes, and some have been shown to impact on specific aspects of DISC1 biology (1,2,17). Because DISC1 is a multicompartmentalized protein, we first assessed the impact of a panel of such disease-associated amino acid substitutions upon its subcellular distribution. We generated expression constructs ($n = 20$) carrying 37W, 432L or 603I (rare/ultra rare) or 607F (common) variants (1,2,18) in all possible combinations with the common polymorphisms R264Q and S704C (1,2). With the exception of R264Q and P432L, all of these DISC1 variants are at highly conserved positions, and all have the potential to influence the subcellular distribution of DISC1, either because they are predicted to disrupt critical structural motifs, or because they occur in regions of DISC1 that mediate binding to key partner proteins (16).

In a pilot experiment, we used immunocytochemistry to quantify the relative nuclear abundance of exogenous DISC1 in COS7 cells transfected with either one of the 20 DISC1 expression constructs. We found no evidence for an effect of substitutions at positions 264, 432, 603 or 704 on the nuclear targeting of DISC1 (Supplementary Material, Fig. S1), nor for gross alteration of the overall subcellular distribution of DISC1 (not shown). In contrast, both the R37W and the L607F substitutions result in depletion of exogenous DISC1 from the nucleus (Supplementary Material, Fig. S1). Additional variation at positions 264 and 704 does not modify the effect of 37W or 607F on the nuclear abundance of DISC1 (Supplementary Material, Fig. S1). These preliminary observations were confirmed by further immunocytochemical analysis on larger samples of cells (Fig. 1A and B). Both sequence variants reduce nuclear expression of DISC1 by ~50% ($P < 0.01$). The observed decrease in nuclear expression of DISC1-37W or DISC1-607F is not due to decreased overall expression of these DISC1 variants (Supplementary Material, Fig. S2), which confirms that DISC1 carrying R or L at positions 37 and 607, respectively, is targeted to the nucleus more efficiently. DISC1-37W also induces formation of perinuclear mitochondrial clusters (Fig. 1B), which are the subject of a separate study (F. Ogawa, unpublished data). In addition, when compared with wild-type DISC1, DISC1-607F assumes a more diffuse distribution in the cytoplasm (Fig. 1B and Supplementary Material, Fig. S3). Since we found no evidence for an effect of amino acid variation at positions 264 and 704 on the subcellular distribution of DISC1, we performed all the subsequent experiments using DISC1 constructs encoding the common variants at these positions (264R and 704S). The common full-length DISC1 variant, to which all other variants analysed here are compared, will henceforth be referred to in the text as 'wild-type (WT) DISC1'.

To further examine the effect of DISC1 variants 37W and 607F on the subcellular distribution of the protein, we prepared whole-cell lysates and subcellular protein fractions from transfected and untransfected SH-SY5Y neuroblastoma cells and analysed them by western blotting. While the total protein levels of exogenous wild-type, DISC1-37W and DISC1-607F were comparable, we detected a ~50% decrease in the relative nuclear abundance of DISC1-37W and DISC1-607F ($P < 0.01$, Fig. 1C), and observed a similar effect by immunocytochemistry (Supplementary Material, Fig. S4). This reduction in nuclear expression in SH-SY5Y cells is equivalent to that observed in COS7 cells. Besides being clearly detectable in the soluble nuclear protein extract, the full-length 100 kDa DISC1 isoform (both endogenous and exogenous) is also present in the cytoplasmic, membrane-bound and cytoskeletal extracts, but not in the chromatin-bound protein fraction (Fig. 1D). While endogenous DISC1 is predominantly enriched in the cytoplasmic and membrane-associated fractions, the vast majority of exogenous wild-type DISC1 is present in the cytoskeletal fraction (Fig. 1D). Interestingly, the relative protein abundance of DISC1-WT, DISC1-37W and DISC1-607F is comparable in the cytoplasmic and membrane-associated fractions;

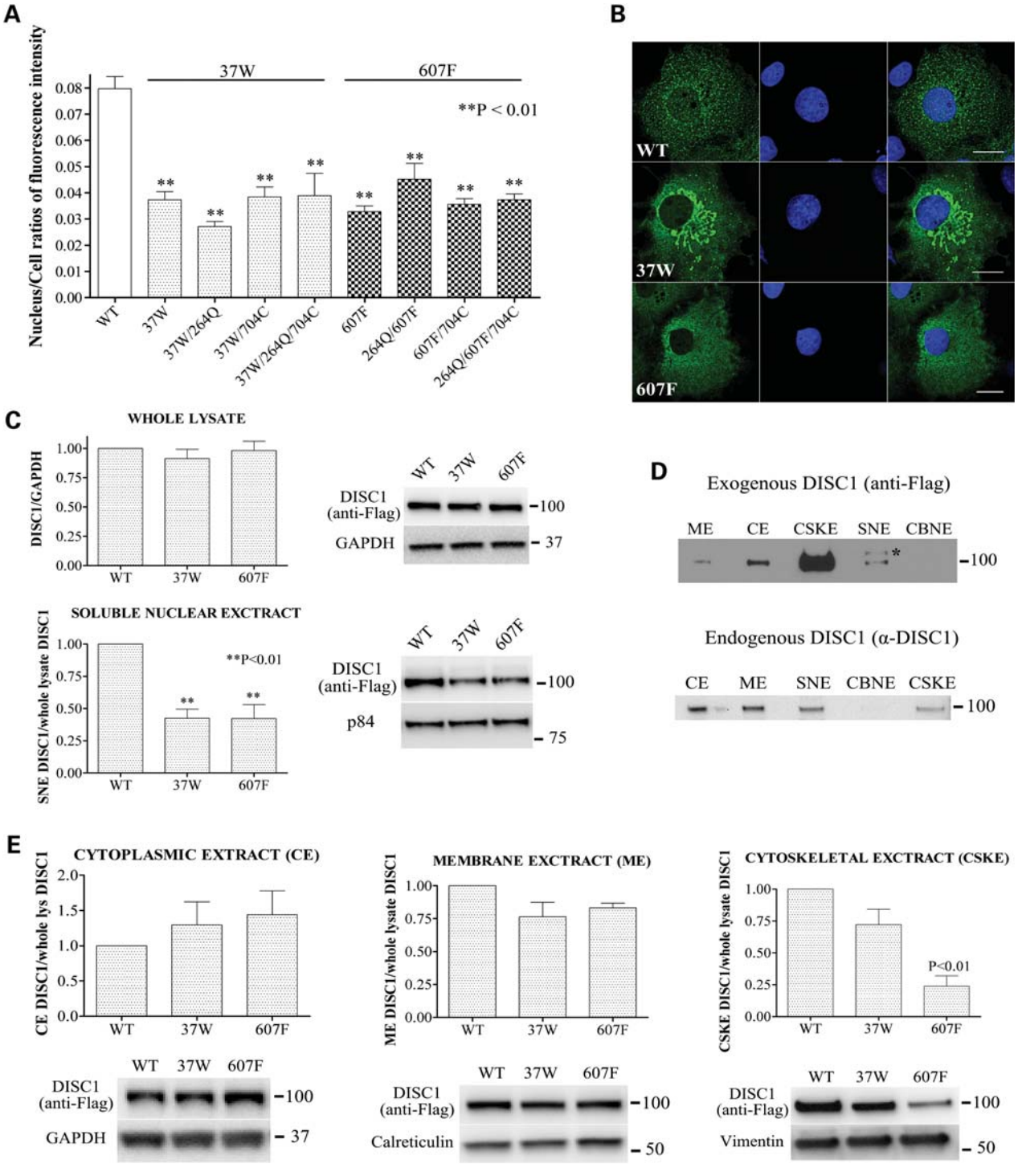

Figure 1. Effect of DISC1 variants on its subcellular distribution. (**A**) Relative abundance of DISC1 variants in the nucleus of transfected COS7 cells calculated as the ratio between the total pixel intensity of DISC1 staining in the nucleus and the total pixel intensity of DISC1 staining in the whole cell. The bars represent the mean values measured in three independent experiments in which 50 cells/variant were analysed. (**B**) Representative confocal images of COS7 cells expressing wild-type DISC1, DISC1-37W or DISC1-607F. DISC1 is in green, and the nuclei are stained with DAPI (blue). Scale bars are 20 μm. (**C**) Distribution of wild-type DISC1, DISC1-37W or DISC1-607F in whole-cell lysates and soluble nuclear extracts (SNE) prepared from transfected SH-SY5Y cells. Each bar represents the average of four independent experiments. (**D**) Equal amounts of sub-cellular protein extracts obtained from SH-SY5Y cells that were either untransfected (bottom) or transfected with wild-type DISC1 (top) were analysed by western blotting using antibodies to detect endogenous or exogenous DISC1, respectively. ME, membrane extract; CE, cytoplasmic extract; CSKE, cytoskeletal extract; CBNE, chromatin-bound nuclear extract. *Non-specific band. (**E**) The indicated sub-cellular protein extracts were obtained from SH-SY5Y cells transfected with wild-type, 37W or 607F DISC1 and analysed by western blotting to detect exogenous DISC1, followed by band densitometry. The loading controls are proteins known to be preferentially enriched in either of the different subcellular fractions analysed. The bars represent the average of four independent experiments. All the densitometry data are normalized to the relative band intensity of wild-type DISC1. The position and size (kDa) of the protein markers is indicated.

however, variant 607F is strongly depleted from the cytoskeletal fraction ($P < 0.01$, Fig. 1E), consistent with its aberrant cytoplasmic distribution (Fig. 1B and Supplementary Material, Fig. S3).

Dominant-negative effect of 37W and 607F upon wild-type DISC1 nuclear distribution

Next, due to the propensity of DISC1 to oligomerize (19–22), we asked if risk-conferring DISC1 variants 37W and 607F act in a dominant-negative fashion. Whole-cell lysates and nuclear protein extracts from SH-SY5Y cells expressing wild-type DISC1 alone or in combination with either DISC1-37W or DISC1-607F were analysed by western blotting. We verified that the different DISC1 expression constructs used in these experiments achieved comparable levels of protein expression in SH-SY5Y cells (Supplementary Material, Fig. S5). As shown in Figure 2A, co-expression of DISC1-37W or DISC1-607F results in a significant decrease in nuclear abundance of wild-type DISC1 ($P < 0.01$), with this effect being particularly pronounced for the 37W variant when compared with 607F ($P < 0.05$). To further examine this, we co-expressed DISC1-37W or DISC1-607F with wild-type DISC1 in COS7 and SH-SY5Y cells and analysed the sub-cellular distribution of each variant by immunocytochemistry, using cells transfected with wild-type DISC1 only as a control. As expected, when wild-type DISC1 is expressed alone, it translocates to the nucleus, where it is detectable as numerous bright puncta on a more diffuse background (Fig. 2B and Supplementary Material, Fig. S6). Consistent with the results of our subcellular protein fractionation experiment, both DISC1-37W and DISC1-607F reduce the formation of wild-type DISC1 puncta in the nucleus (Fig. 2B and Supplementary Material, Fig. S6). Furthermore, we noted that the cytoplasmic distribution of wild-type DISC1 appears more diffuse in the majority of cells co-expressing DISC1-607F (Fig. 2B and Supplementary Material, Fig. S6). Our results predict that 37W or 607F carriers will have substantially reduced nuclear DISC1 expression, and that 607F homozygotes will be similar to 607F heterozygotes in this particular respect.

Differential effect of DISC1 variants 37W and 607F on ATF4-mediated transcription

Sawamura *et al*. (3) showed that co-expression of DISC1 suppresses Gal4-ATF4-mediated transcription and that it enhances the ATF4-mediated inhibition of CRE-dependent transcription in response to increased intracellular cAMP levels. Since ATF4 has also been reported to activate CRE-mediated transcription under basal (low cAMP) conditions (23–25), we asked whether DISC1 regulates ATF4-mediated activation of the CRE at basal cAMP levels. As expected, in luciferase reporter assays carried out in HEK293 cells, we detected activation of CRE-driven transcription upon overexpression of ATF4, but not its dominant-negative mutant ATF4ΔRK, which lacks the DNA-binding domain (26,27) (Supplementary Material, Fig. S7). At basal cAMP levels, co-expression of DISC1 inhibits the ATF4-mediated transactivation of CRE-driven transcription in a dose-dependent manner ($P < 0.01$, Fig. 3A). Importantly, overexpression of DISC1 alone has no effect on the basal activity of the Som-CRE-luc reporter (Supplementary Material, Fig. S8), indicating that DISC1 acts via ATF4.

Next, we tested the effect of DISC1 variants 37W and 607F. Both retain the ability to inhibit ATF4 transcriptional activity, but their inhibitory effect is significantly weaker compared with wild-type DISC1 ($P < 0.05$ for 37W, $P < 0.01$ for 607F, Fig. 3B). This is not caused by differences in expression levels (Supplementary Material, Fig. S9) nor it is limited to HEK293 cells, as we observed this same effect in MO3.13 human oligodendrocytes ($P < 0.05$ for both variants, Fig. 3C).

The transactivation activity of ATF4 is not limited to CRE-containing promoters. In fact, several ATF4 target genes involved in the response to cellular stresses such as amino acid limitation, oxidative stress or endoplasmic reticulum stress are activated through C/EBP-ATF Response Elements (CARE) in their promoters (28). For example, ATF4 induces expression of its target gene C/EBP homology protein (CHOP) by binding to a particular type of CARE in its promoter, the Amino Acid Response Element (AARE) (9,29,30). Thus, we sought to test whether DISC1 modulates the activity of ATF4 at the CHOP AARE. As expected, ATF4 strongly activates transcription from a CHOP AARE-luciferase reporter, but not from its mutant, non-responsive counterpart (31) (Supplementary Material, Fig. S10). As with the CRE, wild-type DISC1 significantly represses the ATF4-dependent transactivation of the CHOP AARE ($P < 0.01$, Fig. 3D). This inhibitory effect is reduced by DISC1-607F ($P < 0.05$, Fig. 3D) and DISC1-37W ($P < 0.05$, Fig. 3D).

To further investigate the likely relationship between the decreased ability of DISC1 variants 37W and 607F to inhibit the transcriptional activity of ATF4 and their defective nuclear targeting, we tested a mutant form of DISC1 lacking the predicted leucine zipper in exon 9 (DISC1ΔLZ9), located between amino acids 607 and 628. Alanine substitutions at positions 614 and 621 prevent translocation of DISC1 to the nucleus (3), consistent with LZ9 being required for nuclear targeting. As expected, when expressed in COS7 cells, DISC1ΔLZ9 fails to accumulate in the nucleus, and assumes a diffuse distribution in the cytoplasm (Fig. 4A), closely resembling that of DISC1-607F (Fig. 1B, Supplementary Material, Figs S3 and S4). The remarkably similar effects of 607F and DISC1ΔLZ9 upon DISC1 nuclear localization are likely related to the predicted structural disruption of LZ9 by 607F (16). Consistent with its exclusion from the nucleus, DISC1ΔLZ9 does not significantly inhibit ATF4-mediated activation of CRE-dependent transcription ($P < 0.05$, Fig. 4B).

ATF4 plays a central role in mediating the cellular response to a range of damaging stimuli, including endoplasmic reticulum stress (7). Following on from our finding that DISC1 represses the transcriptional activity of exogenous ATF4, we examined the effect of DISC1 on the transcriptional activity of endogenously induced ATF4 using the endoplasmic reticulum stress inducer thapsigargin. In line with previously reported observations (32), thapsigargin treatment induces expression of endogenous ATF4 (Supplementary Material, Fig. S11) and determines a ~2-fold activation of CRE-

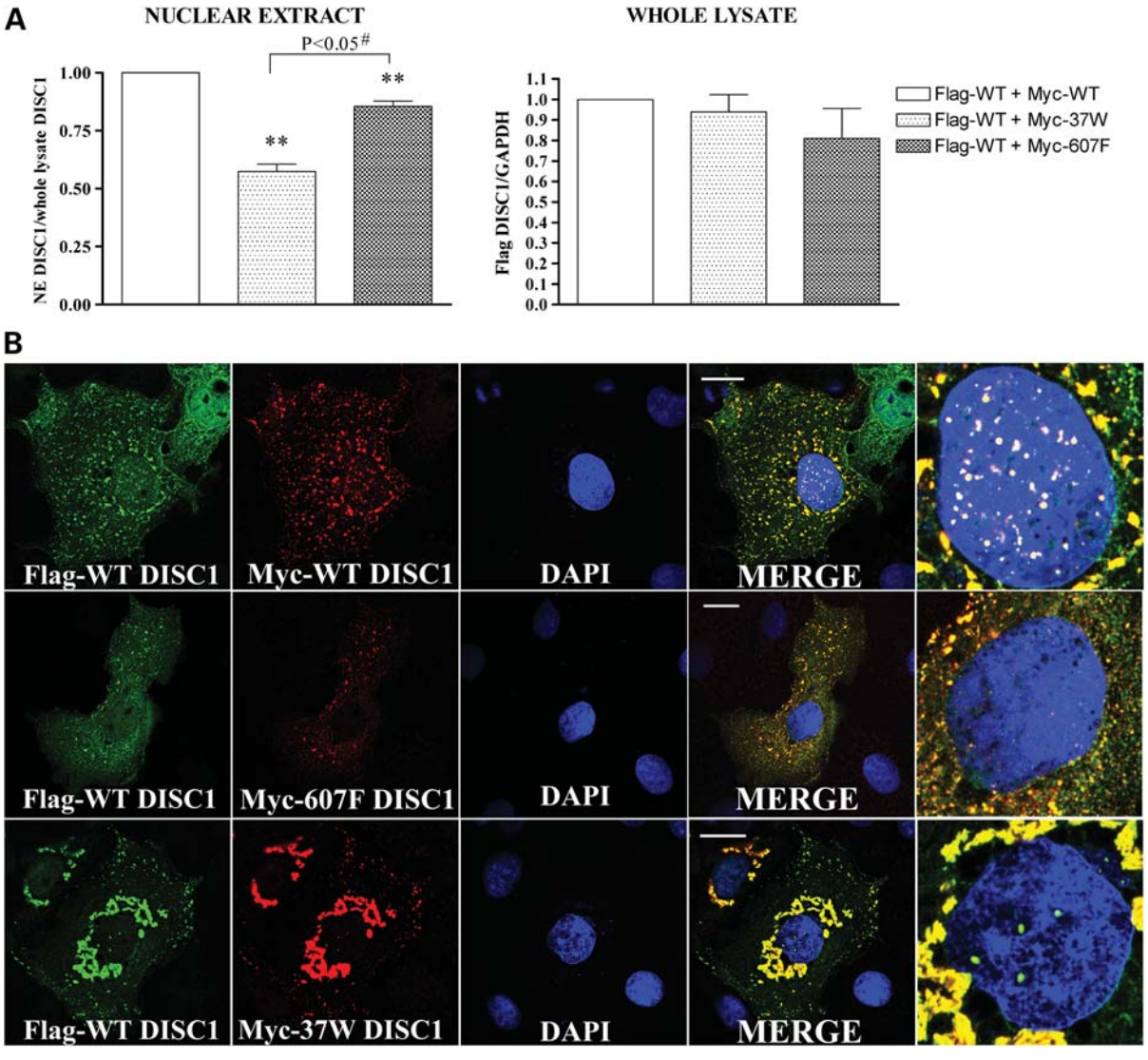

Figure 2. Dominant-negative effect of 37W and 607F DISC1. (**A**) SH-SY5Y cells were transfected with Flag-WT DISC1 and an equal amount of either Myc-DISC1-WT, Myc-DISC1-37W or Myc-DISC1-607F. The relative abundance of Flag-WT DISC1 was then quantified by western blotting in whole-cell lysates and nuclear extracts (NE) prepared from the transfected cells. The bars represent the average of three independent experiments. The data are normalized to the relative band density of Flag-DISC1 in samples expressing WT DISC1 only. (**B**) Sub-cellular distribution of Flag-DISC1 (green) and Myc-DISC1 (red) in representative COS7 cells expressing Flag-WT DISC1 in combination with an equal amount of Myc-DISC1-WT (top), Myc-DISC1-607F (middle) or Myc-DISC1-37W (bottom). Magnifications of the cell nuclei are shown in the far-right panels. $^{**}P < 0.01$; $^{\#}$two-tailed paired Student's *t*-test. Scale bars are 20 μm.

dependent transcription (Fig. 5). Overexpression of wild-type DISC1, but not variants 37W and 607F or the mutant DISC1ΔLZ9, significantly inhibits the thapsigargin-induced activation of CRE-dependent transcription (Fig. 5).

Morris *et al*. (4) showed that co-expression of full-length DISC1 inhibits accumulation of ATF5 in the cell nucleus. Since ATF4 and ATF5 are structurally closely related (33), we asked whether DISC1 impacts on the nuclear distribution and/or protein levels of ATF4, which may contribute to the observed transcriptional inhibition. Surprisingly, in cells transfected using the same ATF4/DISC1 DNA ratio used in the luciferase reporter assays, co-expression of DISC1 does not decrease the overall protein expression or nuclear targeting of exogenous ATF4, but instead seems to have the opposite effect, although this does not reach statistical significance (Fig. 6A and B). DISC1 therefore apparently does not inhibit ATF4-mediated transcription by reducing nuclear ATF4 expression.

Although exogenous ATF4 is highly enriched in the nucleus, we noticed that it is also detectable in the perinuclear region in a pattern closely resembling the typical morphology of mitochondria (Fig. 6A), an organelle to which DISC1 is known to localize (34–36). Cytoplasmic ATF4 partially co-localizes with exogenous DISC1 in this location (Fig. 6A). To better test for a potential mitochondrial localization of exogenous ATF4, we used four different antibodies to detect the protein (both tagged and untagged) in transfected COS7 cells. In each case, we observed partial co-localization

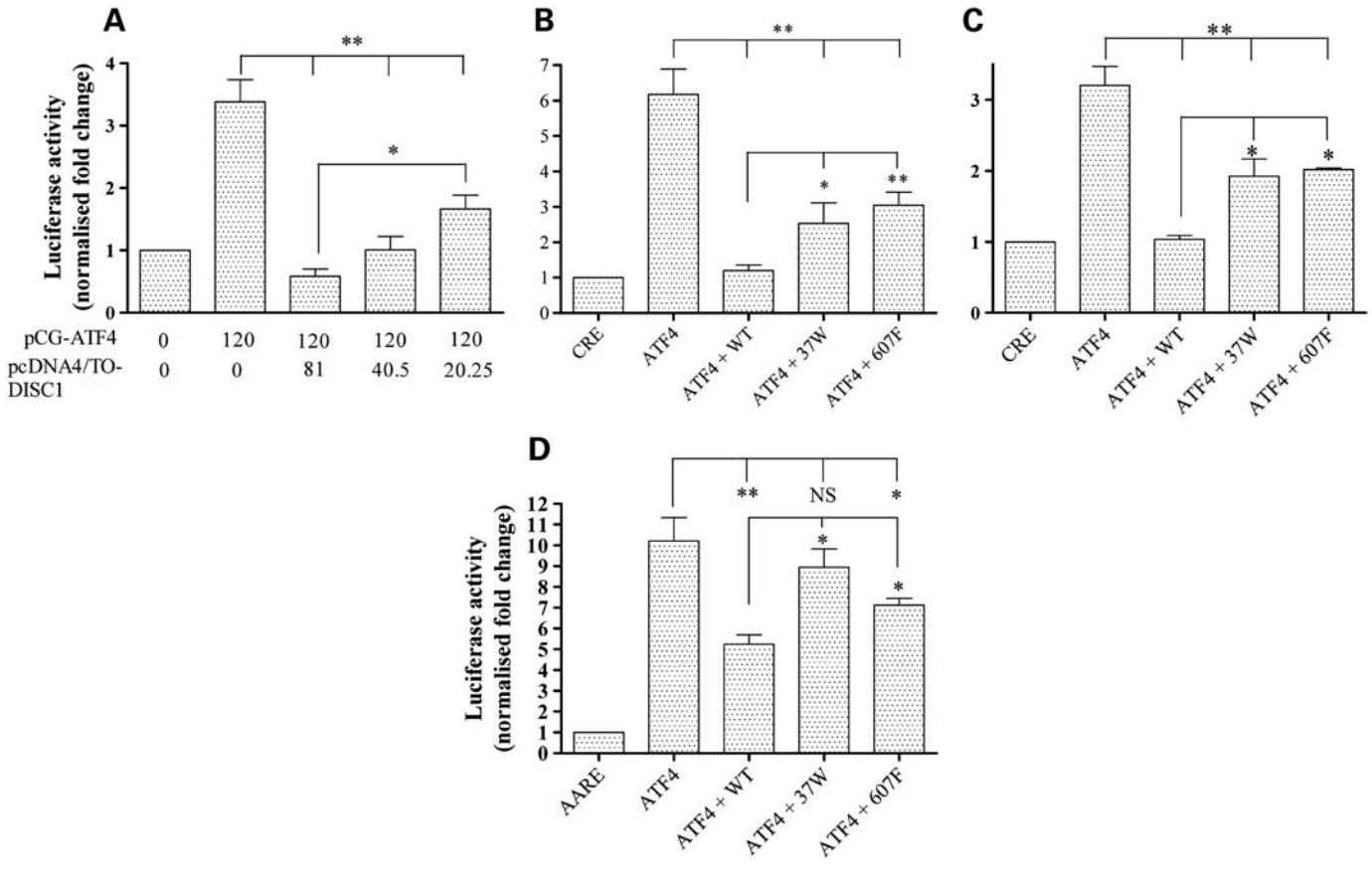

Figure 3. Differential effect of DISC1 variants on ATF4-mediated transcription. (**A**) Relative CRE-dependent luciferase activity in HEK293 cells transfected with a fixed amount of pCG-ATF4 and decreasing amounts of wild-type DISC1. The numbers indicate the amount (ng/well) of plasmid DNA used for transfection. (**B** and **C**) Relative CRE-driven luciferase activity in HEK293 (B) or human oligodendrocyte MO3.13 cells (C) transfected with ATF4 only or in combination with the indicated DISC1 variants. (**D**) Relative CHOP AARE-driven luciferase activity in HEK293 cells transfected with ATF4 only or in combination with the indicated DISC1 variants. All data are normalized to the relative luciferase activity in cells transfected with the reporters only (CRE or AARE). The bars represent the average of at least three independent experiments. $^{*}P < 0.05$, $^{**}P < 0.01$.

of ATF4 with mitochondria, particularly in the perinuclear region (Supplementary Material, Fig. S12).

DISC1 variants affect its interaction with ATF4

The L607F substitution is predicted to disrupt the Leucine packing in DISC1 LZ9, a region identified as essential to mediate binding to ATF4 (3), and could therefore directly impair the DISC1–ATF4 interaction. In addition, by introducing a physical segregation between the two proteins, the defective nuclear localization of DISC1 variants 37W and 607F might in itself impair their interaction with ATF4, the majority of which is found in the nucleus. This mechanism could contribute to their blunted inhibitory effect on ATF4-mediated transcription. As expected, in co-immunoprecipitation assays performed with exogenous proteins in HEK293 cells, DISC1-607F shows significantly impaired binding to ATF4 (Fig. 7A). However, the R37W substitution produces only a slight, non-significant decrease in DISC1 binding to ATF4 (Fig. 7A).

The observed discrepancy between the defective nuclear targeting of DISC1-37W and its largely preserved interaction with ATF4 prompted us to analyse the sub-cellular distribution of the two proteins in co-transfected cells. Interestingly, unlike wild-type DISC1 and DISC1-607F, which exhibit limited co-localization with ATF4 outside the nucleus, DISC1-37W clearly co-distributes with ATF4 at mitochondria (Fig. 7B). We therefore conclude that the reduced capacity of DISC1-37W to inhibit ATF4-mediated transcription is due to its exclusion from the nucleus, rather than to reduced interaction with ATF4.

DISCUSSION

Growing evidence indicates that by establishing dynamic interactions with multiple binding partners, DISC1 functions as a hub protein whose principal role is to modulate various cellular processes in a space- and time-regulated manner. Sequence changes in DISC1 that disrupt its normal compartmentalization and protein interactions are therefore likely to have functional consequences, and may highlight biological processes involved in psychopathology.

In this study, we demonstrated that the putatively causal variant 37W and the common variant 607F both induce a ~50% depletion of the nuclear pool of DISC1, and perturb

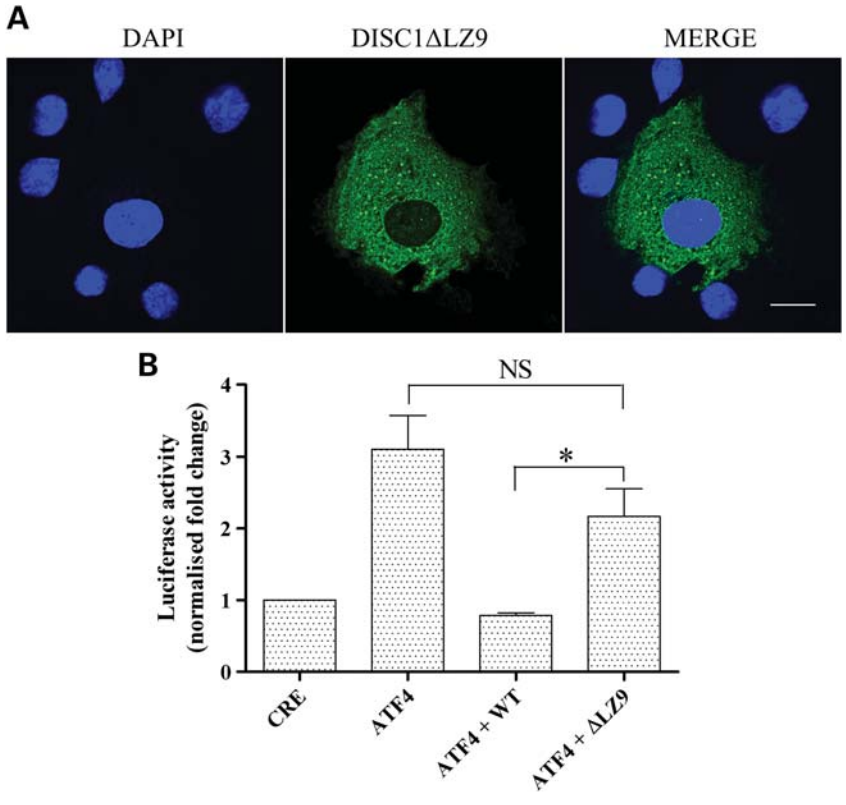

Figure 4. Effect of DISC1 LZ9 on nuclear distribution of DISC1 and transcriptional regulation of ATF4. (**A**) Confocal image of a representative COS7 cell expressing DISC1ΔLZ9 (green). Nuclei are stained with DAPI (blue). (**B**) Relative luciferase activity in HEK293 cells transfected with the reporters only (CRE) or in combination with ATF4 with or without wild-type DISC1 or DISC1ΔLZ9. The bars represent the average of four independent experiments. The data are normalized to the relative luciferase activity in cells expressing the reporters only (CRE). $^{*}P < 0.05$, two-tailed paired Student's *t*-test. The scale bar is 20 μm.

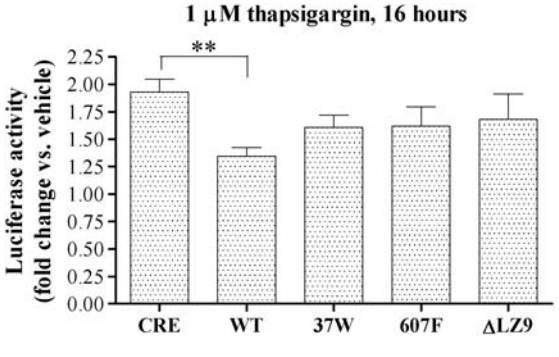

Figure 5. Effect of DISC1 on the CRE-mediated transcriptional response to thapsigargin. HEK293 cells were transfected with the reporters only (CRE) or in combination with the indicated expression constructs. Starting from 32 h post-transfection, the cells were exposed to thapsigargin or vehicle (DMSO) for the indicated time before being assayed for luciferase activity. The bars represent the average of at least three independent experiments. $^{**}P < 0.01$.

the nuclear targeting of wild-type DISC1 in a dominant-negative fashion. In addition, both variants negatively impact on the ability of DISC1 to regulate transcription in response to exogenous ATF4 and endoplasmic reticulum stress. 37W was identified in a patient diagnosed with schizophrenia and not in 10 000 control alleles (18), and is thus a rare, putatively causal variant. In contrast, 607F is a common variant, present in ~10% of the population. The single nucleotide polymorphism (SNP) determining variation at this position, or haplotypes including this SNP, is associated with schizophrenia, schizoaffective disorder, bipolar disorder and depression and correlate with symptom severity in schizophrenia, the P300 waveform mental illness endophenotype and influence brain structure and function (37–46). Singh *et al*. (17) recently assayed several DISC1 variants, including L607F and two other common variants R264Q and S704C for their effect on *wnt* signalling. Interestingly, they reported abnormal *wnt* signalling for 264Q and 607F, but not 704C, while we report abnormal nuclear localization and ATF4 binding for 607F, but not 264Q or 704C, consistent with a differential effect of non-synonymous amino acid substitutions on the varied and distinct functions of DISC1.

The 37W sequence change disrupts a highly conserved tetra-arginine nuclear localization signal in the otherwise poorly conserved head region of DISC1 (3), while the common variant 607F is located in a conserved predicted leucine zipper which was previously shown to contribute to DISC1 nuclear targeting and to be essential for interaction with ATF4 (3). The predicted disruption of this leucine zipper structural feature by L607F (16) therefore likely explains the reduced nuclear targeting and ATF4 binding of DISC1-607F, two effects that may potentially be interrelated.

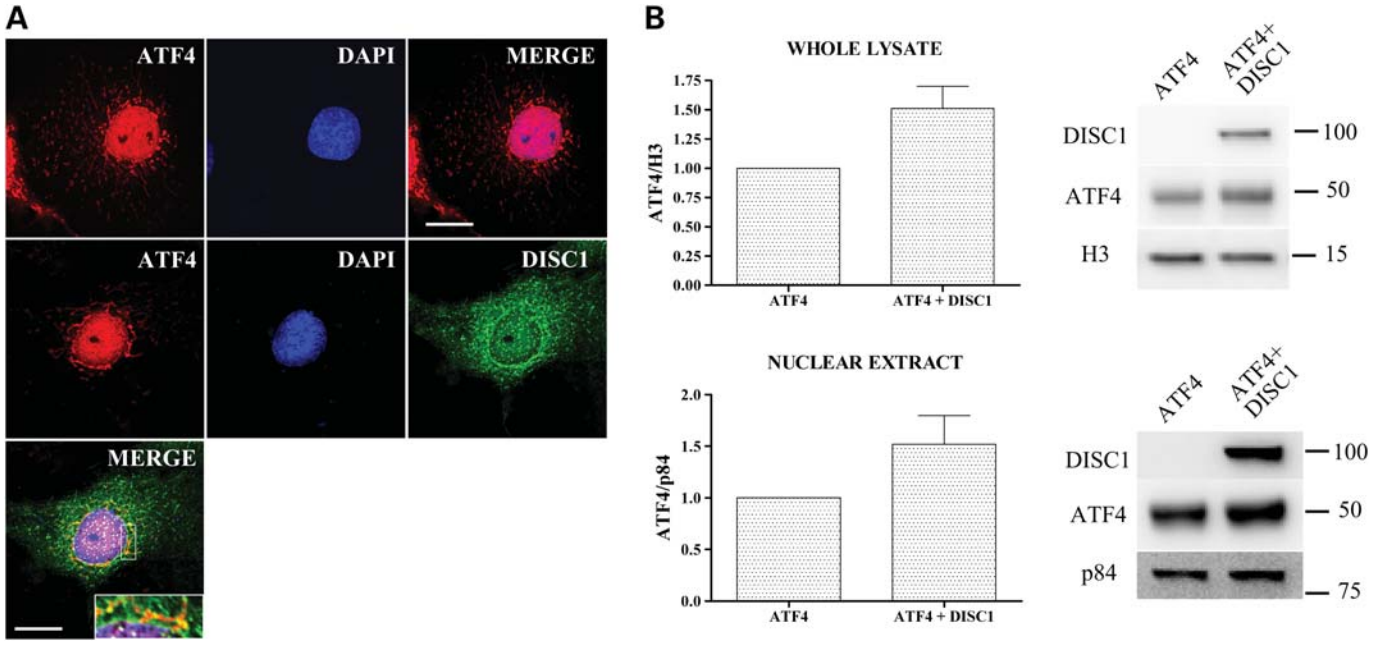

Figure 6. DISC1 does not affect nuclear targeting and protein levels of ATF4. (**A**) Representative COS7 cells transfected with ATF4 alone (top panels) or in combination with DISC1 (lower panels). The area delimited by a white rectangle is magnified in the inset. (**B**) ATF4 protein levels in whole-cell lysates or nuclear extracts prepared from HEK293 cells transfected with ATF4 alone or in combination with DISC1. The ATF4/DISC1 DNA ratio used in these experiments was the same as that used for the luciferase reporter assays. Loading controls are histone 3 (H3) for whole-cell lysates and nuclear matrix protein p84 for nuclear extracts. The bars represent the average of three independent experiments. Scale bars are 20 μm. The position and size (kDa) of the protein markers is indicated.

For both 37W and 607F sequence variants, the end result of reduced nuclear DISC1 expression most likely explains their decreased ability to repress ATF4 transcriptional activity.

Depending on the construct tested, DISC1 is capable of forming dimers, octamers and other oligomers and multimers (19,20,22,47,48). Thus, in heterozygous cells expressing wild-type and variant DISC1, hetero/oligomerization will likely occur, accounting for the dominant-negative effects reported here. Indeed, we have recently observed that DISC1-37W recruits wild-type DISC1 to perinuclear mitochondrial aggregates (F. Ogawa, unpublished data). It is therefore possible that the dominant-negative effect exerted by DISC1-37W on the nuclear targeting of wild-type DISC1 results from redistribution of wild-type DISC1 to mitochondria. We observed a significant, but milder reduction in nuclear abundance of wild-type DISC1 upon co-expression of 607F DISC1, and a change in the cytoplasmic distribution of wild-type DISC1 from punctate to diffuse. 607F is located close to a region of DISC1 (668–747) identified as essential for oligomerization (20) and it resides within a predicted oligomerization-promoting leucine zipper (16). Thus, the dominant-negative effect of DISC1-607F on the nuclear and cytoplasmic distribution of wild-type DISC1 may be related to the potentially altered oligomerization propensity of this variant form of DISC1. These observations indicate that nuclear expression of wild-type and variant DISC1 will likely be reduced in 37W or 607F carriers, with consequent effects for the role of DISC1 in transcription.

ATF4 transcriptional activity is modulated at multiple levels, including transcription and translation, post-translational modification and repression of its transcriptional activity through protein interactions (7,8,23,49–51). Mammalian cells respond to different types of environmental stressors by activating distinct stress-responsive kinases, all converging on phosphorylation of the α subunit of eukaryotic initiation factor 2 α (eIF2-α) (52). Phosphorylation of eIF2-α inhibits general protein synthesis while favouring the preferential translation of ATF4 (11,53,54). The regulation of ATF4 expression in response to stress also occurs at the transcriptional level, with different environmental stressors either activating or suppressing ATF4 mRNA synthesis (8). At the post-translational level, ATF4 is regulated by phosphorylation at multiple sites, which controls both the protein stability by regulating its ubiquitination (55–57), and its transcriptional activity (49,51). One further level of control of ATF4 resides in its interaction with binding partners that can directly inhibit its transcriptional activity, such as CHOP (58), neuronal cell death inducible putative kinase (NIPK) (23) and, as we and others (3) have reported, DISC1. The existence of multiple mechanisms controlling the production, persistence and activity of ATF4 indicates the critical importance of tight regulation of ATF4-mediated gene transcription. We and others (23–25,29,30) have demonstrated that ATF4 activates CRE- and AARE-mediated transcription at basal cAMP levels, while, in contrast, ATF4 represses CRE-mediated transcription in response to elevated cAMP (3,59). DISC1 inhibits both the transactivation and repression (3) activities of ATF4, and is thus likely to be an important modulator of ATF4-mediated transcription in the brain. Our observation that the repressive activity of DISC1 is weakened by sequence variants that influence risk of mental illness suggests that altered ATF4-mediated transcription may be a contributing factor to the overall disease risk.

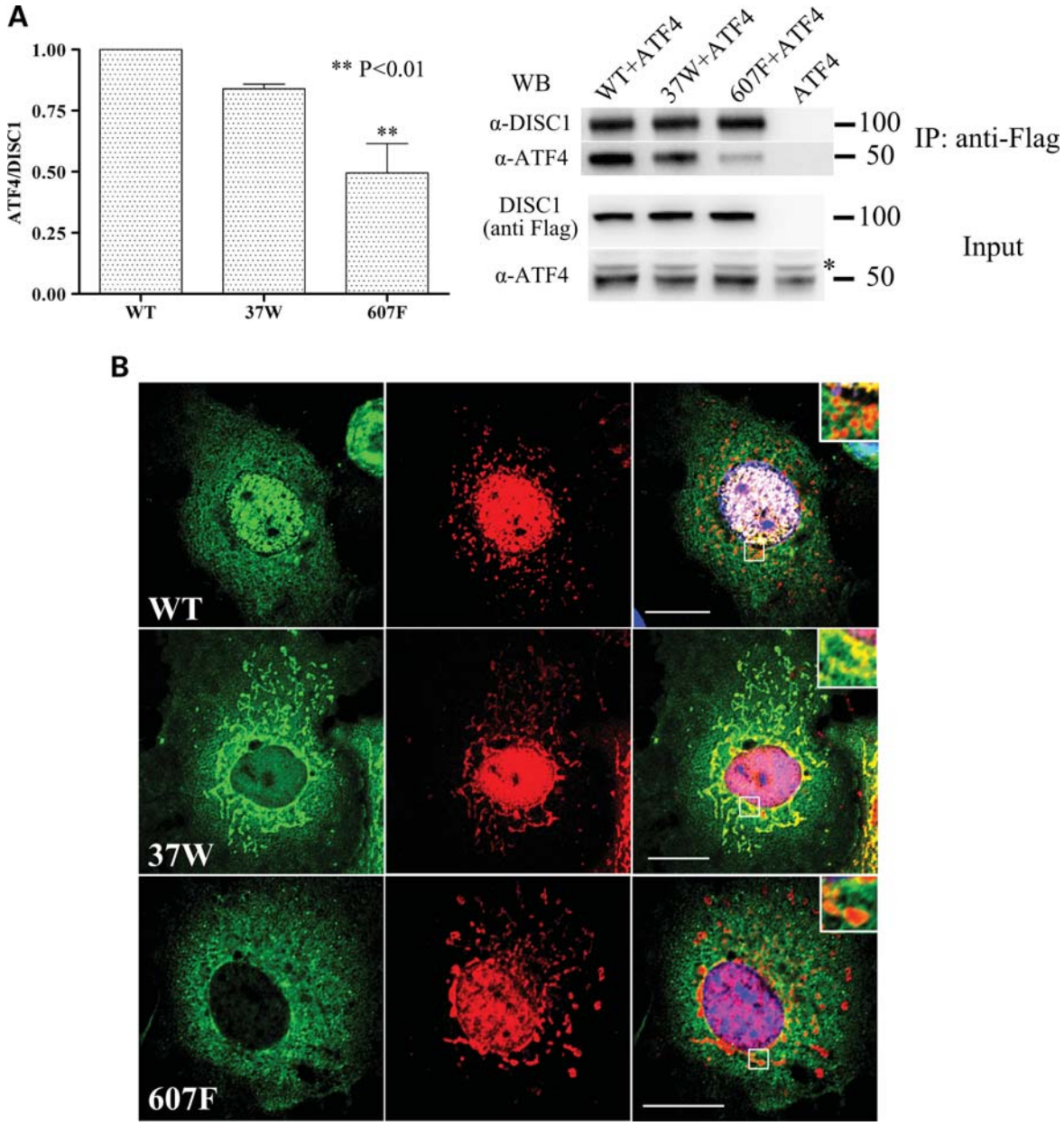

Figure 7. Effect of DISC1 variants on the interaction between DISC1 and ATF4. (**A**) HEK293 cells were transfected with pCG-ATF4 alone or in combination with the indicated DISC1variants. Exogenous DISC1 was immunoprecipitated using an anti-Flag antibody and detected using an anti-DISC1 antibody (α-DISC1). Co-precipitating ATF4 was detected with an anti-ATF4 antibody (sc-200). The bars represent the average of three independent experiments. *Non-specific band. The position and size (kDa) of the protein markers is indicated. (**B**) COS7 cells transfected with the indicated variants of DISC1 (green) and ATF4 (red). The right-hand panels represent the corresponding merged images. The areas delimited by a white square are magnified in the insets. Scale bars are 20 μm.

ATF4 antagonizes the transcriptional activity of CREB, a key mediator of LTP and LTM (13,15,60,61). Therefore, through its modulatory effect on ATF4, DISC1 might be involved in the regulation of the transcriptional events that mediate synaptic plasticity. This in turn implies that DISC1 variants 37W and 607F may deregulate synaptic plasticity and cognitive processes through their defective modulation of ATF4 transcriptional activity. Since cognitive impairment is a core feature of schizophrenia, this is a potential route by which these DISC1 variants influence risk of mental illness.

Both DISC1 and ATF4 are implicated in the regulation of emotional behaviour in rodent models (12,62–67). ATF4 expression in the nucleus accumbens (NA), a key reward region in the brain, is induced by amphetamine administration or restraint stress, and ATF4 overexpression in this region decreases the behavioural responsiveness to amphetamine (12). Like its related transcription factor CREB, ATF4 attenuates emotional reactivity and induces depression-like behaviours when overexpressed in the NA, clearly indicating that ATF4 functions as an activator of CRE-driven transcription

in this brain area (12). Like ATF4, DISC1 modulates the behavioural responsiveness to amphetamine in rodent models (66,68,69), and DISC1 mutations or altered expression are associated with depression-like behaviours in several mouse models (62–67). In the light of these findings, it is tempting to speculate that the role of DISC1 in emotional behaviour may be at least partly mediated by its modulation of ATF4 transcriptional activity on the CRE. If true, this would imply that DISC1 variants that interfere with this particular function of DISC1, such as 37W and 607F, may directly impact on the regulation of emotional behaviour.

ATF4 is also a key mediator of the integrated stress response, and its transcription and translation are strongly upregulated in response to a range of stressors, including amino acid deprivation, oxidative stress, hypoxia, viral infections, endoplasmic reticulum stress and mitochondrial dysfunction (28,70–73). The contribution of damaging environmental exposures to the risk of developing schizophrenia is well established, but mechanistically unclear. Maternal starvation, viral infections and perinatal hypoxia are among the best supported risk factors for schizophrenia (74), and each of these exposures could potentially activate the stress responses mediated by ATF4. It is intriguing to speculate that, by modulating the transcriptional activity of ATF4, DISC1 might contribute to regulation of cellular responses to stress, tipping the balance towards adaptation or apoptosis. In this scenario, 37W and 607F substitutions in DISC1 could increase the risk of mental illness by rendering the brain more susceptible to stress.

In conclusion, we have identified novel cellular and molecular phenotypes associated with common and rare DISC1 variants, and highlighted routes by which these psychiatric illness-associated variants could influence emotional and cognitive processes that are characteristically dysfunctional in mental illness, and the effects of environmental stressors that increase the risk of mental illness. Formal testing of gene–environment interactions has rarely been possible (75), but is of fundamental importance. Identification of a molecular mechanism that links the common DISC1 L607F polymorphism to the ATF4-mediated stress response provides an exciting opportunity to do so in cohorts with appropriate epidemiological data.

MATERIALS AND METHODS

Reagents and antibodies

DMSO and thapsigargin were from Sigma. Primary antibodies were: anti-Flag (F7425 and F3165) (Sigma), c-Myc (sc-40), anti-ATF4 (sc-200) (Santa Cruz) and anti-ATF4 (WH0000468M1) (Sigma), α-DISC1 (76), anti-p84 (ab487), anti-H3 (ab1791), anti-Calreticulin (ab22683), anti-Vimentin (ab8978) (Abcam) and anti-GAPDH (MAB347) (Millipore). TO-PRO3 and Mito Tracker Red were from Invitrogen.

Cell culture and transfection

MO3.13 cells (77) were a gift from Adrian Walmsley (Novartis Institute for Biomedical Research, Basel). All cell lines were cultured in DMEM supplemented with 10% FBS (Gibco) and maintained in a humidified incubator at 37°C and 5% CO_2. Unless otherwise stated, HEK293 and COS7 cells were transfected with Lipofectamine 2000 (Invitrogen) and SH-SY5Y cells were transfected with FugeneHD (Roche), according to the manufacturer's directions.

Plasmids

The ATF4 expression construct pCG-ATF4 (24), encoding human ATF4, was donated by Adrian Harris (University of Oxford). pCG-ATF4ΔRK was obtained by mutating the DNA-binding domain of human ATF4 in pCG-ATF4 (^{294}RYRQKKR^{300} to ^{294}GYLEAAA^{300}) by site-directed mutagenesis. The reporter Som-CRE-luc (Stratagene) and the TK-Renilla control luciferase vector were gifted by Richard Killick (King's College London). The reporter pGL4.23-CRE was generated by inserting four copies of the Somatostatin CRE (underlined) and its flanking regions (5′-AGCCTGACGTCAGAG-3′) upstream of the minimal promoter of the vector pGL4.23[luc2/minP] (Promega). The reporter vector pGL4.23-CHOP AARE and its mutant, non-responsive version pGL4.23-mutCHOP AARE, were generated by site-directed mutagenesis from pGL4.23[luc2/minP]. Mutagenic primers contained two copies of the core CHOP AARE (underlined) and its flanking regions: CHOP AARE, 5′-AACA**T**TGCATCATCCCCGC-3′ and mut CHOP AARE, 5′-AACA**A**TGCATCATCCCCGC-3′ (31), which only differed for the base in bold. All DISC1 expression constructs were generated from the plasmid pcDNA4/TO-Flag DISC1, coding for N-terminus Flag-tagged full-length human DISC1 (isoform L), by site-directed mutagenesis. All the site-directed mutagenesis reactions were performed using the QuikChange II or QuikChange Lightning site-directed mutagenesis kit (Stratagene), according to the manufacturer's directions. All the reporters and expression constructs were verified by direct sequencing.

Luciferase reporter assays

Most luciferase reporter assays were performed in HEK293 cells because they are a well-characterized model for the study of the transcriptional effects of ATF4 (30,78) and they consistently achieve high transfection rates, generating a strong and replicable luminescence signal. Cells were seeded in black-walled 96-well plates at a density of 6×10^4/well (HEK293) or 2.5×10^4/well (MO3.13) and transfected with Fugene HD (Roche Applied Science) or Lipofectamine 2000 (Invitrogen) according to the manufacturer's instructions. Cells were transfected with 90 ng/well of CRE-luciferase reporter plasmid and 9 ng/well of TK Renilla luciferase vector to control for variation in transfection efficiency. The CRE-luciferase reporters were Som-CRE-luc for HEK293 cells and pGL4.23-CRE for MO3.13 cells. The ATF4 expression plasmids were used at a concentration of 120 ng/well and 15 ng/well for CRE-reporter and CHOP AARE-reporter assays, respectively. Unless otherwise stated, DISC1 expression plasmids were used at 81 ng/well. Where necessary, the empty vector pcDNA4/TO was added to the transfection mix to bring the total amount of transfected DNA to 300 ng/well. Background luminescence was measured in cells transfected with the empty vector pcDNA4/TO, and subtracted from the

mean readings of each sample. Each transfection was performed in triplicate. Where indicated, drug treatments were started 32 h after transfection. When DMSO was used as vehicle, its final concentration in the medium was 0.1% or lower, and it did not affect cell viability or morphology. Luciferase activity was measured with the Dual Glo Luciferase Assay System (Promega), following the manufacturer's protocol.

Immunocytochemistry

To stain mitochondria, cells were incubated in 50 nM Mito Tracker Red in DMEM 10% FBS for 30 min before fixation. Cells were then fixed in methanol for 5 min at −20°C, followed by four washes in cold PBS. Fixed cells were blocked for 30 min in PBS containing 3% bovine serum albumin (PBS/BSA), and then incubated for 2 h at room temperature with the primary antibodies diluted in PBS/BSA. Anti-Flag antibodies F7425 and F3165 were used at 1:2000 and 1:10.000, respectively. The anti-c-Myc antibody was used at 1:500. The anti-ATF4 antibodies were used at 1:4000 (sc-200) and 1:2.500 (WH0000468M1). Secondary antibodies were Alexa Fluor goat anti-rabbit IgG 488 and 594 and Alexa Fluor goat anti-mouse IgG 488 and 594, all used at 1:1000. TO-PRO3 was used at 1:500. Images were acquired with a Zeiss LSM510 or a Nikon A1R confocal microscope.

Analysis of DISC1 subcellular distribution by immunofluorescence

COS7 cells transfected with equal amounts of the indicated DISC1 expression constructs were stained using an anti-Flag antibody (F7425) to detect exogenous DISC1, and nuclei were counterstained with TO-PRO3. Single plane confocal images of individual transfected cells were acquired using a Zeiss LSM510 confocal microscope (Zeiss). In each experiment, all the images were acquired using the same confocal settings. The investigator who acquired the images and performed the analysis was blinded to which variant of DISC1 had been transfected in each cell sample analysed. Image analysis was performed with IPLab version 3.9.5 r5 (BD Biosciences). For each cell image analysed, the total pixel intensity of DISC1 staining was measured both in the whole cell and in the nucleus only. The proportion of DISC1 staining localized in the nucleus was then calculated as the nucleus/cell ratio of total pixel intensities in individual cells.

Subcellular fractionation

Subcellular fractions were prepared from SH-SY5Y or HEK293 cells transfected with the indicated constructs for 72 or 24 h, respectively. In each fractionation experiment, a small proportion of the cell sample was lysed in RIPA buffer (150 mM NaCl, 50 mM Tris–HCl, pH 7.5, 1% Nonidet P-40, 0.1% SDS, 0.5% sodium deoxycholate) supplemented with a protease inhibitor cocktail (Roche) for subsequent analysis of the expression level of exogenous proteins by western blotting. Subcellular fractions were obtained using the Subcellular Protein Fractionation Kit or the NE-PER Nuclear and Cytoplasmic Extraction Kit (Pierce Thermo Scientific) according to the manufacturer's instructions.

Immunoprecipitation and immunoblotting

For immunoprecipitation, HEK293 cells were lysed in PBS containing 1% Triton X-100 supplemented with a protease inhibitor cocktail (Roche) 24 h after transfection with the indicated plasmids. Immunoprecipitation was performed using an anti-Flag (F3165) antibody, following a standard protocol (79). Immunoblotting was performed as described (36). Chemiluminescent images were captured using the GeneGnome imaging system and densitometry was performed using the Gene Tools software, both from Syngene (Cambridge, UK). Densitometry was performed in parallel on duplicate western blots, in a minimum of three independent experiments. For the western blotting analysis of subcellular fractions, exogenous DISC1 band densities were first corrected using appropriate loading controls (nuclear matrix protein p84 for nuclear extracts, GAPDH for cytoplasmic extracts, calreticulin for membrane-bound extracts, vimentin for cytoskeletal extracts), and then divided for the respective GAPDH-corrected DISC1 band intensities in the corresponding whole-cell lysates.

Statistical analysis

Unless otherwise specified, data were analysed by one-way ANOVA followed by Dunnett's multiple comparison test.

SUPPLEMENTARY MATERIAL

Supplementary Material is available at HMG online.

ACKNOWLEDGEMENTS

We thank Dinesh Soares for critical comments on the manuscript. We also thank Richard Killick for providing reagents and technical advice on luciferase assays, and Paul Perry for advice and technical support on image analysis.

Conflict of Interest statement. The authors declare no conflict of interest.

FUNDING

This research was supported by grants from The Wellcome Trust (083210/Z/07/Z) and the Medical Research Council (G0600214, G0902166). Funding to pay the Open Access publication charges for this article was provided by the Wellcome Trust (083210/Z/07/Z) and the Medical Research Council (G0902166).

REFERENCES

1. Chubb, J.E., Bradshaw, N.J., Soares, D.C., Porteous, D.J. and Millar, J.K. (2008) The DISC locus in psychiatric illness. *Mol. Psychiatry*, **13**, 36–64.
2. Bradshaw, N.J. and Porteous, D.J. (2012) DISC1-binding proteins in neural development, signalling and schizophrenia. *Neuropharmacology*, **31**, 9043–9054.

3. Sawamura, N., Ando, T., Maruyama, Y., Fujimuro, M., Mochizuki, H., Honjo, K., Shimoda, M., Toda, H., Sawamura-Yamamoto, T., Makuch, L.A. *et al.* (2008) Nuclear DISC1 regulates CRE-mediated gene transcription and sleep homeostasis in the fruit fly. *Mol. Psychiatry*, **13**, 1138–1148, 1069.
4. Morris, J.A., Kandpal, G., Ma, L. and Austin, C.P. (2003) DISC1 (Disrupted-In-Schizophrenia 1) is a centrosome-associated protein that interacts with MAP1A, MIPT3, ATF4/5 and NUDEL: regulation and loss of interaction with mutation. *Hum. Mol. Genet.*, **12**, 1591–1608.
5. Ozeki, Y., Tomoda, T., Kleiderlein, J., Kamiya, A., Bord, L., Fujii, K., Okawa, M., Yamada, N., Hatten, M.E., Snyder, S.H. *et al.* (2003) Disrupted-in-Schizophrenia-1 (DISC-1): mutant truncation prevents binding to NudE-like (NUDEL) and inhibits neurite outgrowth. *Proc. Natl Acad. Sci. USA*, **100**, 289–294.
6. Millar, J.K., Christie, S. and Porteous, D.J. (2003) Yeast two-hybrid screens implicate DISC1 in brain development and function. *Biochem. Biophys. Res. Commun.*, **311**, 1019–1025.
7. Ameri, K. and Harris, A.L. (2008) Activating transcription factor 4. *Int. J. Biochem. Cell Biol.*, **40**, 14–21.
8. Dey, S., Baird, T.D., Zhou, D., Palam, L.R., Spandau, D.F. and Wek, R.C. (2010) Both transcriptional regulation and translational control of ATF4 are central to the integrated stress response. *J. Biol. Chem.*, **285**, 33165–33174.
9. Fawcett, T.W., Martindale, J.L., Guyton, K.Z., Hai, T. and Holbrook, N.J. (1999) Complexes containing activating transcription factor (ATF)/cAMP-responsive-element-binding protein (CREB) interact with the CCAAT/enhancer-binding protein (C/EBP)-ATF composite site to regulate Gadd153 expression during the stress response. *Biochem. J.*, **339**, 135–141.
10. Ohoka, N., Yoshii, S., Hattori, T., Onozaki, K. and Hayashi, H. (2005) TRB3, a novel ER stress-inducible gene, is induced via ATF4-CHOP pathway and is involved in cell death. *EMBO J.*, **24**, 1243–1255.
11. Harding, H.P., Zhang, Y., Zeng, H., Novoa, I., Lu, P.D., Calfon, M., Sadri, N., Yun, C., Popko, B., Paules, R. *et al.* (2003) An integrated stress response regulates amino acid metabolism and resistance to oxidative stress. *Mol. Cell*, **11**, 619–633.
12. Green, T.A., Alibhai, I.N., Unterberg, S., Neve, R.L., Ghose, S., Tamminga, C.A. and Nestler, E.J. (2008) Induction of activating transcription factors (ATFs) ATF2, ATF3, and ATF4 in the nucleus accumbens and their regulation of emotional behavior. *J. Neurosci.*, **28**, 2025–2032.
13. Costa-Mattioli, M., Gobert, D., Stern, E., Gamache, K., Colina, R., Cuello, C., Sossin, W., Kaufman, R., Pelletier, J., Rosenblum, K. *et al.* (2007) eIF2alpha phosphorylation bidirectionally regulates the switch from short- to long-term synaptic plasticity and memory. *Cell*, **129**, 195–206.
14. Abel, T., Martin, K.C., Bartsch, D. and Kandel, E.R. (1998) Memory suppressor genes: inhibitory constraints on the storage of long-term memory. *Science*, **279**, 338–341.
15. Chen, A., Muzzio, I.A., Malleret, G., Bartsch, D., Verbitsky, M., Pavlidis, P., Yonan, A.L., Vronskaya, S., Grody, M.B., Cepeda, I. *et al.* (2003) Inducible enhancement of memory storage and synaptic plasticity in transgenic mice expressing an inhibitor of ATF4 (CREB-2) and C/EBP proteins. *Neuron*, **39**, 655–669.
16. Soares, D.C., Carlyle, B.C., Bradshaw, N.J. and Porteous, D.J. (2011) DISC1: structure, function, and therapeutic potential for major mental illness. *ACS Chem. Neurosci.*, **2**, 609–632.
17. Singh, K.K., De Rienzo, G., Drane, L., Mao, Y., Flood, Z., Madison, J., Ferreira, M., Bergen, S., King, C., Sklar, P. *et al.* (2011) Common DISC1 polymorphisms disrupt Wnt/GSK3beta signaling and brain development. *Neuron*, **72**, 545–558.
18. Song, W., Li, W., Feng, J., Heston, L.L., Scaringe, W.A. and Sommer, S.S. (2008) Identification of high risk DISC1 structural variants with a 2% attributable risk for schizophrenia. *Biochem. Biophys. Res. Commun.*, **367**, 700–706.
19. Leliveld, S.R., Bader, V., Hendriks, P., Prikulis, I., Sajnani, G., Requena, J.R. and Korth, C. (2008) Insolubility of disrupted-in-schizophrenia 1 disrupts oligomer-dependent interactions with nuclear distribution element 1 and is associated with sporadic mental disease. *J. Neurosci.*, **28**, 3839–3845.
20. Leliveld, S.R., Hendriks, P., Michel, M., Sajnani, G., Bader, V., Trossbach, S., Prikulis, I., Hartmann, R., Jonas, E., Willbold, D. *et al.* (2009) Oligomer assembly of the C-terminal DISC1 domain (640–854) is controlled by self-association motifs and disease-associated polymorphism S704C. *Biochemistry*, **48**, 7746–7755.
21. Ottis, P., Bader, V., Trossbach, S.V., Kretzschmar, H., Michel, M., Leliveld, S.R. and Korth, C. (2011) Convergence of two independent mental disease genes on the protein level: recruitment of dysbindin to cell-invasive disrupted-in-schizophrenia 1 aggresomes. *Biol. Psychiatry*, **70**, 604–610.
22. Narayanan, S., Arthanari, H., Wolfe, M.S. and Wagner, G. (2011) Molecular characterization of disrupted in schizophrenia-1 risk variant S704C reveals the formation of altered oligomeric assembly. *J. Biol. Chem.*, **286**, 44266–44276.
23. Ord, D. and Ord, T. (2003) Mouse NIPK interacts with ATF4 and affects its transcriptional activity. *Exp. Cell Res.*, **286**, 308–320.
24. Liang, G. and Hai, T. (1997) Characterization of human activating transcription factor 4, a transcriptional activator that interacts with multiple domains of cAMP-responsive element-binding protein (CREB)-binding protein. *J. Biol. Chem.*, **272**, 24088–24095.
25. Vallejo, M., Ron, D., Miller, C.P. and Habener, J.F. (1993) C/ATF, a member of the activating transcription factor family of DNA-binding proteins, dimerizes with CAAT/enhancer-binding proteins and directs their binding to cAMP response elements. *Proc. Natl Acad. Sci. USA*, **90**, 4679–4683.
26. Siu, F., Bain, P.J., LeBlanc-Chaffin, R., Chen, H. and Kilberg, M.S. (2002) ATF4 is a mediator of the nutrient-sensing response pathway that activates the human asparagine synthetase gene. *J. Biol. Chem.*, **277**, 24120–24127.
27. He, C.H., Gong, P., Hu, B., Stewart, D., Choi, M.E., Choi, A.M. and Alam, J. (2001) Identification of activating transcription factor 4 (ATF4) as an Nrf2-interacting protein. Implication for heme oxygenase-1 gene regulation. *J. Biol. Chem.*, **276**, 20858–20865.
28. Kilberg, M.S., Shan, J. and Su, N. (2009) ATF4-dependent transcription mediates signaling of amino acid limitation. *Trends Endocrinol. Metab.*, **20**, 436–443.
29. Ma, Y., Brewer, J.W., Diehl, J.A. and Hendershot, L.M. (2002) Two distinct stress signaling pathways converge upon the CHOP promoter during the mammalian unfolded protein response. *J. Mol. Biol.*, **318**, 1351–1365.
30. Shan, J., Ord, D., Ord, T. and Kilberg, M.S. (2009) Elevated ATF4 expression, in the absence of other signals, is sufficient for transcriptional induction via CCAAT enhancer-binding protein-activating transcription factor response elements. *J. Biol. Chem.*, **284**, 21241–21248.
31. Bruhat, A., Averous, J., Carraro, V., Zhong, C., Reimold, A.M., Kilberg, M.S. and Fafournoux, P. (2002) Differences in the molecular mechanisms involved in the transcriptional activation of the CHOP and asparagine synthetase genes in response to amino acid deprivation or activation of the unfolded protein response. *J. Biol. Chem.*, **277**, 48107–48114.
32. Luo, S., Baumeister, P., Yang, S., Abcouwer, S.F. and Lee, A.S. (2003) Induction of Grp78/BiP by translational block: activation of the Grp78 promoter by ATF4 through and upstream ATF/CRE site independent of the endoplasmic reticulum stress elements. *J. Biol. Chem.*, **278**, 37375–37385.
33. Vinson, C., Myakishev, M., Acharya, A., Mir, A.A., Moll, J.R. and Bonovich, M. (2002) Classification of human B-ZIP proteins based on dimerization properties. *Mol. Cell Biol.*, **22**, 6321–6335.
34. Park, Y.U., Jeong, J., Lee, H., Mun, J.Y., Kim, J.H., Lee, J.S., Nguyen, M.D., Han, S.S., Suh, P.G. and Park, S.K. (2010) Disrupted-in-schizophrenia 1 (DISC1) plays essential roles in mitochondria in collaboration with Mitofilin. *Proc. Natl Acad. Sci. USA*, **107**, 17785–17790.
35. Millar, J.K., James, R., Christie, S. and Porteous, D.J. (2005) Disrupted in schizophrenia 1 (DISC1): subcellular targeting and induction of ring mitochondria. *Mol. Cell Neurosci.*, **30**, 477–484.
36. James, R., Adams, R.R., Christie, S., Buchanan, S.R., Porteous, D.J. and Millar, J.K. (2004) Disrupted in Schizophrenia 1 (DISC1) is a multicompartmentalized protein that predominantly localizes to mitochondria. *Mol. Cell Neurosci.*, **26**, 112–122.
37. Hodgkinson, C.A., Goldman, D., Jaeger, J., Persaud, S., Kane, J.M., Lipsky, R.H. and Malhotra, A.K. (2004) Disrupted in schizophrenia 1 (DISC1): association with schizophrenia, schizoaffective disorder, and bipolar disorder. *Am. J. Hum. Genet.*, **75**, 862–872.
38. Lepagnol-Bestel, A.M., Dubertret, C., Benmessaoud, D., Simonneau, M., Ades, J., Kacha, F., Hamdani, N., Gorwood, P. and Ramoz, N. (2010)

Association of DISC1 gene with schizophrenia in families from two distinct French and Algerian populations. *Psychiatr. Genet.*, **20**, 298–303.
39. Schosser, A., Gaysina, D., Cohen-Woods, S., Chow, P.C., Martucci, L., Craddock, N., Farmer, A., Korszun, A., Gunasinghe, C., Gray, J. *et al.* (2009) Association of DISC1 and TSNAX genes and affective disorders in the depression case-control (DeCC) and bipolar affective case-control (BACCS) studies. *Mol. Psychiatry*, **15**, 844–849.
40. Szeszko, P.R., Hodgkinson, C.A., Robinson, D.G., Derosse, P., Bilder, R.M., Lencz, T., Burdick, K.E., Napolitano, B., Betensky, J.D., Kane, J.M. *et al.* (2008) DISC1 is associated with prefrontal cortical gray matter and positive symptoms in schizophrenia. *Biol. Psychol.*, **79**, 103–110.
41. Shaikh, M., Hall, M.H., Schulze, K., Dutt, A., Li, K., Williams, I., Walshe, M., Constante, M., Broome, M., Picchioni, M. *et al.* (2011) Effect of DISC1 on the P300 waveform in psychosis. *Schizophr. Bull.* [Epub ahead of print]. doi: 10.1093/schbul/sbr101.
42. Cannon, T.D., Hennah, W., van Erp, T.G., Thompson, P.M., Lonnqvist, J., Huttunen, M., Gasperoni, T., Tuulio-Henriksson, A., Pirkola, T., Toga, A.W. *et al.* (2005) Association of DISC1/TRAX haplotypes with schizophrenia, reduced prefrontal gray matter, and impaired short- and long-term memory. *Arch. Gen. Psychiatry*, **62**, 1205–1213.
43. Raznahan, A., Lee, Y., Long, R., Greenstein, D., Clasen, L., Addington, A., Rapoport, J.L. and Giedd, J.N. (2011) Common functional polymorphisms of DISC1 and cortical maturation in typically developing children and adolescents. *Mol. Psychiatry*, **16**, 917–926.
44. Brauns, S., Gollub, R.L., Roffman, J.L., Yendiki, A., Ho, B.C., Wassink, T.H., Heinz, A. and Ehrlich, S. (2011) DISC1 is associated with cortical thickness and neural efficiency. *Neuroimage*, **57**, 1591–1600.
45. Whalley, H.C., Sussmann, J.E., Johnstone, M., Romaniuk, L., Redpath, H., Chakirova, G., Mukherjee, P., Hall, J., Johnstone, E.C., Lawrie, S.M. *et al.* (2012) Effects of a mis-sense DISC1 variant on brain activation in two cohorts at high risk of bipolar disorder or schizophrenia. *Am. J. Med. Genet. B Neuropsychiatr. Genet.* [Epub ahead of print]. doi: 10.1002/ajmg.b.32035.
46. Hennah, W., Thomson, P., McQuillin, A., Bass, N., Loukola, A., Anjorin, A., Blackwood, D., Curtis, D., Deary, I.J., Harris, S.E. *et al.* (2009) DISC1 association, heterogeneity and interplay in schizophrenia and bipolar disorder. *Mol. Psychiatry*, **14**, 865–873.
47. Kamiya, A., Kubo, K., Tomoda, T., Takaki, M., Youn, R., Ozeki, Y., Sawamura, N., Park, U., Kudo, C., Okawa, M. *et al.* (2005) A schizophrenia-associated mutation of DISC1 perturbs cerebral cortex development. *Nat. Cell Biol.*, **7**, 1167–1178.
48. Brandon, N.J., Handford, E.J., Schurov, I., Rain, J.C., Pelling, M., Duran-Jimeniz, B., Camargo, L.M., Oliver, K.R., Beher, D., Shearman, M.S. *et al.* (2004) Disrupted in Schizophrenia 1 and Nudel form a neurodevelopmentally regulated protein complex: implications for schizophrenia and other major neurological disorders. *Mol. Cell Neurosci.*, **25**, 42–55.
49. Elefteriou, F., Ahn, J.D., Takeda, S., Starbuck, M., Yang, X., Liu, X., Kondo, H., Richards, W.G., Bannon, T.W., Noda, M. *et al.* (2005) Leptin regulation of bone resorption by the sympathetic nervous system and CART. *Nature*, **434**, 514–520.
50. Lassot, I., Estrabaud, E., Emiliani, S., Benkirane, M., Benarous, R. and Margottin-Goguet, F. (2005) p300 modulates ATF4 stability and transcriptional activity independently of its acetyltransferase domain. *J. Biol. Chem.*, **280**, 41537–41545.
51. Yang, X., Matsuda, K., Bialek, P., Jacquot, S., Masuoka, H.C., Schinke, T., Li, L., Brancorsini, S., Sassone-Corsi, P., Townes, T.M. *et al.* (2004) ATF4 is a substrate of RSK2 and an essential regulator of osteoblast biology; implication for Coffin-Lowry Syndrome. *Cell*, **117**, 387–398.
52. Dever, T.E. (2002) Gene-specific regulation by general translation factors. *Cell*, **108**, 545–556.
53. Harding, H.P., Novoa, I., Zhang, Y., Zeng, H., Wek, R., Schapira, M. and Ron, D. (2000) Regulated translation initiation controls stress-induced gene expression in mammalian cells. *Mol. Cell*, **6**, 1099–1108.
54. Vattem, K.M. and Wek, R.C. (2004) Reinitiation involving upstream ORFs regulates ATF4 mRNA translation in mammalian cells. *Proc. Natl Acad. Sci. USA*, **101**, 11269–11274.
55. Lassot, I., Segeral, E., Berlioz-Torrent, C., Durand, H., Groussin, L., Hai, T., Benarous, R. and Margottin-Goguet, F. (2001) ATF4 degradation relies on a phosphorylation-dependent interaction with the SCF(betaTrCP) ubiquitin ligase. *Mol. Cell Biol.*, **21**, 2192–2202.
56. Pons, J., Evrard-Todeschi, N., Bertho, G., Gharbi-Benarous, J., Benarous, R. and Girault, J.P. (2007) Phosphorylation-dependent structure of ATF4 peptides derived from a human ATF4 protein, a member of the family of transcription factors. *Peptides*, **28**, 2253–2267.
57. Frank, C.L., Ge, X., Xie, Z., Zhou, Y. and Tsai, L.H. (2010) Control of activating transcription factor 4 (ATF4) persistence by multisite phosphorylation impacts cell cycle progression and neurogenesis. *J. Biol. Chem.*, **285**, 33324–33337.
58. Gachon, F., Gaudray, G., Thebault, S., Basbous, J., Koffi, J.A., Devaux, C. and Mesnard, J. (2001) The cAMP response element binding protein-2 (CREB-2) can interact with the C/EBP-homologous protein (CHOP). *FEBS Lett.*, **502**, 57–62.
59. Karpinski, B.A., Morle, G.D., Huggenvik, J., Uhler, M.D. and Leiden, J.M. (1992) Molecular cloning of human CREB-2: an ATF/CREB transcription factor that can negatively regulate transcription from the cAMP response element. *Proc. Natl Acad. Sci. USA*, **89**, 4820–4824.
60. Costa-Mattioli, M. and Sonenberg, N. (2006) Translational control of long-term synaptic plasticity and memory storage by eIF2alpha. *Crit. Rev. Neurobiol.*, **18**, 187–195.
61. Bartsch, D., Ghirardi, M., Skehel, P.A., Karl, K.A., Herder, S.P., Chen, M., Bailey, C.H. and Kandel, E.R. (1995) Aplysia CREB2 represses long-term facilitation: relief of repression converts transient facilitation into long-term functional and structural change. *Cell*, **83**, 979–992.
62. Clapcote, S.J., Lipina, T.V., Millar, J.K., Mackie, S., Christie, S., Ogawa, F., Lerch, J.P., Trimble, K., Uchiyama, M., Sakuraba, Y. *et al.* (2007) Behavioral phenotypes of Disc1 missense mutations in mice. *Neuron*, **54**, 387–402.
63. Shen, S., Lang, B., Nakamoto, C., Zhang, F., Pu, J., Kuan, S.L., Chatzi, C., He, S., Mackie, I., Brandon, N.J. *et al.* (2008) Schizophrenia-related neural and behavioral phenotypes in transgenic mice expressing truncated Disc1. *J. Neurosci.*, **28**, 10893–10904.
64. Hikida, T., Jaaro-Peled, H., Seshadri, S., Oishi, K., Hookway, C., Kong, S., Wu, D., Xue, R., Andrade, M., Tankou, S. *et al.* (2007) Dominant-negative DISC1 transgenic mice display schizophrenia-associated phenotypes detected by measures translatable to humans. *Proc. Natl Acad. Sci. USA*, **104**, 14501–14506.
65. Li, W., Zhou, Y., Jentsch, J.D., Brown, R.A., Tian, X., Ehninger, D., Hennah, W., Peltonen, L., Lonnqvist, J., Huttunen, M.O. *et al.* (2007) Specific developmental disruption of disrupted-in-schizophrenia-1 function results in schizophrenia-related phenotypes in mice. *Proc. Natl Acad. Sci. USA*, **104**, 18280–18285.
66. Ayhan, Y., Abazyan, B., Nomura, J., Kim, R., Ladenheim, B., Krasnova, I.N., Sawa, A., Margolis, R.L., Cadet, J.L., Mori, S. *et al.* (2011) Differential effects of prenatal and postnatal expressions of mutant human DISC1 on neurobehavioral phenotypes in transgenic mice: evidence for neurodevelopmental origin of major psychiatric disorders. *Mol. Psychiatry*, **16**, 293–306.
67. Mao, Y., Ge, X., Frank, C.L., Madison, J.M., Koehler, A.N., Doud, M.K., Tassa, C., Berry, E.M., Soda, T., Singh, K.K. *et al.* (2009) Disrupted in schizophrenia 1 regulates neuronal progenitor proliferation via modulation of GSK3beta/beta-catenin signaling. *Cell*, **136**, 1017–1031.
68. Niwa, M., Kamiya, A., Murai, R., Kubo, K., Gruber, A.J., Tomita, K., Lu, L., Tomisato, S., Jaaro-Peled, H., Seshadri, S. *et al.* (2010) Knockdown of DISC1 by in utero gene transfer disturbs postnatal dopaminergic maturation in the frontal cortex and leads to adult behavioral deficits. *Neuron*, **65**, 480–489.
69. Lipina, T.V., Niwa, M., Jaaro-Peled, H., Fletcher, P.J., Seeman, P., Sawa, A. and Roder, J.C. (2010) Enhanced dopamine function in DISC1-L100P mutant mice: implications for schizophrenia. *Genes Brain Behav.*, **9**, 777–789.
70. Badiola, N., Penas, C., Minano-Molina, A., Barneda-Zahonero, B., Fado, R., Sanchez-Opazo, G., Comella, J.X., Sabria, J., Zhu, C., Blomgren, K. *et al.* (2011) Induction of ER stress in response to oxygen-glucose deprivation of cortical cultures involves the activation of the PERK and IRE-1 pathways and of caspase-12. *Cell Death Dis.*, **2**, e149.

71. Granberg, F., Svensson, C., Pettersson, U. and Zhao, H. (2006) Adenovirus-induced alterations in host cell gene expression prior to the onset of viral gene expression. *Virology*, **353**, 1–5.
72. Lange, P.S., Chavez, J.C., Pinto, J.T., Coppola, G., Sun, C.W., Townes, T.M., Geschwind, D.H. and Ratan, R.R. (2008) ATF4 is an oxidative stress-inducible, prodeath transcription factor in neurons in vitro and in vivo. *J. Exp. Med.*, **205**, 1227–1242.
73. Silva, J.M., Wong, A., Carelli, V. and Cortopassi, G.A. (2009) Inhibition of mitochondrial function induces an integrated stress response in oligodendroglia. *Neurobiol. Dis.*, **34**, 357–365.
74. Brown, A.S. (2011) The environment and susceptibility to schizophrenia. *Prog. Neurobiol.*, **93**, 23–58.
75. Caspi, A., Moffitt, T.E., Cannon, M., McClay, J., Murray, R., Harrington, H., Taylor, A., Arseneault, L., Williams, B., Braithwaite, A. *et al.* (2005) Moderation of the effect of adolescent-onset cannabis use on adult psychosis by a functional polymorphism in the catechol-O-methyltransferase gene: longitudinal evidence of a gene X environment interaction. *Biol. Psychiatry*, **57**, 1117–1127.
76. Ogawa, F., Kasai, M. and Akiyama, T. (2005) A functional link between Disrupted-In-Schizophrenia 1 and the eukaryotic translation initiation factor 3. *Biochem. Biophys. Res. Commun.*, **338**, 771–776.
77. McLaurin, J., Trudel, G.C., Shaw, I.T., Antel, J.P. and Cashman, N.R. (1995) A human glial hybrid cell line differentially expressing genes subserving oligodendrocyte and astrocyte phenotype. *J. Neurobiol.*, **26**, 283–293.
78. Ord, D., Meerits, K. and Ord, T. (2007) TRB3 protects cells against the growth inhibitory and cytotoxic effect of ATF4. *Exp. Cell Res.*, **313**, 3556–3567.
79. Bradshaw, N.J., Ogawa, F., Antolin-Fontes, B., Chubb, J.E., Carlyle, B.C., Christie, S., Claessens, A., Porteous, D.J. and Millar, J.K. (2008) DISC1, PDE4B, and NDE1 at the centrosome and synapse. *Biochem. Biophys. Res. Commun.*, **377**, 1091–1096.

“DISC1 variants 37W and 607F disrupt its nuclear targeting and regulatory role in ATF4-mediated transcription”

Supplementary material

Supplementary Material

DISC1 variants 37W and 607F disrupt its nuclear targeting and regulatory role in ATF4-mediated transcription

Elise L.V. Malavasi, Fumiaki Ogawa, David J. Porteous and J. Kirsty Millar

Supplementary Figure 1 (Figure S1)

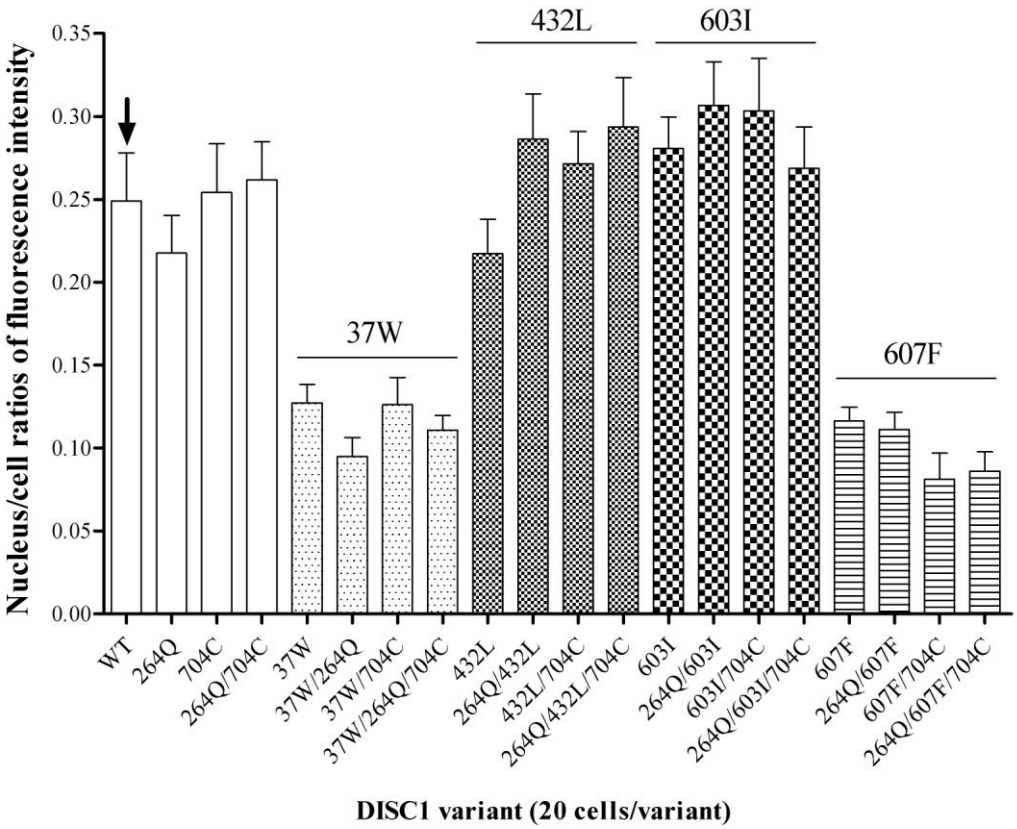

Relative abundance of DISC1 variants in the nucleus of transfected COS7 cells, calculated as the ratio between the total pixel intensity of DISC1 staining in the nucleus and the total pixel intensity of DISC1 staining in the whole cell. The bars represent mean measurements of 20 cells/variant carried out in a single experiment. The black arrow indicates the common long isoform of wild-type (WT) DISC1, to which all other variants are compared.

Supplementary Figure 2 (Figure S2)

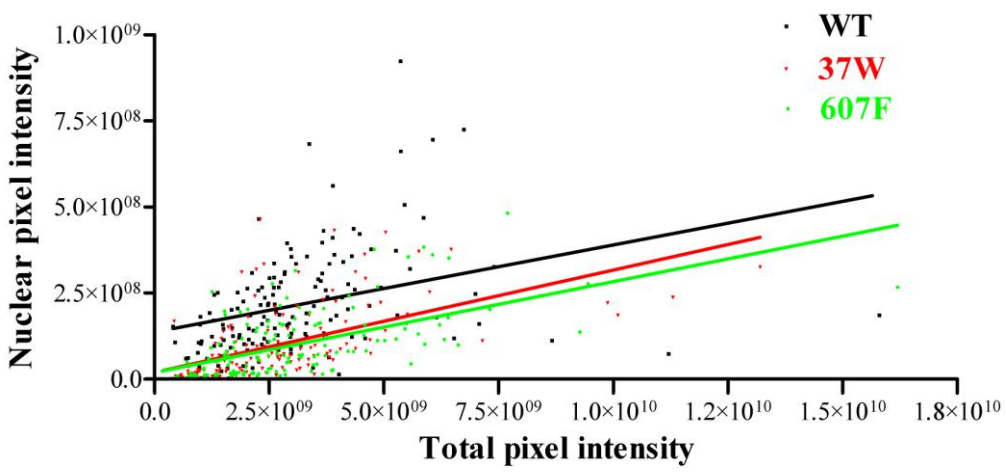

Scatterplot and regression lines of total pixel intensity of DISC1 staining in the whole cell (x-axis, independent variable) vs. nucleus (y-axis, dependent variable) in individual COS7 cells transfected with wild-type DISC1, DISC1-37W or DISC1-607F. The graph was generated by pooling measurements obtained from 50 cells/variant in 3 independent experiments (150 cells/variant in total). Pearson r (95% confidence interval) = 0.3337, P<0.0001 (wild-type DISC1); 0.5648, P<0.0001 (DISC1-37W); 0.5760, P<0.0001 (DISC1-607F).

Supplementary Figure 3 (Figure S3)

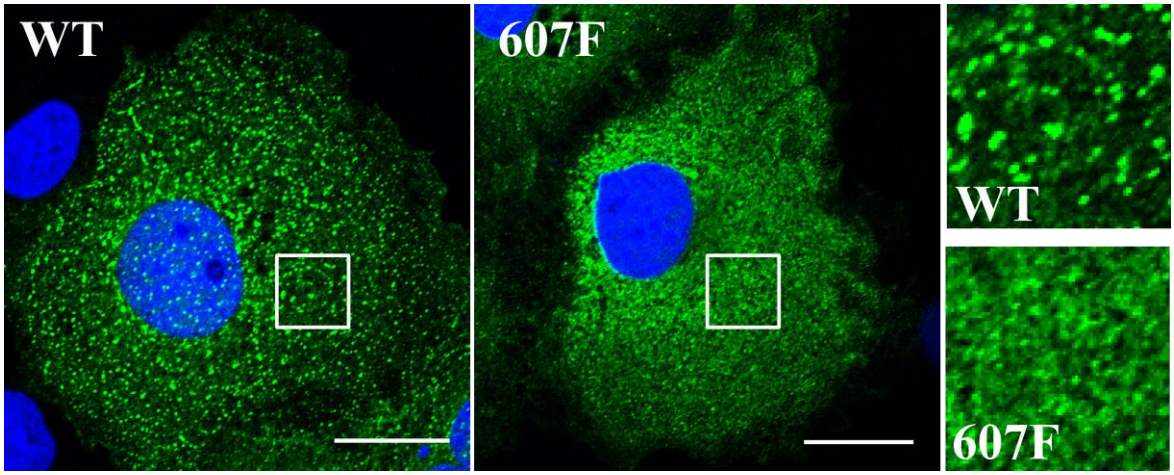

Representative COS7 cells expressing either wild-type DISC1 or DISC1-607F (green). Nuclei (blue) are stained with DAPI. The cytoplasmic regions delimited by the white squares are magnified in the panels on the right. Scale bars are 20 μm.

Supplementary Figure 4 (Figure S4)

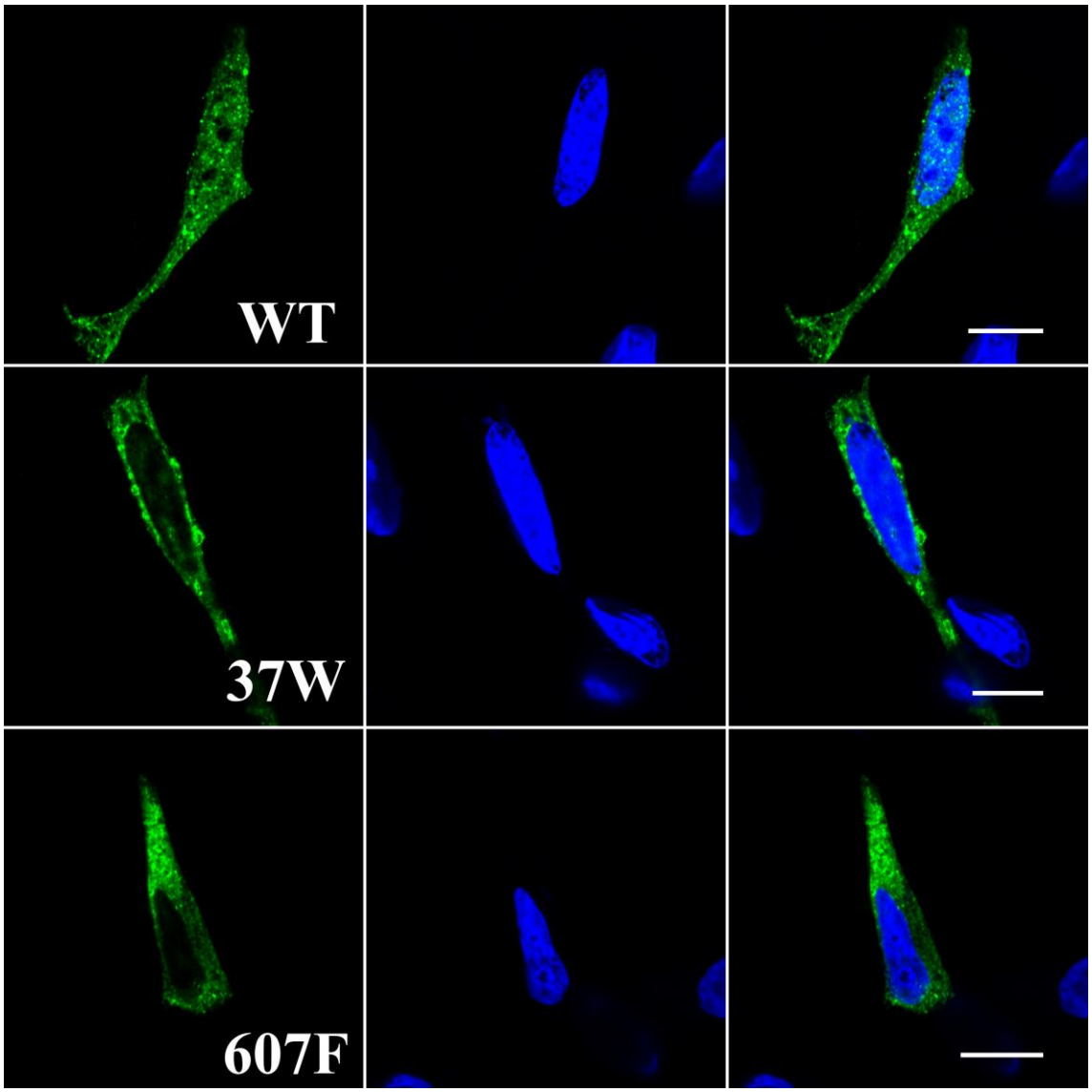

Representative SH-SY5Y cells expressing wild-type DISC1, DISC1-37W or DISC1-607F (green). Nuclei (blue) are stained with DAPI. Scale bars are 10 μm.

Supplementary Figure 5 (Figure S5)

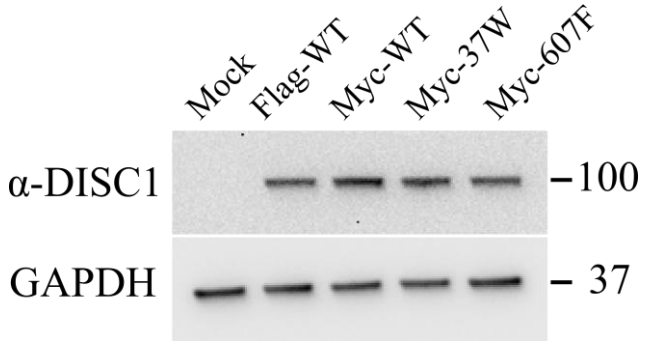

Whole cell lysates were obtained from SH-SY5Y cells that were either mock transfected or transfected with equal amounts of the indicated DISC1 expression constructs, and analysed by Western blotting. DISC1 expression was assessed using the α-DISC1 antibody to ensure that comparable total exogenous DISC1 expression was achieved, and the antibody concentration used was adjusted so that only exogenous DISC1 could be detected. The position and size (kDa) of the protein markers is shown.

Supplementary Figure 6 (Figure S6)

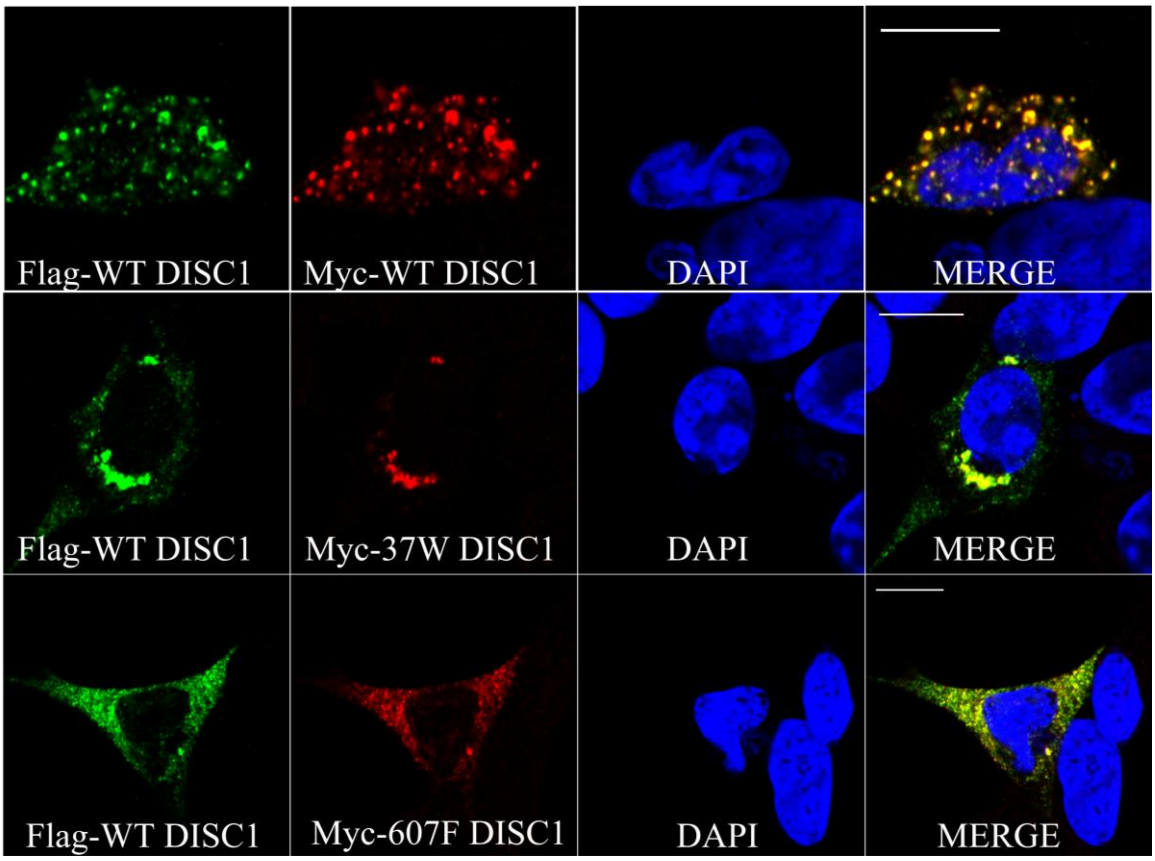

Subcellular distribution of Flag-DISC1 (green) and Myc-DISC1 (red) in representative SH-SY5Y cells expressing Flag-WT DISC1 in combination with an equal amount of Myc-WT DISC1 (top), Myc-37W DISC1 (middle) or Myc-607F DISC1 (bottom). Scale bars are 10 μm.

Supplementary Figure 7 (Figure S7)

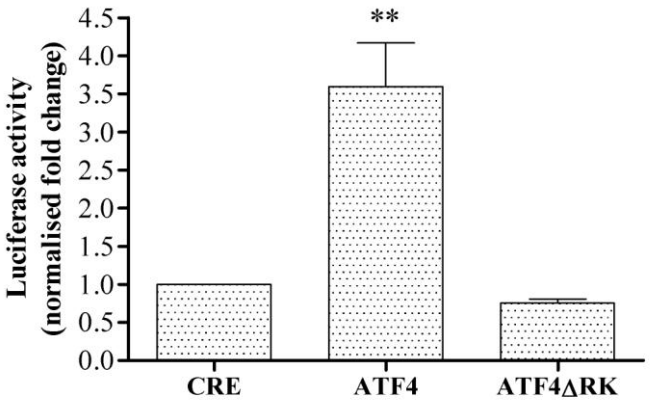

Relative luciferase activity in HEK293 cells transfected with the reporters only (CRE) or in combination with either human ATF4 or its dominant-negative mutant form ATF4ΔRK. The data are normalised to the relative luciferase activity in cells transfected with the reporters only (CRE). **P < 0.01.

Supplementary Figure 8 (Figure S8)

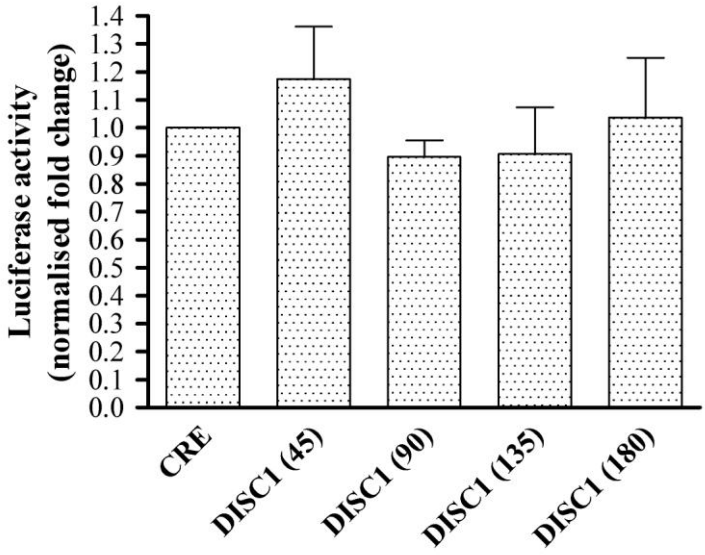

HEK293 cells were transfected with the reporters only (CRE) or in combination with increasing amounts of wild-type DISC1 (reported in brackets as ng/well). Forty-eight hours after transfection, the cells were lysed and the relative luciferase activity was measured. The data are normalised to the relative luciferase activity in cells transfected with the reporters only. The bars represent the average of 4 independent experiments.

Supplementary Figure 9 (Figure S9)

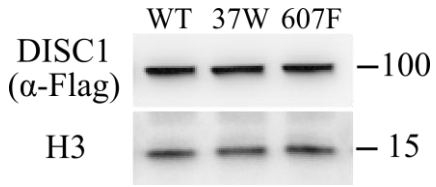

To compare the expression levels of WT DISC1, DISC1-37W and DISC1-607F, whole cell lysates were obtained from HEK293 cells transfected with equal amounts of the indicated DISC1 expression constructs, and analysed by Western blotting. The loading control is histone 3 (H3). The position and size (kDa) of the protein markers is shown.

Supplementary Figure 10 (Figure S10)

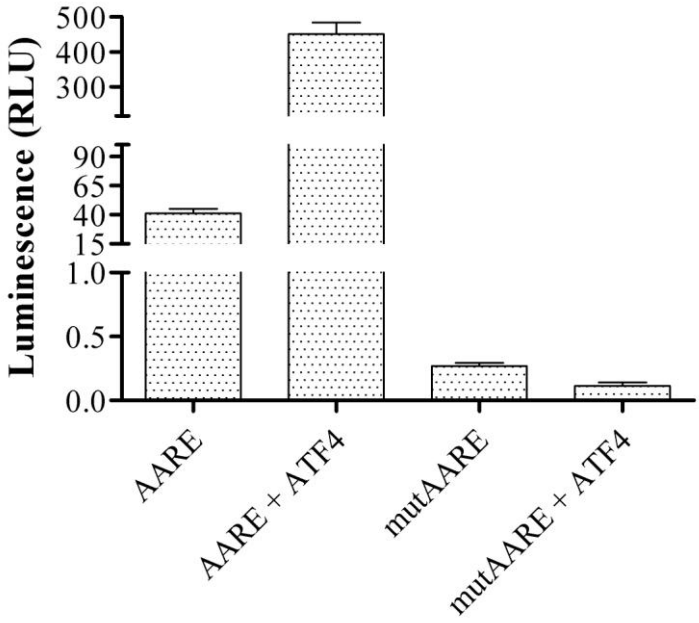

HEK293 cells were transfected with the reporters only (AARE or mutAARE) or in combination with ATF4. Forty-eight hours after transfection, the cells were lysed and the relative luciferase activity was measured. The bars represent the average of 4 independent experiments. RLU: Relative Light Units.

Supplementary Figure 11 (Figure S11)

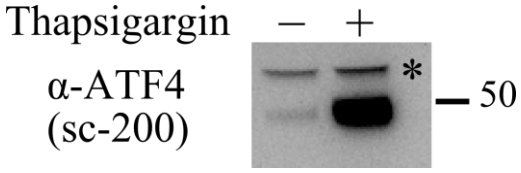

HEK293 cells were treated with 1 μM thapsigargin for 16 hours. At the end of the drug treatment, nuclear protein extracts were prepared from the transfected cells and analysed by Western blotting. Endogenous ATF4 was detected with the sc-200 antibody. The position and size (kDa) of the protein markers is indicated. * Non-specific band.

Supplementary Figure 12 (Figure S12)

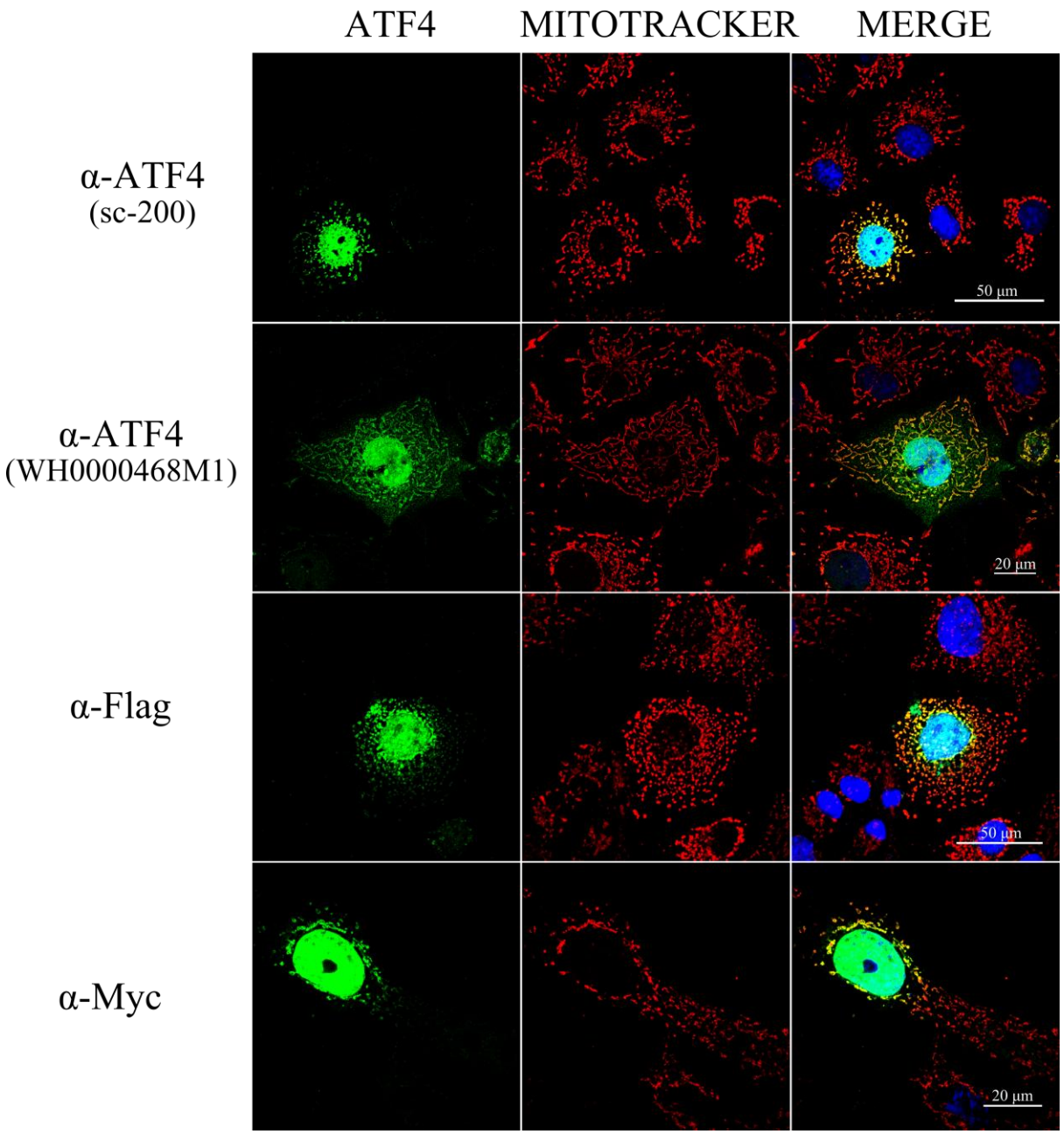

COS7 cells were transfected with pCGATF4 (top two rows), ATF4-Flag (third row) or ATF4-Myc (bottom row). Exogenous ATF4 was detected using either anti-ATF4 or anti-tag antibodies, as indicated in the figure, and mitochondria were stained with Mitotracker Red.